agggaccaaggtggaaatcaaacgtgagtagaatttaaactttgcggccgcctagacgtttaagtgggagatttggaggg
gatgaggaatgaaggaacttcaggatagaaaagggctgaagtcaagttcagctcctaaaatggatgtgggagcaaacttt
gaagataaactgaatgacccagaggatgaaacagcgcagatcaaagaggggcctggagctctgagaagagaaggaga
ctcatccgtgttgagtttccacaagtactgtcttgagttttgcaataaaagtgggatagcagagttgagtgagccgtaggctg
agttctctcttttgtctcctaagtttttatgactacaaaaatcagtagtatgtcctgaaataatcattaagctgtttgaaagtatgac
tgcttgccatgtagataccatgtcttgctgaatgatcagaagaggtgtgactcttattctaaaatttgtcacaaaatgtcaaaat
gagagactctgtaggaacgagtccttgacagacagctcaaggggttttttttcctttgtctcatttctacatgaaagtaaatttga
aatgatctttttttattataagagtagaaatacagttgggtttgaactatatgttttaatggccacggttttgtaagacatttggtcct
ttgttttcccagttattactcgattgtaattttatatcgccagcaatggactgaaacggtccgcaacctcttctttacaactgggt
gacctcgcggctgtgccagccatttggcgttcaccctgccgctaagggccatgtgaacccccgcggtagcatcccttgctc
cgcgtggaccactttcctgaggcacagtgataggaacagagccactaatctgaagagaacagagatgtgacagactaca
ctaatgtgagaaaaacaaggaaagggtgacttattggagatttcagaaataaaatgcatttattattatattcccttattttaatttt
ctattagggaattagaaagggcataaactgctttatccagtgttatattaaaagcttaatgtatataatcttttagaggtaaaatct
acagccagcaaaagtcatggtaaatattctttgactgaactctcactaaactcctctaaattatatgtcatattaactggttaaatt
aatataaatttgtgacatgaccttaactggttaggtaggatatttttcttcatgcaaaaatatgactaataataatttagcacaaaa
atatttcccaatactttaattctgtgatagaaaaatgtttaactcagctactataatcccataattttgaaaactatttattagcttttg
tgtttgacccttccctagccaaaggcaactatttaaggacccctttaaaactcttgaaactactttagagtcattaagttatttaac
cacttttaattactttaaaatgatgtcaattccctttttaactattaatttattttaaggggggaaaggctgctcataattctattgttttt
cttggtaaagaactctcagttttcgtttttactacctctgtcacccaagagttggcatctcaacagaggggactttccgagagg
ccatctggcagttgcttaagatcagaagtgaagtctgccagttcctcccaggcaggtggcccagattacagttgacctgttct
ggtgtggctaaaaattgtcccatgtggttacaaaccattagaccagggtctgatgaattgctcagaatatttctggacaccca
aatacagaccctggcttaaggccctgtccatacagtaggtttagcttggctacaccaaaggaagccatacagaggctaata
tcagagtattcttggaagagacaggagaaaatgaaagccagtttctgctcttaccttatgtgcttgtgttcagactcccaaaca
tcaggagtgtcagataaactggtctgaatctctgtctgaagcatggaactgaaaagaatgtagtttcagggaagaaaggca
atagaaggaagcctgagaatacggatcaattctaaactctgaggggtcggatgacgtggccattctttgcctaaagcatt
gagtttactgcaaggtcagaaaagcatgcaaagccctcagaatggctgcaaagagctccaacaaaacaatttagaacttta
ttaaggaataggggaagctaggaagaaactcaaaacatcaagattttaaatacgcttcttggtctccttgctataattatctg
ggataagcatgctgttttctgtctgtccctaacatgccctgtgattatccgcaaacaacacacccaagggcagaactttgttac
ttaaacaccatcctgtttgcttctttcctcaggaactgtggctgcaccatctgtcttcatcttcccgccatctgatgagcagttga
aatctggaactgcctctgttgtgtgcctgctgaataacttctatcccagagaggccaaagtacagtggaaggtggataacgc
cctccaatcgggtaactcccaggagagtgtcacagagcaggacagcaaggacagcacctacagcctcagcagcaccct
gacgctgagcaaagcagactacgagaaacacaaagtctacgcctgcgaagtcacccatcagggcctgagctcgcccgt
cacaaagagcttcaacaggggagagtgttag (SEQ ID NO: 24)

**Example 1.1 Vector construction**

Sequences for ANTIBODY A originated from the 2nd maturation round after primary screening of the MorphoSys HuCAL Library, a synthetic phage display library. The DNA for ANTIBODY A was originally provided in vectors pMorph from MorphoSys, Germany and corresponds to Fab expressing vectors in Figure 2 in WO 03/070760, appendix p 6/43. In the vector construction for the purposes of the present invention, vectors pEE6.1 and pEE 14.4 (both commercially available from Lonza Biologics are encoded to obtain a construct with both chains in one vector, see appended Figure 1; see WO 87/04462 or WO 89/01036 . The following cloning strategy was applied:

The Ig kappa chain was isolated from vector MS-Roche #7.9.H7_Ig_kappa chain (as described in WO 03/070760) by PCR with primer ACGTAAGCTTGCCGCCACCATGGTGTTGCAG (sense, HindIII; SEQ ID NO. 29) and primer ACGTGAATTCCTAACACTCTCCCCTGTT (antisense, EcoRI; SEQ ID NO. 30), inserted into pCR 2.1 Topo TA and the insert was completely sequenced. The Ig kappa chain insert was removed from pCR Topo 2.1 by HinDIII/EcoRI digest and ligated into vector pEE14.4 as HindIII/EcoRI insert.

The Ig gamma 1 heavy chain was cloned from vector pMorph MS-Roche #7.9.H7_IgG1 by PCR with primer ACGTAAGCTTGCCGCCACCATGAAACACCTG (sense, HindIII; SEQ ID NO: 31) and primer ACGTGAATTCTCATTTACCCGGAGACAG (antisense, EcoRI; SEQ ID NO: 32), inserted into pCR 2.1 Topo TA, and the insert was completely sequenced. The Ig gamma1 heavy chain insert was removed from pCR Topo 2.1 by HindIII/EcoRI digest and ligated into vector pEE 6.4 as HindIII/EcoRI insert. The heavy chain expression cassette was removed from pEE 6.4 IgG1 by NotI/SalI digest and the isolated fragment was inserted into SalI/NotI digested pEE14.4 kappa resulting in the final double-gene construct pEE 14.4 mAb-31.

**Example 1.2: Transfection of CHO cells and expression of ANTIBODY A**

Transfections were carried out according to standard protocols. The host cell line CHO K1 was derived from the Lonza Biologics working cell bank (WCB) # 028-W2 (Lonza, 2002, 1-179) and the host cell line CHO K1 SV was derived from the Lonza Biologics master cell bank (MCB) #269-M (Lonza, 2003, 1-87).

Adherent CHO K1 cells derived from the WCB # 028-W2 were transfected with the vector pEE 14.4 MAb31 containing both heavy and kappa light chain genes by liposomal transfection

(Fugene, Roche Diagnostics). Transfection isolates were selected in DMEM, GS supplement (both JRH Biosciences), 10% dialysed FCS (PAA Laboratories, CoS#R0-CEP 2001-083-Rev 00) and 50μM methionine sulphoximine (MSX from Sigma). 2 weeks later, colonies were picked and transferred to 96well plates and tested with ELISA for antibody production. 4 colonies with the highest expression of ANTIBODY A were cloned by serial limited dilution to obtain single-cell derived cultures, of which 82 clones were derived after one week and expanded.

One of these clones was selected as the one with the highest specific production rate of 48pg/cell/day in adherent state. It was further sub-cloned by limiting dilution to obtain the good producers expressing ANTIBODY A with high stability (Pu, (1998) Mol Biotechnol, 10, 17-25). Additionally, a suspension variant of the CHO K1 cells, the CHO K1 SV cells from MCB #269-M were transfected with the vector pEE 14.4 MAb31 by electroporation. Transfectants were selected as before and the resulting clones were subjected to single cell cloning by limiting dilution resulting in several high producer clones of ANTIBODY A.

**Example 1.3 Adaptation of clones expressing ANTIBODY A to suspension culture**

Best growth properties of CHO K1 clones were determined in DHI media with different protein hydrolysates: Cells were finally adapted to DHI media w/o glutamine (Invitrogen), which is a mixture of DMEM, Ham's F12 and IMDM in the respective proportions of 1:1:2 (v:v:v) (Schlaeger and Schumpp, 1992, J Immunol Methods, 146, 111-20) with the following modifications: soy and rice hydrolysate: *0.2% soy HyPep 1510 and 0.2% rice HyPep* 5603 (Kerry Bioscience), 0.03% Pluronic F68 (Invitrogen), 25μM MSX (Sigma) and 5% dialysed FCS (PAA Laboratories). FCS concentration was decreased gradually until cells did grow exponentially in serum-free media DHI media. Primary seed banks in serum-free DHI media were frozen for the several recombinant cell clones

CHO K1 SV clones were adapted from DMEM containing 10% dialysed FCS to suspension culture in the chemically defined CD-CHO media with 25μM MSX (Gibco-Invitrogen) in a two step procedure (Lonza). Cell banks were created in CD-CHO. Optionally, any other serum-free and protein-free media for CHO cells could be used for suspension culture and as a base for expressing the antibody.

**Example 2: Production of ANTIBODY A**

**Production of ANTIBODY A (by fed-batch fermentation)**

CHO clones were prepared for fermentation from stock cultures in either shake flasks or spinner cultures as follows:

A cryo vial of the respective clones was thawed in the respective culture media containing 25μM MSX in a 100ml shake flask or spinner with a nominal volume of 50-75ml.

Cells were then expanded in consecutive splits of 1:5 to reach a stock culture of 400-500ml volume in either shake flasks or spinners. Cells used for inoculation of fermenters could be derived from these stock cultures up to 90 days after thawing. The seed train constitutes of a 2x 1000ml step in 2L shake flasks or spinners, followed by inoculation of a 10L fermenter as a further vessel. Alternatively, the 10L fermenter could function as the fed-batch vessel itself or as inoculate for the 100L fed-batch fermenter. MSX was present in the culture media for selection until the inoculation of the 10L fermenter where it was exluded.

Fermentation process:

Day 0: Start with $3\text{-}4x10^5$/ml cells (1:4 -1:5 split from seed culture)

Day 2-3: start of feeding, cell density should be above $1.5x10^6$/ml.

Feeding: Continuous or bolus feed at 2% per day.

The isoform composition of ANTIBODY A was monitored throughout the fermentation by ion exchange chromatography (see below).

Day 14-18: When the viability of the cells started to drop (50%) and the expected titers were reached, the cell supernatant was harvested by centrifugation and/or filtration and filter-sterilised. It was stored aseptically and further processed as described in the next section.

The fermentation was carried out in accordance with standard protocols, see e.g. Werner, (1993), Arzneimittelforschung, 43, 1242-9 or Rendall, (2003). Proceedings of the 18th ESACT meeting, May 11-14, 2003, 1, 701-704).

**Example 3: Purification of ANTIBODY A**

The purification process was based on three chromatographic steps and a diafiltration step: Protein A affinity chromatography, cation exchange chromatography, anion exchange

chromatography and diafiltration using a 100kD membrane. The gel types and column sizes were 1 l MabSelect (GE Healthcare, Art. 17-5199, column diameter 9 cm, bed length 18 +/- 2 cm), 0.4 l CM-Toyopearl 650M (Toso Bioscience, Art. 007972, small ion capacity = 85 microequivalents/ml, diameter 5.0 cm, bed length 20 +/- 2 cm), 1.3 l Q-Sepharose FF (GE Healthcare, Art.17-0510-04), diameter 9 cm, bed length 20 +/- 2 cm. Columns were run at room temperature. Fractions were stored at 2 – 8 °C. Detection was at 280 nm. A Biomax 100 ultrafiltration module with an area of 0.1 $m^2$ (Millipore Corp. Art. P2B100A01) was used for concentration and diafiltration.

Protein A chromatography

The following solutions were prepared using purified water:

Solution A (equilibration buffer): 25 mM Tris, 25 mM NaCl, 5 mM EDTA, adjusted to pH 7.1 +/0.1 by HCl

Solution B (washing buffer 1): 100 mM acetic acid adjusted to pH 4.5 +/-0.1 by NaOH

Solution C (elution buffer): 100 mM acetic acid adjusted to pH 3.2 +/-0.1 by NaOH

Solution D (washing buffer 2): 100 mM acetic acid, 75 mM NaCl, pH 3 +/- 0.1

Solution E: (regeneration buffer): 2 M guanidinium hydrochloride, 100 mM Tris, adjusted to pH 7.5 +/-0.1 by HCl

Solution F (storage buffer): 200 mM benzyl alcohol, 100 mM acetic acid, adjusted to pH 5.0 +/- 0.1 by sodium hydroxide

The column was first equilibrated with 3 bed volumes of solution A

In the following it was charged with the clarified cell culture supernatant (45 l, 386 mg/l antibody)
washed with 5 bed volumes of solution A,

washed with 3 bed volumes of solution B,
eluted with 3.5 bed volumes of solution C and the eluate was collected,
washed with 3 column volumes of solution D and
regenerated with 2 column volumes of solution E
equilibrated with 3 bed volumes of buffer A
and washed with bed volumes of buffer F for storage.

A linear flow rate of 100 cm/h was used for all chromatographic steps.

The column load was 17.4 g antibody /l Mabselect gel and the yield for the total mixture of isoforms was 96 %.

Viral inactivation

The following solution was prepared using purified water:

Solution G (adjusting solution): 2 M sodium acetate

The pH of the protein A eluate was adjusted to a pH between 3.5 to 3.7 by addition of concentrated acetic acid or 2 M sodium acetate (solution G). It was stirred for 15 min and than adjusted to pH 4 +/- 0.1 by adding 2 M sodium acetate (solution G).

Cation exchange chromatography

The following solutions were prepared using purified water:
Solution H (equilibration buffer): 100 mM acetic acid, adjusted to pH 4.0 +/-0.1 by NaOH

Solution I (elution buffer 1): 250 mM sodium acetate without pH-adjusting, pH 7.8 - 8.5

Solution J: (elution buffer 2): 500 mM sodium acetate without pH adjusting,, pH 7.8 – 8.5

Solution K (regeneration solution): 0.5 M sodium hydroxide

Solution L (storage buffer): 0.01 M sodium hydroxide

The column was first regenerated with 2 bed volumes of solution K and then equilibrated with 5 bed volumes of solution H.

In the following it was charged with an aliquot of the protein A eluate and washed with 1 bed volume of solution H.

Enclosed it was eluted with 6 bed volumes of solution I. In this step a mixture of the double-glycosylated and the mono-glycosylated isoforms eluted. In the next step 3 bed volumes of solution J were used to elute the non-glycosylated isoforms.

After use the column was regenerated with 2 bed volumes of solution K, stored for 24 h in this buffer and was then washed again with 2 bed volumes of solution K. For storing it was washed with 3 bed volumes of solution L.

An example chromatogram is shown in Fig. 3.

Fractions of the chromatography were analyzed by analytical IEX as described below.

A linear flow rate of 100 cm/h was used for all chromatographic steps.

The column load was 14.3 g antibody /l CM-Toyopearl 650 M, and the yield was 79 % for the mixture of double-glycosylated and mono-glycosylated isoforms and 6.2 % for the non-glycosylated isoforms.

Flow through chromatography using Q-Sepharose FF

The following solutions were prepared in purified water:

Solution M (dilution buffer): 37,5 mM Tris, adjusted to pH 7.9 +/- 0.1 by acetic acid

Solution N (adjusting solution): 2 M Tris

Solution O (equilibration buffer): 83 mM sodium acetate, 25 mM Tris, pH 7.5 +/- 0.1

Solution P (regeneration buffer 1): 0.5 M NaOH / 1M NaCl

Solution Q (regeneration buffer 2): 0.2 M acetic acid / 1 M NaCl

Solution R (storage buffer): 0.01 M NaOH

The eluate from the CMT column (acidic) was first diluted 1 : 3 with solution M and then adjusted to pH 7.5 with solution N.

The column was first equilibrated with 2 bed volumes of solution O and in the following the diluted eluate from the CMT column was processed over the column and the flow through was collected. Product was washed off the column with solution with solution O until the absorption at 280 nm was lower than 0.1 (flow through collected).

The column was regenerated with 1.5 bed volumes of solution P, stored for 1 h and then regenerated with another 1.5 bed volumes of solution P. Then the column was regenerated with 2 bed volumes of solution Q and washed with 3 bed volumes of solution R and stored.

A linear flow rate of 100 cm/h was used for all chromatographic steps.

The column load was 3.5 g antibody /l Q Sepharose FF, and the yield was 91 % for the mixture of double-glycosylated and mono-glycosylated isoforms.

Diafiltration

The following solution was prepared using purified water:

Solution S (diafiltration buffer): 20 mM Histidine, adjusted to pH 5.5 by HCl

A filter holder Pellicon 2 (Millipore Corp.) was equipped with 1 ultrafiltration module type Biomax 100 (Millipore Corp., area = 0.1 $m^2$ , Art.P2B100A01). A WATSON-MARLOW 501 U pump equipped with a silicone tubing was used for pumping. The system was rinsed with buffer O and then 3.8 litres (1.1 g antibody/l) of the flow through from QS chromatography (adjusted tp pH 5.5 by concentrated acetic acid) were concentrated to 250-300 ml within 1 h at 4 – 11°C. In the following a diafiltration (V = const.) against 3 litres of buffer S (about 10 volumes) was performed (4 – 11°). Finally the product was sterile filtrated using a Millipac 20 filter (Millipore Corp.). The yield of the ultrafiltration/ diafiltration step was 91 %. The concentration of the product was 15 mg/ml. The product could be frozen at -70°C.

Analytical IEX method for analysis of fractions

Column: Mono-S HR 5/5 (GE Healthcare, Art. 17-0547-01)
Buffer 1: 50 mM Morpholinoethansulfonic acid, adjusted to pH 5.8 by sodium hydroxide
Buffer 2: 50 mM Morpholinoethansulfonic acid, 1 M NaCl adjusted to pH 5.8 by sodium hydroxide

Flow rate: 1 ml/min
Detection: 280 nm
Sample load: 36 – 72 µ
Gradient: Time % Buffer 2

| | |
|---|---|
| 0 min | 0 |
| 1 | 0 |
| 25 | 63 |
| 27 | 63 |
| 28 | 0 |
| 35 | 0 |

An exemplary chromatogram is given in Fig. 2

Yields

| Step | Isoform | Step yield |
|---|---|---|

| | | |
|---|---|---|
| MabSelect (Protein A) | Mixture of all isoforms | 96 % |
| CM-Toyopearl 650 M | Mixture of mono-glycosylated ANTIBODY A and double-glycosylated ANTIBODY A Content of non-glycosylated ANTIBODY A <0.5% | 79 % |
| | Non-glycosylated ANTIBODY A | 6,2 % |
| Q-Sepharose FF | Mixture of mono-glycosylated ANTIBODY A and double-glycosylated ANTIBODY A Content of non-glycosylated ANTIBODY A <0.5% | 91 % |
| Concentration and Diafiltration | Mixture of mono-glycosylated ANTIBODY A and double-glycosylated ANTIBODY A Content of non-glycosylated ANTIBODY A <0.5% | 91 % |

**Example 4: Characterization of ANTIBODY A isoforms by SDS-PAGE**

SDS-PAGE analysis was carried out using standard protocols with 4-12% NuPage gradient Bis-Tris gel (Invitrogen) and marker MARK12 (Invitrogen) as control. 1-3ug of ProteinA purified supernatants from fermentations (Prod 01, 02, 03) or spinner cultures (all other lanes) were loaded per well. The analysis under reducing conditions resulted in a single band for peak 1 (double-glycosylated ANTIBODY A), a double band for peak 2 (mono-glycosylated ANTIBODY A) and a single band for peak 3 (non-glycosylated ANTIBODY A) in the range of the molecular weight of the heavy chains. The molecular weights of the two bands of peak 2 corresponded to the molecular weights of peak 1 and peak 2, respectively.

Similar results were obtained employing several expression systems like: transient transfection in HEK 293 EBNA cells, transient transfection in CHO cells, and stable expression in CHO cells.

**Example 5: Characterization of ANTIBODY A isoforms by Mass Spectrometric (MS) Analysis.**

A complete antibody mass profile of all ANTIBODY A isoforms was determined by electron spray ionization mass spectroscopy (ESI-MS).

For this, samples of ANTIBODY A were prepared under non-reducing conditions. The samples were desalted into 2% formic acid and 40% acetonitril by G25 gel filtration and used for ESI-MS analysis in a Q-Tof2 or LCT-mass spectrometer instrument from Waters.

A separation by molecular mass is obtained with a difference of 1623 between non-glycosylated ANTIBODY A and mono-glycosylated ANTIBODY A. The expected mass for non-glycosylated ANTIBODY A from the amino acid sequence is 145,987 Da, which is in good agreement with the experimentally determined mass of 145,979 Da. Similarly, mono- and double-glycosylated ANTIBODY A isoforms differ by 1624 Da as indicated in Figure 4. The observed differences in molecular masses are compatible with N-glycosylation patterns that are described in more detail herein below.

**Example 6: Asn-52 glycosylation structure of ANTIBODY A**

Asn52 is part of the sequence aaa-aaa-Asn-Ala-Ser-aaa-aaa of the variable part of the heavy chain, which corresponds to the N-glycosylation consensus sequence Asn-aaa-Ser/Thr. N-linked glycosylation of Asn52 was confirmed by tryptic peptide mapping of ANTIBODY A isoforms and mass spectrometric evaluation of peptide HC/T4 containing Asn52. In tryptic peptide maps of non-glycosylated ANTIBODY A, exclusively a peptide corresponding by mass to non-glycosylated HC/T4 peptide appears, indicating that Asn52 was not glycosylated, whereas in the mono- or double glycosylated ANTIBODY A peptides were detected corresponding by mass to HC/T4 containing N-linked sugar structures.

To further confirm glycosylation of the consensus sequence in the tryptic peptide HC/T4 of the heavy chain, the glycosylated HC/T4 peptide was isolated from peptide maps of glycosylated ANTIBODY A isoforms and analysed by MALDI-mass spectrometry before and after incubation with N-glycosidase F. Before N-Glycosidase F treatment, masses were obtained corresponding to HC/T4 peptide containing N-linked sugar structures. However, the mass of HC/T4 peptide treated with N-Glycosidase F corresponded to the mass expected to non-

glycosylated HC/T4 +1Da, as expected if a sugar chain was removed from the asparagine by N-Glycosidase F (Asn to Asp-conversion).

The presence of N-acetyl-neuraminic acids at the sugar structures attached to Asn52, furthermore, indicates the presence of N-linked complex and hybride type sugar structures. For this, glycosylated ANTIBODY A isoforms were treated with N-Glycosidase F , which removes N-sugar at Asn306, but not at Asn52 and with or without Neuraminidase and analysed after separation of HC and LC by denaturation and reduction and desalting. The masses obtained for the HC from both approaches differed by about 291 Da or 582 Da corresponding to one or 2 sialic acids. From this, it also was concluded that N-linked sugars of the complex and/or hybride type were attached to Asn52.

This Asn-52 glycosylation, an N-glycosylation, predominantly consisted of sugar structures of the biantennary complex type (≥ 75%; mainly 80 – 90%) without core fucosylation and highly sialidated with up to 80% of the complex type antennae containing N-acetyl-neuraminic acids. Minor sugar structures belonged to the biantennary hybrid and the oligomannose type (≤ 25%), respectively (Figure 5 or Figure 27). Common to all Asn52 glycosylation structures was the resistance to cleavage by N-glycosidase F from intact ANTIBODY A.

**Example 7: Asn306 glycosylation structure of ANTIBODY A**

As pointed out above, ANTIBODY A contained attached to asparagine 306 (Asn306) in the Fc-part of the heavy chain (HC) an antibody type glycosylation consisting of a complex biantennary oligosaccharide chain. It is well known that antibodies contain different isoforms of such a complex bi-antennenary oligosaccharide chain, varying in the degree of terminal galactosylation, sialyation and in the degree of core fucosylation. In addition it is known that the degree of lacking core fucosylation in the Fc-located sugar chain is important for *in vivo* efficacy of antibodies, as it is well accepted that the degree of core fucosylation modulates effector functions of antibodies.

For ANTIBODY A major, antibody typical variations (Routier (1997), Glyoconjugate 14(2), 201-207; Raju (2003), BioProcess International, 44-52) in the Fc-located sugar chains attached to Asn306 were found regarding terminal galactosylation and core fucosylation.

The heterogeneity in the degree of terminal galactosylation (G0 : G1 : G2 structures) was

determined to about 35-40% G0-structures, about 45% G1-structures and about 15-20% G2-structures (for schematic demonstration of the structures see Figure 6 or Figure 27).

The content of Fc-sugar structures lacking core fucosylation, i.e. lacking the fucose unit attached to the innermost N-acetyl-glucosamine of the core sugar structure, probably is important for an antibody, as the presence or absence of this fucose unit may modulate the binding of the antibody to Fc-receptors of effector cells, thereby influencing activity of these cells.

For ANTIBODY A the relative content of sugar chain isoforms lacking core fucosylation at Asn 306 was determined by two different methods, as described in the following:

A) Mass spectrometry of complete, glycosylated HC:

Samples of ANTIBODY A were denatured and reduced into light chain (LC) and glycosylated HC in the presence of 6M guanidine-hydrochloride and 250mM TCEP. The reduced samples were desalted into 2% formic acid and 40% acetonitrile and used for ESI-MS analysis in a Q-Tof2 or LCT-mass spectrometer instrument from Waters. From the m/z spectra obtained the relative content of the individual oligosaccharide isoforms were calculated by peak height of glycosylated HCs containing the individual oligosaccharide isoforms from selected single m/z states. For calculation of the relative content of sugar structures lacking core fucosylation, peak height of G0-structure lacking core fucose (G0-Fuc) related to the sum of G0 + (G0-Fuc).

The respective carbohydrate structures were assigned according to the differences of the masses obtained for glycosylated HC and for HC, whose oligosaccharide structures were removed by incubation with N-Glycosidase F prior to MS-analysis in control experiments.

B) Chromatographic analysis of released oligosaccharides by HPEAC-PAD:

Samples of ANTIBODY A were incubated with N-Glycosidase F in sodium phosphate buffer at pH 7.2 in order to release the oligosaccharide chains from Asn306 (the sugar structures at Asn52 were not removed from the intact, non-denatured antibody under the conditions used). The released sugar chains were separated from the ANTIBODY A protein by centrifugation filtration and were analysed on a Carbo Pac PA200 column from Dionex in a BioLC system, using a sodium acetate gradient at strong alkaline pH (pH, 13). The column used was capable of resolving non-fucosylated from fucosylated oligosaccharide chains. Assignment of the individual peaks obtained to respective carbohydrate structures was done by comparing the

retention times to the ones of suitable oligosaccharide standards analysed on the Carbo Pac PA200 column and by determining the molar mass of the peaks separated and collected by MALDI mass spectrometry, respectively. For calculation of the relative content of sugar structures lacking core fucosylation, the sum of area-% of all structures lacking core fucose was formed.

The analysis of several batches ( combinations of double- and mono-glycosylated ANTIBODY A isoforms) and of purified ANTIBODY A isoforms, respectively, revealed that the content of non-fucosylated Asn306 linked oligosaccharide chains was in the range of ~ 14% – 27% (measured by MS) and 6% - 26 % (measured by HPAEC-PAD), respectively.

**Example 8: Determination of $K_D$ values for ANTIBODY A COMPOSITION and isoforms (e.g. non-, mono- or double-glycosylated antibody of the invention) binding to Aβ1-40 and Aβ1-42 fibers *in vitro* by surface plasmon resonance (SPR)**

Binding of ANTIBODY A to fibrillar Aβ was measured online by surface plasmon resonance (SPR), and the affinities of the molecular interactions were determined as follows: Biacore2000 and Biacore3000 instruments were used for these measurements. Aβ1-40 and Aβ1-42 fibers were generated *in vitro* by incubation of synthetic peptides at a concentration of 200 μg/ml in 10 mM Na-acetate buffer (pH 4.0) for three days at 37°C. Electron microscopic analysis confirmed a fibrillar structure for both peptides, Aβ1-40 showing predominantly shorter (< 1 micron) and Aβ1-42 predominantly longer (> 1 micron) fibers. These fibers were assumed to represent aggregated Aβ peptides in human AD brain more closely than ill-defined mixtures of amorphous aggregates and unstructured precipitates. The fibers were diluted 1:10 and directly coupled to a CM5 as described in the Instruction Manual of the manufacturer (BIAapplication Handbook, version AB, Biacore AB, Uppsala, 1998).

This coupling procedure included an activation step, during which the carboxylic acid groups on the surface were transferred into chemically reactive succinimide ester groups by contacting the surface with an aqueous mixture of N-hydroxysuccinimide and 1-ethyl-1-(3-diaminopropyl)-carbodiimide hydrochloride, and an immobilization step, during which the activated surface was contacted with the fibres dissolved in 10 mM acetate buffer (pH 4.5) at 200-350 resonance units (1 resonance unit (RU) corresponds approximately to a surface loading of 1 picogram/mm2). The fiber loaded surface was then contacted with the antibody solutions in the concentration

range 200 nM ≥ C ≥ 0.15 nM. Typical time dependent response curves (= sensograms) monitored during the association phase (during contact with buffer) and the dissociation phase (subsequent contact with buffer) are shown in Figure 7.

The $K_D$ values for binding to Aβ1-40 and Aβ1-42 fibers of the ANTIBODY A isoforms are given in the table below. Briefly, $K_D$ values were calculated by Scatchard type analysis using concentration dependent equilibrium binding responses. These equilibrium binding constants could be obtained in two ways.

Due to the very slow association process at low antibody concentration contact intervals to reach equilibrium were very long (Figure 7). Nevertheless, such contact intervals could be realized on Biacore instruments and the experimental equilibrium responses could be subjected to a Scatchard analysis.

Equilibrium binding data were also obtained by extrapolating shorter time dependent association curves to infinity. These theoretically obtained equilibrium binding levels were then again used for the determination of the $K_D$ values.

Independently from the way of determining equilibrium sensor responses curvilinear Scatchard plots were obtained. From the curvilinear Scatchard plot a higher (bivalent) and lower (monovalent) affinity interaction was derived for ANTIBODY A isoforms derived from the second affinity maturation cycle. These two affinities represent the lower and upper $K_D$ values of the range indicated the following table:

| | | 1-40 high affinity $K_D$ values (nM) | 1-40 low affinity $K_D$ values (nM) |
|---|---|---|---|
| ANTIBODY A COMPOSITION (mixture of mono- and double-glycosylated ANTIBODY A) | extrapolation | 0.49 | 27.25 |
| | stdev | 0.10 | 8.40 |
| | equilibrium | 0.41 | 21.00 |
| double-glycosylated | extrapolation | 1.43 | 18.51 |
| | stdev | 0.02 | 22.33 |

| | | | |
|---|---|---|---|
| ANTIBODY A | equilibrium | 1.54 | 29.00 |
| mono-glycosylated ANTIBODY A | extrapolation | 0.25 | 7.55 |
| | stdev | 0.02 | 2.06 |
| | equilibrium | 0.12 | 11.10 |
| non-glycosylated ANTIBODY A | extrapolation | 0.19 | 1.99 |
| | stdev | 0.03 | 0.15 |
| | equilibrium | 0.42 | 2.82 |

The table above shows $K_D$ values of the low affinity complex (monovalent) and the high affinity complex (bivalent) formed by the interaction of ANTIBODY A isoforms and Aβ1-40 fibrils as determined by surface plasmon resonance. $K_D$ determined by using extrapolated equilibrium responses (marked "extrapolation") and KD values determined by using experimentally determined equilibrium responses (marked "experimental") are given. The extrapolated values were determined at least six times and a standart deviation is given. The $K_D$'s based on experimental and extrapolated equilibrium sensor responses are equal within the limits given by these standard deviations.

**Example 9: Epitope mapping of ANTIBODY A COMPOSITION and isoforms (e.g. non-, mono- or double-glycosylated antibody of the invention) by pepspot analysis with decapeptides**

An epitope (antigenic determinant) can be linear or conformational. The herein described dual epitope specificity was defined by reactivity of the antibody with two non-sequential linear peptides.

Epitope mapping approaches which were used to define specific epitope recognition are based on ELISA technology with hexapeptide conjugates coated on to microplates or on pepspot technology. The latter technology allows the detection and quantitation of the antibody by protocols that are commonly known for Western Blotting of proteins to PVDF membranes.

Applied epitope mapping technologies are designed to specifically detect linear epitopes, whereas they cannot be applied to map more spatially complex epitopes like discontinuous or conformational epitopes. Techniques available for conformational or discontinuous epitope

mapping, like domain scanning and combinatorial peptide arrays require long peptides up to 36 amino acids (domains) or combined peptides each consisting of 12 amino acids.

The applied techniques are therefore considered to be specific for linear epitopes, excluding that conformational epitopes either discontinuous or discontinuously scattered epitopes are involved.

In conclusion, the presented data show that the two regions within the Aβ peptide defined herein resemble independent linear epitopes simultaneously recognized based on the unique dual epitope specificity of the investigated antibodies on single hexameric or decameric Aβ - peptides.

The following amino acid sequence encompassing Aβ (1-42) was divided into 43 overlapping decapeptides with a frameshift of 1 amino acid. The numbers refer to the essential amino acids from the Aβ1-40 sequence which have to be present in the decapeptide for optimal binding of antibody.

ISEVKM$^{1}$DAEF RHDSGYEVHH QKLVFFAEDV GSNKGAIIGL MVGGVVI$^{42}$ATV IV (SEQ ID NO: 4). Accordingly, DAEF RHDSGYEVHH QKLVFFAEDV GSNKGAIIGL MVGGVVIA (SEQ ID NO: 3) represents amino acids 1 to 42 of Aβ4/β-A4 peptide.

The 43 decapeptides were synthesized with N-terminal acetylation and C-terminal covalent attachment to a cellulose sheet ("pepspot") by a commercial supplier (Jerini BioTools, Berlin). The cellulose sheet was incubated for 2 hours on a rocking platform with monoclonal antibody (1 μg/ml) in blocking buffer (50 mM Tris·HCl, 140 mM NaCl, 5 mM NaEDTA, 0.05% NP40 (Fluka), 0.25% gelatin (Sigma), 1% bovine serum albumin fraction V (Sigma), pH 7.4). The sheet was washed 3 times 3 minutes on a rocking platform with TBS (10 mM Tris.HCl, 150 mM NaCl, pH 7.5). It was then pressed on filter paper, wetted with cathode buffer (25 mM Tris base, 40 mM 6-aminohexane acid, 0.01% SDS, 20% methanol) and transferred to a semi-dry blotting stack with the peptide side facing a PVDF membrane (Biorad) of equal size.

The semi-dry blotting stack consisted of freshly wetted filter papers (Whatman No.3) slightly larger than the peptide sheet:
3 papers wetted with Cathode buffer
the peptide sheet
a sheet of PVDF membrane wetted with methanol

3 papers wetted with Anode buffer 1 (30mM Tris base, 20% methanol)

3 papers wetted with Anode buffer 2 (0.3 mM Tris base, 20% methanol)

The transfer was conducted at a current density between Cathode and Anode of 0.8 $mA/cm^2$ for one hour which was sufficient to elute the antibody completely from the cellulose sheet and transfer it on the PVDF membrane. The PVDF membrane was immersed in blocking buffer for 10 minutes. Goat anti-human IgG(H+L) labeled with fluorochrome IRdye800 (Rockland code# 609-132-123) was added at 1:10'000 dilution in Odyssey blocking buffer (Li-Cor) and further diluted 1:1 with PBS, 0.05% Tween20. The membrane was incubated on a rocking platform for 1 hour. It was washed 3x10 minutes with TBST (TBS with 0.005% Tween20). The membrane was dried and scanned for 800nm fluorescence using a long wavelength fluorescence scanner (Odyssey) as shown in Figure 8.

The exact assignment of antibody-reactive spots was achieved by marking the PVDF membrane with a needle puncture. The epitopes of the antibody in question was defined as the minimal amino acid sequence in reactive peptides. The fluorescence intensity was integrated over each spot and recorded as relative fluorescence unit (RFU). For comparison two mouse monoclonal antibodies (BAP-1 which is equivalent to antibody 6E10 (Kim (1998),.) with specificity for the N-terminal domain, and BAP-44 which is equivalent to antibody 4G8 (Kim (1998),) with specificity for the middle domain) were analyzed in the same way, except for using anti-mouse Ig instead of anti-human Ig for detection.

It is of note that affinity maturation and conversion of the monovalent Fab fragments into full-length IgG1 antibodies results usually in some broadening of the epitope recognition sequence as indicated by pepspot and ELISA analyses. This may be related to the recruitment of more contact points in the antibody-antigen interaction area as a consequence of the affinity maturation or to a stronger binding to the minimal epitope such that also weak interactions with adjacent amino acids can be detected. The latter may be the case when Aβ-derived peptides are probed with full-length IgG antibodies. As illustrated in the table below, the recognition sequences of the N-terminal and middle epitopes were extended by up to three amino acids when parent Fabs and corresponding fully maturated IgG antibodies were compared. However, it has to be kept in mind that the decapeptides were modified for covalent attachment at the C-terminal amino acid and this amino acid may therefore not easily be accessible to the full-length antibody due to steric hindrance. If this is the case the last C-terminal amino acid does not significantly

contribute to the epitope recognition sequence and a potential reduction of the minimal recognition sequence by one amino acid at the C-terminal end has to be considered in the pepspot analysis as used in the present invention.

| **antibody** | **Amino acid position** | **Amino acid position** |
|---|---|---|
| double-glycosylated ANTIBODY A | 3-4 (1-10) | 18-24 (17-26) |
| mono-glycosylated ANTIBODY A | 4-5 (3-11) | 20-26 |
| non-glycosylated ANTIBODY A | 3-4 | 20-24 |
| ANTIBODY A COMPOSITION (Mixture of mono- and double-glycosylated ANTIBODY A isoforms (1:1)) | 3-5 (3-11) | 19-26 |
| BAP-44 (mouse monoclonal) | | 19-21 |
| BAP-1 (mouse monoclonal) | 4-6 | |

The table above relates to a pepspot analysis of binding full-length IgG antibodies to decapeptides on a cellulose sheet. The numbers refer to the amino acid position in the Aβ1-40 sequence which have to be present in the decapeptide for binding of antibody. A further extension to the epitope is indicated in brackets in order to indicate the flanking amino acids that are required to achieve maximum binding.

**Example 10: De-polymerization assay employing ANTIBODY A isoforms (e.g. non-, mono- or double-glycosylated antibody of the invention) which induces release of biotinylated Aβ from aggregated Aβ.**

The experimental setup to test the potential of ANTIBODY A isoforms to induce dissociation of aggregated Aβ was as follows:

Biotinylated Aβ1-40 was first incorporated into preformed Aβ1-40/Aβ1-42 fibers before treatment with ANTIBODY A isoforms. Liberation of biotinylated Aβ was measured using an assay employing a streptavidin-POD conjugate as described below.

Synthetic Aβ when incubated in aqueous buffer over several days spontaneously aggregates and forms fibrillar structures which are similar to those seen in amyloid deposits in the brains of Alzheimer's Disease patients. The following *in vitro* assay is suitable to measure incorporation or liberation of biotinylated Aβ into preformed Aβ aggregates in order to analyze the Aβ-neutralizing potential of anti-Aβ antibodies and other Aβ-binding proteins such as albumin (Bohrmann (1999) J. Biol. Chem. 274, 15990-15995). ANTIBODY A isoforms induced de-polymerization of aggregated Aβ as measured by the release of incorporated biotinylated Aβ1-40.

*Experimental procedure:*

NUNC Maxisorb microtiter plates (MTP) were coated with a 1:1 mixture of Aβ1-40 and Aβ1-42 (2 μM each, 100 μl per well) at 37°C for three days. Under these conditions highly aggregated, fibrillar Aβ was adsorbed and immobilized on the surface of the well. The coating solution was then removed and the plates were dried at room temperature for 2-4 hours. The dried plates could be stored at –20°C. For incorporation of biotinylated Aβ the coated plates were incubated with 200 μl/well 20 nM biotinylated Aβ1-40 in TBS containing 0.05 % $NaN_3$ at 37°C overnight. After washing the plate with 3 x 300 μl/well T-PBS, antibodies serially diluted in TBS containing 0.05 % $NaN_3$ were added and incubated at 37°C for 3 hours. The plate was washed and analyzed for the presence of biotinylated Aβ1-40. After washing 3 x with 300 μl T-PBS a streptavidin-POD conjugate (Roche Molecular Biochemicals), diluted 1:1000 in T-PBS containing 1% BSA, was added (100 μl/well) and incubated at room temperature for 2 hours. The wells were washed 3 x with T-PBS and 100 μl/well of a freshly prepared tetramethyl-benzidine (TMB) solution were added. [Preparation of the TMB solution: 10 ml 30 mM citric acid pH 4.1 (adjusted with KOH) + 0.5 ml TMB (12 mg TMB in 1 ml acetone + 9 ml methanol) + 0.01 ml 35 % $H_2O_2$]. The reaction was stopped by adding 100 μl/well 1 N $H_2SO_4$ and absorbance was read at 450 nm in a microtiter plate reader.

As documented in appended Figure 9, ANTIBODY A isoforms induced dissociation of aggregated Aβ as measured by the release of incorporated biotinylated Aβ1-40. ANTIBODY A

isoforms and the mouse monoclonal antibody BAP-1 were similarly active (Figure 9)., whereas the BAP-2, BAP-17 and 4G8 antibodies were clearly less efficient in liberating biotinylated Aβ from the bulk of immobilized Aβ (data not shown). BAP-1 could clearly be differentiated from the glycosylated ANTIBODY A isoforms by its reactivity with cell surface full-length APP. Antibodies like BAP-1 with such properties are not useful for therapeutic applications as potential autoimmunological reactions may be induced. It is interesting to note that BAP-2, despite its specificity for amino acid residue 4-6 which was exposed in aggregated Aβ has a clearly lower activity in this assay indicating that not all N-terminus specific antibodies a priori are equally efficient in releasing Aβ from preformed aggregates. The relatively low efficiency of BAP-17 (C-terminus-specific) and 4G8 (amino acid residues 16-24-specific) in this assay was due to the cryptic nature of these two epitopes in aggregated Aβ. BSA at the concentrations used here had no effect on aggregated Aβ.

The mono-glycosylated isoform exerted higher capacity compared to the double-glycosylated isoform to depolymerize aggregated Aβ peptide in vitro that may be relevant also in vivo.

**Example 11: ANTIBODY A COMPOSITION and comprising isoforms (mono- and double-glycosylated antibody of the invention) capture soluble Aβ from human cerebrospinal fluid (CSF)**

The capacity to capture soluble Aβ from human CSF samples was determined by immunoprecipitation (IP) and semi-quantitative Western blot (WB) analysis. *Experimental procedure:*

Immunoprecipitation of human CFS samples was done according to the following scheme:

| | |
|---|---|
| 70 ul | human CSF |
| 20 ul | Incubation buffer (50mM Tris,140mM NaCl, 5mM EDTA, 0.05% NP-40, 1% BSA, 0.25% Gelatin, 0.25% milk powder, pH 7.2 |
| 10 ul | ANTIBODY A isoforms from stock solutions (1000- 10 ug/ml) |
| 100 ul | |

The solution was kept for one hour at 4°C. 40ul protein G Sepharose beads (Amersham Biosciences #17-0618-01; washed with PBS, 50% slurry) were added and incubated for 2 hours at 4°C on rotator. After centrifugation at 500g for 3minutes at 4°C the supernatant was removed and 200ul PBS were added to the beads, transferred to Millipore filter tubes 0.45um (Millipore

#UFC3OHVNB) and centrifuged at 500g for 3minutes at 4°C. Additional 200ul PBS was added to beads, vortexed and centrifuged at 2000g for 3minutes at 4°C. 45ul sample buffer 1xNuPage with DTT was added and kept for 10 minutes at 70°C followed by centrifugation at 2000g for 3 minutes at 4°C.

For SDS-PAGE, 18ul protein G eluate was applied to NuPage gel 10% Bis-Tris gel together with $A\beta_{1-42}$ (Bachem) as internal standard directly in sample buffer as standard and run in MES buffer system.

The gel was transferred to Hybond C extra membrane (semi-dry system Novex) dry membrane 3' at room temperature. The membrane was transferred into pre-heated PBS and heated in microwave for 3min. at 600W. Blocking was done for 1 hour with SuperBlock Solution (Pierce) and additional blocking for 1hour with 5% Milk Powder (Bio Rad) in T-PBS (0.1% Tween20 in PBS).

Incubation was done over night with anti Aβ antibody W02 Antibody (1:1500-1:2000 from The Genetics, Inc. Zürich, Switzerland) at 4°C on a rotator, followed by washing 3x with T-PBS for 5min and incubation for 2 hours at RT with anti-mouse IgG-HRP (Dako) 1:5000 in T-PBS. Another washing 3 x with T-PBS for 5min was followed by incubation with LumiLight Plus for 5minutes at RT. Western blots were digitized and analysed by densometry with an Alpha Innotech Digital Camera System.

As documented in Figure 10, ANTIBODY A COMPOSITION (comprising mono- and double-glycosylated ANTIBODY A isoforms) bound efficiently to soluble Aβ in human CSF as demonstrated by immunoprecipitation and Western blotting experiments. Notably, in this assay, mono-glycosylated ANTIBODY A was more efficient in capturing soluble Aβ than double-glycosylated ANTIBODY A (Figure 10).

**Example 12: In vitro immunostaining of human amyloid plaques by ANTIBODY A COMPOSITION and isoforms (e.g. non-, mono- or double-glycosylated antibody of the invention)**

Glycosylated ANTIBODY A isoforms were tested for the ability to stain genuine human β-amyloid plaques obtained from brain sections of patients with severe Alzheimer's Disease by

immunohistochemistry analysis using indirect immunofluorescence. Specific and sensitive staining of genuine human β-amyloid plaques was demonstrated.

Cryostat sections of unfixed tissue from the temporal cortex obtained postmortem from a patient that was positively diagnosed for Alzheimer's disease were labeled by indirect immunofluorescence. A successive two-step incubation was used to detect bound ANTIBODY A isoforms, which were revealed by affinity-purified goat anti-human (GAH) IgG (H+L) conjugated to Cy3 (# 109-165-003, lot 49353, Jackson Immuno Research). Controls included unrelated human IgG1 antibodies (Sigma) and the secondary antibody alone, which all gave negative results.

All types of β-amyloid plaques were sensitively and specifically detected and consistently revealed at an ANTIBODY A concentration of 10 ng/ml (Figure 11).

Specific and sensitive staining of genuine human amyloid-β plaques is demonstrated for the glycosylated ANTIBODY A isoforms at a concentration up to 1 μg/ml.

At a concentration of 10 μg/ml a background staining was observed, most prominent with the non-glycosylated ANTIBODY A isoform. The non-glycosylated isoform exerted considerable unspecific stickiness observed at the surface of glass slides and almost all tissue components that were exposed after the sectioning process in vitro. This appeared to be due to unspecific binding involving ionic and/or hydrophobic interactions.

**Example 13: In vivo β-amyloid plaque decoration by ANTIBODY A in a mouse model of Alzheimer's disease**

Glycosylated ANTIBODY A isoforms were tested in a single dose study in PS2APP double transgenic mice (Richards (2003), J. Neuroscience, 23, 8989-9003) for their ability to immuno-decorate β-amyloid plaques *in vivo*. The glycosylated ANTIBODY A isoforms were administered i.e. at a dose of 1 mg/mouse and after 3 days animals were perfused with phosphate-buffered saline and the brains frozen on dry ice and prepared for cryosectioning.

Both glycosylated isoforms showed improved and highly effective brain penetration in vivo (as compared to the non-glycosylated form). Effective brain penetration and specific binding to

amyloid-β plaques was demonstrated in PS2APP mice, a mouse model for AD-related amyloidosis.

The presence of the antibodies bound to β-amyloid plaques was assessed using unfixed cryostat sections either by single-labeled indirect immunofluorescence with goat anti-human IgG (H+L) conjugated to Cy3 (#109-165-003, Jackson Immuno Research) shown in Figure 12 or followed by counterstaining with BAP-2-Alexa488 immunoconjugate to visualize the position and distribution of all β-amyloid plaques types present in the tissue.

An immuno-fluorescence staining approach was used to detect bound ANTIBODY A. After adhesion to precooled glass slides, sections were hydrated in PBS and treated with 100% acetone precooled at -20°C for 2 min. Washing with PBS was done twice for two minutes. Blocking of unspecific binding sites was done either with PBS containing 1% BSA or by sequential incubation in Ultra V block (LabVision) for 5 min followed by a PBS wash and incubation in power block solution (BioGenex) with 10 % normal sheep serum for 20 min. After washing with PBS with 10% normal sheep serum slides were incubated with affinity-purified goat anti-human (GAH) IgG (H+L) conjugated to Cy3 (# 109-165-003, lot 49353, Jackson Immuno Research) at a concentration of 15 μg /ml for 1 hour at room temperature. A counterstaining for amyloid plaques was by incubation with BAP-2, a mouse monoclonal antibody against Ab conjugated to Alexa 488 at a concentration of 0.5 μg /ml for 1 hour at room temperature. Autofluorescence of lipofuscin was quenched by incubation in 4mM CuSO4 in 50 mM ammonium acetate. After rinsing the slides in bidistilled water and washing with 2 x 500 μl/slide PBS, slides were embedded with fluorescence mounting medium (S3023 Dako).

Imaging was done by confocal laser microscopy and image processing for quantitative analysis of colocalizations by IMARIS and COLOCALIZATION software (Bitplane, Switzerland).

After a single dose of 1 mg per mouse glycosylated ANTIBODY A isoforms were found to penetrate across the blood brain barrier and to effectively immuno-decorate/bind all β-amyloid plaques after three days *in vivo*. Representative images are shown in Figure 12. This is in clear contrast to the non-glycosylated form which is not detectable at amyloid plaques.

**Example 14: Investigation of binding of ANTIBODY A isoforms to amyloid precursor protein (APP) expressed on the surface of HEK293 cells:**

The method of flow cytometry is well known in the art. Relative units of fluorescence (e.g. FL1-H) measured by flow cytometry indicated cell surface binding of the respective antibody. A fluorescence shift on APP transfected HEK293 compared to untransfected HEK293 cells indicated the unwanted reaction with cell surface APP. As an example, antibodies BAP-1 and BAP-2 against the N-terminal domain showed a significant shift of FL-1 signal in HEK293/APP (Figure 13, thick line, right hand panel) compared to untransfected HEK293 cells (Figure 13, dotted line, right hand panel). Similarly, BAP-44 antibody (specific for the middle A-beta epitope) showed a similar size shift. In contrast, all ANTIBODY A isoforms (Figure 13 left hand panel) (specific for N-terminal and middle A-beta epitopes) showed no significant shift in fluorescence. The untransfected HEK293 cells had a higher basal fluorescence than the APP transfected cells due to different cell size and surface properties. A FACScan instrument was used in combination with the Cellquest Pro Software package (both Becton Dickinson).

ANTIBODY A isoforms were devoid of reactivity towards cell surface APP (Figure 13).

**Example 15: Morphometrical analysis of Aβ plaque deposition in a mouse model of Alzheimer's disease**

The capability of ANTIBODY A COMPOSITION or the ANTIBODY A isoforms to lower amyloidosis in vivo was studied in various brain regions (thalamus, neocortex, hippocampus and subiculum) using quantitative computer-assisted image analysis of brains of PS2APP mice that received a five-month treatment with ANTIBODY A COMPOSITION or ANTIBODY A isoforms.

Therefore, PS2APP transgenic male mice were injected i.v. with ANTIBODY A COMPOSITION or ANTIBODY A isoforms and vehicle. Seventy-five 5-6-month-old PS2APP mice were divided into five groups (A–E), consisting of 15 mice each. Beginning on day 0, each mouse received either 0.1 mL of vehicle (0 mg/kg), or ANTIBODY A preparations (20 mg/kg) by bolus i.v. injection via the tail vein. Groups A, B, C, D and E of PS2APP mice received vehicle (histidine-buffered saline), ANTIBODY A COMPOSITION which comprises mono-glycosylated ANTIBODY A and double-glycosylated ANTIBODY A and is devoid of non-glycosylated ANTIBODY A as defined above, double-glycosylated ANTIBODY A, mono-glycosylated ANTIBODY A and non-glycosylated ANTIBODY A, respectively.

Immunotolerance against the administered human anti-Aβ antibodies was induced by injecting anti-CD-4 antibody (hybridome clone GK 1.5 as commercially available from ATCC). Monitoring of anti-drug antibodies indicated that antibody treated animals only develop a moderate immune-response after more than 16 weeks of treatment and that the detectable antibodies are either of low affinity or are produced only in low amounts (data not shown).

After 5 month treatment mice were sacrificed. Unfixed brains were sectioned sagitally, including thalamus, hippocampal formation and cortical areas. From each brain hemisphere 50 sections were prepared as follows: Starting at lateral level ~1.92, 5 consecutive series of 5x 10 μm and 5x 20 μm sections were obtained. There was no gap between consecutive sections, resulting in a total tissue usage of 750 μm. The section series therefore ends approximately on lateral level 1.20 (Paxinos and Franklin, 2003). For quantitative morphometrical analysis every 10th section was used.

Sections were stained for amyloid deposits with the double-glycosylated ANTIBODY A isoform at a concentration of 5 μg/ml. Stainings against Aβ using a mouse monoclonal antibody (BAP-2) conjugated to Alexa-488 fluorophore at 5 μg/ml showed comparable results although with significant intracellular and background staining of neurons which interfered with the image processing routine described below. For detection an affinity-purified goat anti-human (GAH) IgG (H+L) conjugated to Cy3 (# 109-165-003, lot 49353, Jackson Immuno Research) at a concentration of 15 μg /ml for 1 hour at room temperature was applied. After washing with 2 x 500 μl PBS/slide, slides were embedded with fluorescence mounting medium (S3023, Dako).

Images were acquired using a GenePix Personal 4100A microarray scanner (Axon Instruments, now Molecular Devices, CA, USA). Amyloid-β plaque load and number was measured using two parameters, namely percentage of area covered by amyloid-β plaques and number of amyloid-β plaques using an unbiased morphometrical method by means of computer assisted image analysis. Quantification of plaque load and number was done with MCID M7 Elite software (Imaging Research Inc., St. Catherines / Ontario, Canada). The scanned images were enhanced by a detail extractor filter followed by a target accent filter. The resulting image was then binarized, adjusting the threshold according to the staining intensity. Artefacts, blood vessels and edge effects were identified on the original reference image and then removed from the binarized image. Regions of interest were outlined on the reference image. For final quantification, the area of these regions and the area occupied by plaques as well as the plaque

number were then measured in the binarized image. Single pixels were ignored. Calculations were made with common spreadsheet software (Microsoft Excel, Redmond / WA, U.S.A.). The size of plaques was separated into 11 groups ranging from <100 to > 1000 $\mu$m2. Statistical evaluation was done using a twotailed, heteroscedastic t-test.

For comparison and statistical evaluation, the baseline of amyloidosis (amyloid-β plaque pathology) was determined at study begin with a cohort (15 animals) of non-treated 6 month old PS2APP mice. Results are depicted in Figures 15 to 18 with levels of significance (*: $p \leq 0.05$; **: $p \leq 0.01$; ***: $p \leq 0.001$).

Amyloid plaque reduction was most pronounced in the thalamus region (Figure 15). The mean reduction of total amyloid-β plaque surface was determined for the antibody treated groups: 64 % for ANTIBODY A COMPOSITION, 70 % for double-glycosylated ANTIBODY A, 81 % for mono-glycosylated ANTIBODY A and 44 % for non-glycosylated ANTIBODY A. The mean reduction in total amyloid-β plaque number was found to be 70 % for ANTIBODY A COMPOSITION, 78 % for double-glycosylated ANTIBODY A, 82 % for mono-glycosylated ANTIBODY A and 36 % for non-glycosylated ANTIBODY A. Note that significance for non-glycosylated ANTIBODY A was low and observed variations were considerable.

Amyloid plaque reduction in the neocortical region together with the corpus callosum is depicted in Figure 16. The mean reduction of total amyloid-β plaque surface was determined for the antibody treated groups: 19 % for ANTIBODY A COMPOSITION, 27 % for double-glycosylated ANTIBODY A, 30 % for mono-glycosylated ANTIBODY A and 10 % for non-glycosylated ANTIBODY A. The mean reduction in total amyloid-β plaque number was found to be 40 % for ANTIBODY A COMPOSITION, 46 % for double-glycosylated ANTIBODY A, 42 % for mono-glycosylated ANTIBODY A and 11 % for non-glycosylated ANTIBODY A.

Amyloid plaque reduction in the entire hippocampal region is depicted in Figure 17. The mean reduction of total amyloid-β plaque surface was determined for the antibody treated groups: 12 % for ANTIBODY A COMPOSITION, 24 % for double-glycosylated ANTIBODY A, 24 % for mono-glycosylated ANTIBODY A and 6 % for non-glycosylated ANTIBODY A. The mean reduction in total amyloid-β plaque number was found to be 36 % for ANTIBODY A COMPOSITION, 46 % for double-glycosylated ANTIBODY A, 37 % for mono-glycosylated ANTIBODY A and 3 % for non-glycosylated ANTIBODY A.

Amyloid plaque reduction in the subiculum, a high susceptibility region for amyloidosis is shown in Figure 18. The mean reduction of total amyloid-β plaque surface was determined for the antibody treated groups: 2 % for ANTIBODY A COMPOSITION, 12 % for double-glycosylated ANTIBODY A, 5 % for mono-glycosylated ANTIBODY A and 1 % for non-glycosylated ANTIBODY A. The mean reduction in total amyloid-β plaque number was found to be 22 % for ANTIBODY A COMPOSITION, 36 % for double-glycosylated ANTIBODY A, 13 % for mono-glycosylated ANTIBODY A and 1 % for non-glycosylated ANTIBODY A. ANTIBODY A COMPOSITION and the main N-glycosylation isoforms (double-glycosylated ANTIBODY A and mono-glycosylated ANTIBODY A) showed a comparable effectivity to decrease amyloid-β plaque load and plaque number. Reduction of plaque load was most pronounced and statistically significant in regions with low or moderate amyloidosis.

Overall, reduction of amyloid-β plaque number was found statistically significant after treatment with ANTIBODY A COMPOSITION and both comprising Asn52 glycosylated isoforms of ANTIBODY A in all measured brain regions. In contrast thereto, only a minor effect on amyloid-β plaque number was found in the thalamus and no significant effects on amyloid-β plaque number in the other investigated brain regions was found after treatment with the non-glycosylated isoform of Antibody A, which is excluded from ANTIBODY A COMPOSITION after the purification as detailed in the invention.

We also investigated potency of plaque clearance in relation to the plaque size. Generally, effectivity of tested human anti-Aβ antibodies was found most pronounced for the clearance of small amyloid-β plaques. This was observed in all brain regions (Figures 15 C, 16 C, 17 C and 18 C). In contrast, there was only a minimal or non-significant trend observed for the non-glycosylated isoform of ANTIBODY A.

Comparative analysis of ANTIBODY A and the major Asn52 glycosylation isoforms demonstrate a comparable capacity to lower plaque load, while the non-glycosylated isoform has no significant effect on plaque lowering.

**Example 16: Pharmacokinetics of in vivo binding of ANTIBODY A COMPOSITION to amyloid-β plaques.**

Two dosing frequencies were compared in order to investigate the binding kinetics of ANTIBODY A COMPOSITION which comprises mono-glycosylated ANTIBODY A and

double-glycosylated ANTIBODY A and is devoid of non-glycosylated ANTIBODY A as defined above.

Therefore, PS2APP transgenic male mice were injected i.v. with ANTIBODY A COMPOSITION via the tail vein either 4 times at biweekly intervals at 0.05, 0.1 and 0.3 mg/kg or 3 times at monthly interval with 0.075, 0.15 and 0.45 mg/kg. For comparison, 0.1 mg/kg was administered once and twice at biweekly intervals and 0.15 mg/kg twice at monthly interval. Following administration all mice were sacrificed two weeks after last dosing. Unfixed PS2APP brain tissue was prepared for sagital sectioning between lateral ~ 1.92 and 1.2 mm according to Paxinos and Franklin, including thalamus, hippocampal formation and cortical areas. Brains were sectioned at 40 µm using a cryostat.

An immuno-fluorescence ex vivo immuno-staining approach was used to detect bound ANTIBODY A COMPOSITION antibodies. Therefore, brains were sectioned and incubated with the detection antibody, an affinity-purified goat anti-human (GAH) IgG (H+L) conjugated to Cy3 (# 109-165-003, lot 49353, Jackson Immuno Research) at a concentration of 15 µg /ml for 1 hour at room temperature. A counterstaining for amyloid-β plaques was done by incubation with BAP-2, a mouse monoclonal antibody against Aβ conjugated to Alexa488 fluorophore at a concentration of 0.5 µg /ml for 1 hour at room temperature.

Images were recorded in the occipital cortex close to the cerebellum using a Leica TCS SP2 AOBS confocal laser scanning microscope as described above. Computer-assisted image processing was performed using the IMARIS software (Bitplane, Switzerland). Images of plaques were first selected using the crop function of the software for the lower doses except the two highest doses of 0.3 and 0.45 mg/kg which required a different gain setting for linear signal recording. The SURPASS function was used to select the positive voxels after thresholding (T) as readout for bound GAH-Cy3 at the site of amyloid-β plaques. Threshold settings were 19 and 12 for lower and higher dose groups, respectively. As a control for amyloid-β plaque specificity, images of the GAH-Cy3 stainings were compared after double labeling with images of plaques stained by mouse monoclonal BAP2 conjugated to Alexa488 and recorded in a different channel.

Descriptive statistics to quantitative description of all images was done with the IMARIS MeasurementPro software modul. Mean voxel fluorescence intensity (MVI) values were determined from selected amyloid-β plaques in the low dose groups or total signal from images

in the high dose groups. The baseline MVI (B) is due to instrumental noise, tissue scatter signal and autofluorescence of lipofuscin. For background correction, B was determined by measuring the average signal intensity at areas apart from amyloid- β plaques and subsequently subtracted from the MVI of all measured images (MVI - B = S). Signal intensity (S) values resembling averaged intensities on plaques obtained from 3 to 4 images from each one brain section per mouse and dose group. For comparability, signal intensities were normalized to a reference sample obtained from a previous study. As reference we used PS2APP mouse brain sections after a single dose administration of 0.25 mg/kg. Measurement endpoint was one week after dosing

All measured intensity values were normalized to the average intensity at amyloid- β plaques obtained after a single dose administration of ANTIBODY A COMPOSITION at 0.25 mg/kg that was measured one week after dosing (see following table). The normalized values for mean relative fluorescence intensity of immunopositive amyloid-β plaques were obtained by CLSM after immunostaining and measuring signal intensities averaged from 3 animals per dose group. Plaques without detectable ANTIBODY A COMPOSITION derived ANTIBODY A were observed only in the lower dose groups, most likely due to limited or partial occupancy of ANTIBODY A COMPOSITION derived ANTIBODY A at the plaque surface, which might have been lost during the sectioning process. Therefore, only immunopositive plaques were included for the comparative analysis.

Mean relative fluorescence intensity per dose group after multiple i.v. (BOLUS) administration of ANTIBODY A COMPOSITION in PS2APP transgenic mice is shown in the following table:

| Dose – interval/injections | Normalized Average Mean Fluorescence Intensity of immunopositive ANTIBODY A COMPOSITION Amyloid-β Plaques | | Percentage of ANTIBODY A COMPOSITION immunonegative amyloid-β plaques |
|---|---|---|---|
| | % | SD | % |
| 0.25mg - single[1] | 100 | 6 | 0 |
| 0.05mg - biweekly / 4x | 53 | 2 | 58 |
| 0.075mg - monthly / 3x | 57 | 6 | 39 |
| 0.15mg - monthly / 2x | 106 | 6 | 19 |
| 0.1mg - biweekly / 1x | 59 | 8 | 45 |

| | | | |
|---|---|---|---|
| 0.1mg - biweekly / 2x | 83 | 26 | 21 |
| 0.1mg - biweekly / 4x | 88 | 12 | 2 |
| 0.15mg - monthly / 3x | 93 | 19 | 1 |
| 0.3mg - biweekly / 4x | 148 | 24 | 0 |
| 0.45mg - monthly / 3x | 184 | 20 | 0 |

[1] Experimental values represent intensity values normalized to the value obtained from a single dose of 0.25 mg/kg after 1 week.

Figure 19 shows binding of ANTIBODY A COMPOSITION in relation to the number of successive biweekly doses at 0.1 mg/kg. After two applications mean intensity appeared increased, although the extent of immunostaining varies considerably and therefore did not reach significance. After 4 injections, amyloid-β plaques are immunostained more homogenously, but mean intensity is only slightly increased. Overall, the data for biweekly application clearly indicate a tendency of increased plaque binding that is correlated with the number of applications.

Figure 20 shows binding of ANTIBODY A COMPOSITION in relation to the number of successive monthly doses at 0.15 mg/kg. Interestingly, comparable levels are obtained after 2 and 3 applications. This was not necessarily expected and might indicate initiation of early effects which contribute to time-dependent differences in clearance mechanism, like delayed microglia cell activation.

The binding efficacy of ANTIBODY A COMPOSITION in relation to administered dose is shown in Figure 21 and 22 . Biweekly doses at 0.05, 0.1 and 0.3 mg/kg (Figure 21) and monthly doses of 0.075, 0.15 and 0.45 mg/kg (Figure 22) clearly showed a dose relationship. It is also evident that the response is not linear and additional factors like a temporally delayed activation of microglia cells might contribute to the observed non-linearity.

It thus can be concluded that ANTIBODY A COMPOSITION-binding to mouse Aβ plaques is dose-related with indications that multiple doses are accumulative.

**Example 17: Analysis of antigen-dependent cellular phagocytosis.**

In order to determine the ANTIBODY A COMPOSITION-mediated phagocytic effect, genuine Aβ plaques from AD brain slices were pre-incubated with different concentrations of ANTIBODY A COMPOSITION which comprises mono-glycosylated ANTIBODY A and double-glycosylated ANTIBODY A and is devoid of non-glycosylated ANTIBODY A as defined above and exposed to living human primary monocytes.

Unfixed human AD brain tissue sections from the occipital cortex region were prepared from a severe AD case (Braak stage IV). Before adding living cells sections were rehydrated with PBS for 5 minutes. ANTIBODY A COMPOSITION antibodies were applied by incubation at defined concentrations in PBS for 1 hour. After washing with PBS living cells were added. Prestimulated human primary monocytes were used at 0.8 and 1.5 x 106/ ml in RPMI 1640 (Gibco # 61870-044) medium with 1% antibiotic solution from a stock solution containing 10'000 U/ml penicillin and 10'000 mg/ml streptomycin (Gibco # 15140-122) and incubated at 37°C with 5% carbon dioxide for 2 to 4 days. Methods for the preparation of prestimulated human primary monocytes are well known in the art e.g. by use of stimulating factors, like macrophage colony-stimulating factor (M-CSF).

After incubation, culture medium was gently removed and sections preserved by chemical fixation with 2% formaldehyde in PBS for 10 minutes. Staining of residual Aβ plaque load was done by incubation with BAP-2, a mouse monoclonal antibody against Aβ conjugated to Alexa488 fluorophore (Molecular Probes: A-20181, monoclonal antibody labeling kit) at a concentration of 10 mg/ml for 1 hour at room temperature.

Quantification of plaque removal was determined by measuring the immunofluorescence of residual stained Aβ plaques. Images were recorded on a Leica TCS SP2 AOBS confocal laser scanning microscope. One optical layer was recorded at excitation wavelength of 488 nm at a pinhole setting of 4 Airy using a HCX PL FL 20x/0.40 correction objective except in one experiment, where a HCPL Fluotar 10x/0.30 objective at a pinhole setting of 3 was used instead. Instrument settings were kept constant for all images to allow a relational quantitative comparison. Specifically, laser power, gain and offset were adjusted to allow for signal intensity monitoring within the dynamic range. For each ANTIBODY A COMPOSITION concentration grey matter regions were recorded at comparable positions from consecutive sections in order to minimize fluctuations possibly coming from anatomical differences in plaque load. Potential competitive binding of ANTIBODY A COMPOSITION and the detection antibody BAP-2, was

measured in the absence of cells at all ANTIBODY A COMPOSITION concentrations. An unrelated human IgG1 (Serotec, PHP010) antibody was used as an additional control. Images analysis was performed using the IMARIS Software (Bitplane, Switzerland). The isosurface of BAP-2 positive pixels representing objects of BAP-2 s bound to the plaques were created by intensity tresholding. Surface area and total fluorescence intensity values were calculated using the "iso surface function" of the SurpassPro software module. Data were expressed as averaged staining area and total staining intensity values obtained from 5 grey matter regions of one brain section. The signal baseline is composed by the instrumental noise and tissue scatter signal was found negligible and was therefore not subtracted from the total intensity signal.

The qualitative effect of ANTIBODY A COMPOSITION was visualized by a decrease in Aβ plaque stain that indicates increased phagocytosis of Aβ plaques from human AD brain sections as shown in Figure 23. Immunohistochemistry revealed a reduction in stainable Aβ plaques clearly visible after a pre-incubation with 100 ng/ml ANTIBODY A COMPOSITION already after 40 hours. The effect is very pronounced and at ANTIBODY A COMPOSITION concentrations of 1 and 5 mg/ml. Aβ plaques are substantially and increasingly cleared by cellular phagocytosis with only few large Aβ plaques remaining at 5 mg/ml. A quantitative measurement based on the immunoreactivity signals expressed as area and intensity of the same experiment is shown in Figure 24 .

Alternatively, the ANTIBODY A COMPOSITION-mediated phagocytic effect was determined using Aβ conjugated fluorescent polystyrene beads. Therefore, fluorescent beads (3 mm, Fluoresbrite carboxy YG, Polysciences Inc.) were coupled with Aβ. Briefly, beads were washed 2x by suspension and centrifugation in coupling buffer (50 mM MES buffer, pH 5.2, 1% DMSO). The pellet (approx. 10 ul) was suspended in 200 ul coupling buffer and activated by addition of 20 ul of a 20% solution of EDC (Ethyl-diaminopropyl-carbodiimide, Pierce) in coupling buffer. Immediate addition of 20 µg Aβ (1-40) or Aβ (1-42) (in 0.1% ammonium hydroxide, Bachem) started the coupling reaction. After one night incubation the beads were washed with 3x 0.5 ml 10mM Tris.HCl pH 8.0 and 3x 0.5ml storage buffer (10 mm Tris.HCl pH 8.0, 0.05% BSA, 0.05% NaN3). The 1% suspension was stored at 4oC until use. As a negative control Fluoresbrite carboxy NYO (red fluorescence) beads were coupled with all-D amino acid Aβ (1-40). (in 0.1% ammonium hydroxide, Bachem).

Murine monocytes/macrophages (cell line P388D1) were grown in C24 transparent tissue culture clusters or C96 black microplates to approx. 50% confluency. The culture medium was IMEM with 5% FBS, glutamine and antibiotics. To block unspecific scavenger receptors 10 ml fucoidan (Fluka, 10 mg/ml in water) was added to 200 ml culture volume and incubated for 2 hours. ANTIBODY A COMPOSITION was added in serial dilutions and pre-incubated for 30 minutes. Fluorescent Aβ bead suspension (20 µl) was added and incubated for 3 hrs to allow phagocytosis. The adherent cells were washed vigorously 1x with ice cold EDTA and 2x with PBS in order to remove adhering agglutinates from the cell surface. The residual beads were either monitored by visual inspection at a Zeiss Axiovert 405 or for quantification by using a microplate fluorimeter (Fluoroscan, Labsystems) with 444nm (Exc) and 485nm (Em) filter settings

The qualitative effect of ANTIBODY A COMPOSITION on the phagocytosis of synthetic Aβ aggregates coupled to fluorescent fluorobeads by P388D1 cells is shown in Figure 25 . The quantitative determination of the dose response of ANTIBODY A COMPOSITION is shown in Figure 26 . Two independent experiments revealed a range from 30 to 200 ng/ml for EC50 and 10 to 60 ng/ml for MEC. The observed variability is likely caused by differences of the incubation stoichiometry, i.e. ratio of beads to cells. The observed decline of bead phagocytosis above a concentration > 200 ng/ml is due to monovalent antibody interaction with limited antigen.

It thus can be concluded that ANTIBODY A COMPOSITION efficiently induces phagocytosis of Aβ plaques from AD brain tissue sections in a dose related manner.

# CLAIMS

1. A purified antibody molecule being characterized in that at least one antigen binding site of said antibody molecule comprises a glycosylated asparagine (Asn) in the variable region of the heavy chain ($V_H$).

2. The purified antibody molecule of claim 1, wherein said glycosylated asparagine (Asn) in the variable region of the heavy chain ($V_H$) is in the CDR2 region.

3. The purified antibody molecule of claim 1 or 2, wherein said glycosylated asparagine (Asn) in the variable region of the heavy chain ($V_H$) is in position 52 of SEQ ID NO: 2 or position 52 of SEQ ID NO: 6.

4. The purified antibody molecule of any one of claim1 1 to 3, whereby said antibody molecule is capable of specifically recognizing the β-A4 peptide/Aβ4.

5. The purified antibody molecule of claim 4, whereby said β-A4 peptide/Aβ4 has the following sequence:

   DAEFRHDSGYEVHHQKLVFFAEDVGSNKGAIIGLMVGGVVIA (SEQ ID NO: 3)

   or a part of at least 15 amino acids of said sequence.

6. The antibody molecule of any one of claims 1 to 5, being characterized in that at least one antigen binding site of said antibody molecule comprises a glycosylated asparagine (Asn) in the variable region of the heavy chain ($V_H$) and said $V_H$ being encoded by:

   (a) a nucleic acid molecule comprising the nucleotide sequence as shown in SEQ ID NO: 1

   CAGGTGGAATTGGTGGAAAGCGGCGGCGGCCTGGTGCAACCGGGCGGCA
   GCCTGCGTCTGAGCTGCGCGGCCTCCGGATTTACCTTTAGCAGCTATGCG
   ATGAGCTGGGTGCGCCAAGCCCCTGGGAAGGGTCTCGAGTGGGTGAGCG
   CTATTAATGCTTCTGGTACTCGTACTTATTATGCTGATTCTGTTAAGGGTC
   GTTTTACCATTTCACGTGATAATTCGAAAAACACCCTGTATCTGCAAATG
   AACAGCCTGCGTGCGGAAGATACGGCCGTGTATTATTGCGCGCGTGGTA
   AGGGTAATACTCATAAGCCTTATGGTTATGTTCGTTATTTTGATGTTTGGG

GCCAAGGCACCCTGGTGACGGTTAGCTCA;

(b) a nucleic acid molecule which encodes a polypeptide having the amino acid sequence as shown in SEQ ID NO: 2

QVELVESGGGLVQPGGSLRLSCAASGFTFSSYAMSWVRQAPGK
GLEWVSAINASGTRTYYADSVKGRFTISRDNSKNTLYLQMNSL
RAEDTAVYYCARGKGNTHKPYGYVRYFDVWGQGTLVTVSS
(SEQ ID NO. 2);

(c) a nucleic acid molecule that hybridizes to the nucleic acid molecule of (a) or (b) and which encodes a polypeptide which is capable of binding to the β-A4 peptide/Aβ4 as shown in the following amino acid sequence

DAEFRHDSGYEVHHQKLVFFAEDVGSNKGAIIGLMVGGVVIA
(SEQ ID NO: 3)

or is capable of binding to a fragment thereof which comprises at least 15 amino acids;

(d) a nucleic acid molecule that hybridizes to the nucleic acid molecule of (a) or (b) and which encodes a polypeptide which is capable of binding to at least two regions on the β-A4 peptide/Aβ4 as shown in the following amino acid sequence

DAEFRHDSGYEVHHQKLVFFAEDVGSNKGAIIGLMVGGVVIA
(SEQ ID NO: 3)

or to at least two regions of a fragment of SEQ ID NO. 3 which comprises at least 15 amino acids whereby said two regions on the β-A4 peptide Aβ4 or said fragment thereof comprise the amino acids on position 3 to 6 and on position 18 to 26; or

(e) a nucleic acid sequence that is degenerate to a nucleic acid sequence as defined in any one of (a) to (d).

7. The antibody molecule of any of claims 1 to 5, wherein the variable region comprising a glycosylated asparagine (Asn) is comprised in a heavy chain selected from the group consisting of:

(a) a heavy chain polypeptide encoded by a nucleic acid molecule as shown in SEQ ID NOS: 5, 23 or 25;

(b) a heavy chain polypeptide having the amino acid sequence as shown in SEQ ID NO: 6 or 26;

(c) a heavy chain polypeptide encoded by a nucleic acid molecule that hybridizes to the nucleic acid molecule defined in (a) and which encodes a polypeptide which is capable of binding to the β-A4 peptide/Aβ4 as shown in the following amino acid sequence

DAEFRHDSGYEVHHQKLVFFAEDVGSNKGAIIGLMVGGVVIA
(SEQ ID NO: 3)

or a fragment thereof which comprises at least 15 amino acids; or

(d) a heavy chain polypeptide encoded by a nucleic acid molecule that hybridizes to the nucleic acid molecule defined in (a) and which encodes a polypeptide which is capable of binding to at least two regions on the β-A4 peptide/Aβ4 as shown in the following amino acid sequence

DAEFRHDSGYEVHHQKLVFFAEDVGSNKGAIIGLMVGGVVIA
(SEQ ID NO: 3)

or to at least two regions of a fragment of SEQ ID NO. 3 which comprises at least 15 amino acids

whereby said two regions on the β-A4 peptide Aβ4 or said fragment thereof comprise the amino acids on position 3 to 6 and on position 18 to 26.

8. The antibody molecule of anyone of claims 1 to 7, wherein two antigen binding sites comprise the glycosylated Asn in the variable region of the heavy chain ($V_H$).

9. The antibody molecule of claim 8, wherein the CDR2 regions of the heavy chains ($V_H$) comprise the glycosylated Asn.

10. The antibody molecule of any one of claims 1 to 9, wherein said Asn is Asn on position

52 of SEQ ID NO: 2 or is the Asn on position 52 of SEQ ID NO: 6.

11. The antibody molecule of any one of claims 1 to 10, whereby said glycosylation on Asn in the $V_H$ region is selected from the group consisting of

(a) a sugar structure of the biantennary complex type;

(b) a sugar structure of the biantennary hybrid type;

(c) a sugar structure of the biantennary oligomannose type; and

(d) a sugar bi-antennary structure of the any of the structures as provided in figure 5 or figure 27.

12. The antibody molecule of claim 11, whereby said sugar structure does not comprise a core fucosylation.

13. The antibody molecule of any one of claims 2 to 12, whereby said CDR-2 region has an amino acid sequence as shown in SEQ ID NO: 12.

14. The antibody molecule of any one of claims 1 to 13, which is recombinantly produced.

15. The antibody molecule of any one of claims 1 to 14 which is produced in a CHO-cell.

16. The antibody molecule of claim 15, whereby said CHO cell is CHO K1 or CHO K1 SV.

17. A method for the preparation of an antibody molecule as defined in any one of claims 1 to 16 comprising the steps of

(a) recombinantly expressing a heterologous nucleic acid molecule encoding an antibody molecule as defined in any one of claims 1 to 13 in a mammalian cultured cell;

(b) purifying said recombinantly expressed antibody molecule by a method comprising the steps of

(b1) protein A column purification;

(b2) ion exchange column purification; and

(b3) size exclusion column purification.

18. The method of claim 17, wherein said ion exchange column purification comprises a cation exchange chromatography.

19. The method of claim 17 or 18, further comprising as an additional step (c) an analytical chromatography and/or a further concentration step.

20. A composition comprising an antibody molecule being characterized in that one antigen binding site of said antibody molecule comprises a glycosylated asparagine (Asn) in the variable region of the heavy chain ($V_H$) and comprising an antibody molecule being characterized in that the two antigen binding sites of said antibody molecule comprise a glycosylated asparagine (Asn) in the variable region of the heavy chain ($V_H$), and which comprises less than 5 % of an antibody molecule being characterized in that none antigen binding site of said antibody molecule comprises a glycosylated asparagine (Asn) in the variable region of the heavy chain ($V_H$).

21. A composition comprising an antibody molecule of any one of claims 1 to 16 or an antibody molecule prepared by the method of any one of claims 17 to 19.

22. The composition of claim 20 or 21, which is a diagnostic or a pharmaceutical composition.

23. Use of an antibody molecule of any one of claims 1 to 16 or the composition of any one of claims 20 to 22 for the preparation of a medicament for the prevention and/or treatment of a disease associated with amyloidogenesis and/or amyloid-plaque formation.

24. Use of an antibody molecule of any one of claims 1 to 16 or the composition of any one of claims 20 to 22 for the preparation of a diagnostic kit for the detection of a disease associated with amyloidogenesis and/or amyloid-plaque formation.

25. Use of an antibody molecule of any one of claims 1 to 16 or a composition of any one of claims 20 to 22 for the preparation of a medicament for the disintegration of β-amyloid plaques.

26. Use of an antibody molecule of any one of claims 1 to 16 or a composition of any one of claims 20 to 22 for the preparation of a pharmaceutical composition for passive

immunization against β-amyloid plaque formation.

27. Use of an antibody molecule of any one of claims 1 to 16 or a composition of any one of claims 20 to 22 for the preparation of a pharmaceutical composition for the preventive treatment against a disease associated with amyloidogenesis and/or amyloid-plaque formation

28. The use of claim 27, wherein pre-existing plaques or aggregation intermediates of amyloid-β are to be reduced.

29. Use of an antibody molecule of any one of claims 1 to 16 or a composition of any one of claims 20 to 22 for the preparation of a diagnostic kit for the diagnosis of a disease associated with amyloidogenesis and/or amyloid-plaque formation in a patient or for the diagnosis of the susceptibility of a patient for the development of a disease associated with amyloidogenesis and/or amyloid-plaque formation.

30. The use of any one of claims 23, 24 or 27 to 29, wherein said disease is dementia, Alzheimer's disease, motor neuropathy, Down's syndrome, Creutzfeld Jacob disease, hereditary cerebral hemorrhage with amyloidosis Dutch type, dementia associated with Lewy body formation, Parkinson's disease, HIV-related dementia, ALS or neuronal disorders related to aging.

31. A kit comprising an antibody molecule of any one of claims 1 to 16 or as prepared by the method of any one of claims 17 to 19 or a composition as defined in claims 20 to 22.

32. Method for the prevention, treatment or amelioration of a disease associated with amyloidogenesis and/or amyloid-plaque formation, comprising administering the antibody molecule of any one of claims 1 to to 16 or the composition of any one of claims 20 to 22 to a mammal in need of such prevention or treatment.

33. The method of claim 32, wherein said disease is dementia, Alzheimer's disease, motor neuropathy, Down's syndrome, Creutzfeld Jacob disease, hereditary cerebral hemorrhage with amyloidosis Dutch type, dementia associated with Lewy body formation, Parkinson's disease, HIV-related dementia, ALS or neuronal disorders related to aging.

34. The method of claim 32 or 33, wherein said mammal is a human.

Fujirebio Diagnostics, Inc. v. Quanterix Corp.
EX-1045
5640

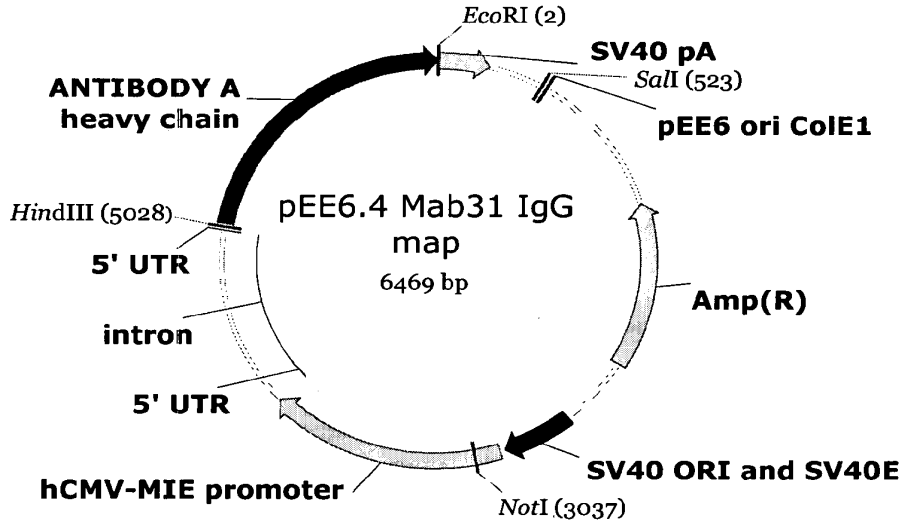



Figure 1A

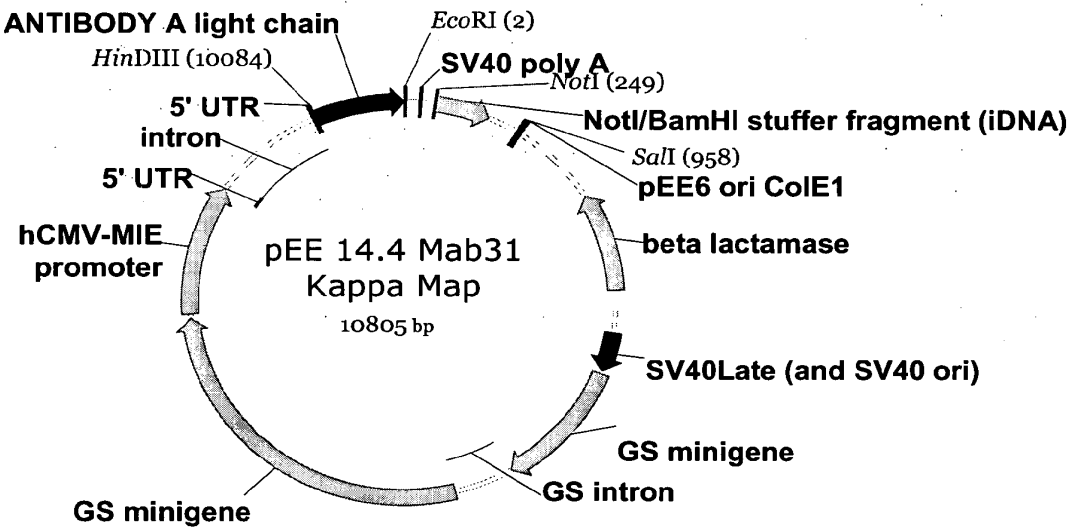



Figure 1B

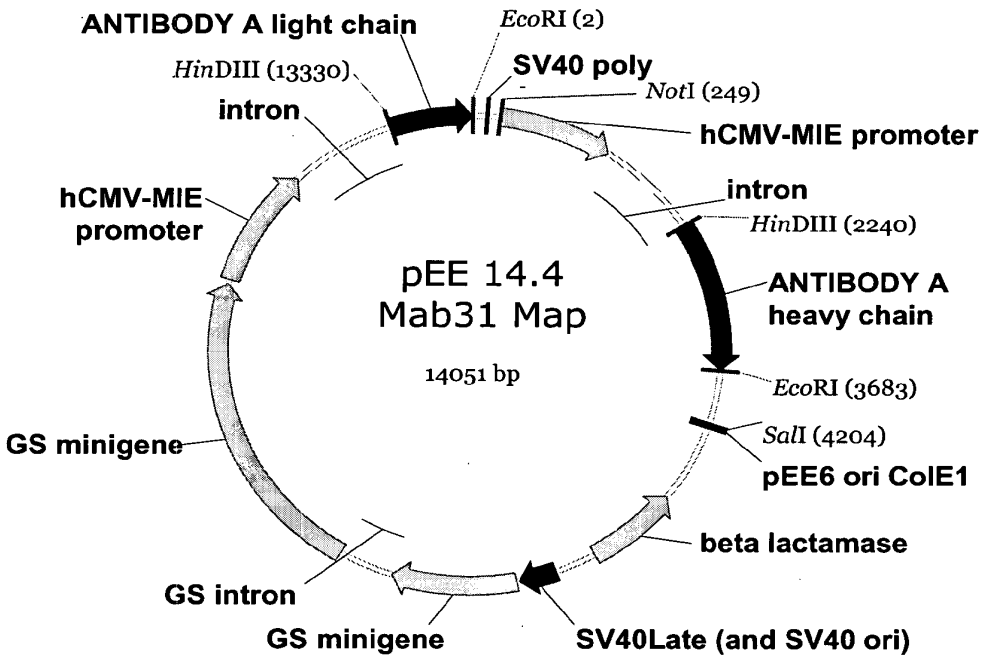

ANTIBODY A light chain
EcoRI (2)
SV40 poly
HinDIII (13330)
NotI (249)
intron
hCMV-MIE promoter
intron
hCMV-MIE promoter
HinDIII (2240)
pEE 14.4
Mab31 Map
14051 bp
ANTIBODY A heavy chain
EcoRI (3683)
SalI (4204)
GS minigene
pEE6 ori ColE1
beta lactamase
GS intron
GS minigene
SV40Late (and SV40 ori)

Figure 1C

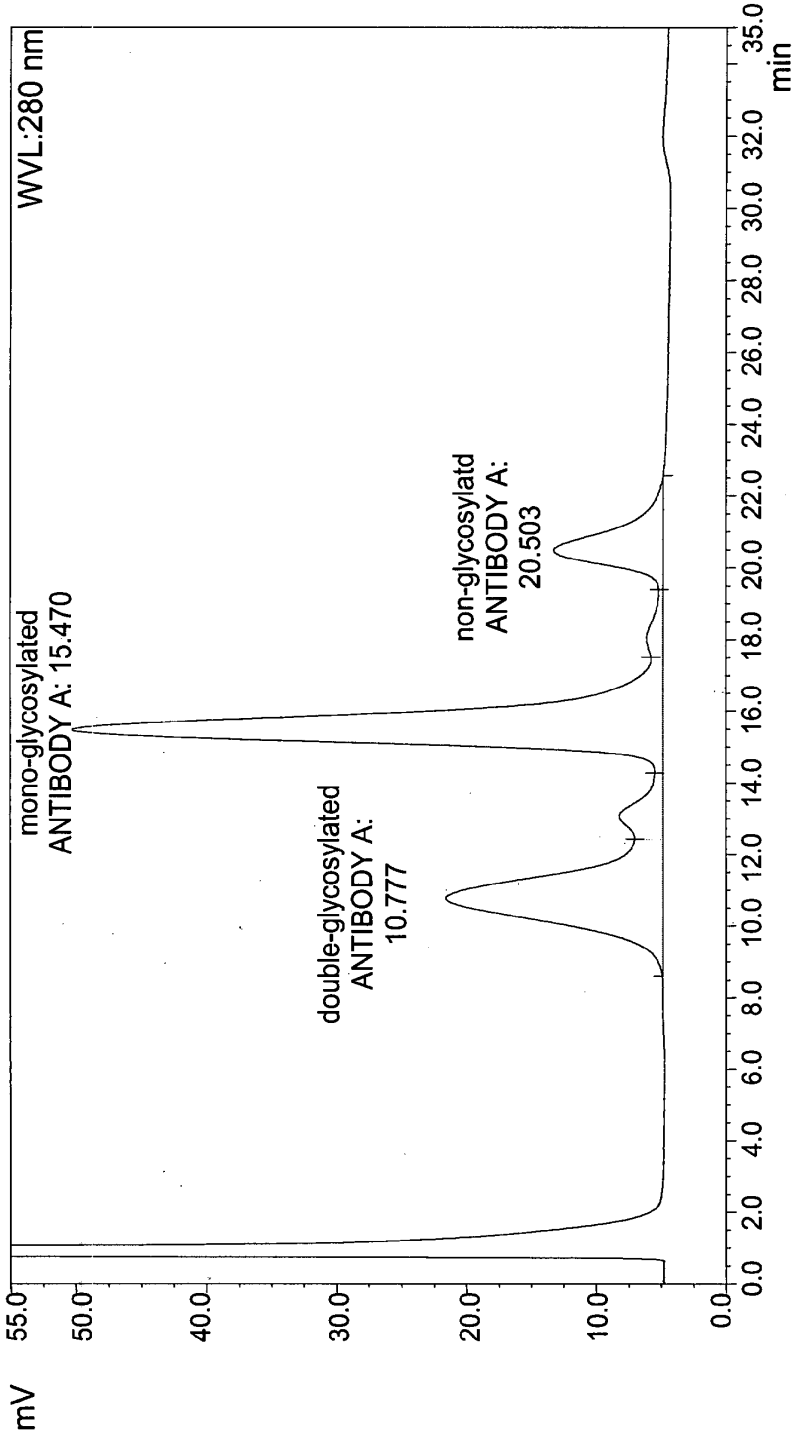

WVL:280 nm
mono-glycosylated ANTIBODY A: 15.470
double-glycosylated ANTIBODY A: 10.777
non-glycosylatd ANTIBODY A: 20.503
mV
55.0
50.0
40.0
30.0
20.0
10.0
0.0
0.0
2.0
4.0
6.0
8.0
10.0
12.0
14.0
16.0
18.0
20.0
22.0
24.0
26.0
28.0
30.0
32.0
35.0
min

Figure 2

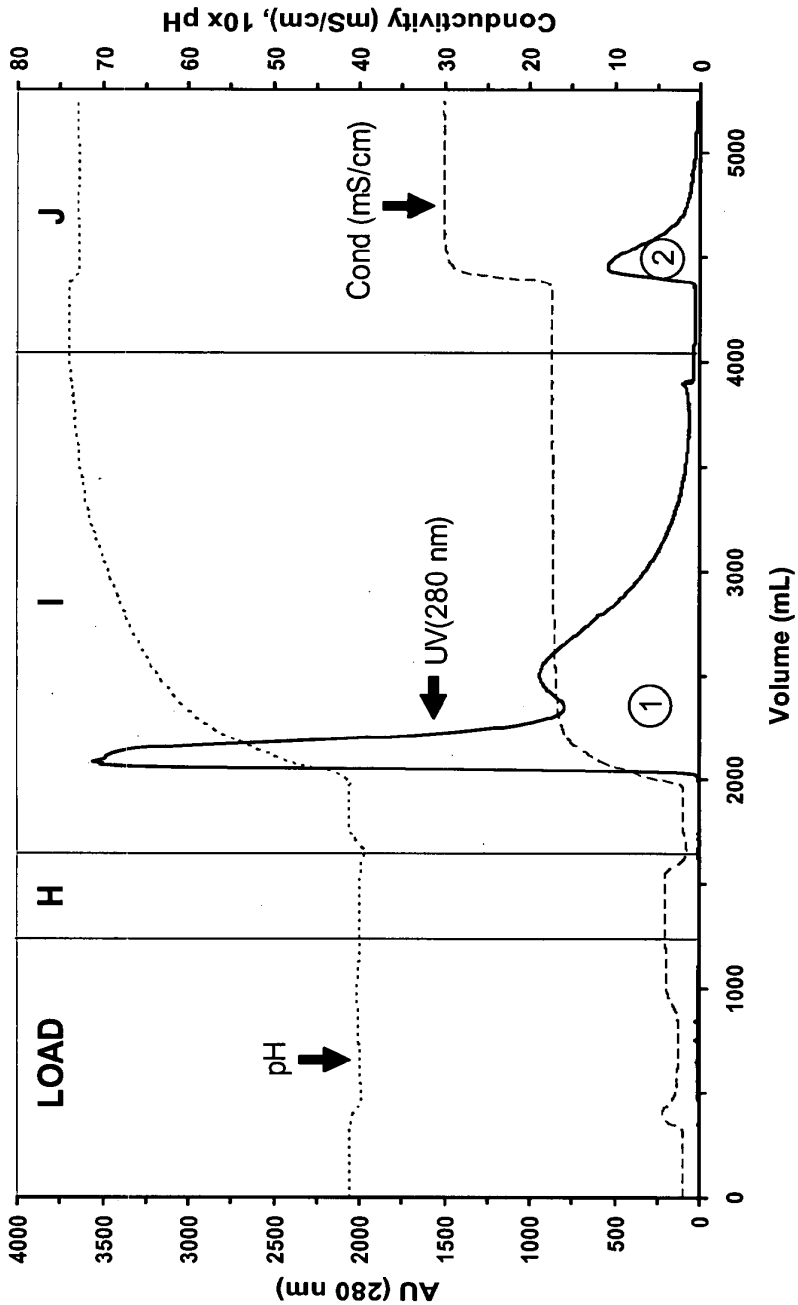

LOAD
H
I
J
pH
UV(280 nm)
Cond (mS/cm)
1
2
AU (280 nm)
Conductivity (mS/cm), 10x pH
Volume (mL)
0
500
1000
1500
2000
2500
3000
3500
4000
0
10
20
30
40
50
60
70
80
0
1000
2000
3000
4000
5000

Figure 3

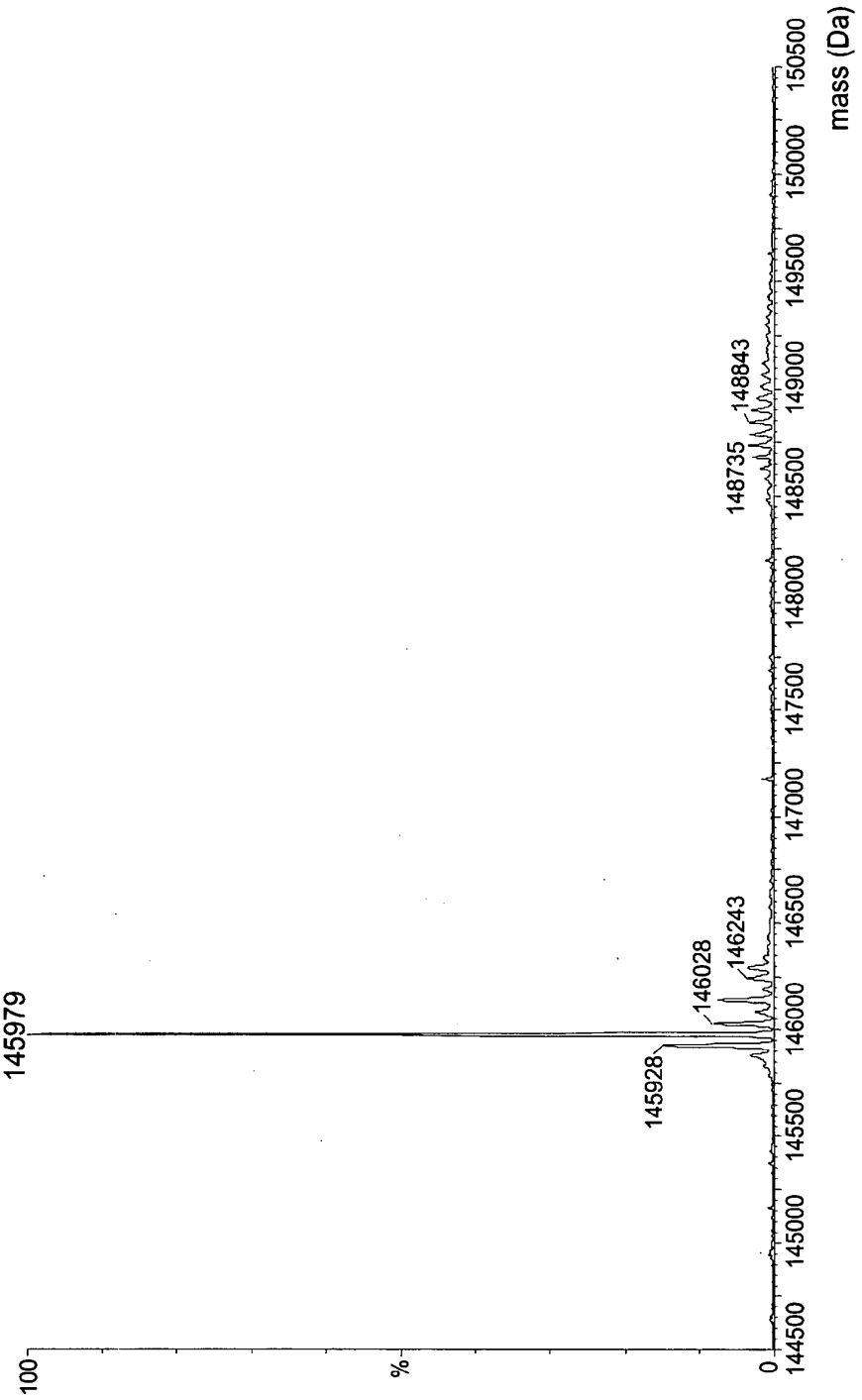



Figure 4A non-glycosylated ANTIBODY A

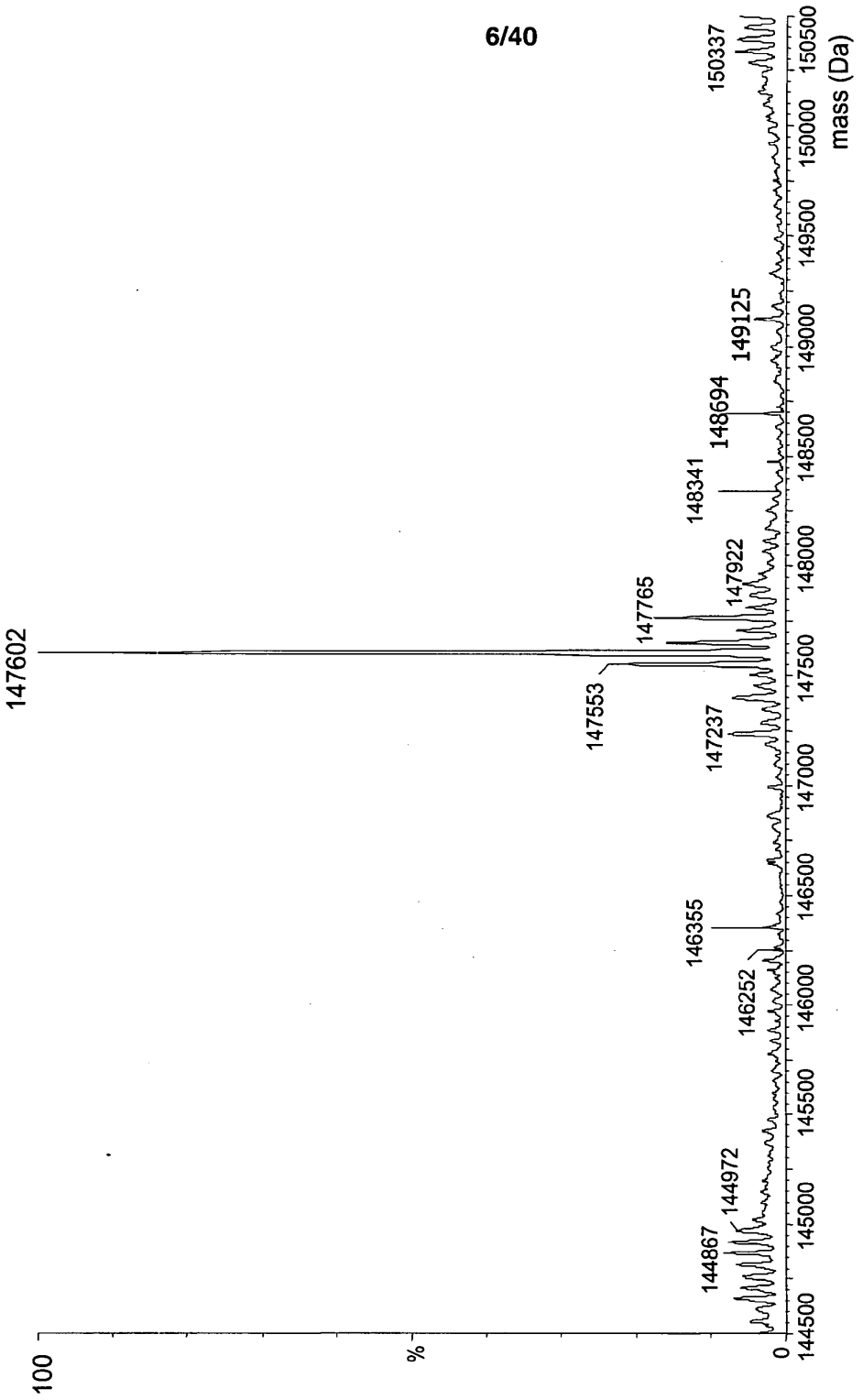



**Figure 4B mono-glycosylated ANTIBODY A**

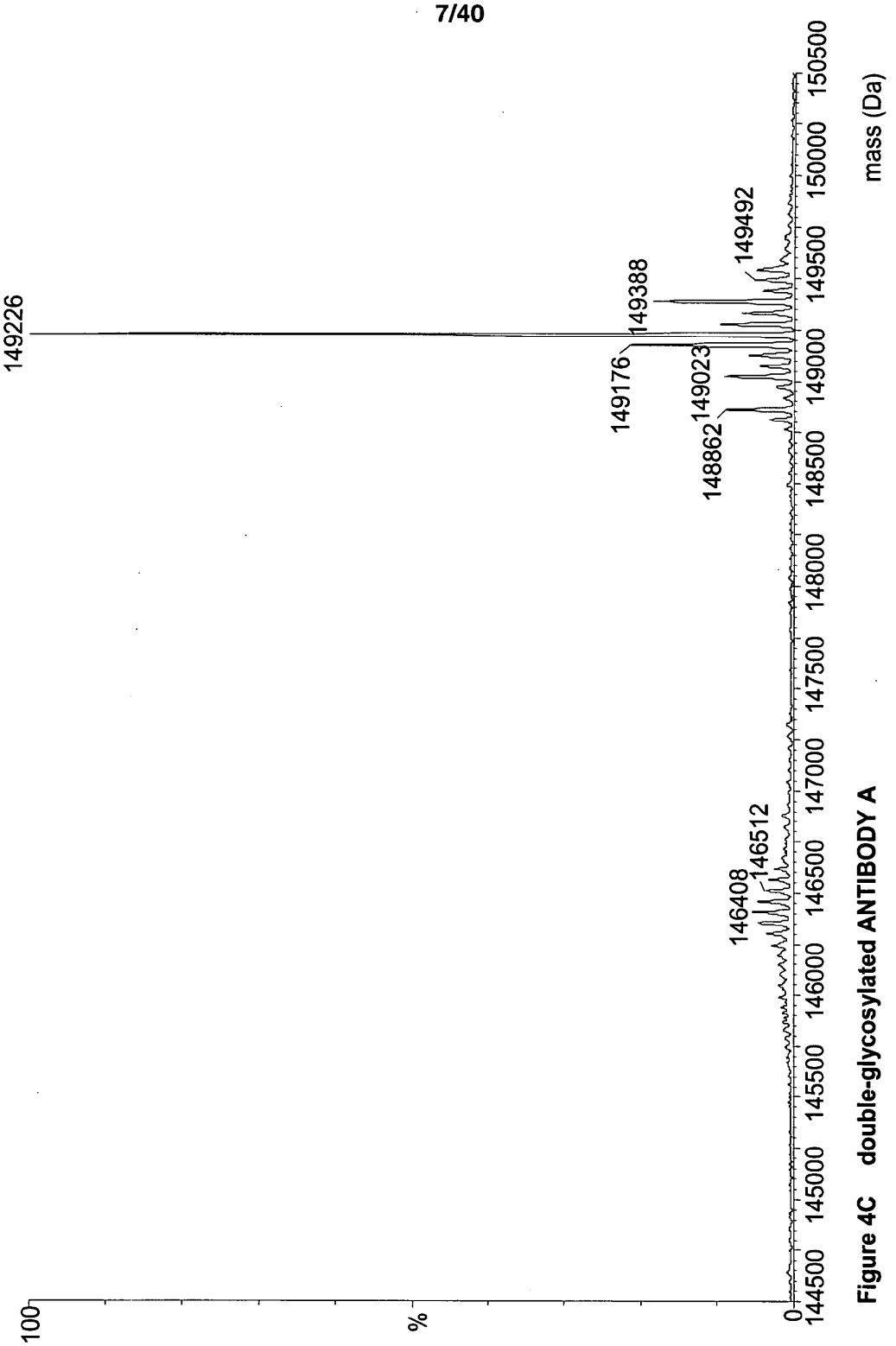
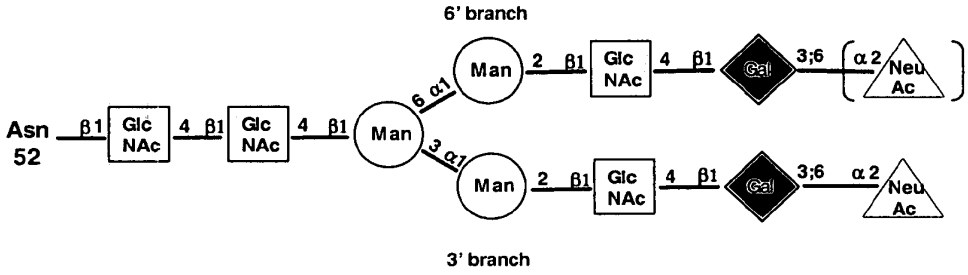
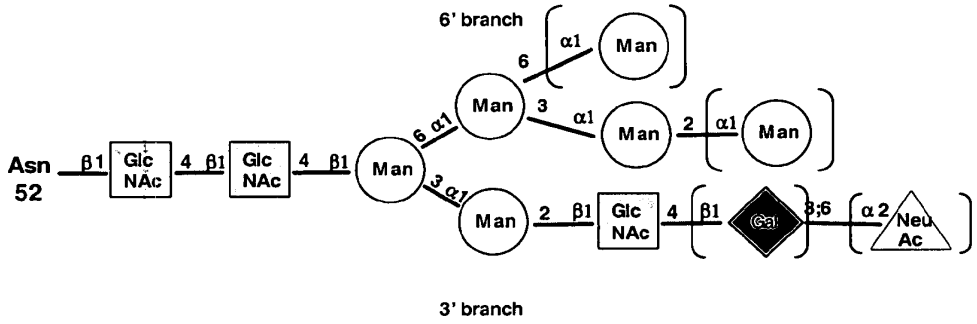



Figure 4C double-glycosylated ANTIBODY A

A


6' branch
Asn 52
β1
Glc NAc
4 β1
Glc NAc
4 β1
Man
6 α1
3 α1
Man
2 β1
Glc NAc
4 β1
Gal
3;6
α2
Neu Ac
Man
2 β1
Glc NAc
4 β1
Gal
3;6
α2
Neu Ac
3' branch

B


6' branch
α1
Man
6
Man
3
α1
Man
2
α1
Man
Asn 52
β1
Glc NAc
4 β1
Glc NAc
4 β1
Man
6 α1
3 α1
Man
2 β1
Glc NAc
4 β1
Gal
3;6
α2
Neu Ac
3' branch

C

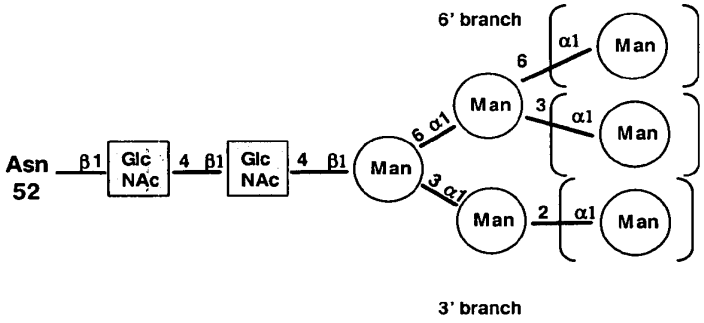

6' branch
α1
Man
6
Man
3
α1
Man
2
α1
Man
Asn 52
β1
Glc NAc
4 β1
Glc NAc
4 β1
Man
6 α1
3 α1
3' branch

Figure 5

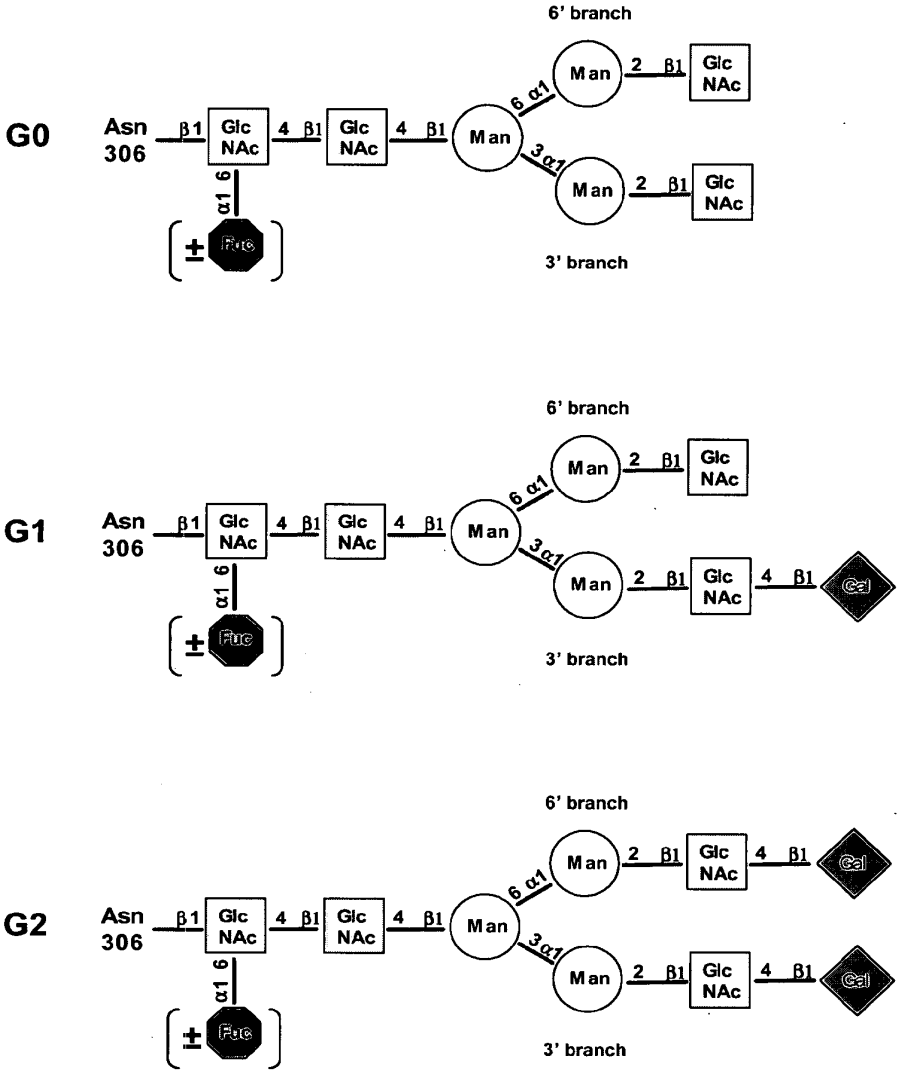

G0
G1
G2
Asn 306
β1
Glc NAc
4 β1
Glc NAc
4 β1
Man
6 α1
3 α1
Man
2 β1
Glc NAc
α1 6
± Fuc
6' branch
3' branch
Gal
4 β1

Figure 6

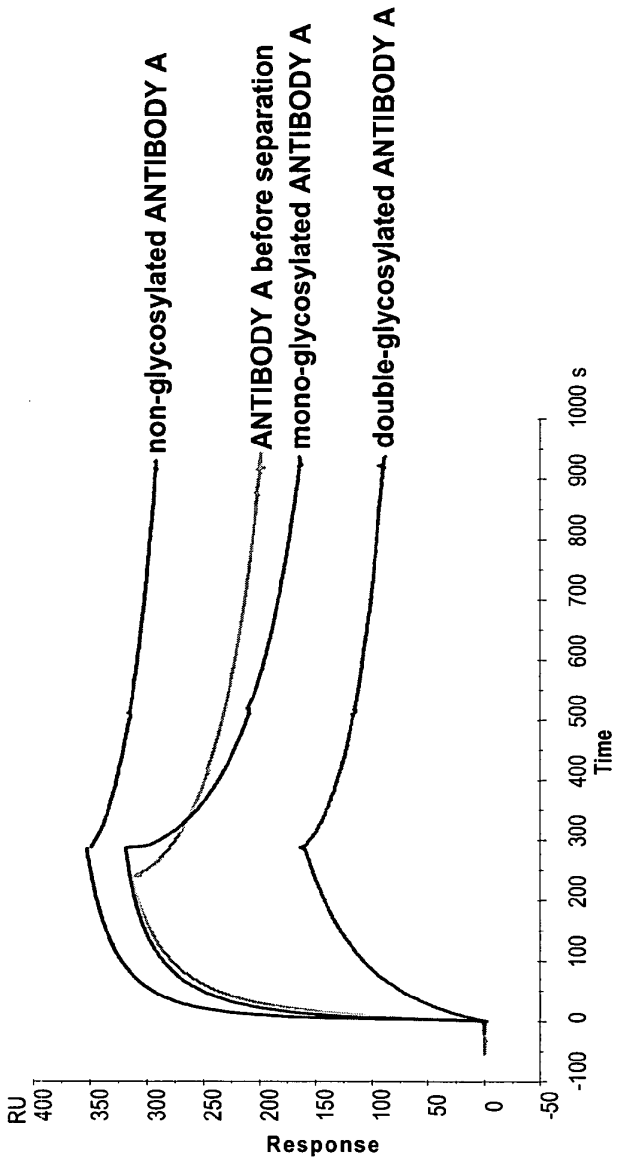
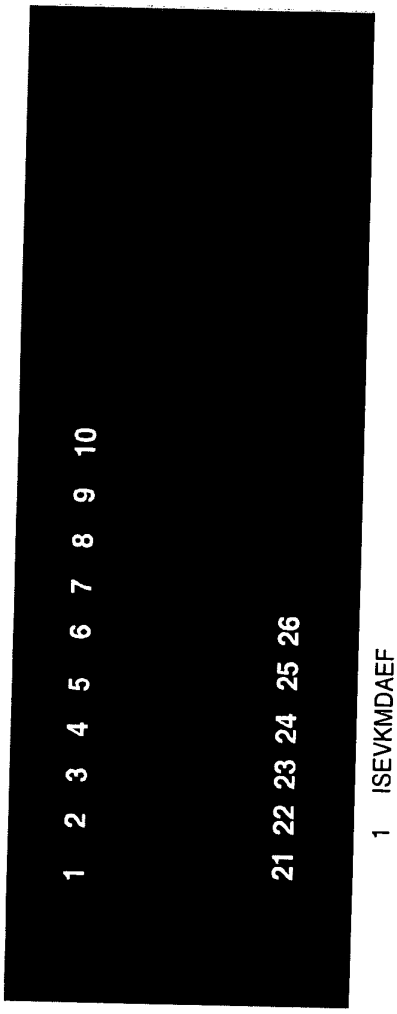

non-glycosylated ANTIBODY A
ANTIBODY A before separation
mono-glycosylated ANTIBODY A
double-glycosylated ANTIBODY A
RU
400
350
300
250
200
150
100
50
0
-50
Response
-100
0
100
200
300
400
500
600
700
800
900
1000 s
Time

Figure 7




| | | | |
|---|---|---|---|
| 1 | ISEVKMDAEF | 21 | QKLVFFAEDV |
| 2 | SEVKMDAEFR | 22 | KLVFFAEDVG |
| 3 | EVKMDAEFRH | 23 | LVFFAEDVGS |
| 4 | VKMDAEFRHD | 24 | **VFFAEDVGSN** |
| 5 | KMDAEFRHDS | 25 | FFAEDVGSNK |
| 6 | MDAEFRHDS | 26 | FAEDVGSNK |
| 7 | DAEFRHDSGY | | |
| 8 | AEFRHDSGYE | | |
| 9 | **EFRHDSGYEV** | | |
| 10 | FRHDSGYEVH | | |

**Figure 8A**

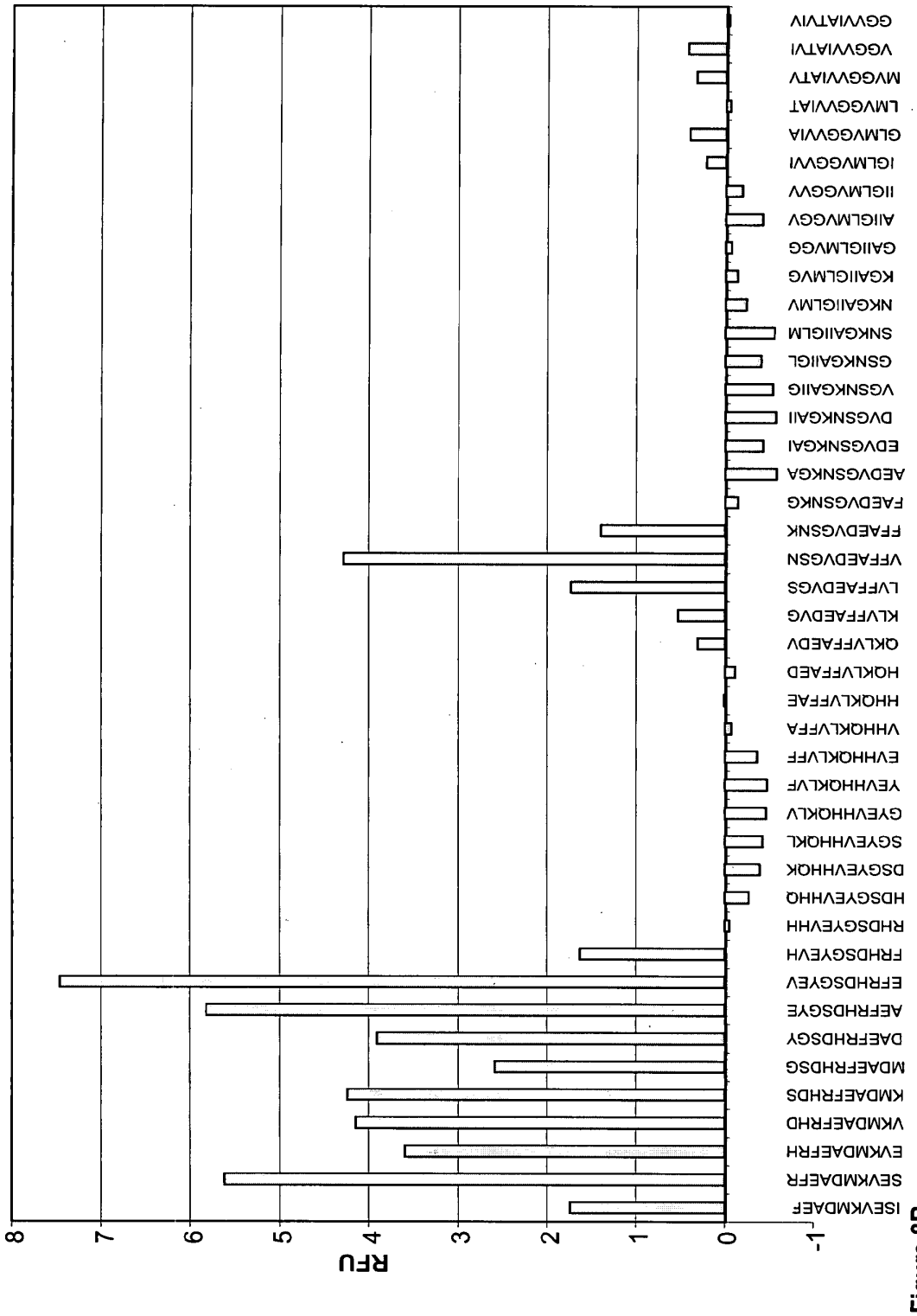

RFU
8
7
6
5
4
3
2
1
0
-1
ISEVKMDAEF
SEVKMDAEFR
EVKMDAEFRH
VKMDAEFRHD
KMDAEFRHDS
MDAEFRHDSG
DAEFRHDSGY
AEFRHDSGYE
EFRHDSGYEV
FRHDSGYEVH
RHDSGYEVHH
HDSGYEVHHQ
DSGYEVHHQK
SGYEVHHQKL
GYEVHHQKLV
YEVHHQKLVF
EVHHQKLVFF
VHHQKLVFFA
HHQKLVFFAE
HQKLVFFAED
QKLVFFAEDV
KLVFFAEDVG
LVFFAEDVGS
VFFAEDVGSN
FFAEDVGSNK
FAEDVGSNKG
AEDVGSNKGA
EDVGSNKGAI
DVGSNKGAII
VGSNKGAIIG
GSNKGAIIGL
SNKGAIIGLM
NKGAIIGLMV
KGAIIGLMVG
GAIIGLMVGG
AIIGLMVGGV
IIGLMVGGVV
IGLMVGGVVI
GLMVGGVVIA
LMVGGVVIAT
MVGGVVIATV
VGGVVIATVI
GGVVIATVIV

Figure 8B

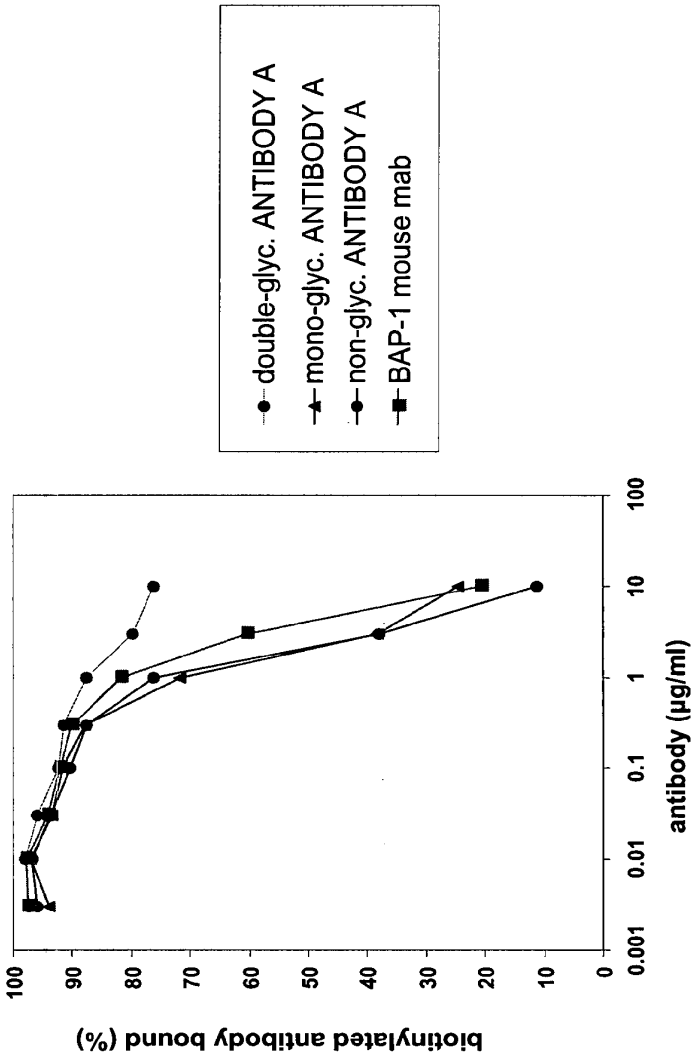

double-glyc. ANTIBODY A
mono-glyc. ANTIBODY A
non-glyc. ANTIBODY A
BAP-1 mouse mab
biotinylated antibody bound (%)
100
90
80
70
60
50
40
30
20
10
0
0.001
0.01
0.1
1
10
100
antibody (µg/ml)

Figure 9

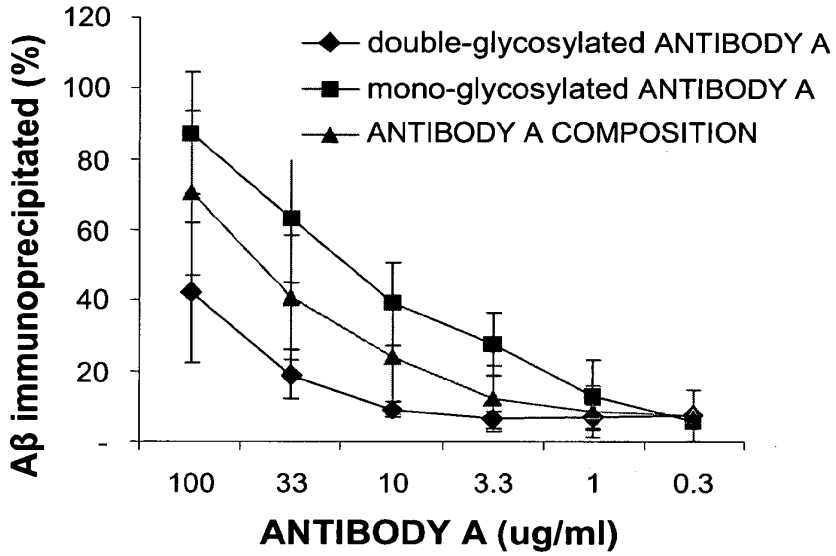

120
100
80
60
40
20
-
Aβ immunoprecipitated (%)
double-glycosylated ANTIBODY A
mono-glycosylated ANTIBODY A
ANTIBODY A COMPOSITION
100
33
10
3.3
1
0.3
ANTIBODY A (ug/ml)

**Figure 10**

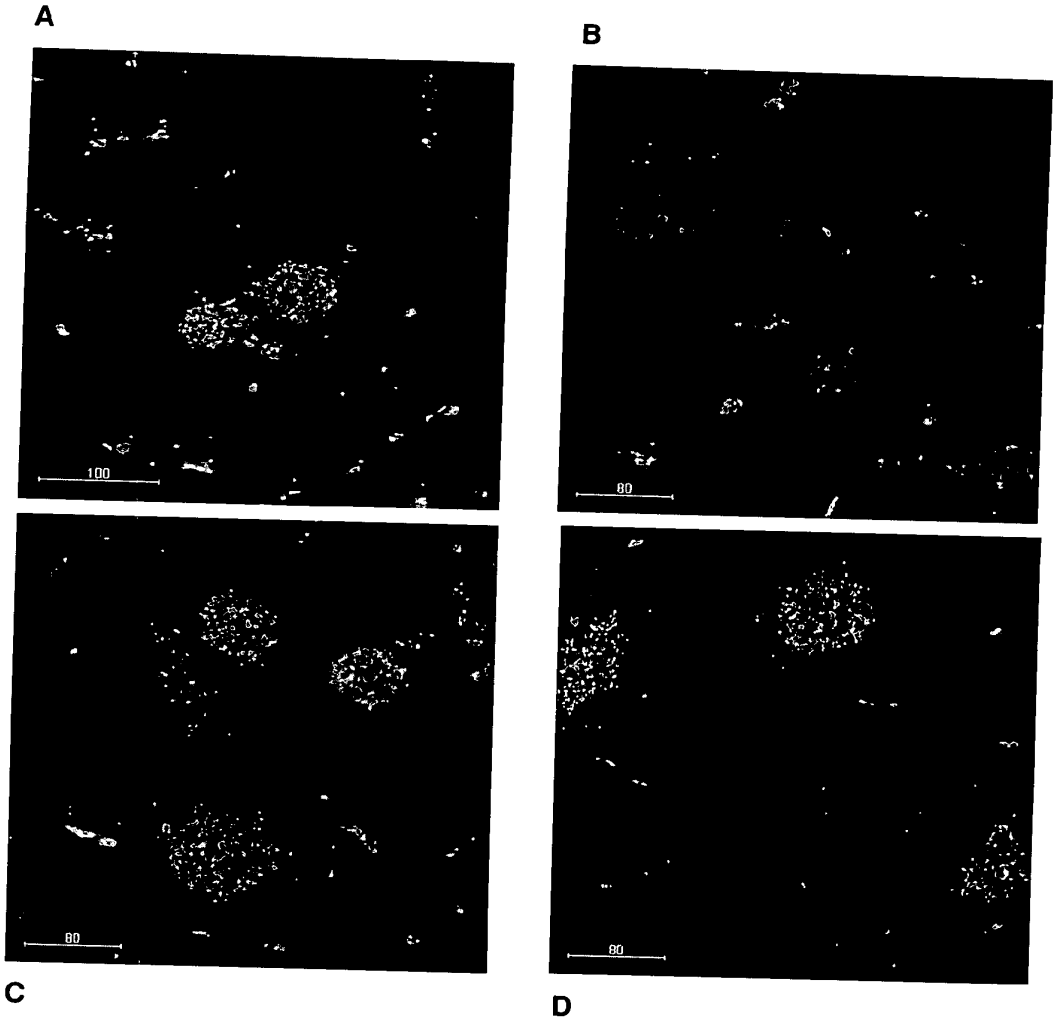



Figure 11

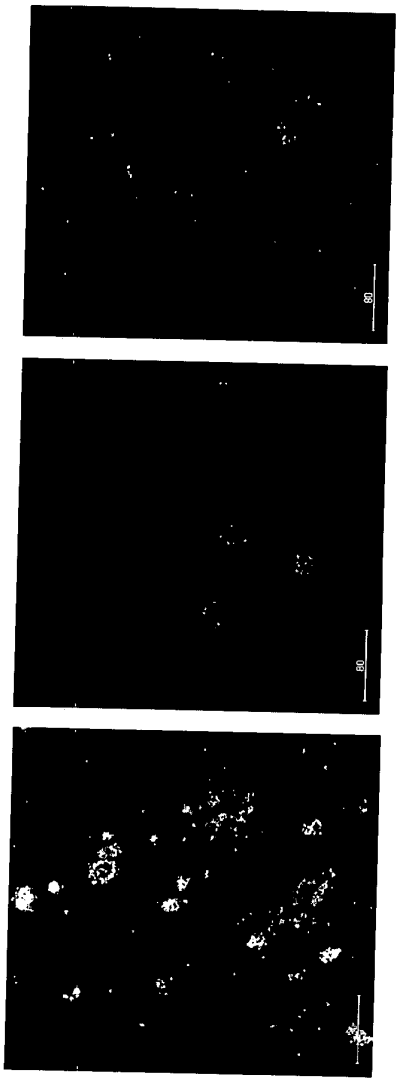


Figure 12

Fujirebio Diagnostics, Inc. v. Quanterix Corp.
EX-1045
5656

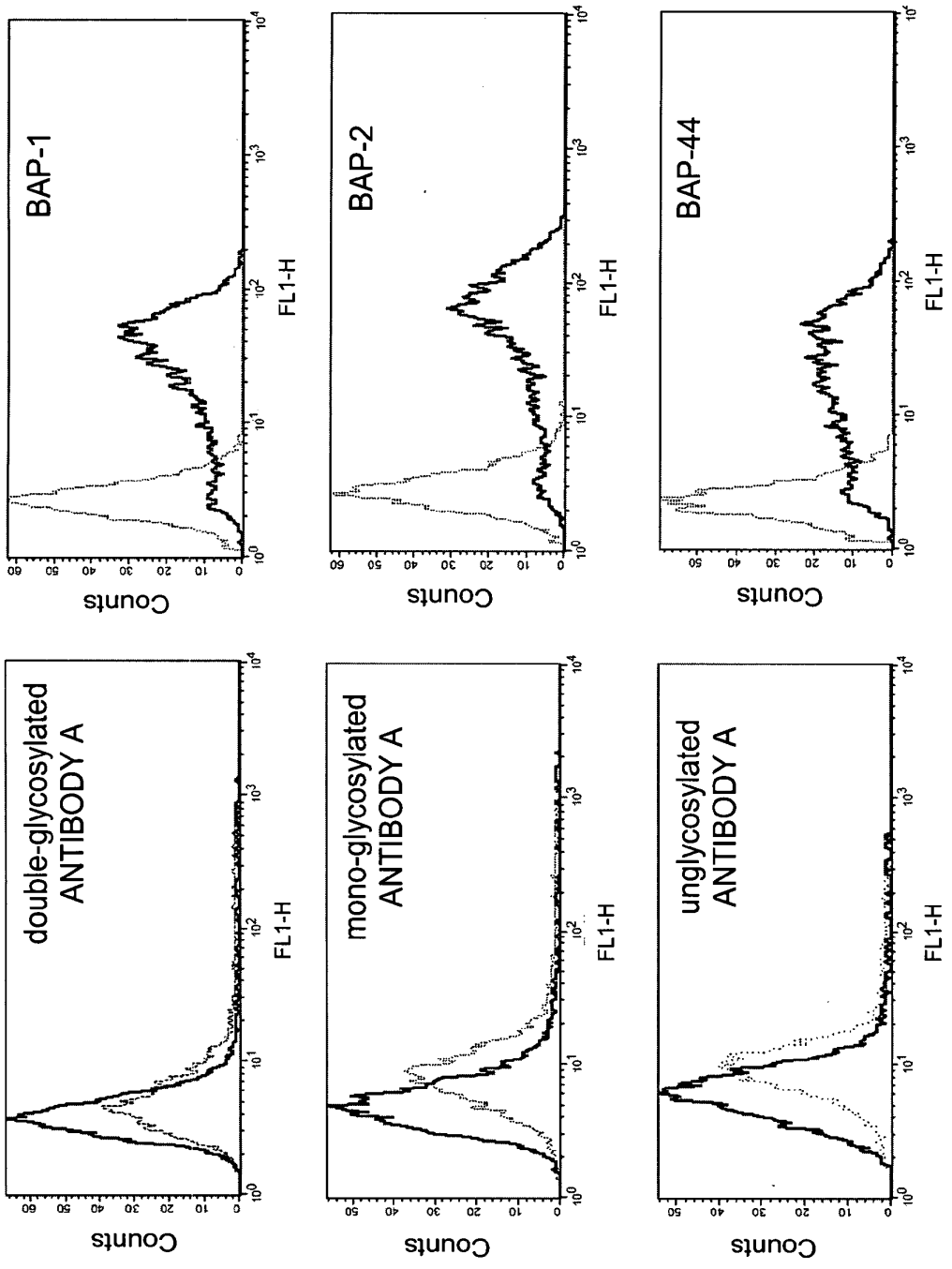

BAP-1
BAP-2
BAP-44
double-glycosylated ANTIBODY A
mono-glycosylated ANTIBODY A
unglycosylated ANTIBODY A
Counts
FL1-H

Figure 13

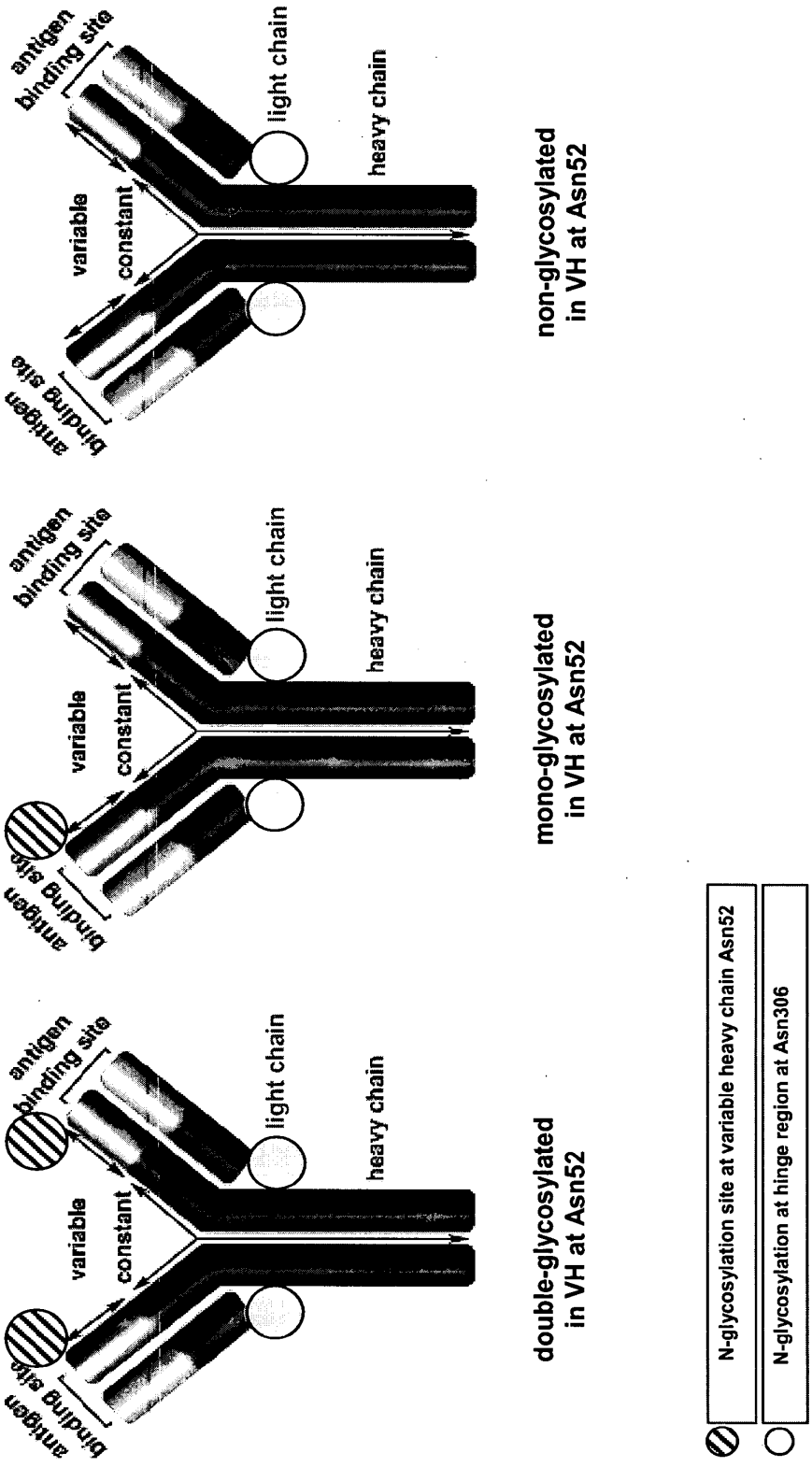

antigen binding site
light chain
heavy chain
variable
constant
antigen binding site
non-glycosylated in VH at Asn52
antigen binding site
light chain
heavy chain
variable
constant
antigen binding site
mono-glycosylated in VH at Asn52
antigen binding site
light chain
heavy chain
variable
constant
antigen binding site
double-glycosylated in VH at Asn52
N-glycosylation site at variable heavy chain Asn52
N-glycosylation at hinge region at Asn306

Figure 14

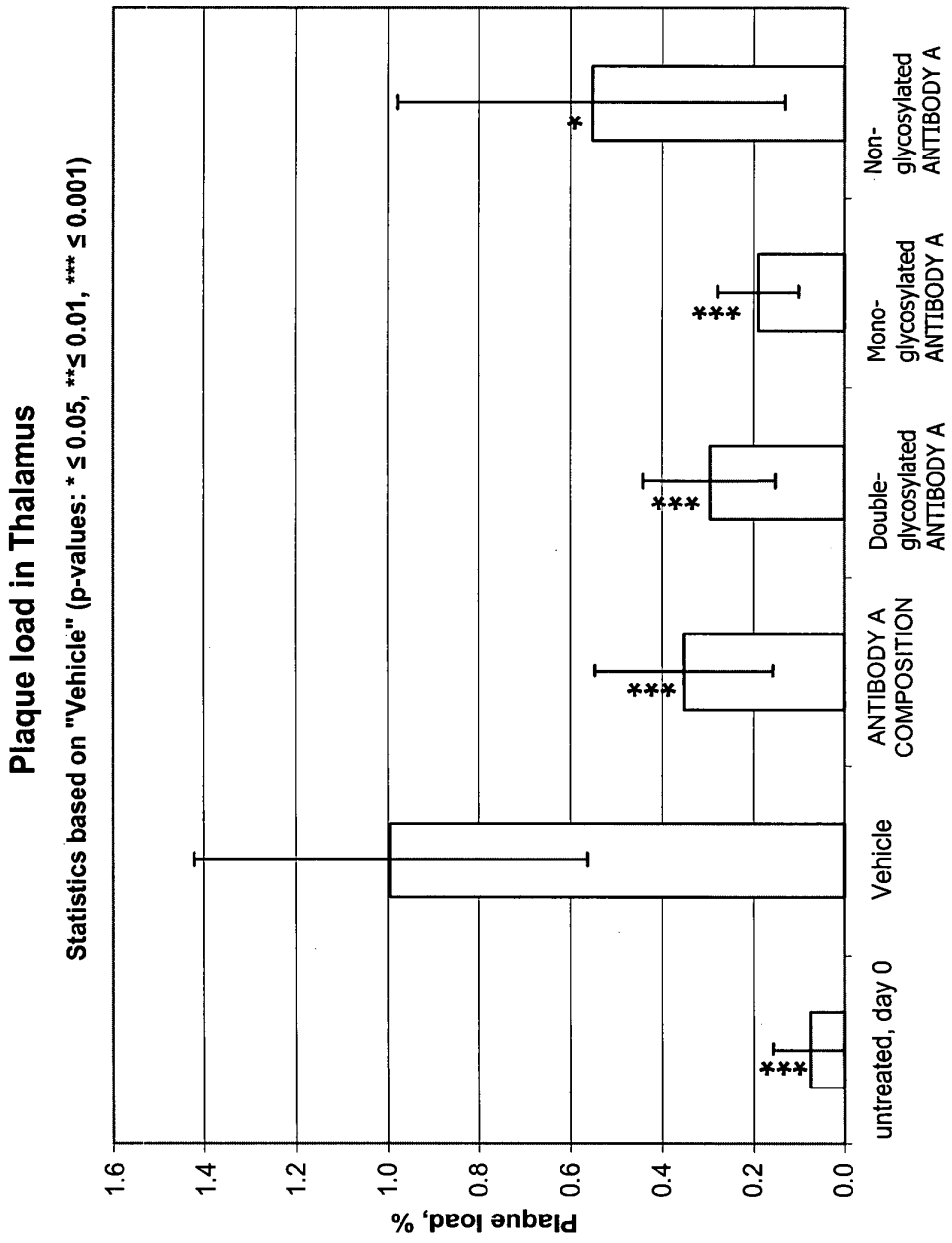

Plaque load in Thalamus
Statistics based on "Vehicle" (p-values: * ≤ 0.05, ** ≤ 0.01, *** ≤ 0.001)
Plaque load, %
1.6
1.4
1.2
1.0
0.8
0.6
0.4
0.2
0.0
***
***
***
***
*
untreated, day 0
Vehicle
ANTIBODY A COMPOSITION
Double-glycosylated ANTIBODY A
Mono-glycosylated ANTIBODY A
Non-glycosylated ANTIBODY A

Figure 15A

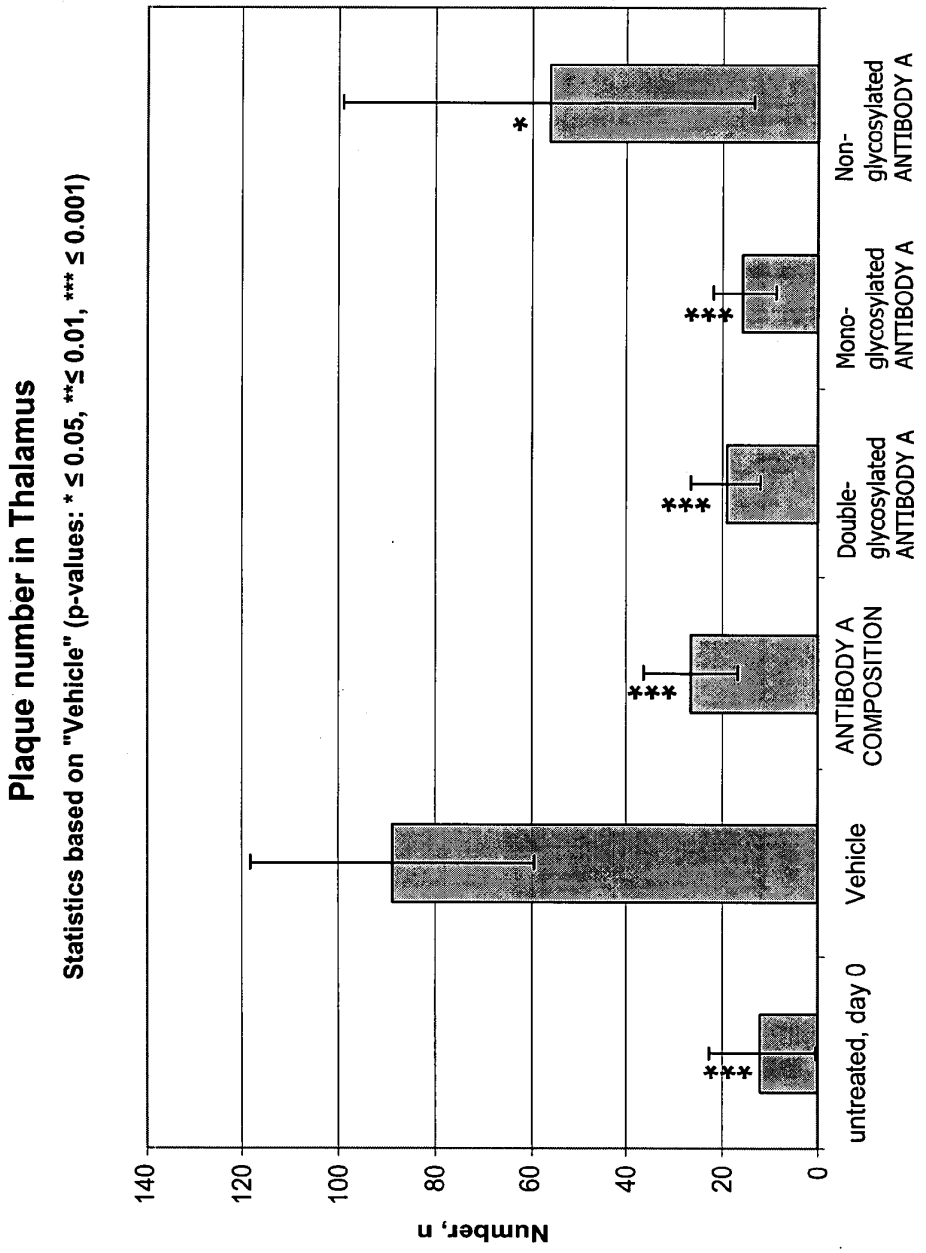

Plaque number in Thalamus
Statistics based on "Vehicle" (p-values: * ≤ 0.05, ** ≤ 0.01, *** ≤ 0.001)
Number, n
0
20
40
60
80
100
120
140
***
Vehicle
***
***
***
*
untreated, day 0
ANTIBODY A COMPOSITION
Double-glycosylated ANTIBODY A
Mono-glycosylated ANTIBODY A
Non-glycosylated ANTIBODY A

Figure 15B

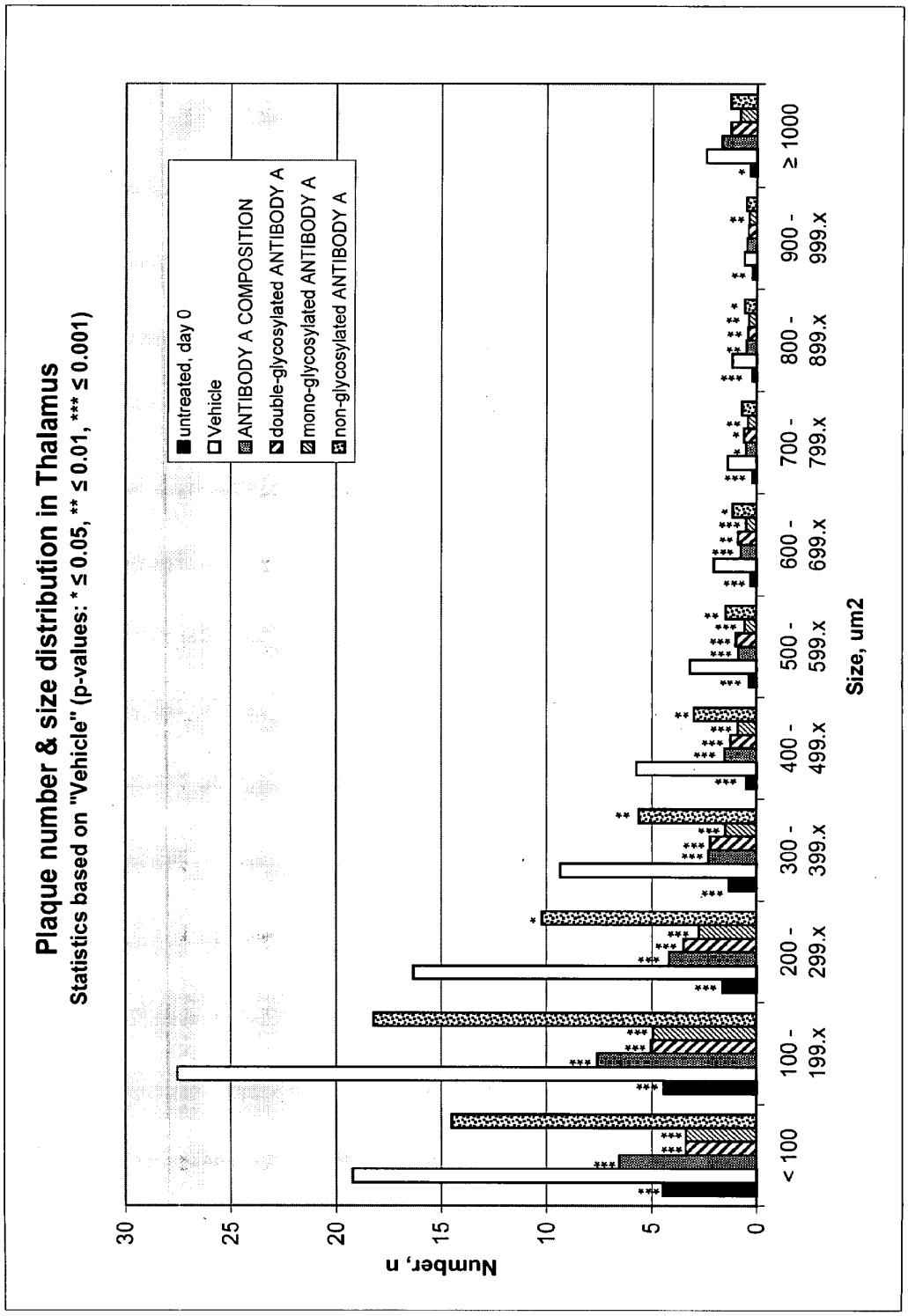

Plaque number & size distribution in Thalamus
Statistics based on "Vehicle" (p-values: * ≤ 0.05, ** ≤ 0.01, *** ≤ 0.001)
untreated, day 0
Vehicle
ANTIBODY A COMPOSITION
double-glycosylated ANTIBODY A
mono-glycosylated ANTIBODY A
non-glycosylated ANTIBODY A
Number, n
0
5
10
15
20
25
30
< 100
100 - 199.x
200 - 299.x
300 - 399.x
400 - 499.x
500 - 599.x
600 - 699.x
700 - 799.x
800 - 899.x
900 - 999.x
≥ 1000
Size, um2

Figure 15C

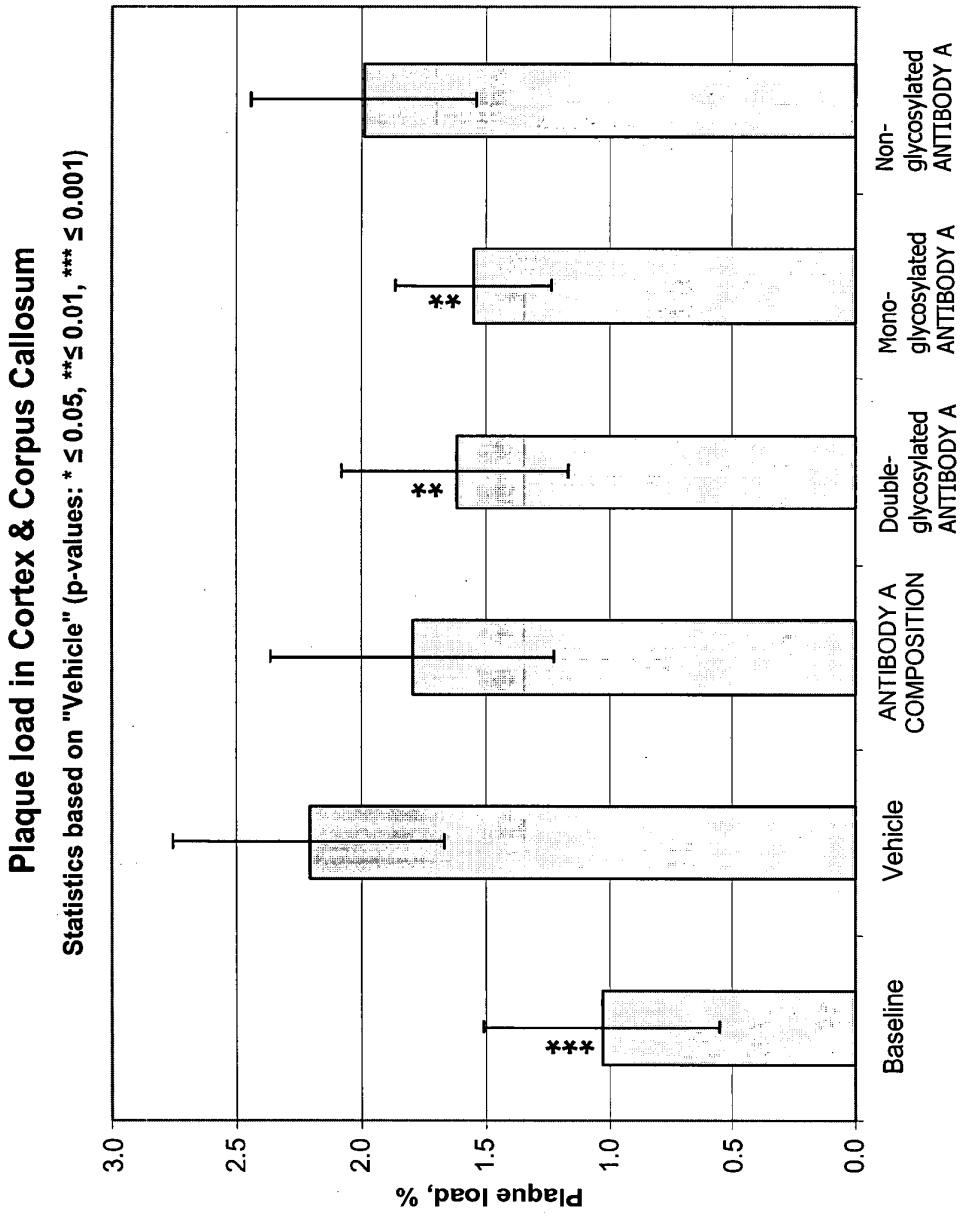

Plaque load in Cortex & Corpus Callosum
Statistics based on "Vehicle" (p-values: * ≤ 0.05, **≤ 0.01, *** ≤ 0.001)
Plaque load, %
3.0
2.5
2.0
1.5
1.0
0.5
0.0
***
**
**
Baseline
Vehicle
ANTIBODY A COMPOSITION
Double-glycosylated ANTIBODY A
Mono-glycosylated ANTIBODY A
Non-glycosylated ANTIBODY A

Figure 16A

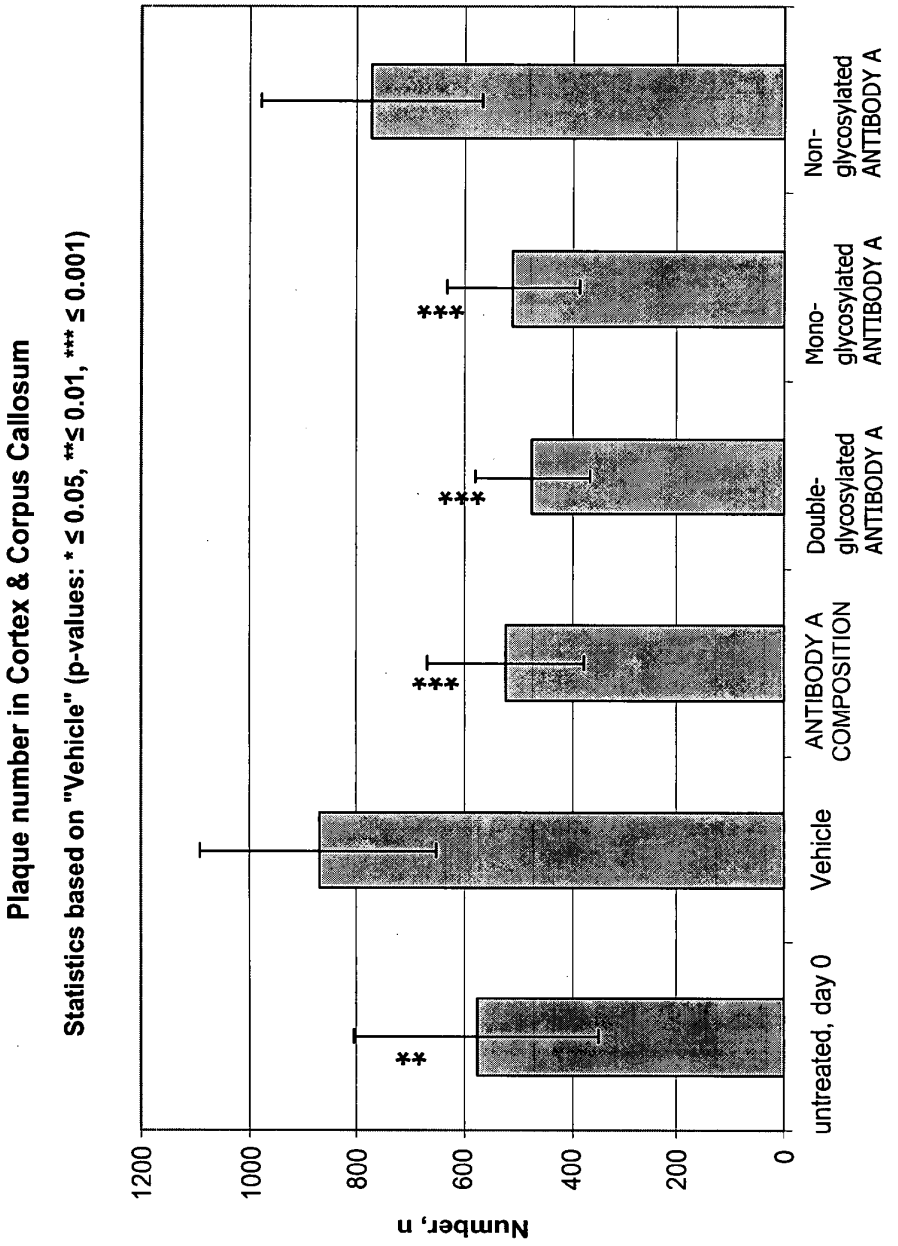

Plaque number in Cortex & Corpus Callosum
Statistics based on "Vehicle" (p-values: * ≤ 0.05, ** ≤ 0.01, *** ≤ 0.001)
Number, n
1200
1000
800
600
400
200
0
**
***
***
***
untreated, day 0
Vehicle
ANTIBODY A COMPOSITION
Double-glycosylated ANTIBODY A
Mono-glycosylated ANTIBODY A
Non-glycosylated ANTIBODY A

Figure 16B

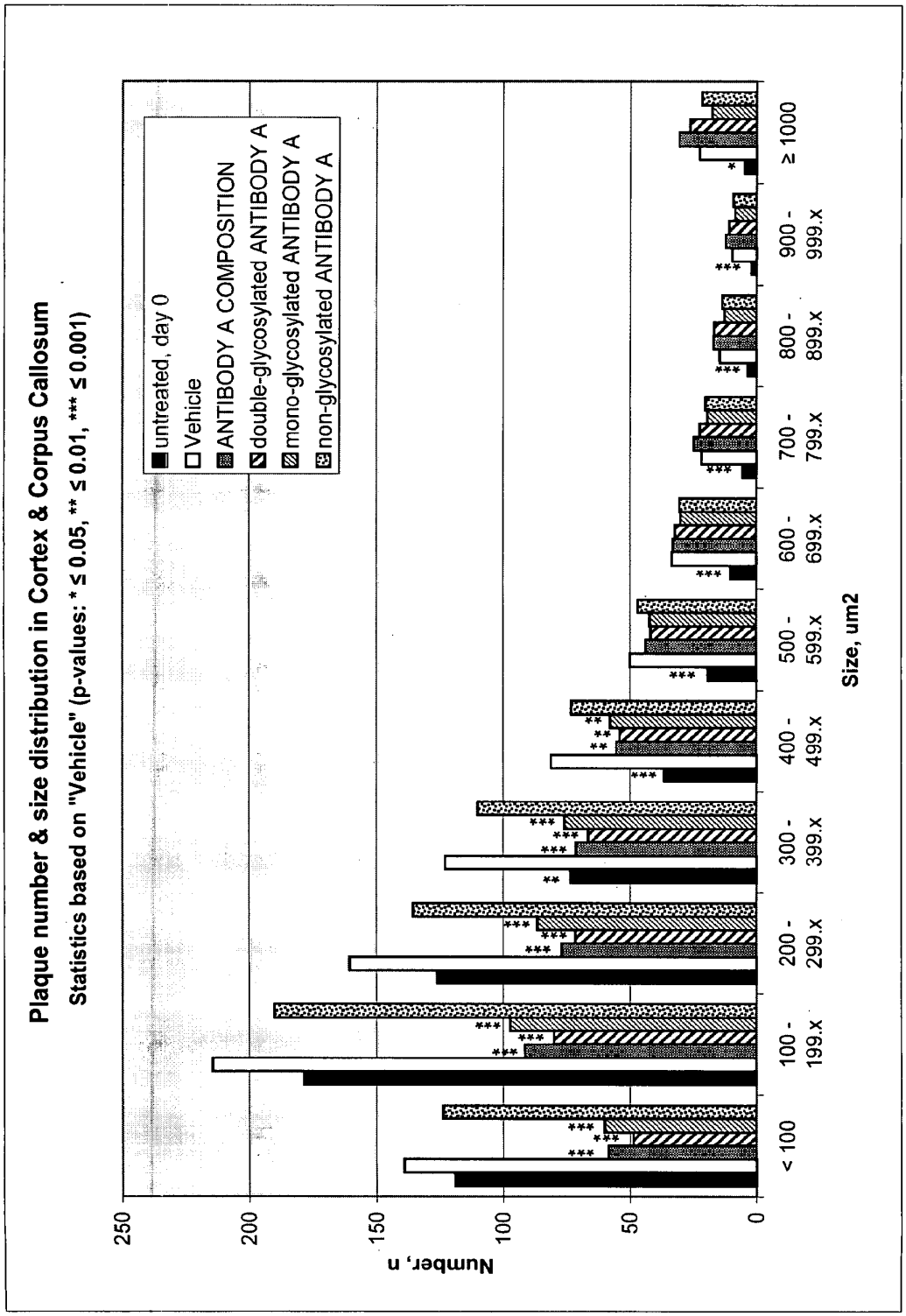

Plaque number & size distribution in Cortex & Corpus Callosum
Statistics based on "Vehicle" (p-values: * ≤ 0.05, ** ≤ 0.01, *** ≤ 0.001)
untreated, day 0
Vehicle
ANTIBODY A COMPOSITION
double-glycosylated ANTIBODY A
mono-glycosylated ANTIBODY A
non-glycosylated ANTIBODY A
Number, n
0
50
100
150
200
250
< 100
100 - 199.x
200 - 299.x
300 - 399.x
400 - 499.x
500 - 599.x
600 - 699.x
700 - 799.x
800 - 899.x
900 - 999.x
≥ 1000
Size, um2

Figure 16C

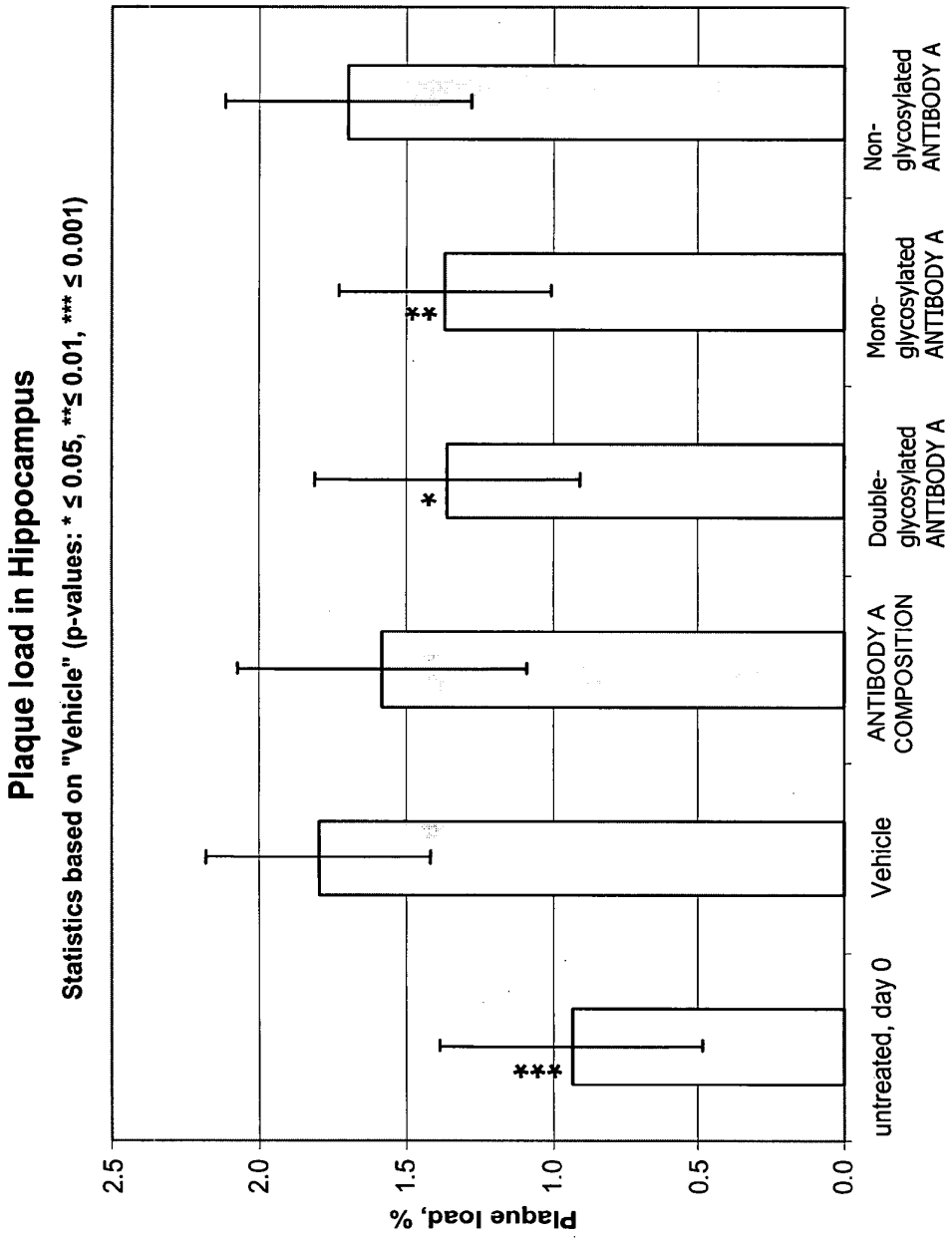

Plaque load in Hippocampus
Statistics based on "Vehicle" (p-values: * ≤ 0.05, ** ≤ 0.01, *** ≤ 0.001)
Plaque load, %
2.5
2.0
1.5
1.0
0.5
0.0
***
**
*
untreated, day 0
Vehicle
ANTIBODY A COMPOSITION
Double-glycosylated ANTIBODY A
Mono-glycosylated ANTIBODY A
Non-glycosylated ANTIBODY A

Figure 17A

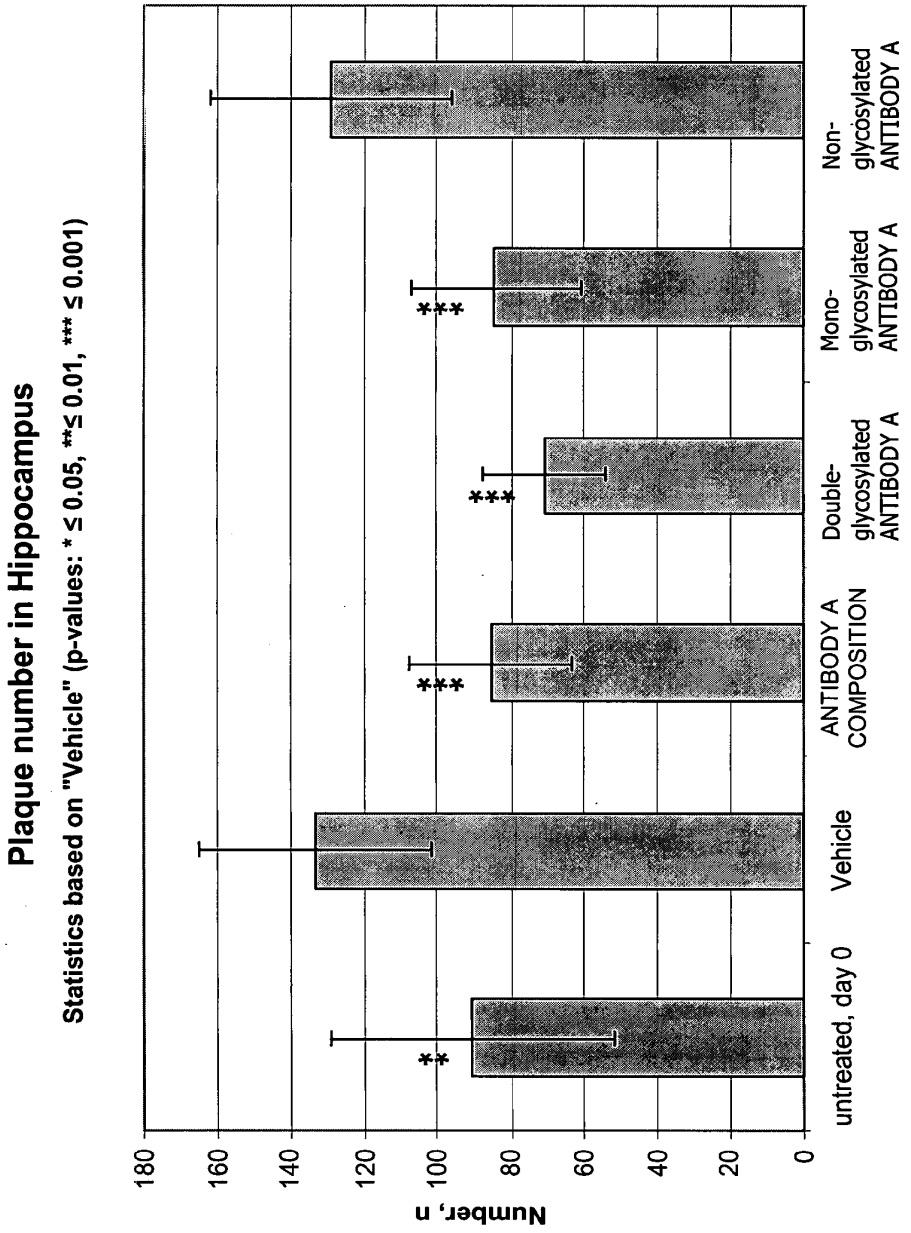

Plaque number in Hippocampus
Statistics based on "Vehicle" (p-values: * ≤ 0.05, **≤ 0.01, *** ≤ 0.001)
Number, n
0
20
40
60
80
100
120
140
160
180
**
***
***
***
untreated, day 0
Vehicle
ANTIBODY A COMPOSITION
Double-glycosylated ANTIBODY A
Mono-glycosylated ANTIBODY A
Non-glycosylated ANTIBODY A

Figure 17B

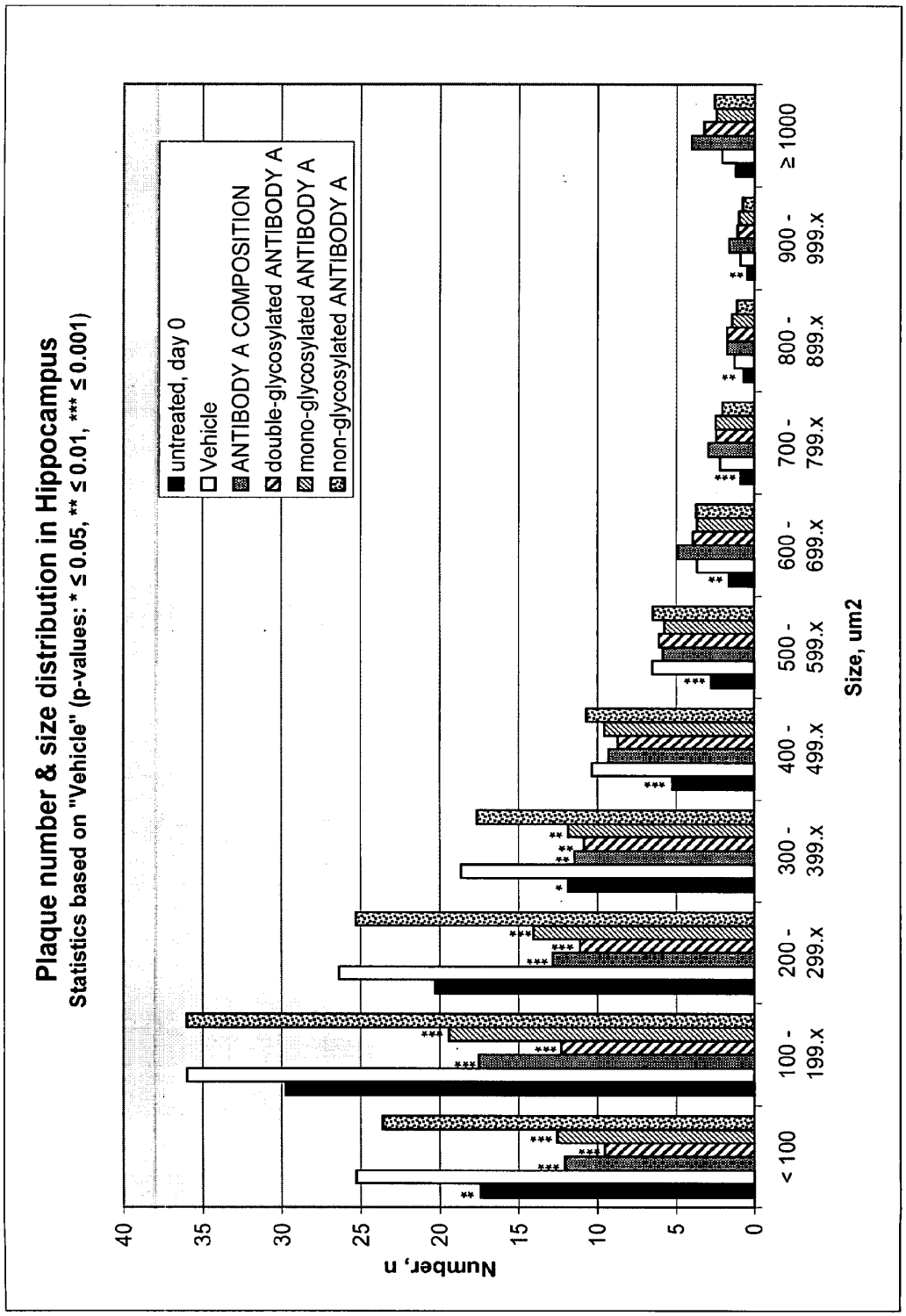

Plaque number & size distribution in Hippocampus
Statistics based on "Vehicle" (p-values: * ≤ 0.05, ** ≤ 0.01, *** ≤ 0.001)
untreated, day 0
Vehicle
ANTIBODY A COMPOSITION
double-glycosylated ANTIBODY A
mono-glycosylated ANTIBODY A
non-glycosylated ANTIBODY A
Number, n
0
5
10
15
20
25
30
35
40
< 100
100 - 199.x
200 - 299.x
300 - 399.x
400 - 499.x
500 - 599.x
600 - 699.x
700 - 799.x
800 - 899.x
900 - 999.x
≥ 1000
Size, um2

Figure 17C

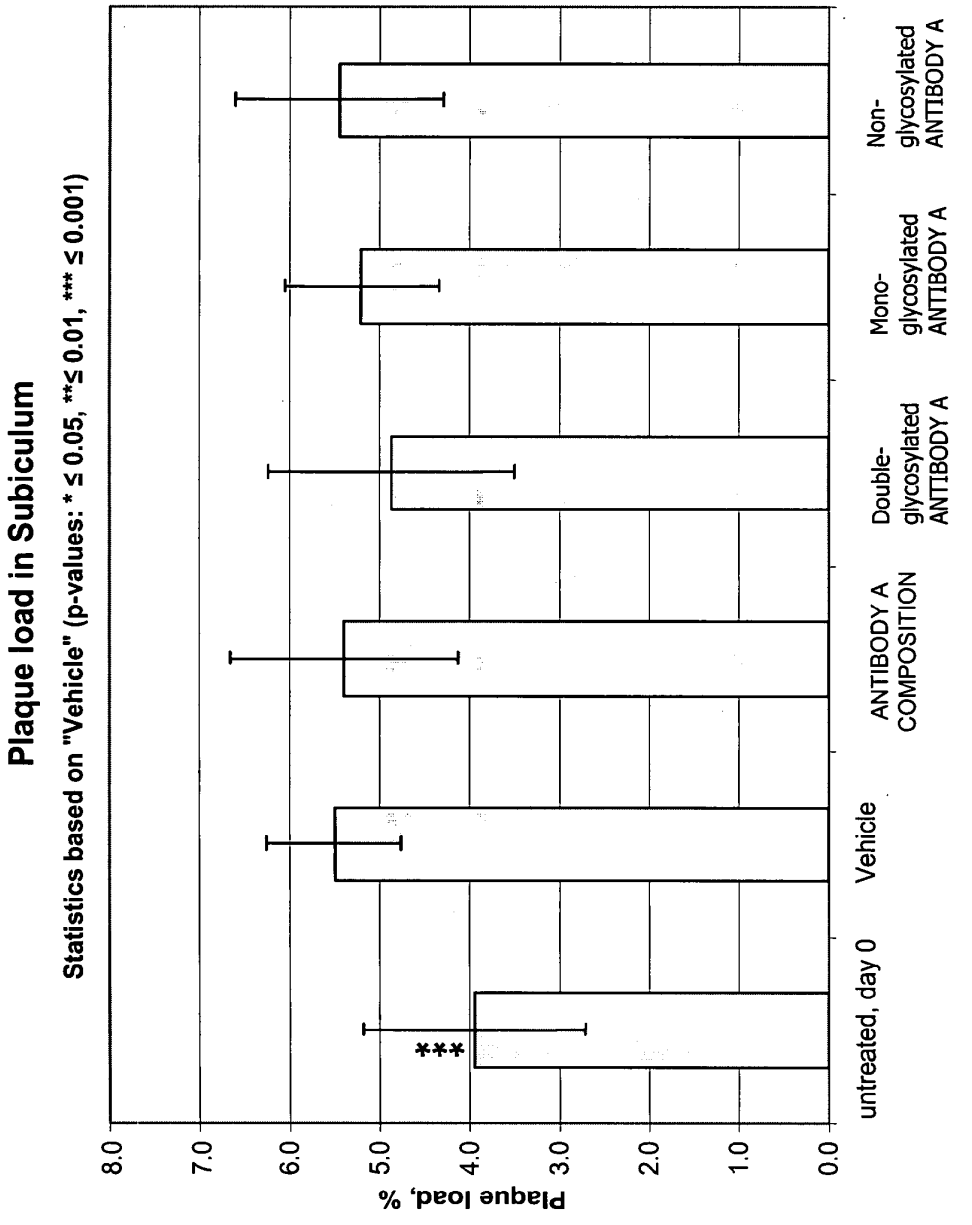

Plaque load in Subiculum
Statistics based on "Vehicle" (p-values: * ≤ 0.05, ** ≤ 0.01, *** ≤ 0.001)
Plaque load, %
8.0
7.0
6.0
5.0
4.0
3.0
2.0
1.0
0.0
***
untreated, day 0
Vehicle
ANTIBODY A COMPOSITION
Double-glycosylated ANTIBODY A
Mono-glycosylated ANTIBODY A
Non-glycosylated ANTIBODY A

Figure 18A

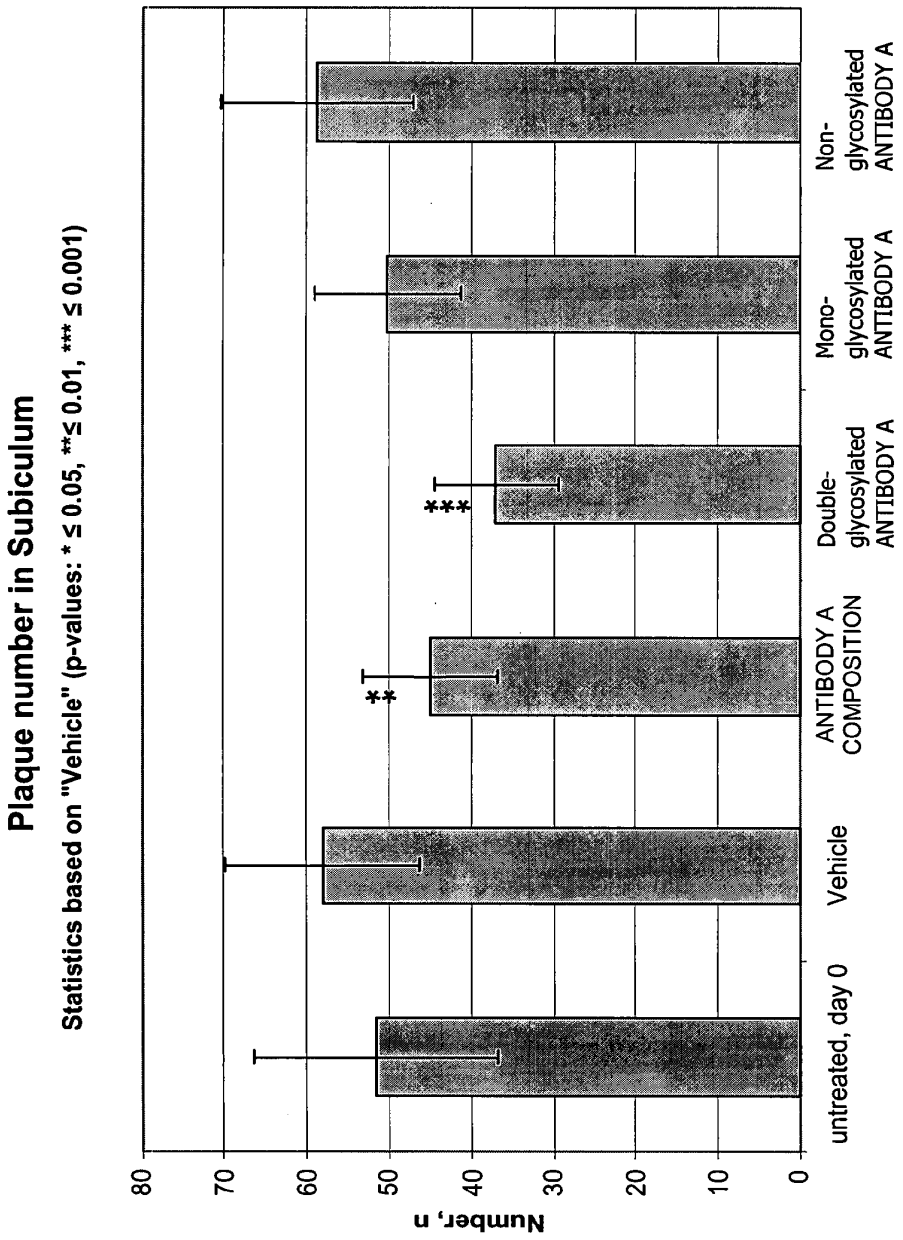

Plaque number in Subiculum
Statistics based on "Vehicle" (p-values: * ≤ 0.05, **≤ 0.01, *** ≤ 0.001)
Number, n
0
10
20
30
40
50
60
70
80
**
***
untreated, day 0
Vehicle
ANTIBODY A COMPOSITION
Double-glycosylated ANTIBODY A
Mono-glycosylated ANTIBODY A
Non-glycosylated ANTIBODY A

Figure 18B

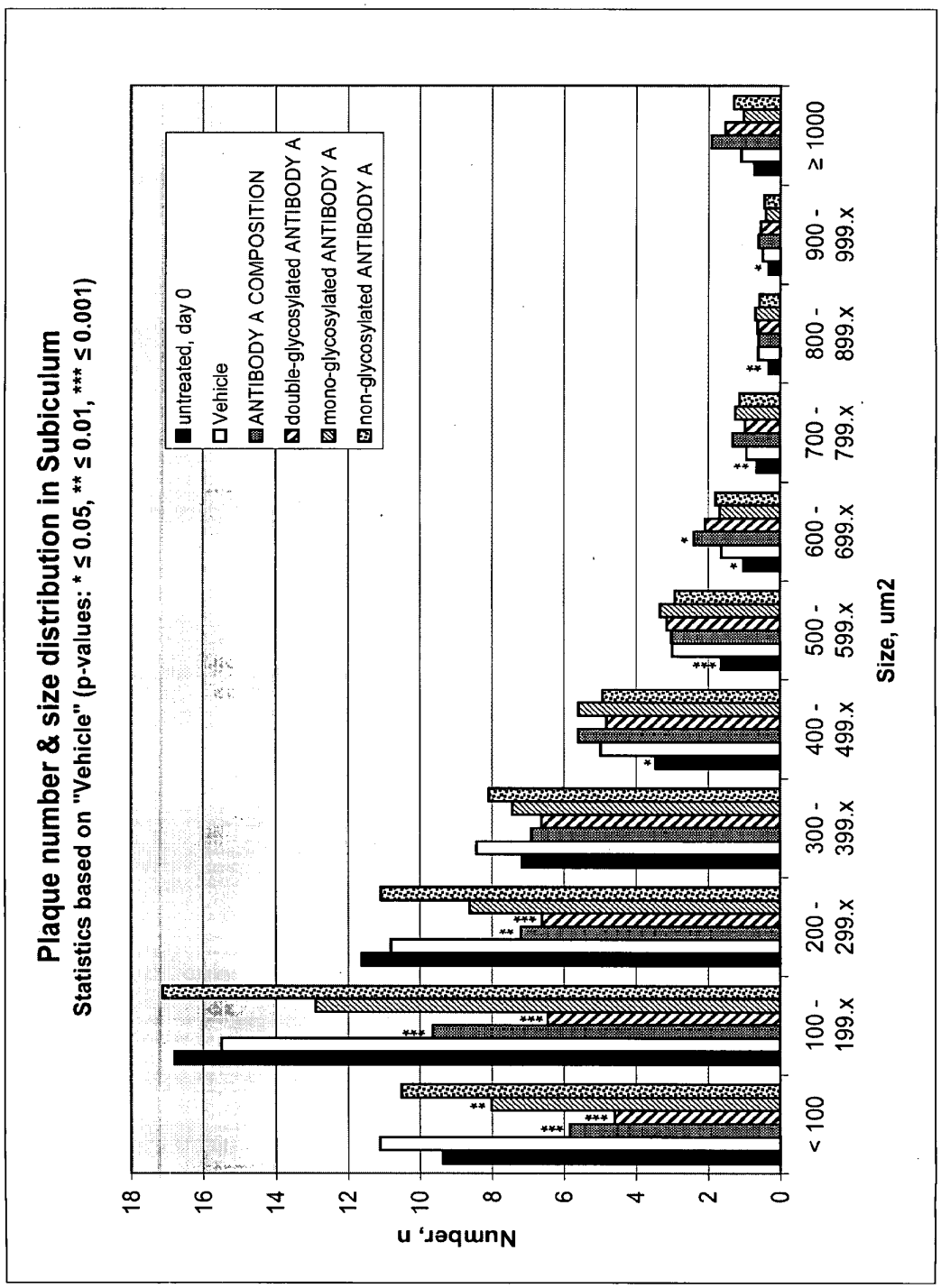

Plaque number & size distribution in Subiculum
Statistics based on "Vehicle" (p-values: * ≤ 0.05, ** ≤ 0.01, *** ≤ 0.001)
untreated, day 0
Vehicle
ANTIBODY A COMPOSITION
double-glycosylated ANTIBODY A
mono-glycosylated ANTIBODY A
non-glycosylated ANTIBODY A
Number, n
0
2
4
6
8
10
12
14
16
18
< 100
100 - 199.x
200 - 299.x
300 - 399.x
400 - 499.x
500 - 599.x
600 - 699.x
700 - 799.x
800 - 899.x
900 - 999.x
≥ 1000
Size, um2

Figure 18C

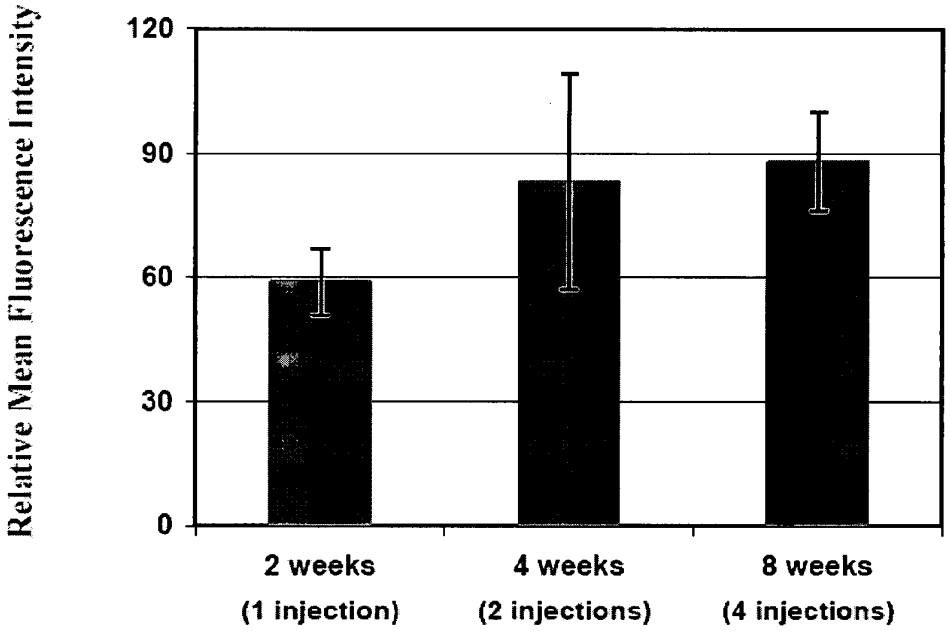

Relative Mean Fluorescence Intensity
120
90
60
30
0
2 weeks
(1 injection)
4 weeks
(2 injections)
8 weeks
(4 injections)

Figure 19

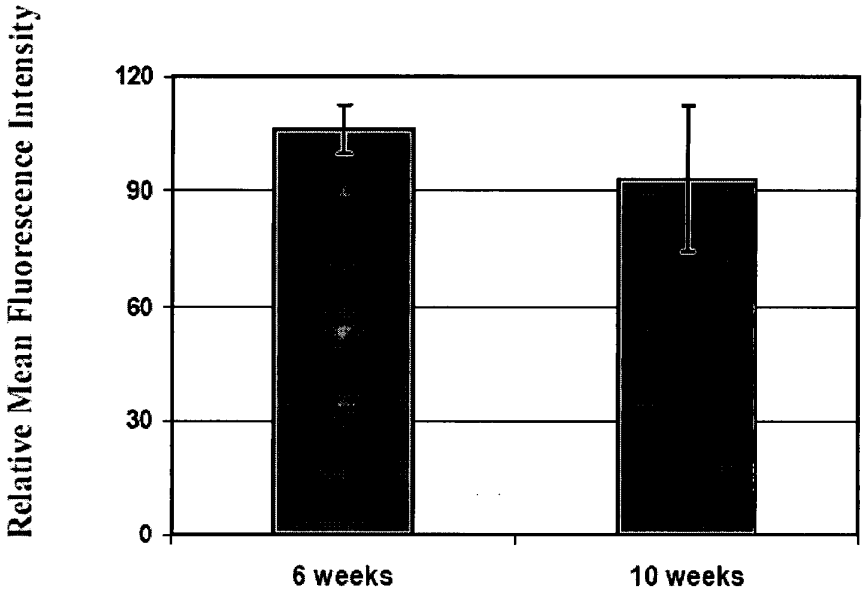

Relative Mean Fluorescence Intensity
120
90
60
30
0
6 weeks
10 weeks

Figure 20

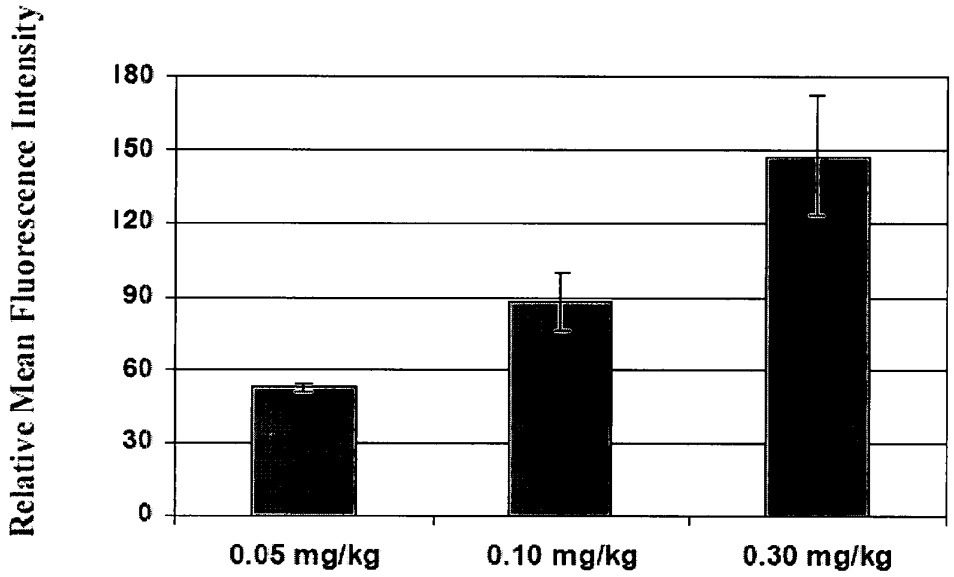

Relative Mean Fluorescence Intensity
180
150
120
90
60
30
0
0.05 mg/kg
0.10 mg/kg
0.30 mg/kg

Figure 21

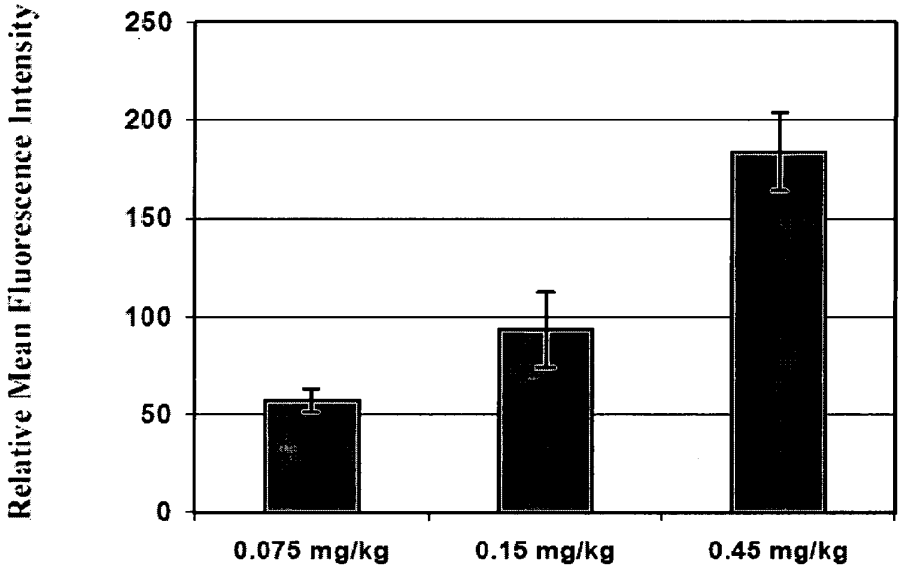

Relative Mean Fluorescence Intensity
250
200
150
100
50
0
0.075 mg/kg
0.15 mg/kg
0.45 mg/kg

Figure 22

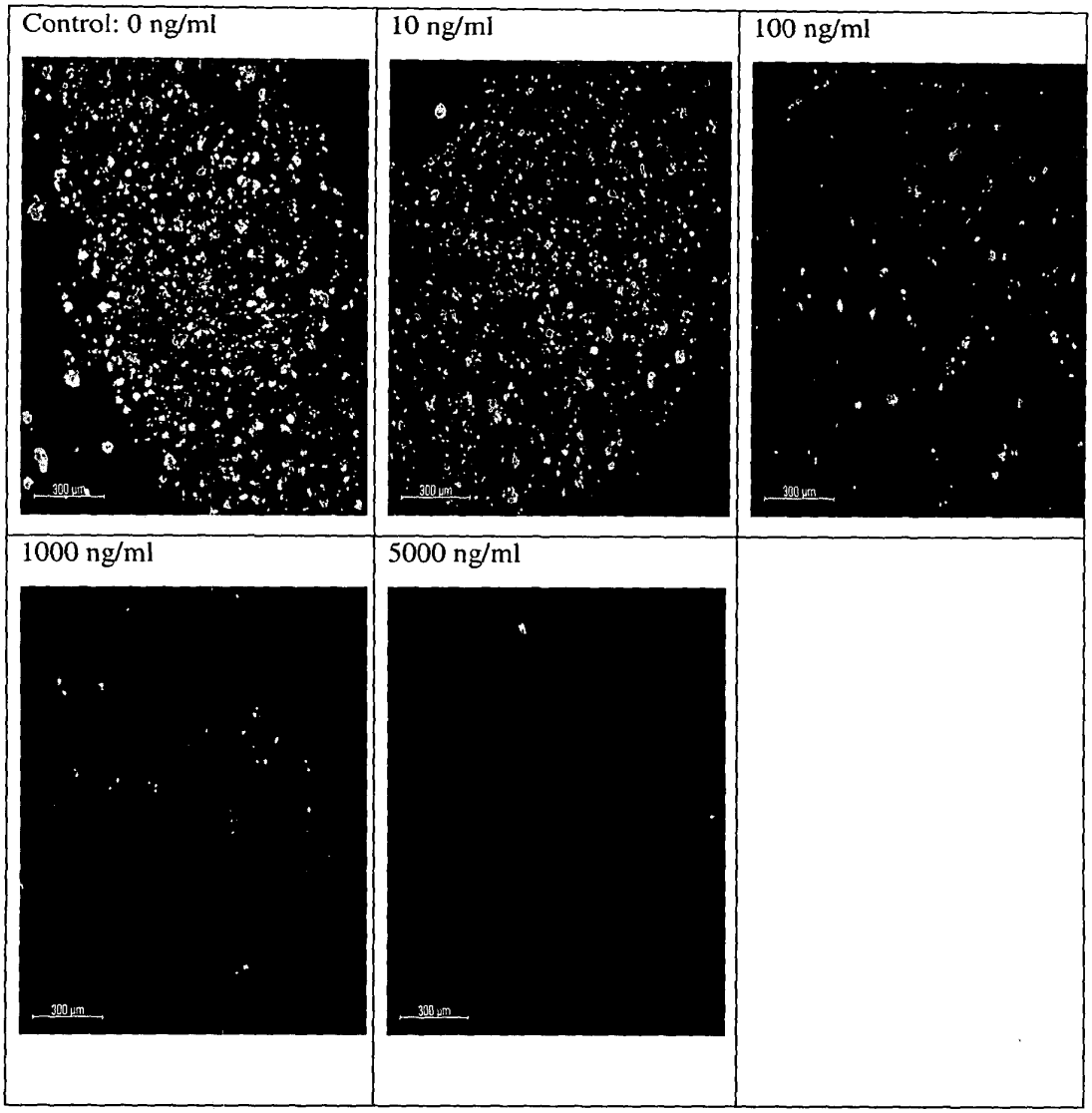



**Figure 23**

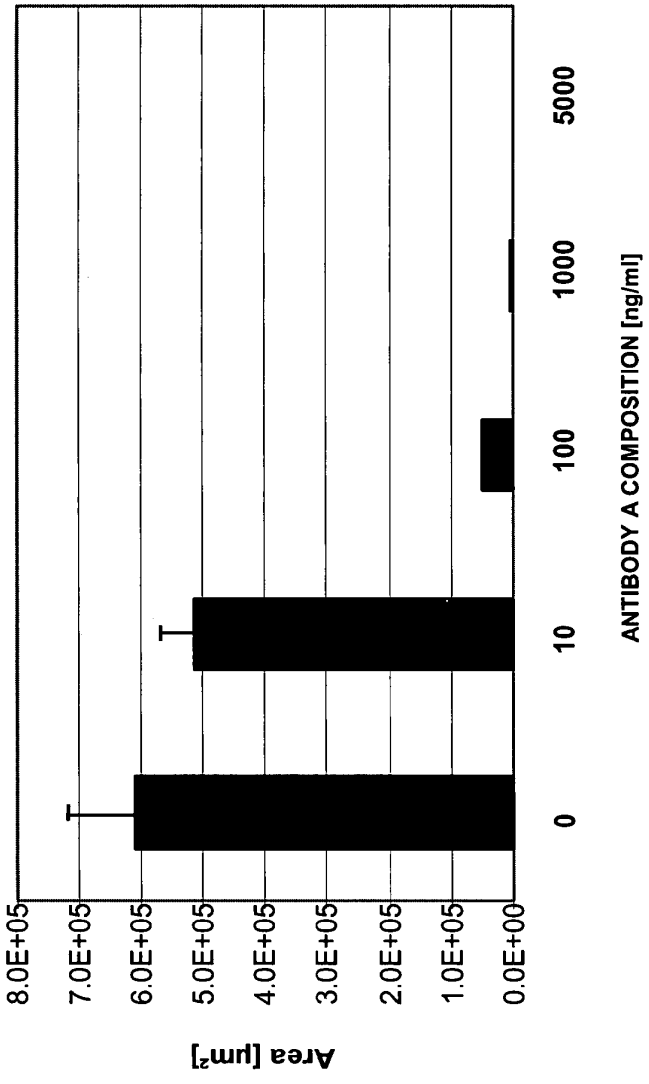



Figure 24A

Fujirebio Diagnostics, Inc. v. Quanterix Corp.
EX-1045
5676

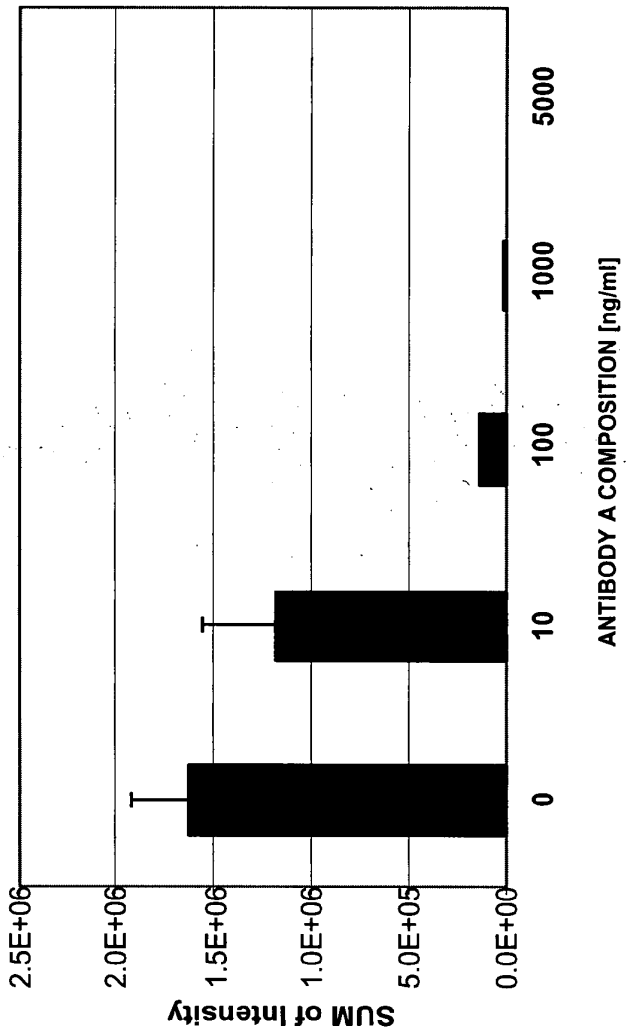

SUM of Intensity
2.5E+06
2.0E+06
1.5E+06
1.0E+06
5.0E+05
0.0E+00
0
10
100
1000
5000
ANTIBODY A COMPOSITION [ng/ml]

Figure 24B

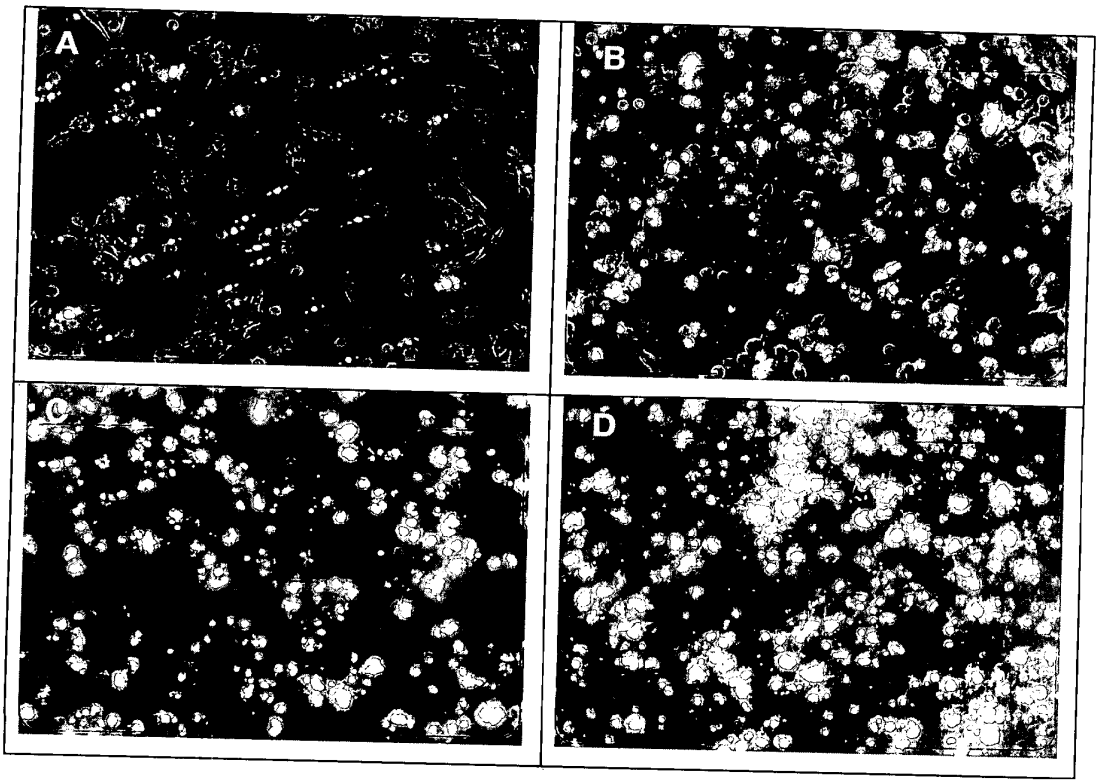



Figure 25

Fujirebio Diagnostics, Inc. v. Quanterix Corp.
EX-1045
5678

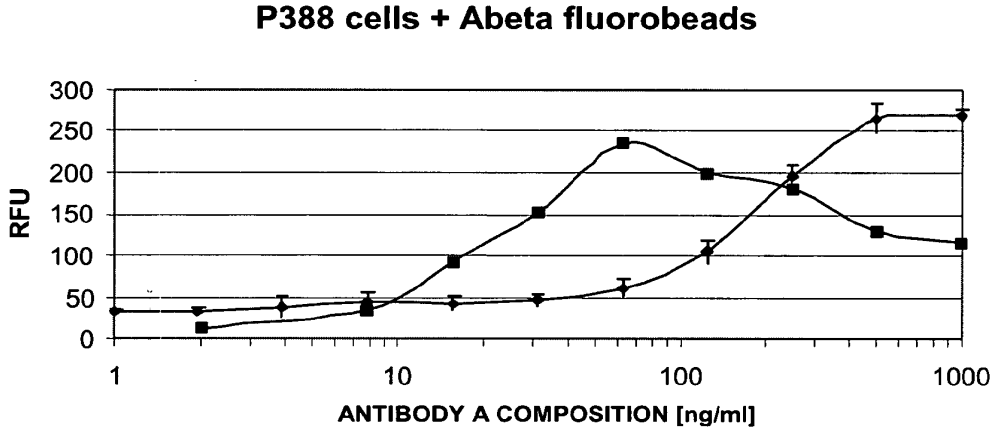
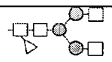
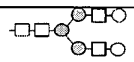
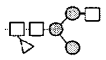
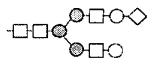
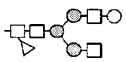
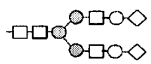
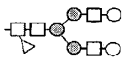
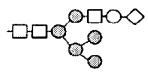
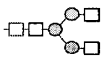
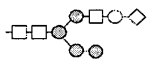
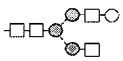
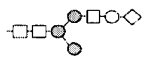
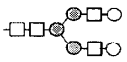
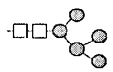

P388 cells + Abeta fluorobeads
RFU
300
250
200
150
100
50
0
1
10
100
1000
ANTIBODY A COMPOSITION [ng/ml]

**Figure 26**

| Name | Structure[1)] | Name[2)] | Structure[1)] |
|---|---|---|---|
| Asn 306_G0 |  | Asn 52_G2_0NANA-F |  |
| Asn 306_G0-GlcNac |  | Asn 52_G2_1NANA-F |  |
| Asn 306_G1 |  | Asn 52_G2_2NANA-F |  |
| Asn 306_G2 |  | Asn 52_hyb_Man5_1NANA |  |
| Asn 306_G0-F |  | Asn 52_hyb_Man4_1NANA |  |
| Asn 306_G1-F |  | Asn 52_hyb_Man3_1NANA |  |
| Asn 306_G2-F |  | Asn 52_Man5 |  |
| Asn 306_Man5 |  | | |

[1)] Fucose △, Mannose ●, N-Acetylglucosamine □, Galactose○, N-Acetylneuraminic acid ◇
[2)] "hyb" denotes hybrid structures

**Figure 27**

SEQUENCE LISTING

<110> F. Hoffmann-La Roche AG

<120> Antibody glycosylation in the variable region

<130> K1314 PCT S3

<150> EP 05 02 7090.9
<151> 2005-12-12

<160> 32

<170> PatentIn version 3.3

<210> 1
<211> 378
<212> DNA
<213> artificial sequence

<220>
<223> VH-region of ANTIBODY A

<400> 1
caggtggaat tggtggaaag cggcggcggc ctggtgcaac cgggcggcag cctgcgtctg 60

agctgcgcgg cctccggatt tacctttagc agctatgcga tgagctgggt gcgccaagcc 120

cctgggaagg gtctcgagtg ggtgagcgct attaatgctt ctggtactcg tacttattat 180

gctgattctg ttaagggtcg ttttaccatt tcacgtgata attcgaaaaa caccctgtat 240

ctgcaaatga acagcctgcg tgcggaagat acggccgtgt attattgcgc gcgtggtaag 300

ggtaatactc ataagcctta tggttatgtt cgttattttg atgtttgggg ccaaggcacc 360

ctggtgacgg ttagctca 378

<210> 2
<211> 126
<212> PRT
<213> artificial sequence

<220>
<223> VH-region of ANTIBODY A

<400> 2

Gln Val Glu Leu Val Glu Ser Gly Gly Gly Leu Val Gln Pro Gly Gly
1 5 10 15

Ser Leu Arg Leu Ser Cys Ala Ala Ser Gly Phe Thr Phe Ser Ser Tyr
20 25 30

Ala Met Ser Trp Val Arg Gln Ala Pro Gly Lys Gly Leu Glu Trp Val
35 40 45

```
Ser Ala Ile Asn Ala Ser Gly Thr Arg Thr Tyr Tyr Ala Asp Ser Val
    50                  55                  60

Lys Gly Arg Phe Thr Ile Ser Arg Asp Asn Ser Lys Asn Thr Leu Tyr
65                  70                  75                  80

Leu Gln Met Asn Ser Leu Arg Ala Glu Asp Thr Ala Val Tyr Tyr Cys
                85                  90                  95

Ala Arg Gly Lys Gly Asn Thr His Lys Pro Tyr Gly Tyr Val Arg Tyr
            100                 105                 110

Phe Asp Val Trp Gly Gln Gly Thr Leu Val Thr Val Ser Ser
        115                 120                 125
```

<210> 3
<211> 42
<212> PRT
<213> artificial sequence

<220>
<223> A-beta

<400> 3

```
Asp Ala Glu Phe Arg His Asp Ser Gly Tyr Glu Val His His Gln Lys
1               5                   10                  15

Leu Val Phe Phe Ala Glu Asp Val Gly Ser Asn Lys Gly Ala Ile Ile
            20                  25                  30

Gly Leu Met Val Gly Gly Val Val Ile Ala
        35                  40
```

<210> 4
<211> 52
<212> PRT
<213> artificial sequence

<220>
<223> A-beta comprising peptide sequence

<400> 4

```
Ile Ser Glu Val Lys Met Asp Ala Glu Phe Arg His Asp Ser Gly Tyr
1               5                   10                  15

Glu Val His His Gln Lys Leu Val Phe Phe Ala Glu Asp Val Gly Ser
            20                  25                  30
```

Asn Lys Gly Ala Ile Ile Gly Leu Met Val Gly Gly Val Val Ile Ala
35 40 45

Thr Val Ile Val
50

<210> 5
<211> 1391
<212> DNA
<213> artificial sequence

<220>
<223> heavy chain with Fc-region of ANTIBODY A

<400> 5
caggtggaat tggtggaaag cggcggcggc ctggtgcaac cgggcggcag cctgcgtctg 60

agctgcgcgg cctccggatt tacctttagc agctatgcga tgagctgggt gcgccaagcc 120

cctgggaagg gtctcgagtg ggtgagcgct attaatgctt ctggtactcg tacttattat 180

gctgattctg ttaagggtcg ttttaccatt tcacgtgata attcgaaaaa caccctgtat 240

ctgcaaatga acagcctgcg tgcggaagat acggccgtgt attattgcgc gcgtggtaag 300

ggtaatactc ataagcctta tggttatgtt cgttattttg atgtttgggg ccaaggcacc 360

ctggtgacgg ttagctcagc ctccaccaag ggtccatcgg tcttcccccc ggcaccctcc 420

tccaagagca cctctggggg cacagcggcc ctgggctgcc tggtcaagga ctacttcccc 480

gaaccggtga cggtgtcgtg gaactcaggc gccctgacca gcggcgtgca caccttcccg 540

gctgtcctac agtcctcagg actctactcc ctcagcagcg tggtgaccgt gccctccagc 600

agcttgggca cccagaccta catctgcaac gtgaatcaca agcccagcaa caccaaggtg 660

gacaagaaag ttgagcccag atatcgtgcg atatcgtgca atcttgtgac aaaactcaca 720

catgcccacc gtgcccagca cctgaactcc tgggggggacc gtcagtcttc ctcttccccc 780

caaaacccaa ggacaccctc atgatctccc ggaccctga ggtcacatgc gtggtggtgg 840

acgtgagcca cgaagaccct gaggtcaagt tcaactggta cgtggacggc gtggaggtgc 900

ataatgccaa gacaaagccg cgggaggagc agtacaacag cacgtaccgg gtggtcagcg 960

tcctcaccgt cctgcaccag gactggctga atggcaagga gtacaagtgc aaggtctcca 1020

acaaagccct cccagccccc atcgagaaaa ccatctccaa agccaaaggg cagccccgag 1080

aaccacaggt gtacaccctg cccccatccc gggatgagct gaccaagaac caggtcagcc 1140

tgacctgcct ggtcaaaggc ttctatccca gcgacatcgc cgtggagtgg gagagcaatg 1200

ggcagccgga gaacaactac aagaccacgc ctcccgtgct ggactccgac ggctccttct 1260

tcctctacag caagctcacc gtggacaaga gcaggtggca gcaggggaac gtcttctcat 1320

gctccgtgat gcatgaggct ctgcacaacc actacacgca gaagagcctc tccctgtctc 1380

cgggtaaatg a 1391

<210> 6
<211> 456
<212> PRT
<213> artificial sequence

<220>
<223> heavy chain with Fc-region of ANTIBODY A

<400> 6

Gln Val Glu Leu Val Glu Ser Gly Gly Gly Leu Val Gln Pro Gly Gly
1 5 10 15

Ser Leu Arg Leu Ser Cys Ala Ala Ser Gly Phe Thr Phe Ser Ser Tyr
20 25 30

Ala Met Ser Trp Val Arg Gln Ala Pro Gly Lys Gly Leu Glu Trp Val
35 40 45

Ser Ala Ile Asn Ala Ser Gly Thr Arg Thr Tyr Tyr Ala Asp Ser Val
50 55 60

Lys Gly Arg Phe Thr Ile Ser Arg Asp Asn Ser Lys Asn Thr Leu Tyr
65 70 75 80

Leu Gln Met Asn Ser Leu Arg Ala Glu Asp Thr Ala Val Tyr Tyr Cys
85 90 95

Ala Arg Gly Lys Gly Asn Thr His Lys Pro Tyr Gly Tyr Val Arg Tyr
100 105 110

Phe Asp Val Trp Gly Gln Gly Thr Leu Val Thr Val Ser Ser Ala Ser
115 120 125

Thr Lys Gly Pro Ser Val Phe Pro Leu Ala Pro Ser Ser Lys Ser Thr
130 135 140

Ser Gly Gly Thr Ala Ala Leu Gly Cys Leu Val Lys Asp Tyr Phe Pro
145 150 155 160

Glu Pro Val Thr Val Ser Trp Asn Ser Gly Ala Leu Thr Ser Gly Val
165 170 175

```
His Thr Phe Pro Ala Val Leu Gln Ser Ser Gly Leu Tyr Ser Leu Ser
            180                 185                 190

Ser Val Val Thr Val Pro Ser Ser Ser Leu Gly Thr Gln Thr Tyr Ile
        195                 200                 205

Cys Asn Val Asn His Lys Pro Ser Asn Thr Lys Val Asp Lys Lys Val
    210                 215                 220

Glu Pro Lys Ser Cys Asp Lys Thr His Thr Cys Pro Pro Cys Pro Ala
225                 230                 235                 240

Pro Glu Leu Leu Gly Gly Pro Ser Val Phe Leu Phe Pro Pro Lys Pro
                245                 250                 255

Lys Asp Thr Leu Met Ile Ser Arg Thr Pro Glu Val Thr Cys Val Val
            260                 265                 270

Val Asp Val Ser His Glu Asp Pro Glu Val Lys Phe Asn Trp Tyr Val
        275                 280                 285

Asp Gly Val Glu Val His Asn Ala Lys Thr Lys Pro Arg Glu Glu Gln
    290                 295                 300

Tyr Asn Ser Thr Tyr Arg Val Val Ser Val Leu Thr Val Leu His Gln
305                 310                 315                 320

Asp Trp Leu Asn Gly Lys Glu Tyr Lys Cys Lys Val Ser Asn Lys Ala
                325                 330                 335

Leu Pro Ala Pro Ile Glu Lys Thr Ile Ser Lys Ala Lys Gly Gln Pro
            340                 345                 350

Arg Glu Pro Gln Val Tyr Thr Leu Pro Pro Ser Arg Asp Glu Leu Thr
        355                 360                 365

Lys Asn Gln Val Ser Leu Thr Cys Leu Val Lys Gly Phe Tyr Pro Ser
    370                 375                 380

Asp Ile Ala Val Glu Trp Glu Ser Asn Gly Gln Pro Glu Asn Asn Tyr
385                 390                 395                 400

Lys Thr Thr Pro Pro Val Leu Asp Ser Asp Gly Ser Phe Phe Leu Tyr
                405                 410                 415
```

Ser Lys Leu Thr Val Asp Lys Ser Arg Trp Gln Gln Gly Asn Val Phe
420 425 430

Ser Cys Ser Val Met His Glu Ala Leu His Asn His Tyr Thr Gln Lys
435 440 445

Ser Leu Ser Leu Ser Pro Gly Lys
450 455

<210> 7
<211> 648
<212> DNA
<213> artificial sequence

<220>
<223> light chain of ANTIBODY A

<400> 7
gatatcgtgc tgacccagag cccggcgacc ctgagcctgt ctccgggcga acgtgcgacc 60

ctgagctgca gagcgagcca gagcgtgagc agcagctatc tggcgtggta ccagcagaaa 120

ccaggtcaag caccgcgtct attaatttat ggcgcgagca gccgtgcaac tggggtcccg 180

gcgcgtttta gcggctctgg atccggcacg gattttaccc tgaccattag cagcctggaa 240

cctgaagact ttgcgactta ttattgcctt cagatttata atatgcctat tacctttggc 300

cagggtacga aagttgaaat taaacgtacg gtggctgcac catctgtctt catcttcccg 360

ccatctgatg agcagttgaa atctggaact gcctctgttg tgtgcctgct gaataacttc 420

tatcccagag aggccaaagt acagtggaag gtggataacg ccctccaatc gggtaactcc 480

caggagagtg tcacagagca ggacagcaag gacagcacct acagcctcag cagcaccctg 540

acgctgagca aagcagacta cgagaaacac aaagtctacg cctgcgaagt cacccatcag 600

ggcctgagct cgcccgtcac aaagagcttc aacaggggag agtgttag 648

<210> 8
<211> 215
<212> PRT
<213> artificial sequence

<220>
<223> light chain of ANTIBODY A

<400> 8

Asp Ile Val Leu Thr Gln Ser Pro Ala Thr Leu Ser Leu Ser Pro Gly
1 5 10 15

```
Glu Arg Ala Thr Leu Ser Cys Arg Ala Ser Gln Ser Val Ser Ser Ser
            20                  25                  30

Tyr Leu Ala Trp Tyr Gln Gln Lys Pro Gly Gln Ala Pro Arg Leu Leu
        35                  40                  45

Ile Tyr Gly Ala Ser Ser Arg Ala Thr Gly Val Pro Ala Arg Phe Ser
    50                  55                  60

Gly Ser Gly Ser Gly Thr Asp Phe Thr Leu Thr Ile Ser Ser Leu Glu
65                  70                  75                  80

Pro Glu Asp Phe Ala Thr Tyr Tyr Cys Leu Gln Ile Tyr Asn Met Pro
                85                  90                  95

Ile Thr Phe Gly Gln Gly Thr Lys Val Glu Ile Lys Arg Thr Val Ala
            100                 105                 110

Ala Pro Ser Val Phe Ile Phe Pro Pro Ser Asp Glu Gln Leu Lys Ser
        115                 120                 125

Gly Thr Ala Ser Val Val Cys Leu Leu Asn Asn Phe Tyr Pro Arg Glu
    130                 135                 140

Ala Lys Val Gln Trp Lys Val Asp Asn Ala Leu Gln Ser Gly Asn Ser
145                 150                 155                 160

Gln Glu Ser Val Thr Glu Gln Asp Ser Lys Asp Ser Thr Tyr Ser Leu
                165                 170                 175

Ser Ser Thr Leu Thr Leu Ser Lys Ala Asp Tyr Glu Lys His Lys Val
            180                 185                 190

Tyr Ala Cys Glu Val Thr His Gln Gly Leu Ser Ser Pro Val Thr Lys
        195                 200                 205

Ser Phe Asn Arg Gly Glu Cys
    210                 215
```

<210> 9
<211> 30
<212> DNA
<213> artificial sequence

<220>
<223> CDR1 heavy chain

<400> 9
ggatttacct ttagcagcta tgcgatgagc 30

<210> 10
<211> 10
<212> PRT
<213> artificial sequence

<220>
<223> CDR1 heavy chain

<400> 10

Gly Phe Thr Phe Ser Ser Tyr Ala Met Ser
1 5 10

<210> 11
<211> 51
<212> DNA
<213> artificial sequence

<220>
<223> CDR2 heavy chain

<400> 11
gctattaatg cttctggtac tcgtacttat tatgctgatt ctgttaaggg t 51

<210> 12
<211> 17
<212> PRT
<213> artificial sequence

<220>
<223> CDR2 heavy chain

<400> 12

Ala Ile Asn Ala Ser Gly Thr Arg Thr Tyr Tyr Ala Asp Ser Val Lys
1 5 10 15

Gly

<210> 13
<211> 51
<212> DNA
<213> artificial sequence

<220>
<223> CDR3 heavy chain

<400> 13
ggtaagggta atactcataa gccttatggt tatgttcgtt attttgatgt t 51

<210> 14
<211> 17
<212> PRT
<213> artificial sequence

<220>
<223> CDR3 heavy chain

<400> 14

Gly Lys Gly Asn Thr His Lys Pro Tyr Gly Tyr Val Arg Tyr Phe Asp
1 5 10 15

Val

<210> 15
<211> 36
<212> DNA
<213> artificial sequence

<220>
<223> CDR1 light chain

<400> 15
agagcgagcc agagcgtgag cagcagctat ctggcg 36

<210> 16
<211> 12
<212> PRT
<213> artificial sequence

<220>
<223> CDR1 light chain

<400> 16

Arg Ala Ser Gln Ser Val Ser Ser Ser Tyr Leu Ala
1 5 10

<210> 17
<211> 21
<212> DNA
<213> artificial sequence

<220>
<223> CDR2 light chain

<400> 17
ggcgcgagca gccgtgcaac t 21

<210> 18
<211> 7
<212> PRT
<213> artificial sequence

<220>
<223> CDR2 light chain

<400> 18

Gly Ala Ser Ser Arg Ala Thr
1 5

<210> 19
<211> 24
<212> DNA
<213> artificial sequence

<220>
<223> CDR3 light chain

<400> 19
cttcagattt ataatatgcc tatt 24

<210> 20
<211> 8
<212> PRT
<213> artificial sequenze

<220>
<223> CDR3 light chain

<400> 20

Leu Gln Ile Tyr Asn Met Pro Ile
1 5

<210> 21
<211> 648
<212> DNA
<213> artificial sequence

<220>
<223> light chain of ANTIBODY A

<400> 21
gatatcgtgc tgacccagag cccggcgacc ctgagcctgt ctccgggcga acgtgcgacc 60

ctgagctgca gagcgagcca gagcgtgagc agcagctatc tggcgtggta ccagcagaaa 120

ccaggtcaag caccgcgtct attaatttat ggcgcgagca gccgtgcaac tggggtcccg 180

gcgcgtttta gcggctctgg atccggcacg gattttaccc tgaccattag cagcctggaa 240

cctgaagact ttgcgactta ttattgcctt cagatttata atatgcctat tacctttggc 300

cagggtacga aagttgaaat taaacgtacg gtggctgcac catctgtctt catcttcccg 360

ccatctgatg agcagttgaa atctggaact gcctctgttg tgtgcctgct gaataacttc 420

tatcccagag aggccaaagt acagtggaag gtggataacg ccctccaatc gggtaactcc 480

caggagagtg tcacagagca ggacagcaag gacagcacct acagcctcag cagcaccctg 540

acgctgagca aagcagacta cgagaaacac aaagtctacg cctgcgaagt cacccatcag 600

ggcctgagct cgcccgtcac aaagagcttc aacaggggag agtgttag 648

<210> 22
<211> 215
<212> PRT
<213> artificial sequence

<220>
<223> light chain of ANTIBODY A

<400> 22

Asp Ile Val Leu Thr Gln Ser Pro Ala Thr Leu Ser Leu Ser Pro Gly
1 5 10 15

Glu Arg Ala Thr Leu Ser Cys Arg Ala Ser Gln Ser Val Ser Ser Ser
20 25 30

Tyr Leu Ala Trp Tyr Gln Gln Lys Pro Gly Gln Ala Pro Arg Leu Leu
35 40 45

Ile Tyr Gly Ala Ser Ser Arg Ala Thr Gly Val Pro Ala Arg Phe Ser
50 55 60

Gly Ser Gly Ser Gly Thr Asp Phe Thr Leu Thr Ile Ser Ser Leu Glu
65 70 75 80

Pro Glu Asp Phe Ala Thr Tyr Tyr Cys Leu Gln Ile Tyr Asn Met Pro
85 90 95

Ile Thr Phe Gly Gln Gly Thr Lys Val Glu Ile Lys Arg Thr Val Ala
100 105 110

Ala Pro Ser Val Phe Ile Phe Pro Pro Ser Asp Glu Gln Leu Lys Ser
115 120 125

Gly Thr Ala Ser Val Val Cys Leu Leu Asn Asn Phe Tyr Pro Arg Glu
130 135 140

Ala Lys Val Gln Trp Lys Val Asp Asn Ala Leu Gln Ser Gly Asn Ser
145 150 155 160

Gln Glu Ser Val Thr Glu Gln Asp Ser Lys Asp Ser Thr Tyr Ser Leu
165 170 175

Ser Ser Thr Leu Thr Leu Ser Lys Ala Asp Tyr Glu Lys His Lys Val
180 185 190

Tyr Ala Cys Glu Val Thr His Gln Gly Leu Ser Ser Pro Val Thr Lys
195 200 205

Ser Phe Asn Arg Gly Glu Cys
210 215

<210> 23
<211> 3984
<212> DNA
<213> artificial sequence

<220>
<223> alternative sequence encoding heavy chain with Fc-region of ANTIBODY A

<400> 23
atggagtttg ggctgagctg ggttttcctc gttgctcttt taagaggtga ttcatggaga 60

aatagagaga ctgagtgtga gtgaacatga gtgagaaaaa ctggatttgt gtggcatttt 120

ctgataacgg tgtccttctg tttgcaggtg tccagtgtca ggtggagctg gtggagtctg 180

ggggaggcct ggtccagcct ggggggtccc tgagactctc ctgtgcagcg tctggattca 240

ccttcagtag ctatgccatg agctgggtcc gccaggctcc aggcaagggg ctcgagtggg 300

tgtccgccat aaacgccagc ggtacccgca cctactatgc agactccgtg aagggccgat 360

tcaccatctc cagagacaat tccaagaaca cgctgtatct gcaaatgaac agcctgagag 420

ccgaggacac ggctgtgtat tactgtgcga gaggcaaggg gaacacccac aagccctacg 480

gctacgtacg ctactttgac gtgtggggcc aaggaaccct ggtcaccgtc tcctcaggtg 540

agtcctcaca acctctctcc tgcggccgca gcttgaagtc tgaggcagaa tcttgtccag 600

ggtctatcgg actcttgtga gaattagggg ctgacagttg atggtgacaa tttcagggtc 660

agtgactgtc tggtttctct gaggtgagac tggaatatag gtcaccttga agactaaaga 720

ggggtccagg ggcttttctg cacaggcagg gaacagaatg tggaacaatg acttgaatgg 780

ttgattcttg tgtgacacca agaattggca taatgtctga gttgcccaag ggtgatctta 840

gctagactct ggggtttttg tcgggtacag aggaaaaacc cactattgtg attactatgc 900

tatggactac tggggtcaag gaacctcagt caccgtctcc tcaggtaaga atggcctctc 960

caggtcttta tttttaacct ttgttatgga gttttctgag cattgcagac taatcttgga 1020

tatttgccct gagggagccg gctgagagaa gttgggaaat aaatctgtct agggatctca 1080

gagcctttag gacagattat ctccacatct ttgaaaaact aagaatctgt gtgatggtgt 1140

tggtggagtc cctggatgat gggataggga ctttggaggc tcatttgagg gagatgctaa 1200

aacaatccta tggctggagg gatagttggg gctgtagttg gagattttca gtttttagaa 1260

tgaagtatta gctgcaatac ttcaaggacc acctctgtga caaccatttt atacagtatc 1320

caggcatagg gacaaaaagt ggagtggggc actttcttta gatttgtgag gaatgttcca 1380

cactagattg tttaaaactt catttgttgg aaggagctgt cttagtgatt gagtcaaggg 1440

agaaaggcat ctagcctcgg tctcaaaagg gtagttgctg tctagagagg tctggtggag 1500

cctgcaaaag tccagctttc aaaggaacac agaagtatgt gtatggaata ttagaagatg 1560

ttgcttttac tcttaagttg gttcctagga aaaatagtta aatactgtga ctttaaaatg 1620

tgagagggtt ttcaagtact catttttta aatgtccaaa atttttgtca atcaatttga 1680

ggtcttgttt gtgtagaact gacattactt aaagtttaac cgaggaatgg gagtgaggct 1740

ctctcatacc ctattcagaa ctgactttta acaataataa attaagttta aaatattttt 1800

aaatgaattg agcaatgttg agttgagtca agatggccga tcagaaccgg aacacctgca 1860

gcagctggca ggaagcaggt catgtggcaa ggctatttgg ggaagggaaa ataaaaccac 1920

taggtaaact tgtagctgtg gtttgaagaa gtggttttga aacactctgt ccagccccac 1980

caaaccgaaa gtccaggctg agcaaaacac cacctgggta atttgcattt ctaaaataag 2040

ttgaggattc agccgaaact ggagaggtcc tcttttaact tattgagttc aacctttaa 2100

ttttagcttg agtagttcta gtttccccaa acttaagttt atcgacttct aaaatgtatt 2160

tagaattcga gctcggtaca gctttctggg gcaggccagg cctgaccttg gctttggggc 2220

agggaggggg ctaaggtgag gcaggtggcg ccagcaggtg cacacccaat gcccatgagc 2280

ccagacactg gacgctgaac ctcgcggaca gttaagaacc caggggcctc tgcgcctggg 2340

cccagctctg tcccacaccg cggtcacatg gcaccacctc tcttgcagcc tccaccaagg 2400

gcccatcggt cttccccctg gcaccctcct ccaagagcac ctctgggggc acagcggccc 2460

tgggctgcct ggtcaaggac tacttccccg aaccggtgac ggtgtcgtgg aactcaggcg 2520

ccctgaccag cggcgtgcac accttcccgg ctgtcctaca gtcctcagga ctctactccc 2580

tcagcagcgt ggtgaccgtg ccctccagca gcttgggcac ccagacctac atctgcaacg 2640

tgaatcacaa gcccagcaac accaaggtgg acaagaaagt tggtgagagg ccagcacagg 2700

gagggagggt gtctgctgga agccaggctc agcgctcctg cctggacgca tcccggctat 2760

gcagccccag tccagggcag caaggcaggc cccgtctgcc tcttcacccg gagcctctgc 2820

ccgccccact catgctcagg gagagggtct tctggctttt tcccaggctc tgggcaggca 2880

caggctaggt gcccctaacc caggccctgc acacaaaggg gcaggtgctg ggctcagacc 2940

tgccaagagc catatccggg aggaccctgc ccctgaccta agcccacccc aaaggccaaa 3000

ctctccactc cctcagctcg gacaccttct ctcctcccag attccagtaa ctcccaatct 3060

tctctctgca gagcccaaat cttgtgacaa aactcacaca tgcccaccgt gcccaggtaa 3120

gccagcccag gcctcgccct ccagctcaag gcgggacagg tgccctagag tagcctgcat 3180

ccagggacag gccccagccg ggtgctgaca cgtccacctc catctcttcc tcagcacctg 3240

aactcctggg gggaccgtca gtcttcctct tccccccaaa acccaaggac accctcatga 3300

tctcccggac ccctgaggtc acatgcgtgg tggtggacgt gagccacgaa gaccctgagg 3360

tcaagttcaa ctggtacgtg gacggcgtgg aggtgcataa tgccaagaca aagccgcggg 3420

aggagcagta caacagcacg taccgtgtgg tcagcgtcct caccgtcctg caccaggact 3480

ggctgaatgg caaggagtac aagtgcaagg tctccaacaa agccctccca gcccccatcg 3540

agaaaaccat ctccaaagcc aaaggtggga cccgtggggt gcgagggcca catggacaga 3600

ggccggctcg gcccaccctc tgccctgaga gtgaccgctg taccaacctc tgtccctaca 3660

gggcagcccc gagaaccaca ggtgtacacc ctgccccccat cccgggatga gctgaccaag 3720

aaccaggtca gcctgacctg cctggtcaaa ggcttctatc ccagcgacat cgccgtggag 3780

tgggagagca atgggcagcc ggagaacaac tacaagacca cgcctcccgt gctggactcc 3840

gacggctcct tcttcctcta cagcaagctc accgtggaca agagcaggtg gcagcagggg 3900

aacgtcttct catgctccgt gatgcatgag gctctgcaca accactacac gcagaagagc 3960

ctctccctgt ccccgggcaa atga 3984

<210> 24
<211> 3202
<212> DNA
<213> artificial sequence

<220>
<223> alternative sequence encoding light chain of ANTIBODY A

<400> 24
atggacatga gggtcctcgc tcagctcctg gggctcctgc tgctctgttt cccaggtaag 60

gatggagaac actagcagtt tactcagccc agggtgctca gtactgcttt actattcagg 120

gaaattctct tacaacatga ttaattgtgt ggacatttgt ttttatgttt ccaatctcag 180

gcgccagatg tgatatcgtg ttgacgcagt ctccagccac cctgtctttg tctccagggg 240

aaagagccac cctctcctgc cgggccagtc agagtgttag cagcagctac ttagcctggt 300

accagcagaa acctggccag gcgcccaggc tcctcatcta tggcgcatcc agcagggcca 360

ctggcgtgcc agccaggttc agtggcagtg ggtctgggac agacttcact ctcaccatca 420

gcagcctgga gcctgaagat ttcgcgacct attactgtct gcagatttac aacatgccta 480

tcacgttcgg ccaagggacc aaggtggaaa tcaaacgtga gtagaattta aactttgcgg 540

ccgcctagac gtttaagtgg gagatttgga ggggatgagg aatgaaggaa cttcaggata 600

gaaaagggct gaagtcaagt tcagctccta aaatggatgt gggagcaaac tttgaagata 660

aactgaatga cccagaggat gaaacagcgc agatcaaaga ggggcctgga gctctgagaa 720

gagaaggaga ctcatccgtg ttgagtttcc acaagtactg tcttgagttt tgcaataaaa 780

gtgggatagc agagttgagt gagccgtagg ctgagttctc tcttttgtct cctaagtttt 840

tatgactaca aaaatcagta gtatgtcctg aaataatcat taagctgttt gaaagtatga 900

ctgcttgcca tgtagatacc atgtcttgct gaatgatcag aagaggtgtg actcttattc 960

taaaatttgt cacaaaatgt caaaatgaga gactctgtag gaacgagtcc ttgacagaca 1020

gctcaagggg ttttttttcct ttgtctcatt tctacatgaa agtaaatttg aaatgatctt 1080

ttttattata agagtagaaa tacagttggg tttgaactat atgttttaat ggccacggtt 1140

ttgtaagaca tttggtcctt tgttttccca gttattactc gattgtaatt ttatatcgcc 1200

agcaatggac tgaaacggtc cgcaacctct tctttacaac tgggtgacct cgcggctgtg 1260

ccagccattt ggcgttcacc ctgccgctaa gggccatgtg aacccccgcg gtagcatccc 1320

ttgctccgcg tggaccactt tcctgaggca cagtgatagg aacagagcca ctaatctgaa 1380

gagaacagag atgtgacaga ctacactaat gtgagaaaaa caaggaaagg gtgacttatt 1440

ggagatttca gaaataaaat gcatttatta ttatattccc ttattttaat tttctattag 1500

ggaattagaa agggcataaa ctgctttatc cagtgttata ttaaaagctt aatgtatata 1560

atcttttaga ggtaaaatct acagccagca aaagtcatgg taaatattct ttgactgaac 1620

tctcactaaa ctcctctaaa ttatatgtca tattaactgg ttaaattaat ataaatttgt 1680

gacatgacct taactggtta ggtaggatat ttttcttcat gcaaaaatat gactaataat 1740

aatttagcac aaaaatattt cccaatactt taattctgtg atagaaaaat gtttaactca 1800

gctactataa tcccataatt ttgaaaacta tttattagct tttgtgtttg acccttccct 1860

agccaaaggc aactatttaa ggacccttta aaactcttga aactacttta gagtcattaa 1920

gttatttaac cacttttaat tactttaaaa tgatgtcaat tccctttaa ctattaattt 1980

attttaaggg gggaaaggct gctcataatt ctattgtttt tcttggtaaa gaactctcag 2040

ttttcgtttt tactacctct gtcacccaag agttggcatc tcaacagagg ggactttccg 2100

agaggccatc tggcagttgc ttaagatcag aagtgaagtc tgccagttcc tcccaggcag 2160

gtggcccaga ttacagttga cctgttctgg tgtggctaaa aattgtccca tgtggttaca 2220

aaccattaga ccagggtctg atgaattgct cagaatattt ctggacaccc aaatacagac 2280

cctggcttaa ggccctgtcc atacagtagg tttagcttgg ctacaccaaa ggaagccata 2340

cagaggctaa tatcagagta ttcttggaag agacaggaga aaatgaaagc cagtttctgc 2400

tcttaccttа tgtgcttgtg ttcagactcc caaacatcag gagtgtcaga taaactggtc 2460

tgaatctctg tctgaagcat ggaactgaaa agaatgtagt ttcagggaag aaaggcaata 2520

gaaggaagcc tgagaatacg gatcaattct aaactctgag ggggtcggat gacgtggcca 2580

ttctttgcct aaagcattga gtttactgca aggtcagaaa agcatgcaaa gccctcagaa 2640

tggctgcaaa gagctccaac aaaacaattt agaactttat taaggaatag ggggaagcta 2700

ggaagaaact caaaacatca agattttaaa tacgcttctt ggtctccttg ctataattat 2760

ctgggataag catgctgttt tctgtctgtc cctaacatgc cctgtgatta tccgcaaaca 2820

acacacccaa gggcagaact ttgttactta aacaccatcc tgtttgcttc tttcctcagg 2880

aactgtggct gcaccatctg tcttcatctt cccgccatct gatgagcagt tgaaatctgg 2940

aactgcctct gttgtgtgcc tgctgaataa cttctatccc agagaggcca aagtacagtg 3000

gaaggtggat aacgccctcc aatcgggtaa ctcccaggag agtgtcacag agcaggacag 3060

caaggacagc acctacagcc tcagcagcac cctgacgctg agcaaagcag actacgagaa 3120

acacaaagtc tacgcctgcg aagtcaccca tcagggcctg agctcgcccg tcacaaagag 3180

cttcaacagg ggagagtgtt ag 3202

<210> 25
<211> 1428
<212> DNA
<213> artificial sequence

<220>
<223> heavy chain with Fc region of ANTIBODY A and with leader sequence

<400> 25
atgaaacacc tgtggttctt cctcctgctg gtggcagctc ccagatgggt cctgtcccag 60

gtggaattgg tggaaagcgg cggcggcctg gtgcaaccgg gcggcagcct gcgtctgagc 120

tgcgcggcct ccggatttac ctttagcagc tatgcgatga gctgggtgcg ccaagcccct 180

gggaagggtc tcgagtgggt gagcgctatt aatgcttctg gtactcgtac ttattatgct 240

gattctgtta agggtcgttt taccatttca cgtgataatt cgaaaaacac cctgtatctg 300

caaatgaaca gcctgcgtgc ggaagatacg gccgtgtatt attgcgcgcg tggtaagggt 360

aatactcata agccttatgg ttatgttcgt tattttgatg tttggggcca aggcaccctg 420

gtgacggtta gctcagcctc caccaagggt ccatcggtct tccccctggc accctcctcc 480

aagagcacct ctgggggcac agcggccctg ggctgcctgg tcaaggacta cttccccgaa 540

ccggtgacgg tgtcgtggaa ctcaggcgcc ctgaccagcg gcgtgcacac cttcccggct 600

gtcctacagt cctcaggact ctactccctc agcagcgtgg tgaccgtgcc ctccagcagc 660

ttgggcaccc agacctacat ctgcaacgtg aatcacaagc ccagcaacac caaggtggac 720

aagaaagttg agcccaaatc ttgtgacaaa actcacacat gcccaccgtg cccagcacct 780

gaactcctgg ggggaccgtc agtcttcctc ttccccccaa aacccaagga caccctcatg 840

atctcccgga cccctgaggt cacatgcgtg gtggtggacg tgagccacga agaccctgag 900

gtcaagttca actggtacgt ggacggcgtg gaggtgcata atgccaagac aaagccgcgg 960

gaggagcagt acaacagcac gtaccgggtg gtcagcgtcc tcaccgtcct gcaccaggac 1020

tggctgaatg gcaaggagta caagtgcaag gtctccaaca aagccctccc agcccccatc 1080

gagaaaacca tctccaaagc caaagggcag ccccgagaac cacaggtgta caccctgccc 1140

ccatcccggg atgagctgac caagaaccag gtcagcctga cctgcctggt caaaggcttc 1200

tatcccagcg acatcgccgt ggagtgggag agcaatgggc agccggagaa caactacaag 1260

accacgcctc ccgtgctgga ctccgacggc tccttcttcc tctacagcaa gctcaccgtg 1320

gacaagagca ggtggcagca ggggaacgtc ttctcatgct ccgtgatgca tgaggctctg 1380

cacaaccact acacgcagaa gagcctctcc ctgtctccgg gtaaatga 1428

<210> 26
<211> 475
<212> PRT
<213> artificial sequence

<220>
<223> heavy chain with Fc region of ANTIBODY A and with leader sequence

<400> 26

Met Lys His Leu Trp Phe Phe Leu Leu Leu Val Ala Ala Pro Arg Trp
1 5 10 15

Val Leu Ser Gln Val Glu Leu Val Glu Ser Gly Gly Gly Leu Val Gln
20 25 30

Pro Gly Gly Ser Leu Arg Leu Ser Cys Ala Ala Ser Gly Phe Thr Phe
35 40 45

```
Ser Ser Tyr Ala Met Ser Trp Val Arg Gln Ala Pro Gly Lys Gly Leu
    50                  55                  60

Glu Trp Val Ser Ala Ile Asn Ala Ser Gly Thr Arg Thr Tyr Tyr Ala
65                  70                  75                  80

Asp Ser Val Lys Gly Arg Phe Thr Ile Ser Arg Asp Asn Ser Lys Asn
                85                  90                  95

Thr Leu Tyr Leu Gln Met Asn Ser Leu Arg Ala Glu Asp Thr Ala Val
            100                 105                 110

Tyr Tyr Cys Ala Arg Gly Lys Gly Asn Thr His Lys Pro Tyr Gly Tyr
        115                 120                 125

Val Arg Tyr Phe Asp Val Trp Gly Gln Gly Thr Leu Val Thr Val Ser
    130                 135                 140

Ser Ala Ser Thr Lys Gly Pro Ser Val Phe Pro Leu Ala Pro Ser Ser
145                 150                 155                 160

Lys Ser Thr Ser Gly Gly Thr Ala Ala Leu Gly Cys Leu Val Lys Asp
                165                 170                 175

Tyr Phe Pro Glu Pro Val Thr Val Ser Trp Asn Ser Gly Ala Leu Thr
            180                 185                 190

Ser Gly Val His Thr Phe Pro Ala Val Leu Gln Ser Ser Gly Leu Tyr
        195                 200                 205

Ser Leu Ser Ser Val Val Thr Val Pro Ser Ser Ser Leu Gly Thr Gln
    210                 215                 220

Thr Tyr Ile Cys Asn Val Asn His Lys Pro Ser Asn Thr Lys Val Asp
225                 230                 235                 240

Lys Lys Val Glu Pro Lys Ser Cys Asp Lys Thr His Thr Cys Pro Pro
                245                 250                 255

Cys Pro Ala Pro Glu Leu Leu Gly Gly Pro Ser Val Phe Leu Phe Pro
            260                 265                 270

Pro Lys Pro Lys Asp Thr Leu Met Ile Ser Arg Thr Pro Glu Val Thr
        275                 280                 285
```

```
Cys Val Val Val Asp Val Ser His Glu Asp Pro Glu Val Lys Phe Asn
    290                 295                 300

Trp Tyr Val Asp Gly Val Glu Val His Asn Ala Lys Thr Lys Pro Arg
305                 310                 315                 320

Glu Glu Gln Tyr Asn Ser Thr Tyr Arg Val Val Ser Val Leu Thr Val
                325                 330                 335

Leu His Gln Asp Trp Leu Asn Gly Lys Glu Tyr Lys Cys Lys Val Ser
            340                 345                 350

Asn Lys Ala Leu Pro Ala Pro Ile Glu Lys Thr Ile Ser Lys Ala Lys
        355                 360                 365

Gly Gln Pro Arg Glu Pro Gln Val Tyr Thr Leu Pro Pro Ser Arg Asp
    370                 375                 380

Glu Leu Thr Lys Asn Gln Val Ser Leu Thr Cys Leu Val Lys Gly Phe
385                 390                 395                 400

Tyr Pro Ser Asp Ile Ala Val Glu Trp Glu Ser Asn Gly Gln Pro Glu
                405                 410                 415

Asn Asn Tyr Lys Thr Thr Pro Pro Val Leu Asp Ser Asp Gly Ser Phe
            420                 425                 430

Phe Leu Tyr Ser Lys Leu Thr Val Asp Lys Ser Arg Trp Gln Gln Gly
        435                 440                 445

Asn Val Phe Ser Cys Ser Val Met His Glu Ala Leu His Asn His Tyr
    450                 455                 460

Thr Gln Lys Ser Leu Ser Leu Ser Pro Gly Lys
465                 470                 475
```

<210> 27
<211> 708
<212> DNA
<213> artificial sequence

<220>
<223> light chain of ANTIBODY A with leader sequence

<400> 27
atggtgttgc agacccaggt cttcatttct ctgttgctct ggatctctgg tgcctacggg 60

gatatcgtgc tgacccagag cccggcgacc ctgagcctgt ctccgggcga acgtgcgacc 120

ctgagctgca gagcgagcca gagcgtgagc agcagctatc tggcgtggta ccagcagaaa 180

ccaggtcaag caccgcgtct attaatttat ggcgcgagca gccgtgcaac tggggtcccg 240

gcgcgtttta gcggctctgg atccggcacg gattttaccc tgaccattag cagcctggaa 300

cctgaagact ttgcgactta ttattgcctt cagatttata atatgcctat tacctttggc 360

cagggtacga aagttgaaat taaacgtacg gtggctgcac catctgtctt catcttcccg 420

ccatctgatg agcagttgaa atctggaact gcctctgttg tgtgcctgct gaataacttc 480

tatcccagag aggccaaagt acagtggaag gtggataacg ccctccaatc gggtaactcc 540

caggagagtg tcacagagca ggacagcaag gacagcacct acagcctcag cagcaccctg 600

acgctgagca aagcagacta cgagaaacac aaagtctacg cctgcgaagt cacccatcag 660

ggcctgagct cgcccgtcac aaagagcttc aacaggggag agtgttag 708

<210> 28
<211> 235
<212> PRT
<213> artificial sequence

<220>
<223> light chain of ANTIBODY A with leader sequence

<400> 28

Met Val Leu Gln Thr Gln Val Phe Ile Ser Leu Leu Leu Trp Ile Ser
1 5 10 15

Gly Ala Tyr Gly Asp Ile Val Leu Thr Gln Ser Pro Ala Thr Leu Ser
20 25 30

Leu Ser Pro Gly Glu Arg Ala Thr Leu Ser Cys Arg Ala Ser Gln Ser
35 40 45

Val Ser Ser Ser Tyr Leu Ala Trp Tyr Gln Gln Lys Pro Gly Gln Ala
50 55 60

Pro Arg Leu Leu Ile Tyr Gly Ala Ser Ser Arg Ala Thr Gly Val Pro
65 70 75 80

Ala Arg Phe Ser Gly Ser Gly Ser Gly Thr Asp Phe Thr Leu Thr Ile
85 90 95

Ser Ser Leu Glu Pro Glu Asp Phe Ala Thr Tyr Tyr Cys Leu Gln Ile
100 105 110

```
Tyr Asn Met Pro Ile Thr Phe Gly Gln Gly Thr Lys Val Glu Ile Lys
        115                 120                 125

Arg Thr Val Ala Ala Pro Ser Val Phe Ile Phe Pro Pro Ser Asp Glu
    130                 135                 140

Gln Leu Lys Ser Gly Thr Ala Ser Val Val Cys Leu Leu Asn Asn Phe
145                 150                 155                 160

Tyr Pro Arg Glu Ala Lys Val Gln Trp Lys Val Asp Asn Ala Leu Gln
                165                 170                 175

Ser Gly Asn Ser Gln Glu Ser Val Thr Glu Gln Asp Ser Lys Asp Ser
            180                 185                 190

Thr Tyr Ser Leu Ser Ser Thr Leu Thr Leu Ser Lys Ala Asp Tyr Glu
        195                 200                 205

Lys His Lys Val Tyr Ala Cys Glu Val Thr His Gln Gly Leu Ser Ser
    210                 215                 220

Pro Val Thr Lys Ser Phe Asn Arg Gly Glu Cys
225                 230                 235


<210>  29
<211>  31
<212>  DNA
<213>  artificial sequence

<220>
<223>  MS-Roche #7.9.H7_Ig_kappa sense primer

<400>  29
acgtaagctt gccgccacca tggtgttgca g                                    31


<210>  30
<211>  28
<212>  DNA
<213>  artificial sequence

<220>
<223>  MS-Roche #7.9.H7_Ig_kappa antisense primer

<400>  30
acgtgaattc ctaacactct cccctgtt                                        28


<210>  31
<211>  31
<212>  DNA
<213>  artificial sequence
```

<220>
<223> MS-Roche #7.9.H7_IgG1 sense primer

<400> 31
acgtaagctt gccgccacca tgaaacacct g 31

<210> 32
<211> 28
<212> DNA
<213> artificial sequence

<220>
<223> MS-Roche #7.9.H7_IgG1 antisense primer

<400> 32
acgtgaattc tcatttaccc ggagacag 28

# INTERNATIONAL SEARCH REPORT

International application No
PCT/EP2006/011914

A. CLASSIFICATION OF SUBJECT MATTER
INV. C07K16/18 A61K39/395 A61P25/28

According to International Patent Classification (IPC) or to both national classification and IPC

B. FIELDS SEARCHED

Minimum documentation searched (classification system followed by classification symbols)
C07K

Documentation searched other than minimum documentation to the extent that such documents are included in the fields searched

Electronic data base consulted during the international search (name of data base and, where practical, search terms used)
EPO-Internal, WPI Data, BIOSIS, EMBASE, Sequence Search

C. DOCUMENTS CONSIDERED TO BE RELEVANT

| Category* | Citation of document, with indication, where appropriate, of the relevant passages | Relevant to claim No. |
|---|---|---|
| X | ENDO T ET AL: "Glycosylation of the variable region of immunoglobulin G--site specific maturation of the sugar chains." MOLECULAR IMMUNOLOGY SEP 1995, vol. 32, no. 13, September 1995 (1995-09), pages 931-940, XP000983494 ISSN: 0161-5890 abstract<br>-----<br>-/-- | 1-3, 14-34 |

[X] Further documents are listed in the continuation of Box C. [X] See patent family annex.

* Special categories of cited documents :

"A" document defining the general state of the art which is not considered to be of particular relevance
"E" earlier document but published on or after the international filing date
"L" document which may throw doubts on priority claim(s) or which is cited to establish the publication date of another citation or other special reason (as specified)
"O" document referring to an oral disclosure, use, exhibition or other means
"P" document published prior to the international filing date but later than the priority date claimed

"T" later document published after the international filing date or priority date and not in conflict with the application but cited to understand the principle or theory underlying the invention
"X" document of particular relevance; the claimed invention cannot be considered novel or cannot be considered to involve an inventive step when the document is taken alone
"Y" document of particular relevance; the claimed invention cannot be considered to involve an inventive step when the document is combined with one or more other such documents, such combination being obvious to a person skilled in the art.
"&" document member of the same patent family

| Date of the actual completion of the international search | Date of mailing of the international search report |
|---|---|
| 26 February 2007 | 09/03/2007 |

| Name and mailing address of the ISA/ | Authorized officer |
|---|---|
| European Patent Office, P.B. 5818 Patentlaan 2<br>NL - 2280 HV Rijswijk<br>Tel. (+31-70) 340-2040, Tx. 31 651 epo nl,<br>Fax: (+31-70) 340-3016 | Le Flao, Katell |

4

Form PCT/ISA/210 (second sheet) (April 2005)



Fujirebio Diagnostics, Inc. v. Quanterix Corp.
EX-1045
5703

## INTERNATIONAL SEARCH REPORT

International application No
PCT/EP2006/011914

C(Continuation). DOCUMENTS CONSIDERED TO BE RELEVANT

| Category* | Citation of document, with indication, where appropriate, of the relevant passages | Relevant to claim No. |
|---|---|---|
| X | LEIBIGER H ET AL: "Variable domain-linked oligosaccharides of a human monoclonal IgG: structure and influence on antigen binding." THE BIOCHEMICAL JOURNAL 1 MAR 1999, vol. 338 ( Pt 2), 1 March 1999 (1999-03-01), pages 529-538, XP002422080 ISSN: 0264-6021 figure 1 | 1,14-34 |
| X | WO 03/070760 A (HOFFMANN LA ROCHE [CH]; MORPHOSYS AG [DE]; BARDROFF MICHAEL [DE]; BOHR) 28 August 2003 (2003-08-28) example 6 | 1-34 |
| A | ROUTIER F H ET AL: "The glycosylation pattern of a humanized IgGI antibody (D1.3) expressed in CHO cells" GLYCOCONJUGATE JOURNAL, LUND, SE, vol. 14, no. 2, 1997, pages 201-207, XP002375244 ISSN: 0282-0080 cited in the application page 202 - page 203 page 205 - page 206 figures 3,4 table 2 | 1-34 |
| A | SHEELEY DOUGLAS M ET AL: "Characterization of monoclonal antibody glycosylation: Comparison of expression systems and identification of terminal alpha-linked galactose" ANALYTICAL BIOCHEMISTRY, vol. 247, no. 1, 1997, pages 102-110, XP002385237 ISSN: 0003-2697 pages 104-107 page 108, column 2 figures 2,3,6 | 1-34 |

4



Fujirebio Diagnostics, Inc. v. Quanterix Corp.
EX-1045
5704

# INTERNATIONAL SEARCH REPORT

International application No.
PCT/EP2006/011914

**Box II Observations where certain claims were found unsearchable (Continuation of item 2 of first sheet)**

This International Search Report has not been established in respect of certain claims under Article 17(2)(a) for the following reasons:

1. [X] Claims Nos.:
because they relate to subject matter not required to be searched by this Authority, namely:

Although claims 32-34 are directed to a method of treatment of the human/animal body, the search has been carried out and based on the alleged effects of the compound/composition.

2. [ ] Claims Nos.:
because they relate to parts of the International Application that do not comply with the prescribed requirements to such an extent that no meaningful International Search can be carried out, specifically:

3. [ ] Claims Nos.:
because they are dependent claims and are not drafted in accordance with the second and third sentences of Rule 6.4(a).

**Box III Observations where unity of invention is lacking (Continuation of item 3 of first sheet)**

This International Searching Authority found multiple inventions in this international application, as follows:

1. [ ] As all required additional search fees were timely paid by the applicant, this International Search Report covers all searchable claims.

2. [ ] As all searchable claims could be searched without effort justifying an additional fee, this Authority did not invite payment of any additional fee.

3. [ ] As only some of the required additional search fees were timely paid by the applicant, this International Search Report covers only those claims for which fees were paid, specifically claims Nos.:

4. [ ] No required additional search fees were timely paid by the applicant. Consequently, this International Search Report is restricted to the invention first mentioned in the claims; it is covered by claims Nos.:

**Remark on Protest**

[ ] The additional search fees were accompanied by the applicant's protest.

[ ] No protest accompanied the payment of additional search fees.



Fujirebio Diagnostics, Inc. v. Quanterix Corp.
EX-1045
5705

## INTERNATIONAL SEARCH REPORT

Information on patent family members

International application No
PCT/EP2006/011914

| Patent document cited in search report | Publication date | Patent family member(s) | Publication date |
|---|---|---|---|
| WO 03070760 A | 28-08-2003 | AU 2003218995 A1 | 09-09-2003 |
| | | BR 0307837 A | 07-12-2004 |
| | | CA 2477012 A1 | 28-08-2003 |
| | | CN 1630665 A | 22-06-2005 |
| | | HR 20040712 A2 | 30-06-2005 |
| | | JP 2005527199 T | 15-09-2005 |
| | | MX PA04008077 A | 14-12-2005 |
| | | US 2005169925 A1 | 04-08-2005 |
| | | ZA 200406604 A | 14-06-2005 |

(12) INTERNATIONAL APPLICATION PUBLISHED UNDER THE PATENT COOPERATION TREATY (PCT)

(19) World Intellectual Property Organization
International Bureau

(43) International Publication Date
26 July 2007 (26.07.2007)

PCT

(10) International Publication Number
WO 2007/082750 A1

(51) International Patent Classification:
*G01N 33/68* (2006.01) *C07K 16/00* (2006.01)

(21) International Application Number:
PCT/EP2007/000423

(22) International Filing Date: 18 January 2007 (18.01.2007)

(25) Filing Language: English

(26) Publication Language: English

(30) Priority Data:
06000969.3 18 January 2006 (18.01.2006) EP

(71) Applicant *(for all designated States except US)*: **FRIEDRICH-ALEXANDER-UNIVERSITÄT ERLANGEN-NÜRNBERG** [DE/DE]; Schlossplatz 4, 91054 Erlangen (DE).

(72) Inventors; and

(75) Inventors/Applicants *(for US only)*: **WILTFANG, Jens** [DE/DE]; Hoferstr. 15a, 91056 Erlangen (DE). **KORNHUBER, Johannes** [DE/DE]; Klopstockstrasse 15, 90491 Nürnberg (DE). **HENKEL, Andreas, Wolfram** [DE/DE]; Am Europakanal 1, 91056 Erlangen (DE). **LEWCZUK, Piotr** [DE/DE]; Buschhornweg 2, 91341 Röttenbach (DE). **KLAFKI, Hans-Wolfgang** [DE/DE]; Stubenlohstr. 14e, 91052 Erlangen (DE).

(74) Agent: **REHBERG HÜPPE+PARTNER**; Nikolausberger Weg 62, 37073 Göttingen (DE).

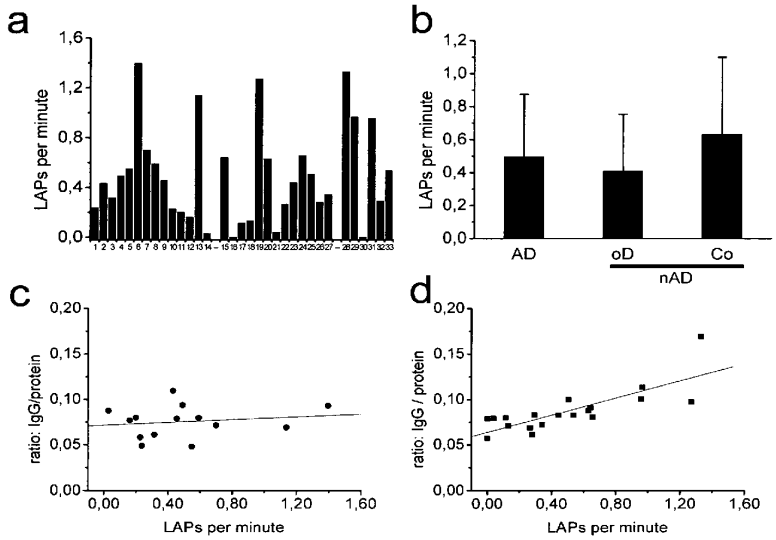
(81) Designated States *(unless otherwise indicated, for every kind of national protection available)*: AE, AG, AL, AM, AT, AU, AZ, BA, BB, BG, BR, BW, BY, BZ, CA, CH, CN, CO, CR, CU, CZ, DE, DK, DM, DZ, EC, EE, EG, ES, FI, GB, GD, GE, GH, GM, GT, HN, HR, HU, ID, IL, IN, IS, JP, KE, KG, KM, KN, KP, KR, KZ, LA, LC, LK, LR, LS, LT, LU, LV, LY, MA, MD, MG, MK, MN, MW, MX, MY, MZ, NA, NG, NI, NO, NZ, OM, PG, PH, PL, PT, RO, RS, RU, SC, SD, SE, SG, SK, SL, SM, SV, SY, TJ, TM, TN, TR, TT, TZ, UA, UG, US, UZ, VC, VN, ZA, ZM, ZW.

(84) Designated States *(unless otherwise indicated, for every kind of regional protection available)*: ARIPO (BW, GH, GM, KE, LS, MW, MZ, NA, SD, SL, SZ, TZ, UG, ZM, ZW), Eurasian (AM, AZ, BY, KG, KZ, MD, RU, TJ, TM), European (AT, BE, BG, CH, CY, CZ, DE, DK, EE, ES, FI, FR, GB, GR, HU, IE, IS, IT, LT, LU, LV, MC, NL, PL, PT, RO, SE, SI, SK, TR), OAPI (BF, BJ, CF, CG, CI, CM, GA, GN, GQ, GW, ML, MR, NE, SN, TD, TG).

**Published:**
— *with international search report*

*[Continued on next page]*

(54) **Title:** IMMUNOGLOBULIN-BOUND Aβ-PEPTIDES AND IMMUNOGLOBULINS-BINDING Aβ- PEPTIDES IN DIAGNOSIS AND THERAPY OF ALZHEIMER'S DEMENTIA




(57) **Abstract:** A method of analyzing a sample obtained from a patient for indications that the patient has or is susceptible to Alzheimer's dementia comprises the step of determining at least one concentration in the sample, the concentration being selected from the group of concentrations of Aβ-peptide- and immunoglobulin-including particles, of immunoglobulin-bound Aβ-peptides, and of Aβ-peptide-bound immunoglobulins. Certain Aβ-peptide-bound immunoglobulins can further be used in producing an immune therapy agent suitable for treating or preventing Alzheimer's dementia.

WO 2007/082750 A1

— *before the expiration of the time limit for amending the claims and to be republished in the event of receipt of amendments*

*For two-letter codes and other abbreviations, refer to the "Guidance Notes on Codes and Abbreviations" appearing at the beginning of each regular issue of the PCT Gazette.*

Fujirebio Diagnostics, Inc. v. Quanterix Corp.
EX-1045
5708

# IMMUNOGLOBULIN-BOUND Aβ-PEPTIDES AND IMMUNOGLOBULINS-BINDING Aβ-PEPTIDES IN DIAGNOSIS AND THERAPY OF ALZHEIMER'S DEMENTIA

The present invention generally relates to a method of analyzing a sample obtained from a patient for indications that the patient has or is susceptible to Alzheimer's dementia, the method comprising the step of determining at least one concentration in the sample.

Further, the present invention relates to an assay for analyzing a sample obtained from a patient for indications that the patient has or is susceptible to Alzheimer's dementia, and to a method of producing an immunotherapy agent suitable for treating or preventing Alzheimer's dementia.

## Prior Art

In view of novel therapies that may enter clinical trials in the near future, early and reliable diagnosis of Alzheimer's disease (AD) and other neurodegenerative diseases is gaining more and more importance. Any changes in biochemical composition of the brain metabolism should be predominantly reflected in the cerebrospinal fluid (CSF), because of its direct contact with the extracellular fluids of the central nervous system [1,2]. Therefore, determination of biomarkers in CSF, including beta-amyloid peptides (Aβ-peptides, in the following sometimes abbreviated as Aβ), tau and phospho-tau proved to be very important for differential diagnosis of dementias [3,4]. Commonly, Aβ-peptides are quantified by ELISA

technique for AD diagnosis. Decrease of Aβ1-42 (in the following sometimes abbreviated as Aβ42) in CSF of AD patients was reported by many groups; however, this decrease is not AD specific but also observed in Lewy-body dementia, and Creutzfeldt-Jakob disease [5-7]. Precipitation of Aβ into amyloid plaques has been proposed as one potential mechanism for reduction of Aβ in CSF [8]; however, since CJD patients with decreased CSF Aβ1-42 levels do not have brain beta-amyloid plaques, other mechanisms than plaque-mediated precipitation may be responsible [5]. Such mechanisms could be high-avidity binding to carrier proteins, IgGs or formation of detergent-stable soluble oligomers, conditions which would result in decreased CSF concentrations of the monomeric fraction due to epitope masking [5]. There is evidence that Aβ-peptides exist in several structural conformations, one of these being the beta sheet structure [9]. This form which tends to have strong aggregation potency is considered to be the pathological form, occurring in AD-patients.

In 1998, Pitschke and colleagues reported [10] that exclusively CSF of AD patients, but not of controls, contained large amounts of large Aβ-peptide binding particles (LAPs). Detection of LAPs in CSF by confocal spectroscopy (ConSP) was therefore interpreted as a positive diagnosis for AD. This method was based on 'seeded polymerization' of fluorescent synthetic Aβ-peptides on preexisting Aβ aggregates and fibrils in CSF of AD patients. These kind of aggregates are supposedly the main component of amyloid plaques that are associated with Alzheimer's disease [11]. In the optical setup, the fluorescence of labeled molecules was detected as they entered a small illuminated confocal volume of approximately one femtoliter [12]. Large single aggregates deliver high intensive fluorescent flashes (peaks) when they pass through the confocal volume, making them easy to detect against the much lower background of monomers.

Recently, antibodies against Aβ peptides were found in CSF in AD patients but also in non-demented individuals [13]. Immune responses and auto-antibodies directed against aggregated forms of Aβ-peptides may not only be of diagnostic interest but may also have therapeutic potential. Schenk and coworkers reported striking effects of Aβ vaccination in transgenic mice [14] and subsequently, a clinical trial was launched [15].

A method of analyzing a sample obtained from a patient for indications that the patient has or is susceptible to Alzheimer's dementia, which comprises the step of determining at least one concentration in the sample, is known from EP 1 270 592 A1. Here, the concentrations of different Aβ-peptides are measured in a fraction of the sample which binds to a monoclonal antibody mbAb 1E8 specific for Aβ1-x and Aβ2-x. The concentrations of the Aβ-peptides are measured using SDS-PAGE. Besides the concentrations of Aβ1-42 and Aβ1-40, a ratio of these concentrations denominated as Aβ42/40 is determined to discriminate the samples derived from AD patients from the samples derived from non AD patients. A suitable Aβ42/40 threshold value for this discrimination may be in the range of 0.09 to 0.11 but there is an overlap of the Aβ42/40 values of both groups.

Two standard ELISA assays for determining the concentrations both of Aβ1-42 and of Aβ1-40 in a sample obtained from a patient could be combined into one assay for analyzing the sample for indications that the patient has or is susceptible to Alzheimer's dementia, in which the ratio Aβ42/40 is calculated from the individual concentrations.

## Problem of the Invention

It is a problem of the present invention to provide a new and better discriminating method of analyzing a sample obtained from a patient for indications that the patient has or is susceptible to Alzheimer's dementia. It is a further problem of the present invention to

provide a method of producing a new and promising immunotherapy agent suitable for treating or preventing Alzheimer's dementia.

## Solution of the Invention

The problems of the present invention are solved by a method of analyzing a sample obtained from a patient having the features of independent claim 1, by an assay for analyzing a sample obtained from a patient having the features of independent claim 9, and by a method of producing an immunotherapy agent having the features of independent claim 10. Preferred embodiments of the first method are described in dependent claims 2 to 8.

## General Description of the Invention

Originally, the inventors of the present invention improved the detection sensitivity of the known ConSP setup by means of a microchannel flow-through about 20-fold to evaluate the potential of the detection of LAPs in CSF for clinical AD standard diagnostics. Surprisingly, the inventors found that LAPs are detected in both groups with high inter-individual variation, rendering this method useless for AD diagnosis.

To gain insight into molecular details of LAPs the inventors employed confocal microscopy for molecular imaging of LAPs, which revealed that LAPs are heterogeneous super-aggregates that can be subdivided in at least 4 subtypes. Particularly, it is possible to identify a subtype of immunoglobulin (IgG) containing LAPs that binds very tightly to aggregated Aβ1-42 peptides (LAP-4 subtype), and that was detected in 42.1 % of all non AD controls but is virtually absent from CSF of AD patients.

Further, a close correlation exists between LAPs and IgG concentration in CSF in controls but not in AD patients. Aβ-peptides (Aβ1-40 and Aβ1-42) copurify with immunoglobulins from

CSF on beads which are, for example, impregnated with protein A or protein G acting as an antibody binding the immunoglobulins.

The ratio Aβ42/40 in IgG-bound Aβ-peptides discriminates AD patients and controls without overlap. Importantly, the discrimination is significantly improved as compared to direct Aβ1-40 and Aβ1-42 quantification in the same set of CSF samples by standard ELISA.

These results not only offer improved early diagnosis of AD but also indicate an involvement of the immune system in regulating Aβ1-42 homeostasis. Thus, the present results are regarded as evidence that a potential Aβ1-42–clearing system involves immune complexes, patrols the CSF of some nAD controls, and is absent in all AD patients.

Based on these findings, the new method of analyzing a sample obtained from a patient for indications that the patient has or is susceptible to Alzheimer's dementia comprises the step of determining at least one concentration in the sample, the concentration being selected from the group of concentrations of Aβ-peptide- and immunoglobulin-including particles, of immunoglobulin-bound Aβ-peptides, and of Aβ-peptide-bound immunoglobulins. Thus, the first new method makes use of the fact that Aβ-peptides are bound to a different extent by IgGs present in AD patients and in nAD patients. This difference in the binding properties can by quantified by the concentrations of Aβ-peptide- and immunoglobulin-including particles as well as by the concentrations of both the Aβ-peptides and the IgGs bound in these particles.

It is preferred to directly determine the at least one concentration in the first new method, but is also possible to indirectly determine each of the above stated concentrations in that, for example, the ratio of the Aβ-peptides and/or the IgGs not bound in Aβ-peptide- and

immunoglubolin-including particles on the one hand and of the total Aβ-peptides and/or IgGs on the other hand is determined.

The data presented here have been obtained from cerebrospinalfluid as the sample obtained from AD and nAD patients. However, it is expected that similar data can also be obtained using other body fluids or body tissue homogenates as the sample obtained from the patient.

Preferably, the at least one concentration which is determined according to the first new method is selected from the group of concentrations consisting of concentrations of Aβ1-42-peptide- and immunoglobulin-including particles, of a concentration of immunoglobulin-bound Aβ1-42-peptides, of a concentration of immunoglobulin-bound Aβ1-40-peptides, and of concentrations of immunoglobulins bound to Aβ1-40-peptides and Aβ1-42-peptides. I.e. the new method focuses on Aβ1-42 bound by IgGs. The particles including Aβ1-42 and IgGs also include Aβ1-40.

The concentration of Aβ1-42- and IgGg-including particles, which is determined according to the new method can be a concentration of large Aβ1-42-peptide-binding particles (LAPs). According to the findings of the inventors LAPs can be subdivided into at least four subtypes. Two of this subtypes which are denominated as subtype 3 and subtype 4 here include Aβ1-42 and IgGs. These two LAP-subtypes are of particular interest in the new method.

Particularly it is preferred, if the first new method concentrates on the determination of the concentration of LAPs of LAP-subtype 4. The LAPs of LAP-subtype 4 have a round shape in single molecule imaging, whereas LAPs of LAP-subtype 3 have a more ellipsoids shape in single molecule imaging. The LAPs of LAP-subtype 4 are not found in samples from AD patients. They are only found in some of the samples of none AD patients. The nAD patients

from which the samples including LAPs of LAP-subtype 4 have been taken may be regarded as not susceptible to Alzheimer's disease whereas the other nAD patients may have a susceptibility to AD. At least, the existence of LAPs of LAP-subtype 4 in a sample from a particular patient indicates that the patient even if having a dementia has no AD.

The LAPs of the different LAP-subtypes may be differentiated in image morphometry by well established parameters of area, brightness, shape and texture. The LAPs of LAP-subtypes 3 and 4 clearly only differ from each other with regard to the shape-parameter. Only the LAPs of LAP-subtype 4 show a shape-parameter of 0,7 to 1,0. The shape-parameter is calculated as ( $\frac{4\Pi A}{P^2}$) and varies from 0 to 1, the difference to 1 indicating the difference with regard to a round shape.

In one particularly preferred group of embodiments of the new method, a fraction binding to an immunoglobulin-binding substance is separated from the remainder of the sample. The substance binding IgGs can, for example, be Protein A or Protein G, both binding to IgGs of various kinds. A more specific antibody to selected IgGs may also be used.

In a particular embodiment of the first new method, a ratio of the concentrations of Aβ1-42 and Aβ1-40 is determined in the separated fraction of the sample binding to the immunoglobulin-binding substance. It has been found that the value of this ratio is able to clearly differentiate between AD patients and nAD patients. A suitable upper threshold value for the ratio Aβ42/40 above which no AD patients are found may be set within a range of 0.12 to 0.20. Particularly the upper threshold value should be within a range of 0,125 to 0,130. This latter range is the observed gap between the values of AD patients and nAD patients.

For applying the first new method in an easy way, the assay may be used comprising an immunoglobulin-binding substance for separating a fraction binding to this substance from the remainder of the sample, and two marker substances which selectively bind to Aβ1-40-peptides and Aβ1-42-peptides in the fraction of the sample bound to the immunoglobulin-binding substance and which allow for a determination of the concentrations of the Aβ1-40-peptides and of the Aβ1-42-peptides in the fraction of the sample. The immunoglobulin-binding substance may, for example be Protein A or Protein G. Suitable marker substances can be constructed according to known methods.

The new method of producing an immune therapy agent suitable for treating or preventing Alzheimer's dementia comprises the step of purifying an immunoglobulin from a subtype of immunoglobulin-including large Aβ1-42-peptide-binding particles (LAPs) having a round shape in single molecule imaging (LAP-subtype 4). It is expected that the IgGs included in the LAPs of LAP-subtype 4 have certain properties binding Aβ-peptides, particularly Aβ1-42, into these LAPs. Further, it is expected that the Aβ-peptides bound by these IgGs are no longer able to be involved in an outbreak of AD. This may have the reason that the LAPs of LAP-subtype 4 are cleared by an immune system.

Other features and advantages of the present invention will become apparent to one with skill in the art upon examination of the following figures and the detailed description.

## Brief Description of the Figures

The invention can be better understood with reference to the attached figures.

**Fig. 1** illustrates the identification of auto-aggregated Aβ1-42*:

a. Confocal spectroscopy: Fluorescence peaks resulting from LAPs in CSF of a nAD patient that bind Aβ1-42*,

b. peaks of Aβ1-42* in physiological buffer,

c. Confocal microscopy: Four examples of LAPs, formed from of auto-aggregated Aβ1-42* in physiological buffer (scale bar = 2 µm),

d. synthetic Aβ1-42, pre-aggregated for 24 h in physiological buffer, incubated with Aβ1-42* (scale bar = 5 µm),

e. LAP-area versus LAP-texture plot of auto-aggregated Aβ1-42* shows two groups of auto-Aβ1-42* aggregates,

f. low LAP-texture values discriminate auto-aggregates from other LAP types.

**Fig. 2** shows that LAP frequency is AD independent but correlates with IgG concentration:

a. Frequency of LAPs above 3000 kHz photon count in individual patients. ICD-10 diagnoses are specified: patients 1-14 comprise the patient group "AD", and patients 15-33 comprise "nAD", 1-10 = AD, 11-14 = AD of mixed type, 15 = dementia with aphasia, 16 = dementia with Parkinson's disease, 17 –18 = vascular dementia, 19 = dementia, not specified, 20+21 = fronto-temporal dementia, 22-24 = Lewy-body dementia, 25-27 = Morbus Pick's disease, 28-32 = personality disorders, 33 = alcohol dependence;

b. Mean values ± standard deviation of 3 diagnostic groups show no significant differences at a threshold of 3000 kHz photon count;

c. Confocal spectroscopy: Linear correlation between LAP frequency and specific IgG concentration shows a highly significant correlation in nAD controls,

d. but no significant correlation in AD patients.

**Fig. 3** illustrates how confocal imaging discriminates four different LAP subtypes in CSF

a. Aβ1-42, 24 h pre-aggregated, labeled with Aβ1-42*;

b.; 1 % albumin in PBS forms aggregates with Aβ1-42*;

c. IgG-containing LAP-3 subtype;

d. IgG-containing LAP-4 subtype;

e. single confocal image, showing examples LAP subtypes: 1 = Aβ1-42* auto-aggregates, 2 = LAP-3 subtype, 3 = LAP-4 subtype

scale bars: a.- d. = 2 µm, e. =3.5 µm.

**Fig. 4** shows how protein A based depletion of IgG reduces LAPs:

a. Box plots show LAP-3 subtype frequency does not discriminate between diagnostic groups. LAP-4 subtype was detected only in a subgroup of nAD controls while AD patients had this subtype only within the background level;

b. Patient-specific changes in LAP subtype counts. LAP counts in individual patients before (solid bars), and after (shaded bars) protein A precipitation, (AD = Alzheimer's dementia, Co = non demented controls, oD = other dementias, nAD = Co and oD combined);

c. LAP-4 subtype is found in a subgroup of nAD controls only (solid bars). Protein A - precipitation (shaded bars) reduces LAP-4 subtype in these subjects.

**Fig. 5** depicts how the protein A precipitation improves AD diagnosis based on Aβ42/40 ratio:

a. Urea-based Aβ-SDS-PAGE-immunoblot with antibody 1E8 against Aβ peptides. A = AD patient, C = nAD control Q3 – Q7 = dilution series of a mixture of synthetic Aβ peptides;

b. Absolute concentrations of Aβ 1-42 and Aβ 1-40, co-precipitated with IgGs by protein A. Protein A beads bind IgG-Aβ 1-42 complexes significantly more effective in nAD controls while IgG-Aβ 1-40 complexes were significantly more precipitated in AD patients.

c. Elisa shows a highly significant separation between AD patients and nAD controls, directly measured in CSF, based on the Aβ42/40 ratio. Aβ-SDS-PAGE-immunoblot after

protein A precipitation clearly improves separation between AD patients and nAD controls when Aβ42/40 ratio was calculated from IgG-bound Aβ peptides. Two Lewy-body dementia patients (⊗) have the lowest Aβ42/40 ratio within the nAD group. The ratio for one LBD-patient was not available. The black bar indicates the range of 5 controls without dementia.

## Detailed Description

### Results

Large Aβ-peptide binding particles in CSF are not specific for AD.

Synthetic Aβ1-42 was fluorescently labeled with CY3 or FluorX (referred to Aβ1-42* in this application) and used for seeded aggregation studies. Analysis by confocal spectroscopy (ConSP) revealed that incubation of Aβ1-42* with CSF induced seeded aggregation of the probe on particles preexisting in CSF and produced many bright fluorescent peaks, as shown in figure 1a, b.

ConSP and additionally confocal imaging (ConIM) were employed in order to analyze LAPs in CSF of AD patients and nAD controls. Confocal images of LAPs were analyzed by completely autonomic working computer algorithms which determined LAP-properties like area (size), brightness, shape and texture. The concentration of LAPs, determined by ConSP alone, varied considerably between individual patients but was not specific for AD.

Self-aggregation of fluorescent Aβ1-42 probe

The first problem encountered by using the ConSP setup was that the frequency of peaks with a brightness of less than 1000 kHz photon counts varied among different Aβ1-42* preparations, pointing to auto-aggregation of the fluorescent probe. Confocal imaging of Aβ1-42* auto-aggregates (figure 1c) showed that the majority consisted of small, irregular

shaped structures with low brightness. In contrast, pre-aggregated synthetic Aβ1-42 which was not fluorescently labeled, formed large super-auto-aggregates *in vitro* that provided seeds for labeled Aβ1-42*. These structures were much larger than Aβ1-42* auto-aggregates which usually measured less than 2 µm, consisted of flat, punctuated structures that sometimes contained elongated tube-like fibrils. Figure 1d gives an example of such structures that were also rather dim but nevertheless quite large. Self-aggregation of the Aβ1-42* probe could be greatly reduced by filtering it through a 0.22 µm membrane spin filter, right before usage in the experiment.

Auto-aggregates of Aβ1-42* could easily be identified by ConIM analysis because they were very inhomogeneous in texture. Figure 1e shows that virtually all Aβ1-42* auto-aggregates had texture values of more than 2, indicating a very heterogeneous brightness distribution, and were smaller than 4 µm² when texture was plotted against area. By contrast, when the fluorescent probe was mixed with CSF (figure 1f) of a patient or control person, many homogeneously bright LAPs became visible, which were clearly no auto-aggregates, because they had texture values of less than 2.

Frequency of LAPs varies among individual patients

In order to exclude Aβ1-42* auto-aggregates from ConSP analysis, only bright LAPs of more than 3000 kHz photon counts were included in the analysis, a value three times the threshold used by Pitschke and colleagues. Figure 2a illustrates that large individual differences in LAP frequency were found when patients were analyzed by ConSP.

Although there were striking and consistent inter-individual variations (triplicate determination) no significant differences (Kruskal-Wallis test, p=0.51) were found in LAP frequency between diagnostic groups, as shown in figure 2b. It was clearly apparent that

CSF of some individual patients contained a large number of bright particles while others had virtually none that could surpass the applied strict criteria for LAP- brightness.

Close correlation between LAPs and immunoglobulins

In order to determine whether there was any correlation between LAPs, measured by ConSP and other CSF parameters, several neurochemical parameters were compared with the LAP frequency in individual patients (Table 1).

LAP frequency was significantly correlated to Aβ1-42 and tau only in nAD controls but the AD-specific CSF biomarker phospho-tau showed no correlation at all. Significant positive correlations were found between LAP frequency and immunoglobulin concentrations in nAD subjects only, while AD patients showed no correlation at all. In particular, the specific IgG concentration (IgG / protein) which corresponds to the relative contribution of IgG to total protein, was correlated ($r=0.83$; $p<0.0001$) to LAP frequency in nAD controls (figure 2c) but not in AD patients (figure 2d).

Individuals with normal or only minor elevated IgG concentrations of less than 50 mg/l in CSF had a significantly ($p<0.0001$) lower LAP frequency ($10.4 \pm 7.9$) than patients with pathologically (more than 50 mg/l) high IgG ($28.7 \pm 10.7$). In line with this result, the only patient in the nAD group, who was positive for oligoclonal bands, had the highest IgG concentration and also the highest LAP frequency.

Structural analysis of LAPs by confocal microscopy

To gain insight into structural details of LAPs, all samples were rescanned by the ConIM technique. LAPs were detected in all investigated CSF samples and in agreement with the results from ConSP, large inter-individual variations were observed in LAP frequency. ConIM allowed us to differentiate between auto-aggregates of Aβ1-42* and at least four structurally

distinct LAP subtypes (figure 3). Auto-aggregates comprised 46% - 56 % of all detected fluorescent particles. They were clearly defined by heterogeneous texture, low brightness and small size (table 2).

LAP-1 subtype, rarely found in CSF, resembled structures that were observed when fluorescent Aβ1-42* was added to pre-aggregated synthetic, not labeled, Aβ1-42 seeds *in vitro*. The LAP-2 subtype consisted of probably protein-bound Aβ1-42* aggregates which were also small and heterogeneously textured but round shaped particles of variable brightness. It resembled particles generated in vitro by adding Aβ1-42* to physiological buffer, containing 1 % albumin as a seed.

The third and the fourth subtype comprised very bright LAPs that were either ellipsoid (LAP-3 subtype) or round-shaped (LAP-4 subtype). The fourth subtype did also comprise super-aggregates that appeared as chains of large (~10 $\mu m^2$) round pearls (figure 3d). Only a minute portion of these chains were expected to reveal this pearl chain like structure, since the LAPs were imaged by confocal microscopy. This technique retrieves image series, consisting of narrow frames of the scanned volume. The "chain of pearls" is not visible unless it is oriented exactly in the same orientation as the confocal layer. Therefore images of LAP-4 subtype were usually observed as large, bright and round spheres. Figure 4a, b shows that LAP-3 subtype was found in AD patients and nAD controls, while LAP-4 subtype was exclusively found in some nAD controls (figure 4a, c). AD patients had a LAP-4 frequency within the background level. Figure 4b shows that LAP-3 subtype was removed by protein A precipitation in the majority of individuals but there was no significant difference between AD and nAD groups. LAPs of subtype 4, only found in nAD controls, were also removed by protein A precipitation.

LAP-3, -4 contain Aβ1-42 binding IgGs

LAPs that were grouped into either the third or the fourth type resembled immune complexes, which are observed in autoimmune diseases. In order to test if LAP-3, -4 subtypes contained immunoglobulins, protein A precipitation of IgG and IgG-bound antigens were performed.

IgGs were almost completely removed from aliquots of CSF samples by protein A precipitation (data not shown). The IgG-depleted CSF was spiked with Aβ1-42* subsequently and ConIM images were taken. Both LAP-3, -4 subtype counts were substantially decreased in all individuals who had shown high LAP counts before IgG depletion (figure 4b, c).

IgG depletion improves Aβ1-42/1-40 ratio based AD diagnosis

Aβ40 and Aβ42 concentrations measured by Elisa before IgG depletion showed the well known decrease of Aβ-42 and virtually unchanged concentration of Aβ-40 in AD patients with respect to nAD controls. Moreover, tau and phospho-tau 181 were in the range as expected for AD patients, confirming that the available patients were a representative selection.

In order to determine if Aβ peptides were prominent antigens of protein A-bound IgG-antibodies, the fraction of co-precipitated Aβ peptides by urea-based SDS-PAGE/immunoblot were measured [16]. Figure 5a shows that indeed, the quintet of Aβ peptides (Aβ 1-37/38/39/40/42)[17] was detected in precipitated fractions, indicating the presence of Aβ-binding antibodies. Figure 5b shows that a significant ($p = 0.029$) decrease of Aβ 1-42 and surprisingly a significant ($p = 0.009$) increase of Aβ1-40 was found in the protein A bound IgG fraction in AD patients as compared to nAD controls. Figure 5c shows a

highly significant $p = 4.5 \times 10^{-8}$) 2.5 fold difference in the Aβ-42/40 ratios between AD patients and nAD controls that allowed clear separation of diagnostic groups without overlap. Noteworthy a subgroup of nAD controls without any cognitive deficits showed the highest values for the ratio of IgG-bound Aβ42/40, whereas two patients with Lewy body dementia were closest to the AD values (fig. 5c).

**Discussion**

Biomarkers in the CSF have become valuable tools in the early and reliable diagnosis of Alzheimer's disease and other dementias which is of importance to initiate suitable treatments. The levels of total tau protein, phospho-tau, and Aβ42 in CSF were shown to be of diagnostic value, in particular when evalutated in combination with each other[4]. Novel therapeutics for AD with strong disease modifying properties are expected to become available in the future, for review, see[18] and this will further emphasize the importance of accurate early diagnosis of AD and the predictive diagnosis of incipient AD in MCI patients.

In 1998, Pitschke and coworkers reported the detection of Aβ binding particles in CSF of AD patients by "seeded aggregation" of fluorescently labeled synthetic Aβ1-42* probes by confocal spectroscopy (ConSp). Importantly, these particles were claimed to exist exclusively in CSF from AD patients but not in samples from age matched controls, suggesting that they might be of diagnostic value. To the knowledge of the inventors, these highly promising findings have never been confirmed by other groups so far. Using an improved dynamic "flow through" setup, the detection probability for Aβ binding particles was substantially increased, and it was possible to detect 5-10 LAPs per minute, a frequency about 20 times higher than that reported in the original study. However, the exclusive confinement of LAPs to AD patients reported by Pitschke and colleagues could not be confirmed. Instead, large inter-individual variations with regard to the number of LAPs in CSF were observed independent of diagnosis. In order to

exclude auto-aggregates of synthetic Aβ1-42* probes, the threshold was raised threefold over background level, but again virtually no difference in average LAP frequency between AD patients and nAD subjects was found. Thus, ConSP as such is not suitable for use in AD diagnostics.

Confocal microscopy for single molecule imaging (ConIM) was used to classify distinct subtypes of LAPs, based on brightness, area, shape and texture. Accordingly, the total population of CSF LAPs in all patients of the available collective was analyzed by fully automated quantitative computer-assisted morphometry. By this, four different LAP subtypes were clearly identified in CSF samples.

Images of LAP-3 and LAP-4 subtypes showed large multicentric supermolecular –structures, composed of multiple smaller core units which were secondarily attached to each other. These structures resembled immune complexes which have been observed in autoimmune diseases and in antigen-antibody aggregates generated *in-vitro* [19]. LAP-3 and LAP-4 particles were substantially reduced after treatment of CSF samples with protein A coated magnetic beads, a finding that indicated the presence of immunoglobulins.

The elongated and relatively dim LAP-3 subtypes were not correlated to the diagnosis of the patients. LAP-4 subtypes were particularly interesting, because they were virtually absent in AD patients while they were detected in 42.1 % of all nAD controls.

Further support for the involvement of immunoglobulins in the composition of LAP-3 and LAP-4 subtypes came from the observation that LAP frequencies in CSF of nAD controls but not of AD patients, were positively correlated to immunoglobulin concentration. In addition significant correlations were observed between Aβ42, tau and LAPs in nAD controls. However, after Bonferroni correlation that accounts for multiple testing, only the the specific IgG/protein parameter remained significant. Several other CSF proteins and peptides did not show any

significant correlations (table 1), suggesting a high specificity. Next, protein A precipitation was performed and the protein A bound fraction was analyzed by SDS-PAGE-immunoblot. At least 5 Aβ-peptides corresponding to Aβ (1-42, 1-40, 1-39, 1-38 and 1-37) were detected in this fraction and all of them have been observed as regularly constituents of CSF[17].

Taken together, these findings suggest that LAP-3 and LAP-4 probably contain auto-antibodies against Aβ-peptides with their bound antigens. Naturally occurring auto-antibodies directed against Aβ-peptides were detected preferentially in CSF of nAD controls and with significantly lower titers in CSF from AD patients, however without diagnostic value because of considerable overlap between diagnostic groups [13]. When the amounts of Aβ42 and Aβ40 peptides in the protein A enriched fraction were compared, it became obvious that the relative contributions of these C-terminal variants showed significant differences between nAD controls and AD patients. The observation that immunoglobulin bound Aβ42 was lower in AD patients as compared to controls, probably reflects the well known general decrease in Aβ42 in CSF which could also be confirmed in the available collective by standard ELISA. It is also possible that the increased amount of IgG-bound Aβ1-42 in nAD controls indicates the presence of auto-antibodies against this highly amyloidogenic species which may protect from AD onset. Recently, Hock and coworkers showed that the presence of auto-antibodies against Aβ1-42 were not correlated to the therapeutic benefit of active Aβ1-42 immunization, but a specific subfraction of auto-anti-antibodies against aggregated plaque-derived Aβ1-42 was[20]. Further evidence for a protective role of Ab42 auto-antibodies comes from a large, long-term epidemiological study, which demonstrated that these auto-antibodies were commonly detected in plasma of AD patients and age-matched healthy subjects. In those cases where auto-antibodies did not prevent the outbreak of AD, this was explained by low antibody titers and inadequate affinity and avidity of the antibodies to their antigens [21]. Moreover, immune senescence was also frequently observed in aged people [22].

Several studies, performed by Elisa, indicated no change in Aβ1-40 concentration in AD [23,24]. Surprisingly, it was found that the amount of Aβ40 in the protein A enriched fraction was highly significant elevated in the AD patients. This observation supports the hypothesis that AD patients carry auto-antibodies against Aβ1-40 which do not protect them from AD. As a consequence from both observations, decreased Aβ42 plus increased Aβ40 in the immunoglobulin bound fraction, AD patients and nAD controls could be clearly discriminated without overlap when Aβ42/40 ratios were compared. This clear non-overlapping separation was found in spite of two LBD-patients included in the control group which are known to have also lower Aβ42/40 ratios [25]. Importantly, the discrimination was substantially better as compared to the discrimination on the basis of Aβ42/40 ratios calculated from standard ELISA tests.

In summary findings reported here provide evidence for a putative circulating immune (IgG)-based clearance system for soluble amyloidogenic proteins/peptides patrolling the central nervous system. A deficiency of this circulating IgG-clearance system in neurodegenerative disorders would result in increased tissue concentrations of soluble and finally precipitated amyloidogenic proteinaceous compounds but reduced concentrations of these amyloidogenic species within the clearing pool, e.g. IgG-bound Aβ1-42 in human body fluids. Future experiments might be directed towards a more detailed characterization of anti-Aβ auto-antibodies and the evaluation of their use for differential diagnosis of neurodegenerative disorders. Furthermore, the findings reported here are also be of interest in view of potential novel immunological therapeutic approaches for AD.

## Methods

### Patients

The experiments were performed as double blind trials. CSF was obtained from all patients by a lumbar puncture. CSF was centrifuged (1600 x g, 15 min, RT), aliquoted, immediately frozen and stored at −80°C until assay. The patients (*n*=33) were diagnosed according to the criteria of ICD-10 and National Institute of Neurological and Communicative Disorders and Stroke-Alzheimer's Disease and Related Disorders Association (NINCDS-ADRDA) [26]. The diagnostic work-up included either cranial CT or predominantly MRI and routine blood assays. The extensive neuropsychological characterisation of the dementia patients followed the diagnostic criteria of the German Competence Net Dementias [27]. Only patients with early dementias (Mini Mental State Examination ≥ 20) were included in the study. The patients were divided into 3 subgroups: (1) AD (n=14): This group comprised patients with AD (n=8) and AD of mixed type (n=6); (2) oD (n=13): A group of patients with dementia of other origin, including Morbus Pick's disease (n=3), Lewy-body-dementia (n=3), and vascular dementia (n=4); (3) Co (n=6): Non-demented disease controls, comprising patients with heterogenous neurological or psychiatric diseases but without memory complaints. The patient groups (2) and (3) were summarized as "nAD" in the course of this article. CSF dementia markers like Aβ1-40, Aβ1-42, total Tau and phospho-Tau181 were measured in all patients. CSF aliquots for the analysis of IgG-bound Aβ-peptides were available in 9 of the AD patients, 13 of the oD patients and 5 of the Co patients. The results are presented in table 3.

### Fluorescence labeling of synthetic Aβ1-42

The peptide was dissolved in water-free DMSO to a final concentration of 400 µM and centrifuged for 10 minutes at 14000 rpm at RT to remove large insoluble particles and kept

on ice during the course of the experiments. 1 mg FluorX (Amersham Biosciences, Freiburg, Germany) was dissolved in a total volume of 1 ml reaction buffer (50 mM $NaPO_3$, pH=9.2, 0.2% SDS) and 20 µg of peptide (11 µl) was add to 100 µl FluorX solution and 9 µl reaction buffer for 30 min at RT. FluorX –labeled Aβ1-42 was used in all experiments on the confocal spectroscopy setup.

For confocal imaging of LAPs, 20 µg Aβ1-42 were labeled with Cy3 (Amersham Biosciences, Freiburg, Germany) according to manufacturer's instruction. Fluorescent Aβ1-42 is indicated as "Aβ1-42*" in this article.

The conjugated Aβ1-42* was separated from free fluorescent label by NAP5 column (Amersham Biosciences, Freiburg, Germany). The sample (120 µl) was allowed to sink into the gel bed and was eluted with 5 ml elution buffer (10 mM $NaPO_3$, pH 7.2, 0.2% SDS, 200 mM NaCl). The fluorescence in the fractions was determined by Fluorescence Correlation Spectroscopy (FCS) by mixing of 2 µl Aβ1-42* with 20 µl physiological buffer. 10 FCS curves were recorded for 1 minute each. By means of this technique, the free fluorescent molecules could be clearly discriminated from Aβ1-42*, based on different diffusion coefficients. Fractions containing exclusively conjugates were pooled and centrifuged through Micropore Ultrafree MC (BioRad) sterile spin filter (0.22 µm) for 5 minutes at 14000 RPM in order to remove auto-aggregates of Aβ1-42*.

'Seeded aggregation' assay in CSF with Aβ1-42*

CSF was collected according to the standardized guidelines for CSF-collection and storage of the German Competence Net Dementias [27], centrifuged (1600 g, 15 min, RT) and immediately frozen (–80°C), and it was used in all experiments. After thawing, 20 µl CSF was mixed with 2 µl of Aβ1-42* and allowed to bind to LAPs for 15–25 minutes at room

temperature. In all confocal spectroscopy experiments, 20 µl were filled in the reservoir of the silicon elastomer microstructure which was connected to a microstructured channel. The confocal spot was centered 2-4 mm from the reservoir outlet of the channel in the middle of the channel. All experiments were performed as double blind trials in triplicate and baselines were normalized for analysis. The velocity of the sample (of 0.72 ± 0.20 mm/s) was controlled and recorded by FCS for each measurement [28]. All recorded data were normalized for different flow speeds by dividing the number of recorded fluorescent counts by the corresponding values from the FCS measurements.

Fast-flow confocal spectroscopy measurements

Fabrication of microstructures for fast-flow measurements was described in detail earlier [28,29]. In brief, the microstructures were cast from a silicone mold comprising the channel geometry and topology in the negative (upstanding) form. The silicon wafer was partly custom-made (GeSim, Großerkmannsdorf), coated with a thin 200-nm Teflon layer. The lengths of all microchannels were about 1.5 cm. Disposable microstructure channels could then easily be obtained by imprinting the complementary mold topology into silicon elastomer. In this routine, 2-3 ml of viscous elastomer kit (Sylgard 184, Dow Corning) was poured onto the silicon wafers and hardened on a heating plate for 30 min at 110 °C. The hardened silicon elastomer could then easily be peeled off the wafer, cut to the desired sizes, and punched at the end of the microchannels for filling-in of the Aβ-spiked CSF. Finally, it was sealed to a thin glass plate by manually pressing a coverslip of 170 µm thickness to the channel top, and mounted on an inverted microscope (Olympus IX 70).

The fluorescence from the flowing sample was detected in a self-made confocal setup. The 488 nm line of an Ar laser (Lasos, Jena, Germany) was adjusted into the microscope and focused by an objective (Olympus UplanApo 60 x, NA 1.2 W). Epifluorescence was collected

by an optical fiber, and detected by an avalanche photodiode (SPCM CD3017, EG&G, Canada). Optical filters were introduced into the beam path (dichroic mirror 496 DCLP, and band pass filter 525 DF 50, both AHF, Tübingen, Germany). FCS was performed with the correlator card ALV-5000 (ALV Langen, Germany).

Confocal imaging and quantification of LAPs

20 µl CSF sample was spiked with Aβ1-42*, as described above and transferred onto a cover slip. The spiked CSF drop was scanned by a confocal laser microscope (LS 410, Leica, Wetzlar, Germany) in the 2-line scan average mode, using the 543 nm line of the argon laser. An immersion objective Fluotar 63 x, a long pass filter LP 570 was used, the zoom was set to 8 in all experiments and the pinhole was set to 1 airy. 50 image planes, separated by 1 µm in Z-direction, were collected at 2 different areas of the drop, resulting in 2 image stacks that measured 30 x 30 x 100 µm. The image planes were processed and low-pass filtered with Metamorph® imaging software (Universal Imaging Co, USA). The 'Integrated Morphology Analysis' routine from Metamorph® determined automatically the area, shape, brightness and texture. The algorithm for quantification in brief: LAPs were detected by thresholding the image to a sensitivity of 10 % above the average background. Detected objects were then masked and the brightness (Σgray value / # of pixels) was calculated. The brightness was proportional to the amount of Aβ1-42*, bound to the LAP. The area of an object represented the sum of all pixels in calibrated units. The shape factor ($\frac{4\Pi A}{P^2}$), a value from 0 to 1, allowed to characterize an object as elongated = 0 or as a perfect circle = 1. The texture measured the uniformity of the gray levels in an object ($\sum_{i=1}^{N}\sum_{j=1}^{N}(i-j)^2 P_L\left(i/j\right)$). Objects with uniform gray level have a texture difference moment (TDM) close to 0 while objects with greater variation of gray level have a larger TDM value. These four parameters were recorded for every detected LAP and subtypes of LAPs were

characterized by setting specific parameter limits, examples were shown in table 2. These classifications were performed by a custom software ALDES, ver. 4.6.

Depletion of IgG from CSF and analysis of IgG-bound Aβ peptides

Magnetic microbeads (12.5 µL) pre-coated with protein A (Dynabeads® Protein A, Dynal, Germany) were transferred to a 1.5 ml reaction tube, briefly centrifuged and placed in a magnetic stand for one minute. The resulting supernatant was removed and 50 µL of CSF was added to the semi-dry beads. Samples were incubated at room temperature under rotation for 30 min, briefly centrifuged and magnetically collected. Bead-bound complexes were drawn to the side of the tube facing the magnet, and the CSF supernatant was removed with a pipette and used for further analysis. Beads were washed with 200 µl phosphate-buffered saline (PBS) / 0.1% bovine serum albumin (BSA). For Aβ SDS-PAGE / immunoblot, bound complexes were eluted by heating the sample at 95 °C for 5 min with 25 µl of sample buffer (0.36 M bis-Tris, 0.16 M N,N-bis- (2-hydroxyethyl)-glycine, 1% (w/v) SDS, 15% (w/v) sucrose, and 0.004% (w/v) bromphenol blue) [17,30]. Urea-based SDS-PAGE/immunoblot for Aβ peptide analysis was performed as described [30]

Quantification of routine CSF parameters and conventional neurochemical dementia markers

CSF concentrations of immunoglobulins, albumin, and total CSF-protein were measured, according to manufacturer's instructions by means of the following commercially available assays: Albumin, IgG, IgA and IgM were quantified by nephelometry with the Immunochemistry System IMMAGE™ (Beckman-Coulter, Krefeld, Germany) and total protein quantification was performed with the Tina-quant™ assay (Roche/Hitachi, Basel, Switzerland).

The neurochemical dementia markers Aβ1-42 and Aβ1-40 were determined by ELISA from

"The Genetics Company, Inc.", Schlieren, Switzerland and total Tau and phospho-Tau by ELISA from "Innogenetics", Gent, Belgium.

Data analysis and statistical calculation

Non-parametric statistical tests (rank correlation, Mann-Whitney-U, Kruskal – Wallis) were calculated with the statistical software package SPSS™ for Windows 12 (SPSS Inc., Chicago, Il, USA). Additionally, the significance of the correlation coefficients was adjusted for multiple testing by the Bonferroni method (p-values multiplied with factor 17). All tests were two-sided. The level of significance was set at $\alpha$=0.05.

## Tables

**Table 1:** Linear correlation between LAP frequency and CSF parameters

| | nAD patients | | AD patients | |
|---|---|---|---|---|
| **Parameter** | ***r*** | ***p*** | ***r*** | ***P*** |
| Aβ1-42 | 0.50 | 0.031* | -0.21 | 0.464 |
| Aβ1-40 | 0.43 | 0.073 | -0.28 | 0.364 |
| Protein | 0.29 | 0.223 | -0.14 | 0.642 |
| Albumin | 0.35 | 0.137 | -0.16 | 0.578 |
| Tau | 0.53 | 0.021* | 0.09 | 0.765 |
| pTau | 0.07 | 0.794 | 0.07 | 0.830 |
| IgG | 0.56 | 0.012* | -0.13 | 0.670 |
| IgM | 0.48 | 0.037* | 0 | 0.988 |
| IgA | 0.60 | 0.007** | 0.06 | 0.850 |
| Aβ1-42/1-40 | 0.27 | 0.283 | 0.02 | 0.957 |
| Aβ1-42/protein | 0.15 | 0.540 | -0.13 | 0.648 |
| Aβ1-40/protein | 0 | 0.987 | -0.10 | 0.748 |
| pTau/protein | -0.03 | 0.893 | 0.30 | 0.316 |
| IgG/protein | 0.83 | <0.001*** | 0.03 | 0.923 |
| IgG/albumin | 0.49 | 0.033* | 0.20 | 0.503 |
| IgM/protein | 0.43 | 0.069 | 0.15 | 0.615 |
| IgA/protein | 0.62 | 0.005** | 0.37 | 0.199 |

r = correlation coefficient, p = probability, calculated by Mann-Whitney U-test;

* = $p < 0.05$, ** = $p < 0.01$, *** = $p < 0.001$

5

**Table 2:** LAP definition by image-morphometry parameters

| LAP type | Area ($\mu m^2$) | Brightness (1-100) | Shape (0-1) | Texture (0-20) |
|---|---|---|---|---|
| Aβ-auto-aggregates | 0.01 – 0.20 | 1 – 25 | 0.2 - 1.0 | 2 - 20 |
| Type 1: pre-aggregated Aβ | 3.40 – 6.80 | 1 – 25 | 0.0 - 0.5 | 0 - 4.5 |
| Type 2: protein/albumin | 0.07 – 0.34 | 5 – 25 | 0.5 - 1.0 | 2 - 4.5 |
| Type 3:IgG- Aβ1-42 | 0.34 – 4.10 | 2 – 100 | 0.1 - 0.7 | 0 - 1.3 |
| Type 4:IgG- Aβ1-42 | 0.34 – 4.10 | 15 – 100 | 0.7 - 1.0 | 0 - 2.0 |

**Table 3:** Clinical diagnostic parameters

| Parameter | mean | s.d. | p-value |
|---|---|---|---|
| AD Aβ1-40 | 8042,4 (pg/ml) | 2785,19 | 0.167 |
| nAD Aβ1-40 | 6705,1 (pg/ml) | 2037,29 | |
| nAD Aβ1-42 | 439,2 (pg/ml) | 211,14 | >0.001 |
| nAD Aβ1-42 | 733,4 (pg/ml) | 291,93 | |
| AD Aβ1-42/1-40 | 0,054 | 0,0237 | >0.001 |
| nAD Aβ 1-42/1-40 | 0,116 | 0,0466 | |
| AD Tau | 697,92 (pg/ml) | 334,85 | >0.001 |
| nAD Tau | 273,73 (pg/ml) | 203,55 | |
| AD pTau | 93,48 (pg/ml) | 40,07 | >0.001 |
| nAD pTau | 41,21 (pg/ml) | 22,72 | |
| AD age | 70,6 (years) | 6,55 | 0.012 |
| nAD age | 58,8 (years) | 15,21 | |

AD men: 6, AD women:8; nAD men: 10, nAD women: 9

## References

1. Lewczuk, P. et al. Tau protein phosphorylated at threonine 181 in CSF as a neurochemical biomarker in Alzheimer's disease: original data and review of the literature. *Journal of Molecular Neuroscience* **23**, 115-122 (2004).

2. Kropp, S. et al. [Diagnostic steps in Alzheimer dementia before treatment with new antidimentives]. *Fortschr Neurol Psychiatr* **68**, 257-61. (2000).

3. Verbeek, M.M., De Jong, D. & Kremer, H.P. Brain-specific proteins in cerebrospinal fluid for the diagnosis of neurodegenerative diseases. *Ann Clin Biochem* **40**, 25-40 (2003).

4. Andreasen, N. & Blennow, K. CSF biomarkers for mild cognitive impairment and early Alzheimer's disease. *Clin Neurol Neurosurg* **107**, 165-73 (2005).

5. Wiltfang, J. et al. Beta-amyloid peptides in cerebrospinal fluid of patients with Creutzfeldt-Jakob disease. *Ann Neurol* **54**, 263-7 (2003).

6. Hulstaert, F. et al. Improved discrimination of AD patients using beta-amyloid(1-42) and tau levels in CSF. *Neurology* **52**, 1555-62. (1999).

7. Otto, M. et al. Decreased beta-amyloid1-42 in cerebrospinal fluid of patients with Creutzfeldt-Jakob disease. *Neurology* **54**, 1099-102. (2000).

8. Selkoe, D.J. Cell biology of the amyloid beta-protein precursor and the mechanism of Alzheimer's disease. *Annu Rev Cell Biol* **10**, 373-403 (1994).

9. Antzutkin ON, B.J., Tycko R. Site-specific identification of non-beta-strand conformations in Alzheimer's beta-amyloid fibrils by solid-state NMR. *Biophysical Journal* **84**, 3326-3335. (2003).

10. Pitschke, M., Prior, R., Haupt, M. & Riesner, D. Detection of single amyloid beta-protein aggregates in the cerebrospinal fluid of Alzheimer's patients by

fluorescence correlation spectroscopy. *Nat Med* **4**, 832-4. (1998).

11. Atwood, C.S., Martins, R.N., Smith, M.A. & Perry, G. Senile plaque composition and posttranslational modification of amyloid-beta peptide and associated proteins. *Peptides* **23**, 1343-50 (2002).

12. Schwille, P., Bieschke, J. & Oehlenschlager, F. Kinetic investigations by fluorescence correlation spectroscopy: the analytical and diagnostic potential of diffusion studies. *Biophys Chem* **66**, 211-28. (1997).

13. Du, Y. et al. Reduced levels of amyloid beta-peptide antibody in Alzheimer disease. *Neurology* **57**, 801-5 (2001).

14. Schenk, D. et al. Immunization with amyloid-beta attenuates Alzheimer-disease-like pathology in the PDAPP mouse. *Nature* **400**, 173-7 (1999).

15. Hock, C. et al. Generation of antibodies specific for beta-amyloid by vaccination of patients with Alzheimer disease. *Nat Med* **8**, 1270-5 (2002).

16. Klafki, H.W., Wiltfang, J. & Staufenbiel, M. Electrophoretic separation of betaA4 peptides (1-40) and (1-42). *Anal Biochem* **237**, 24-9. (1996).

17. Wiltfang, J. et al. Highly conserved and disease-specific patterns of carboxyterminally truncated Abeta peptides 1-37/38/39 in addition to 1-40/42 in Alzheimer's disease and in patients with chronic neuroinflammation. *J Neurochem* **81**, 481-96. (2002).

18. Citron, M. Strategies for disease modification in Alzheimer's disease. *Nat Rev Neurosci* **5**, 677-85 (2004).

19. Ljunghusen, O., Johansson, A. & Skogh, T. Hepatic immune complex elimination studied with FITC-labelled antigen. *J Immunol Methods* **128**, 1-7 (1990).

20. Hock, C. et al. Antibodies against beta-amyloid slow cognitive decline in Alzheimer's disease. *Neuron* **38**, 547-54 (2003).

21. Hyman, B.T. et al. Autoantibodies to amyloid-beta and Alzheimer's disease. *Ann Neurol* **49**, 808-10 (2001).

22. Pawelec, G., Adibzadeh, M., Pohla, H. & Schaudt, K. Immunosenescence: ageing of the immune system. *Immunol Today* **16**, 420-2 (1995).

23. Shoji, M. et al. Combination assay of CSF tau, A beta 1-40 and A beta 1-42(43) as a biochemical marker of Alzheimer's disease. *J Neurol Sci* **158**, 134-40 (1998).

24. Mehta, P.D. et al. Plasma and cerebrospinal fluid levels of amyloid beta proteins 1-40 and 1-42 in Alzheimer disease. *Arch Neurol* **57**, 100-5 (2000).

25. Lewczuk, P. et al. Neurochemical diagnosis of Alzheimer's dementia by CSF Abeta42, Abeta42/Abeta40 ratio and total tau. *Neurobiol Aging* **25**, 273-81 (2004).

26. McKhann, G. et al. Clinical diagnosis of Alzheimer's disease: report of the NINCDS-ADRDA Work Group under the auspices of Department of Health and Human Services Task Force on Alzheimer's Disease. *Neurology* **34**, 939-44. (1984).

27. KND. German Competence Nets Dementia, http://www.kompetenznetze.de/navi/de/Kompetenznetze/demenzen.html. (2002).

28. Dittrich, P.S. & Schwille, P. An integrated microfluidic system for reaction, high-sensitivity detection, and sorting of fluorescent cells and particles. *Anal Chem* **75**, 5767-74 (2003).

29. Dittrich, P.S. & Schwille, P. Spatial two-photon fluorescence cross-correlation spectroscopy for controlling molecular transport in microfluidic structures. *Anal Chem* **74**, 4472-9 (2002).

30. Wiltfang, J. et al. Molecular biology of Alzheimer's dementia and its clinical relevance to early diagnosis and new therapeutic strategies. *Gerontology* **47**, 65-71. (2001).

## CLAIMS

1. A method of analyzing a sample obtained from a patient for indications that the patient has or is susceptible to Alzheimer's dementia, the method comprising the step of determining at least one concentration in the sample, the concentration being selected from the group of concentrations

- of Aβ-peptide- and immunoglobulin-including particles,
- of immunoglobulin-bound Aβ-peptides, and
- of Aβ-peptide-bound immunoglobulins.

2. The method of claim 1, wherein the sample includes cerebrospinal fluid.

3. The method of claim 1 or 2, wherein the at least one concentration is selected from the group of concentrations consisting

- of concentrations of Aβ1-42-peptide- and immunoglobulin-including particles,
- of a concentration of immunoglobulin-bound Aβ1-42-peptides,
- of a concentration of immunoglobulin-bound Aβ1-40-peptides, and
- of concentrations of immunoglobulins bound to Aβ1-40-peptides and Aβ1-42-peptides.

4. The method of claim 3, wherein the concentration of Aβ1-42-peptide- and immunoglobulin-including particles is a concentration of immunoglobulin-including large Aβ1-42-peptide-binding particles (LAPs).

5. The method of claim 4, wherein the concentration of immunoglobulin-including LAPs is a concentration of LAPs of a LAP-subtype having a round shape in single molecule imaging, the round shape showing a shape-parameter in image morphometry of at least 0.7.

6. The method of claim 1, 2 or 3, wherein a fraction binding to an immunoglobulin-binding substance is separated from the remainder of the sample.

7. The method of claim 6, wherein a ratio Aβ42/40 of the concentrations of the Aβ1-42-peptides and of the Aβ1-40-peptides is determined in the fraction of the sample.

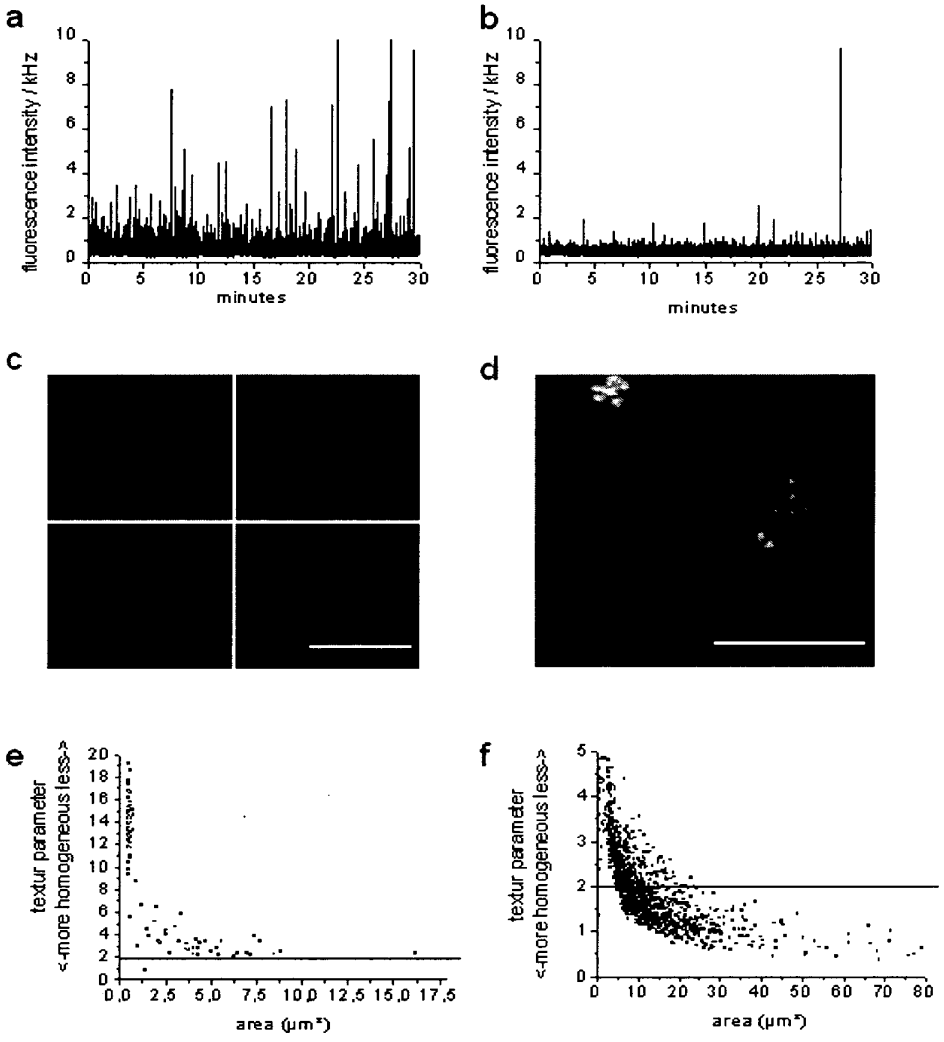
8. The method of claim 7, wherein a threshold value within a range of 0.12 to 0.20 is set to determine whether the ratio Aβ42/40 in the fraction of the sample is indicative of the patient having Alzheimer's dementia.

9. An assay for analyzing a sample obtained from a patient for indications that the patient has or is susceptible to Alzheimer's dementia, the assay comprising an immunoglobulin-binding substance for separating a fraction binding to this substance from the remainder of the sample, and two marker substances which selectively bind to Aβ1-40-peptides and Aβ1-42-peptides in the fraction of the sample bound to the immunoglobulin-binding substance and which allow for a determination of the concentrations of the Aβ1-40-peptides and of the Aβ1-42-peptides in the fraction of the sample.

10. A method of producing an immune therapy agent suitable for treating or preventing Alzheimer's dementia, the method comprising the step of purifying an immunoglobulin from a subtype of immunoglobulin-including large Aβ1-42-peptide-binding particles (LAPs) having a round shape in single molecule imaging.

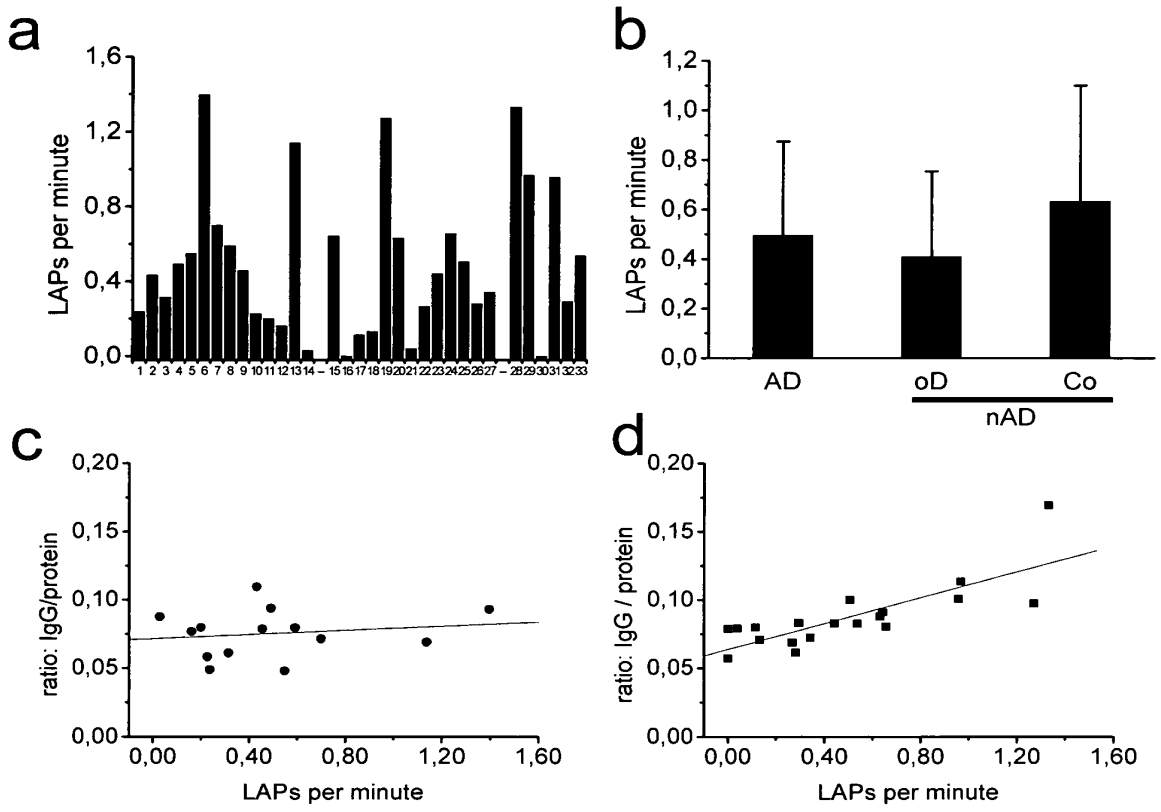
1/5

**Fig. 1**


a
b
fluorescence intensity / kHz
minutes
c
d
e
f
textur parameter
<-more homogeneous less->
area (µm²)

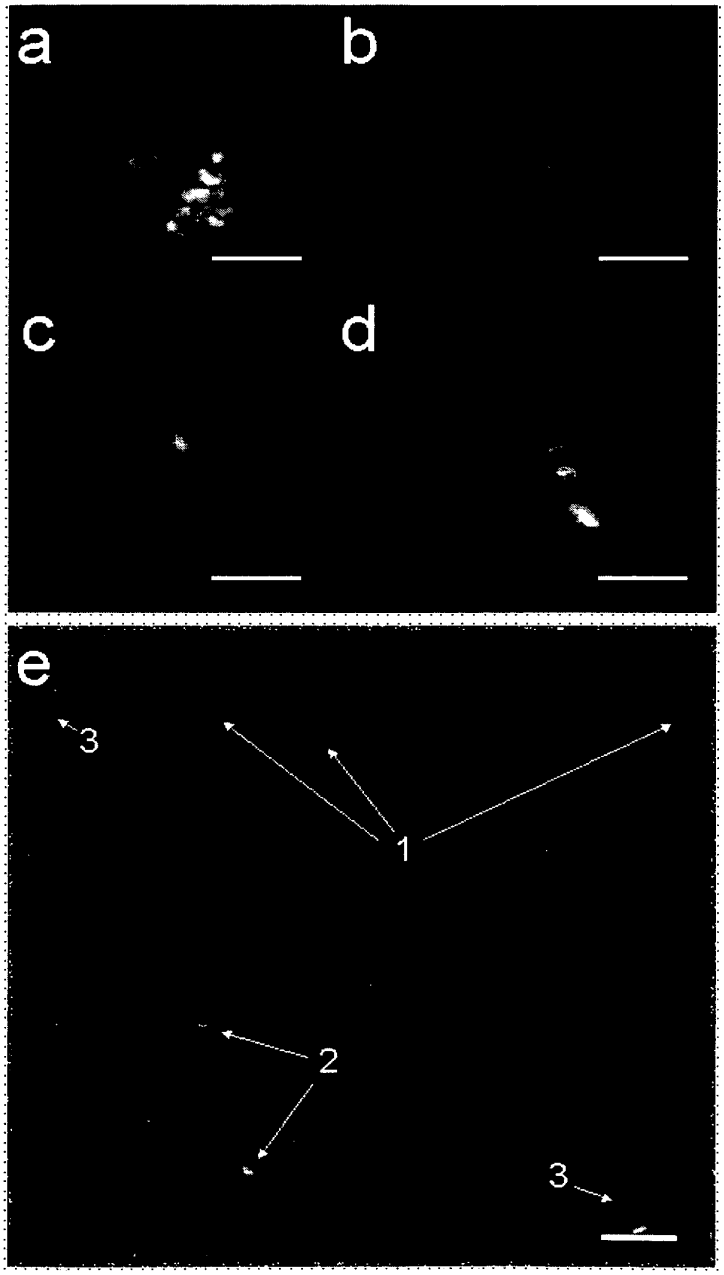
2/5

**Fig. 2**


a
LAPs per minute
1,6
1,2
0,8
0,4
0,0
1 2 3 4 5 6 7 8 9 10 11 12 13 14 – 15 16 17 18 19 20 21 22 23 24 25 26 27 – 28 29 30 31 32 33
b
LAPs per minute
1,2
1,0
0,8
0,6
0,4
0,2
0,0
AD
oD
Co
nAD
c
ratio: IgG/protein
0,20
0,15
0,10
0,05
0,00
0,00
0,40
0,80
1,20
1,60
LAPs per minute
d
ratio: IgG / protein
0,20
0,15
0,10
0,05
0,00
0,00
0,40
0,80
1,20
1,60
LAPs per minute

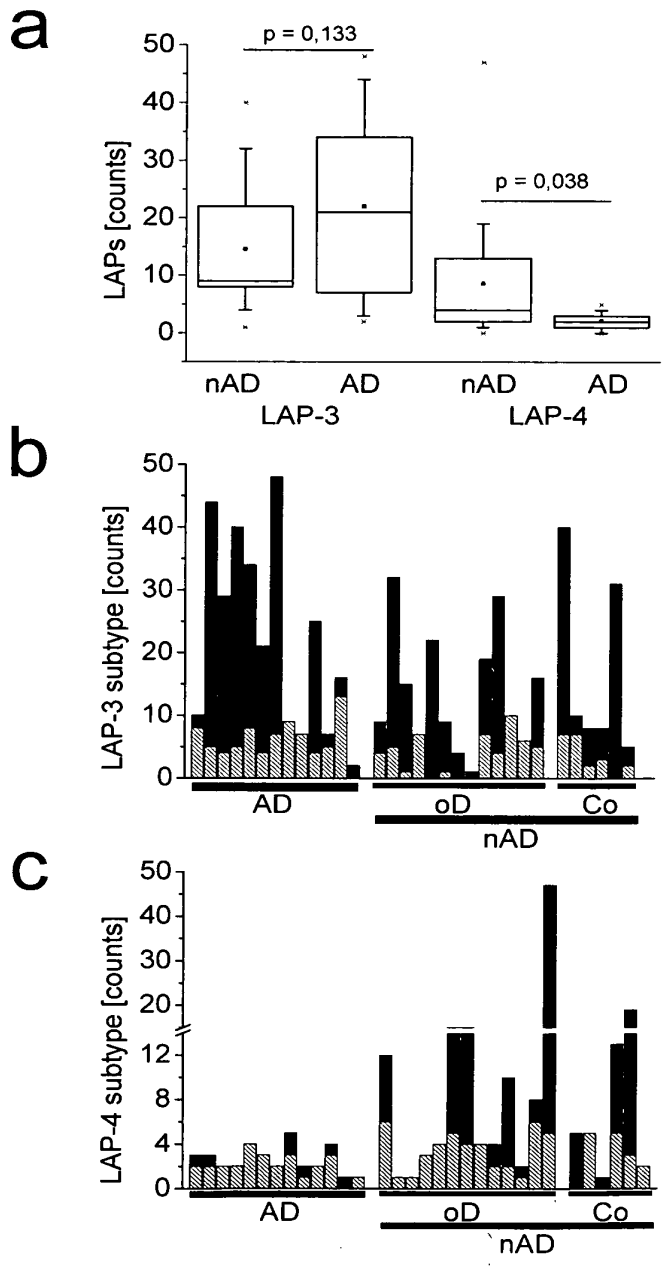
3/5

**Fig. 3**



4/5

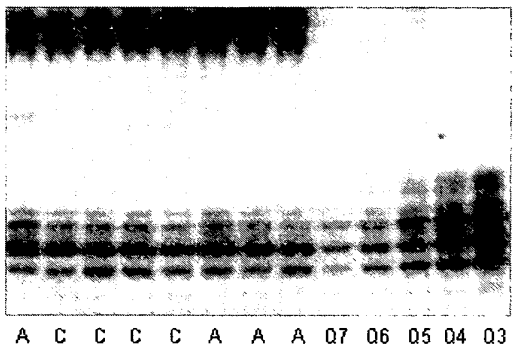
**Fig. 4**


a
p = 0,133
p = 0,038
LAPs [counts]
50
40
30
20
10
0
nAD
AD
nAD
AD
LAP-3
LAP-4
b
LAP-3 subtype [counts]
50
40
30
20
10
0
AD
oD
Co
nAD
c
LAP-4 subtype [counts]
50
40
30
20
12
8
4
0
AD
oD
Co
nAD

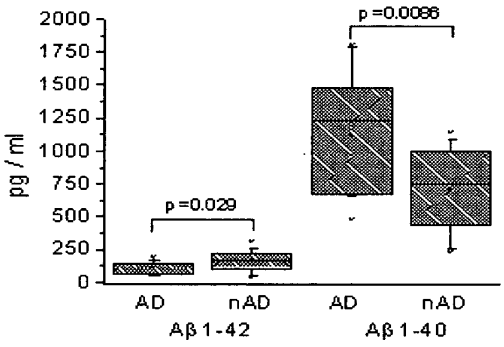
5/5

**Fig 5**

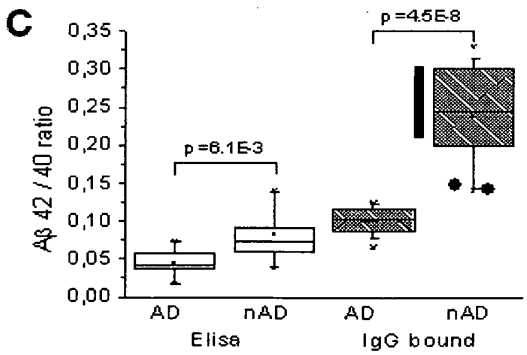
a


A C C C C A A A Q7 Q6 Q5 Q4 Q3

b


pg / ml
2000
1750
1500
1250
1000
750
500
250
0
p =0.0086
p =0.029
AD
nAD
AD
nAD
Aβ 1-42
Aβ 1-40

c


Aß 42 / 40 ratio
0,35
0,30
0,25
0,20
0,15
0,10
0,05
0,00
p =4.5E-8
p =6.1E-3
AD
nAD
AD
nAD
Elisa
IgG bound

# INTERNATIONAL SEARCH REPORT

International application No
PCT/EP2007/000423

A. CLASSIFICATION OF SUBJECT MATTER
INV. G01N33/68 C07K16/00

According to International Patent Classification (IPC) or to both national classification and IPC

B. FIELDS SEARCHED

Minimum documentation searched (classification system followed by classification symbols)
G01N

Documentation searched other than minimum documentation to the extent that such documents are included in the fields searched

Electronic data base consulted during the international search (name of data base and, where practical, search terms used)
EPO-Internal, PAJ, WPI Data, BIOSIS

C. DOCUMENTS CONSIDERED TO BE RELEVANT

| Category* | Citation of document, with indication, where appropriate, of the relevant passages | Relevant to claim No. |
|---|---|---|
| X | TSUYOSHI ISHII ET AL: "IDENTIFICATION OF COMPONENTS OF IMMUNOGLOBULINS IN SENILE PLAQUES BY MEANS OF FLUORESCENT ANTIBODY TECHNIQUE" ACTA NEUROPATHOLOGICA, SPRINGER VERLAG, BERLIN, DE, vol. 32, no. 2, 11 August 1975 (1975-08-11), pages 157-162, XP009013619 ISSN: 0001-6322 abstract page 158, lines 9-12; figure 1a | 1-4,6-10 |

-/--

[X] Further documents are listed in the continuation of Box C.

[X] See patent family annex.

* Special categories of cited documents :

"A" document defining the general state of the art which is not considered to be of particular relevance

"E" earlier document but published on or after the international filing date

"L" document which may throw doubts on priority claim(s) or which is cited to establish the publication date of another citation or other special reason (as specified)

"O" document referring to an oral disclosure, use, exhibition or other means

"P" document published prior to the international filing date but later than the priority date claimed

"T" later document published after the international filing date or priority date and not in conflict with the application but cited to understand the principle or theory underlying the invention

"X" document of particular relevance; the claimed invention cannot be considered novel or cannot be considered to involve an inventive step when the document is taken alone

"Y" document of particular relevance; the claimed invention cannot be considered to involve an inventive step when the document is combined with one or more other such documents, such combination being obvious to a person skilled in the art.

"&" document member of the same patent family

| Date of the actual completion of the international search | Date of mailing of the international search report |
|---|---|
| 20 June 2007 | 28/06/2007 |

| Name and mailing address of the ISA/ | Authorized officer |
|---|---|
| European Patent Office, P.B. 5818 Patentlaan 2<br>NL – 2280 HV Rijswijk<br>Tel. (+31-70) 340-2040, Tx. 31 651 epo nl,<br>Fax: (+31-70) 340-3016 | VADOT-VAN GELDRE, E |

Form PCT/ISA/210 (second sheet) (April 2005)



Fujirebio Diagnostics, Inc. v. Quanterix Corp.
EX-1045
5747

# INTERNATIONAL SEARCH REPORT

International application No
PCT/EP2007/000423

C(Continuation). DOCUMENTS CONSIDERED TO BE RELEVANT

| Category* | Citation of document, with indication, where appropriate, of the relevant passages | Relevant to claim No. |
|---|---|---|
| X | KAMETANI F ET AL: "A MONOCLONAL ANTIBODY HY20-54-16-3L TO LAMBDA (LAMBDA) LIGHT CHAIN OF HUMAN IMMUNOGLOBULIN REACTS WITH AMYLOID IN ALZHEIMER'S DISEASE BRAIN" NEUROSCIENCE LETTERS, LIMERICK, IE, vol. 117, no. 1/2, 4 September 1990 (1990-09-04), pages 62-67, XP009013620 ISSN: 0304-3940 | 1-4,6-10 |
| A | abstract; figure 3 page 65, lines 14-22 page 66, lines 9-11 | 5 |
| | ----- | |
| X | PARDRIDGE W M ET AL: "HIGH MOLECULAR WEIGHT ALZHEIMER'S DISEASE AMYLOID PEPTIDE IMMUNOREACTIVITY IN HUMAN SERUM AND CSF IS AN IMMUNOGLOBULIN G" BIOCHEMICAL AND BIOPHYSICAL RESEARCH COMMUNICATIONS, ACADEMIC PRESS INC. ORLANDO, FL, US, vol. 145, no. 1, 29 May 1987 (1987-05-29), pages 241-248, XP008019434 ISSN: 0006-291X page 246, last paragraph - page 247, paragraph 1 abstract | 1-4,6-10 |
| | ----- | |
| X | EIKELENBOOM P ET AL: "IMMUNOGLOBULINS AND COMPLEMENT FACTORS IN SENILE PLAQUES AN IMMUNOPEROXIDASE STUDY" ACTA NEUROPATHOLOGICA, SPRINGER VERLAG, BERLIN, DE, vol. 57, no. 2/3, 1982, pages 239-242, XP008019447 ISSN: 0001-6322 abstract page 239, column 1 page 240, column 1, last paragraph - column 2, paragraph 1 | 1-4,6-10 |
| | ----- | |
| X | PITSCHKE M ET AL: "DETECTION OF SINGLE AMYLOID BETA-PROTEIN AGGREGATES IN THE CEREBROSPINAL FLUID OF ALZHEIMER'S PATIENTS BY FLUORESCENCE CORRELATION SPECTROSCOPY" NATURE MEDICINE, NATURE PUBLISHING GROUP, NEW YORK, NY, US, vol. 4, no. 7, July 1998 (1998-07), pages 832-834, XP001073409 ISSN: 1078-8956 cited in the application page 833, column 2, paragraph 3; figures 2,3 | 1-4,6-10 |
| | ----- | |
| | -/-- | |



Fujirebio Diagnostics, Inc. v. Quanterix Corp.
EX-1045
5748

# INTERNATIONAL SEARCH REPORT

International application No
PCT/EP2007/000423

C(Continuation). DOCUMENTS CONSIDERED TO BE RELEVANT

| Category* | Citation of document, with indication, where appropriate, of the relevant passages | Relevant to claim No. |
|---|---|---|
| X | BARELLI H ET AL: "CHARACTERIZATION OF NEW POLYCLONAL ANTIBODIES SPECIFIC FOR 40 AND 42 AMINO ACID-LONG AMYLOID BETA PEPTIDES: THEIR USE TO EXAMINE THE CELL BIOLOGY OF PRESENILINS AND THE IMMUNOHISTOCHEMISTRY OF SPORADIC ALZHEIMER'S DISEASE AND CEREBRAL AMYLOID ANGIOPATHY CASES" MOLECULAR MEDICINE, BLACKWELL SCIENCE, CAMBRIDGE, MA, US, vol. 3, no. 10, October 1997 (1997-10), pages 695-707, XP001030449 ISSN: 1076-1551 figure 5 | 9 |
| X | NUNAN JANELLE ET AL: "The C-terminal fragment of the Alzheimer's disease amyloid protein precursor is degraded by a proteasome-dependent mechanism distinct from gamma-secretase" EUROPEAN JOURNAL OF BIOCHEMISTRY, vol. 268, no. 20, October 2001 (2001-10), pages 5329-5336, XP002437217 ISSN: 0014-2956 page 5330, column 2, paragraph 3; figure 1 | 9 |
| A | US 2003/166019 A1 (WILTFANG JENS ET AL) 4 September 2003 (2003-09-04) cited in the application paragraphs [0014], [0018], [0025]; figures 4,5,12 | 1-10 |
| A | GEYLIS V ET AL: "Human monoclonal antibodies against amyloid-beta from healthy adults" NEUROBIOLOGY OF AGING, TARRYTOWN, NY, US, vol. 26, no. 5, May 2005 (2005-05), pages 597-606, XP004748495 ISSN: 0197-4580 page 599, paragraph 3.2 | 10 |



Fujirebio Diagnostics, Inc. v. Quanterix Corp.
EX-1045
5749

# INTERNATIONAL SEARCH REPORT

**Information on patent family members**

**International application No**
PCT/EP2007/000423

| Patent document cited in search report | Publication date | Patent family member(s) | Publication date |
|---|---|---|---|
| US 2003166019 A1 | 04-09-2003 | AT 277952 T | 15-10-2004 |
| | | DE 50103881 D1 | 04-11-2004 |
| | | EP 1270592 A1 | 02-01-2003 |
| | | ES 2228697 T3 | 16-04-2005 |
| | | JP 2003012700 A | 15-01-2003 |



Fujirebio Diagnostics, Inc. v. Quanterix Corp.
EX-1045
5750

(12) INTERNATIONAL APPLICATION PUBLISHED UNDER THE PATENT COOPERATION TREATY (PCT)

(19) World Intellectual Property Organization
International Bureau

(43) International Publication Date
9 August 2007 (09.08.2007)

PCT

(10) International Publication Number
WO 2007/090126 A2

(51) International Patent Classification: Not classified

(21) International Application Number:
PCT/US2007/061321

(22) International Filing Date: 30 January 2007 (30.01.2007)

(25) Filing Language: English

(26) Publication Language: English

(30) Priority Data:
60/763,247 30 January 2006 (30.01.2006) US

(71) Applicant *(for all designated States except US)*: **INVITROGEN CORPORATION** [US/US]; 1600 Faraday Avenue, Carlsbad, California 92008 (US).

(72) Inventors; and

(75) Inventors/Applicants *(for US only)*: **BEERNICK, Hans T.** [US/US]; 5977 Palomar Circle, CamariLLo, California 93012 (US). **BRODEY, Mary M.** [US/US]; 9554 Coosa Street, Ventura, California 93004 (US).

(74) Agent: **ANDERSON, Koren J.**; Invitrogen Corporation, c/o intellevate, P.O. Box 52050, Minneapios. Minnesota 55402 (US).

(81) Designated States *(unless otherwise indicated, for every kind of national protection available)*: AE, AG, AL, AM, AT, AU, AZ, BA, BB, BG, BR, BW, BY, BZ, CA, CH, CN, CO, CR, CU, CZ, DE, DK, DM, DZ, EC, EE, EG, ES, FI, GB, GD, GE, GH, GM, GT, HN, HR, HU, ID, IL, IN, IS, JP, KE, KG, KM, KN, KP, KR, KZ, LA, LC, LK, LR, LS, LT, LU, LV, LY, MA, MD, MG, MK, MN, MW, MX, MY, MZ, NA, NG, NI, NO, NZ, OM, PG, PH, PL, PT, RO, RS, RU, SC, SD, SE, SG, SK, SL, SM, SV, SY, TJ, TM, TN, TR, TT, TZ, UA, UG, US, UZ, VC, VN, ZA, ZM, ZW.

(84) Designated States *(unless otherwise indicated, for every kind of regional protection available)*: ARIPO (BW, GH, GM, KE, LS, MW, MZ, NA, SD, SL, SZ, TZ, UG, ZM, ZW), Eurasian (AM, AZ, BY, KG, KZ, MD, RU, TJ, TM), European (AT, BE, BG, CH, CY, CZ, DE, DK, EE, ES, FI, FR, GB, GR, HU, IE, IS, IT, LT, LU, LV, MC, NL, PL, PT, RO, SE, SI, SK, TR), OAPI (BF, BJ, CF, CG, CI, CM, GA, GN, GQ, GW, ML, MR, NE, SN, TD, TG).

**Published:**
— *without international search report and to be republished upon receipt of that report*

*For two-letter codes and other abbreviations, refer to the "Guidance Notes on Codes and Abbreviations" appearing at the beginning of each regular issue of the PCT Gazette.*

WO 2007/090126 A2

(54) Title: COMPOSITIONS AND METHODS FOR DETECTING AND QUANTIFYING TOXIC SUBSTANCES IN DISEASE STATES

(57) Abstract: The present invention relates to compositions comprising synthetic aggregated peptides (SAPs). The present invention also relates to the use of these SAPs as standards in methods for quantifying substances in a sample. The present invention also relates to methods of detecting, diagnosing and monitoring the progression of an abnormal condition in a subject with the methods comprising determining levels of an aggregated biomarker in a subject by measuring levels of the aggregated biomarker in the subject and correlating these levels to a standard curve, where the standard curve is established using a SAP peptide as the standard.

# COMPOSITIONS AND METHODS FOR DETECTING AND QUANTIFYING TOXIC SUBSTANCES IN DISEASE STATES

## Background of the Invention

*Cross Reference to Related Applications*

**[0001]** This application claims priority to U.S. Provisional Application No. 60/763,247, filed January 30, 2006, the contents of which are incorporated by reference as if set forth fully herein.

*Field of the Invention*

[0002] The present invention relates to compositions comprising synthetic aggregate peptides ("SAP peptides or SAPs"). The present invention also relates to the use of these SAPs as standards in methods for quantifying substances in a sample. The present invention also relates to methods of detecting, diagnosing and monitoring the progression of an abnormal condition in a subject with the methods comprising determining levels of an aggregated biomarker in a subject by measuring levels of the aggregated biomarker in the subject and correlating these levels to a standard curve, where the standard curve is established using a SAP peptide as the standard. The present invention also provides a method of screening antibodies and chemical compounds as potential therapeutics developed for the treatment, prevention or diagnosis of abnormal conditions involving aggregated biomarkers.

*Background of the Invention*

**[0003]** Aggregated peptides are gaining recognition as potential toxins involved in a variety of disease states. For example, there is increasing evidence that soluble aggregates of beta-amyloid (Aβ) (1-42) may be responsible for neuronal cell death in Alzheimer's rather than plaques. Interestingly, Aβ is present in Alzheimer-related plaques formation, but it is present in the well-known fibrillized form as well as smaller oligomeric forms.

**[0004]** Similarly, aggregates of alpha-synuclein are being implicated in cell death associated with Parkinson's disease; aggregates of huntingtin peptide are being implicated in cell death associated with Huntington's Disease and aggregates of superoxide dismutase 1 are being implicated in cell death associated with amyotropic lateral sclerosis (ALS). Aggregates of prion protein are implicated in several prion diseases, such as bovine spongiform encephalopathy, variant Creutzfeldt-Jakob disease, Gerstmann-Sträussler-Scheinke Syndrome, Fatal Familial Insomnia, kuru, scrapie, transmissible mink encephalopathy, chronic wasting disease of cervids, feline spongiform encephalopathy, exotic ungulate encephalopathy, and prion–mediated protein misfolding in yeast and other organisms. Aggregates of stefin B are implicated in myoclonus epilepsy. Aggregates of tau are implicated in frontotemporal dementia/tauopathy. Aggregates of transthyretin are implicated in senile systemic amyloidosis and familial amyloid polyneuropathy. Aggregates of ataxin-1 are implicated in spinocerebellar ataxia type-1. Aggregates of gelsolin are implicated in familial amyloidosis of the Finnish type. Aggregates of BRI are implicated in familial Brisith dementia. In fact, aggregated peptides are now being implicated in other disease states. In heart disease, aggregated HSP is implicated in desmin-related cardiomyopathy. Aggregates of alphaB crystallin are implicated in desmin-related cardiomyopathy, dilated cardiomyopathy, and hypertrophic cardiomyopathy. Aggregates of amylin as well as islet amyloid peptide are implicated in type II diabetes melletis. Aggregates of beta2-microglobulin are implicated in a systemic amyloidosis known as dialysis-related amyloidosis. Aggregates immunoglobulin light chain are implicated in a systemic amyloidosis known as light-chain amyloidosis. Aggregates of antithrombin are implicated in thrombosis. Protein aggregates are also implicated in cystic fibrosis, rheumatoid arthritis, and cirrhosis of the liver.

**[0005]** With the increased awareness that these aggregated proteins may be playing a role in disease states, it becomes increasingly important to accurately measure these aggregated peptides. Indeed, to aid in the diagnosis and monitoring of patients suffering from or at risk of suffering from a disease state characterized by the presence of these aggregated peptides, it is becoming critical to quantitatively assess levels of these aggregated peptides. To that end, peptide standards are needed to standardize and calibrate assays used to quantify these aggregated peptides.



Fujirebio Diagnostics, Inc. v. Quanterix Corp.
EX-1045
5753

**[0006]** There are, however, difficulties in obtaining pure forms of the aggregated peptides to use as standards in these developing assays. First, the general structure of the aggregated peptides themselves makes these compositions highly soluble. The high solubility of these aggregated peptides, in turn, makes it quite challenging to isolate large enough quantities of sufficiently purified aggregated peptides that can be used as standards in quantitative assays. Aggregated peptides are generally held together by non-covalent interaction, thus making the aggregates dynamic in size and complexity. Recent evidence, however, suggests that cytotoxic forms of aggregates may be more homogeneous in nature, yet purification and storage of these components is, in fact, complicated by the dynamic nature of aggregate assembly. In addition, these aggregated peptides often do not survive the freeze-thaw cycle, thus putting a damper on the number of assays that can be standardized with a single lot of isolated aggregated peptide.

**[0007]** What is needed in the art, therefore, is a synthetic standard that circumvents these difficulties in using isolated, naturally occurring aggregated peptides. The standards should be easy to synthesize, stable over time, stable within solution, and able to withstand repeated freeze-thaw cycles. In addition, it is critical that the synthetic standard present an epitope to an antibody or aptamer that is identical to or closely mimics the naturally occurring epitope present on the aggregated peptide.

## Summary of the Invention

**[0008]** The present invention relates to methods for quantifying a known biomarker in a sample, with the methods comprising an assay that compares the binding activity of a binding agent towards the known biomarker with the binding activity of the binding agent towards a composition comprising a branched synthetic aggregate peptide (SAP peptide or SAP).

**[0009]** The present invention also relates to methods of detecting and diagnosing an abnormal condition is a subject, with the methods comprising detecting the binding activity of a binding agent towards at least one standard to establish a standard curve, where the standard comprises a SAP peptide. The methods further comprise contacting a sample from the subject with at least one binding agent that is capable of binding an aggregated biomarker, detecting the level binding activity of the binding agent in the sample and correlating the binding activity in the sample to the established standard curve to determine the levels of the aggregated biomarker in the subject.



Fujirebio Diagnostics, Inc. v. Quanterix Corp.
EX-1045
5754

The determined levels of the aggregated biomarker, using SAP as a standard, are then compared to normal levels of the aggregated biomarker to determine if a difference exists between the measured levels of the aggregated biomarker and normal levels of the aggregated biomarker.

**[0010]** The present invention also relates to methods of monitoring the progression of an abnormal condition in a subject and methods of monitoring the efficacy of a treatment in a subject with an abnormal condition, with the methods comprising detecting the binding activity of a binding agent towards at least one standard to establish one or more standard curves, where the standard comprises a SAP peptide. The methods further comprise contacting more than one sample from a subject with at least one binding agent that is capable of binding an aggregated biomarker, where the multiple samples are taken from the subject at different time points. The level binding activity of the binding agent in the samples is detected and the binding activity in each sample is correlated to the established standard curve(s) to determine the levels of the aggregated biomarker in the subject. The determined levels of the aggregated biomarker from each time point, using SAP as a standard, are then compared to each other to determine if the measured levels of the aggregated biomarker are changing over time.

**[0011]** The present invention also relates to compositions comprising a branched SAP peptide, where at least one branch of the SAP peptide comprises the N-terminus of amyloid beta peptide.

## Brief Description of the Drawings

**[0012]** FIGURE 1 depicts one specific embodiment of the present invention, which is a 4-branched SAP peptide. The particular embodiment depicted is commonly referred to as a multiple antigenic peptide (or MAP). The MAP core comprises a β-alanine amino acid with a single lysine. The amino group of the β-alanine is attached through the α-carboxyl group of the lysine residue. The lysine provides two amino groups for attachment of additional residues. To each of the amine groups is attached an additional lysine residue, expanding the number of amine terminals to four. One or more peptide chains of interest can then be covalently attached to each of the 4 amino terminals. In this way, the MAP may comprise 4 separate peptide chains of interest. A MAP with 8 branches would be established by adding one additional layer of lysine residues to the 4 amino terminals prior to attachment of any peptide chains of interest. MAPs



Fujirebio Diagnostics, Inc. v. Quanterix Corp.
EX-1045
5755

with 16, 32, 64 or more branches would be established by adding subsequent layers of lysine residues to the core structure prior to addition of any peptide(s) of interest.

**[0013]** FIGURE 2 depicts a standard curve generated using one embodiment of MAP peptides presented herein. The standard curve generated using the MAP peptide comprising the N-terminus (1-20) of the amyloid beta peptide on each of the 4 arms of the MAP (MAP-$A\beta_{1-20}$) closely mimics that standard curve generated using pure aggregated amyloid beta (1-42) peptide.

**[0014]** FIGURE 3 depicts the results of an assay measuring levels of aggregated amyloid beta in subjects with a standard curve generated with MAP-$A\beta_{1-20}$ peptide.

**[0015]** FIGURE 4 depicts the results of an assay measuring levels of aggregated amyloid beta in subjects with a standard curve generated with MAP-$A\beta_{1-20}$ peptide.

**[0016]** FIGURE 5 depicts the time course for aggregation of alpha-synuclein in laboratory conditions at 37°C.

**[0017]** FIGURE 6 depicts a standard curve generated using one embodiment of MAP peptides presented herein. The standard curve generated using the MAP peptide comprising a portion of the C-terminus of the alpha-synuclein peptide on each of the 4 arms of the MAP (MAP-alpha-synuclein) closely mimics that standard curve generated using laboratory-aggregated alpha-synuclein.

## Detailed Description of the Invention

**[0018]** The present invention relates to methods for quantifying a known biomarker in a sample, with the methods comprising an assay that compares the binding activity of a binding agent towards the known biomarker with the binding activity of the binding agent towards a composition comprising a branched synthetic aggregate peptide (SAP).

**[0019]** As used herein, a sample can be any environment that may be suspected of containing the antigen of interest. Thus, a sample includes, but is not limited to, a solution, a cell or a portion thereof, tissue culture medium, a body fluid, a tissue or portion thereof, and an organ or portion thereof. Examples of cells include, but are not limited to, bacteria, yeast, plant, insect, avian, fish, reptilian, amphibian, and mammalian such as, for example, bovine, ovine, equine, porcine,



Fujirebio Diagnostics, Inc. v. Quanterix Corp.
EX-1045
5756

canine, feline, human and nonhuman primates. Other examples include non-animal organisms that may harbor similar antigens of interest, include but are not limited to molds, viruses, and other model systems for the study of biological processes. The scope of the invention should not be limited by the cell type assayed or the media in which these cells are cultured or processed (*e.g.,* for the production of cellular or tissue lysates). Examples of biological samples to be assayed include, but are not limited to, blood, plasma, serum, urine, saliva, milk, seminal plasma, synovial fluid, interstitial fluid, cerebrospinal fluid, lymphatic fluids, bile, and amniotic fluid, tissue culture medium, tissue homogenates, cell lysates, chemical solutions. The scope of the methods of the present invention should not be limited by the type of sample assayed. The terms "subject" "patient" and "organism" are used interchangeably herein and are used to mean any animal. In one embodiment the animal is a mammal. In a more particular embodiment, the animal is a human or nonhuman primate.

**[0020]** The samples may or may not have been removed from their native environment. Thus, the portion of sample assayed need not be separated or removed from the rest of the sample or from a subject that may contain the sample. For example, the blood of a subject may be assayed for the known biomarker without removing any of the blood from the patient. Of course, the sample may also be removed from its native environment. Furthermore, the sample may be processed prior to being assayed. For example, the sample may be diluted or concentrated; the sample may be purified and/or at least one compound, such as an internal standard, may be added to the sample. The sample may also be physically altered (*e.g.*, centrifugation, size exclusion chromatography, size permeation chromatography, filtered, including ultrafiltration, affinity separation) or chemically altered (*e.g.*, adding an acid, base, buffer, solvent, treating with a chemically reactive resin, heating) prior to or in conjunction with the methods of the current invention. Processing also includes freezing and/or preserving the sample prior to assaying, extracting secreted cellular products from surrounding medium, or physical disruption of cells and/or tissue to actively extract the analyte of interest.

**[0021]** As used herein the term SAP, or synthetic aggregated peptide, is used to mean a synthetic compound comprising a core component with one more peptide or single amino acid branches extending from the core. Unlike typical hapten-carrier complexes, *e.g.,* keyhole limpet hemocyanin (KLH) where the carrier is generally immunogenic even in the absence of hapten, it



Fujirebio Diagnostics, Inc. v. Quanterix Corp.
EX-1045
5757

is possible that the core of the SAPs of the present invention may be administered to an animal without causing a detectable immunogenic reaction. To be clear, the SAPs of the present invention will be useful in the methods of the present invention even if the core of the SAPs is able to cause a detectable immunogenic reaction. The peptides or amino acid arms extending from the core are referred to as the peptide(s) of interest. Examples of core components include, but are not limited to, amino acids, saccharides, oligosaccharides, polysaccharides, other polymers, such as but not limited to, polyethylene glycol, and any combination of the above. The invention should not be limited by the composition of the core, provided that the core is capable of attachment with one or more arms for the peptide(s) of interest. The attachment of the peptide arm to the SAP core may be covalent or non-covalent. In one embodiment, the core of the SAPs may comprise 2 or more branches or arms with the peptide(s) of interest attached thereto. In one embodiment, the SAP comprises 4 arms. In another embodiment, the SAP comprises more than 4 arms, such as, but not limited to, 8, 16, 32, 64 or more arms. It is conceivable that the SAPs may also comprise a number that is not an even power of 2, such as, but not limited to, 3, 5, 6, 7, 9, 10, 11, 12, 13, 14, 15, 17, 18, 19, 20 etc.

**[0022]** In one embodiment, the SAP comprises a core, where the core comprises one or more amino acids. In this particular embodiment, where the core comprises one or more amino acids, the SAP is commonly referred to as a multiple antigenic peptide, or MAP. Methods of producing MAPs are well known in the art. See Tam, JP, *Proc. Nat'l Acad. Sci. USA*, 85:5409-5413 (1988), which is incorporated by reference. In one specific embodiment, the MAP is 4-armed MAP with the core of the MAP comprising an amino acid, such as, but not limited to, β-alanine that is attached to a first lysine reside *via* a typical peptide bond. This first lysine residue, *i.e.*, the first layer of the MAP, provides 2 amino groups to which are attached a second and third lysine residue. These second and third lysine groups (the second layer of the MAP), in turn, provides 4 amino groups to which can be attached the peptide sequence(s) of interest.

**[0023]** Variations of this core structure are readily obtained by altering the number and identity of the amino acids that form the core of the MAP. For example, if a MAP with 3 arms is desired, the second layer of the MAP may, for example, comprise a second lysine residue and another residue that does not provide 2 amino groups. Examples of such amino acid residues include, but are not limited to alanine, valine, phenylalanine, methionine, leucine, isoleucine, aspartate,



Fujirebio Diagnostics, Inc. v. Quanterix Corp.
EX-1045
5758

glutamate, serine, threonine, tyrosine, cysteine and other non-naturally occurring amino acids. In this way, the second layer terminates in 2 amino groups offered by the second lysine and a third amino group offered by the other amino acid residue.

**[0024]** To the core of the SAP is attached to the peptide arm or peptide arms. As used herein, a peptide arm means a peptide or amino acid that is intended to be incorporated onto the core of the SAP as an arm extending therefrom. A peptide, in turn, is used to mean a chain of 2 or more amino acids joined together by peptide bonds. Thus, for the purposes of the present invention, a peptide includes di-peptides, tri-peptides, oligopeptides, polypeptides, full length protein chains, and proteins. The length of the peptide arm may vary depending on the intended use and can be any size, provided that the binding agent can specifically bind the SAP.

**[0025]** In one embodiment, each arm of the SAP comprises an identical peptide arm. In another embodiment, each arm of the SAP comprises peptides of interest where the peptides are not identical to each other. For example, a SAP comprising 4 arms may possess 4, 3 or 2 non-identical peptides of interest. As used herein, the phrase "identical peptides of interest" means peptides chains that have the identical primary structure as well as any post-translational modifications, such as, but not limited to, glycosylation, oxidation, acetylation, methylation, phosphorylation, acylation, nitrosylation, citrullination. The "post-translational modifications" may be natural or they may be synthetic modifications that normally do not take place in a native cellular environment. For example, the peptides of interest or portions thereof may possess polyethylene glycol (PEG) (*i.e.,* the peptide is PEGylated), be amidated with succinimyl ester or be cysteine alkylated. Additional protein modifications include, but are not limited to, ubiquinylation, prenylation and modifications resulting from the action of enzymes such as, but not limited to transglutaminase, and glutathione transferase. Thus, two peptide chains that are identical in amino acid sequence, but have, for example, different glycosylation patterns, different phosphorylation patterns are considered non-identical peptides of interest for the purposes of the present invention. For example, at least one arm of the SAP may comprise a peptide chain where the chain is unphosphorylated, and at least one arm of the SAP, where the peptide chain is phosphorylated. A single SAP may thus be used to monitor phosphorylation (or other enzymatic) events and/or may be used to determine proportions of phosphorylated (or differently modified) peptides within a system. Such other modifications include, but are not



Fujirebio Diagnostics, Inc. v. Quanterix Corp.
EX-1045
5759

limited to cleavage events involving such enzymes as, but not limited to, proteases such as caspases and secretases. An example of a cleavage even includes, but is not limited to, the cleavage of Aβ1-42 to Aβ1-20.

**[0026]** The inventors have discovered that the SAPs can serve as standards in binding assays that employ binding agents that bind to known biomarkers. As used herein, the term binding agent is used to mean a composition that binds specifically to the known biomarker. Examples of binding agents include, but are not limited to, natural proteins such as receptors, antibodies and functional fragments thereof, as well as synthetic molecules, such as but not limited to, aptamers and protein fragments screened by phage-display or other methods. As used herein, the term "antibody" is used to mean immunoglobulin molecules and functional fragments thereof, regardless of the source or method of producing the fragment. As used herein, a "functional fragment" of an immunoglobulin is a portion of the immunoglobulin molecule that specifically binds to a binding target. Thus, the term "antibody" as used herein encompasses whole antibodies, such as antibodies with isotypes that include but are not limited to IgG, IgM, IgA, IgD, IgE and IgY , and even single-chain antibodies found in some animals *e.g.,* camels. Whole antibodies may be monoclonal or polyclonal, and they may be humanized or chimeric. The term "monoclonal antibody" as used herein is not limited to antibodies produced through hybridoma technology. Rather the term "monoclonal antibody" refers to an antibody that is derived from a single clone, including any eukaryotic, prokaryotic, or phage clone, and not the method by which it is produced. The term "antibody" also encompasses functional fragments of immunoglobulins, including but not limited to Fab fragments, Fab′ fragments, $F(ab')_2$ fragments and Fd fragments. "Antibody" also encompasses fragments of immunoglobulins that comprise at least a portion of a $V_L$ and/or $V_H$ domain, such as single chain antibodies, a single-chain Fv (scFv), disulfide-linked Fvs and the like.

**[0027]** The antibodies used in the present invention may be monospecific, bispecific, trispecific or of even greater multispecificity. In addition the antibodies may be monovalent, bivalent, trivalent or of even greater multivalency. Furthermore, the antibodies of the invention may be from any animal origin including, but not limited to, birds and mammals. In specific embodiments, the antibodies are human, murine, rat, sheep, rabbit, goat, guinea pig, horse, or chicken. As used herein, "human" antibodies include antibodies having the amino acid sequence



Fujirebio Diagnostics, Inc. v. Quanterix Corp.
EX-1045
5760

of a human immunoglobulin and include antibodies isolated from human immunoglobulin libraries or from animals transgenic for one or more human immunoglobulin and that do not express endogenous immunoglobulins, as described in United States Patent No. 5,939,598, which is herein incorporated by reference.

**[0028]** The antibodies used in the present invention may be described or specified in terms of the epitope(s) or portion(s) of a polypeptide to which they recognize or specifically bind. Or the antibodies may be described based upon their ability to bind to specific conformations of the antigen, or specific modification (*e.g.,* cleavage or chemical, natural or otherwise, modification of sequence). In one embodiment, a single antibody used in the methods of the present invention is specific towards an epitope presented on a SAP and towards an epitope presented on the known biomarker that is being assayed.

**[0029]** The specificity of the antibodies used in present invention may also be described or specified in terms of their binding affinity towards the antigen (epitope) or of by their cross-reactivity. Specific examples of binding affinities encompassed in the present invention include but are not limited to those with a dissociation constant (Kd) less than $5\times10^{-2}$ M, $10^{-2}$ M, $5\times10^{-3}$ M, $10^{-3}$ M, $5\times10^{-4}$ M, $10^{-4}$ M, $5\times10^{-5}$ M, $10^{-5}$ M, $5\times10^{-6}$ M, $10^{-6}$ M, $5\times10^{-7}$ M, $10^{-7}$ M, $5\times10^{-8}$ M, $10^{-8}$ M, $5\times10^{-9}$ M, $10^{-9}$ M, $5\times10^{-10}$ M, $10^{-10}$ M, $5\times10^{-11}$ M, $10^{-11}$ M, $5\times10^{-12}$ M, $10^{-12}$ M, $5\times10^{-13}$ M, $10^{-13}$ M, $5\times10^{-14}$ M, $10^{-14}$ M, $5\times10^{-15}$ M, or $10^{-15}$ M. In one embodiment, the antibody that is used in the methods of the present invention has a substantially equivalent binding affinity towards the epitope presented on a SAP and towards an epitope presented on the known biomarker that is being assayed. As used herein, a substantially equivalent binding affinity means within the same order of magnitude of the dissociation constant.

**[0030]** The antibodies used in the invention also include derivatives that are modified, for example, by covalent attachment of any type of molecule to the antibody such that covalent attachment does not prevent the antibody from generating an anti-idiotypic response. Examples of modifications to antibodies include but are not limited to, glycosylation, acetylation, pegylation, phosphorylation, amidation, derivatization by known protecting/blocking groups, proteolytic cleavage, linkage to a cellular ligand or other composition, such as a signaling moiety, a label etc. In addition, the antibodies may be linked or attached to solid substrates, such



Fujirebio Diagnostics, Inc. v. Quanterix Corp.
EX-1045
5761

as, but not limited to, beads, particles, glass surfaces, plastic surfaces, ceramic surfaces, metal surfaces. Any of numerous chemical modifications may be carried out by known techniques, including, but not limited to, specific chemical cleavage, acetylation, biotinylation, farnesylation, formylation, inhibition of glycosylation by tunicamycin and the like. Additionally, the derivative may contain one or more non-classical or synthetic amino acids.

**[0031]** The antibodies used in the present invention may be generated by any suitable method known in the art. Polyclonal antibodies can be produced by various procedures well known in the art. For example, a SAP or an epitope on the SAP can be administered to various host animals including, but not limited to, rabbits, goats, chickens, mice, rats, to induce the production of sera containing polyclonal antibodies specific for the antigen. Various adjuvants may be used to increase the immunological response, depending on the host species, and include but are not limited to, Freund's (complete and incomplete), mineral gels such as aluminum hydroxide, surface active substances such as lysolecithin, pluronic polyols, polyanions, peptides, oil emulsions, keyhole limpet hemocyanins, dinitrophenol, and potentially useful human adjuvants such as BCG (bacille Calmette-Guerin) and *Corynebacterium parvum*. Such adjuvants are also well known in the art.

**[0032]** Monoclonal antibodies can be prepared using a wide variety of techniques known in the art including the use of hybridoma, recombinant, and phage display technologies, or a combination thereof. For example, monoclonal antibodies can be produced using hybridoma techniques including those known in the art and taught, for example, in Harlow *et al.*, Antibodies: A Laboratory Manual, (Cold Spring Harbor Laboratory Press, 2nd ed. 1988); Hammerling, *et al.*, in: Monoclonal Antibodies and T-Cell Hybridomas 563-681 (Elsevier, N.Y., 1981) (both of which are incorporated by reference).

**[0033]** Methods for producing and screening for specific antibodies using hybridoma technology are routine and well known in the art such as, but not limited to, immunizing a mouse, hamster, or rat. Additionally, newer methods to produce rabbit and other mammalian monoclonal antibodies may be available to produce and screen for antibodies. In short, methods of producing and screening antibodies, and the animals used therein, should not limit the scope of the invention. Once an immune response is detected, the mouse spleen is harvested and



Fujirebio Diagnostics, Inc. v. Quanterix Corp.
EX-1045
5762

splenocytes isolated. The splenocytes are then fused by well known techniques to any suitable myeloma cells, for example cells from cell line SP2/0 available from the ATCC. Hybridomas are selected and cloned by limited dilution. The hybridoma clones can then be assayed by methods known in the art for cells that secrete antibodies capable of binding a biomarker of the present invention. Ascites fluid, which generally contains high levels of antibodies, can be generated by immunizing mice with positive hybridoma clones. In addition, antibodies can be produced using a variety of alternate methods, including but not limited to bioreactors and standard tissue culture methods, to name a few.

**[0034]** The antibodies used the present invention can also be generated using various phage display methods known in the art. In phage display methods, functional antibody domains are displayed on the surface of phage particles which carry the polynucleotide sequences encoding them. In a particular embodiment, such phage can be utilized to display antigen binding domains expressed from a repertoire or combinatorial antibody library. Phage expressing an antigen binding domain that binds the antigen of interest can be selected or identified with the antigen of interest, such as using a labeled antigen or antigen bound or captured to a solid surface or bead. The phage used in these methods are typically filamentous phage including, but not limited to, fd and M13 binding domains expressed from phage with Fab, Fv or disulfide stabilized Fv antibody domains recombinantly fused to either the phage gene III or gene VIII protein. Examples of phage display methods that can be used to make the antibodies of the present invention include those disclosed in Brinkman *et al., J. Immunol. Methods* 182:41-50 (1995); Ames *et al., J. Immunol. Methods* 184:177-186 (1995); Kettleborough *et al., Eur. J. Immunol.* 24:952-958 (1994); Persic *et al., Gene* 187 9-18 (1997); Burton *et al., Advances in Immunology* 57:191-280 (1994); PCT application No. PCT/GB91/01134; PCT publications WO 90/02809; WO 91/10737; WO 92/01047; WO 92/18619; WO 93/11236; WO 95/15982; WO 95/20401; and United States Patent Nos. 5,698,426; 5,223,409; 5,403,484; 5,580,717; 5,427,908; 5,750,753; 5,821,047; 5,571,698; 5,427,908; 5,516,637; 5,780,225; 5,658,727; 5,733,743 and 5,969,108, all of which are incorporated by reference.

**[0035]** Antibody fragments which recognize specific epitopes may be generated by known techniques. For example, Fab and $F(ab')_2$ fragments of the invention may be produced by proteolytic cleavage of immunoglobulin molecules, using enzymes such as papain (to produce



Fujirebio Diagnostics, Inc. v. Quanterix Corp.
EX-1045
5763

Fab fragments) or pepsin (to produce $F(ab')_2$ fragments). $F(ab')_2$ fragments contain the variable region, the light chain constant region and the CH1 domain of the heavy chain.

**[0036]** Other methods, such as recombinant techniques, may be used to produce Fab, Fab' and $F(ab')_2$ fragments and are disclosed in PCT publication WO 92/22324; Mullinax *et al., BioTechniques* 12(6):864-869 (1992); and Sawai *et al., AJRI* 34:26-34 (1995); and Better *et al., Science* 240:1041-1043 (1988), which are herein incorporated by reference. After phage selection, for example, the antibody coding regions from the phage can be isolated and used to generate whole antibodies, including human antibodies, or any other desired antigen binding fragment, and expressed in any desired host, including mammalian cells, insect cells, plant cells, yeast, and bacteria.

**[0037]** Examples of techniques which can be used to produce other types of fragments, such as scFvs and include those described in United States Patent Nos. 4,946,778 and 5,258,498; Huston *et al., Methods in Enzymology* 203:46-88 (1991); Shu *et al., Proc. Nat'l Acad. Sci. (USA)* 90:7995-7999 (1993); and Skerra *et al., Science* 240:1038-1040 (1988), all of which are incorporated by reference. For some uses, including *in vivo* use of antibodies in humans and *in vitro* detection assays, it may be preferable to use chimeric, humanized, or human antibodies. A chimeric antibody is a molecule in which different portions of the antibody are derived from different animal species, such as antibodies having a variable region derived from a murine monoclonal antibody and a human immunoglobulin constant region. Methods for producing chimeric antibodies are known in the art. *See e.g.,* Morrison, *Science* 229:1202 (1985); Oi *et al., BioTechniques* 4:214 (1986); Gillies *et al., J. Immunol. Methods* 125:191-202(1989); United States Patent Nos. 5,807,715; 4,816,567; and 4,816,397, all of which are herein incorporated by reference. Humanized antibodies are antibody molecules from non-human species antibody that bind the desired antigen having one or more complementarity determining regions (CDRs) from the non-human species and framework regions from a human immunoglobulin molecule. Often, framework residues in the human framework regions will be substituted with the corresponding residue from the CDR donor antibody to alter, preferably improve, antigen binding. These framework substitutions are identified by methods well known in the art, *e.g.,* by modeling of the interactions of the CDR and framework residues to identify framework residues important for antigen binding and sequence comparison to identify unusual framework residues at particular



Fujirebio Diagnostics, Inc. v. Quanterix Corp.
EX-1045
5764

positions. (*See* United States Patent No. 5,585,089; Riechmann *et al., Nature* 332:323 (1988), both of which are herein incorporated by reference. Antibodies can be humanized using a variety of techniques known in the art including, for example, CDR-grafting (EP 239,400; PCT publication WO 91/09967; United States Patent Nos. 5,225,539; 5,530,101; and 5,585,089), veneering or resurfacing (EP 592,106; EP 519,596; Padlan, *Molecular Immunology* 28(4/5):489-498 (1991); Studnicka *et al., Protein Engineering* 7(6):805-814 (1994); Roguska. *et al., Proc. Nat'l. Acad. Sci.* 91:969-913 (1994)), and chain shuffling (United States Patent No. 5,565,332), all of which are hereby incorporated by reference.

**[0038]** Completely human antibodies may be particularly desirable for therapeutic treatment or diagnosis of human patients. Human antibodies can be made by a variety of methods known in the art including phage display methods described above using antibody libraries derived from human immunoglobulin sequences. See also. U.S. Pat. Nos. 4,444,887 and 4,716,111; and PCT publications WO 98/46645, WO 98/50433, WO 98/24893, WO 98/16654, WO 96/34096, WO 96/33735, and WO 91/10741; each of which is incorporated by reference.

**[0039]** Human antibodies can also be produced using transgenic mice which are incapable of expressing functional endogenous immunoglobulins, but which can express human immunoglobulin genes. For example, the human heavy and light chain immunoglobulin gene complexes may be introduced randomly or by homologous recombination into mouse embryonic stem cells. Alternatively, the human variable region, constant region, and diversity region may be introduced into mouse embryonic stem cells in addition to the human heavy and light chain genes. The mouse heavy and light chain immunoglobulin genes may be rendered non-functional separately or simultaneously with the introduction of human immunoglobulin loci by homologous recombination. In particular, homozygous deletion of the JH region prevents endogenous antibody production. The modified embryonic stem cells are expanded and microinjected into blastocysts to produce chimeric mice. The chimeric mice are then bred to produce homozygous offspring which express human antibodies. The transgenic mice are immunized in the normal fashion with a selected antigen. Monoclonal antibodies directed against the antigen can be obtained from the immunized, transgenic mice using conventional hybridoma technology. The human immunoglobulin transgenes harbored by the transgenic mice rearrange during B cell differentiation, and subsequently undergo class switching and somatic



Fujirebio Diagnostics, Inc. v. Quanterix Corp.
EX-1045
5765

mutation. Thus, using such a technique, it is possible to produce therapeutically useful IgG, IgA, IgM and IgE antibodies. For an overview of this technology for producing human antibodies, see Lonberg and Huszar, *Int. Rev. Immunol.* 13:65-93 (1995), which is hereby incorporated by reference. For a detailed discussion of this technology for producing human antibodies and human monoclonal antibodies and protocols for producing such antibodies, see, e.g., PCT publications WO 98/24893; WO 92/01047; WO 96/34096; WO 96/33735; European Patent No. 0 598 877; United States Patent Nos. 5,413,923; 5,625,126; 5,633,425; 5,569,825; 5,661,016; 5,545,806; 5,814,318; 5,885,793; 5,916,771; and 5,939,598, which are incorporated by reference.

**[0040]** Still another approach for generating human antibodies utilizes a technique referred to as guided selection. In guided selection, a selected non-human monoclonal antibody, *e.g.,* a mouse antibody, is used to guide the selection of a completely human antibody recognizing the same epitope. (Jespers *et al., Biotechnology* 12:899-903 (1988), herein incorporated by reference).

**[0041]** Accordingly, using the binding agents and SAP standards described herein, the present invention provides methods of detecting and quantifying a known biomarker in a sample, with the methods comprising contacting the sample with a binding agent that is specific for both the known biomarker and the SAP standard, and detecting the binding of the binding agent to the known biomarker and SAP standard. The binding agent may be coated onto a cell culture surface or a 96-well plate, such as an ELISA plate, or the capture antibody may be bound to or coated on beads or columns, or any surface or environment capable of housing the capture antibody such that it is available to bind to the antigen of interest.

**[0042]** Examples of an assay used in the methods of the present invention to assess the quantity of a known biomarker include, but are not limited to, immunosorbence assays and competitive binding assays. Specific embodiments of some of the assays listed include, but are not limited to, direct and indirect assays, as well as binary and tertiary sandwich assays. In one embodiment, the assay is an immunosorbence assay. In more specific embodiments, the immunosorbence assay is a colorimetric assay, an enzyme-linked immunosorbence assay (ELISA), a planar array or a radioimmunoassay. Other examples of assays that may be used in the methods of the present invention include, but are not limited to, bead or particle-based immunoassays, chemiluminescient assays, surface plasmon resonance (SPR) based assays, fluorescence assays,



Fujirebio Diagnostics, Inc. v. Quanterix Corp.
EX-1045
5766

rolling-circle amplification assays, assays using dendrimers, and other enzyme or non-enzymatic amplification schemes.

**[0043]** The methods of the present invention utilize SAPs as standards to quantify and standardize assays that are designed to quantify known biomarkers. The invention is not limited to the identity or class of known biomarkers. Examples of classes of biomarkers include but are not limited to, carbohydrates such as monosaccharides, disaccharides, oligosaccharides and polysaccharides, proteins, peptides and amino acids, including, but not limited to, oligopeptides, polypeptides and mature proteins, nucleic acids, oligonucleotides, polynucleotides, lipids, fatty acids, lipoproteins, proteoglycans, carbohydrates, glycoproteins, organic compounds, inorganic compounds, ions, and synthetic and natural polymers, peptides, proteins, sacchraides, carbohydrates.

**[0044]** In one embodiment, the biomarker is a peptide. Examples of biomarker peptides include but are not limited to, beta amyloid (Aβ), huntingtin peptide, alpha-synuclein, tau, superoxide-dismutase 1 (SOD-1), prion peptide, stefin B, transthyretin, ataxin-1, gelsolin, BRI, HSP, alphaB crystalline, amylin, beta2-microglobulin, immunoglobulin light chain, antithrombin, and portions thereof. The phrase "portion of a peptide" is readily understood in the art. The above listed peptides are well-known for their association with disease states. For example, Aβ is associated with Alzheimer's Disease, alpha-synuclein is associated with Parkinson's Disease and Alzheimer's Disease, SOD-1 is associated with amytropic lateral sclerosis (ALS), huntingtin is associated with Huntington's Disease, and prion is associated with Creutzfeldt-Jakob Disease and other spongiform encephalopathies.

**[0045]** In a more specific embodiment, the biomarker is an aggregated peptide. As used herein, an aggregated peptide is an aggregation of peptides that form a distinct globular , ball-like structure, or annular structure. The aggregated peptide is thought to form by an initial nucleation process where hydrophobic regions of the individual peptide chains aggregate in the center of the globule to form a hydrophobic core. The aggregated core then polymerizes additional peptide chains onto the core. In general, the aggregated peptide will polymerize until it forms a stable globular or annular structure with a hydrophobic core and hydrophilic surface. Once the stable aggregated peptide forms, the aggregated peptide will, in general, cease polymerization. The



Fujirebio Diagnostics, Inc. v. Quanterix Corp.
EX-1045
5767

structure of the aggregated peptide accounts for its generally high solubility and stability. An example of an aggregated peptide is illustrated in Barghorn, S. *et al.*, *J. Neurochem.* 95(3):834-47 (2005), which is incorporated by reference. For example, aggregated Aβ peptide ($A\beta_{1-42}$) is gaining attention as a potential toxin that is associated with Alzheimer's Disease. Similarly, aggregated forms of huntingtin peptide, alpha-synuclein, superoxide-dismutase 1 (SOD-1) and prion peptide are gaining attention as potential toxins in Huntington's Disease, Parkinson's Disease, ALS, and Creutzfeld-Jakob Disease, respectively. In particular the compositions and methods of the present invention can be used in any abnormal condition that may be characterized by amyloidogenesis. Table 1 and 2 list a representative of diseases attributed to toxic protein aggregates, the list is not intended to be inclusive as many other disease are also know to be attributed to toxic protein aggragates.

**[0046]** Table 1:

| **Disease** | **Protein** | **Reference** |
|---|---|---|
| Alzheimer's disease | beta amyloid | Lambert, M., et al. (1998) PNAS 95: 6448.<br><br>Kayed, R., et al. (2003) Science 300: 486.<br><br>Demuro, A., et al. (2005) J. Biol. Chem. 280: 17294. |
| Parkinson's disease | alpha-synuclein | El-Agnaf, A., et al. (2006) FASEB J. 20: 419. |
| Huntington's disease | huntingtin peptide | Demuro, A., et al. (2005) J. Biol. Chem. 280: 17294. |
| Amyotropic lateral sclerosis (ALS) | superoxide dismutase 1 | Cleveland, D.W. and R.J. Rothstein (2001) Nat. Rev. |



Fujirebio Diagnostics, Inc. v. Quanterix Corp.
EX-1045
5768

| | | |
|---|---|---|
| | | Neurosci. 2: 806. |
| Bovine spongiform encephalopathy, variant Creutzfeldt-Jakob disease | prion | Demuro, A., et al. (2005) J. Biol. Chem. 280: 17294. |
| Myoclonus epilepsy | stefin B | Lalioti, M.D., et al. (1997) Nature 286: 767. |
| Frontotemporal dementia/tauopathy | tau | Spillantini, M.G. and M. Goedert (1998) Trends Neurosci. 21: 428. |
| Senile systemic amyloidosis and familial amyloid polyneuropathy | transthyretin | Quintas, A., et al. (1997) FEBS Lett. 418: 297-300. |
| Spinocerebellar ataxia type-1 | ataxin-1 | de Chiara, C., et al. (2005) J. Mol. Biol. 354: 883. |
| Familial amyloidosis of the Finnish type | gelsolin | Huff, M.E., et al. (2003) J. Mol. Biol. 334: 119. |
| Familial British dementia | BRI | El-Agnaf, O.M., et al. (2001) Biochemistry 40: 3449. |

**[0047]**

**[0048]** Table 2 ***Protein Aggregates in Other Diseases***

| **Disease** | **Protein** | **Reference** |
|---|---|---|
| Familial Mediterranean fever, systemic AA amyloidosis, visceral amyloidosis | serum amyloid A | Van der Hilst, J.C., et al. (2005) Clin. Exp. Med. 5: 87. |



Fujirebio Diagnostics, Inc. v. Quanterix Corp.
EX-1045
5769

| | | |
|---|---|---|
| Desmin-related cardiomyopathy, dilated cardiomyopathy, and hypertrophic cardiomyopathy | alphaB crystallin/HSP | Atsushi Sanbe, A., et al. (2005) PNAS 102: 13592.<br>**[0049]** Kumarapeli, A.R. and X. Wang (2004). J. Mol. Cell Cardiol. 376: 1097. |
| Diabetes | islet amyloid polypeptide | Demuro, A., et al. (2005) J. Biol. Chem. 280: 17294. |
| Dialysis-related amyloidosis | beta2-microglobulin | Buxbaum, J.N. (2004) Curr. Opin. Rheumatol. 16: 67. |
| Light-chain amyloidosis | immunoglobulin light chain | Buxbaum, J.N. (2004) Curr. Opin. Rheumatol. 16: 67. |
| Senile systemic amyloidosis | transthyretin | Buxbaum, J.N. (2004) Curr. Opin. Rheumatol. 16: 67. |
| Thrombosis | antithrombin | Corral, J., et al. (2005) Haematologica 90: 238. |
| Cirrhosis of the liver | antitrypsin | Corral, J., et al. (2005) Haematologica 90: 238. |
| Emphysema | serpine family of proteinase inhibitors | Lomas, D.A. and R.W Carrell (2002) Nat. Rev. Genet. 3: 759. |
| Hereditary Systemic Amyloidosis | Lysozyme | Pepys, M.B., et al. (1993) Nature 362: 553. |

:

**[0050]** In one embodiment, the methods of the present invention are directed towards the quantification of a known aggregated peptide as the biomarker. Thus, the binding agent must be



Fujirebio Diagnostics, Inc. v. Quanterix Corp.
EX-1045
5770

capable of specifically binding the known aggregated biomarker. To quantify the binding activity of the binding agent towards the known aggregated biomarker, the methods depend upon the use of a SAP as a standard. As discussed, the arms of the SAP comprise a peptide arm. In a specific embodiment, the SAP comprises at least a portion of the same peptide that makes up the aggregated peptide as the biomarker. Thus, if the biomarker to be quantified is aggregated Aβ, the SAP may comprise at least a portion of the Aβ peptide on at least one arm of the SAP. In one specific embodiment, aggregated $A\beta_{1-42}$ is the known biomarker and the SAP standard comprises a hydrophilic portion of the Aβ peptide on each of 4 arms of the SAP. In a more specific embodiment, the SAP comprises the N-terminus of $A\beta_{1-42}$. In an even more specific embodiment, the SAP comprises at least 6 contiguous amino acids from amino acids 1-20 of SEQ ID NO. 1. In other specific embodiments, the SAP comprises at least 7, 8, 9, 10, 11, 12, 13, 14, 15, 16, 17, 18, 19 and 20 contiguous amino acids from amino acids 1-20 of SEQ ID NO. 1, below. The amino acid sequence of SEQ ID NO.1 represents the amino acid sequence of human $A\beta_{1-42}$ peptide.

SEQ ID NO.1: daefrhdsgy evhhqklvff aedvgsnkga iiglmvggvv ia

**[0051]** In another specific embodiment aggregated huntingtin peptide is the biomarker and the SAP standard comprises a portion of the huntingtin peptide on at least one arm of the SAP standard. The full length huntingtin peptide can be accessed under GenBank Accession No NM 002111, which is hereby incorporated by reference, and the SAP standard may comprise any portion of the huntingtin peptide. Furthermore, "huntingtin peptide", as used herein indicates a peptide with an amino acid sequence that is at least 80%, 85%, 90%, 95%, 96%, 97%, 98% or 99% identical to the huntingtin peptide as disclosed by GenBank Accession No. NM 002111. The "huntingtin peptide" may also include the expanded poly-glutamine tracts that characterize the toxic protein species found in Huntington's disease. In another specific embodiment, the SAP standard comprises a portion of the huntingtin peptide on each arm of the SAP. In a more specific embodiment, the SAP standard comprises a portion of the N-terminus of the huntingtin peptide on one or more arms of the SAP and may include expanded polyglutamine tracts or portions thereof. In other specific embodiments, the SAP standard comprises a portion of the center or the C-terminus of the huntingtin peptide on one or more arms of the SAP.



Fujirebio Diagnostics, Inc. v. Quanterix Corp.
EX-1045
5771

**[0052]** In another specific embodiment aggregated alpha-synuclein peptide is the biomarker and the SAP standard comprises a portion of the alpha-synuclein peptide on at least one arm of the SAP standard. The full length human alpha-synuclein peptide and splice variants can be accessed under GenBank Accession Nos. P37840, NM 000345, NM 0077308, NP 009292, NP 000336, which are hereby incorporated by reference, and the SAP standard may comprise any portion of the alpha-synuclein peptide. Furthermore, "alpha-synuclein peptide," as used herein indicates a peptide with an amino acid sequence that is at least 80%, 85%, 90%, 95%, 96%, 97%, 98% or 99% identical to the alpha-synuclein peptide as disclosed by GenBank Accession Nos. P37840, NM 000345, NM 0077308, NP 009292, NP 000336. In another specific embodiment, the SAP standard comprises a portion of the alpha-synuclein peptide on each arm of the SAP. In a more specific embodiment, the SAP standard comprises a portion of the C-terminus of the alpha-synuclein peptide on one or more arms of the SAP. In an even more specific embodiment, the SAP standard comprises at least 7, 8, 9, 10, 11, 12, 13, 14, 15, 16, 17, 18, 19 and 20 contiguous amino acids of SEQ ID NO:2, below. In particular, the SAP standard comprises amino acids 116-130 of SEQ ID NO:2, where SEQ ID NO:2 represents the amino acid sequence of human alpha-synuclein. In other specific embodiments, the SAP standard comprises a portion of the center or the N-terminus of the alpha-synuclein peptide on one or more arms of the SAP.

```
  1 mdvfmkglsk akegvvaaae ktkqgvaeaa gktkegvlyv gsktkegvvh gvatvaektk
 61 eqvtnvggav vtgvtavaqk tvegagsiaa atgfvkkdql gkneegapqe giledmpvdp
121 dneayempse egyqdyepea (SEQ ID NO:2)
```

**[0053]** In another specific embodiment aggregated SOD-1 peptide is the biomarker and the SAP standard comprises a portion of the SOD-1 peptide on at least one arm of the SAP standard. The full length human SOD-1 peptide can be accessed under GenBank Accession Nos. NM 000454 and NC 000021, which are hereby incorporated by reference, and the SAP standard may comprise any portion of the SOD-1. Furthermore, "SOD-1 peptide," as used herein indicates a peptide with an amino acid sequence that is at least 80%, 85%, 90%, 95%, 96%, 97%, 98% or 99% identical to the SOD-1 peptide as disclosed by GenBank Accession Nos. NM 000454 and NC 000021. In another specific embodiment, the SAP standard comprises a portion of the SOD-1 peptide on each arm of the SAP. In a more specific embodiment, the SAP standard comprises a portion of the N-terminus of the SOD-1 peptide on one or more arms of the SAP. In other



Fujirebio Diagnostics, Inc. v. Quanterix Corp.
EX-1045
5772

specific embodiments, the SAP standard comprises a portion of the center or the C-terminus of the SOD-1 peptide on one or more arms of the SAP.

**[0054]** In another specific embodiment aggregated prion peptide is the biomarker and the SAP standard comprises a portion of the prion peptide on at least one arm of the SAP standard. The full length human prion peptide can be accessed under GenBank Accession No. P04156, which is hereby incorporated by reference, and the SAP standard may comprise any portion of the prion peptide. Furthermore, "prion peptide," as used herein indicates a peptide with an amino acid sequence that is at least 80%, 85%, 90%, 95%, 96%, 97%, 98% or 99% identical to the prion peptide as disclosed by GenBank Accession No. P04156. In another specific embodiment, the SAP standard comprises a portion of the prion peptide on each arm of the SAP. In a more specific embodiment, the SAP standard comprises a portion of the N-terminus of the prion peptide on one or more arms of the SAP. In other specific embodiments, the SAP standard comprises a portion of the center or the C-terminus of the prion peptide on one or more arms of the SAP.

**[0055]** In another specific embodiment aggregated islet amyloid polypeptide is the biomarker and the SAP standard comprises a portion of the islet amyloid polypeptide on at least one arm of the SAP standard. The full length human islet amyloid polypeptide can be accessed under GenBank Accession No. NM 000415, which is hereby incorporated by reference, and the SAP standard may comprise any portion of the islet amyloid polypeptide. Furthermore, "islet amyloid polypeptide," as used herein indicates a peptide with an amino acid sequence that is at least 80%, 85%, 90%, 95%, 96%, 97%, 98% or 99% identical to the islet amyloid polypeptide as disclosed by GenBank Accession No. NM 000415. In another specific embodiment, the SAP standard comprises a portion of the islet amyloid polypeptide on each arm of the SAP. In a more specific embodiment, the SAP standard comprises a portion of the N-terminus of the islet amyloid polypeptide on one or more arms of the SAP. In other specific embodiments, the SAP standard comprises a portion of the center or the C-terminus of the islet amyloid polypeptide on one or more arms of the SAP.

**[0056]** As used herein, "identity" is a measure of the identity of nucleotide sequences or amino acid sequences compared to a reference nucleotide or amino acid sequence, usually a wild-type



Fujirebio Diagnostics, Inc. v. Quanterix Corp.
EX-1045
5773

sequence. In general, the sequences are aligned so that the highest order match is obtained. "Identity" per se has an art-recognized meaning and can be calculated using published techniques. (See, *e.g.,* Computational Molecular Biology, Lesk, A. M., ed., Oxford University Press, New York (1988); Biocomputing: Informatics And Genome Projects, Smith, D. W., ed., Academic Press, New York (1993); Computer Analysis of Sequence Data, Part I, Griffin, A. M., and Griffin, H. G., eds., Humana Press, New Jersey (1994); von Heinje, G., Sequence Analysis In Molecular Biology, Academic Press (1987); and Sequence Analysis Primer, Gribskov, M. and Devereux, J., eds., M Stockton Press, New York (1991)). While several methods exist to measure identity between two polynucleotide or polypeptide sequences, the term "identity" is well known in the art (Carillo, H. & Lipton, D., Siam J Applied Math 48:1073 (1988)). Methods commonly employed to determine identity or similarity between two sequences include, but are not limited to, those disclosed in Guide to Huge Computers, Martin J. Bishop, ed., Academic Press, San Diego (1994) and Carillo, H. & Lipton, D., Siam J Applied Math 48:1073 (1988). Computer programs may also contain methods and algorithms that calculate identity and similarity. Examples of computer program methods to determine identity and similarity between two sequences include, but are not limited to, GCS program package (Devereux, J., et al., Nucleic Acids Research 12(i):387 (1984)), BLASTP, BLASTN, FASTA (Atschul, S. F., et al., J Molec Biol 215:403 (1990)).

**[0057]** A polypeptide having an amino acid sequence at least, for example, about 95% "identical" to a reference nucleotide sequence encoding a peptide of interest, for example Aβ, is understood to mean that the amino acid sequence of the peptide is identical to the reference sequence except that the amino acid sequence may include up to about five mutations per each 100 amino acids of the reference peptide sequence encoding the Aβ peptide being used as the reference sequence. In other words, to obtain a polypeptide having an amino acid sequence at least about 95% identical to a reference amino acid sequence, up to about 5% of the amino acids in the reference sequence may be deleted or substituted with another amino acid, or a number of amino acids up to about 5% of the total amino acids in the reference sequence may be inserted into the reference sequence. These mutations of the reference sequence may occur at the N- or C- terminal positions of the reference amino acid sequence or anywhere between those terminal positions, interspersed either individually among amino acids in the reference sequence or in one or more contiguous groups within the reference sequence.



Fujirebio Diagnostics, Inc. v. Quanterix Corp.
EX-1045
5774

**[0058]** In another embodiment, the peptide arm(s) is (are) intended to mimic the structural motif, *e.g.,* alpha helices, beta sheets, etc., of the aggregated biomarker, rather than the peptide sequence of the aggregated peptide. The secondary and tertiary structural motifs of proteins can be readily determined using current technology, and peptide arms can also be designed to mimic the target structural motif(s) of the aggregated peptides.

**[0059]** Of course, the methods of detecting known biomarkers can be combined with detecting other biomarkers that are also indicative of particular disease states or abnormal conditions. For example, the methods of the present invention can be combined with methods of detecting biomarkers such as, but not limited to, tau protein and cytokines, to name a few. In fact, the SAP compositions of the present invention may be used as standards in multiplex assays, where more than one biomarker is being assayed. In one embodiment, aggregates composed of more than one biomarker is being assayed, and a single SAP standard is used to calibrate or standardize the muliplex assay, where the single SAP comprises at least two non-identical peptides of interest.

**[0060]** The present invention also relates to methods of detecting and diagnosing an abnormal condition in a subject. As used herein, an abnormal condition indicates that the subject is exhibiting one or more signs not present in a normal, healthy individual. The signs of the abnormal condition may be asymptomatic, in that none of the signs are readily apparent to the subject or healthcare provider in the absence of testing. Of course, the abnormal condition may also manifest itself in one or more signs that are readily apparent to the subject or healthcare provider.

**[0061]** The methods of detecting and diagnosing an abnormal condition in a subject comprise detecting the binding activity of a binding agent towards at least one concentration of at least one standard to establish a standard curve, where the standard comprises a SAP peptide. Methods of generating a standard curve are well known in the art. In general, establishing a standard curve involves detecting the levels of binding activity of the binding agent to various known concentrations of the SAP standard. The curve is then generated by plotting the levels of binding activity against the known concentrations of SAP standards. The curve may be generated by simply plotting the coordinates on an appropriate graph, or the curve may be generated using an



Fujirebio Diagnostics, Inc. v. Quanterix Corp.
EX-1045
5775

algorithm to compute the equation of the curve. The standard curve can be any shape, including but not limited to linear, parabolic, hyperbolic and sigmoidal.

**[0062]** The methods further comprise contacting a sample from the subject with at least one binding agent that is capable of binding an aggregated biomarker, detecting the level binding activity of the binding agent in the sample and correlating the binding activity in the sample to the established standard curve to determine the levels of the aggregated biomarker in the subject.

**[0063]** The invention is not limited by the method of detecting the binding of the binding agent to the biomarker and/or SAP standard. The detection method may require a specific label, or may be label-independent as in SPR, TRF, interferometry, nephelometry, or waveguide biorefringence interferometry. For example, the detection of binding may include, but is not limited to, using a second detection antibody that binds to the binding agent-biomarker complex, such as in a "sandwich ELISA," using spectroscopy, such as mass spectroscopy or fluorescence spectrophotometry, and electrophoresis or other separation method, such as Western Blotting, chromatography, capillary electrophoresis, capillary immunodetection, or other separation-based methods. The use of subsequent detection antibodies to detect binding of the binding agent to the biomarker may include, but is not limited to, radioactive isotopes and enzymes, such as horse radish peroxidase or alkaline phosphatase, as has been described herein. Additionally, if the binding agent, for example, is bound to a bead or particle, methods of detecting and measuring bound antigen may also include flow cytometry (FACS), colorimetric or other "encoded" particle technologies, or magnetic separation technologies.

**[0064]** In ELISAs, the capture molecule, *i.e.,* the binding agent that initially binds to the biomarker does not have to be conjugated to a label; instead, a labeled subsequent detection molecule (which may recognize the capture molecule) may be added to the well. One of skill in the art would be knowledgeable as to the parameters that can be modified to increase the signal detected as well as other variations of ELISAs known in the art. As used herein the term "capture molecule" is used mean a binding agent that immobilizes the biomarker by its binding to the biomarker. Further, a biomarker is "immobilized" if the biomarker or biomarker-capture molecule complex is separated or is capable of being separated from the remainder of the sample. When the capture molecule is coated to a well or other surface, a detection molecule



Fujirebio Diagnostics, Inc. v. Quanterix Corp.
EX-1045
5776

may be added following the addition of the biomarker of interest to the wells. As used herein, a detection molecule is used to mean a molecule, such as an antibody or receptor, comprising a label. In a specific embodiment, the methods of the present invention comprise the use of a capturing antibody and a detection antibody to detect the biomarker. In a more specific embodiment, the capture antibody and the detection antibody are the same antibodies with the same binding specificities. In another specific embodiment, the capture antibody and the detection antibody are different antibodies.

**[0065]** A label, as used herein, is intended to mean a chemical compound or ion that possesses or comes to possess or is capable of generating a detectable signal. The labels of the present invention may be conjugated to the primary binding agent, *e.g.,* primary antibody, or secondary binding agent, *e.g.,* secondary antibody, the biomarker or a surface onto which the label and/or binding agent is attached. Examples of labels includes, but are not limited to, radiolabels, such as, for example, $^{3}H$ and $^{32}P$, that can be measured with radiation-counting devices; pigments, biotin, dyes or other chromogens that can be visually observed or measured with a spectrophotometer; spin labels that can be measured with a spin label analyzer; and fluorescent labels (fluorophores), where the output signal is generated by the excitation of a suitable molecular adduct and that can be visualized by excitation with light that is absorbed by the dye or can be measured with standard fluorometers or imaging systems. Additional examples of labels include, but are not limited to, a phosphorescent dye, a tandem dye and a particle. The label can be a chemiluminescent substance, where the output signal is generated by chemical modification of the signal compound; a metal-containing substance; or an enzyme, where there occurs an enzyme-dependent secondary generation of signal, such as the formation of a colored product from a colorless substrate. The term label also includes a "tag" or hapten that can bind selectively to a conjugated molecule such that the conjugated molecule, when added subsequently along with a substrate, is used to generate a detectable signal. For example, one can use biotin as a label and subsequently use an avidin or streptavidin conjugate of horseradish peroxidate (HRP) to bind to the biotin label, and then use a colorimetric substrate (e.g., tetramethylbenzidine (TMB)) or a fluorogenic substrate such as Amplex Red reagent (Molecular Probes, Inc.) to detect the presence of HRP. Numerous labels are know by those of skill in the art and include, but are not limited to, particles, fluorophores, haptens, enzymes and their colorimetric, fluorogenic and chemiluminescent substrates and other labels that are described in



Fujirebio Diagnostics, Inc. v. Quanterix Corp.
EX-1045
5777

RICHARD P. HAUGLAND, MOLECULAR PROBES HANDBOOK OF FLUORESCENT PROBES AND RESEARCH PRODUCTS (9th edition, CD-ROM, (September 2002), which is herein incorporated by reference.

**[0066]** A fluorophore of the present invention is any chemical moiety that exhibits an absorption maximum beyond 280 nm, and when covalently attached to a labeling reagent retains its spectral properties. Fluorophores of the present invention include, without limitation; a pyrene (including any of the corresponding derivative compounds disclosed in US Patent 5,132,432, incorporated by reference), an anthracene, a naphthalene, an acridine, a stilbene, an indole or benzindole, an oxazole or benzoxazole, a thiazole or benzothiazole, a 4-amino-7-nitrobenz-2-oxa-1, 3-diazole (NBD), a cyanine (including any corresponding compounds in US Serial Nos. 09/968,401 and 09/969,853, incorporated by reference), a carbocyanine (including any corresponding compounds in US Serial Nos. 09/557,275; 09/969,853 and 09/968,401; U.S.; Patents Nos. 4,981,977; 5,268,486; 5,569,587; 5,569,766; 5,486,616; 5,627,027; 5,808,044; 5,877,310; 6,002,003; 6,004,536; 6,008,373; 6,043,025; 6,127,134; 6,130,094; 6,133,445; and publications WO 02/26891, WO 97/40104, WO 99/51702, WO 01/21624; EP 1 065 250 A1, incorporated by reference), a carbostyryl, a porphyrin, a salicylate, an anthranilate, an azulene, a perylene, a pyridine, a quinoline, a borapolyazaindacene (including any corresponding compounds disclosed in US Patent Nos. 4,774,339; 5,187,288; 5,248,782; 5,274,113; and 5,433,896 , incorporated by reference), a xanthene (including any corresponding compounds disclosed in U.S. Patent No. 6,162,931; 6,130,101; 6,229,055; 6,339,392; 5,451,343 and US serial No. 09/922,333, incorporated by reference), an oxazine (including any corresponding compounds disclosed in US Patent No. 4,714,763, incorporated by reference) or a benzoxazine, a carbazine (including any corresponding compounds disclosed in US Patent No. 4,810,636, incorporated by reference), a phenalenone, a coumarin (including an corresponding compounds disclosed in US Patent Nos. 5,696,157; 5,459,276; 5,501,980 and 5,830,912, incorporated by reference), a benzofuran (including an corresponding compounds disclosed in US Patent Nos. 4,603,209 and 4,849,362, incorporated by reference) and benzphenalenone (including any corresponding compounds disclosed in US Patent No. 4,812,409, incorporated by reference) and derivatives thereof. As used herein, oxazines include resorufins (including any corresponding compounds disclosed in 5,242,805, incorporated by reference), aminooxazinones, diaminooxazines, and their benzo-substituted analogs.



Fujirebio Diagnostics, Inc. v. Quanterix Corp.
EX-1045
5778

**[0067]** When the fluorophore is a xanthene, the fluorophore is optionally a fluorescein, a rhodol (including any corresponding compounds disclosed in US Patent Nos. 5,227,487 and 5,442,045, incorporated by reference), or a rhodamine (including any corresponding compounds in US Patent Nos. 5,798,276; 5,846,737; US serial no. 09/129,015, incorporated by reference). As used herein, fluorescein includes benzo- or dibenzofluoresceins, seminaphthofluoresceins, or naphthofluoresceins. Similarly, as used herein rhodol includes seminaphthorhodafluors (including any corresponding compounds disclosed in U.S. Patent No. 4,945,171, incorporated by reference). Alternatively, the fluorophore is a xanthene that is bound via a linkage that is a single covalent bond at the 9-position of the xanthene. Preferred xanthenes include derivatives of 3*H*-xanthen-6-ol-3-one attached at the 9-position, derivatives of 6-amino-3*H*-xanthen-3-one attached at the 9-position, or derivatives of 6-amino-3*H*-xanthen-3-imine attached at the 9-position.

**[0068]** Fluorophores for use in the invention include, but are not limited to, xanthene (rhodol, rhodamine, fluorescein and derivatives thereof) coumarin, cyanine, pyrene, oxazine and borapolyazaindacene. Most preferred are sulfonated xanthenes, fluorinated xanthenes, sulfonated coumarins, fluorinated coumarins and sulfonated cyanines. The choice of the fluorophore attached to the labeling reagent will determine the absorption and fluorescence emission properties of the labeling reagent and immuno-labeled complex. Physical properties of a fluorophore label include spectral characteristics (absorption, emission and stokes shift), fluorescence intensity, lifetime, polarization and photo-bleaching rate all of which can be used to distinguish one fluorophore from another.

**[0069]** Typically the fluorophore contains one or more aromatic or heteroaromatic rings, that are optionally substituted one or more times by a variety of substituents, including without limitation, halogen, nitro, cyano, alkyl, perfluoroalkyl, alkoxy, alkenyl, alkynyl, cycloalkyl, arylalkyl, acyl, aryl or heteroaryl ring system, benzo, or other substituents typically present on fluorophores known in the art.

**[0070]** In one aspect of the invention, the fluorophore has an absorption maximum beyond 480 nm. In a particularly useful embodiment, the fluorophore absorbs at or near 488 nm to 514 nm



Fujirebio Diagnostics, Inc. v. Quanterix Corp.
EX-1045
5779

(particularly suitable for excitation by the output of the argon-ion laser excitation source) or near 546 nm (particularly suitable for excitation by a mercury arc lamp).

**[0071]** Many of fluorophores can also function as chromophores and thus the described fluorophores are also preferred chromophores of the present invention.

**[0072]** In addition to fluorophores, enzymes also find use as labels. Enzymes are desirable labels because amplification of the detectable signal can be obtained resulting in increased assay sensitivity. The enzyme itself may not produce a detectable signal but is capable of generating a signal by, for example, converting a substrate to produce a detectable signal, such as a fluorescent, colorimetric or luminescent signal. Enzymes amplify the detectable signal because one enzyme on a labeling reagent can result in multiple substrates being converted to a detectable signal. This is advantageous where there is a low quantity of target present in the sample or a fluorophore does not exist that will give comparable or stronger signal than the enzyme. The enzyme substrate is selected to yield the preferred measurable product, e.g. colorimetric, fluorescent or chemiluminescence. Such substrates are extensively used in the art, many of which are described in the MOLECULAR PROBES HANDBOOK, *supra*.

**[0073]** In a specific embodiment, a colorimetric or fluorogenic substrate and enzyme combination uses oxidoreductases such as horseradish peroxidase and a substrate such as 3,3'-diaminobenzidine (DAB) and 3-amino-9-ethylcarbazole (AEC), which yield a distinguishing color (brown and red, respectively). Other colorimetric oxidoreductase substrates that yield detectable products include, but are not limited to: 2,2-azino-bis(3-ethylbenzothiazoline-6-sulfonic acid) (ABTS), *o*-phenylenediamine (OPD), 3,3',5,5'-tetramethylbenzidine (TMB), *o*-dianisidine, 5-aminosalicylic acid, 4-chloro-1-naphthol. Fluorogenic substrates include, but are not limited to, homovanillic acid or 4-hydroxy-3-methoxyphenylacetic acid, reduced phenoxazines and reduced benzothiazines, including Amplex® Red reagent and its variants (U.S. Pat. No. 4,384,042) and reduced dihydroxanthenes, including dihydrofluoresceins (U.S. Pat. No. 6,162,931, incorporated by reference) and dihydrorhodamines including dihydrorhodamine 123. Peroxidase substrates that are tyramides (U.S. Pat. Nos. 5,196,306; 5,583,001 and 5,731,158, incorporated by reference) represent a unique class of peroxidase substrates in that they can be intrinsically detectable before action of the enzyme but are "fixed in place" by the action of a



Fujirebio Diagnostics, Inc. v. Quanterix Corp.
EX-1045
5780

peroxidase in the process described as tyramide signal amplification (TSA). These substrates are extensively utilized to label targets in samples that are cells, tissues or arrays for their subsequent detection by microscopy, flow cytometry, optical scanning and fluorometry.

**[0074]** Another preferred colorimetric (and in some cases fluorogenic) substrate and enzyme combination uses a phosphatase enzyme such as an acid phosphatase, an alkaline phosphatase or a recombinant version of such a phosphatase in combination with a colorimetric substrate such as 5-bromo-6-chloro-3-indolyl phosphate (BCIP), 6-chloro-3-indolyl phosphate, 5-bromo-6-chloro-3-indolyl phosphate, *p*-nitrophenyl phosphate, or *o*-nitrophenyl phosphate or with a fluorogenic substrate such as 4-methylumbelliferyl phosphate, 6,8-difluoro-7-hydroxy-4-methylcoumarinyl phosphate (DiFMUP, U.S. Pat. No. 5,830,912, incorporated by reference) fluorescein diphosphate, 3-*O*-methylfluorescein phosphate, resorufin phosphate, *9H*-(1,3-dichloro-9,9-dimethylacridin-2-one-7-yl) phosphate (DDAO phosphate), or ELF 97, ELF 39 or related phosphates (U.S. Pat. Nos. 5,316,906 and 5,443,986, incorporated by reference).

**[0075]** Glycosidases, in particular beta-galactosidase, beta-glucuronidase and beta-glucosidase, are additional suitable enzymes. Appropriate colorimetric substrates include, but are not limited to, 5-bromo-4-chloro-3-indolyl beta-D-galactopyranoside (X-gal) and similar indolyl galactosides, glucosides, and glucuronides, *o*-nitrophenyl beta-D-galactopyranoside (ONPG) and p-nitrophenyl beta-D-galactopyranoside. Preferred fluorogenic substrates include resorufin beta-D-galactopyranoside, fluorescein digalactoside (FDG), fluorescein diglucuronide and their structural variants (U.S. Pat. Nos. 5,208,148; 5,242,805; 5,362,628; 5,576,424 and 5,773,236, incorporated by reference), 4-methylumbelliferyl beta-D-galactopyranoside, carboxyumbelliferyl beta-D-galactopyranoside and fluorinated coumarin beta-D-galactopyranosides (U.S. Pat. No. 5,830,912, incorporated by reference).

**[0076]** Additional enzymes include, but are not limited to, hydrolases such as cholinesterases and peptidases, oxidases such as glucose oxidase and cytochrome oxidases, and reductases for which suitable substrates are known.

**[0077]** Specific embodiments of the present invention comprise enzymes and their appropriate substrates to produce a chemiluminescent signal, such as, but not limited to, natural and recombinant forms of luciferases and aequorins. Chemiluminescence-producing substrates for



Fujirebio Diagnostics, Inc. v. Quanterix Corp.
EX-1045
5781

phosphatases, glycosidases and oxidases such as those containing stable dioxetanes, luminol, isoluminol and acridinium esters are additionally useful.

**[0078]** Additional embodiments comprise haptens such as biotin. Biotin is useful because it can function in an enzyme system or fluorogenic system to further amplify the detectable signal, and it can function as a tag to be used in affinity chromatography for isolation purposes. For detection purposes, an enzyme conjugate that has affinity for biotin is used, such as avidin-HRP or streptavidin-HRP. Subsequently a peroxidase substrate is added to produce a detectable signal. Alternatively, a colorimetric or fluorimetric reporter dye or protein that has affinity for biotin is used, such as streptavidin-R-Phycoerythrin.

**[0079]** Haptens also include hormones, naturally occurring and synthetic drugs, pollutants, allergens, affector molecules, growth factors, chemokines, cytokines, lymphokines, amino acids, peptides, chemical intermediates, nucleotides and the like.

**[0080]** Fluorescent proteins also find use as labels for the labeling reagents of the present invention. Examples of fluorescent proteins include green fluorescent protein (GFP) and the phycobiliproteins and the derivatives thereof. The fluorescent proteins, especially phycobiliprotein, are particularly useful for creating tandem dye labeled labeling reagents. These tandem dyes comprise a fluorescent protein and a fluorophore for the purposes of obtaining a larger stokes shift wherein the emission spectra is farther shifted from the wavelength of the fluorescent protein's absorption spectra. This is particularly advantageous for detecting a low quantity of a target in a sample wherein the emitted fluorescent light is maximally optimized, in other words little to none of the emitted light is reabsorbed by the fluorescent protein. For this to work, the fluorescent protein and fluorophore function as an energy transfer pair wherein the fluorescent protein emits at the wavelength that the fluorophore absorbs at and the fluorophore then emits at a wavelength farther from the fluorescent proteins than could have been obtained with only the fluorescent protein. A particularly useful combination is the phycobiliproteins disclosed in US Patents 4,520,110; 4,859,582; 5,055,556, incorporated by reference, and the sulforhodamine fluorophores disclosed in 5,798,276, or the sulfonated cyanine fluorophores disclosed in US serial Nos. 09/968/401 and 09/969/853, incorporated by reference; or the sulfonated xanthene derivatives disclosed in 6,130,101, incorporated by reference and those



Fujirebio Diagnostics, Inc. v. Quanterix Corp.
EX-1045
5782

combinations disclosed in US Patent 4,542,104, incorporated by reference. Alternatively, the fluorophore functions as the energy donor and the fluorescent protein is the energy acceptor.

**[0081]** In one embodiment, the label is a fluorophore selected from the group consisting of fluorescein, coumarins, rhodamines, 5-TMRIA (tetramethylrhodamine-5-iodoacetamide), (9-(2(or4)-(N-(2-maleimdylethyl)-sulfonamidyl)-4(or 2)-sulfophenyl)-2,3,6,7,12,13,16,17-octahydro-(1H,5H,11H,15H-xantheno(2,3,4-ij:5,6,7-i'j')diquinolizin-18-ium salt) (Texas Red®), 2-(5-(1-(6-(N-(2-maleimdylethyl)-amino)-6-oxohexyl)-1,3-dihydro-3,3-dimethyl-5-sulfo-2H-indol-2-ylidene)-1,3-propyldienyl)-1-ethyl-3,3-dimethyl-5-sulfo-3H-indolium salt (Cy™3), N,N'-dimethyl-N-(iodoacetyl)-N'-(7-nitrobenz-2-oxa- 1,3-diazol-4-yl)ethylenediamine (IANBD amide), 6-acryloyl-2-dimethylaminonaphthalene (acrylodan), pyrene, 6-amino-2,3-dihydro-2-(2-((iodoacetyl)amino)ethyl)-1,3-dioxo-1H-benz(de)isoquinoline-5,8-disulfonic acid salt (lucifer yellow), 2-(5-(1-(6-(N-(2-maleimdylethyl)-amino)-6-oxohexyl)-1,3-dihydro-3,3-dimethyl-5-sulfo-2H-indol-2-ylidene)-1,3-pentadienyl)-1-ethyl-3,3-dimethyl-5-sulfo-3H-indolium salt (Cy™5), 4-(5-(4-dimethylaminophenyl)oxazol-2-yl)phenyl-N- (2-bromoacetamidoethyl)sulfonamide (Dapoxyl® (2-bromoacetamidoethyl)sulfonamide)), (*N*- (4,4-difluoro-1,3,5,7-tetramethyl- 4-bora-3a,4a-diaza-*s*-indacene- 2-yl)iodoacetamide (BODIPY® 507/545 IA), *N*-(4,4-difluoro-5,7-diphenyl- 4-bora-3a,4a-diaza-*s*-indacene- 3-propionyl)- *N'*-iodoacetylethylenediamine (BODIPY 530/550 IA), 5-((((2-iodoacetyl)amino)ethyl) amino)naphthalene-1-sulfonic acid (1,5-IAEDANS), and carboxy-X-rhodamine, 5/6-iodoacetamide (XRIA 5,6). Another example of a label is BODIPY-FL-hydrazide. Other luminescent labels include lanthanides such as europium (Eu3+) and terbium (Tb3+), as well as metal-ligand complexes of ruthenium [Ru(II)], rhenium [Re(I)], or osmium [Os(II)], typically in complexes with diimine ligands such as phenanthroline.

**[0082]** Once levels of the known biomarker are measured, these measured levels are compared to normal levels of the biomarker to determine a difference, if any, between the measured levels and the normal levels of the biomarker. A difference between normal levels and the measured levels of the biomarker may indicate that the subject has a disease or abnormal condition or has a higher (or lower) probability of developing a disease or abnormal condition than normal subjects. In addition the magnitude of difference between measured levels and normal levels of the



Fujirebio Diagnostics, Inc. v. Quanterix Corp.
EX-1045
5783

biomarker may also indicate the severity of disease or abnormal condition or the level of probability of developing a disease or abnormal condition, compared to normal subjects.

**[0083]** The difference between measured levels of the biomarker and normal levels may be a relative or absolute quantity. In addition, "levels of biomarkers" is used to mean any measure of the quantity of the biomarker such as, but not limited to, mass, concentration, biological activity. Example of biological activities that may be used to quantify biomarkers include, but are not limited to, chemotactic, cytotoxic, enzymatic or other biological activities, such as quantifiable activities that are used, for example, by the National Institute for Biological Standards and Control (NIBSC) in the United Kingdom for the quantification of interferon, cytokine and growth-factor activity. The difference in levels of biomarker may be equal to zero, indicating that the patient is normal, or that there has been no change in levels of biomarker since the previous assay. The difference may simply be, for example, a measured fluorescent value, radiometric value, densitometric value, mass value *etc.*, without any additional measurements or manipulations. Alternatively, the difference may be expressed as a percentage or ratio of the measured value of the antigen to a measured value of another compound including, but not limited to, a standard, such as the SAP standard. The difference may be negative, indicating a decrease in the amount of measured biomarker over normal value or from a previous measurement, and the difference may be positive, indicating an increase in the amount of measured antigen over normal values or from a previous measurement. The difference may also be expressed as a difference or ratio of the biomarker to itself, measured at a different point in time. The difference may also be determined using in an algorithm, wherein the raw data is manipulated.

**[0084]** "Normal levels" of a given biomarker may be assessed by measuring levels of the biomarker in a known healthy subject, including the same subject that is later screened or being diagnosed. Normal levels may also be assessed over a population sample, where a population sample is intended to mean either multiple samples from a single patient or at least one sample from a multiple of subjects. Normal levels of a biomarker, in terms of a population of samples, may or may not be categorized according to characteristics of the population including, but not limited to, sex, age, weight, ethnicity, geographic location, fasting state, state of pregnancy or



Fujirebio Diagnostics, Inc. v. Quanterix Corp.
EX-1045
5784

post-pregnancy, menstrual cycle, general health of the patient, alcohol or drug consumption, caffeine or nicotine intake and circadian rhythms.

**[0085]** The present invention also relates to methods of diagnosing or testing for an abnormal condition in a patient. As used herein the term "diagnose" means to confirm the results of other tests or to simply confirm suspicions that the patient may have a particular abnormal condition. A "test," on the other hand, is used to indicate a screening method where the patient or the healthcare provider has no indication that the patient may, in fact, have a particular disease or particular abnormal condition. The methods of testing herein may be used for a definitive diagnosis, or the tests may be used to assess a patient's likelihood or probability of developing a disease or abnormal condition.

**[0086]** The methods of the present invention, therefore, may be used for diagnostic or screening purposes. Both diagnostic and testing can be used to "stage" a condition or disease in a patient. As used herein, the term "stage" is used to indicate that the abnormal condition or disease can be categorized, either arbitrarily or rationally, into distinct degrees of severity. The categorization may be based upon any quantitative characteristic that can be separated, such as, but not limited to, a numerical value of a biomarker, or it may be based upon qualitative characteristics that can be separated. The term "stage" may or may not involve disease progression. In addition, the assay or measurement may be used to stratify a population into relevant cohorts of similarly classified individuals, such as for a clinical trial or other study.

**[0087]** The present invention also relates to methods of monitoring the progression of an abnormal condition in a subject, as well as methods of monitoring the efficacy of a treatment or a potential treatment in a subject with an abnormal condition, with the methods comprising establish one or more standard curves, where the standard comprises a SAP peptide. The methods further comprise contacting more than one sample from a subject with at least one binding agent that is capable of binding an aggregated biomarker, where the multiple samples are taken from the subject at different time points. The level binding activity of the binding agent in the samples is detected and the binding activity in each sample is correlated to the established standard curve(s) to determine the levels of the aggregated biomarker in the subject. The determined levels of the aggregated biomarker from each time point, using SAP as a standard,



Fujirebio Diagnostics, Inc. v. Quanterix Corp.
EX-1045
5785

are then compared to each other to determine if the measured levels of the aggregated biomarker are changing over time.

**[0088]** Thus, the present invention also relates to methods of screening potential therapeutics for their ability to prevent or reverse protein aggregation *in vitro*. The methods may comprise, for example, monitoring the rate of aggregation of a biomarker in the presence or absence of a test compound and determining if the test compound alters the rate of aggregation. The SAPs of the present invention, could, of course, be used to establish binding curves and aggregation rate curves as well.

[**0089**] The invention may also be used to screen antibodies that have been developed as potential therapeutics, such as, but not limited to, humanized antibodies. Currently, vaccination studies are underway that have the intent of generating antibodies in the subject that bind and antagonize the effect of aggregated beta amyloid, and possibly promote the clearance of beta amyloid aggregates. The administration of humanized antibodies raised against aggregates of beta amyloid, as well as other proteins or peptides that have a tendency to form toxic aggregates, may permit active immunization programs to be circumvented. The compositions of the present invention may be used to compare the affinity or other characteristics of generated antibodies.

**[0090]** Similarly, the SAPs of the present invention may also be used as vaccinations themselves. Accordingly, the SAPs, which may less toxic or even non-toxic to the host cell or organism, may be administered in such a manner as to elicit an immune response from the cell or organism, while reducing risks associated with administering traditional vaccines. The vaccines may be in the form of single dose preparations or in multi-dose flasks which can be used for mass vaccination programs. Reference is made to Remington's Pharmaceutical Sciences, Mack Publishing Co., Easton, Pa., Osol (ed.) (1980); and New Trends and Developments in Vaccines, Voller et al. (eds.), University Park Press, Baltimore, Md. (1978), for methods of preparing and using vaccines. Thus, in one embodiment, the present invention provides for methods of vaccinating a subject, with the method comprising administering to the subject a protection-inducing amount of a SAP vaccine, with the vaccine comprising a SAP and an adjuvant. In specific embodiments, the SAP of the SAP vaccine is a MAP. In even more specific embodiments, the MAP of the SAP vaccine is comprises at least a portion of the Aβ peptide, the



Fujirebio Diagnostics, Inc. v. Quanterix Corp.
EX-1045
5786

huntingtin peptide, the alpha-synuclein peptide, the SOD-1 peptide, islet amyloid polypeptide and the prion peptide or mutants thereof.

**[0091]** The following examples are for illustrative purposes and are not intended to limit the scope of the subject matter of the present invention.

*Examples*

**[0092]** *Example 1 – Preparation of a 4-Branched MAP-Aβ$_{1-20}$*

**[0093]** The MAP-Aβ$_{1-20}$ peptide was constructed using Fmoc protein synthesis chemistry, which is described in Tam, J.P. and Lu, Y.-A., *Proc. Nat'l. Acad. Sci.*, 85:9084-9088 (1989); Ahlborg, N., *J. Immunol. Methods*, 179:269-275 (1995); and Espanel, X., *et al.*, J. Biol. Chem. 278(17):15162-15167 (2003), all of which are incorporated by reference in their entirety. The β-alanine was first immobilized, and the lysine residues were added to the immobilized β-alanine. Through a series of addition of protected amino acid residues, the chains were elongated in the C to N terminal direction.

**[0094]** *Example 2 – Quantification of Aggregated Aβ$_{1-42}$ Using MAP-Aβ$_{1-20}$*

**[0095]** As described in United States Patent Nos. 6, 696,304, 6,649,414, 6,632,536 and 6,599,331, which are incorporated by reference, antibody specific for Aβ1-20 was conjugated to color encoded beads, composed of polystyrene, which were licensed from Luminex™ Corporation (Austin, TX). Wells of a 96-well plate were pre-wet with 200 µL working buffer/wash solution. The wash solution is available from Biosource International (Camarillo, CA, USA). After about 15 to 30 seconds, the wash solution was aspirated from the wells using vacuum manifold.

**[0096]** The bead conjugation method used yields a 100X stock solution, containing approximately 20 x $10^6$ beads/mL. The beads used in the assay were prepared from the 100X stock solution. Just prior to use, the stock solution was vortexed for 30 seconds, and then sonicated for 30 seconds. The working solution of the conjugated beads, containing about 2 x $10^5$ beads/mL, was prepared by diluting the stock solution in wash buffer 1:100. Just prior to use, the working solution of conjugated beads was again vortexed for 30 seconds and sonicated



Fujirebio Diagnostics, Inc. v. Quanterix Corp.
EX-1045
5787

for 30 seconds. About 25 μL (5000 beads) of conjugated bead solution was added to each well designated for the assay (including wells designated for the standard curve and for the samples) and the wells were subsequently shielded from light.

**[0097]** Next, 200 μL of wash solution was added to each well and the beads were allowed to soak for about 15 to 30 seconds. The wash solution was then aspirated with the vacuum manifold. The washing step was repeated. The residual liquid on the bottom of the plate was blotted on a clean paper towel.

**[0098]** The MAP-$A\beta_{1-20}$ standards were prepared in the following concentrations: 20 ng/mL; 6.67 ng/mL, 2.22ng/mL, 0.74 ng/mL, 0.25 ng/mL, 0.082 ng/mL; 0.027 ng/mL and a blank. Each well designated for standard received 100 μL of standard.

**[0099]** Next, 50 μL buffer was pipetted into each of the well and then 50 μL of each sample was pipetted into designated wells in duplicate. The plate was incubated for about 2 hours at room temperature on an orbital shaker at about 500-600 rpm. After incubation, the liquid was aspirated from the wells with a vacuum manifold at a pressure of less than about 5 inches Hg. The wells were washed three times with 200 μl of wash solution buffer.

**[00100]** For detection, 100 μL of a biotinylated detector antibody at a concentration of about 5 μg/mL, was added to each well the plate and incubated for about 1 hour at room temperature on an orbital shaker at about 500-600 rpm. The detector antibody is specific for an epitope of the $A\beta_{1-20}$.

**[00101]** Ten to fifteen minutes before the end of the incubation period, a streptavidin-R-Phycoerythrin solution was prepared. The concentration of the steptavidin-R-Phycoerythrin was about 12 μg/mL.

**[00102]** After the 1 hour incubation, the biotinylated detector antibody solution was aspirated from the wells with a vacuum manifold at a pressure of less than about 5 inches Hg. The beads were washed three times and the residual liquid was blotted from the bottom of the plate on clean paper towels.



Fujirebio Diagnostics, Inc. v. Quanterix Corp.
EX-1045
5788

**[00103]** After removal of the detector antibody solution and subsequent washing, about 100 μL of the streptavidin-R-Phycoerythrin solution was added to each well and incubated for about 30 minutes at room temperature on an orbital shaker at 500-600 rpm.

**[00104]** The streptavidin-R-Phycoerythrin solution was aspirated from the wells using a vacuum manifold at a pressure of less than about 5 inches Hg, and the wells were washed four times.

**[00105]** After washing, the beads were resuspended in buffer solution and fluorescence was read on a Luminex 100™.

**[00106]** From the known concentrations of MAP-$A\beta_{1-20}$ and the corresponding fluorescence values, a standard curve was generated using standard curve fitting software SOFTmaxPro. From the generated standard curve, concentration of samples were determined and then multiplied by 2 to correct for the 1:2 dilution in the wells.

**[00107]** Figure 2 provides representative standard curves obtained in the aggregated Aβ assay for the Luminex™ platform, using the MAP-$A\beta_{1-20}$ as the standard.

**[00108]** Also depicted in Figure 2 is the comparison of the reactivity of the MAP-$A\beta_{1-20}$ with the reactivity of the indicated concentrations of Glabe's oligomer. In this example, Glabe's oligomer is an aggregated form of Aβ that is synthesized in vitro that is postulated to have a similar conformation to the natural Aβ aggregates found in biological samples. The following reference describes the production of Glabe's oligomer and is incorporated by reference: Demuro, A., *J. Biol. Chem.* 280(17):17294-17300 (2005).

**[00109]** Figures 3 and 4 depict levels of natural aggregated Aβ in samples, using the MAP-$A\beta_{1-20}$ as a standard. Figures 3 depicts the detection of natural aggregated Aβ in ventricular fluid samples from a cohort of elderly patients with Alzheimer's disease and elderly, non-demented control patients. The samples of Figure 3 were collected into tubes, centrifuged briefly to sediment cells contained in the samples, then frozen until analyzed for aggregated Aβ with the aggregated Aβ assay described here.



Fujirebio Diagnostics, Inc. v. Quanterix Corp.
EX-1045
5789

**[00110]** Also depicted in Figure 3 are correlations of concentrations of Aβ with concentrations of inflammatory cytokines that were measured with commercially available reagents from BioSource International, Inc. Figure 4 depicts the detection of natural aggregated Aβ in tissue homogenates prepared from various brain regions of patients with Alzheimer's disease, patients with Alzheimer's disease with Lewy Bodies, and elderly, non-demented controls, using the assay described here. The samples of Figure 4 were collected, weighed, homogenized in Tris buffered saline supplemented with protease inhibitors, then centrifuged for 1 hour at 100,000 x g at 4 °C. This procedure has been shown to minimize Aβ fibrils and protofibrils. The following references have used an ultracentrifugation step to eliminate Aβ fibrils from samples and are incorporated by reference: Gong, Y., et al., *Proc. Natl. Acad. Sci.* 199(18):10417-10422; Barghorn, S., et al. *J. Neurochem.* 95(3):834-847 (2005). Following the centrifugation step, the clear liquid that formed the middle layer of the sample was carefully extracted using a syringe to avoid the upper fatty layer and the pellet that comprised the bottom layer of the. Samples prepared in this manner were assayed with the aggregated Aβ assay described here, and concentrations of Aβ were correlated with concentrations of inflammatory cytokines, measured with commercially available reagents from BioSource, International, Inc.

**[00111]** *Example 3 – Preparation of a 4-Branched MAP-Alpha-Synuclein*

**[00112]** The MAP-alpha-synuclein 116-130 peptide was constructed using Fmoc protein synthesis chemistry, which is described in Tam, J.P. and Lu, Y.-A., *Proc. Nat'l. Acad. Sci.*, 85:9084-9088 (1989); Ahlborg, N., *J. Immunol. Methods*, 179:269-275 (1995); and Espanel, X., *et al.*, J. Biol. Chem. 278(17):15162-15167 (2003), all of which are incorporated by reference in their entirety. As used herein, the phrase MAP-alpha-synuclein 116-130 peptide indicates a peptide with amino acids 116-130 of SEQ ID NO:2. Following the same general construction of the 4-branched MAP-$A\beta_{1-20}$ standard, a β-alanine moiety was first immobilized, and the lysine residues were added to the immobilized β-alanine. Through a series of addition of protected amino acid residues, the chains were elongated in the C to N terminal direction.

**[00113]** *Example 4 - Time Course Aggregation of Alpha-Synuclein*

**[00114]** Aggregated Alpha-Synuclein was generated according to the following procedure. Recombinant Alpha-Synuclein A53T (Recombinant Peptide Technologies Cat. # S-1002-2) was



Fujirebio Diagnostics, Inc. v. Quanterix Corp.
EX-1045
5790

reconstituted with deionized water to a concentration of 1 mg/mL. An aliquot (100 µL) of the recombinant protein was then dispensed into a 2 mL Corning Cryogenic vial and diluted to a final concentration of about 100 µg/mL in PBS containing 0.02% sodium azide. The vial was then capped, sealed with Parafilm, and placed on a rocker in a 37°C incubator. At various times, aliquots of the protein were removed from the mixture, and stored at -20°C. At the completion of the incubation step, samples were defrosted at room temperature, then diluted to a final concentration of 1 µg/mL in Assay Diluent. The diluted samples were then assayed using the 211 mAb (Invitrogen Corp., Carlsbad, California, USA, Cat. # 32-8100) as both the capturing and detecting (biotinylated) antibody. The results are presented in the Figure 5.

**[00115]** *Example 5 - Quantification of Aggregated Alpha-Synuclein Using MAP-Alpha-Synuclein*

**[00116]** As described in United States Patent Nos. 6, 696,304, 6,649,414, 6,632,536 and 6,599,331, which are incorporated by reference, antibody specific for alpha-synuclein was conjugated to color encoded beads, composed of polystyrene, which were licensed from Luminex™ Corporation (Austin, TX). Wells of a 96-well plate were pre-wet with 200 µL working buffer/wash solution. The wash solution is available from Biosource International (Camarillo, CA, USA). After about 15 to 30 seconds, the wash solution was aspirated from the wells using vacuum manifold.

**[00117]** The bead conjugation method used yields a 100X stock solution, containing approximately 20 x $10^6$ beads/mL. The beads used in the assay were prepared from the 100X stock solution. Just prior to use, the stock solution was vortexed for 30 seconds, and then sonicated for 30 seconds. The working solution of the conjugated beads, containing about 2 x $10^5$ beads/mL, was prepared by diluting the stock solution in wash buffer 1:100. Just prior to use, the working solution of conjugated beads was again vortexed for 30 seconds and sonicated for 30 seconds. About 25 µL (5000 beads) of conjugated bead solution was added to each well designated for the assay (including wells designated for the standard curve and for the samples) and the wells were subsequently shielded from light.



Fujirebio Diagnostics, Inc. v. Quanterix Corp.
EX-1045
5791

**[00118]** Next, 200 μL of wash solution was added to each well and the beads were allowed to soak for about 15 to 30 seconds. The wash solution was then aspirated with the vacuum manifold. The washing step was repeated. The residual liquid on the bottom of the plate was blotted on a clean paper towel.

**[00119]** The MAP-alpha synuclein standards were prepared in the following concentrations: 0.738 ng/mL; 0.246 ng/mL, 0.0819 ng/mL and 0.0273 ng/mL, in addition to a blank. Each well designated for standard received 100 μL of standard.

**[00120]** Next, 50 μL buffer was pipetted into each of the well and then 50 μL of each sample was pipetted into designated wells in duplicate. The plate was incubated for about 2 hours at room temperature on an orbital shaker at about 500-600 rpm. After incubation, the liquid was aspirated from the wells with a vacuum manifold at a pressure of less than about 5 inches Hg. The wells were washed three times with 200 μL of wash solution buffer.

**[00121]** For detection, 100 μL of a biotinylated detector antibody at a concentration of about 2 μg/mL, was added to each well the plate and incubated for about 1 hour at room temperature on an orbital shaker at about 500-600 rpm. The detector antibody (211 mAb) is specific for an epitope of alpha synuclein.

**[00122]** Ten to fifteen minutes before the end of the incubation period, a streptavidin-R-Phycoerythrin solution was prepared. The concentration of the steptavidinR-Phycoerythrin was about 5 μg/mL.

**[00123]** After the 1 hour incubation, the biotinylated detector antibody solution was aspirated from the wells with a vacuum manifold at a pressure of less than about 5 inches Hg. The beads were washed three times and the residual liquid was blotted from the bottom of the plate on clean paper towels.

**[00124]** After removal of the detector antibody solution and subsequent washing, about 100 μL of the streptavidin-R-Phycoerythrin solution was added to each well and incubated for about 30 minutes at room temperature on an orbital shaker at 500-600 rpm.



Fujirebio Diagnostics, Inc. v. Quanterix Corp.
EX-1045
5792

**[00125]** The streptavidin-R-Phycoerythrin solution was aspirated from the wells using a vacuum manifold at a pressure of less than about 5 inches Hg, and the wells were washed four times.

**[00126]** After washing, the beads were resuspended in buffer solution and fluorescence was read on a Luminex 100™.

**[00127]** From the known concentrations of MAP-alpha-synuclein and the corresponding fluorescence values, a standard curve was generated using standard curve fitting software SOFTmaxPro. From the generated standard curve, concentration of samples were determined and then multiplied by 2 to correct for the 1:2 dilution in the wells.

**[00128]** Figure 6 provides representative standard curves obtained in the aggregated alpha-synuclein assay for the Luminex™ platform, using the MAP-alpha-synuclein as the standard.

**[00129]** Also depicted in Figure 6 is the comparison of the reactivity of the MAP-alpha-synuclein with the reactivity of the indicated concentrations of laboratory-aggregated alpha-synuclein from Example 4.



Fujirebio Diagnostics, Inc. v. Quanterix Corp.
EX-1045
5793

## What is Claimed is:

1. A method for quantifying a known biomarker in a sample, said method comprising an assay comparing the binding activity of a binding agent to said known biomarker with the binding activity of said binding agent to a synthetic aggregated peptide (SAP).

2. The method of claim 1 wherein said known biomarker is a peptide.

3. The method of claim 2, wherein said known peptide is selected from the group consisting of beta amyloid (Aβ), huntingtin, alpha-synuclein, superoxide dismutase-1, (SOD1) and prion peptide.

4. The method of claim 3, wherein said known peptide is an aggregated oligomer.

5. The method of claim 4, wherein said aggregated oligomer is an aggregated oligomer of Aβ.

6. The method of claim 3, wherein said binding agent is an antibody or functional fragment thereof.

7. The method of claim 6, wherein said assay is an assay selected from the group consisting of a colorimetric assay and a radiometric assay.

8. The method of claim 7, wherein said assay is a colorimetric assay that is an enzyme-linked immunosorbence assay (ELISA).

9. The method of claim 8, wherein said SAP is a multiple antigenic peptide (MAP).

10. The method of claim 9, wherein said MAP with more than 4 branches.

11. The method of claim 9, wherein said MAP is a 4-branched MAP.

12. The method of claim 11, wherein said MAP comprises at least a portion of a peptide selected from the group consisting of beta amyloid (Aβ), huntingtin, alpha-synuclein, superoxide dismutase-1, (SOD1) and prion peptide.



Fujirebio Diagnostics, Inc. v. Quanterix Corp.
EX-1045
5794

13. The method of claim 11, wherein said MAP comprises at least a portion of the Aβ peptide.

14. The method of claim 13, wherein said portion of Aβ is the N-terminus said Aβ peptide.

15. The method of claim 14, wherein said N-terminus of said Aβ comprises amino acids 1-10 of SEQ ID NO. 1.

16. The method of claim 15, wherein said N-terminus of said Aβ comprises amino acids 1-20 of SEQ ID NO:1.

17. The method of claim 11, wherein said MAP comprises at least a portion of the alpha-synuclein peptide.

18. The method of claim 17, wherein said portion of alpha-synuclein is near the C-terminus said alpha synuclein peptide.

19. The method of claim 18, wherein said C-terminus of said alpha-synuclein comprises amino acids 121-125 of SEQ ID NO. 2.

20. The method of claim 19, wherein said N-terminus of said alpha-synuclein comprises amino acids 116-130 of SEQ ID NO. 2.

21. A method of detecting an abnormal condition in a subject, said method comprising

a) detecting the binding activity of a binding agent towards at least one standard to establish a standard curve, said standard comprising a synthetic aggregated peptide (SAP);

b) contacting a sample from said subject with at least one binding agent that is capable of binding a biomarker, wherein said biomarker is an aggregated biomarker;

c) detecting the level binding activity of said binding agent in said sample;

d) correlating said level of binding activity in said sample to said standard curve to determine the levels of said aggregated biomarker in said subject; and



Fujirebio Diagnostics, Inc. v. Quanterix Corp.
EX-1045
5795

e) comparing the levels of said aggregated biomarker in said subject to normal levels of said aggregated biomarker to determine a difference between measured levels of said aggregated biomarker and normal levels of said aggregated biomarker;

wherein a difference between said measured levels of said aggregated biomarker and said normal levels of said aggregated biomarker, is indicative of an abnormal condition in said subject.

22. The method of claim 21, wherein said abnormal condition is selected from the group consisting of Alzheimer's Disease, Huntington's Disease, Parkinson's Disease, Cruetzfeldt-Jakob Disease, and heart disease or any stage thereof.

23. The method of claim 22, wherein said aggregated biomarker is selected from the group consisting of aggregated beta amyloid (Aβ), aggregated huntingtin, aggregated alpha-synuclein, aggregated superoxide dismutase-1, (SOD1) and aggregated prion peptide.

24. The method of claim 23, wherein said SAP is a multiple antigenic peptide (MAP).

25. The method of claim 24 wherein said MAP comprises 4 branches.

26. The method of claim 25 wherein at least one branch of said MAP standard comprises at least a portion of a peptide selected from the group consisting of beta amyloid (Aβ), huntingtin, alpha-synuclein, superoxide dismutase-1, (SOD1) and prion peptide.

27. The method of claim 26 wherein said abnormal condition is Alzheimer's Disease, said aggregated biomarker is aggregated Aβ and at least one branch of said MAP standard comprises at least a portion of the beta amyloid (Aβ) peptide.

28. The method of claim 27 wherein said at least one branch of said MAP standard comprises the N-terminus of said amyloid beta (Aβ) peptide.

29. The method of claim 28 wherein said N-terminus of Aβ peptide comprises amino acids 1-20 of SEQ ID NO:1.



Fujirebio Diagnostics, Inc. v. Quanterix Corp.
EX-1045
5796

30. The method of claim 26 wherein said abnormal condition is Parkinson's Disease, said aggregated biomarker is aggregated alpha-synuclein and at least one branch of said MAP standard comprises at least a portion of an alpha-synuclein peptide.

31. The method of claim 30 wherein said at least one branch of said MAP standard comprises a portion of the C-terminus of said alpha-synuclein peptide.

32. The method of claim 31, wherein said C-terminus of said alpha-synuclein peptide comprises amino acids 121-125 of SEQ ID NO:2.

33. A composition comprising a branched MAP peptide, wherein at least one branch of said MAP peptide comprises the N-terminus of amyloid beta (Aβ) peptide.

34. The composition of claim 30, wherein said MAP peptide comprises 4 branches.

35. The composition of claim 31, wherein each of said 4 branches comprises said N-terminus of Aβ peptide.

36. The composition of claim 32, wherein said N-terminus of Aβ peptide comprises amino acids 1-20 of SEQ ID NO:1.

37. The peptide of claim 33, wherein at least one of said 4 branches comprises a peptide other than said N-terminus of Aβ peptide.

38. A composition comprising a branched MAP peptide, wherein at least one branch of said MAP peptide comprises a portion of the C-terminus of alpha-synuclein peptide.

39. The composition of claim 38, wherein said MAP peptide comprises 4 branches.

40. The composition of claim 39, wherein each of said 4 branches comprises said portion of said C-terminus of alpha-synuclein peptide.

41. The composition of claim 30, wherein said portion of said C-terminus of alpha-synuclein peptide comprises amino acids 121-125 of SEQ ID NO:1.



Fujirebio Diagnostics, Inc. v. Quanterix Corp.
EX-1045
5797

42. The peptide of claim 41, wherein at least one of said 4 branches comprises a peptide other than said portion of said C-terminus of alpha-synuclein peptide.



Fujirebio Diagnostics, Inc. v. Quanterix Corp.
EX-1045
5798

FIGURE 1

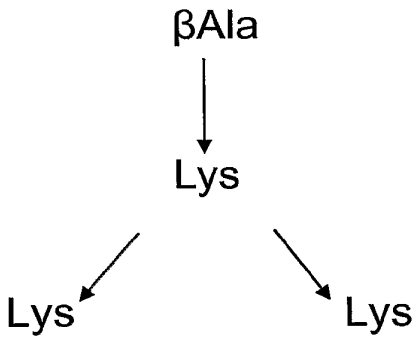


FIGURE 2

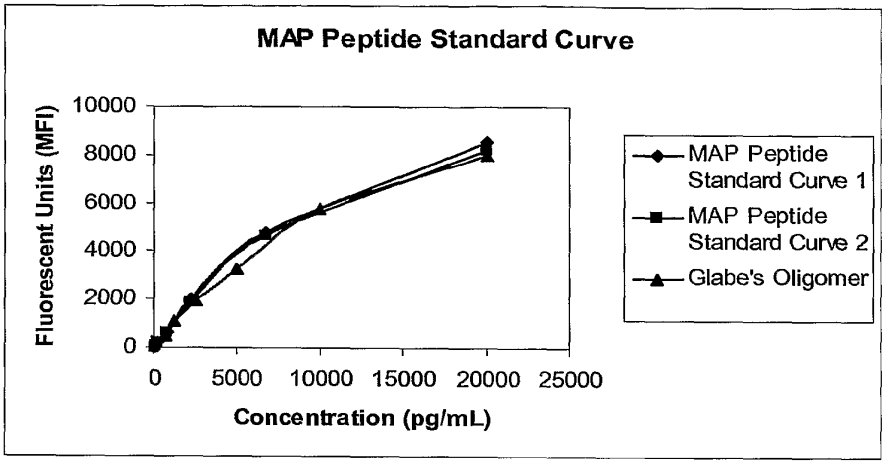
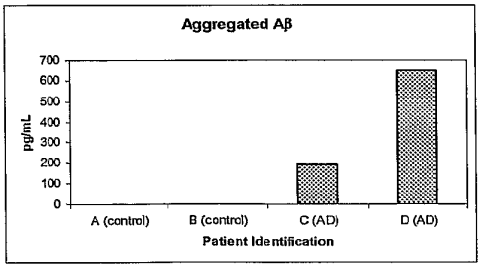
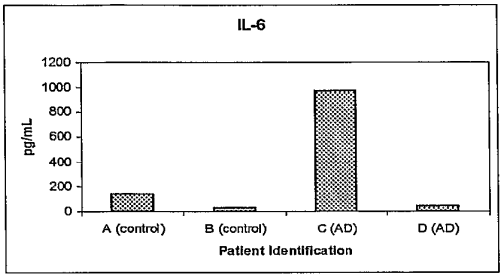
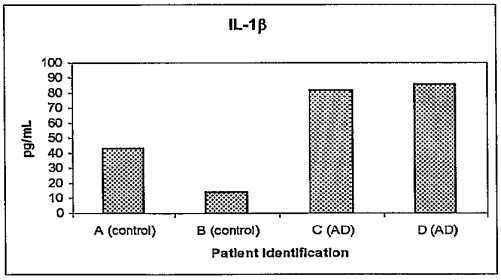

MAP Peptide Standard Curve
Fluorescent Units (MFI)
10000
8000
6000
4000
2000
0
0
5000
10000
15000
20000
25000
Concentration (pg/mL)
MAP Peptide Standard Curve 1
MAP Peptide Standard Curve 2
Glabe's Oligomer

FIGURE 3


Aggregated Aβ
pg/mL
700
600
500
400
300
200
100
0
A (control)
B (control)
C (AD)
D (AD)
Patient Identification


IL-6
pg/mL
1200
1000
800
600
400
200
0
A (control)
B (control)
C (AD)
D (AD)
Patient Identification


IL-1β
pg/mL
100
90
80
70
60
50
40
30
20
10
0
A (control)
B (control)
C (AD)
D (AD)
Patient Identification

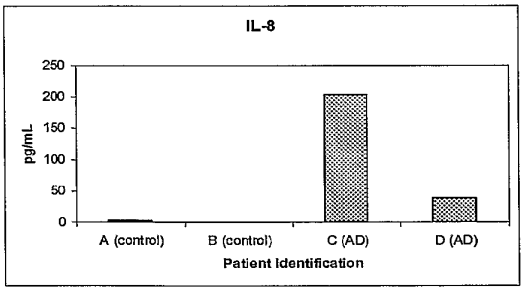
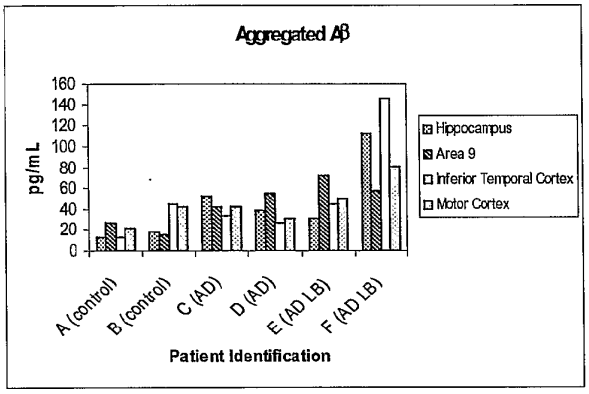
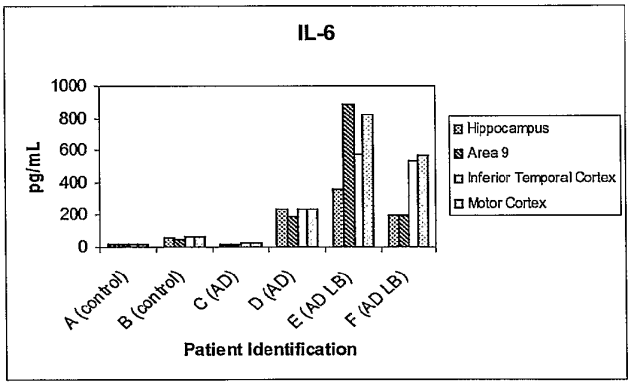

IL-8
pg/mL
250
200
150
100
50
0
A (control)
B (control)
C (AD)
D (AD)
Patient Identification

FIGURE 4


Aggregated Aβ
pg/mL
160
140
120
100
80
60
40
20
0
A (control)
B (control)
C (AD)
D (AD)
E (AD LB)
F (AD LB)
Patient Identification
Hippocampus
Area 9
Inferior Temporal Cortex
Motor Cortex


IL-6
pg/mL
1000
800
600
400
200
0
A (control)
B (control)
C (AD)
D (AD)
E (AD LB)
F (AD LB)
Patient Identification
Hippocampus
Area 9
Inferior Temporal Cortex
Motor Cortex

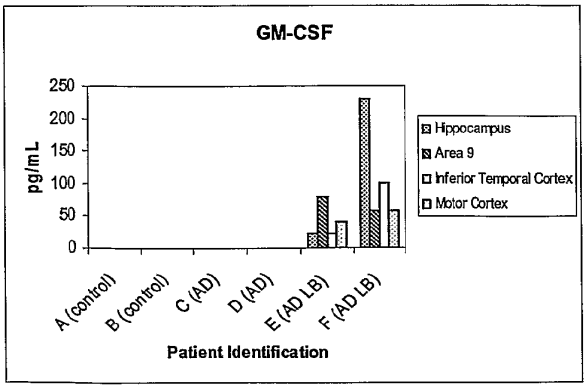

GM-CSF
pg/mL
250
200
150
100
50
0
A (control)
B (control)
C (AD)
D (AD)
E (AD LB)
F (AD LB)
Patient Identification
Hippocampus
Area 9
Inferior Temporal Cortex
Motor Cortex

FIGURE 5

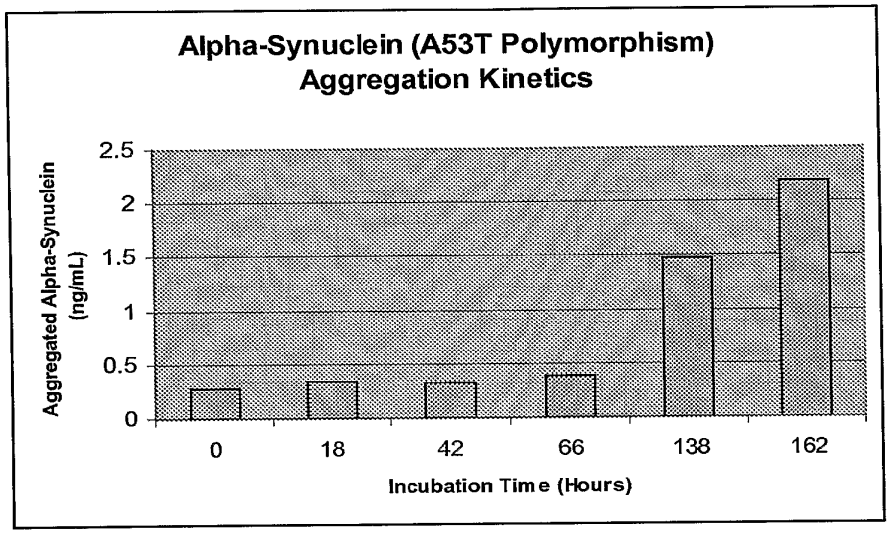
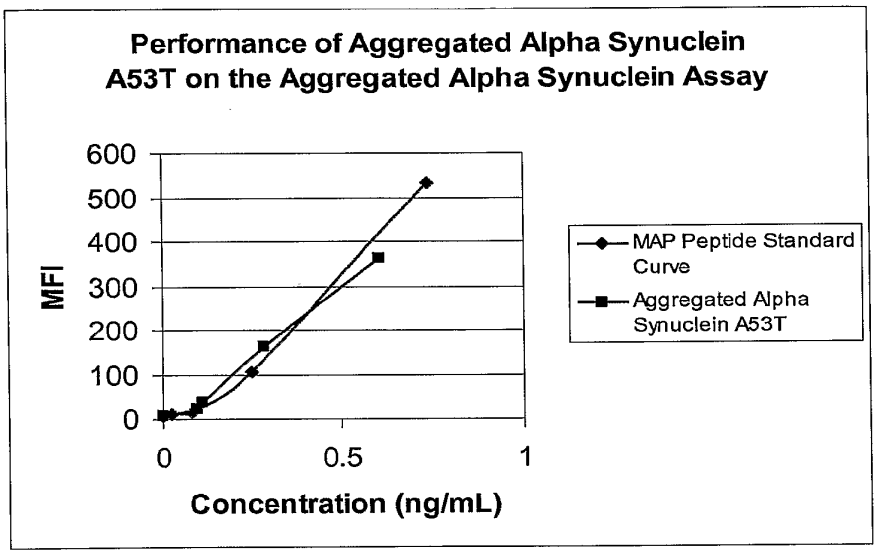

Alpha-Synuclein (A53T Polymorphism)
Aggregation Kinetics
Aggregated Alpha-Synuclein (ng/mL)
2.5
2
1.5
1
0.5
0
0
18
42
66
138
162
Incubation Time (Hours)

FIGURE 6


Performance of Aggregated Alpha Synuclein A53T on the Aggregated Alpha Synuclein Assay
600
500
400
300
200
100
0
MFI
0
0.5
1
Concentration (ng/mL)
MAP Peptide Standard Curve
Aggregated Alpha Synuclein A53T

(12) INTERNATIONAL APPLICATION PUBLISHED UNDER THE PATENT COOPERATION TREATY (PCT)

(19) World Intellectual Property Organization
International Bureau

(43) International Publication Date
20 September 2007 (20.09.2007)

PCT

(10) International Publication Number
WO 2007/106762 A2

(51) International Patent Classification:
*G01N 33/53* (2006.01)

(21) International Application Number:
PCT/US2007/063762

(22) International Filing Date: 12 March 2007 (12.03.2007)

(25) Filing Language: English

(26) Publication Language: English

(30) Priority Data:
60/782,175 14 March 2006 (14.03.2006) US

(71) Applicant *(for all designated States except US)*: **WASHINGTON UNIVERSITY IN ST. LOUIS** [US/US]; One Brookings Drive, St. Louis, Missouri 63110 (US).

(72) Inventors; and
(75) Inventors/Applicants *(for US only)*: **HOLTZMAN, David** [US/US]; 6 Hortense Place, St. Louis, Missouri 63108 (US). **HU, Yan** [CN/US]; 1712 Pineberry Court, St. Louis, Missouri 63146 (US). **TOWNSEND, Robert Reid** [US/US]; 3463 Ongfellow Boulevard, St. Louis, Missouri 63104 (US).

(74) Agent: **DOTY, Kathryn**; Polsinelli Shalton Flanigan Suelthaus, 100 South Fourth Street, Suite 1100, St. Louis, Missouri 63102-1825, (US).

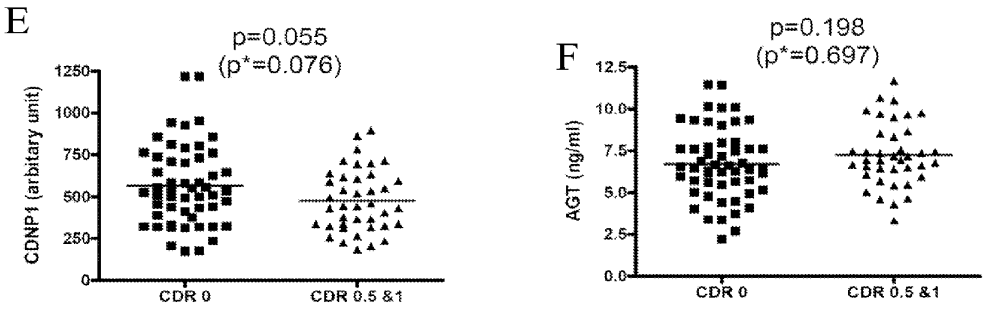
(81) Designated States *(unless otherwise indicated, for every kind of national protection available)*: AE, AG, AL, AM, AT, AU, AZ, BA, BB, BG, BR, BW, BY, BZ, CA, CH, CN, CO, CR, CU, CZ, DE, DK, DM, DZ, EC, EE, EG, ES, FI, GB, GD, GE, GH, GM, GT, HN, HR, HU, ID, IL, IN, IS, JP, KE, KG, KM, KN, KP, KR, KZ, LA, LC, LK, LR, LS, LT, LU, LY, MA, MD, MG, MK, MN, MW, MX, MY, MZ, NA, NG, NI, NO, NZ, OM, PG, PH, PL, PT, RO, RS, RU, SC, SD, SE, SG, SK, SL, SM, SV, SY, TJ, TM, TN, TR, TT, TZ, UA, UG, US, UZ, VC, VN, ZA, ZM, ZW.

(84) Designated States *(unless otherwise indicated, for every kind of regional protection available)*: ARIPO (BW, GH, GM, KE, LS, MW, MZ, NA, SD, SL, SZ, TZ, UG, ZM, ZW), Eurasian (AM, AZ, BY, KG, KZ, MD, RU, TJ, TM), European (AT, BE, BG, CH, CY, CZ, DE, DK, EE, ES, FI, FR, GB, GR, HU, IE, IS, IT, LT, LU, LV, MC, MT, NL, PL, PT, RO, SE, SI, SK, TR), OAPI (BF, BJ, CF, CG, CI, CM, GA, GN, GQ, GW, ML, MR, NE, SN, TD, TG).

**Published:**
— *without international search report and to be republished upon receipt of that report*

*For two-letter codes and other abbreviations, refer to the "Guidance Notes on Codes and Abbreviations" appearing at the beginning of each regular issue of the PCT Gazette.*

(54) Title: ALZHEIMER'S DISEASE BIOMARKERS AND METHODS OF USE




(57) Abstract: The invention encompasses biomarkers for AD, a method for detecting AD, a method of monitoring AD, and a kit for quantifying biomarkers for AD.

WO 2007/106762 A2

# ALZHEIMER'S DISEASE BIOMARKERS AND METHODS OF USE

## GOVERNMENTAL RIGHTS

[0001] This invention was made with government support under AG025662 awarded by the NIH. The government has certain rights in the invention.

## FIELD OF THE INVENTION

[0002] The invention generally relates to biomarkers for Alzheimer's disease, methods of detecting Alzheimer's disease, methods of monitoring Alzheimer's disease, and kits for detecting biomarkers for Alzheimer's disease.

## BACKGROUND OF THE INVENTION

[0003] Alzheimer's disease (AD) will likely become the greatest public health crisis in the United States within the next 2-3 decades if left unchecked. There are currently no proven treatments that delay the onset or prevent the progression of AD, although a few promising candidates are being developed. During the development of these therapies, it will be very important to have biomarkers that can identify individuals at high risk for AD or at the earliest clinical stage of AD in order to target them for therapeutic trials, disease-modifying therapies and to monitor their therapy. Clinicopathological studies suggest that AD pathology (particularly the buildup of amyloid plaques) begins 10-20 years before cognitive symptoms. Even the earliest clinical symptoms of AD are accompanied by, and likely due to, neuronal/synaptic dysfunction and/or cell death. Thus, it will be critical to identify individuals with "preclinical" and very early stage AD, prior to marked clinical symptoms and neuronal loss, so new therapies will have the greatest clinical impact.

[0004] A definitive diagnosis of AD can still only be obtained via neuropathologic evaluation at autopsy. Investigators at the Washington University School of Medicine (WUSM) developed a Clinical Dementia Rating (CDR) scale in which an individual's cognition is rated as normal (CDR 0), or demented with severities of very mild, mild, moderate or severe (CDR 0.5, 1, 2 or 3, respectively) (See Morris, *Neurology*, 1993; 43:2412, hereby included by reference).



Fujirebio Diagnostics, Inc. v. Quanterix Corp.
EX-1045
5806

Individuals diagnosed with possible/probable dementia of the Alzheimer's type (DAT) are usually CDR 1 or greater. One challenge has been to diagnose individuals at earlier stages, when clinical symptoms are less severe. During these early stages (CDR 0.5, often lasting 2-5 years or longer), the majority of individuals meet clinical criteria for mild cognitive impairment (MCI) (Peterson et al., Arch. Neurol, 1999; 56:303). Data suggest an early and insidious pathogenesis of AD, the clinical manifestation of which becomes apparent only after substantial neuronal cell death and synapse loss has taken place. These findings have profound implications for AD therapeutic and diagnostic strategies.

[0005] At present, a few AD biomarkers have been identified that may differentiate individuals with clinical disease (i.e., DAT) from those who are cognitively normal. Mean cerebral spinal fluid (CSF) amyloid beta (Aβ42) levels have been consistently reported to be decreased in AD, including cases of mild dementia, although this decrease may not be specific for AD. CSF Aβ42 is also decreased in MCI, but there is great overlap with control group values. Many studies have reported elevated levels of CSF total tau (and phosphorylated forms) in AD patients. However, similar to Aβ42, there is significant overlap between individual tau values in MCI/AD and control groups, and this increase is not specific for AD. In addition to Aβ42 and tau, differences in other candidate AD biomarkers that likely reflect CNS damage have been observed, including isoprostanes, and 4-hydroxy-2-nonenal (markers of oxidative damage), and sulfatide, a sphingolipid produced by oligodendrocytes. To date, however, none of these individual candidate markers have achieved levels of sensitivity and specificity acceptable for use in disease diagnosis.

## SUMMARY OF THE INVENTION

[0006] One aspect of the invention encompasses a biomarker for AD. The biomarker comprises the level of antithrombin III in a bodily fluid of a subject.

[0007] Another aspect of the invention encompasses a method for detecting AD. Generally speaking, the method comprises quantifying the level of antithrombin III in a bodily fluid of the subject and determining if the quantified



Fujirebio Diagnostics, Inc. v. Quanterix Corp.
EX-1045
5807

level of antithrombin III is elevated in comparison to the average antithrombin III level for a subject with a CDR of 0.

[0008] Yet another aspect of the invention encompasses a method for monitoring AD. Typically, the method comprises quantifying the level of antithrombin III in a bodily fluid of the subject and comparing the quantified level of antithrombin III to a previously quantified antithrombin III level of the subject.

[0009] Still another aspect of the invention encompasses a kit for quantifying antithrombin III in a bodily fluid of a subject. The kit comprises the means to quantify antithrombin III and instructions.

## BRIEF DESCRIPTION OF THE FIGURES

[0010] **FIG. 1** depicts the 2-D DIGE analysis of CSF prior to and following depletion of high abundance proteins. The same amount of protein (19 micrograms) in CSF prior to depletion (A) and following depletion (B) and in the retained proteins (C) was labeled with Cy2 (blue), Cy3 (green), and Cy5 (red), respectively, and analyzed on a single gel (10% isocratic SDS-PAGE gel). (D) overlay of all three fluorescent images demonstrates the position of the depleted proteins (pink) with respect to the low abundance proteins revealed by the depletion method.

[0011] **FIG. 2** depicts a representative 2-D DIGE image (Cy2-labeled) of CSF that has been depleted of six high abundance proteins. 50 micrograms of protein was labeled and resolved first on a pH 3–10 IPG strip and further separated on a 10–20% gradient SDS-PAGE gel.

[0012] **FIG. 3** depicts representative gel images and 3-D representations of one of the apoE spots that displayed intraindividual variation. Shown here are the data from Subject 2. There is a 3.1-fold change of the levels of this apoE spot between the two time points. (A) represents timepoint 1; (B) represents timepoint 2.

[0013] **FIG. 4** depicts the hierarchical clustering of the 2-D DIGE profiles of 306 matched proteins spots from the 12 CSF samples from six individual subjects at time 1 (T1) and 2 weeks (T2). Each 2-D DIGE profile (column) contains 306 matched protein spots. Lines correspond to individual proteins, and colors represent their standard abundance after a log transformation



Fujirebio Diagnostics, Inc. v. Quanterix Corp.
EX-1045
5808

and Z-score normalization (red, more abundant; green, less abundant). The CDR 0.5 samples are marked with an asterisk. Spotfire software was used to generate the cluster tree and the heat map. Distance in the cluster tree depicted here is not a reflection of similarity or strength of association.

[0014] **FIG. 5** depicts the multidimensional scaling analysis of the 2-D DIGE profiles of 12 CSF samples from six individual subjects at time 1 (T1) and then 2 weeks later (T2). A 2-D projection of the 3-D scatter plot is shown. The proteomic profile of each sample is represented by a point. The axes correspond to the first three principal components. A single color has been used to label two intraindividual CSF samples.

[0015] **FIG. 6** depicts graphs showing the CSF levels of biomarkers in CDR group of 0, 0.5, and 1. The graphs were generated using unadjusted raw data. One-way ANOVA analysis was performed to compare the average levels of candidate biomarkers in the three groups and where overall $p<0.05$, Bonferroni's multiple comparison test was done to examine which comparisons generate statistically significant differences (denoted by asterisks). (A) ACT; (B) ATIII; (C) ZAG; (D) CDNP1.

[0016] **FIG. 7** depicts graphs showing that the mean levels of CSF $A\beta_{42}$ are decreased (A) and levels of total tau are increased (B) in very mild AD vs. control subjects. Clinical dementia rating (CDR) 0 equals no cognitive impairment, CDR 0.5 represents very mild dementia, and CDR 1 represents mild dementia due to AD. P values calculated using the raw data (P) and those calculated using the log-transformed and adjusted dataset (P*) are also displayed.

[0017] **FIG. 8** depicts graphs showing the levels of selected candidate biomarkers in a large CSF sample set as assayed by ELISA. P values calculated using the raw data (P) and those calculated using the log-transformed and adjusted dataset (P*) are displayed. ACT, ATIII, and ZAG are significantly increased in AD (CDR 0.5 and 1) vs. control (CDR 0) samples. (A) ACT; (B) ZAG; (C) Gelsolin; (D) ATIII; (E) CDNP1; (F) AGT.

[0018] **FIG. 9** depicts graphs showing that the levels of ACT, ATIII, and ZAG are not significantly different in plasma between AD (CDR 0.5 and 1) vs. control (CDR 0) samples. (A) ACT; (B) ATIII; (C) ZAG



Fujirebio Diagnostics, Inc. v. Quanterix Corp.
EX-1045
5809

[0019] **FIG. 10** depicts graphs showing the correlations between the CSF and plasma levels of candidate biomarkers, including ACT (A), ATIII (B), and ZAG (C).

[0020] **FIG. 11** depicts a graph showing the receiver operating characteristic curve (ROC) for the normalized and adjusted CSF concentrations of each biomarker candidate and the optimum linear combination (Optimum) combining data from all biomarkers.

## DETAILED DESCRIPTION OF THE PREFERRED EMBODIMENTS

[0021] Given the early, insidious pathogenesis of AD, combined with the theory that neuronal degeneration is easier to slow or halt than to reverse, it is vital to identify biomarkers that can detect the disease before or during the early development of symptoms and irreversible pathologic damage. Such biomarkers could be used for AD screening and diagnosis, as well as potentially for assessing response to new therapies. Despite the existence of a few promising CSF biomarkers for early stage AD as described above, these candidate markers have not fulfilled the consensus criteria necessary for use in individual diagnosis. Given the probability of multiple underlying pathogenic mechanisms of late-onset AD, it is likely that a battery of biomarkers will be more useful than an individual marker. Therefore, new and better biomarkers must be identified.

[0022] To this end, the present invention provides novel AD biomarkers present in the bodily fluid of a subject. The level of these biomarkers correlate with CDR score, and therefore may allow a more accurate diagnosis or prognosis of AD in subjects that are at risk for AD, that show no clinical signs of AD, or that show minor clinical signs of AD. Furthermore, the biomarkers may allow the monitoring of AD, such that a comparison of biomarker levels allows an evaluation of disease progression in subjects that have been diagnosed with AD, or that do not yet show any clinical signs of AD. Moreover, the AD biomarkers of the invention may be used in concert with known AD biomarkers such that a more accurate diagnosis or prognosis of AD may be made.



Fujirebio Diagnostics, Inc. v. Quanterix Corp.
EX-1045
5810

## I. *Biomarkers to Detect Alzheimer's Disease*

[0023] One aspect of the present invention provides biomarkers to detect AD. A biomarker is typically a protein, found in a bodily fluid, whose level varies with disease state and may be readily quantified. The quantified level may then be compared to a known value. The comparison may be used for several different purposes, including but not limited to, diagnosis of AD, prognosis of AD, and monitoring treatment of AD.

[0024] Through proteomic screening performed as detailed in the examples, several novel biomarkers have been identified for AD. In one embodiment, the level of a serine protease inhibitor is a biomarker for AD. Examples of serine protease inhibitors include alpha 1-antitrypsin, alpha 1-antichymotrypsin, alpha 2-antiplasmin, antithrombin III, complement 1-inhibitor, neuroserpin, plasminogen activator inhibitor-1 and 2, and protein Z-related protease inhibitor (ZPI). In another embodiment the biomarker is the level of α1-antichymotrypsin (ACT). In yet another embodiment, the biomarker is the level of antithrombin III (ATIII). In an alternative embodiment, the biomarker is the level of zinc-alpha-2-glycoprotein (ZAG). In another alternative embodiment, the biomarker is the level of carnosinase 1 (CNDP1).

[0025] Each of the biomarkers identified above may be used in concert with another biomarker for purposes including but not limited to diagnosis of AD, prognosis of AD, and monitoring treatment of AD. For instance, two or more, three or more, four or more, five or more, or six or more AD biomarkers may be used in concert. As explained above, there are several known biomarkers for AD. In one embodiment, two or more biomarkers from the group comprising ACT, ATIII, ZAG, CNDP1, Aβ42 and tau are used in concert. In yet another embodiment, three or more biomarkers from the group comprising ACT, ATIII, ZAG, CNDP1, Aβ42 and tau are used in concert. In still another embodiment, four or more biomarkers from the group comprising ACT, ATIII, ZAG, CNDP1, Aβ42 and tau are used in concert. In yet still another embodiment, ACT, ATIII, ZAG, CNDP1, Aβ42 and tau are used in concert as biomarkers for AD.



Fujirebio Diagnostics, Inc. v. Quanterix Corp.
EX-1045
5811

**a. bodily fluids**

[0026] The levels of AD biomarkers of the invention may be quantified in several different bodily fluids. Non-limiting examples of bodily fluid include whole blood, plasma, serum, bile, lymph, pleural fluid, semen, saliva, sweat, urine, and CSF. In one embodiment, the bodily fluid is selected from the group comprising whole blood, plasma, and serum. In another embodiment, the bodily fluid is whole blood. In yet another embodiment, the bodily fluid is plasma. In still yet another embodiment, the bodily fluid is serum. In an exemplary embodiment, the bodily fluid is CSF.

[0027] As will be appreciated by a skilled artisan, the method of collecting a bodily fluid from a subject can and will vary depending upon the nature of the bodily fluid. Any of a variety of methods generally known in the art may be utilized to collect a bodily fluid from a subject. Generally speaking, the method preferably maintains the integrity of the AD biomarker such that it can be accurately quantified in the bodily fluid. One method of collecting CSF is detailed in the examples. Methods for collecting blood or fractions thereof are well known in the art. For example, see US Patent No. 5,286,262, which is hereby incorporated by reference in its entirety.

[0028] A bodily fluid may be tested from any mammal known to suffer from Alzheimer's disease or used as a disease model for Alzheimer's disease. In one embodiment, the subject is a rodent. Examples of rodents include mice, rats, and guinea pigs. In another embodiment, the subject is a primate. Examples of primates include monkeys, apes, and humans. In an exemplary embodiment, the subject is a human. In some embodiments, the subject has no clinical signs of AD. In other embodiments, the subject has mild clinical signs of AD, for instance, corresponding to a CDR score of 0.5. In yet other embodiments, the subject may be at risk for AD. In still other embodiments, the subject has been diagnosed with AD.

**b. level of biomarker**

[0029] The level of the biomarker may encompass the level of protein concentration or the level of enzymatic activity. In either embodiment, the



Fujirebio Diagnostics, Inc. v. Quanterix Corp.
EX-1045
5812

level is quantified, such that a value, an average value, or a range of values is determined. In one embodiment, the level of protein concentration of the AD biomarker is quantified. In another embodiment, the concentration of ATIII is quantified. In yet another embodiment, the concentration of ACT is quantified. In still another embodiment, the concentration of ZAG is quantified. In still yet another embodiment, the concentration of CNDP1 is quanitified.

[0030] There are numerous known methods and kits for measuring the amount or concentration of a protein in a sample, including ELISA, western blot, absorption measurement, colorimetric determination, Lowry assay, Bicinchoninic acid assay, or a Bradford assay. Commercial kits include ProteoQwest™ Colorimetric Western Blotting Kits (Sigma-Aldrich, Co.), QuantiPro™ bicinchoninic acid (BCA) Protein Assay Kit (Sigma-Aldrich, Co.), FluoroProfile™ Protein Quantification Kit (Sigma-Aldrich, Co.), the Coomassie Plus - The Better Bradford Assay (Pierce Biotechnology, Inc.), and the Modified Lowry Protein Assay Kit (Pierce Biotechnology, Inc.). In certain embodiments, the protein concentration is measured by ELISA. For instance, the level of ATIII may be quantified by ELISA as described in the examples.

[0031] In another embodiment, the level of enzymatic activity of the biomarker is quantified. Generally, enzyme activity may be measured by means known in the art, such as measurement of product formation, substrate degradation, or substrate concentration, at a selected point(s) or time(s) in the enzymatic reaction. In one embodiment, the enzyme activity of ATIII is quantified. In another embodiment, the enzyme activity of ACT is quantified. In yet another embodiment, the enzyme activity of CNDP1 is quantified. There are numerous known methods and kits for measuring enzyme activity. For example, see US Patent No. 5,654,152. Some methods may require purification of the AD biomarker prior to measuring the enzymatic activity of the biomarker. A pure biomarker constitutes at least about 90%, preferably, 95% and even more preferably, at least about 99% by weight of the total protein in a given sample. AD biomarkers of the invention may be purified according to methods known in the art, including, but not limited to, ion-exchange chromatography, size-exclusion chromatography, affinity chromatography, differential solubility, differential



Fujirebio Diagnostics, Inc. v. Quanterix Corp.
EX-1045
5813

centrifugation, and HPLC. (See Current Protocols in Molecular Biology, Eds. Ausubel, et al., Greene Publ. Assoc., Wiley-Interscience, New York)

## II. *Methods of Using the Biomarkers*

### a. using biomarkers for the diagnosis or prognosis of AD

[0032] In one embodiment, the invention encompasses a method for detecting AD comprising quantifying the level of an AD biomarker in a bodily fluid of a subject and subsequently determining if the quantified level of the biomarker is elevated or depressed in comparison to the average level of the biomarker for a subject with a CDR of 0. The subject may have no clinical signs of AD, the subject might be at risk for AD, or alternatively, the subject might show mild dementia (CDR of 0.5). The average level of the biomarker for a subject with a CDR of 0 refers to the arithmetic average of the biomarker level in a bodily fluid of at least 50 subjects with a CDR of 0.

[0033] An elevated or depressed biomarker level may lead to either a diagnosis or prognosis of AD. In one embodiment, an elevated biomarker level indicates a diagnosis of AD. In another embodiment, an elevated biomarker level indicates a prognosis of AD. In yet another embodiment, a depressed biomarker level indicates a diagnosis of AD. In still yet another embodiment, a depressed biomarker level indicates a prognosis of AD.

[0034] A skilled artisan will realize that whether an elevated or a depressed biomarker level in comparison to the average level of the biomarker for a subject with a CDR of 0 is indicative of AD will depend on the biomarker in question. In one embodiment, an elevated level of ATIII indicates a diagnosis or prognosis of AD. In another embodiment, an elevated level of ACT indicates a diagnosis or prognosis of AD. In yet another embodiment, an elevated level of tau indicates a diagnosis or prognosis of AD. In still another embodiment, a depressed level of Aβ42 indicates a diagnosis or prognosis of AD. In yet still another embodiment, a modulated level of ZAG indicates a diagnosis or prognosis of AD. In an alternative embodiment, a depressed level of CNDP1 indicates a diagnosis or prognosis of AD.



Fujirebio Diagnostics, Inc. v. Quanterix Corp.
EX-1045
5814

[0035] An AD biomarker of the invention may be quantified in concert with another known AD biomarker as detailed in Part I above. For example, ATIII may be used as an AD biomarker in concert with Aβ42. In this example, a simultaneously elevated ATIII level and a depressed Aβ42 level in a bodily fluid of a subject would be indicative of a diagnosis or prognosis of AD.

[0036] The percent elevation or depression of an AD biomarker compared to the average level of the biomarker for a subject with a CDR of 0 is typically greater than 15% to indicate a diagnosis or prognosis of AD. In some instances, the percent elevation or depression is 15%, 16%, 17%, 18%, 19%, 20%, 21%, or 22%. In other instances, the percent elevation or depression is 23%, 24%, 25%, 26%, 27%, 28%, 29% or 30%. In still other instances, the percent elevation or depression is greater than 30%. In alternative instances, the percent elevation or depression is greater than 50%.

**b. using biomarkers to monitor AD**

[0037] Another embodiment of the invention encompasses a method for monitoring AD comprising quantifying the level of an AD biomarker in a bodily fluid of a subject and comparing the quantified level of the biomarker to a previously quantified biomarker level of the subject to determine if the quantified level is elevated or depressed in comparison to the previous level. The subject may be diagnosed with AD, or alternatively, may have no clinical signs of AD. The comparison may give an indication of disease progression. Therefore, the comparison may serve to measure the effectiveness of a chosen therapy. Alternatively, the comparison may serve to measure the rate of disease progression. For example, a depressed ATIII level, in comparison to a previous level, may indicate an abatement of disease progression.

[0038] In the context of monitoring AD, the percent elevation or depression of an AD biomarker compared to a previous level may be from 0% to greater than about 50%. In one embodiment, the percent elevation or depression is from about 1% to about 10%. In another embodiment, the percent elevation or depression is from about 10% to about 20%. In yet another embodiment, the percent elevation or depression is from about 20% to about 30%. In still another embodiment, the percent elevation or depression is from about 30% to about



Fujirebio Diagnostics, Inc. v. Quanterix Corp.
EX-1045
5815

40%. In yet still another embodiment, the percent elevation or depression is from about 40% to about 50%. In a further embodiment, the percent elevation or depression is greater than 50%.

### III. *Kits for Detecting or Monitoring AD*

[0039] Another aspect of the invention encompasses kits for detecting or monitoring AD in a subject. A variety of kits having different components are contemplated by the current invention. Generally speaking, the kit will include the means for quantifying one or more AD biomarkers in a subject. In another embodiment, the kit will include means for collecting a bodily fluid, means for quantifying one or more AD biomarkers in the bodily fluid, and instructions for use of the kit contents. In certain embodiments, the kit comprises a means for quantifying AD biomarker enzyme activity. Preferably, the means for quantifying biomarker enzyme activity comprises reagents necessary to detect the biomarker enzyme activity. In certain aspects, the kit comprises a means for quantifying the amount of AD biomarker protein. Preferably, the means for quantifying the amount of biomarker protein comprises reagents necessary to detect the amount of biomarker protein.

[0040] In one embodiment, the kit comprises means to quantify the level of ATIII in a bodily fluid of a subject. The level of ATIII refers to either the enzyme activity of ATIII or the protein concentration of ATIII. In another embodiment, the kit comprises a means to quantify the level of at least one AD biomarker. In yet another embodiment, the kit comprises means to quantify the level of at least two, at least three, at least four, at least five or at least six AD biomarkers. In still yet another embodiment, the kit comprises means to quantify the level of at least seven, at least eight, at least nine, or at least ten AD biomarkers. In still another embodiment, the kit comprises means to quantify the level of ten or more biomarkers. In certain embodiments, the kit comprises the means to quantify the level of one or more biomarkers from the group consisting of ATIII, ACT, ZAG, CNDP1, Aβ42, and tau. In each of the above embodiments, the AD biomarker level refers to either the biomarker enzyme activity or the biomarker protein concentration. The means necessary to detect either enzyme activity or protein concentration are discussed in Part II above.



Fujirebio Diagnostics, Inc. v. Quanterix Corp.
EX-1045
5816

[0041] As various changes could be made in the above compounds, products and methods without departing from the scope of the invention, it is intended that all matter contained in the above description and in the examples given below, shall be interpreted as illustrative and not in a limiting sense.

## EXAMPLES

[0042] The following examples illustrate the invention.

### Example 1:

*Materials and Methods for Example 1:*

[0043] CSF Sampling: Human CSF samples were obtained by lumbar puncture (LP) from subjects enrolled in the Memory and Aging Project at Washington University as part of an ongoing biomarker study. The study protocol was approved by the Human Studies Committee at Washington University, and written and verbal informed consent was obtained from each participant at enrollment. In 6 individuals, two samples were obtained from the same individual 2 weeks apart. Two weeks is an arbitrary time span, chosen to allow the skin, subcutaneous tissue, and meninges to have adequate time for repair prior to a second LP. Other time periods may certainly be used. All LPs were performed at the same time of the day with no fasting requirement. 25- 35 ml of CSF was obtained from all participants with either a 22 or a 25 guage spinal needle. All CSF samples were free of blood contamination. After collection, CSF samples were briefly centrifuged at 1,000 x g to pellet any cell debris, frozen, and stored in polypropylene tubes at -80 °C in 0.5-ml aliquots until analysis. The age of these six individuals ranged from 64 to 91 years. The cognitive state of the subjects was rated using a Clinical Dementia Rating (CDR) scale in which an individual's cognition is rated as normal (CDR 0), or demented with severities of very mild, mild, moderate or severe (CDR 0.5, 1, 2 or 3, respectively). Individuals diagnosed with possible/probable dementia of the Alzheimer's type (DAT) are usually CDR 1 or greater. Of the 6 individuals who had CSF sampling on 2 occasions, 2 weeks apart, four of these subjects had a CDR score of 0, and the other two were rated



Fujirebio Diagnostics, Inc. v. Quanterix Corp.
EX-1045
5817

as CDR 0.5. The protein content in each CSF sample was determined with the micro-BCA protein assay kit (Pierce), and it ranged from 570 to 1,000 μg/ml.

[0044] Multiaffinity Immunodepletion of CSF Proteins: Because albumin, IgG, α1-antitrypsin, IgA, transferrin, and haptoglobin collectively account for ~80% of the total CSF protein content, these proteins were selectively removed to enrich for proteins of lower abundance. An antibody-based multiaffinity removal system (Agilent Technologies, Palo Alto, CA) was used according to the manufacturer's instructions. Briefly 1.5–2 ml of CSF was concentrated and buffer-exchanged with Agilent Buffer A to a final volume of 50 μl using Amicon Ultra-4 centrifugal filter units (10-kDa cut-off) (Millipore). Samples were then diluted to 200 μl with Buffer A and passed through an Ultra-free MC microcentrifuge filter (0.22 μm) (Millipore) to remove particulates. The filtrate was injected at 0.25 ml/min onto a 4.6 x 50-mm multiple affinity removal column equilibrated at room temperature with Agilent Buffer A on a Microtech (Vista, CA) Ultra-Plus HPLC system. CSF devoid of high abundance proteins (flow-through) was collected between 1.5 and 6 min. After 9 min of elution with Buffer A, the eluant was changed to Agilent Buffer B at 1 ml/min. The six bound proteins were eluted from the column between 10 and 14 min. After 3.5 min, the column was regenerated with Buffer A.

[0045] *2-D DIGE:* Depleted CSF samples were buffer-exchanged and concentrated with lysis buffer (30 mM Tris-Cl, pH 7.8, 7 M urea, 2 M thiourea, 4% CHAPS containing protease inhibitors (catalog number 697498, Roche Diagnostics) and phosphatase inhibitors (catalog numbers 524624 and 524625, EMD Biosciences, Darmstadt, Germany) using Amicon Ultra-4 centrifugal filter units (10-kDa cut-off) (Millipore). The protein concentration was determined with a modified Lowry method (PlusOne 2D-Quant kit, Amersham Biosciences). Fifty micrograms of protein from each sample was labeled with 400 pmol of one of three N-hydroxysuccinimide cyanine dyes for proteins (Amersham Biosciences), diluted with rehydration buffer (7 M urea, 2 M thiourea, 4% CHAPS, 2.5% DTT, 10% isopropanol, 5% glycerol, and 2% PharmalytepH 3–10), combined according to experimental design, and equilibrated with IPG strips (24 cm; pH 3–10, nonlinear). The three samples that were equilibrated with each IPG strip consisted



Fujirebio Diagnostics, Inc. v. Quanterix Corp.
EX-1045
5818

of two depleted CSF samples from the same individual (Cy2 and Cy5) and a pooled sample (pooled using an equal volume aliquot of each of the 12 CSF samples) (Cy3) as the internal standard. First dimension isoelectric focusing was performed at 65.6 kV-h in an Ettan IPGphor system (Amersham Biosciences). The strips were then treated with reducing and alkylating solutions prior to the second dimension (SDS-PAGE). After equilibration with a solution containing 6 M urea, 30% glycerol, 2% SDS, 50 mM Tris-Cl, pH 7.8, 32 mM DTT, the strips were treated with the same solution containing 325 mM iodoacetamide instead of DTT. The strips were overlayered onto a 10% isocratic or gradient SDS-PAGE gel (20 x 24 cm), immobilized to a low fluorescence glass plate and electrophoresed for ~18 h at 1 watt/gel. The Cy2-, Cy3-, and Cy5-labeled images were acquired on a Typhoon 9400 scanner (Amersham Biosciences) at the excitation/emission values of 488/520, 532/580, 633/670 nm, respectively.

[0046] Image Analyses: Intragel spot detection and quantification and intergel matching and quantification were performed using Differential In-gel Analysis (DIA) and Biological Variation Analysis (BVA) modules of DeCyder software version 5.01 (Amersham Biosciences) as described previously (Alban et al., (2003) Proteomics 3, 36–44; Tonge et al., (2001) Proteomics 1, 377–396). Briefly in DIA, the Cy2, Cy3, and Cy5 images for each gel were merged, spot boundaries were automatically detected, and normalized spot volumes (protein abundance) were calculated. During spot detection, the estimated number of spots was set at 3,500, and the exclude filter was set as follows: slope, >1.1; area, <100; peak height, <100; and volume, <10,000. This analysis was used to calculate abundance differences in given proteins between two samplings from the same individual. The resulting spot maps were exported to BVA. Matching of the protein spots across six gels was performed after several rounds of extensive land marking and automatic matching. Dividing each Cy2 or Cy5 spot volume with the corresponding Cy3 (internal standard) spot volume within each gel gave a standard abundance, thereby correcting intergel variations. For each of the CSF samples, a profile was created that consisted of standard abundance for all of the matched spots.

[0047] Protein Digestion and Mass Spectrometry: Gel features were selected in the DeCyder software and the X and Y coordinates were saved in a



Fujirebio Diagnostics, Inc. v. Quanterix Corp.
EX-1045
5819

file for spot excision. After translation using in-house software (Imagemapper), the central core (1.8 mm) of the selected gel features was excised with a ProPic robot (Genomics Solutions, Ann Arbor, MI) and transferred to a 96-well PCR plate. The gel pieces were then digested in situ with trypsin using a modification of a published method (Havlis et al., (2003) Anal. Chem. 75, 1300–1306). To maximize specificity, sensitivity, and sequence coverage of the digested proteins, the resulting peptide pools were analyzed by tandem MS using both MALDI and ESI. Spectra of the peptide pools were obtained on a MALDI-TOF/TOF instrument (Proteomics 4700, Applied Biosystems, Foster City, CA). The initial spectra were used to determine the molecular weights of the peptides (to within 20 ppm of their theoretical masses). Selected precursor ions were then focused in the instrument using a timed ion selector, and peptide fragmentation spectra were produced after high energy (1.5-keV) collision-induced dissociation. ESI-MS was performed using an advanced capillary LC-MS/MS system (Eksigent nano-LC 1D Proteomics, Eksigent Technologies, Livermore, CA). A nanoflow (200 nl/min) pulse-free liquid chromatograph was interfaced to a quadrupole time-of-flight mass spectrometer (Q-STAR XL, Applied Biosystems) using a PicoView system (New Objective, Woburn, MA). Sample injection was performed with an Endurance autosampler (Spark Holland, Plainsboro, NJ). The peptide fragmentation spectra were processed using Data Explorer version 4.5 or Analyst software (Applied Biosystems). After centroiding and background subtraction, the peak lists were used to search databases with MASCOT version 1.9 (Matrix Sciences, Boston, MA). Peptide sequences were qualified by manual interpretation of raw non-centroided spectra.

[0048] CSF Biomarker Assessment (ELISA): CSF samples were analyzed for total tau, amyloid β42 (Aβ42), α1-chymotrypsin (ACT), antithrombin III (ATIII), and gelsolin by commercial enzyme-linked immunosorbant assay (ELISA) (Innotest, Innogenetics, Ghent, Belgium). For all biomarker measures, samples were continuously kept on ice, and assays were performed on sample aliquots after a single thaw from initial freezing.

[0049] Threshold Selection: The DIA software performs a log transformation of the volume ratios and uses them to generate a frequency histogram. A normal distribution is fitted to the main peak of the frequency



Fujirebio Diagnostics, Inc. v. Quanterix Corp.
EX-1045
5820

histogram. After normalization, this fitted distribution curve centers on 0, which represents proteins with unaltered abundance. Model standard deviation (S.D.) is then derived based on the normalized model curve. 2 S.D., the volume ratio for 2 S.D. based on the raw data, is the software-recommended cut-off. In a normally distributed data set, 95% of data points would fall within this value. Based on the observation that 2 S.D. ranged from 1.31 to 1.52 for the six individuals who were compared 2 weeks apart, gel features changing by >1.5 in spot volume were considered significant.

[0050] p Value Determination for Intraindividual Variation: The statistical significance of observing different levels of the same protein in multiple intraindividual comparisons was estimated by describing the data as a binomial distribution and calculating the probability of the observed events. Our null hypotheses are as follows: 1) all intra-individual comparison experiments are independent from each other, and 2) in any intra-individual comparison, protein levels should not change; therefore any observed change should be random and represent system fluctuation rather than a property of an individual protein. For any given experiment (intra-individual comparison) that follows the null hypotheses, the probability of any protein changing its expression level is $p_c$. This value can be estimated by maximum a posteriori estimation; i.e. based on the observed number of protein spots detected in a given gel and the observed number of spots determined to have altered abundance (i.e. having a >1.5 spot volume ratio) between the two time points in an intraindividual comparison, we calculated $p_c$. such that the probability of observing the experimental data given $p_c$. is maximized. In N independent trials (in this case six intraindividual comparisons), the probability of observing the same protein having changed abundance in n or more individuals is as follows.

$$p(i \geq n \backslash N) = \sum_{i=n..N} \binom{N}{n} p_c^{\,n}(1 - p_c)^{N-n}$$

(Eq. 1)



Fujirebio Diagnostics, Inc. v. Quanterix Corp.
EX-1045
5821

$p_c$. is determined to be 0.0140, and N is 6. Because not all of the "changed" spots are identified by MS/MS, this p value is likely an underestimation of the significance.

[0051] Hierarchical Clustering and Multidimensional Scaling Analysis: Hierarchical clustering was performed using Spotfire (Spotfire, Somerville, MA) software. Unweighted pair group method with arithmetic mean (UPGMA) was selected as the clustering method, and Euclidean distance was selected as the similarity measure. BRB Arraytools (linus.nci.nih.gov/BRB-ArrayTools.html) were used for multidimensional scaling analysis. Euclidean distance was used to measure similarity.

*Results:*

[0052] Prior to comparing CSF samples between individuals to identify patterns of disease-associated proteins, it is important to examine variation within individuals over a short period of time so that one can better interpret potential changes in CSF between individuals, as well as changes within a given individual over a longer time span. In a first study, we analyzed 12 CSF samples, composed of pairs of samples from six individuals, obtained 2 weeks apart. Multiaffinity depletion, two-dimensional DIGE, and tandem mass spectrometry were used. A number of proteins whose abundance varied between the two time points were identified for each individual. Some of these proteins were commonly identified in multiple individuals. More importantly, despite the intraindividual variations, hierarchical clustering and multidimensional scaling analysis of the proteomic profiles revealed that two CSF samples from the same individual cluster the closest together and that the between-subject variability is much larger than the within-subject variability. Among the six subjects, comparison between the four cognitively normal and the two very mildly demented subjects also yielded some proteins that have been identified in previous AD biomarker studies.

[0053] One objective of this study was to evaluate variability in the CSF proteome associated with longitudinal collection of CSF from individuals. Utilizing single gel, multiple image analysis, we were able to identify within-subject differences with a high degree of confidence. By including a pooled sample in



Fujirebio Diagnostics, Inc. v. Quanterix Corp.
EX-1045
5822

every gel as an internal standard, we were able to match and perform relative quantification of spots across gels and compare the degree of within-subject variation with that of between-subject variation. This study is an important component in the long term research program of the applicants to identify biomarkers for preclinical and very mild AD.

[0054] Because high abundance proteins comprise a large portion of the protein content of CSF and thus dominate 2-D gel images, we removed these proteins to increase our ability to detect and quantify proteins of lower abundance. We used a column-based multiple immunoaffinity system to remove six proteins (albumin, IgG, $\alpha_1$-antitrypsin, IgA, transferrin, and haptoglobin) from human CSF. This depletion technique has been shown in a proteomic study on serum to be superior to three other similar depletion methods and resulted in a 76% increase in the number of protein spots detected (Chromy et al., (2004) J. Proteome Res. 3, 1120–1127). When loading the same amount of total protein, our CSF study showed a 99% increase in the number of spots detected (Fig. 1): up to ~2,100 spots were detected on a gel. Fig. 2 is a representative 2-D DIGE image of a postdepletion CSF sample used in this study.

[0055] Two CSF samples were taken from the same individual 2 weeks apart (time point 1 (T1) and time point 2 (T2)) and were analyzed on the same gel together with a pooled sample as an internal standard. Six individuals were analyzed, translating into 12 CSF samples and six gels. The internal standard was a pool that included an equal volume aliquot of all 12 CSF samples. Pairwise comparisons of individual spots were made between T1 and T2 samplings for each individual to identify differences in protein abundance. A number of spots were selected for MS/MS analysis for each individual based on the following two criteria: 1) the -fold change of the spot volume between the two time points was greater than 1.5 (see “Experimental Procedures” for threshold selection), and 2) the protein spot was well resolved and appeared as a symmetrical peak. A total of 104 spots met these criteria, ranging from eight to 34 spots per gel, and 73 of them were identified by MS/MS. Table I presents some of the identified proteins, along with the number of individuals sharing a greater than 1.5-fold change. The -fold change is the change in protein abundance at T2 compared to T1 (the direction of change was ignored).



Fujirebio Diagnostics, Inc. v. Quanterix Corp.
EX-1045
5823

**Table 1. Proteins identified by MS/MS that vary in abundance within individuals over a 2-week time period.**

| Protein | GenBank™ ID | Number | -Fold change | *p* value |
|---|---|---|---|---|
| Transthyretin | 339685 | 6 | 1.92 ± 0.46 | $7.53 \times 10^{-12}$ |
| Chromogranin A | 180529 | 3 | 1.79 ± 0.09 | $5.32 \times 10^{-5}$ |
| Complement component C4A | 443671 | 3 | 1.73 ± 0.31 | $5.32 \times 10^{-5}$ |
| Hemopexin precursor | 386789 | 3 | 1.63 ± 0.09 | $5.32 \times 10^{-5}$ |
| Osteopontin-a | 992948 | 3 | 1.50 ± 0.11 | $5.32 \times 10^{-5}$ |
| β fibrinogen precursor | 182430 | 2 | 3.33 ± 1.21 | 0.00283 |
| Apolipoprotein E | 178849 | 2 | 3.13 ± 0.03 | 0.00283 |
| Complement component 3 precursor | 4557385 | 2 | 2.81 ± 1.60 | 0.00283 |
| Semaphorin L | 3551779 | 2 | 2.06 ± 0.74 | 0.00283 |
| Aprotinin | 58005 | 2 | 2.05 ± 0.51 | 0.00283 |
| Prostaglandin $D_2$ synthase | 54696706 | 2 | 1.97 ± 0.17 | 0.00283 |
| $a_2$-Macroglobulin | 177872 | 2 | 1.75 ± 0.18 | 0.00283 |
| Fibulin 1 precursor | 106018 | 2 | 1.64 ± 0.31 | 0.00283 |
| Chromogranin B precursor | 4502807 | 2 | 1.64 ± 0.12 | 0.00283 |
| Ubiquitin | 13569612 | 2 | 1.60 ± 0.06 | 0.00283 |
| Fibrinogen γ | 71828 | 1[a] | 3.87±2.55 | 0.0811 |
| Apolipoprotein H precursor | 4557327 | 1[a] | 2.55 ± 0.30 | 0.0811 |
| PRO 1400 | 6650772 | 1[a] | 1.99 ± 0.58 | 0.0811 |
| Transferrin | 31415705 | 1[a] | 1.66±0.18 | 0.0811 |
| Pyruvate kinase | 2117873 | 1 | 6.02 | 0.0811 |
| Complement C8-β propeptide | 29575 | 1 | 5.49 | 0.0811 |
| Angiotensinogen | 532198 | 1 | 4.72 | 0.0811 |
| Coagulation factor XII | 180359 | 1 | 2.15 | 0.0811 |
| Scrapie-responsive protein 1 | 37183198 | 1 | 1.62 | 0.0811 |
| Cerebroside sulfate activator protein | 337760 | 1 | 1.60 | 0.0811 |
| α albumin | 4501987 | 1 | 1.52 | 0.0811 |

[a] Several isoforms were identified in the same individual

[0056] There was a certain degree of variability in the CSF proteome detected within an individual over a 2-week period. Representative gel images and 3-D representations of one of such proteins are shown in Fig. 3. There was a 3.1-fold change of the levels of this ApoE spot between the two time points. Although many protein constituents in the CSF are derived from plasma, some of these changed proteins (Table 1) have been shown to be enriched in CSF or derived from nervous tissue, such as prostaglandin $D_2$ synthase, transthyretin, apolipoprotein E (apoE), chromogranin A, chromogranin B, semaphorin L, and scrapie-responsive protein 1. Interestingly a number of the same proteins are found to vary in multiple individuals. We calculated the *p* value of a given protein



Fujirebio Diagnostics, Inc. v. Quanterix Corp.
EX-1045
5824

appearing as changed by chance in one or more individuals (Table 1) and found that it is statistically significant when a protein is shown as changed in two or more individuals (using a cut-off *p* value of 0.05). The protein found to vary most often is transthyretin (six of six individuals). Other commonly variable (isoforms of) proteins include chromogranins A and B, complement component 3 and C4A, hemopexin precursor, osteopontin a, β fibrinogen precursor, apoE, semaphorin L, prostaglandin $D_2$ synthase, $\alpha_2$-macroglobulin, fibulin precursor, and ubiquitin. Aprotinin, a synthetic peptide present in the lysis buffer, appeared as a changed protein. Transthyretin and apoE have been shown to promote the solubility, transport, and clearance of amyloid-β (Aβ), a molecule important in the pathogenesis of AD. For transthyretin, multiple isoforms were found to vary within individuals (in the same direction for a given individual), whereas only one isoform of apoE was found to vary. In fact, our apoE ELISA data showed that total apoE level does not vary significantly within individuals. The direction of the intra-individual changes (increase versus decrease when comparing the initial and subsequent CSF sampling) did not show any trends among individuals. These findings strongly suggest that intra-individual variations in the CSF proteome reflect the dynamic steady states of those proteins. These data also suggest that the levels of some (isoforms of) proteins in CSF tend to fluctuate more significantly than others due to the nature of their metabolism as opposed to standard errors in experiments. Such intra-individual protein abundance variations are a caveat when considering these proteins as potential disease-related biomarkers.

[0057] An important goal of this study was to quantify the degree of intra-individual variation in relation to variation between individuals. For that purpose, protein spots were matched across all six gels so that a proteomic profile containing matched spots can be created for each sample, allowing for statistical comparisons to be made between individual profiles.

[0058] One advantage of 2-D DIGE is the ability to perform intergel matching and comparison through the inclusion of an internal standard on each gel. Nevertheless the assumption in using 2-D gel image analysis to measure relative protein concentration is that matched spots (spots that are located at the same position in different gels) correspond to the identical protein. This



Fujirebio Diagnostics, Inc. v. Quanterix Corp.
EX-1045
5825

assumption was tested by first matching all six gels using one of the pooled samples (internal standard) as a master image, from which 306 protein spots across all six gels were matched. Sixteen matched spots that were well resolved and distributed across the entire gel were selected and analyzed with MS/MS. For 14 spots, protein identifications were obtained from more than two gels. For 11 of the 14 spots, the identified proteins were the same. Examination of the 3-D gel images revealed that, for the three spots that gave different proteins there was evidence (e.g. a ridge) of another protein underneath the most prominent gel feature or matching/picking aberrations. Our conclusion is that matched, well-resolved gel features correspond to the same protein.

[0059] After intergel matching, a proteomic profile that consisted of standard abundance (i.e. –fold change in protein abundance compared with the pooled internal standard) was generated for matched spots for each of the 12 CSF samples. Because standard abundance is derived using the spot volume of the pooled sample as a denominator, it can be considered as the relative abundance of a protein spot. In this dataset, two statistical analyses were applied to assess the relationship among the CSF samples. First, hierarchical clustering analysis was performed on the proteomic profiles. Hierarchical clustering orders objects in a treelike structure based on similarity (i.e. in this case, “pattern similarity”). Clustering analysis is used extensively in the mining of gene expression data generated by functional genomic studies, but its application to protein expression data remains limited. Through the inclusion of an internal standard, a dataset was created that was very similar to datasets derived from GeneChip or microarray experiments and therefore allowed for the application of clustering algorithms to 2-D gel image analysis. The results, including a dendrogram and a heat map, are presented in Fig. 4. The dendrogram reveals that each pair of intraindividual CSF samples (T1 and T2) was clustered the closest together. As can be visualized in the heat map, the proteomic profiles of intra-individual samples are most similar to each other and distinctively different from other individuals’ profiles. The two CDR subjects with very mild AD (i.e. CDR 0.5, marked with an asterisk) did not cluster the closest together, indicating that there were no obvious global changes of protein expression between the CDR 0.5 and CDR 0 samples in this initial study. To rule out the possibility that the two



Fujirebio Diagnostics, Inc. v. Quanterix Corp.
EX-1045
5826

samplings from the same subject cluster together simply because they were run on the same gel, we analyzed T1 samples from two subjects on one gel and T2 samplings from these two subjects on another gel. Clustering analysis of the proteomic profiles showed that longitudinal samples from the same subject still cluster the closest together. This further demonstrates the validity of the intergel comparison.

[0060] Second, multidimensional scaling analysis was performed on the proteomic profiles. Like hierarchical clustering, multidimensional scaling is commonly used in microarray research as an analysis tool. Its purpose is to capture as much variation in the data as possible in a minimal number of dimensions (two or three) so that trends in data are more obvious. In effect, one is attempting to reduce the dimensionality of the data to summarize the most influential (i.e. defining) components while simultaneously filtering out noise. The distance between two samples can be thought to represent the similarity between them; the smaller the distance, the more similar the samples. Fig. 5 is a 2-D projection of the 3-D scatter plot of the proteomes of the 12 CSF samples. CSF samples from the same subject are represented with the same color. As can be observed from the graph, there is a short distance between two samples from the same individual, and this distance varies among individuals. However, the distance between intraindividual CSF samples is much smaller than between samples from different individuals. These data highlight that intraindividual variation in the CSF proteome is much smaller than the interindividual variation.

[0061] Because our sample set included four CDR 0 subjects (eight CSF samples) and two CDR 0.5 subjects (four CSF samples), we were able to evaluate possible CDR group-associated differences. As mentioned earlier, 306 spots were matched across six gels/12 individual CSF samples. For each spot in a given CSF sample, there is a corresponding standard abundance (representing the relative abundance of this protein spot) that can be compared across the 12 samples. Therefore, we were able to perform a *t* test (in the BVA module of the DeCyder software) on the matched spots by designating the eight CDR 0 CSF samples as group 1 and the four CDR 0.5 samples as group 2. We selected the top ranking ($p < 0.02$) and well resolved spots and subjected them to MS/MS analysis. Eleven of the 13 spots selected were found to represent eight different



Fujirebio Diagnostics, Inc. v. Quanterix Corp.
EX-1045
5827

proteins (Table 2). Interestingly four of these proteins have been shown to have altered levels in AD CSF, including $\alpha_1\beta$-glycoprotein, prostaglandin $D_2$ synthase, cystatin C, and $\beta_2$-microglobulin. Consistent with previous studies, $\alpha_1\beta$-glycoprotein is decreased in the CDR 0.5 group, whereas cystatin C and $\beta_2$-microglobulin are increased. Prostaglandin $D_2$ synthase was found to increase in the CDR 0.5 group, which is consistent with a previous study, whereas another study reported a decrease of prostaglandin $D_2$ synthase. Several isoforms of chitinase 3-like 1, also known as GP-39 cartilage protein, were found to be increased in the CDR 0.5 group. This protein is primarily produced by human chondrocytes and synovial fibroblasts and has been shown to be a target antigen in patients with rheumatoid arthritis.

**Table 2. CSF proteins found to be differentially expressed between CDR 0.5 and CDR 0 groups.**

| Spot ID | Protein | GenBank™ ID | *p* value | Direction of change |
|---|---|---|---|---|
| 1 | $\alpha_1\beta$-Glycoprotein | 69990 | 0.011 | Decrease |
| | Complement component 3 precursor | 4557385 | 0.011 | Decrease |
| 2 | Apolipoprotein H precursor | 4557327 | 0.0071 | Decrease |
| 3 | Chitinase 3-like 1 | 4557018 | 0.011 | Increase |
| 4 | Chitinase 3-like 1 | 4557018 | 0.014 | Increase |
| 5 | Prostaglandin $D_2$ synthase | 55962672 | 0.015 | Increase |
| | Chitinase 3-like 1 | 4557018 | 0.015 | Increase |
| 6 | Prostaglandin $D_2$ synthase | 54696706 | 0.00022 | Increase |
| 7 | Prostaglandin $D_2$ synthase | 54696706 | 0.016 | Increase |
| 8 | Prostaglandin $D_2$ synthase | 54696706 | 0.011 | Increase |
| 9 | Cystatin C | 181387 | 0.019 | Increase |
| 10 | Thioredoxin | 231098 | 0.0058 | Increase |
| 11 | $\beta_2$-Microglobulin | 34616 | 0.0022 | Increase |

[0062] Although this sample size was very small, five of eight differentially expressed proteins identified by MS/MS have been implicated in previous AD biomarker studies, and for three of them, these results (increase *versus* decrease) are consistent with previous reports. Importantly only one of these proteins (*i.e.* prostaglandin $D_2$ synthase) was identified to display intra-individual variation. These preliminary differences that were found need to be validated with a much larger sample set; however, these results suggest that,



Fujirebio Diagnostics, Inc. v. Quanterix Corp.
EX-1045
5828

given appropriate sample selection, protein quantification, and profile comparison, one may not require a large set of samples to identify disease-related biomarkers.

**Example 4:**

*Materials and methods for Example 4*

[0063] Subjects: Research subjects were participants at the Alzheimer's Disease Research Center (ADRC) at the Washington University School of Medicine (WUSM) and were recruited by the ADRC to this study. All subjects gave informed consent to participate in this study and all protocols were approved by the institutional review board for human studies at Washington University. Study investigators were blind to the cognitive status of the participants, which was determined by ADRC clinicians in accordance with standard protocols and criteria, as described previously (Berg et al., Arch Neurol (1998) 55:326-335; Morris et al., Ann Neurol (1988) 24:17-22). Subjects were assessed on clinical grounds to be cognitively normal in accordance with a Clinical Dementia Rating (CDR) of 0 (n =55) or to have very mild (CDR 0.5; n=20) or mild (CDR 1; n=19) dementia that is believed to be caused by AD as described (Morris et al., Arch Neurol (2001) 58:397-405).

[0064] CSF and plasma collection: CSF (20 –35ml) was collected at 8:00 AM after overnight fasting, as described previously (Fagan et al., Ann Neurol (2000) 48:201-210). Lumbar punctures (LPs) (L4/L5) were performed by a trained neurologist using a 22-gauge Sprotte spinal needle. CSF samples were free from any blood contamination. Samples were gently inverted to avoid gradient effects, briefly centrifuged at low speed to pellet any cellular elements, and aliquoted (500 µl) into polypropylene tubes before freezing at -80°C. Fasted blood (10 –15 ml) was also obtained from each subject just before LP, and plasma was prepared by standard centrifugation techniques. Plasma samples were aliquoted (500 µl) into polypropylene tubes before freezing at -80°C.

[0065] Multi-affinity immunodepletion of abundant CSF proteins: Since albumin, IgG, α1-antitrypsin, IgA, transferrin and haptoglobin collectively account for ~80% total CSF protein content, they were selectively removed in order to enrich for proteins of lower abundance. An antibody-based multi-affinity



Fujirebio Diagnostics, Inc. v. Quanterix Corp.
EX-1045
5829

removal system (Agilent Technologies, Palo Alto, CA) was employed according to the manufacturer's instructions, as described in the materials and methods for examples 1-3.

[0066] 2D-DIGE: Twelve CSF samples were analyzed by 2D-DIGE: CDR 1 subjects (n=6) and age-matched CDR 0 controls (n=6). These samples were selected based on Aβ42 concentration, i.e. CDR 1 samples were selected whose Aβ42 concentration is less than 500 pg/ml and the converse for CDR 0 samples. Fifty µg of protein from each depleted CSF sample was labeled with 400 pmol of one of three N-hydroxsuccinimide cyanine dyes for proteins (GE Healthcare, Piscataway, NJ), mixed with 30 µg of unlabled protein from the same sample, diluted with rehydration buffer, combined according to experimental design, and equilibrated with immobilized pH gradient (IPG) strips (24 cm; pH 3-10, nonlinear). The three samples that were equilibrated with each IPG strip consisted of a CDR 0 sample, a CDR 1 sample and a pooled sample (pooled using an equal volume aliquot of each of the 12 CSF samples) (labeled with Cy3) as the internal standard. To avoid possible dye-related bias, half of the CDR 0 samples were labeled with Cy2 and half with Cy5 and the same protocol was used to label the CDR 1 samples. First-dimension isoelectric focusing was performed at 65.6 kV-h in an Ettan IPGphor system (GE Healthcare). The second dimension was performed on a gradient SDS-PAGE gel (10-20%). The Cy2, Cy3, Cy5-labeled images were acquired on a Typhoon 9400 scanner (GE Healthcare).

[0067] Image analysis: Intra-gel spot detection, quantification and inter-gel matching and quantification were performed using Differential In-gel Analysis (DIA) and Biological Variation Analysis (BVA) modules of DeCyder software v5.01 (GE Healthcare), respectively as described previously (Hu et al., Mol Cell Propteomics (2005) 4:2000-9, hereby incorporated by reference in its entirety). A subset of protein spots (n=514) were matched across all six gels. Student's t-test was performed to compare the average (relative) abundance of a given spot between the two groups (CDR 1 vs. CDR 0). Spots that had a p value below 0.05 and were well resolved were selected for subsequent mass spectrometric analysis.

[0068] Protein digestion and mass spectrometry: Gel spots of interest were flagged with the DeCyder software and the X and Y coordinates



Fujirebio Diagnostics, Inc. v. Quanterix Corp.
EX-1045
5830

were used by a robotic spot picker (ProPic; Genomics Solutions, Ann Arbor, MI) to cut and transfer gel features into a 96 well plate for in situ gel digestion with trypsin using a modification of a previously described method (Havlis et al. Anal Chen (2003) 75:1300-6). Briefly, excised gel cylinders (2mm in diameter) were robotically transferred to 96 well plates (Axygen Scientific, Union City, CA) and over-layered with 100 µL of water. After washing and trypsin digestion (Sigma, St. Louis, MO) in 5 µL of 5 mM tri-ethyl-ammonium bicarbonate buffer, (pH 8.0; Sigma), an aliquot (0.5 µL) was removed from each well and placed in a microfuge tube (200 µL) containing 0.5 µL of MALDI Matrix (Agilent Technologies). The tubes were vortexed, spun in a microfuge for 30 s and spotted (1 µL) onto a stainless steel target (192 spot plate) for MALDI -TOF/TOF mass spectrometry as previously described (Bredemeyer et al., PNAS (2004) 101:11785-90). To the remaining gel samples, 12 µL of aqueous acetonitrile/formic acid (1%/1%) (Sigma) was added and the plate was incubated at 37°C for 1 h. The samples (~ 10 µL) were then transferred to polypropylene auto sampler vials, spun at 10,000 x g for 15 min in a Sorvall centrifuge equipped with a HB-6 rotor, and stored at -80°C for analysis by LC-MS/MS. LC-MS/MS was performed using a capillary LC (Eksigent, Livermore, CA) interfaced to a nano-LC-linear quadrupole ion trap Fourier transform ion cyclotron resonance mass spectrometer (nano-LC-FTMS) (King et al., Anal Chem (2006) 78:2171-81).

[0069] Database searching was performed using MASCOT 1.9.05 software (Matrix Science, Oxford, UK) against the NCBI non-redundant database (March 24, 2005). Protein identifications were supported by at least two peptides with Mascot scores of > 40 and accurate measurements of the peptide parent masses within 5 ppm. Protein identifications were confirmed by manual interpretation of the fragmentation spectra with a minimal acceptance criterion of four contiguous b or y ions for each peptide sequence.

[0070] ELISA analyses: Aβ42 and total tau concentrations in the CSF samples were analyzed by a commercially available enzyme-linked immunosorbent assay (Innotest; Innogenetics, Ghent, Belgium). Albumin ELISA was performed with an ELISA kit (Bethyl Laboratories, Montgomery, TX). A sandwich ELISA was developed for ACT measurement: rabbit anti-human ACT antibody (1:1000; DAKO, Carpinteria, CA) was used for capture and a sheep anti-



Fujirebio Diagnostics, Inc. v. Quanterix Corp.
EX-1045
5831

human ACT antibody (1:5000; The binding site, San Diego, CA) was used for detection. ACT purified from human plasma was used as standard (Sigma). For ATIII measurement, a sandwich ELISA was developed: rabbit anti-human ATIII antibody (1:1000; DAKO) was used for capture and a mouse monoclonal anti-human ATIII (clone HYB 230-04, 1:5000; Assay designs, Ann Arbor, MI) was used for detection. ATIII purified from human plasma was used as standard (Sigma). For ZAG, a sandwich ELISA was developed: rabbit anti-human ZAG antibody (1:1000; gift from Dr. Iwao Ohkubo, Shiga University of Medical Science, Japan) was used for capture and a mouse monoclonal anti-human ZAG antibody (clone 1D4, 1:100; Santa Cruz Biotechnology, Santa Cruz, CA) was used for detection. ZAG purified from human seminal plasma was used as standard (gift from Dr. Iwao Ohkubo). For gelsolin ELISA, CSF samples were directly coated on the plate, followed by incubation with a mouse monoclonal anti-gelsolin antibody (clone GS-2C4, 1:2000; Sigma). Gelsolin purified from human plasma was used as standard (Sigma). For AGT measurement, a sandwich ELISA was used: mouse monoclonal anti-AGT antibody (clone F8A2, 1:285; gift from Dr. Claus Oxvig, University of Aarhus, Denmark) was used for capture and a chicken antibody (1:1200; gift from Dr. Claus Oxvig) was used for detection. AGT purified from human plasma was used as standard (Calbiochem, San Diego, CA). For CNDP1 ELISA, CSF samples were directly coated on the plate, followed by incubation with goat anti-human CNDPI antibody (1:500; R&D systems, Minneapolis, MN).

[0071] For all ELISA measurements: 1) Biotinylated secondary antibody (1:5000; Jackson ImmunoResearch, West grove, PA) and poly-HRP streptavidin (1:2000; Research Diagnostics, Concord, MA) were used; for color development, TMB super slow or TMB super sensitive (Sigma) were used; 2) Samples were kept continuously on ice, and assays were performed on sample aliquots after a second thaw after initial freezing; 3) The levels of a given protein in all CSF samples were measured in the same experiment; 4)Data from a single experiment is presented and similar data have been obtained from at least one replicate experiment.

[0072] Statistical analyses: The Shapiro-Wilk test was used to test the hypothesis of a normal distribution for levels of ACT, ATIII, ZAG, CNDP1,



Fujirebio Diagnostics, Inc. v. Quanterix Corp.
EX-1045
5832

Aβ42, and tau. The distributions were log transformed to approximate a normal distribution. Values were then adjusted for age at lumbar puncture, gender, and the number of APOE4 alleles. The residuals were tested for association with case-control status using a t-test.

[0073] The area under the receiver operating characteristic curve (AUC) for each trait was calculated using the ROCR package in R (http://www.R-project.org; (Sing et al, Bioinformatics (2005) 21:3940-41)). A method proposed by Xiong et al (Med Decis Making (2004) 24:659-69) was implemented to determine the optimum linear combination of these traits and calculate confidence intervals on the AUC. This method requires a complete dataset; removal of individuals with missing phenotype data resulted in a slight decrease in the sample size (N=83).

[0074] Immunohistochemistry: ACT immunostaining was performed on ethanol fixed paraffin sections (5μm thickness) of human brain (frontal cortex) with a rabbit anti-human ACT antibody (1:100; Accurate chemical, Westbury, NY). ATIII immunostaining was performed on formalin fixed frozen sections (12μm thickness) of human brain (frontal cortex) using a rabbit anti-human ATIII antibody (1:500; Dako). The staining was developed chromogenically (DAB). Standard immunohistochemical protocol was employed for the above immunostaining (Han et al., Neurobiol Dis (200) 7:38-53). Thioflavine-S and X-34 staining was performed as described (Bales et al., Nature Genetics (1997) 17:263).

*Results:*

[0075] Sample selection: The CSF proteomes of 6 mild AD subjects were compared to those of 6 age-matched cognitively normal subjects. The mild AD subjects were clinically characterized with a CDR score of 1, indicating mild dementia and the controls all had a CDR score of 0, indicating non-demented. To maximize the likelihood of selecting CDR 1 subjects who truly had AD pathology from CDR 0 subjects who did not, selection was based on CSF Aβ42 concentrations. A recent study comparing in vivo amyloid imaging with CSF levels of various biomarkers showed that Aβ42 is an excellent marker of cerebral amyloid deposition, independent of clinical diagnosis Fagan et al., Ann Neurol



Fujirebio Diagnostics, Inc. v. Quanterix Corp.
EX-1045
5833

(2006) 59:512-19). The CSF samples were analyzed individually (as opposed to pooling the samples) to increase the statistical power of the analysis.

[0076] Candidate biomarkers identified. Upon 2D-DIGE analysis, 514 protein spots were matched across all six gels. Since a pooled sample was included on each gel, the relative abundance of the matched spots were normalized in all 12 individual CSF samples. Student's t-test (using $p < .05$ to define statistical significance) was performed to examine whether the average (relative) abundance of a given protein spot in the two CDR groups was significantly different. Twenty-one spots were found that displayed differential abundance (p values < 0.05) between the two groups. Three spots were excluded due to poor gel resolution and the remaining 18 were selected for excision, in gel tryptic digestion, and mass spectrometric identification.

[0077] To estimate whether most of these proteins are truly different in abundance as opposed to artifacts, the false discovery rate (FDR) was assessed in this study by using data from our previous study with this method (see examples 1-3) to approximate a "same-same comparison". In that study, the same comparative proteomic approach (depletion – followed by 2D-DIGE – MS/MS) was applied to the analysis of 12 CSF samples, composed of pairs of samples from the same six individuals, obtained 2 weeks apart. When the 6 CSF samples (as a group) obtained at time point 1 were compared to the 6 samples (as a group) obtained at time point 2, it is similar to a 'same-same comparison' because CSF samples from the same subject should be quite similar. When that comparison was performed, 0 spots were found (out of 306 matched spots) that were differentially expressed between the two groups (using a p value of 0.05 as cutoff). This result indicates that the false positive rate in the study (when using a p value of 0.05 as cut-off) is likely to be very low.

[0078] Protein identifications of the 18 spots are shown in Table 3. The protein identity of 16 of the 18 spots were successfully determined. For some spots, multiple proteins have been identified within one spot, most likely due to comigration of certain proteins. In addition, some proteins were identified in multiple proteins spots, including α1-antichymotrypsin (ACT) and antithrombin III (ATIII), likely reflecting the existence of different protein isoforms (e.g., post-translational modifications). A total of 11 proteins were identified as candidate



Fujirebio Diagnostics, Inc. v. Quanterix Corp.
EX-1045
5834

biomarkers for mild AD. Levels of gelsolin (GSN) and carnosinase I (CNDP1) were found to be lower in the mild AD group compared to the CDR 0 group whereas levels of the other candidate markers were higher in the CDR 1 group compared to controls. The relative difference in abundance between the averages of the two groups observed in 2D-DIGE is moderate, most within ±2 fold.

**Table 3: List of proteins that were identified through 2D-DIGE and mass spectrometry analysis to have differential abundance in mild AD and control CSF samples.**

| Spot | Protein | Change in AD in the CDR 1 group compared to the CDR 0 group | P value (student's t-test) |
|---|---|---|---|
| 1 | Antithrombin III | increased | 0.028 |
| 2 | Antithrombin III | increased | 0.023 |
| 3 | Antithrombin III<br>Angiotensinogen | increased | 0.033 |
| 4 | α-1-antichymotrypsin | increased | 0.031 |
| 5 | Carnosinase I<br>Secretogranin III<br>Kininogen | decreased | 0.018 |
| 6 | α-1-antichymotrypsin | increased | 0.031 |
| 7 | Antithrombin III | increased | 0.022 |
| 8 | α-1-antichymotrypsin | increased | 0.0091 |
| 9 | No ID | increased | 0.0041 |
| 10 | α-1-antichymotrypsin | increased | 0.015 |
| 11 | α-1-antichymotrypsin<br>Secretogranin III | increased | 0.011 |
| 12 | α-1-antichymotrypsin<br>Secretogranin III<br>Kininogen | increased | 0.0013 |
| 13 | Angiotensinogen<br>Kinongen | increased | 0.005 |
| 14 | Zinc α2-glycoprotein | increased | 0.027 |
| 15 | Zinc α2-glycoprotein<br>Chromagranin B | increased | 0.014 |
| 16 | Gelsolin | decreased | 0.028 |
| 17 | No ID | decreased | 0.048 |
| 18 | Neuronal pentraxin<br>Prostaglandin D2 synthase<br>β trace<br>Secretogranin III | decreased | 0.043 |

[0079] Validation of candidate biomarkers with ELISA. In order to confirm the findings with another method and also to be more quantitative, the levels of candidate biomarkers were first assayed in the original 12 CSF samples (CDR 0 (n=6), CDR1 (n=6)) using ELISA. Based on the availability of antibodies, the following candidates were assessed: ACT, ATIII, Zinc-α2-glycoprotein (ZAG),



Fujirebio Diagnostics, Inc. v. Quanterix Corp.
EX-1045
5835

CNDP1, GSN and angiotensinogen (AGT). Then, a larger test set of CSF samples of cognitively normal subjects (CDR 0, n=49) were assayed versus subjects with very mild (CDR 0.5, n=19) or mild dementia (CDR 1, n=13) judged to be due to AD. The goal was to determine whether the findings could be validated in a larger, independent sample set. This level of validation is very important and has not been done before in previous AD proteomic biomarker studies to our knowledge. For all the candidate biomarkers evaluated, when the larger sample set was assayed, the same trend was observed as when the 12 original samples were assayed. Therefore, values from the 12 original samples were combined with the test sample set in the subsequent graphs. In addition, since no differences between the CDR 0.5 and CDR 1 groups were observed, these groups were combined to form the mild AD group and were then compared to the CDR 0 group. ELISA data that display CDR 0.5 and CDR 1 separately can be found in Fig. 6. For reference, the concentrations of Aβ42 and total tau (which have been obtained previously to this study) in these CSF samples were included (Fig. 7).

[0080] As shown in Fig. 8, the CSF levels of ACT, ATIII and ZAG are significantly increased in the very mild/mild AD group, confirming the 2D-DIGE findings. There is a trend for a decrease in CNDP1 levels in the very mild/mild AD group (Fig 8), though this was not quite statistically significant (p=0.055). In contrast to the 2D-DIGE findings, a difference in levels of GSN or AGT between the two groups was not confirmed (Fig. 8). After log transformation (to approximate a normal distribution) the datasets were examined for any possible interactions between CSF concentrations of candidate biomarkers (including Aβ42 and total tau) and age/gender/number of APOE4 alleles. A significant correlation was found between the number of APOE4 alleles and CSF levels of Aβ42, total tau and AGT. There is also a positive correlation between age and CSF levels of ACT and GSN. In addition, an interaction between gender and CSF ZAG concentrations was observed, with males having higher levels than females. The initial observations based on the raw concentration data are not qualitatively different from those using the log-transformed and adjusted traits. The adjusted p values were included in fig. 8 (designated by p*) for comparison. Since the



Fujirebio Diagnostics, Inc. v. Quanterix Corp.
EX-1045
5836

differences in levels of GSN or AGT between the two groups were not confirmed, these two candidates were not included in subsequent analyses.

[0081] Next, whether similar differences exist in plasma as were found in CSF was assessed. Levels of ACT, ATIII and ZAG in paired plasma samples were not significantly different between the very mild/mild AD and control groups (Fig. 9). There was also no significant correlation between the CSF and plasma levels of ACT or ATIII, but there was a weak correlation between the CSF and plasma levels of ZAG (Fig. 10).

[0082] The relationships among the CSF concentrations of the candidate biomarkers (together with Aβ42 and tau) were examined (Table 4). None of the newly identified candidate biomarkers correlate with Aβ42 though ACT, CNDP1 and ZAG moderately correlate with tau. Interestingly, there are very strong, highly significant correlations between ACT, ATIII and ZAG (but not CNDP1) (Table 4). To preliminarily assess the potential use of these candidate biomarkers in differentiating subjects with very mild/mild AD from controls, a method proposed by Xiong et al. (Med Decis Making (2004) 24:659-69) was applied to determine the optimum linear combination of these biomarkers and calculated the confidence intervals on the AUC (the area under the receiver operating characteristic curve). Individual candidates by themselves are very comparable to those of Aβ42 and total tau in differentiating very mild/mild AD from controls (Table 5, Fig. 11). Importantly, when all biomarkers are optimally combined, this results in a higher AUC and sensitivity than for any single biomarker.

**Table 4: Pearson Correlation Coefficients for the normalized, adjusted biomarkers. Coefficients were derived using log-transformed data that were also adjusted for interacting factors (i.e. age, gender or the number of APOE4 allele). P-values are displayed in the parentheses.**

| | ATIII | CNDP1 | ACT | ZAG | Aβ42 | TAU |
|---|---|---|---|---|---|---|
| ATIII | 1 | | | | | |
| CNDP1 | -0.007 (0.95) | 1 | | | | |
| ACT | 0.73 (<.0001) | 0.030 (0.78) | 1 | | | |
| ZAG | 0.66 (<.0001) | 0.026 (0.81) | 0.71 (<.0001) | 1 | | |
| | 0.018 | 0.090 | -0.056 | 0.024 | | |



Fujirebio Diagnostics, Inc. v. Quanterix Corp.
EX-1045
5837

| | | | | | | |
|---|---|---|---|---|---|---|
| Aβ42 | (0.87) | (0.40) | (0.61) | (0.83) | 1 | |
| TAU | 0.092 (0.40) | 0.32 (0.003) | 0.36 (0.0009) | 0.32 (0.0024) | -0.065 (0.55) | 1 |

**Table 5: Comparison of the AUC of the optimum linear combination (Optimum) to that of each individual biomarker (AUC: area under the receiver operating curve).**

| Marker | AUC (SE) | Sensitivity at 80% Specificity | p-value vs. Optumim |
|---|---|---|---|
| ATIII | 0.75 (0.10) | 0.48 | 0.29 |
| CNDP1 | 0.65 (0.12) | 0.24 | 0.099 |
| ACT | 0.75 (0.11) | 0.3 | 0.32 |
| ZAG | 0.72 (0.10) | 0.42 | 0.21 |
| Aβ42 | 0.64 (0.12) | 0.36 | 0.085 |
| tau | 0.68 (0.11) | 0.36 | 0.14 |
| Optimum | 0.88 (0.07) | 0.7 | -- |

[0083] Cellular localization of ACT and ATIII. The cellular localization of some of the candidate biomarkers were examined in human and transgenic AD mouse brain. Consistent with previous reports (Abraham et al., 1998; Abraham et al., Neurobiol aging et al. (1990) 11:123-29), ACT is co-localized with amyloid plaques in human AD brain and is also present in neurons and astrocytes. Also, antibodies to ATIII label amyloid plaques and neurofibrillary tangles (NFT) in human AD brain, in accordance with a previous report (Kalatira et al, Am J Pathol (1993) 143:886-893).

*Discussion*:

[0084] In this study, candidate biomarkers for mild AD were identified by analyzing a small group of CSF samples (mild AD vs. control) with a comparative proteomic approach. Importantly, selected biomarkers were validated with ELISA using a larger sample set. Among the identified biomarkers is ACT, which has been identified previously in other reports. Novel biomarkers such as ATIII, ZAG and CNDP1 were also identified, whose roles as AD biomarkers in CSF have not been previously assessed and validated. This is the first proteomic study on AD biomarkers that not only discovered candidate protein biomarkers, but also validated these candidates in a much larger and independent sample set with a sensitive and quantitative method (i.e. ELISA) in multiple, well characterized individuals. Thus, this proof-of-principle study demonstrates that this proteomic approach can be used to reliably identify AD biomarkers in CSF.



Fujirebio Diagnostics, Inc. v. Quanterix Corp.
EX-1045
5838

[0085] The proteomic approach taken included multi-affinity depletion, 2-D DIGE, and nano-LC-FTMS. The sensitive, high resolution mass spectrometric resulted in the identification in 16 of the 18 gel features that showed significant differential abundances between the two CDR groups. The overall result was the generation of reliable data, which is demonstrated by the low false discovery rate (FDR) in the study. FDR is defined as the number of expected false predictions divided by the number of total predictions, which in the study is 21. The number of expected false predictions was estimated using a previous set of CSF proteomic data (generated using the same approach and performed in the same lab by the same people). A “same-same” comparison was approximated by comparing a set of 6 CSF samples from 6 individuals to a second set of 6 CSF samples from the same individuals, taken 2 weeks apart. Any differentially expressed proteins found in such a comparison would be false positives because in the ideal scenario, there should be no differences detected in a same-same comparison. Interestingly, no protein spots (0 out of 306 matched spots) were found that were significantly different between the two groups. With a close-to-zero FDR when the p value cutoff is set at 0.05, the p value cutoff could potentially be increased to maximize the number of biomarker candidates discovered while still maintaining a low FDR.

[0086] Four of the 6 selected biomarker candidates were validated using ELISA with a much larger characterized sample set. Although protein spots that correspond to GSN and AGT display differential abundance in 2D-DIGE, a difference between the mild AD and control group via ELISA was not detected. One possible explanation is the existence of different isoforms for a single protein. GSN has two isoforms “a” and “b” which differ only by a stretch of 24 amino acids at the N terminus. The unique peptides for the two isoforms were not detected in the MS data and the ELISA is not isoform specific. AGT is known to have different isoforms due to glycosylation Matsubara et al., Ann Neurol (1990) 28:561-67). If the 2D-DIGE observations only reflect differences in certain isoforms, it might not result in a difference in total protein level measured by ELISA. Thus, to the extent that AD is associated with changes in the level of specific protein isoforms, ELISA for total protein levels might not detect such changes.



Fujirebio Diagnostics, Inc. v. Quanterix Corp.
EX-1045
5839

[0087] One of the validated candidate biomarkers, ACT, has been previously proposed as a possible biomarker for AD. An increase in CSF ACT level was observed in the AD group, in agreement with a number of previous studies (Matsubara et al., Ann Neurol (1990) 28:561-67; DeKosky et al., Ann Neurol (2003) 53:81-90; Harigaya et al., Intern Ned (1995) 34:481-84; Licastro et al., Alzheimer Dis Assoc Disord (1995) 9:112-118). There was no significant change in ACT levels in plasma in the dementia group nor a correlation between the CSF and plasma levels of this protein. This is similar to some previous findings [33, 36-39] (Matsubara et al., Ann Neurol (1990) 28:561-67; Licastro et al., Alzheimer Dis Assoc Disord (1995) 9:112-118; Pirttila et al., Neurobiol Aging (1994) 15:313-317; Licastro et al., Dement Geriatr Cogn Disord (2000) 11:25-28; Lanzrein et al., Alzhemier Dis Assoc Disord (1998) 12:215-227) but not others (Matsubara et al., Ann Neurol (1990) 28:561-67; DeKosky et al., Ann Neurol (2003) 53:81-90; Licastro et al., Alzheimer Dis Assoc Disord (1995) 9:112-118; Oishi et al., Ann Clin Lab Sci (1996) 26:340-45; Licastro et al., J Nuroimmunol (2000) 103:97-102). The ACT index (a calculated quotient using the ACT and albumin content of CSF and plasma to detect intrathecal ACT synthesis) was also measured and it was found that 90% of the samples have an index above 1, with an average index of 2.4. These results indicate independent within-CNS production as the main source of ACT in CSF.

[0088] In contrast to ACT, other validated candidates (i.e. ATIII, ZAG and CNDP1) have not been well-studied in AD and therefore represent novel potential biomarkers. ATIII, like ACT, is a serine protease inhibitor. In the present and another study (Kalaria et al., Am J Pathol (1993) 143:886-893), ATIII was shown to localize to both amyloid plaques and NFT in AD brain. However, ATIII has not previously been reported to be increased in AD CSF. It is not clear why ZAG and CNDP1 are altered in AD CSF or their potential roles in AD pathogenesis. ZAG is a soluble glycoprotein and present in a variety of body fluids (Poortmans et al., J Lab Clin Med (1968) 71:807-11). The biological functions of ZAG are largely unknown. One 2D-gel-based proteomic study identified ZAG as one of the proteins that was increased in AD CSF (Davidsson et al., Neuroreport (2002) 13:611-15) though this was not validated in a large sample set. Carnosinase I (CNDP1) hydrolyzes carnosine (β-alanlyl-L-histidine) and



Fujirebio Diagnostics, Inc. v. Quanterix Corp.
EX-1045
5840

homocarnosine (γ-aminobutyryl-L-histidine), both of which are believed to be neuro-protective (Teufel et al., J Biol Chem (2003) 278:6521-31). Decreased serum levels of CNDP1 have been found in patients with Parkinson's disease, multiple sclerosis and in patients after a cerebrovascular accident (Wassif et al., Clin Chim Acta (1994) 225:57-64).

[0089] The degree of the changes of these validated biomarker candidates (in AD CSF) is moderate (within 30%), with overlaps between the AD and control group. However, the magnitude of the difference in levels of ACT, ATIII and ZAG is comparable to that of Aβ42, currently one of the best CSF biomarkers of AD that correlates very well with the presence or absence of amyloid in the brain (Fagan et al., Ann Neurol (2006) 59:512-19). Importantly, changes in these biomarkers are already evident in the very mildly demented CDR 0.5 group (Fig. 7), suggesting the suitability of these candidates for the early detection of AD. Due to the existence of preclinical AD in cognitively normal individuals, the CDR 0 group is likely heterogeneous, containing subjects with and without AD pathology in the brain. Indeed, a recent study demonstrated the presence of brain amyloid and low levels of CSF Aβ42 in a subset of cognitively normal individuals (Fagan et al., Ann Neurol (2006) 59:512-19). Such preclinical AD pathology might in part account for the overlap between AD and control group in terms of biomarker concentrations.

[0090] Statistical analyses demonstrate that the biomarker candidates identified have diagnostic power/accuracy comparable to that of Aβ42 and total tau. When all biomarkers are combined, a greater AUC and sensitivity can be achieved. Although the difference is not statistically significant in this study (including 50 CDR 0 subjects and 33 mild AD subjects), this trend may become significant when larger sample sets are assessed.



Fujirebio Diagnostics, Inc. v. Quanterix Corp.
EX-1045
5841

## CLAIMS

What is claimed is:

1. A biomarker for AD, the biomarker comprising the level of antithrombin III in a bodily fluid of a subject.
2. The biomarker of claim 1, wherein the bodily fluid is CSF.
3. The biomarker of claim 1, wherein the antithrombin III is antithrombin III enzymatic activity.
4. The biomarker of claim 1, wherein the antithrombin III is antithrombin III protein concentration.
5. A method for detecting AD, the method comprising:
    a. quantifying the level of antithrombin III in a bodily fluid of the subject, and
    b. determining if the quantified level of antithrombin III is elevated in comparison to the average antithrombin III level for a subject with a CDR of 0.
6. The method of claim 5, wherein an elevated antithrombin III level in comparison to the average antithrombin III level indicates a diagnosis of AD.
7. The method of claim 5, wherein an elevated antithrombin III level in comparison to the average antithrombin III level indicates a prognosis of AD.
8. The method of claim 5, wherein the antithrombin III measured is antithrombin III enzymatic activity.
9. The method of claim 5, wherein the antithrombin III measured is antithrombin III protein concentration.
10. The method of claim 9, further comprising measuring antithrombin III protein concentration by ELISA.
11. The method of claim 5, wherein the subject is at risk for AD.
12. The method of claim 5, wherein the subject has no clinical signs of AD.
13. The method of claim 5, wherein the subject is human.
14. The method of claim 5, wherein the bodily fluid is CSF.
15. The method of claim 5, further comprising



Fujirebio Diagnostics, Inc. v. Quanterix Corp.
EX-1045
5842

a. quantifying the level of at least one other AD biomarker in a bodily fluid of the subject, and

b. determining if the quantified level of the additional AD biomarker or biomarkers is elevated or depressed in comparison to the average level for that biomarker for a subject with a CDR of 0.

16. The method of claim 5, further comprising quantifying three or more biomarkers.

17. The method of claim 5, further comprising quantifying five or more biomarkers.

18. The method of claim 5, further comprising quantifying ten or more biomarkers.

19. The method of claim 16, further comprising selecting the additional biomarkers from the group comprising ACT, ZAG, CNDP1, Aβ42, and tau.

20. A method for monitoring AD, the method comprising:

a. quantifying the level of antithrombin III in a bodily fluid of the subject, and

b. comparing the quantified level of antithrombin III to a previously quantified antithrombin III level of the subject.

21. The method of claim 20, where the subject's response to AD treatment is monitored.

22. The method of claim 20, wherein the antithrombin III measured is antithrombin III enzymatic activity.

23. The method of claim 20, wherein the antithrombin III measured is antithrombin III protein concentration.

24. The method of claim 23, further comprising measuring antithrombin III protein concentration by ELISA.

25. The method of claim 20, wherein the subject has been diagnosed with AD.

26. The method of claim 20, wherein the subject has no clinical signs of AD.

27. The method of claim 20, wherein the subject is human.

28. The method of claim 20, wherein the bodily fluid is CSF.



Fujirebio Diagnostics, Inc. v. Quanterix Corp.
EX-1045
5843

29. The method of claim 20, further comprising
    a. quantifying the level of at least one other biomarker in a bodily fluid of the subject, and
    b. comparing the quantified level of the additional AD biomarker or biomarkers to a previously quantified level of the subject for that biomarker.
30. The method of claim 20, further comprising quantifying three or more biomarkers.
31. The method of claim 20, further comprising quantifying five or more biomarkers.
32. The method of claim 20, further comprising quantifying ten or more biomarkers.
33. The method of claim 30, further comprising selecting the additional biomarkers from the group comprising ACT, ZAG, CNDP1, Aβ42, and tau.
34. A kit for quantifying antithrombin III in a bodily fluid of a subject comprising means to quantify antithrombin III and instructions.
35. The kit of claim 34, wherein antithrombin III enzymatic activity is quantified.
36. The kit of claim 34, further comprising the means to quantify antithrombin III enzymatic activity.
37. The kit of claim 34, wherein antithrombin III protein is quantified.
38. The kit of claim 34, further comprising the means to quantify antithrombin III protein concentration.
39. The kit of claim 34, further comprising the means to quantify at least one other AD biomarker.
40. The kit of claim 34, further comprising the means to quantify three or more AD biomarkers.
41. The kit of claim 34, further comprising the means to quantify five or more AD biomarkers.
42. The kit of claim 34, further comprising the means to quantify ten or more AD biomarkers.
43. The kit of claim 34, wherein the bodily fluid comprises CSF.



Fujirebio Diagnostics, Inc. v. Quanterix Corp.
EX-1045
5844

44. The kit of claim 34, wherein the subject is human.
45. A biomarker for AD, the biomarker comprising the level of carnosinase 1 in a bodily fluid of a subject.
46. The biomarker of claim 1, wherein the bodily fluid is CSF.
47. The biomarker of claim 1, wherein the carnosinase I is carnosinase I enzymatic activity.
48. The biomarker of claim 1, wherein the carnosinase I is carnosinase I protein concentration.
49. A method for detecting AD, the method comprising:
    a. quantifying the level of carnosinase I in a bodily fluid of the subject, and
    b. determining if the quantified level of carnosinase I is elevated in comparison to the average carnosinase I level for a subject with a CDR of 0.
50. The method of claim 49, wherein an elevated carnosinase I level in comparison to the average carnosinase I level indicates a diagnosis of AD.
51. The method of claim 49, wherein an elevated carnosinase I level in comparison to the average carnosinase I level indicates a prognosis of AD.
52. The method of claim 49, wherein the carnosinase I measured is carnosinase I enzymatic activity.
53. The method of claim 49, wherein the carnosinase I measured is carnosinase I protein concentration.
54. The method of claim 53, further comprising measuring carnosinase I protein concentration by ELISA.
55. The method of claim 49, wherein the subject is at risk for AD.
56. The method of claim 49, wherein the subject has no clinical signs of AD.
57. The method of claim 49, wherein the subject is human.
58. The method of claim 49, wherein the bodily fluid is CSF.
59. The method of claim 49, further comprising
    a. quantifying the level of at least one other AD biomarker in a bodily fluid of the subject, and



Fujirebio Diagnostics, Inc. v. Quanterix Corp.
EX-1045
5845

b. determining if the quantified level of the additional AD biomarker or biomarkers is elevated or depressed in comparison to the average level for that biomarker for a subject with a CDR of 0.

60. The method of claim 49, further comprising quantifying three or more biomarkers.

61. The method of claim 49, further comprising quantifying five or more biomarkers.

62. The method of claim 49, further comprising quantifying ten or more biomarkers.

63. The method of claim 62, further comprising selecting the additional biomarkers from the group comprising ACT, ZAG, ATIII, Aβ42, and tau.

64. A method for monitoring AD, the method comprising:
   a. quantifying the level of carnosinase I in a bodily fluid of the subject, and
   b. comparing the quantified level of carnosinase I to a previously quantified carnosinase I level of the subject.

65. The method of claim 64, where the subject's response to AD treatment is monitored.

66. The method of claim 64, wherein the carnosinase I measured is carnosinase I enzymatic activity.

67. The method of claim 64, wherein the carnosinase I measured is carnosinase I protein concentration.

68. The method of claim 67, further comprising measuring carnosinase I protein concentration by ELISA.

69. The method of claim 64, wherein the subject has been diagnosed with AD.

70. The method of claim 64, wherein the subject has no clinical signs of AD.

71. The method of claim 64, wherein the subject is human.

72. The method of claim 64, wherein the bodily fluid is CSF.

73. The method of claim 64, further comprising
   a. quantifying the level of at least one other biomarker in a bodily fluid of the subject, and



Fujirebio Diagnostics, Inc. v. Quanterix Corp.
EX-1045
5846

b. comparing the quantified level of the additional AD biomarker or biomarkers to a previously quantified level of the subject for that biomarker.

74. The method of claim 64, further comprising quantifying three or more biomarkers.

75. The method of claim 64, further comprising quantifying five or more biomarkers.

76. The method of claim 64, further comprising quantifying ten or more biomarkers.

77. The method of claim 76, further comprising selecting the additional biomarkers from the group comprising ACT, ZAG, ATIII, Aβ42, and tau.

78. A kit for quantifying carnosinase I in a bodily fluid of a subject comprising means to quantify carnosinase I and instructions.

79. The kit of claim 78, wherein carnosinase I enzymatic activity is quantified.

80. The kit of claim 78, further comprising the means to quantify carnosinase I enzymatic activity.

81. The kit of claim 78, wherein carnosinase I protein is quantified.

82. The kit of claim 78, further comprising the means to quantify carnosinase I protein concentration.

83. The kit of claim 78, further comprising the means to quantify at least one other AD biomarker.

84. The kit of claim 78, further comprising the means to quantify three or more AD biomarkers.

85. The kit of claim 78, further comprising the means to quantify five or more AD biomarkers.

86. The kit of claim 78, further comprising the means to quantify ten or more AD biomarkers.

87. The kit of claim 78, wherein the bodily fluid comprises CSF.

88. The kit of claim 78, wherein the subject is human.



Fujirebio Diagnostics, Inc. v. Quanterix Corp.
EX-1045
5847

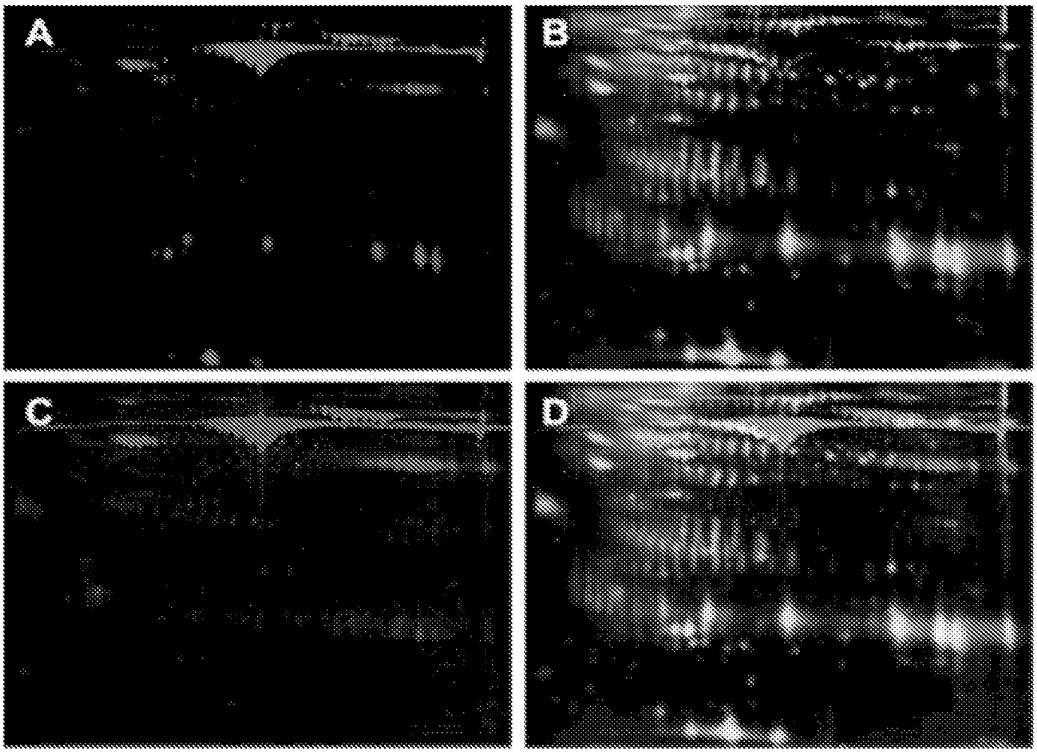



Fig. 1

Fujirebio Diagnostics, Inc. v. Quanterix Corp.
EX-1045
5848

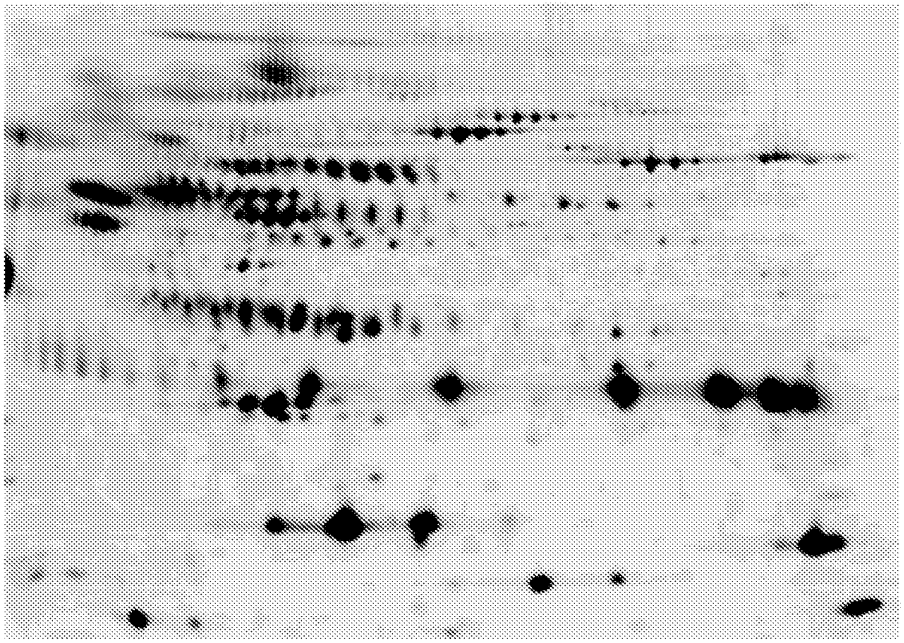
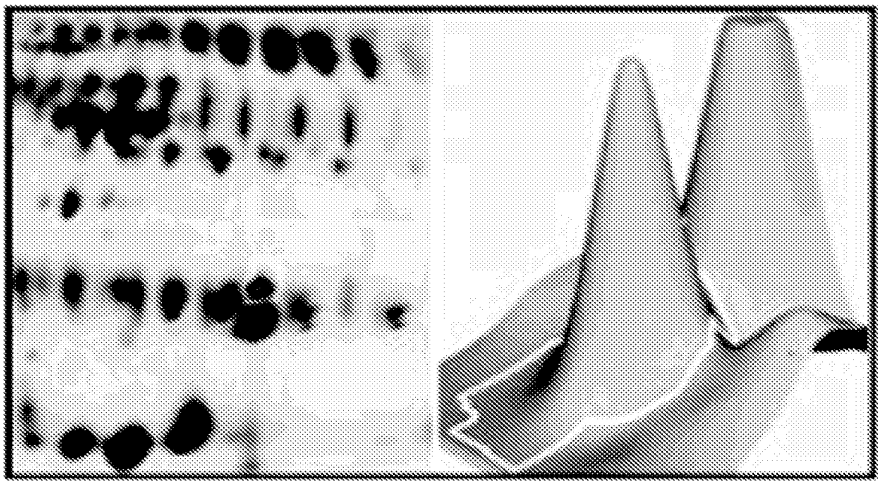


Fig. 2

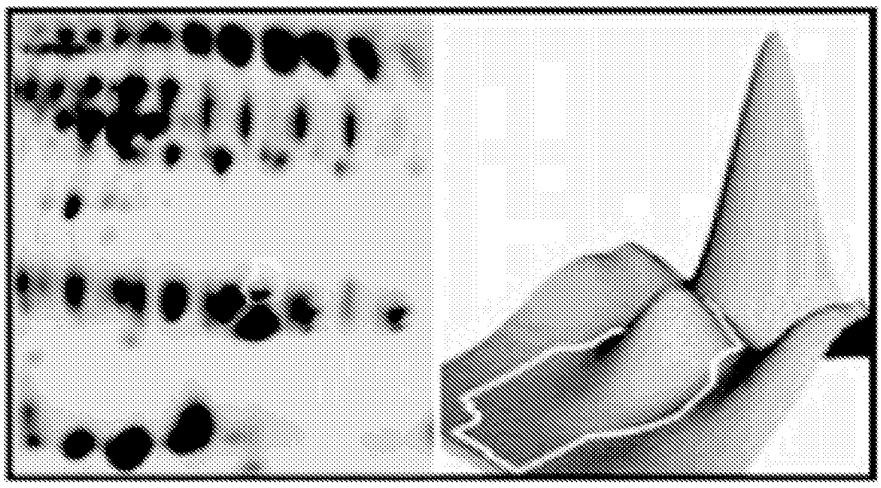
Fujirebio Diagnostics, Inc. v. Quanterix Corp.
EX-1045
5849

A



Time point 1

B



Time point 2

**Fig. 3**

Fujirebio Diagnostics, Inc. v. Quanterix Corp.
EX-1045
5850

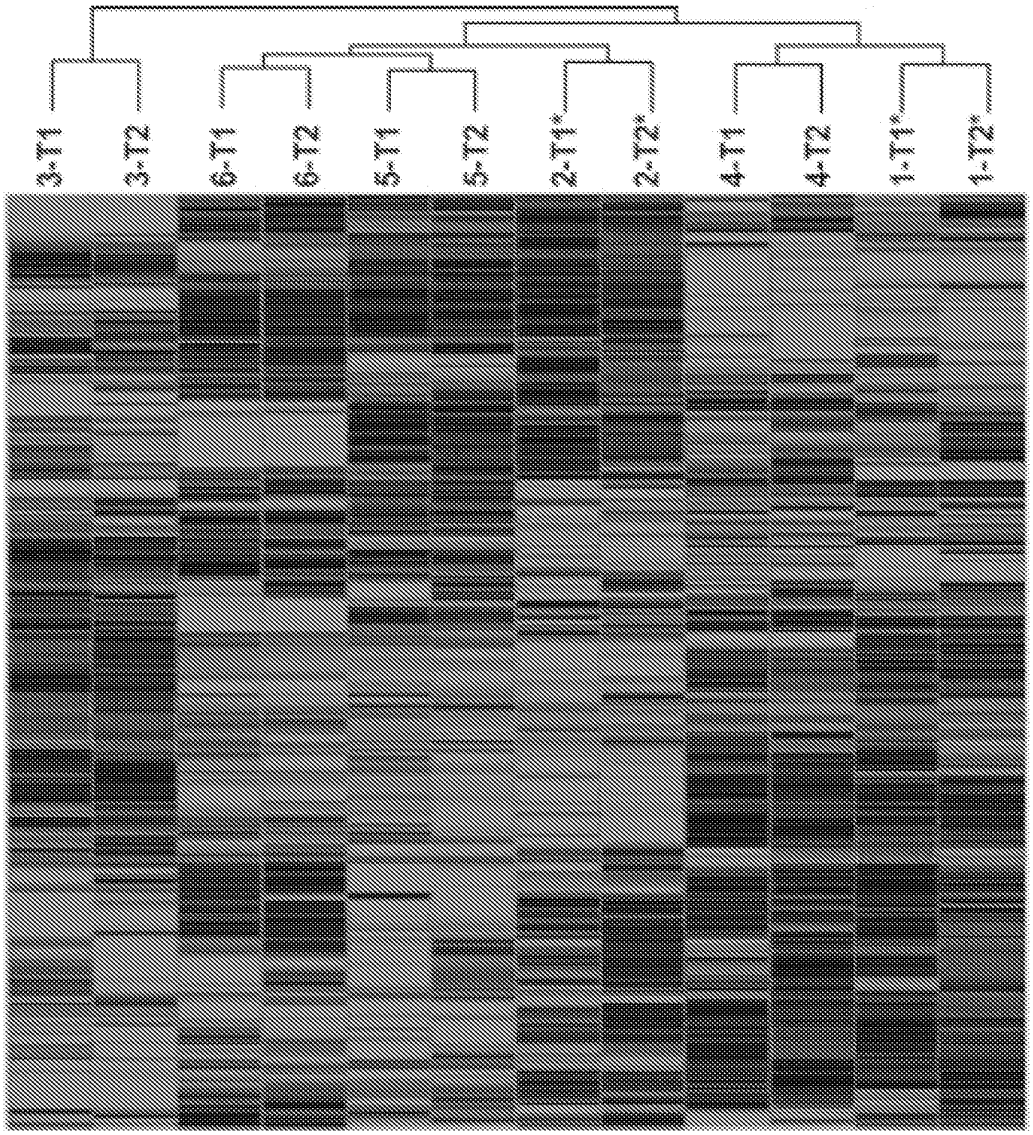



Fig. 4

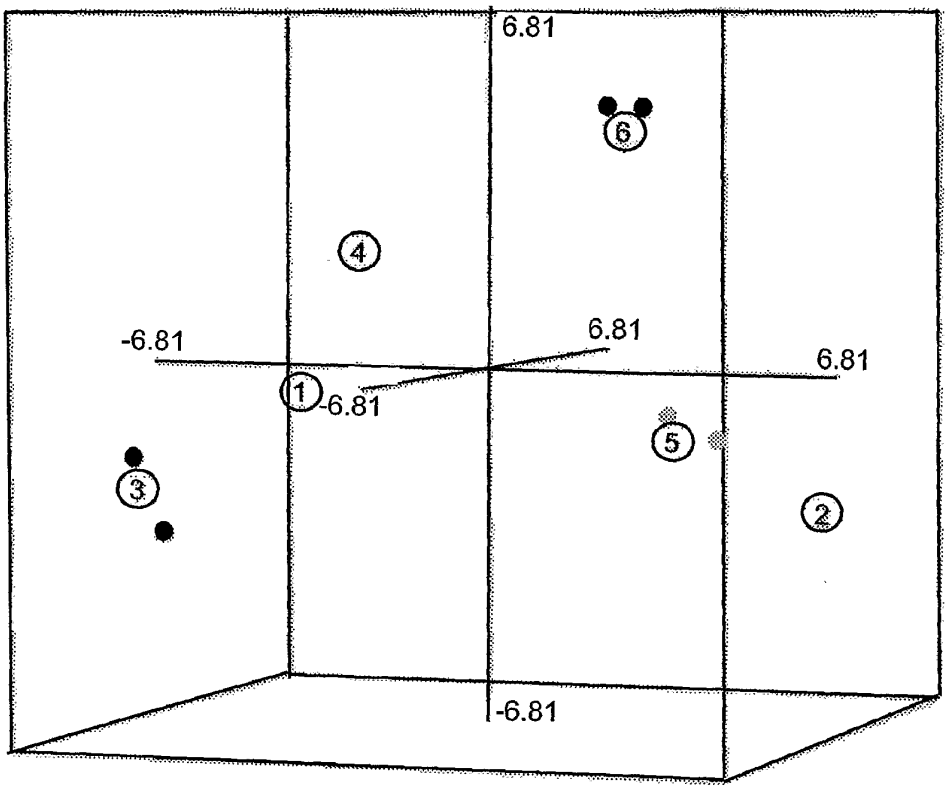



**Fig. 5**



Fujirebio Diagnostics, Inc. v. Quanterix Corp.
EX-1045
5852

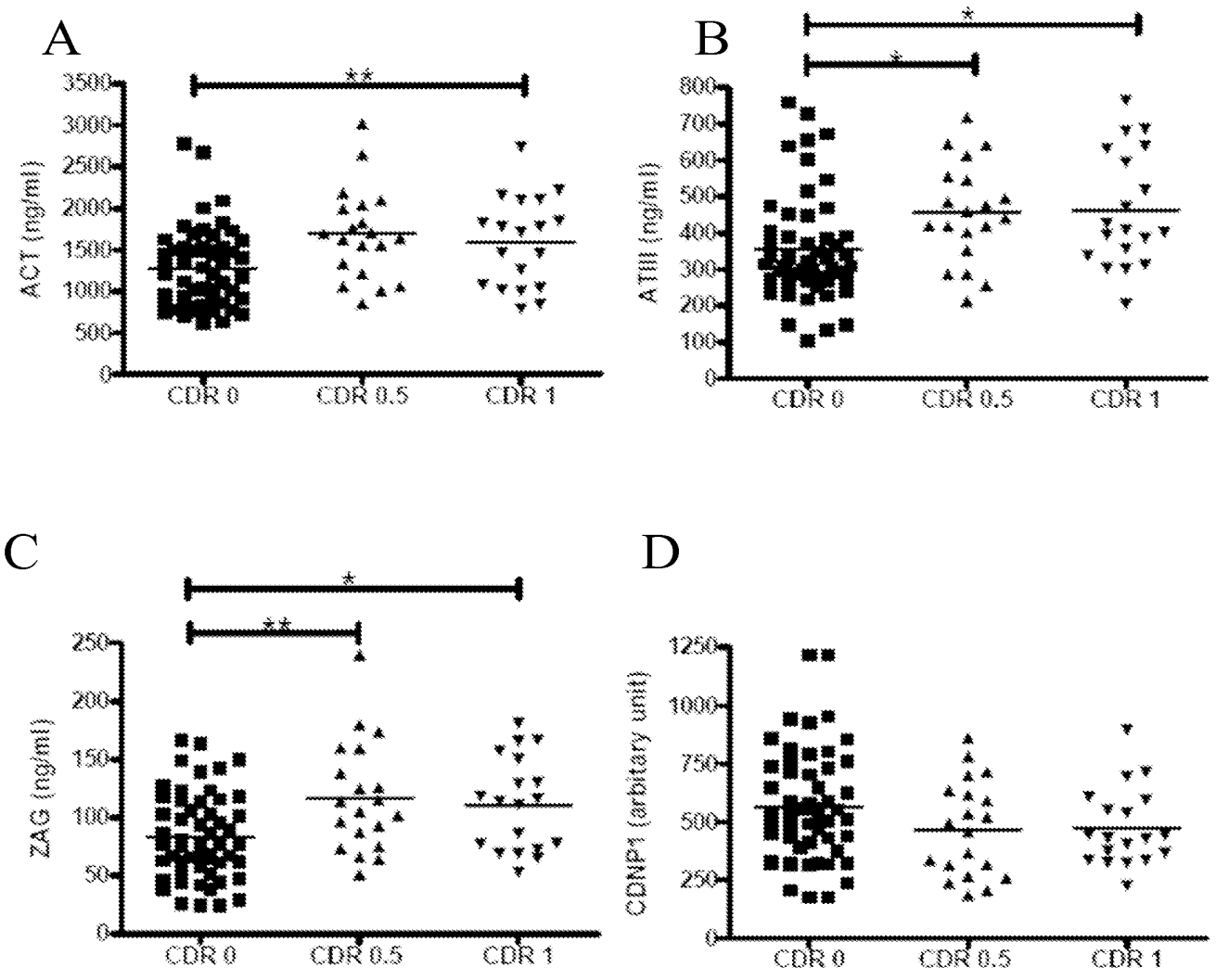

A
ACT (ng/ml)
3500
3000
2500
2000
1500
1000
500
0
**
CDR 0
CDR 0.5
CDR 1
B
ATIII (ng/ml)
800
700
600
500
400
300
200
100
0
*
*
CDR 0
CDR 0.5
CDR 1
C
ZAG (ng/ml)
250
200
150
100
50
0
*
**
CDR 0
CDR 0.5
CDR 1
D
CDNP1 (arbitary unit)
1250
1000
750
500
250
0
CDR 0
CDR 0.5
CDR 1

**Fig. 6**

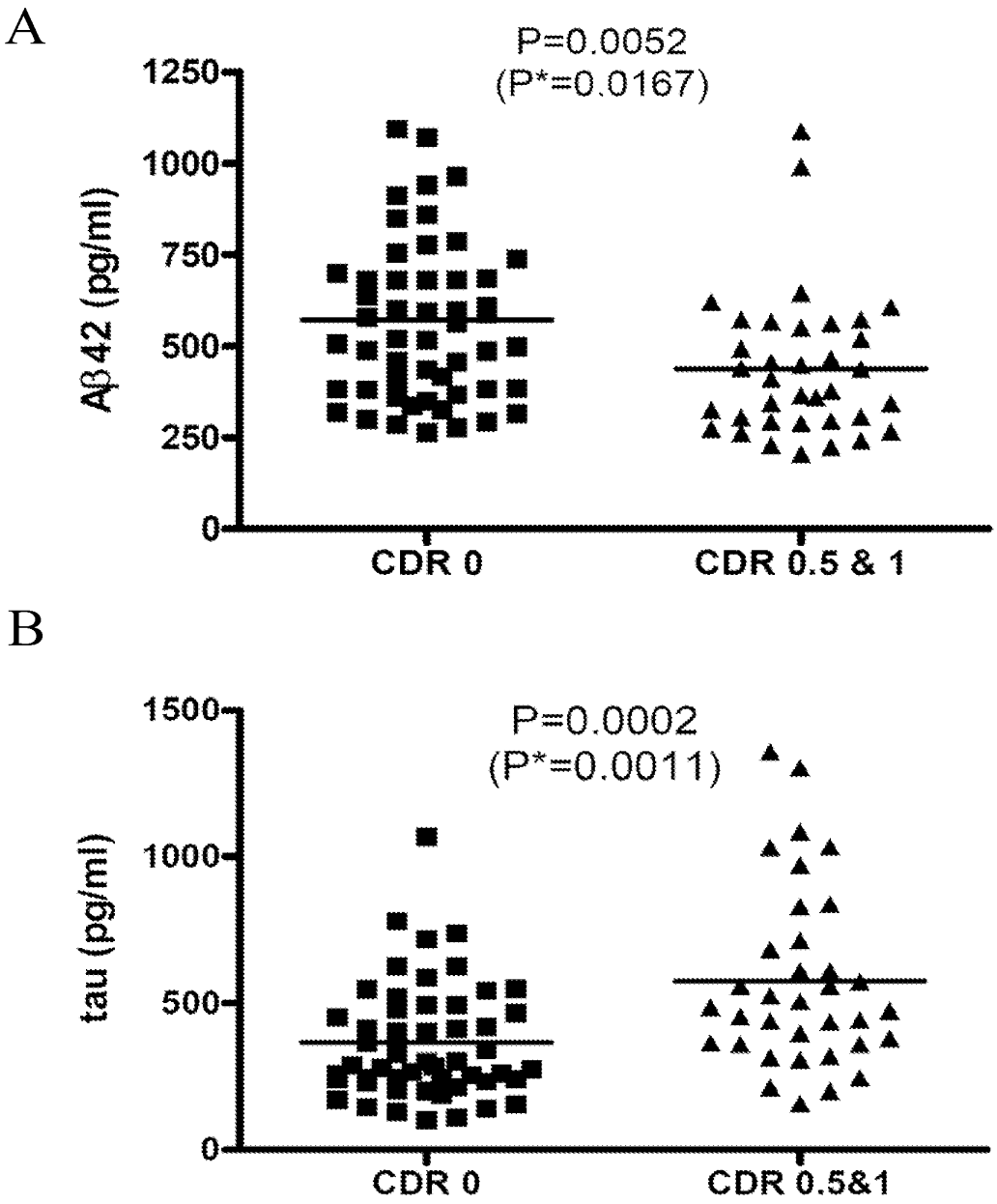
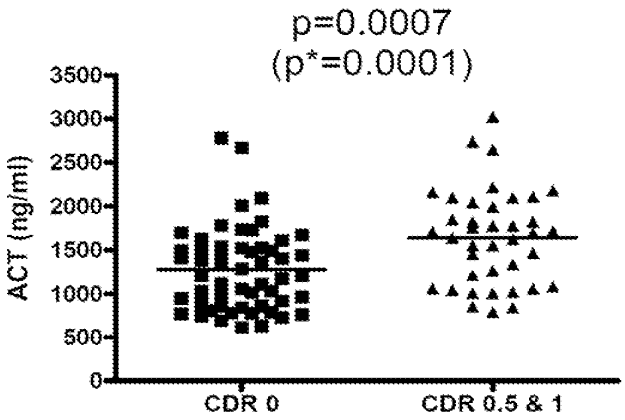
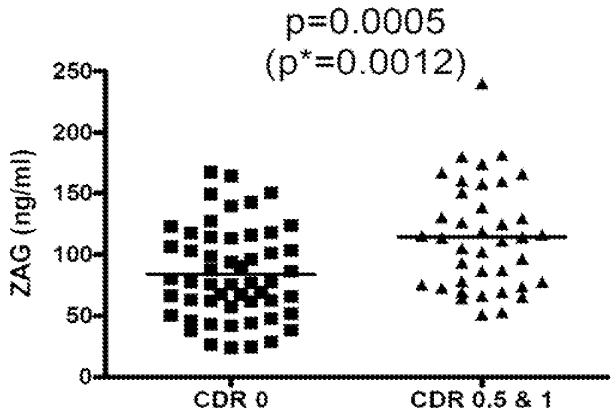

A
P=0.0052
(P*=0.0167)
1250
1000
750
500
250
0
Aβ42 (pg/ml)
CDR 0
CDR 0.5 & 1
B
P=0.0002
(P*=0.0011)
1500
1000
500
0
tau (pg/ml)
CDR 0
CDR 0.5&1

**Fig. 7**

A


p=0.0007
(p*=0.0001)
ACT (ng/ml)
3500
3000
2500
2000
1500
1000
500
0
CDR 0
CDR 0.5 & 1

B


p=0.0005
(p*=0.0012)
ZAG (ng/ml)
250
200
150
100
50
0
CDR 0
CDR 0.5 & 1

C

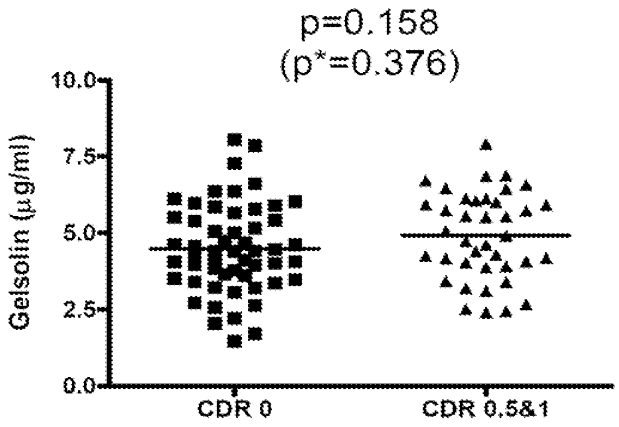
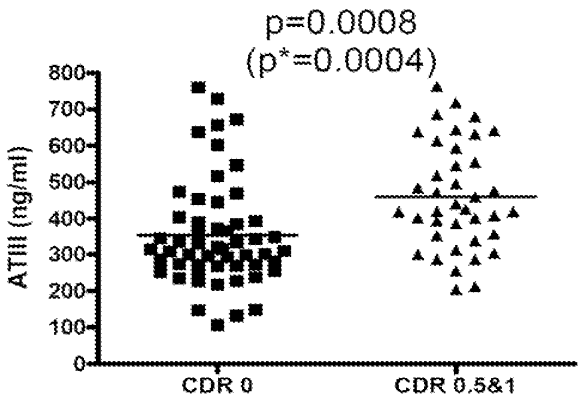
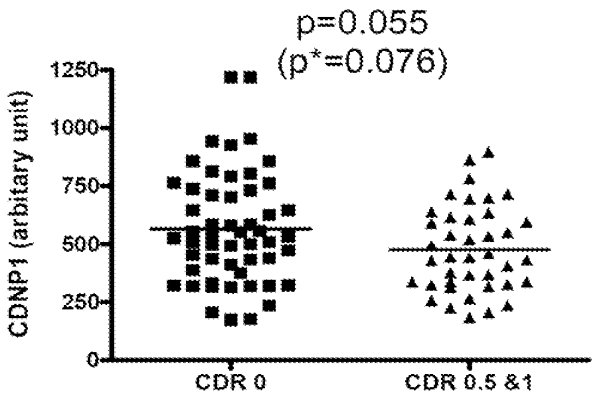

p=0.158
(p*=0.376)
Gelsolin (µg/ml)
10.0
7.5
5.0
2.5
0.0
CDR 0
CDR 0.5&1

**Fig. 8**

D




E




F

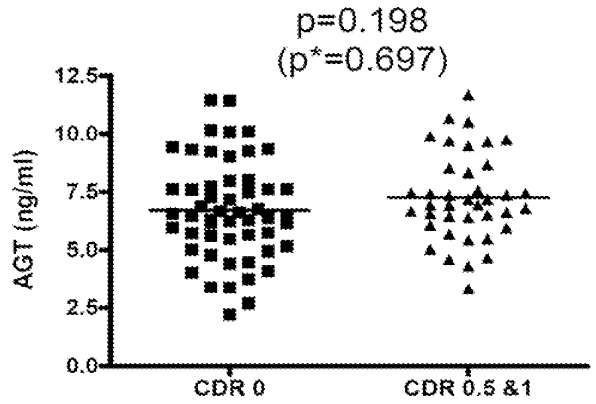



**Fig. 8**

Fujirebio Diagnostics, Inc. v. Quanterix Corp.
EX-1045
5856

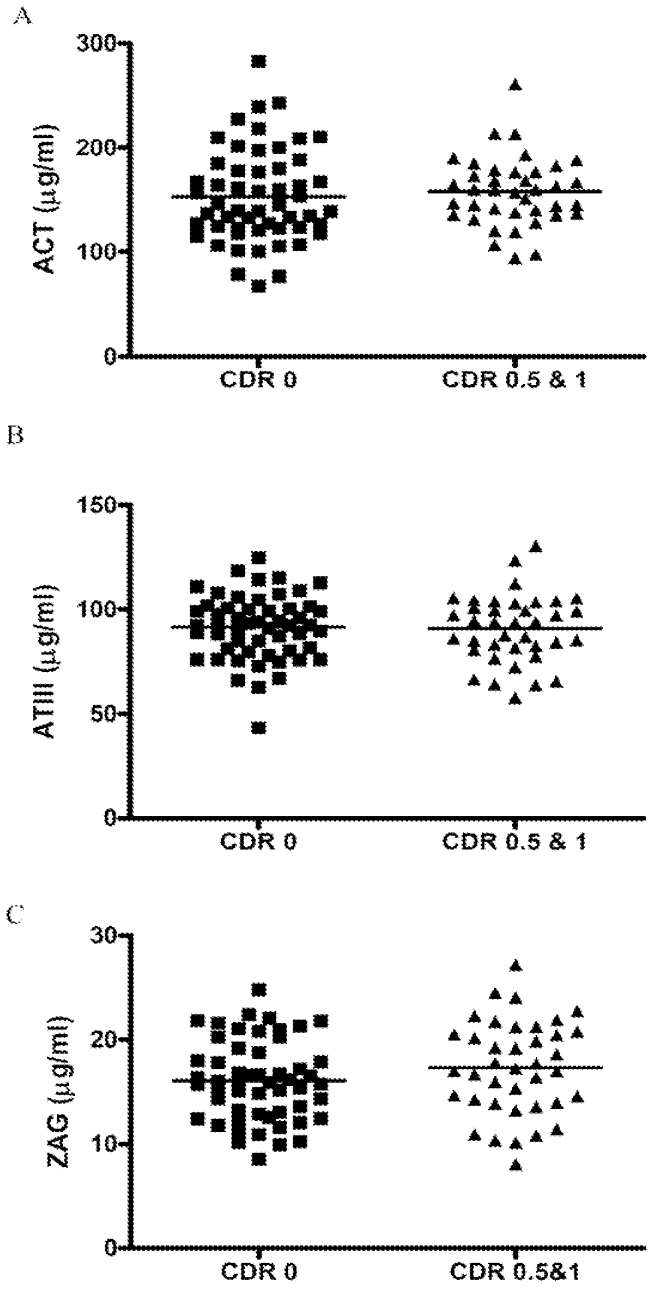

A
300
200
100
0
ACT (µg/ml)
CDR 0
CDR 0.5 & 1
B
150
100
50
0
ATIII (µg/ml)
CDR 0
CDR 0.5 & 1
C
30
20
10
0
ZAG (µg/ml)
CDR 0
CDR 0.5&1

Fig. 9

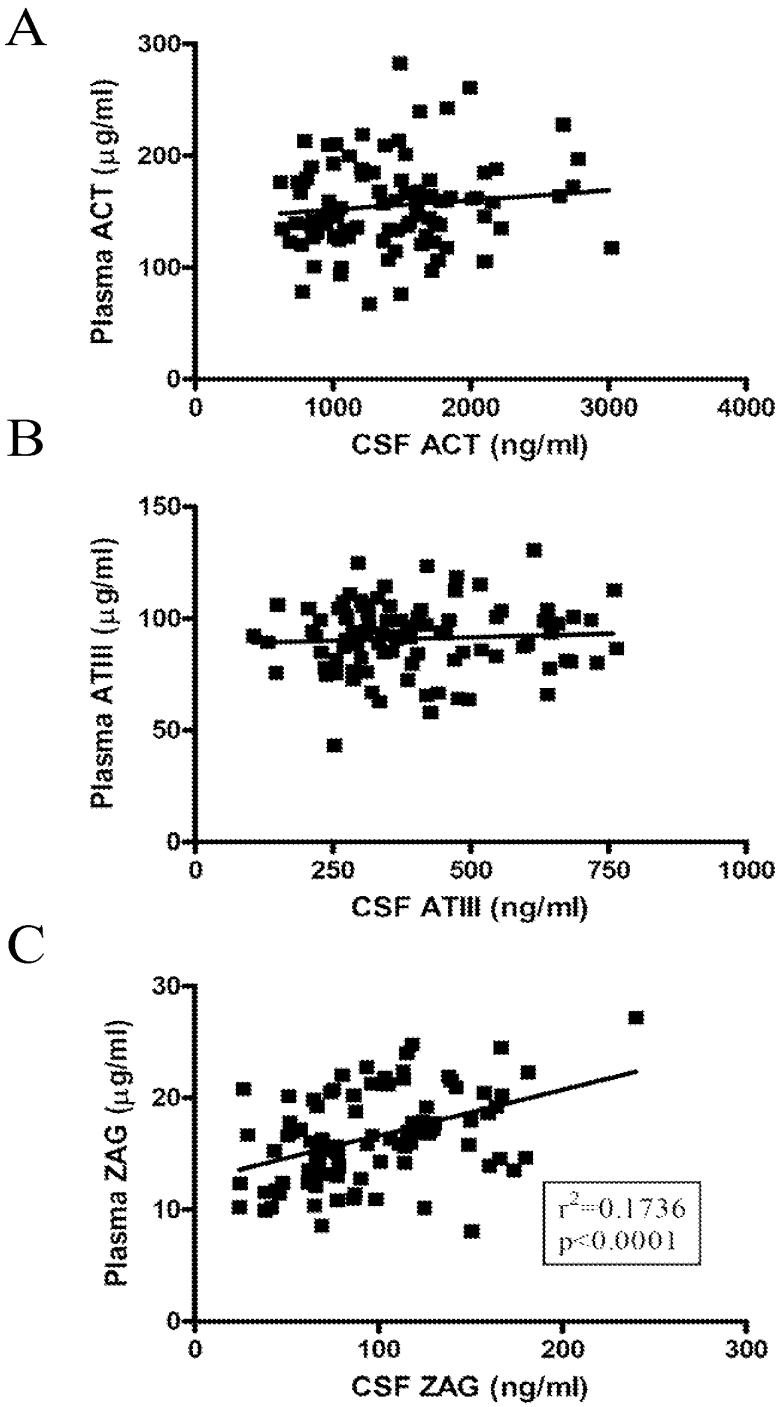

A
Plasma ACT (µg/ml)
300
200
100
0
0
1000
2000
3000
4000
CSF ACT (ng/ml)
B
Plasma ATIII (µg/ml)
150
100
50
0
0
250
500
750
1000
CSF ATIII (ng/ml)
C
Plasma ZAG (µg/ml)
30
20
10
0
0
100
200
300
CSF ZAG (ng/ml)
r²=0.1736
p<0.0001

**Fig. 10**

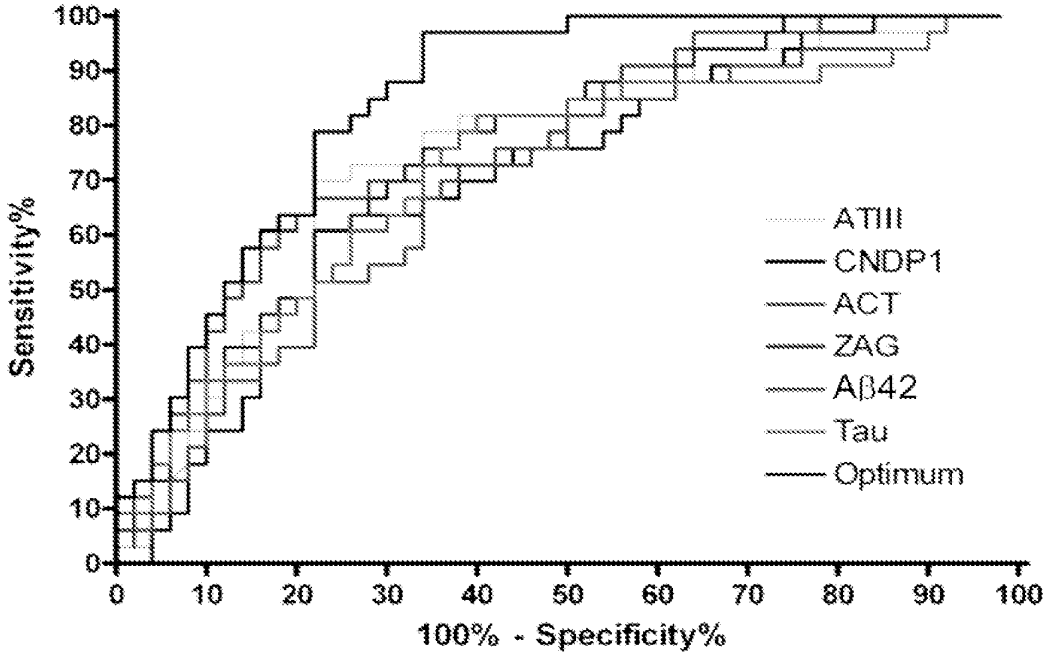

Sensitivity%
100
90
80
70
60
50
40
30
20
10
0
0
10
20
30
40
50
60
70
80
90
100
100% - Specificity%
ATIII
CNDP1
ACT
ZAG
Aβ42
Tau
Optimum

**Fig. 11**

(12) INTERNATIONAL APPLICATION PUBLISHED UNDER THE PATENT COOPERATION TREATY (PCT)

(19) World Intellectual Property Organization
International Bureau

(43) International Publication Date
29 November 2007 (29.11.2007)

PCT

(10) International Publication Number
WO 2007/136614 A2

(51) International Patent Classification:
*G01N 33/53* (2006.01)

(21) International Application Number:
PCT/US2007/011594

(22) International Filing Date: 15 May 2007 (15.05.2007)

(25) Filing Language: English

(26) Publication Language: English

(30) Priority Data:
60/801,962 19 May 2006 (19.05.2006) US
60/900,396 9 February 2007 (09.02.2007) US

(71) Applicant *(for all designated States except US)*: **MERCK & CO., INC.** [US/US]; 126 East Lincoln Avenue, Rahway, NJ 07065-0907 (US).

(72) Inventors; and

(75) Inventors/Applicants *(for US only)*: **DEVANARAYAN, Viswanath** [IN/US]; 126 East Lincoln Avenue, Rahway, NJ 07065-0907 (US). **MODUR, Vijay** [US/US]; 126 East Lincoln Avenue, Rahway, NJ 07065-0907 (US). **SEEBURGER, Jeffrey, L.** [US/US]; 126 East Lincoln Avenue, Rahway, NJ 07065-0907 (US). **ROMANO, Gary, J.** [US/US]; 126 East Lincoln Avenue, Rahway, NJ 07065-0907 (US). **SIMON, Adam, J.** [US/US]; 126 East Lincoln Avenue, Rahway, NJ 07065-0907 (US). **TANAKA, Wesley, K.** [US/US]; 126 East Lincoln Avenue, Rahway, NJ 07065-0907 (US). **LATERZA, Omar** [PY/US]; 126 East Lincoln Avenue, Rahway, NJ 07065-0907 (US).

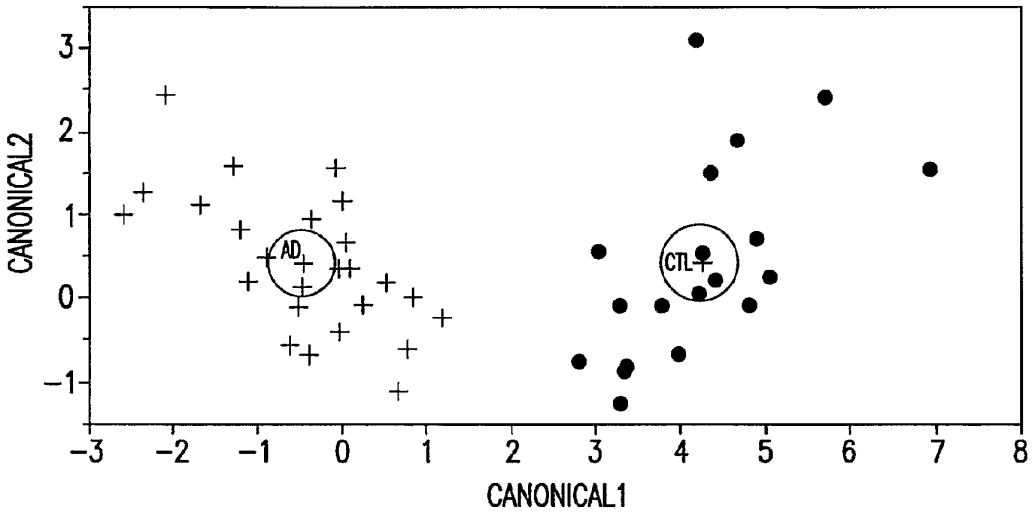
(74) Common Representative: **MERCK & CO., INC.**; 126 East Lincoln Avenue, Rahway, NJ 07065-0907 (US).

(81) Designated States *(unless otherwise indicated, for every kind of national protection available)*: AE, AG, AL, AM, AT, AU, AZ, BA, BB, BG, BH, BR, BW, BY, BZ, CA, CH, CN, CO, CR, CU, CZ, DE, DK, DM, DZ, EC, EE, EG, ES, FI, GB, GD, GE, GH, GM, GT, HN, HR, HU, ID, IL, IN, IS, JP, KE, KG, KM, KN, KP, KR, KZ, LA, LC, LK, LR, LS, LT, LU, LY, MA, MD, ME, MG, MK, MN, MW, MX, MY, MZ, NA, NG, NI, NO, NZ, OM, PG, PH, PL, PT, RO, RS, RU, SC, SD, SE, SG, SK, SL, SM, SV, SY, TJ, TM, TN, TR, TT, TZ, UA, UG, US, UZ, VC, VN, ZA, ZM, ZW.

(84) Designated States *(unless otherwise indicated, for every kind of regional protection available)*: ARIPO (BW, GH, GM, KE, LS, MW, MZ, NA, SD, SL, SZ, TZ, UG, ZM, ZW), Eurasian (AM, AZ, BY, KG, KZ, MD, RU, TJ, TM), European (AT, BE, BG, CH, CY, CZ, DE, DK, EE, ES, FI, FR, GB, GR, HU, IE, IS, IT, LT, LU, LV, MC, MT, NL, PL, PT, RO, SE, SI, SK, TR), OAPI (BF, BJ, CF, CG, CI, CM, GA, GN, GQ, GW, ML, MR, NE, SN, TD, TG).

*[Continued on next page]*

(54) Title: ASSAYS AND METHODS FOR THE DIAGNOSIS AND PROGRESSION OF ALZHEIMER'S DISEASE USING A MULTI-ANALYTE MARKER PANEL




(57) Abstract: The present invention provides a novel and sensitive means of monitoring Alzheimer's disease. The method consists of the construction of statistically relevant multi-analyte panels, through the use of shrunken centroids (SC), simulated annealing algorithm (SAA) and genetic algorithm (GA) within the framework of linear discriminant analysis (LDA) or through the use of random forest (RF) analysis of individual biomarkers, to more accurately and objectively assess the status of an individual for the purposes of disease classification and predicting cognitive endpoints such as MMSE, CAMCOG, or Learning Memory, a subscore of CAMCOG.

WO 2007/136614 A2

**Published:**
— *without international search report and to be republished upon receipt of that report*

*For two-letter codes and other abbreviations, refer to the "Guidance Notes on Codes and Abbreviations" appearing at the beginning of each regular issue of the PCT Gazette.*

TITLE OF THE INVENTION

# ASSAYS AND METHODS FOR THE DIAGNOSIS AND PROGRESSION OF ALZHEIMER'S DISEASE USING A MULTI-ANALYTE MARKER PANEL

## CROSS REFERENCE TO RELATED APPLICATIONS

This application claims the benefit of U.S. Provisional Application No. 60/801,962, filed May 19, 2006 and U.S. Provisional Application No. 60/900,396, filed February 9, 2007, the contents of which are incorporated herein by reference in their entirety.

## FIELD OF THE INVENTION

The present invention relates generally to the diagnosis and prognosis for therapy in the field of Alzheimer's disease. More specifically, it relates to biomarkers that can be used to diagnosis Alzheimer's disease or to determine the efficacy of drugs given to treat Alzheimer's disease.

## BACKGROUND OF THE INVENTION

Alzheimer's disease (AD) is a major neurodegenerative disease of unknown etiology that is characterized by the selective degeneration of basal forebrain cholinergic neurons. The degeneration of these cells leads to a secondary loss of neurons in the limbic system and cortex that control learning and memory. The consequent symptoms of the disease include a progressive loss of memory, the loss of the ability to communicate and the loss of other cognitive functions which occur over a course of approximately eight years. Over the course of this cognitive decline patients often become bedridden and completely unable to care for themselves. Although several symptomatic therapies have been approved to provide some compensation for the cholinergic deficit, for example, Aricept® (donepezil HCl, Eisai Co., Ltd. and Pfizer Inc.), the clinical effects of these are modest and none are able to significantly alter the course of the disease. Improving upon strategies for the treatment of AD has become a focus for the medical and scientific communities due to increases in the average age of the world population, the consequent increase in incidence and prevalence of age-related disorders such as AD, and the severe socioeconomic impact associated with supporting such cognitively impaired patients over the long term.

Requisite to improving the treatment of AD is improving the ability of clinicians to accurately diagnose the disease early in its course and to accurately monitor the progression of



Fujirebio Diagnostics, Inc. v. Quanterix Corp.
EX-1045
5862

the disease. Currently, a diagnosis of possible or probable AD is typically made based on clinical symptoms. A definitive diagnosis of AD can only be made post-mortem and requires a pathological examination of the affected brain tissue. The key pathological hallmarks of the disease are plaques consisting of deposited amyloid beta (Aβ) protein and tangles consisting of degenerated neuronal cells and their cytoskeletal elements (neurofibrillary tangles). There are currently no tests that, in and among themselves, have been validated to identify AD and differentiate it from other diseases affecting cognition. Compared to the pathological diagnosis, the pre-mortem clinical diagnosis can achieve an accuracy of approximately 80% to 90% at the very best of centers. However, this level of diagnostic accuracy more commonly occurs at well-experienced AD centers and for patients who have been manifesting clinical symptoms for several years (Rasmusson, D. X., et al., Alzheimer Dis. Assoc. Disord., 10(4): 180-188 (1996); Frank, R.A. et al., Proceedings of the Biological Markers Working Group: NIA Initiative on Neuroimaging in Alzheimer's Disease, Neurobiol. Ageing, 24: 521-536 (2003)). Following the clinical diagnosis, the progression of the disease is typically monitored through cognitive testing and assessment of everyday function. The course is often variable across patients and may be influenced by both organic and environmental elements.

The last decade has seen an increase in efforts to identify and validate AD-related biomarkers that might increase the sensitivity and specificity of diagnosis and provide a convenient and objective measure of disease progression (Regan Research Institute and National Institute of Ageing (NIA) Consensus Report of the Working Group on: 'Molecular and Biochemical Markers of Alzheimer's Disease,' Neurobiol. Ageing, 19(2): 109-116 (1998); Frank et al., 2003). Among the techniques that currently hold promise in this regard is the biochemical analysis of cerebrospinal fluid (CSF). The value of CSF analysis is based on the fact that the composition of this fluid may reflect brain biochemistry due to its direct contact with brain tissue.

The CSF proteins that have received the most attention are those thought to reflect key features of the disease pathogenesis, including Aβ deposition and neuronal degeneration. Studies have demonstrated reduced levels of the Aβ42 peptide in the CSF of clinically diagnosed AD patients compared to controls (Andreasen, N., et al., Arch. Neurol., 58: 373-379 (2001); NIA Consensus Report, 1998; Frank et al, 2003, Andreasen, N., et al., Clin. Neurol. Neurosurg. 107: 165-173 (2005)). Aβ42 is a cleavage product of the amyloid precursor protein (APP) and is thought to be a major constituent of the senile plaque. One theory of disease progression is that reduced CSF levels in AD patients may be due to increased deposition of the peptide in the brain.



Fujirebio Diagnostics, Inc. v. Quanterix Corp.
EX-1045
5863

In contrast, many studies have shown that the expression of the Aβ40 peptide, another APP cleavage product that is also a plaque component, may be similar in clinically diagnosed AD and control CSF (Frank et al, 2003).

The Tau protein is another CSF protein that has been studied for disease etiology. Tau is an axonal protein that, when hyperphosphorylated, assembles into the paired helical filaments that form neurofibrillary tangles. Whereas the presence of Tau in the CSF is thought to be a general reflection of axonal (i.e., neuronal) degeneration in the brain, the presence of phosphorylated Tau (p-Tau) may be a more specific indicator of AD-related pathology. CSF levels of both Tau and p-Tau in clinically diagnosed AD patients have been shown in many studies to be elevated compared to that in controls (Andreasen, 2001; and for review Consensus Report, 1998; Frank et al, 2003 and Andreasen, 2005).

A recent review article describes not only the status of biochemical biomarkers but also imaging biomarkers and their use in longitudinal clinical trials (Thal, L. J., et al., Alzheimer Dis. Assoc. Disord., 20(1): 6-15 (2006)).

SUMMARY OF THE INVENTION

The present invention relates to a method for classifying disease states in Alzheimer's disease comprising: (a) selecting a statistically relevant multi-analyte panel from human ante- mortem and healthy control fluid samples in which a plurality of biomarkers are differentially expressed to form a reference AD and control multi-analyte panel; (b) conducting a linear discriminate analysis on the multi-analyte data from step (a); (c) obtaining a test fluid sample from a patient; (d) conducting immunoassays on the test sample for the minimal number of analytes needed to specify the panel of step (a); (e) applying the results of step (d) to the linear discriminate analysis of step (b) to obtain an output; and (f) determining from the output of step (e) the classification of the disease state, where the output is either AD or control. In this method the multi-analyte panel is a plurality of biomarkers selected from the group consisting of Aβ40, Aβ42, Tau, pTau, sAPPα, sAPPβ, Aβx-42, Aβx-40, BACE activity, AF, Calcitonin, FABP, IFNγ, SCF, MCP-1, TBG and VEGF. In preferred embodiments of the invention, the multi-analyte panel is selected from the group consisting of (a) Aβ42, sAPPβ and BACE (b) Aβ40, Tau and pTau; (c) Aβ42, pTau and BACE; (d) Aβx-42, Tau and pTau; (e) Aβx-42, Tau, pTau, BACE; (f) Aβx-42, Tau7, pTau; and (g) Aβ42, sAPPβ.

In another embodiment, the invention relates to a method for predicting cognition scores for Alzheimer's disease ("AD") patients comprising: (a) selecting a statistically relevant



Fujirebio Diagnostics, Inc. v. Quanterix Corp.
EX-1045
5864

multi-analyte panel from human ante- mortem and healthy control fluid samples in which a plurality of biomarkers are differentially expressed to form a reference AD and control multi-analyte panel; (b) conducting a random forest analysis on the multi-analyte data from step (a); (c) obtaining a test fluid sample from a patient; (d) conducting immunoassays on the test sample for the minimal number of analytes needed to specify the panel of step (a); (e) applying the results of step (d) to the random forest analysis of step (b) to obtain an output; and (f) determining from the output of step (e) the cognition score, where the output is the assignment of the cognition score. In this method the predicted cognition score is selected from the group consisting of MMSE, Learning Memory and Total CAMCOG. In this method the multi-analyte panel is a plurality of biomarkers selected from the group consisting of Aβ40, Aβ42, Tau, pTau, sAPPα, sAPPβ, Aβx-42, Aβx-40, BACE activity, AF, Calcitonin, FABP, IFNγ, SCF, MCP-1, TBG and VEGF. In a preferred embodiment of the invention, the multi-analyte panel is selected from the group consisting of (a) Aβ42, sAPPβ and BACE (b) β40, Tau and pTau; (c) Aβ42, pTau and BACE; (d) Aβx-42, Tau and pTau; (e) Aβx-42, Tau, pTau, BACE; (f) Aβx-42, Tau7, pTau; and (g) Aβ42, sAPPβ.

BRIEF DESCRIPTION OF THE DRAWINGS

Figures 1A and 1B show the group means and confidence intervals for the expression of various analytes. Figure 1A shows Aβ42 (log-transformed), Figure 1B shows sAPPα (log-transformed), Figure 1C shows sAPPβ (log-transformed) and Figure 1D shows CSF BACE activity (log-transformed) in AD patients versus control subjects. Expression in AD patients is significantly lower than in control subjects in each case, while BACE activity in AD patients is significantly lower than in control subjects after adjusting for the baseline age difference in the ANOVA.

Figure 2 shows show a graphical output from a linear discriminant analysis (LDA) ("•", control; "+", definite AD) for the Expanded 9 marker panel. LDA analysis measures the distance from each point in the data set to each group's multivariate mean and classifies the point to the closest group. The distance measure used is the Mahalanobis distance, which takes into account the variance and covariance between the variables. Each multivariate mean is a labeled circle. The size of the circle corresponds to a 95% confidence limit for the mean. Groups that are significantly different tend to have non-intersecting circles. The markers considered in this analysis include Aβ42, Aβ40, Tau, pTau, sAPPα, and sAPPβ.



Fujirebio Diagnostics, Inc. v. Quanterix Corp.
EX-1045
5865

Figures 3A-3J show a graphical output from a random forest (RF) analysis for an Expanded 9 marker panel for MMSE. In Figure 3A the importance of the marker is scored and ranked with respect to its relative contribution to the prediction of cognition score. Aβ42 appears to be the most important predictor followed by Tau and pTau. In Figures 3B-3J the relative contribution of each marker is plotted after taking into account all of the other markers in the model. The partial residuals, plotted as the vertical axis of these graphs, can be considered as proportional to the MMSE scores and, thus, the plots provide an indication of the nature of contribution of each marker to the prediction of MMSE scores. The small vertical lines on the horizontal axis represent regions of particular importance as these are regions that are rich in data.

Figures 4A-4C show the group means and confidence intervals for the expression of various analytes. Figure 4A shows Fatty Acid Binding Protein ("FABP") (log-transformed), Figure 4B shows Stem Cell Factor ("SCF") (log-transformed) and Figure 4C shows Throxine Binding Globulin ("TBG") (log-transformed) in AD patients versus control subjects.

Figures 5A and 5B are canonical plots that provide a two-dimensional representation of the linear discriminant analysis (LDA) for an optimal 3-analyte panel (Figure 5A) and an optimal 6-analyte panel (Figure 5B). LDA measures the distance from each point in the data set to each group's multivariate mean (called a *centroid*) and classifies the point to the closest group. The distance measure used is the Mahalanobis distance which takes into account the variances and covariances between the variables. In this figure, each multivariate mean is a labeled circle. The size of the circle corresponds to a 95% confidence limit for the mean. As shown in these figures, separation of AD and control subjects is evident using these panels.

Figure 6 is a list of the 90 markers comprising the RBM panel. Among these markers, 27 markers (noted by an asterisk *) were measurable in fewer than five control and five AD subjects. Only markers from this panel that were measurable in at least five control and five AD subjects (63 markers) were used in all data analyses.

Figures 7A and 7B show the computer output from the R statistical software package. Figure 7A shows the software result indicating the sensitivity, specificity and overall classification accuracy of the composite three marker panel (Calcitonin, Fatty Acid Binding Protein, VEGF) as carried out with the SC algorithm (Table 4). Representative results from these computation runs are shown in Tables 3 and 4. Figure 7B shows the software result classifying ten unknown subjects as either AD or control based on their CSF measurements for the three marker panel of Figure 7A.



Fujirebio Diagnostics, Inc. v. Quanterix Corp.
EX-1045
5866

## DETAILED DESCRIPTION OF THE INVENTION

### Definitions

As used herein, the term "analyte" or "marker" or "biomarker" refers to one of the member proteins or protein states comprising the composite or multi-analyte panel, for example, Aβ42 or phosphorylated Tau at amino acid Threonine 181.

As used herein, the term "covariate" refers to variables such as the baseline age and sample storage time that are used as additional independent variables in the univariate analysis of variance (ANOVA).

As used herein, the term "composite" or "multi-analyte panel" or "multivariate panel" refers to any combination of two or more analytes or markers.

As used herein, the term "sensitivity" refers to the ability of an individual marker or a composite of markers to correctly identify patients with the disease, i.e. Alzheimer's disease, which is the probability that the test is positive for a patient with the disease. The current clinical criterion for patients who are deemed as probable for having AD is about 85% sensitive when compared to autopsy confirmed cases.

As used herein, the term "specificity" refers to the ability of an individual marker or a composite of markers to correctly identify patients that do not have the disease, that is, the probability that the test is negative for a patient without disease. The current clinical criterion is about 75% specific.

As used herein, the term "accuracy" or "overall classification accuracy" refers to the computed ability of an individual marker or a composite marker panel to correctly identify Both AD and control cases.

As used herein, the term "percent concordance (%C)" reflects the degree of agreement between the predicted results and their corresponding observed results. This metric is useful for assessing the accuracy of predicting quantitative endpoints such as the cognition scores.

As used herein, the term "prediction" or "prediction of cognitive scores" or "cognitive prediction" or "cognition prediction" refers to the translation or estimation of a cognitive score on a suitable scale from a set biochemical markers in a multi-analyte panel, that is, to assign an equivalent cognitive score based on where they fit within the statistically relevant multi-analyte panel. This can be done for MMSE based on a scale of 0 to 30, for CAMCOG based on a scale of 0 to 107 and for Learning Memory based on a scale of 0 to 17.



Fujirebio Diagnostics, Inc. v. Quanterix Corp.
EX-1045
5867

As used herein, the term "root mean squared error (RMSE)" is an estimate of the standard deviation of the predicted minus the observed results. Similar to percent concordance, it provides an alternative way to characterize the accuracy of the predictions of quantitative endpoints such as the cognition scores.

As used herein, the term "statistically relevant multi-analyte panel" refers to a multi-analyte panel that has been shown to meet an acceptable level of performance by those of ordinary skill in the art. For example, the 1998 National Institute of Ageing (NIA) criteria for classifying Alzheimer's disease from normal comprises sensitivity of greater than 85% and specificity of greater than 75%.

As used herein, the term "optimal multi-analyte panel" refers to a multi-analyte panel that represents the best subset of markers for that size panel using a specified algorithm.

As used herein, the term "Core 6" or "Core 6 marker panel" means the biomarker panel consisting of CSF Aβ40, Aβ2, pTau-181, tTau, sAPPα, and sAPPβ as defined in the examples.

As used herein, the term "Expanded 9" or "Expanded 9 marker panel" means the biomarker panel consisting of the Core 6 marker panel defined above (CSF Aβ40, Aβ42, pTau-181, tTau, sAPPα, and sAPPβ) plus the addition of CSF BACE activity, Aβx-40, Aβx-42 as defined in the examples.

As used herein, the term "RBM antigen panel" or "RBM panel" refers to the collection of markers, biomarkers or analytes comprising the proprietary human Multi-Analyte Profile (MAP®) (Figure 6) from Rules-Based Medicine, Inc., Austin, TX. MAPs, based on Luminex's xMAP bead based technology, consist of at least three pools of beads representing 90 antigens. While the total panel comprises 90 biomarkers, only 63 of these markers were measurable in at least five control and five AD subjects. Thus, in some instances only the 63 measurable markers were used in the data analysis. As a conservative approach the lowest calibrator concentration of the respective marker was used as the value for samples that fell below the lowest calibrator concentration in the standard curve. Designed originally for human plasma analysis of 100 µL samples, the Human MAP® has been analytically validated according to NACLES criteria and successfully used on human CSF when using 200 µL samples in manual mode and 250 µL samples in automated mode.

As used herein, the term "monitoring Alzheimer's disease" means both the ability to classify a subject as AD or control as well as the ability to predict the cognitive status of the individual, including MMSE, LM, and total CAMCOG.



Fujirebio Diagnostics, Inc. v. Quanterix Corp.
EX-1045
5868

As used herein, the term "classifying the disease state" means that a subject is classified as either having the Alzheimer's disease or as being normal.

As used herein, the term "tau" or "total tau" or "tTau" refer to the total Tau protein in a given sample or assay, regardless of phosphorylation state.

As used herein, the term "pTau" refers to the subset of Tau proteins which contain a phosphorylation site at a specified amino acid within the protein, in particular for the assays used herein, at amino acid position 181.

As used herein, the term "MMSE" refers to the Mini-Mental State Examination used in the cognitive assessment community.

As used herein, the term "total CAMCOG" or "CAMCOG" refers to the cognitive and self-contained part of the Cambridge Examination for Mental Disorders of the Elderly used in the cognitive assessment community.

As used herein, the term "Learning Memory" or "LM" refers to the Learning Memory component of the CAMCOG assessment.

As used herein, the term "CERAD" refers to the Consortium to Establish a Registry for Alzheimer's Disease used in the neuropathological community.

As used herein, the term "CSF" refers to cerebrospinal fluid.

The present invention provides a novel and sensitive means of monitoring Alzheimer's disease. The method comprises the construction of statistically relevant multi-analyte panels, through the use of linear discriminant analysis (LDA) or random forest (RF) analysis, of individual biomarkers to more accurately and objectively assess the status of an individual for the purposes of disease classification and predicting cognitive endpoints, such as MMSE, CAMCOG, or Learning Memory, a subscore of CAMCOG.

The National Institute of Aging (NIA) consensus white paper on AD biomarkers (Regan Research Institute and NIA Consensus Report of the working group on 'Molecular and Biochemical Markers of Alzheimer's Disease,' reported at Neurobiology of Aging, 19(2): 109-116 (1998)(hereinafter "1998 NIA Consensus") outlines several non-limiting uses of Alzheimer biomarkers. In particular, biomarkers of AD, either in the form of individual markers or multi-analyte panels can be used for multiple purposes: (1) to aid in the classification or diagnosis of the disease state of an individual to complement traditional clinical diagnosis with an objective measurement; (2) for epidemiological screening to select an enriched population or to characterize the prevalence of disease or demographics of any given epidemiological study; (3) for predictive testing or prognostic purposes of indicating who is susceptible to further



Fujirebio Diagnostics, Inc. v. Quanterix Corp.
EX-1045
5869

neurodegenerative and cognitive decline; (4) for studying brain-behavior relationships; and (5) for monitoring disease progression or response to treatment in clinical trials and clinical practice. In practice the latter purpose has two separate aspects, including, (A) to determine whether a treatment induces a measurable biochemical change and (B) to determine whether treatment changes the progression of the illness, using the biomarker or multi-analyte panel as an index of disease status or state. The 1998 NIA Consensus also stated that a proposed biomarker or multi-analyte panels should include as many of the features of an ideal marker, including: (1) be able to detect a fundamental feature of AD neuropathology; (2) be validated in neuropathologically confirmed AD cases; (3) be precise (ability to detect AD early in its course and distinguish it from other dementias); (4) be reliable; (5) be non-invasive; (6) be simple to perform; and lastly (7) be inexpensive. It has been acknowledged and remains the case that no known biomarker for Alzheimer's meets the 1998 NIA criteria indicated.

The 1998 NIA panel fully recognized the utility of multiple markers, when they specifically highlighted that, "[a] combination of markers may provide greater diagnostic accuracy than any single one individually. Critical evaluation of multiple simultaneous biomarkers should utilize the same principles outlined above, including sensitivity, specificity, prior probability, positive predictive value, and negative predictive value. Of these, high sensitivity and specificity are most important as they indicate the accuracy of the test."

With this guidance, the aim of the present invention was on those multi-analyte panels that meet the 1998 NIA panel criteria for sensitivity and specificity (sensitivity>85%, specificity>75%) and which were previously unknown to the AD biomarker community.

The literature describes other multi-analyte type analyses that have been conducted. For example, WO 2004/104597, "Method for Prediction, Diagnosis, and Differential Diagnosis of AD" describes methods of predicting disease status via an x/y ratio of Aβ peptides. WO 2005/047484, "Biomarkers for Alzheimer's Disease" describes a series of markers that can be used for the assessment of disease state and other scientifically interesting avenues. WO 2005/052592, "Methods and compositions for diagnosis, stratification, and monitoring of Alzheimer's disease and other neurological disorders in body fluids" teaches methods and markers gleaned from plasma for the monitoring of Alzheimer's disease.

Multi-analyte literature articles also include the measurement of 13 biological markers in CSF of Patients with AD and other Dementias (Blasko *et al.*, Dement Geriatr Cogn Disord. 21: 9-15, (2006). Carrette O, *et al.*, "A panel of cerebrospinal fluid potential biomarkers



Fujirebio Diagnostics, Inc. v. Quanterix Corp.
EX-1045
5870

for the diagnosis of Alzheimer's disease," Proteomics 3(8):1486-94 (2003), discusses use of CSF for potential biomarkers.

Sample Summary

Table 1A summarizes the key demographics of the cohort considered in Applicants' analysis. AD subjects are characterized according to the CERAD criteria and post-mortem confirmed. MMSE scores were obtained at the time of CSF sample collection.

Table 1A

| | | Control (n=29) | AD (n=27) |
|---|---|---|---|
| Age | Mean ± SD | 69.3 ± 13.6 | 76.2 ± 7.8 |
| | Range | 35.9 to 94.3 | 56.7 to 87.9 |
| Gender | Male | 18 | 10 |
| | Female | 11 | 17 |
| ApoE-e4 | homozygote (4/4) | 1 | 6 |
| | heterozygote (2/4, 3/4) | (2, 6) | (1, 15) |
| | Other (2/3, 3/3) | (4, 16) | (0, 5) |
| MMSE | Mean | 28.9 ± 1.4 | 9.4 ± 6.4 |
| | Range | 25 to 30 | 0 to 23 |

Table 1B shows the number of AD and control subjects by age: under 73 years of age (<73) and those individuals who are over 73 years of age (>73). Since this provided a roughly even split of the data (n = 26 in age<73 group, and n =30 in age > 30 group), the age groups were used as a baseline factor to reduce confounding in the comparison of AD and Control groups (ANOVA) for each marker.

Table 1B

| Age < 73 | | Age > 73 | |
|---|---|---|---|
| CTL | AD | CTL | AD |
| n=19 | n=7 | n=10 | n=20 |



Fujirebio Diagnostics, Inc. v. Quanterix Corp.
EX-1045
5871

Table 1C lists the number of subjects for whom Applicants obtained measurable data for the biomarkers in the Expanded 9 marker panel. Data from all subjects were available for the first six markers, Aβ42, Aβ40, tTau, pTau, sAPPα, and sAPPβ. Due to limited CSF sample volume, data from some of the subjects were not available for Aβx-42, Aβx-40 and BACE Activity.

Table 1C

| | Number of Subjects | | |
|---|---|---|---|
| | AD | CTL | Total |
| Aβ42, Aβ40, tTau, pTau, sAPPα, sAPPβ | 27 | 29 | 56 |
| Aβx-42 | 26 | 23 | 49 |
| Aβx-40 | 25 | 19 | 44 |
| BACE Activity | 26 | 26 | 52 |

Table 1D lists the number of subjects for whom Applicants obtained measurable data for the eight markers that were statistically significant ($p<0.05$) from the RBM panel. All of these markers except Calcitonin were measurable in all subjects. Calcitonin was not measurable for some subjects due to values falling below the lowest calibration concentration in the standard curve. As a conservative approach, the lowest calibrator concentration was used to impute the values for such samples. Only those markers from the RBM panel that were measurable in at least 5 AD and at least 5 CTL subjects were used in the data analyses. Sixty three (63) markers from the RBM panel met these criteria.

Table 1D

| | Number of Subjects | | |
|---|---|---|---|
| | AD | CTL | Total |
| AFP, FABP, IFN-γ, MCP-1, SCF, TBG, VEGF | 27 | 29 | 56 |
| Calcitonin | 25 | 14 | 39 |

Univariate Marker Analysis for the Expanded 9 marker panel

Table 2 provides the descriptive univariate statistics for individual markers and the ratio of expression of each marker between AD and control (CTL) with respect to both observed (raw) data and the least squares (LS) means from ANOVA. The ratios with respect to



Fujirebio Diagnostics, Inc. v. Quanterix Corp.
EX-1045
5872

LS means derived from the ANOVA is generally considered to be a more accurate reflection of the effect as it takes into account the imbalance in the data and the effect of age as well. The p-values from the ANOVA are also provided, in addition to the False Discovery Rate q-values.

Covariates such as Age and Storage Time (ST) were included in the univariate analysis of variance (ANOVA) for each marker if the p-values corresponding to these covariates were less than 0.1. For each of the markers above, the fold change from AD to control using the raw data and from the least squares (LS) means from the ANOVA are reported, along with their respective false positive rate (FPR) represented by the p-value and their false discovery rate (FDR) represented by the q-value.

The 55% lower Aβ42 values obtained from the univariate analysis was consistent with many published studies to date literature. See, for example, Galasko *et al.*, Arch. Neurol. (1998); Motter *et al.*, Ann. Neurol., 38: 643-648 (1995); Tamaoka *et al.*, J. Neurol. Sci., 148: 41-45 (1997); Scheuner *et al.*, Nat. Med., 2: 864-870 (1996).

Similarly, consistent with the literature (Arai *et al.*, Alz. Res., 3: 211-213 (1997); Trojanowski *et al.*, Alzh. Dis. Review, 1: 77-83 (1996)), our observation was that both total Tau and pTau-181 are elevated in AD compared to control. See, for example, Kahle *et al.*, Neurology, 54: 1498(2000)). t-Tau levels are known to change with age, so age adjustment is required when t-Tau levels are diagnostically employed.

pTau generally has been measured at three different sites, Threonine 231, Serine 199, Threonine 181. Several studies indicate pTau levels may provide an early indicator useful for differential diagnosis.

A number of studies have shown that CSF Aβ40 levels are similar in AD and controls (Mecocci *et al.*, J. Neuroimmunol., 57:165-170 (1995); Tamoaka *et al.*, J. Neurol Sci., 148: 41-45 (1997)). Jensen *et al.*, Ann. Neurol., 45: 504-511 (1999), published a study in which a decrease in CSF Aβ40 was found with significant overlap between the groups, similar to our own results.

sAPP (including both sAPP□ and sAPP□) has been studied in the CSF of AD subjects by Olsson *et al.* (Experimental Neurology 183: 74-80 (2003), Table 2) where they saw no significant differences in either fragment.

Aβx-40 and Aβx-42 have been studied in the context of plaques immuno-reactivity and correlation to cognitive decline by Parvathy *et al.* (Arch. Neurol. 58: 2025-32 (2001)).



Fujirebio Diagnostics, Inc. v. Quanterix Corp.
EX-1045
5873

CSF BACE activity was originally published by Holsinger *et al.*, Ann. Neurol., 55: 898 (2004), and more recently followed up by Verheijen *et al.*, Clin. Chem., 52: E-published April 13, 2006.



Fujirebio Diagnostics, Inc. v. Quanterix Corp.
EX-1045
5874

Table 2. Univariate Marker Analysis for the Expanded 9 marker panel plus the RBM panel

| Markers | Covariates in ANOVA | AD/CTL (raw means) | AD/CTL (LS Means) | FPR (p-value) | FDR (q-value) |
|---|---|---|---|---|---|
| Aβ40 | Age | 0.66 | 0.63 | <0.0001 | <0.0001 |
| Aβ42 | None | 0.46 | 0.45 | <0.0001 | <0.0001 |
| Tau | None | 2.40 | 2.38 | <0.0001 | <0.0001 |
| pTau | Age | 1.76 | 1.63 | <0.0001 | <0.0001 |
| sAPPα | Age & ST | 0.77 | 0.79 | 0.0682 | 0.1994 |
| sAPPβ | Age & ST | 0.72 | 0.74 | 0.0155 | 0.0819 |
| BACE | Age | 0.92 | 0.84 | 0.0383 | 0.1364 |
| Aβx42 | None | 0.47 | 0.49 | <0.0001 | <0.0001 |
| Aβx40 | Age & ST | 0.70 | 0.78 | 0.0112 | 0.0710 |
| AFP | Age | 1.19 | 1.16 | 0.0158 | 0.0819 |
| Calcitonin | Age | 2.43 | 3.17 | 0.0012 | 0.0102 |
| FABP | Age | 1.57 | 1.57 | 0.0097 | 0.0692 |
| IFNγ | Age & ST | 0.87 | 0.72 | 0.0236 | 0.1036 |
| MCP-1 | None | 1.14 | 1.17 | 0.0312 | 0.1187 |
| SCF | Age | 0.92 | 0.83 | 0.0264 | 0.1077 |
| TBG | None | 1.38 | 1.33 | 0.0203 | 0.0965 |
| VEGF | Age | 0.83 | 0.77 | 0.0001 | 0.0011 |

Among the markers in the Expanded 9 marker panel, all except sAPPα were statistically significant at less than 5% false positive rate (FPR), i.e., at $p<0.05$. The effect of sAPPα was marginally significant with $p=0.0682$. Among these markers, Aβ40, Aβ42, Tau, pTau, and Aβx42 had the most robust effect at less than 5% false discovery rate (FDR), i.e., $q<0.05$. In addition, sAPPβ and Aβx40 had a robust effect at less than 10% false discovery rate ($q<0.1$).

Among the 63 measurable analytes in the RBM human MAP that were analyzed Alpha Fetoprotein (AFP) (16% elevated), Calcitonin (217% elevated), Fatty Acid Binding Protein (FABP) (57% elevated), Interferon–gamma (IFNγ (28% reduced), Monocyte Chemotactic Protein-1 (MCP-1) (17% elevated), Stem Cell Factor (SCF) (17% reduced), Thyroxine Binding Globulin (TBG) (33% elevated), and Vascular Endothelial Growth Factor



Fujirebio Diagnostics, Inc. v. Quanterix Corp.
EX-1045
5875

(VEGF) (23% reduced) percentages relative to control are significant with a false positive rate $p<0.05$. Among these, Calcitonin and VEGF have the most robust effect at less than 5% false discovery rate (FDR), i.e., $q<0.05$. In addition, AFP, FABP and TBG had a robust effect at less than 10% false discovery rate ($q<0.1$).

AFP is the major fetal plasma protein. The concentration of AFP peaks in the fetal bloodstream at 2-3 g/l around 12-14 weeks of gestation and then falls. AFP passes into the maternal bloodstream where it may be detected by assay. Fetal malformations such as neural tube defects seen in Down's syndrome elevate the maternal serum levels. Elevated AFP is seen most frequently in adults with germ cell tumours and hepatocellular carcinoma, but also in gastric, colon, biliary, pancreatic and lung cancers (~20% of patients). Swiss-Prot Accession Number: P02771.

Calcitonin is secreted by the parafollicular C-cells of the thyroid gland. Its primary physiological effect is to lower serum calcium levels. Elevated levels of calcitonin (>100 pg/mL) may be encountered in a variety of pathological conditions including leukemias and myeloproliferative disorders. The most notable condition expressing elevated calcitonin levels is medullary thyroid carcinoma (MTC). Swiss-Prot Accession Number: P01258.

FABP is typically a plasma marker of acute myocardial infarction (AMI). The plasma kinetics of FABP closely resemble those of myoglobin in that elevated plasma concentrations are found within 2 hours after AMI and return to normal generally within 18 to 24 hours. The concentration of FABP in skeletal muscle is 20 times lower than in cardiac tissue (for myoglobin the same content for cardiac and skeletal tissue). This makes FABP a useful biochemical marker for the early assessment or exclusion of AMI. FABP also appears to be a useful plasma marker for the estimation of cardiovascular risk. Swiss-Prot Accession Number: P05413.

IFNγ is secreted from T cells (cytotoxic and Th1) and Natural Killer cells. Its major functions are to activate macrophages and to increase the expression of class II MHC on APC. IFNγ stimulated macrophages are more phagocytic, they are more capable of killing intracellular pathogens and they have increased ability to present antigen. IFNγ secreted by Th1 cells has a cross regulatory role in controlling Th2 function, and will induce a class switch to IgG. It actually can inhibit the activities of the Th2 pathway by inducing IL-12 production by macrophages. This cytokine has a role in many different types of immune responses such as delayed type hypersensitivity, inflammation, antibody production and viral infection. Swiss-Prot Accession Number: P01579.



Fujirebio Diagnostics, Inc. v. Quanterix Corp.
EX-1045
5876

MCP-1 plays a role in the recruitment of monocytes to sites of injury and infection. MPC-1 has been found in the joints of people with rheumatoid arthritis where it may serve to recruit macrophages and perpetuate the inflammation in the joints. MPC-1 has also been found elevated in the urine of people with lupus as a sign warning of inflammation of the kidney. MCP-1 has also been called small inducible cytokine A2 (SCYA2) and monocyte chemotactic and activating factor (MCAF). Swiss-Prot Accession Number: P13500.

SCF is a stromal cell-derived cytokine synthesized by fibroblasts and other cell types. It is a glycoprotein that plays a key role in hematopoiesis acting both as a positive and negative regulator, often in synergy with other cytokines. It also plays a key role in mast cell development, gametogenesis, and melanogenesis. Swiss-Prot Accession Number: P21583.

TBG levels are particularly useful for cases in which total thyroid hormone levels do not correlate with the thyro-metabolic status, such as with pregnancy, the use of contraceptive steroids, or in patients with hereditary excesses or deficiencies of TBG. Swiss-Prot Accession Number: P05543

VEGF is important in the pathophysiology of neuronal and other tumors, probably functioning as a potent promoter of angiogenesis. It may be involved also in altering blood-brain-barrier functions under normal and pathological conditions. VEGF secreted from the stromal cells may be responsible for the endothelial cell proliferation in capillary hemangioblastomas which are composed of abundant microvasculature and primitive angiogenic elements represented by stromal cells. Swiss-Prot Accession Number: P15692.

Multi-analyte panels and models for the Expanded 9 markers

The present invention is focused on the determination and use of composite or multi-analyte panels for the monitoring of Alzheimer's disease. Unlike the published literature, which is generally focused on Aβ42, pTau, tTau, Applicants have extended the marker panel with six additional analytes and have discovered unexpectedly that some unique and novel composites can reach the level of performance that meet the criteria for sensitivity and specificity recommended by the 1998 NIA panel (sensitivity>85%, specificity>75%)..

In one embodiment of the invention, a composite or multi-analyte panel comprising Aβ42, sAPPβ and BACE is employed to monitor Alzheimer's disease. As shown in the Examples and Table 3, this multi-analyte panel performs quite well in post mortem confirmed AD cases. In preferred embodiments of the invention the multi-analyte panel is selected from the group consisting of (a) Aβ42, sAPPβ and BACE (b) Aβ40, Tau and pTau; (c)



Fujirebio Diagnostics, Inc. v. Quanterix Corp.
EX-1045
5877

Aβ42, pTau and BACE; (d) Aβx-42, Tau and pTau; (e) Aβx-42, Tau, pTau, BACE; (f) Aβx-42, Tau7, pTau; and (g) Aβ42, sAPPβ.

In another embodiment of the invention, the biomarker composites or multi-analyte panels can be used for classification of Alzheimer's disease. In this embodiment, reference samples are collected from at least 25 patients that have been characterized as post mortem confirmed AD and from at least 25 healthy subjects from a similar age group. The samples are then run in a specific multi-analyte panel to generate data. For example, using the Aβ42, sAPPβ and BACE panel each sample is measured in each assay. Those skilled in the art would understand that each assay of the multi-analyte analyte panel needs to undergo fit-for-purpose assay validation, which includes the assessment of key issues such as freeze-thaw stability, dilution linearity, precision, sensitivity, etc. One then builds a statistical model on the composite biomarker using linear discriminant analysis (LDA). This can be performed using a contributed program library within the R language/environment (A Language and Environment for Statistical Computing, R Development Core Team, R Foundation for Statistical Computing, Vienna, Austria, 2005, ISBN 3-900051-07-0, Reference for the contributed programs within R for performing LDA: Venables, W. N. and Ripley, B. D., Modern Applied Statistics with S. Fourth Edition. Springer, New York (2002) ISBN 0-387-95457-0). The LDA is carried out on this reference dataset, thus creating a model on the specific composite in the R environment.

New samples are collected in the clinic from prospective patients that are awaiting diagnosis. These samples are run in the minimal assays necessary for the specific composite. The data generated from the multi-analyte panel are then inputted into the LDA model/algorithm that was built using the reference dataset as described above with the composite in place in the R environment. The output from this process gives a determination of AD or control for the new subjects to aid in the diagnosis. This classification is useful for doctors and caregivers to aid in determining whether a patient is suffering from Alzheimer's disease as compared to other forms of cognitive decline.

In still another embodiment of the invention, the biomarker composites or multi-analyte panels can be used for predicting cognition scores such as MMSE, Total CAMCOG of Learning Memory, a subscore of CAMCOG. In this embodiment, reference samples are collected from at least 25 patients that have been characterized as post mortem AD and from at least 25 healthy subjects from a similar age group. The samples are then run in the specific multi-analyte panel to generate data. As noted above, those skilled in the art would understand that each assay of the multi-analyte analyte panel needs to undergo fit-for-purpose assay



Fujirebio Diagnostics, Inc. v. Quanterix Corp.
EX-1045
5878

validation. To build a statistical model on the composite biomarker, random forest analysis is performed using a contributed program library within the R language/environment as described above. The random forest analysis is carried out on this reference dataset, thus creating a model on the specific composite in the R environment.

New samples are collected in the clinic from prospective patients that are awaiting assessment of their cognitive ability in terms of MMSE, Learning Memory, Total CAMCOG. The samples are run in the minimal assays necessary for the specific composite. The data generated from this multi-analyte panel are then input into the random forest model/algorithm that was built using the reference dataset as described above with the composite in place in the R environment. The output from this process provides an estimate of the cognitive scores of interest: MMSE, Learning Memory, Total CAMCOG. This analysis is useful for doctors and caregivers to aid in determining if someone has a low cognitive score attributable to Alzheimer's disease as compared to other forms of cognitive impairment.

Table 3 provides a selected list of various individual markers and composites from the Expanded 9 marker panel that were considered in the LDA to determine their utility for correctly classifying AD from control. While the invention described herein may comprise composites other than those shown, one skilled in the art would choose analytes such that the composites would have sensitivities greater than 85% and specificities greater than 75% to meet the 1998 NIA criteria for sensitivity and specificity. Preferred composites from those listed in Table 3 are ones meeting the 1998 NIA criteria for sensitivity and specificity.

One skilled in the art would recognize that the addition of a marker to a composite may sometimes have the undesired effect of lowering the sensitivity and/or specificity. For example, the inclusion of sAPPα in the composite of Aβ42, Tau and pTau lowers the specificity from 95% to 90%. Similarly, the inclusion of sAPPβ in the composite of Aβ40, BACE and sAPPα lowers the specificity from 81% to 73%. On the other hand, adding a marker such as Aβ42 to a composite of Tau and pTau may improve the sensitivity and specificity. For example, the inclusion of BACE Activity to the composite of Aβ40 and sAPPα improved the sensitivity from 74% to 83% and specificity from 75 to 81%. It should be noted that data for BACE was not available from four subjects and these subjects were excluded in the analysis for composites that were of special interest for comparing with and without BACE Activity.



Fujirebio Diagnostics, Inc. v. Quanterix Corp.
EX-1045
5879

Table 3

| Analyte or multi-analyte panels | % Accuracy | % Sensitivity | % Specificity |
|---|---|---|---|
| Aβ42 | 91 | 93 | 90 |
| Aβ40 | 74 | 74 | 74 |
| Tau | 75 | 57 | 93 |
| pTau | 74 | 56 | 92 |
| sAPPα | 66 | 66 | 66 |
| sAPPβ | 68 | 69 | 67 |
| Aβx-42 | 82 | 96 | 66 |
| Aβx-40 | 80 | 86 | 72 |
| BACE | 43 | 51 | 35 |
| Tau, pTau | 75 | 35 | 75 |
| Aβ42, Tau | 94 | 96 | 92 |
| Aβ42, pTau | 96 | 100 | 93 |
| Aβ42, Tau, pTau | 97 | 100 | 95 |
| Aβ42, Tau, pTau, sAPPα | 95 | 100 | 90 |
| Aβ40, Tau, pTau | 95 | 90 | 99 |
| Aβ40, Aβ42, Tau, pTau | 96 | 97 | 96 |
| Aβ42, Tau, pTau* | 99 | 100 | 99 |
| Aβ42, Tau, pTau, BACE | 99 | 100 | 99 |
| Aβ42, pTau, BACE | 98 | 100 | 96 |
| Aβ40, sAPPα * | 75 | 74 | 75 |
| Aβ40, sAPPα, BACE | 82 | 83 | 81 |
| Aβ40, sAPPα, sAPPβ, BACE | 79 | 84 | 73 |
| Aβ40, sAPPβ * | 76 | 75 | 77 |
| Aβ40, sAPPβ, BACE | 81 | 85 | 76 |
| Aβ42, sAPPβ * | 92 | 95 | 90 |
| Aβ42, sAPPβ, BACE | 92 | 96 | 88 |
| Aβx-40, Aβ42, Tau, pTau | 98 | 99 | 97 |
| Aβx-42, Tau, pTau | 96 | 96 | 95 |
| Aβx-42, Aβ42, Tau, pTau | 100 | 100 | 100 |
| Aβx-42, Aβ42, Tau, pTau, BACE | 99 | 99 | 100 |
| Aβx-42, Tau, pTau, BACE | 96 | 94 | 98 |
| Aβx-42, Tau, pTau* | 95 | 96 | 95 |

* excludes 4 subjects with missing BACE activity data



Fujirebio Diagnostics, Inc. v. Quanterix Corp.
EX-1045
5880

Multi-analyte panels and models for the RBM panel

The present invention is focused on the determination and use of composites or multi-analyte panels for the monitoring of Alzheimer's disease. Applicants have further extended the multi-analyte panels or composites based on the Expanded 9 marker panel presented above with the addition of 63 measurable analytes that were measurable from the RBM panel. From the collection of measurable markers, Applicants have discovered unexpectedly that several composites can achieve a level of performance that meet the criteria for sensitivity and specificity recommended by the 1998 NIA panel (sensitivity>85%, specificity>75%).

In various embodiments of the invention, optimal panels of varying sizes have been identified for monitoring Alzheimer's disease. In one embodiment the composite or multi-analyte panel is made up of three analytes/biomarkers, for example, Calcitonin, FABP and VEGF, used to monitor Alzheimer's disease. In other embodiments, composites with additional markers, such as the six marker multi-analyte panel comprising Calcitonin, FABP, MMP-3, Myoglobin, SCFactor and VEGF, provide improved ability to monitor Alzheimer's disease.

Representative optimal panels or composites of varying sizes are shown in Table 4 which can be used for classification of Alzheimer's disease. As is done with the multi-analyte panels for the Expanded 9 markers above, reference samples are collected and analyzed from at least 25 patients that have been characterized as post mortem confirmed AD and from at least 25 healthy subjects from a similar age group. For example, one could select a composite that utilizes Calcitonin, FABP, MMP-3, Myoglobin, SCF and VEGF for a six analyte panel for use with the SAA algorithm and then measure each sample for these anlaytes. As is done with the Expanded 9 marker panels above, one then builds a statistical model for the selected composite analytes using LDA as described above, creating a model of the specific composite in the R environment.

New samples are then collected in the clinic from prospective patients awaiting diagnosis. These samples are run in the minimum number of assays necessary for the specific composite. The data generated from this multi-analyte panel are then inputted into the LDA model/algorithm that was built using the reference dataset. The output from this process gives the determination of AD or control for the new subjects to aid in the diagnosis. This classification is useful for doctors and caregivers to aid in determining whether a patient is suffering from Alzheimer's disease as compared to other forms of cognitive decline.

Multivariate analysis was performed using LDA to examine the collective role of subsets of analytes that distinguish CSF samples from the AD and control subjects. Multi-



Fujirebio Diagnostics, Inc. v. Quanterix Corp.
EX-1045
5881

analyte panels that provide the best predictive performance for each panel size were determined from the collection of measurable analytes in the RBM panel. For each of the panel sizes ranging from three to twelve analytes, optimal multi-analyte panels were determined using the Simulated Annealing Algorithm (SAA) and the Genetic Algorithm (GA) within the framework of the LDA method (Duarte Silva, A.P., Efficient Variable Screening for Multivariate Analysis, J. Multivariate Analysis, 76: 35-62 (2001)). In addition, an optimal panel of three markers from the Shrunken Centroid (SC) method (Tibshirani RJ, Hastie T, Narasimhan B, and G. Chu., Diagnosis of Multiple Cancer Types by Shrunken Centroids of Gene Expression, P.N.A.S.,U.S.A., 99(10): 6567-6572 (2002)) was also derived. These representative optimal multi-analyte panels are listed in Table 4, along with their predictive performance determined from the aggregate of 50 replicates of 10-fold cross-validation.

In a preferred embodiment of the invention, the composite or multi-analyte panel comprises at least three biomarkers and the composite or multi-analyte panel meets the 1998 NIA criteria for sensitivity (>85%) and specificity (>85%). In a more preferred embodiment, the multi-analyte panel comprises three to six biomarkers which meet this criteria and, in an even more preferred embodiment, the multi-analyte panel comprises six biomarkers which meet this criteria. In addition to the composite of three biomarkers derived using the SC method, all composites comprising at least four biomarkers listed in Table 4 meet the 1998 NIA criteria for sensitivity and specificity. The % sensitivity and % specificity metrics reported in this table are within 0.4% standard error. Those skilled in the art would recognize that other composites could be derived that meet the desired criteria and, as such, the invention described herein is not limited to the representative optimal composites listed in Table 4.



Fujirebio Diagnostics, Inc. v. Quanterix Corp.
EX-1045
5882

Table 4: Optimal multi-analyte panels using markers from the RBM panel

| Model | Panel Size | Optimal Panel Search Algorithm | Multi-Analyte Panel | % Accuracy | % Sensitivity | % Specificity |
|---|---|---|---|---|---|---|
| LDA | 3 | SAA | AFP, TNF-RII, VEGF | 84 | 84 | 85 |
| | | GA | AFP, TNF-RII, VEGF | 84 | 84 | 85 |
| | | SC | Calcitonin, FABP, VEGF | 86 | 85 | 87 |
| | 4 | SAA | Calcitonin, FABP, MMP-3, VEGF | 91 | 89 | 92 |
| | | GA | Calcitonin, FABP, MMP-3, VEGF | 91 | 89 | 92 |
| | 5 | SAA | Calcitonin, FABP, IgE, MMP-3, VEGF | 90 | 89 | 91 |
| | | GA | Calcitonin, SHBG, TNF-RII, Thyroid Stimulating Hormone (TSH), VEGF | 86 | 80 | 92 |
| | 6 | SAA | Calcitonin, FABP, MMP-3, Myoglobin, SCF, VEGF | 94 | 93 | 95 |
| | | GA | AFP, MIP-1β, MMP-3, SCF, TNF-RII, VEGF | 88 | 88 | 88 |
| | 7 | SAA | Calcitonin, CD40, IgE, SHBG, TNF-RII, THS, VEGF | 89 | 86 | 92 |
| | | GA | Calcitonin, FABP IgE, MMP-3, Myoglobin, SCF, VEGF | 94 | 93 | 95 |
| | 8 | SAA | Calcitonin, CD40, Creatine Kinase MB (CK-MB), FABP, IgE, SCF TSH, VEGF | 91 | 90 | 91 |
| | | GA | AFP, MIP-1β, Prostatic Acid Phosphatase (PAP), SCF, SHBG, TNF-RII, TSH, VEGF | 88 | 88 | 89 |
| | 9 | SAA | Calcitonin, CD40, FABP, IgE, MMP-3, Myoglobin, SCF, TSH, VEGF | 94 | 91 | 96 |
| | | GA | Calcitonin, FABP, IgE, MMP-3, Myoglobin, PAP, SCF, SGOT, VEGF | 93 | 91 | 93 |
| | 10 | SAA | β-2 Microglobulin (β2M), Calcitonin, FABP, IgE, IL-10, MMP-3, Myoglobin, PAP, SCF, SGOT | 95 | 95 | 96 |
| | | GA | β-2 M, Calcitonin, FABP, IgE, IL-10, MMP-3, Myoglobin, PAP, SCF, SGOT | 95 | 95 | 96 |
| | 11 | manual | β-2 M, Calcitonin, FABP, IgE, IL-10, MMP-3, Myoglobin, PAP, SCF, SGOT, VEGF | 96 | 96 | 96 |
| | 12 | SAA | β-2 M, Calcitonin, FABP, GM.CSF, IgE, IL-16, MMP-3, Myoglobin, PAP, SCF, SGOT, VEGF | 94 | 92 | 96 |

In order to graphically illustrate the performance of these panels, canonical plots from a LDA for an optimal panel for a 3-analyte panel as determined from the Shrunken



Fujirebio Diagnostics, Inc. v. Quanterix Corp.
EX-1045
5883

Centroids (SC) algorithm and an optimal panel for a 6-analyte panel as determined from the Simulated Annealing Algorithm (SAA) are shown in Figures 5A and 5B, respectively. The 3-analyte panel, Calcitonin, FABP and VEGF, provides 86% classification accuracy. The percent accuracy improves to 94% with the addition of MMP-3, Myoglobin and SCF to form the 6-analyte panel.

Those skilled in the art would recognize and understand that the present invention is not limited to either the composites from the Expanded 9 marker panel (Table 3) or the composites from the RBM panel (Table 4), but would also include composites derived using markers from both panels. It is notable that several markers emerged from the multivariate LDA that were not individually statistically significant, but that when combined become important markers in a multi-analyte composites. Examples of analytes that were individually not statistically significant but that emerged as part of an optimal composite include the following:

TNF RII (Tumor Necrosis Factor receptor type 2) is a soluble form of the TNF receptor. Two types of soluble TNF receptors have been identified in human serum and urine that neutralize the biological activities of TNF-α and TNF-β. These binding proteins represent truncated forms of the two types of high-affinity cell surface receptors for TNF (TNFR-p60 Type B and TNFR-p80 Type A). Soluble TNF RI corresponds to TNFR-p60 Type B. Soluble TNF RII corresponds to TNFR-p80 Type A. In the TNF superfamily nomenclature, TNF RI and TNF RII are referred to as TNFRSF1A and TNFRSF1B, respectively. These apparent soluble forms of the receptors appear to arise as a result of shedding of the extracellular domains of the membrane-bound receptors. Swiss-Prot Accession Number: Q92956

MMP-3 (Matrix Metalloproteinase 3), or stromelysin, can degrade numerous extracellular matrix (ECM) substrates, such as collagen. It can also release cell surface molecules such as heparin-binding EGF-like growth factor and TNF-alpha, and it can activate other MMPs, including MMP-9 and collagenases. It can also inactivate several serine proteinase inhibitors. Swiss-Prot Accession Number: P08254

IgE (Immunoglobulin E) levels of circulating IgE in serum are extremely low compared to the other immunoglobulins. Levels at birth are almost non-detectable, but increase with age. IgE has been linked to atopic disease and there is a strong correlation between increased total serum or plasma IgE levels and allergy. The determination of total IgE levels has been found to be useful in the assessment of atopic diseases such as allergic rhinitis, extrinsic asthma, urticaria, and atopic eczema. Patients with pulmonary aspergillosis, parasitic



Fujirebio Diagnostics, Inc. v. Quanterix Corp.
EX-1045
5884

infestations and some immunodeficiencies have also been found to have increased amounts of IgE.

SHBG (Sex Hormone Binding Globulin) is a glycoprotein that binds to sex hormones, specifically testosterone and estradiol. These sex hormones circulate in the bloodstream, bound mostly to SHBG and to some degree bound to albumin. Only a small fraction is unbound, or "free," and thus biologically active and able to enter a cell and activate its receptor. Thus, bioavailability of sex hormones is influenced by the level of SHBG. SHBG levels are controlled by a delicate balance of enhancing and inhibiting factors. Its level is decreased by high levels of insulin and insulin-like growth factor-I (IGF-I). High androgen levels decrease SHBG, while high estrogen and thyroxine levels increase it. Conditions with low SHBG include polycystic ovary syndrome, diabetes, and hypothyroidism. Conditions with high SHBG include pregnancy, hyperthyroidism, and anorexia nervosa. Swiss-Prot Accession Number: P04278.

TSH (Thyroid Stimulating Hormone), or thyrotropin, is a glycoprotein synthesized and secreted by the pituitary gland. It stimulates synthesis and secretion of the thyroid hormones, thyroxine (T4) and triiodothyronine (T3). Secretion of TSH is stimulated by thyrotropin-releasing hormone (TRH), a hypothalamic tripeptide. TSH synthesis and release are regulated via a negative feedback mechanism by the level of thyroid hormones. Increased serum levels of free T4 and T3 depress TSH secretion (hyperthyroidism), while decreased serum levels of free T4 and T3 result in excess TSH secretion (primary hypothyroidism). Serum TSH concentration is inversely proportional to the free T4 (FT4) concentration in a log/linear relationship, making TSH a sensitive marker for monitoring thyroid hormone replacement therapy. Swiss-Prot Accession Number: Alpha P01215; Beta P01222

Myoglobin is a monomeric heme protein that is structurally related to hemoglobin. Very little free myoglobin circulates. It is synthesized and found predominantly in skeletal and cardiac muscle. During the course of a myocardial infarction (MI), myoglobin escapes from the ischemic cardiac muscle and can reach levels 5-10 times normal during the first 5-18 hours. A wide variety of pathological processes damage skeletal muscles, causing release of myoglobin into the circulation. Muscle damage resulting in high levels of myoglobinuria is clinically referred to as rhabdomyolysis. Measurement of myoglobin in rhabdomyolysis may be useful to determine the likelihood of significant renal toxicity. A high serum myoglobin level associated with a low urine myoglobin clearance rate indicates high risk for renal failure. A high serum myoglobin level with high myoglobin clearance rate indicates low risk for renal failure. A



Fujirebio Diagnostics, Inc. v. Quanterix Corp.
EX-1045
5885

relatively low serum myoglobin level indicates minimal risk for renal failure. Swiss-Prot Accession Number: P02144.

MIP-1 β (Macrophage Inflammatory Protein 1 beta) Swiss-Prot Accession Number: P13236. Like, MIP-1 α (Macrophage Inflammatory Protein 1 alpha): the two MIP proteins are the major factors produced by macrophages following their stimulation with bacterial endotoxins. Both proteins are involved in the cell activation of human granulocytes (neutrophils, eosinophils, and basophils) and appear to be involved in acute neutrophilic inflammation. Both forms of MIP-1 stimulate the production of reactive oxygen species in neutrophils and the release of lysosomal enzymes. They also induce the synthesis of other pro-inflammatory cytokines such as IL-1, IL-6 and TNF in fibroblasts and macrophages. Swiss-Prot Accession Number: P10147.

CD40 is a receptor molecule on the cell surface of all mature B cells (B lymphocytes), most B-cell malignancies, and monocytes, dendritic cells (in the nervous system), endothelial cells (within blood vessels), and epithelial cells. CD40 is a member of the tumor necrosis factor superfamily. Together with CD40 ligand, the molecule that binds to it, CD40 is an important contributor to the inflammatory processes that lead to atherosclerosis and thrombosis (clotting). Swiss-Prot Accession Number: Q6P2H9.

CK-MB (Creatine Kinase MB) is released by damaged cardiac tissue 2-6 hours following infarction. CK-MB values peak at 12-24 hours after infarction and return to normal within 24-48 hours. Certain diseases of skeletal muscle result in an increased amount of CK-MB. The various causes of rhabdomyolysis, including the muscular dystrophies, commonly result in an abnormal increase in serum CK-MB activity. Swiss-Prot Accession Number: Brain P12277; Muscle P06732.

PAP (Prostatic Acid Phosphatase) is richly produced in the prostate gland in men. It normally contributes a small amount to the serum concentration. The clinical use of this prostate-specific fraction is in cases of prostatic adenocarcinoma, where it is elevated most commonly in men with metastatic disease (about 60% of the cases). It is a much less sensitive test in men with localized disease (10-40% depending upon clinical grade). PAP will be transiently elevated following prostatic massage, needle biopsy, cystoscopy, and infarction. PAP is not unique to the prostate, but is detected in numerous body tissues. Swiss-Prot Accession Number: P15309.

SGOT Ag (Serum Glutamic Oxaloacetic Transaminase Antigen) is an enzyme that is normally present in liver and heart cells. SGOT is released into blood when the liver or



Fujirebio Diagnostics, Inc. v. Quanterix Corp.
EX-1045
5886

heart is damaged. The blood SGOT levels are thus elevated with liver damage or with an insult to the heart. Some medications can also raise SGOT levels. SGOT is also called aspartate aminotransferase (AST). It is an acute phase reactant suggestive of inflammation. Swiss-Prot Accession Number: P17174.

β-2 M (Beta 2-Microglobulin) is a protein found on the surfaces of all nucleated cells and is shed into the blood, particularly by tumor cells and lymphocytes. Due to its small size, it passes through the glomerular membrane, but normally less than 1% is excreted due to reabsorption in the proximal tubules of the kidney. Therefore, high plasma levels occur in renal failure, inflammation, and neoplasms, especially those associated with B-lymphocytes. Swiss-Prot Accession Number: P01884.

## EXAMPLE 1

Selection of Patients and CSF Samples

OPTIMA (Oxford Project To Investigate Memory and Ageing) is a highly defined longitudinal cohort of community volunteers with interest in the periodic assessment of their memory and cognitive status who have been studied serially since 1988 and includes controls, AD and other dementias. There are over four hundred subjects and over 300 controls that undergo neuropsychological tests, CT and SPECT scans and various biochemical tests on their blood at regular intervals. Cerebrospinal fluid is obtained from a subset of patients who have consented specifically for this procedure. After death, autopsy is performed and the brains are examined by a neuropathologist to define brain pathology. To date, the autopsy rate has been 94%. All of the information and samples of the OPTIMA cohort are stored at the Radcliff Infirmary in Oxford, UK.

In a pilot study, Applicants have analyzed for biomarker expression CSF specimens obtained ante-mortem from 56 subjects: 29 clinical controls and 27 pathologically confirmed amyloid AD. Pathological data was available for all AD patients and for 13 of the control subjects. The remaining control subjects are to date either still living or did not provide consent for postmortem examination. In the AD group, all 27 subjects were considered by neuropathology to have CERAD definite AD. As a preliminary study, samples were arbitrarily chosen based on sample volume available which led to a mismatch in gender between the control and AD groups. Since gender plays a minimal role in the incidence and progression of AD this difference was not considered significant.



Fujirebio Diagnostics, Inc. v. Quanterix Corp.
EX-1045
5887

The demographic characteristics of the pilot population at the time of CSF collection are listed in the Table 1A. The control and confirmed AD groups were similar in age and marital status, but showed differences in gender distribution as described above. The confirmed AD group reported a greater family history of AD and had moderate to severe disease.

## EXAMPLE 2

Aβ40 Expression

Aβ40 was measured in the CSF with a human Aβ 1-40 Colorimetric solid phase sandwich Enzyme Linked Immuno-Sorbent Assay (ELISA) kit (catalogue # KHB3482, BioSource International, Camarillo, CA) following the manufacturer's recommendations. A standard sandwich immunoassay was performed wherein the analyte, Aβ40, was first captured with an antibody specific for the N-terminal half of Aβ and then detected with a second detection antibody specific for the Aβ40 neo-epitope. This sandwich immunoassay can be performed using any suitable antibody pair that measures Aβ40 or its truncated equivalents. The detection antibody consisted of rabbit anti-Aβ40 and a secondary anti-rabbit IgG:horse radish peroxidase (HRP) conjugate. HRP catalyzes the formation of a chromophore, tetramethylbenzidine (TMB), which was quantitatively measured at 450 nm to provide readout of Aβ40 concentration. This procedure was carried out according to the BioSource kit instructions. A blocking buffer was used to minimize non-specific interactions. Standards were used as received in the kit. Determinations of unknowns were made using a four parameter logistic fit to the standards measured in duplicate wells. Quality controls samples (low, mid, and high) were run on all plates to insure valid results consistent with previous measurements.

The results of the Aβ40 analysis in the pilot cohort of control and confirmed AD human CSF samples are summarized in Table 2 and Table 3. One skilled in the art would recognize that there was a clear reduction of Aβ40 in the AD CSF compared to control; this result is consistent with some published findings and inconsistent with others. In this instance Applicants obtained information regarding the amount of Aβ40 processed by β- and γ-secretase from APP and found that there was enhanced APP processing in AD brain compared to normal age match controls.



Fujirebio Diagnostics, Inc. v. Quanterix Corp.
EX-1045
5888

EXAMPLE 3

Aβ42 Expression

Aβ42 was measured with Innotest™ Aβ42 ELISA kit (Innogenetics Inc., Cat. #80040, Ghent, Belgium) following the manufacturer's recommendations with modifications as follows. Similar to the Aβ40 assay above, a standard sandwich immunoassay was performed wherein the analyte, Aβ42, was first captured with an antibody specific for the N-terminal half of Aβ (3D6) and then detected with a second detection antibody (21F12) specific for the Aβ42 neo-epitope. The assay utilized a mouse monoclonal capture antibody specific for the C-terminus of Aβ42. The detection system employed an N-terminal specific biotinylated mouse monoclonal antibody and a secondary conjugate made of horse radish peroxidase (HRP) labeled strepavidin. The HRP was used to convert tetramethyl benzidine to a chromophore which was quantitatively measured at 450 nm to provide readout of AB42 concentration. This sandwich immunoassay can be performed using any suitable antibody pair that measures Aβ42 or its truncated equivalents. A blocking buffer was used to minimize non-specific interactions. After detection of the amount of bound detection antibody with a substrate for a conjugated enzyme to the detection antibody, the amount of analyte was determined against a standard curve generated from a known master stock In an attempt to reduce variability between kit lot numbers, Applicants deviated from the standard manufacturer's protocol by creating a concentrated solution of amino acid analyzed Aβ42 (0.778 mg/mL in DMSO). This was used across different kit lots instead of the standard material supplied by the manufacturer. The range of standards used for sample analysis was 5.45 to 350 pg/mL. Quality controls samples (low, mid, and high) were run on all plates to insure valid results consistent with previous measurements.

The results of the Aβ42 analysis in the pilot cohort of control and confirmed AD human CSF samples are shown in Figure 1A. The data have been log-transformed in order to ensure approximate symmetry in the distribution. One skilled in the art would recognize that there was a clear reduction of Aβ42 in the AD CSF compared to control, a result that is consistent with most of the published findings in the literature. Applicants obtained information regarding the amount of Aβ42 processed by β- and γ-secretase from APP and found that there was enhanced APP processing in the AD brain compared to normal age match controls.



Fujirebio Diagnostics, Inc. v. Quanterix Corp.
EX-1045
5889

EXAMPLE 4

t-Tau Expression

Total Tau (t-Tau) expression was measured with a human Tau (hTAU AG Innotest™ ) ELISA kit (Innogenetics Inc., catalogue number 80226, Ghent, Belgium) following the manufacturer's recommendations. Similar to the Aβ assays in Examples 2 and 3 above, a standard sandwich immunoassay was performed wherein the analyte, total tau protein independent of phoshorylation state, was first captured with a monoclonal antibody specific for all isoforms of Tau and then subsequently bound by two biotinylated tau-specific antibodies. The final detection was performed by peroxidase-labeled streptavidin. This sandwich immunoassay can be performed using any suitable antibody pair that measures all Tau species, including truncated equivalents. A blocking buffer was used to minimize non-specific interactions. After detection of the amount of bound detection antibody with a substrate for a conjugated enzyme to the detection antibody the amount of analyte was determined against a standard curve generated from a known master stock Quality control samples (low, mid, and high) were run on all plates to insure valid results consistent with previous total Tau measurements.

The results of the total Tau analysis in a pilot cohort of control and confirmed AD human CSF samples are summarized in Table 2 and Table 3. There was a clear increase in total Tau protein in the CSF of AD subjects compared to controls, a result that was consistent with most of the published findings in the literature. Applicants obtained information regarding the amount of total Tau protein, information which some have speculated is a marker of the degree of neurodegeneration which is or has occurred in the brain, and found that there was enhanced levels of total Tau protein in the AD brain compared to normal age match controls.

EXAMPLE 5

p-Tau-181 Expression

Phosphorylated Tau-181 (pTau-181) was measured with the Phospho-TAU ($_{181P}$) Innotest™ ELISA kit (Innogenetics Inc., catalogue number 80062, Ghent, Belgium), following the manufacturer's recommendations. Similar to the total Tau assay above, a standard sandwich immunoassay was performed wherein the analyte, tau protein phosporylated at amino acid 181, was first captured with an antibody specific for all isoforms of Tau and then detected with a second detection antibody which specifically detected Tau molecules phosphorylated at threonine 181 (phospho-tau-181). This sandwich immunoassay can be performed using any suitable



Fujirebio Diagnostics, Inc. v. Quanterix Corp.
EX-1045
5890

antibody pair that measures specific phopho-181 Tau species, including truncated equivalents. A blocking buffer was used to minimize non-specific interactions. After detection of the amount of bound detection antibody with a substrate for a conjugated enzyme to the detection antibody the amount of analyte was determined against a standard curve generated from a known master stock Quality controls samples (low, mid, and high) were run on all plates to insure valid results consistent with previous total Tau measurements.

The results of the phosphor-181-Tau analysis in the pilot cohort of control and confirmed AD human CSF samples are summarized in Table 2 and Table 3. There was a clear increase in pT-181 tau protein in the CSF of AD subjects compared to controls, a result that was consistent with most of the published findings in the literature. Applicants obtained information regarding the amount of Tau protein phosphorylated at a specific threonine at position 181, information which some have speculated is a marker of the degree of neurodegeneration which is or has occurred in the AD brain, and found that there was enhanced abundance of pTau-181 protein in the AD brain compared to normal age match controls.

EXAMPLE 6

sAPPα and sAPPβ Expression

When APP is processed by either α-secretase or β-secretase, it is cleaved into two fragments, of which the amino terminal fragment has been called the secreted APPα or β fragment, respectively. These two cleavage products of APP, sAPPα and sAPPβ, were measured with the MSD® sAPPα/sAPPβ Multiplex kit (MesoScale Discovery Cat #N41CB-1, Gaithersburg, MD), following the manufacturer's recommendations. Unlike the previous Examples above, this assay was run in a duplex format whereby two signals were read from a single well of a 96 well plate enabling simultaneous determinations of both sAPPα and sAPPβ. A standard sandwich immunoassay was performed wherein the analyte, either of the sAPPs, was first captured with an antibody specific for the C -terminal region of sAPPα or the sAPPβ C-terminal neo-epitope and then detected with a second detection antibody directed towards an N-terminal region of APP. This sandwich immunoassay can be performed using any suitable antibody pair that measures these analytes specifically, however, Applicants have assessed several antibodies in the literature and found that most have poor immunoreactivity to the naturally occurring isoforms and post-translational modifications of sAPP found in human CSF. A blocking buffer was used to minimize non-specific interactions. After detection of the amount



Fujirebio Diagnostics, Inc. v. Quanterix Corp.
EX-1045
5891

of bound detection antibody using the MSD TPA buffer solution as a substrate for a Ruthinium conjugated enzyme as detection antibody the amount of analyte was determined against a standard curve generated from a known master stock Quality controls samples (low, mid, and high) were run on all plates to insure valid results consistent with previous measurements.

The results of the sAPPα and sAPPβ analysis in the pilot cohort of control and confirmed AD human CSF samples are shown in Figures 1B and 1C, respectively. The data have been log-transformed in order to ensure approximate symmetry in the distribution. Unexpectedly there was a clear reduction of both sAPPα and sAPPβ in the AD CSF compared to controls, a result that Applicants believe has not been found in published findings in the literature. Applicants obtained information regarding the amount of sAPP processed by β- and α-secretase from APP, and found that there was enhanced APP processing in the AD brain compared to normal age match controls.

## EXAMPLE 7

BACE Activity

β-APP Cleaving Enzyme (BACE) (also known as, memapsin or aspartle protease-2 (Asp2)) activity in CSF has been measured using a two-step method. In the first step, cleavage of a biotinylated peptide substrate was accomplished using CSF as the source of BACE enzyme. In the second step, the extent of enzymatic cleavage of substrate was detected using an avidin-biotin complex and enzyme linked immunosorbent assay (ELISA).

In the peptide substrate cleavage step, 25 µl of either purified recombinant baculovirus expressed BACE (amino acid residues 1-460) at a range of concentration from 0.8 pM to 100 pM or human CSF was added to a 96 well assay plate (Costar, Cat#3365, Corning, NY). To each of these wells, 25 µl of reaction buffer containing 50 mM NaOAc, 0.01% BSA, 15 mM EDTA, 0.2% CHAPS ( Pierce, Cat#28300, Rockford, IL), 1 mM Deferoxamine Mesylate (Sigma, Cat# D9533) and 10 µM pepstatin A (Calbiochem, Cat #516481) at pH 4.5 was added. The plate was gently agitated on a shaker for 15 minutes in order to block any non-BACE aspartyl protease activity by pepstatin A. Finally, 100 µl of 200 nM substrate (biotin-KTEEISEVNF-EVEFR, SEQ ID NO.; 1) prepared in reaction buffer with 10 µM pepstatin A was added. The plate was sealed tightly and incubated at 37°C and agitated at 40 rpm for 2.5 hours. The enzymatic reaction was then arrested by adding 50 µl of 1M Tris (pH 8.0).

In the second step, the product of BACE enzymatic cleavage from the above reaction "biotin-KTEEISEVNF" (SEQ ID NO.:2) was measured by ELISA. The above reaction



Fujirebio Diagnostics, Inc. v. Quanterix Corp.
EX-1045
5892

mixture was transferred onto a streptavidin coated black plate (High binding capacity, Pierce, Cat# 15503, Rockford, IL) and incubated overnight at 4°C. The following day, the plate was washed three times with phosphate buffered saline with 0.1% Tween-20 (PBST) at pH 7.4. This was followed by addition of 100 µl of NF C-terminal neo-epitope rabbit polyclonal antibody at 1:30,000 dilution in 0.1% Tween-20 in Superblock PBS (Pierce, Cat#37515, Rockford, IL), and incubated for 1 hour at room temperature. After this incubation the plate was washed three times with PBST. Then 100 µl of Donkey anti-rabbit IgG-HRP or goat anti-rabbit IgG-AP (Bio-Rad, cat# 170-6518) at 1:30,000 dilution in 0.1% Tween 20-superblock was added and incubated for 1 hour at room temperature. The plate was then washed five times with PBST. The reaction was finally developed using 100 µl/well of CDP-Star ready-to-use with HRP substrate (TMB) or Sapphire-II Enhancer substrate (Applied Biosystems, Cat# T2214) for 30 minutes at room temperature. Absorbance or Luminescence counts were measured in LJL-Analyst (Molecular Devices Inc.). The counts from individual CSF samples were converted to BACE concentration using coefficients determined by a quadratic fit to the baculo-BACE standard curve.

The results of the CSF BACE activity analysis in a pilot cohort of control and confirmed AD human CSF samples are shown in Figures 1D. The data have been log-transformed in order to ensure approximate symmetry in the distribution. From the ANOVA on the log transformed BACE data, after adjusting for the baseline age differences by including it as a factor in the model, it was found that there was a meaningful reduction of CSF BACE activity in AD patients compared to controls, which was inconsistent with the literature whereby initial results indicated that BACE activity in the CSF of AD subjects was elevated compared to age matched controls.

## EXAMPLE 8

Aβx-40 and Aβx-42 Expression

Human CSF Aβx-40 and Aβx-42 was measured using a sandwich ELISA consisting of analyte capture with mouse monoclonal antibody 4G8 (epitope Aβ17-24) followed by detection with alkaline phosphatase conjugated neo-epitope antibodies specific for Aβ40 (G210) and Aβ42 (4D7A3), respectively. The 4G8 antibody was purchased from Signet Inc., while G210 was licensed from University of Heidelberg (Heidelberg, Germany) and 4D7A3 was received from Innogenetics Inc. (Ghent, Belgium).



Fujirebio Diagnostics, Inc. v. Quanterix Corp.
EX-1045
5893

The Aβx-40 and Aβx-42 assays consisted of coating black 96 well costar plates (Costar #3365) with capture antibody 4G8 at 2 μg/ml, in carbonate-bicarbonate buffer (Pierce #28382) at pH of about 9.4. After overnight incubation the plates are washed with PBS and then blocked with 0.1% Tween20 in Superblock (Pierce #37515). CSF samples are diluted 1:8 in 0.1% Tween 20-superblock buffer. Pooled human immunodepleted CSF at a 1:8 dilution was used to prepare standard curves with Aβ40 and Aβ42 respectively. 50 μL of standards, QC's and samples, respectively, were added to wells in duplicate followed by 50 μL of detection antibodies G210-AP and 4D7A3-AP at 1:3000 dilution in 0.3%Tween20/Superblock. Isotype control mouse IgG-AP was used at 1:3000 for background subtraction. The plates are incubated overnight at 4°C. The plates are then washed three times with 0.05% PBST and then plates are thoroughly dried. Plates are then washed with Activation buffer (20 mM Tris-HCl, 1 mM MgCl2, pH 9.8) and then dried. 100 μL alkaline phosphatase substrate (Applied Biosystem #T2214) is added all wells and incubated at RT for 30 minutes. Luminescence counts are measured on the LJL Analyst system (Molecular Devices Inc.). All counts are corrected using the mouse isotype control counts. A third order spline fit to the standards on each plate was used to determine the coefficients that were used to calculate of actual Aβ concentrations for the individual samples.

The results of the CSF Aβx-40 and Aβx-42 analysis in the pilot cohort of control and confirmed AD human CSF samples are summarized in Table 2 and Table 3. Consistent with the literature there was a meaningful difference between the AD CSF compared to controls.

## EXAMPLE 9

Multivariate analysis of marker panels -

Expanded 9 markers for the classification AD versus control

The combined ability of the expanded set of nine CSF markers to differentiate AD from control was assessed using Linear Discriminant Analysis (LDA). This analysis measured the distance from each point in the data set to each group's multivariate mean (called a *centroid*) and classified the point to the closest group. The distance measure used was the Mahalanobis distance which takes into account the variances and covariances between the variables. In Figure 2 each multivariate mean is a labeled circle. The size of the circle corresponds to a 95% confidence limit for the mean. Groups that are significantly different tend to have non-intersecting circles.



Fujirebio Diagnostics, Inc. v. Quanterix Corp.
EX-1045
5894

The assessment of relative importance of the biomarkers with respect to their ability to discriminate AD from control subjects was done within the framework of a random forest analysis (Breiman, 2001). In each tree of the forest (i.e., large collection of trees derived from many simulated samples from the original data), data was permuted in one biomarker at a time and predictions on the permuted data from the random forest method were obtained. These were compared to the predictions from the unpermuted data and the loss in accuracy is assessed. A large loss in accuracy, represented as the percent of mean decrease in accuracy ("MeanDecreaseAccuracy"), indicates the relative importance of the corresponding marker.

With respect to LDA, the predictive ability of these markers to separate AD from control for hold-out datasets was investigated using fifty replicates of 10-fold cross validation. This analysis entailed dividing up the data randomly into ten subgroups, using the fitted model from nine of these subgroups to predict the disease classification in the tenth subgroup, repeating this for all ten groups and then averaging the results across all ten repetitions. This analysis was repeated fifty times to generate a reliable estimate of the overall accuracy along with the sensitivity and specificity of the biomarker composites for separating AD from normal, i.e. control, subjects.

These analyses were based on 29 controls and 27 AD subjects. The LDA graph in Figure 2 was generated using JMP software, v5.0.1 from SAS Institute (Cary, NC). All other analyses were performed using R (R: A Language and Environment for Statistical Computing, R Development Core Team, R Foundation for Statistical Computing, Vienna, Austria, 2005, ISBN 3-900051-07-0).

LDA for assessing the performance of the various composites of markers was performed using a contributed library within R (Venables, W. N. and Ripley, B. D., Modern Applied Statistics with S., Fourth Edition, Springer, New York (2002) ISBN 0-387-95457-0). The random forest analysis was performed using a contributed library within R (Andy Liaw and Matthew Wiener, Classification and Regression by Random Forest, R News, 2 (3): 18-22 (2002)). The 10-fold cross-validation for obtaining reliable estimates of the performance metrics of the biomarker composites was performed using a contributed library within R (Andrea Peters and Torsten Hothorn, Improved Predictors, R package version 0.8-3(2004)).

Table 4 lists representative composites of biomarkers from the LDA analysis that met the 1998 NIA criteria on sensitivity and specificity (sensitivity>85%, specificity>75%). For example, the composite of Aβ42, Tau, pTau and BACE activity provide 99.35% overall accuracy, 99.62% sensitivity and 99.08% specificity. One skilled in the art would understand



Fujirebio Diagnostics, Inc. v. Quanterix Corp.
EX-1045
5895

that the addition of a marker to a composite may not improve the performance. For example, inclusion of sAPPβ in the composite of Aβ40, BACE and sAPPα reduced the specificity from 81% to 73%. Conversely, adding a marker to a composite, such as the addition of BACE activity to the composite of Aβ40 and sAPPα, improved the sensitivity from 74% to 83% and specificity from 75 to 81%.

EXAMPLE 10

Multivariate analysis of marker panels –

Expanded 9 markers for cognition prediction (MMSE)

The relationship between CSF markers and the Mini Mental State Exam (MMSE) cognition scores (MMSE) was analyzed using the RF method (Breiman, 2001). This multivariate analysis method entailed an aggregation of results from a forest of decision tree models that were built to ensure maximum prediction accuracy and minimum effect from the correlation (colinearity) between biomarkers. Several (typically 500) bootstrap samples (random samples of the same size as the data set drawn with replacement) were drawn from the original dataset and a decision tree of maximum size was built from each bootstrap dataset resulting in trees with low bias but high imprecision. Only a random subset of a few biomarkers was considered at each tree node for determining the optimal split, helping reduce the effect of correlation/colinearity between the predictor variables. The predictions were obtained from each tree in the forest and then aggregated in the form of a majority vote for a class/event in the classification model (categorical response) or in the form of the average prediction in a regression model (continuous/quantitative response). The high imprecision from a single tree was reduced by aggregating across the large number of trees in the forest. This method of aggregating the results across a forest of several trees, by maintaining high accuracy and minimizing the correlation effect among biomarkers, results in the optimal predictions.

The assessment of relative importance of the biomarkers with respect to their ability to predict the MMSE scores was done within the framework of the RF analysis (Breiman, 2001). In each tree of the forest (i.e., large collection of trees derived from many simulated samples from the original data), data were permuted in one biomarker at a time and predictions on the permuted data from the random forest method were obtained. These were compared to the predictions from the unpermuted data and the increase in the variability of the predictions was assessed. A large increase in the prediction variability, represented as the percent increase in MSE ("%IncMSE"); indicated the relative importance of the corresponding biomarker. Figure



Fujirebio Diagnostics, Inc. v. Quanterix Corp.
EX-1045
5896

3A shows the ranking of the relative importance of the six markers for cognition prediction. Applicants observed that Tau, Aβ42, and pTau were the top three markers for cognition prediction.

The predictive power of the CSF markers from the RF algorithm was assessed using fifty replicates of 10-fold cross validation. Data were divided into ten random parts, each part was used as the hold-out (test) set on which the predictions were obtained from the model fit to the rest of the data and this was repeated for all ten parts. This analysis was replicated fifty times and the prediction errors, such as the root mean squared error (RMSE) and the percent concordance (%C), between the predicted and observed results from the hold-out data were averaged across these repetitions. The composites considered from the nine markers provided RMSE of 7 and %C of 73.6% agreement between the observed and predicted MMSE scores from fifty replicates of 10-fold cross validation as described above.

All of these analyses were carried out using R ( R: A Language and Environment for Statistical Computing, R Development Core Team, R Foundation for Statistical Computing, Vienna, Austria, 2005, ISBN 3-900051-07-0). The random forest analysis was performed using a contributed library within R (Andy Liaw and Matthew Wiener, Classification and Regression by Random Forest, R News 2 (3):18-22 (2002)).

The 10-fold cross-validation for obtaining reliable estimates of the performance metrics of the biomarker composites was performed using a contributed library within R (Improved Predictors, Andrea Peters and Torsten Hothorn, R package version 0.8-3 (2004)).

## EXAMPLE 11

Analysis of samples in the Rules-Based Medicine human Multi-Analyte Profile (MAP)

CSF samples of AD and control were sent to Rules-Based Medicine, Inc. (Austin, TX) for analysis in their proprietary human Multi-Analyte Profile (MAP®) under a fee for service agreement. MAP is a Luminex bead based multi-antigen profile consisting of at least three pools of beads representing some 90 total antigens (Figure 6). Designed originally for human plasma analysis of 100 µL samples, the human MAP has been analytically validated according to NACLES criteria and successfully used on human CSF when using 200 µL samples in manual mode and 250 µL samples in automated mode.

The human CSF samples responded well in the plasma based antigen panel, producing nearly 50 analytes with good measurements in the AD CSF samples. 63 analytes had measurable levels in at least five AD and five control CSF samples.



Fujirebio Diagnostics, Inc. v. Quanterix Corp.
EX-1045
5897

EXAMPLE 12

Univariate analysis of the Expanded 9 plus markers from the RBM panel

The ability of each marker from the Expanded 9 marker panel and the 63 measurable markers as measured from the RBM panel (total of 72 markers) to separate disease from normal (AD versus control) was assessed using analysis of variance (ANOVA) with the disease group as fixed effect. The baseline age group and sample storage time were included as covariates in the ANOVA of each marker if their p-values were less than 0.1. The age groups used in the model was defined by those that are less than and greater than 73 years old at baseline. The analysis was carried out after applying logarithmic transformation (base 10) on the markers to ensure approximate symmetry. The p-values (false positive rate) and q-values (false discovery rates) from this analysis on the 72 markers were determined. False Positive Rate (FPR) or p-value estimates the proportion of false positives among all the proteins that in reality did not change. False discovery rate (FDR) or q-value estimates the proportion of significant changes that are false positives. Analytes from the RBM panel that had $p < 0.05$ are reported in this document, with special reference to those that had a more robust effect at $q < 0.1$. Summary statistics obtained from these analyses for each of the markers included the ratio of AD to control using the observed data and also using the least squares means from the ANOVA after adjusting for baseline age factor and sample storage time (if they were significant at $p<0.1$), the false positive rate (p-value) and the false discovery rate (q value) of the AD versus control comparison. Analysis was carried out using R version 2.4 (R: A Language and Environment for Statistical Computing, R Development Core Team, R Foundation for Statistical Computing, Vienna, Austria, 2005, ISBN 3-900051-07-0). Figures 4A, 4B and 4C were generated using JMP v5.0.1 from the SAS Institute (Cary, NC). The false discovery rate (q values) for each marker was derived using the method proposed by Benjamini & Hockberg (Benjamini & Hockberg, The adaptive control of the false discovery rate in multiple hypotheses testing with independent statistics, *J. Behav. Educ. Statist.* 25: 60–83 (2000)) and determined using a contributed library within R (Strimmer, Estimation and Control of (Local) False Discovery Rates, fdrtool package, version 1, August 8, 2006).

As shown in Table 2 all markers in the Expanded 9 panel significantly differ between AD and control ($p<0.05$) with the exception of sAPPα that is marginally significant ($p=0.0682$). Aβ40, Aβ42, Tau, pTau and Aβx42 have the most robust effect at less than 5%



Fujirebio Diagnostics, Inc. v. Quanterix Corp.
EX-1045
5898

false discovery rate (FDR), i.e., $q<0.05$. In addition, sAPPβ and Aβx40 have a robust effect at less than 10% false discovery rate ($q<0.1$).

Among the measurable markers from the RBM panel, eight markers were statistically significant at $p < 0.05$. These include Alpha Fetoprotein (AF), Calcitonin, Fatty Acid Binding Protein (FABP), Interferon gamma (IFN□, Monocyte Chemotactic Protein-1 (MCP-1), Stem Cell Factor (SCF), Thyroxine Binding Globulin (TBG), and Vascular Endothelial Growth Factor (VEGF). Among these markers, Calcitonin and VEGF have the most robust effect at less than 5% false discovery rate (FDR), i.e., $q<0.05$. In addition, AF, FABP and TBG had a robust effect at less than 10% false discovery rate ($q<0.1$).

EXAMPLE 13

Multivariate results using RBM panel for classifying AD versus control using LDA

Multi-analyte panels that provide the best predictive performance were determined from the collection of measurable analytes in the RBM panel. For each of the panel sizes ranging from three to twelve markers representative optimal multi-analyte panels were determined using the Simulated Annealing Algorithm (SAA) and the Genetic Algorithm (GA) within the framework of the LDA method (Duarte Silva, A.P., Efficient Variable Screening for Multivariate Analysis, Journal of Multivariate Analysis, 76: 35-62 (2001)). In addition, an optimal panel comprising three markers sing the Shrunken Centroid (SC) method (Tibshirani, R.J., Hastie, T., Narasimhan, B. and Chu, G., Diagnosis of Multiple Cancer Types by Shrunken Centroids of Gene Expression. P.N.A.S., USA, 99(10):6567-6572 (2002)) was also derived.

Representative optimal multi-analyte panels are shown in Table 4 along with their predictive performance determined from the aggregate of fifty replicates of 10-fold cross-validation. This analysis entailed dividing up the data randomly into ten subgroups, using the fitted model from nine of these subgroups to predict the disease classification in the tenth subgroup, repeating this for all ten groups and averaging the results across all repetitions. This analysis was repeated fifty times to generate a reliable estimate and standard error of the overall accuracy along with the sensitivity and specificity of the biomarker composites for separating AD from control, i.e. normal subjects.

In addition to the three-marker composite derived from the SC method, all multi-analyte composites of four markers or greater, shown in Table 4, that were derived using the SAA and the GA algorithms met the 1998 NIA criteria for sensitivity and specificity



Fujirebio Diagnostics, Inc. v. Quanterix Corp.
EX-1045
5899

(sensitivity>85%, specificity>75%). The percent sensitivity and percent specificity metrics reported in this table are within 0.4% standard error.

In order to graphically illustrate the performance of these panels, canonical plots for an optimal three-analyte panel determined from the SC method and an optimal six-analyte panel determined from the SAA method are shown in Figures 5A and 5B. The three-analyte panel, Calcitonin, FABP and VEGF, provides 86% classification accuracy. This classification accuracy improves to 96% with the addition of MMP-3, Myoglobin and SCF to form the six-analyte panel.

These analyses were based on 29 controls and 27 AD subjects. The LDA graphs in Figures 5A and 5B was generated using JMP software, v5.0.1 from SAS Institute (Cary, NC). All data analyses were performed using R (R: A Language and Environment for Statistical Computing, R Development Core Team, R Foundation for Statistical Computing, Vienna, Austria, 2005, ISBN 3-900051-07-0).

The linear discriminant analysis for assessing the performance of the various composites of markers was performed using a contributed library within R (Venables, W. N. and Ripley, B. D., Modern Applied Statistics with S., Fourth Edition. Springer, New York (2002) ISBN 0-387-95457-0). The SC method was implemented using a contributed library within R (Hastie, Tibshirani, Narasimhan, Chu, PAM: Prediction Analysis of Microarrays, PAMr package, version 1.25, March 31, 2006). The Simulated Annealing Algorithm was implemented using a contributed library within R (Cerdeira, Duarte-Silva, Cadima and Minhoto, Selecting Variable Subsets, The subselect Package, version 0.9-99, (June 8, 2006)). The 10-fold cross-validation for obtaining reliable estimates of the performance metrics of the biomarker composites was performed using a contributed library within R (Improved Predictors, Andrea Peters and Torsten Hothorn, R package version 0.8-3 (2004)).



Fujirebio Diagnostics, Inc. v. Quanterix Corp.
EX-1045
5900

WHAT IS CLAIMED:

1. A method for classifying disease states in Alzheimer's disease ("AD") comprising:

a. selecting a statistically relevant multi-analyte panel from human ante-mortem and healthy control fluid samples in which a plurality of biomarkers are differentially expressed to form a reference AD and control multi-analyte panel;

b. conducting a linear discriminate analysis on the multi-analyte data from step (a);

c. obtaining a test fluid sample from a patient;

d. conducting immunoassays on the test sample for the minimal number of analytes needed to specify the panel of step (a);

e. applying the results of step (d) to the linear discriminate analysis of step (b) to obtain an output; and

f. determining from the output of step (e) the classification of the disease state, where the output is either AD or control.

2. The method of claim 1 wherein the multi-analyte panel comprises a plurality of at least three biomarkers selected from the group consisting of Aβ40, Aβ42, Tau, pTau, sAPPα, sAPPβ, Aβx-42, Aβx-40, BACE activity, AF, Calcitonin, FABP, IFNγ, SCF, MCP-1, TBG and VEGF.

3. The method of claim 2 wherein the multi-analyte panel results in a composite having >85% sensitivity and >75% specificity.

4. The method of claim 3 wherein the multi-analyte panel comprises an optimal panel as set forth in Table 5.

5. A method for predicting cognition scores for Alzheimer's disease ("AD") patients comprising:

a. selecting a statistically relevant multi-analyte panel from human ante-mortem and healthy control fluid samples in which a plurality of biomarkers are differentially expressed to form a reference AD and control multi-analyte panel;



Fujirebio Diagnostics, Inc. v. Quanterix Corp.
EX-1045
5901

b. conducting a random forest analysis on the multi-analyte data from step (a);

c. obtaining a test fluid sample from a patient;

d. conducting immunoassays on the test sample for the minimal number of analytes needed to specify the panel of step (a);

e. applying the results of step (d) to the random forest analysis of step (b) to obtain an output; and

f. determining from the output of step (e), where the output is the assignment of the cognition score.

6. The method of claim 5 wherein the predicted cognition score is selected from the group consisting of MMSE, Learning Memory and Total CAMCOG.

7. The method of claim 6 wherein the multi-analyte panel comprises a plurality of at least three biomarkers selected from the group consisting of Aβ40, Aβ42, Tau, pTau, sAPPα, sAPPβ, Aβx-42, Aβx-40, BACE activity, AF, Calcitonin, FABP, IFNγ, SCF, MCP-1, TBG and VEGF.

8. The method of claim 7 wherein the multi-analyte panel results in a composite having >85% sensitivity and >75% specificity.

9. The method of claim 8 wherein the multi-analyte panel comprises an optimal panel as set forth in Table 5.



Fujirebio Diagnostics, Inc. v. Quanterix Corp.
EX-1045
5902

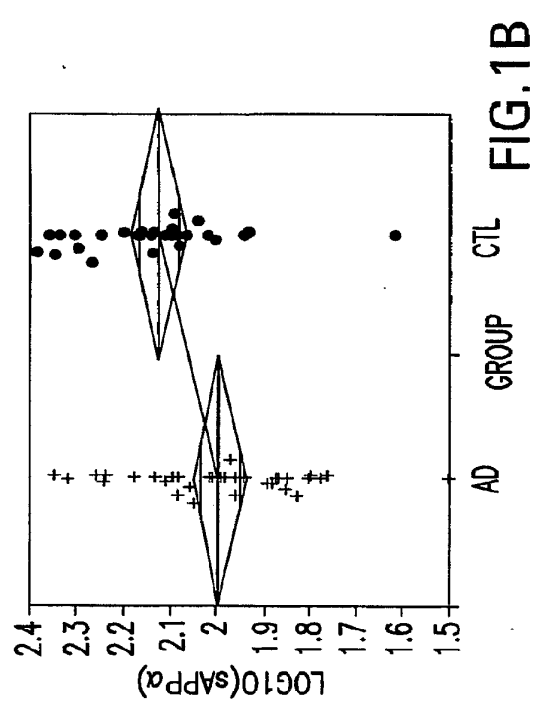



FIG. 1B

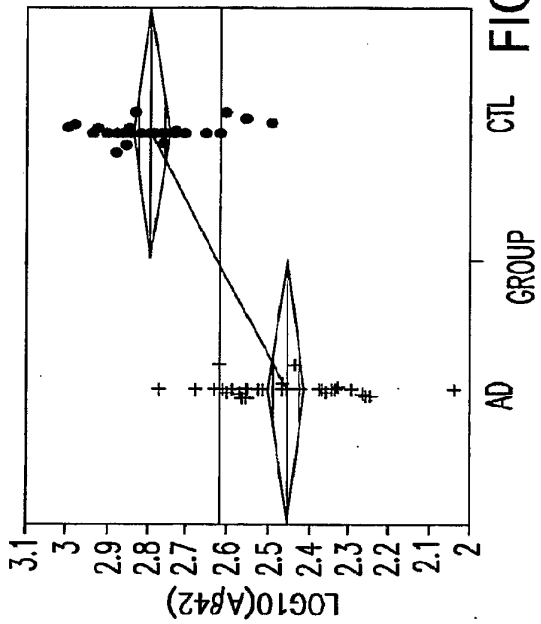



FIG. 1A

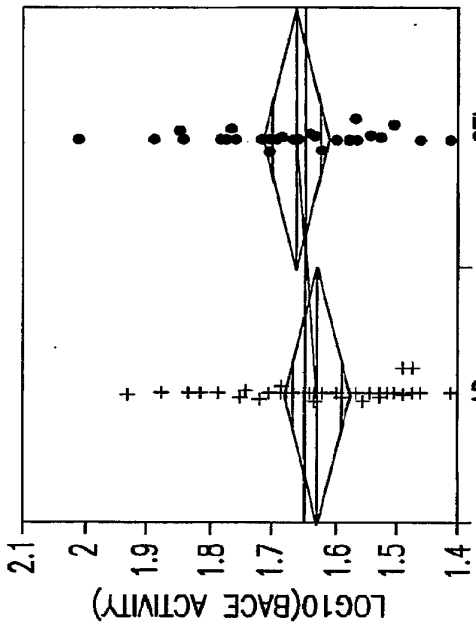



FIG. 1D

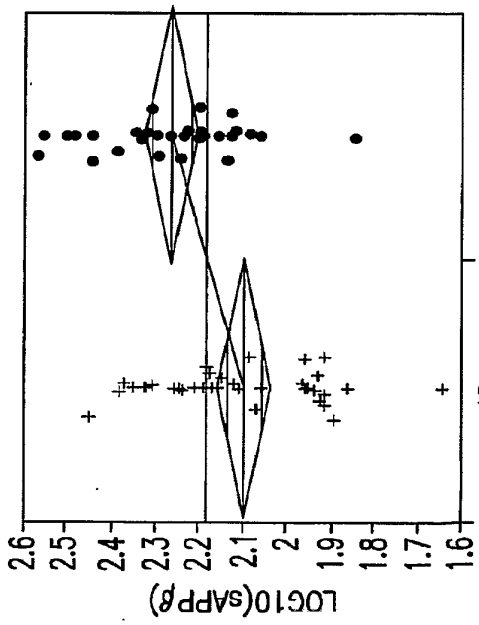



FIG. 1C

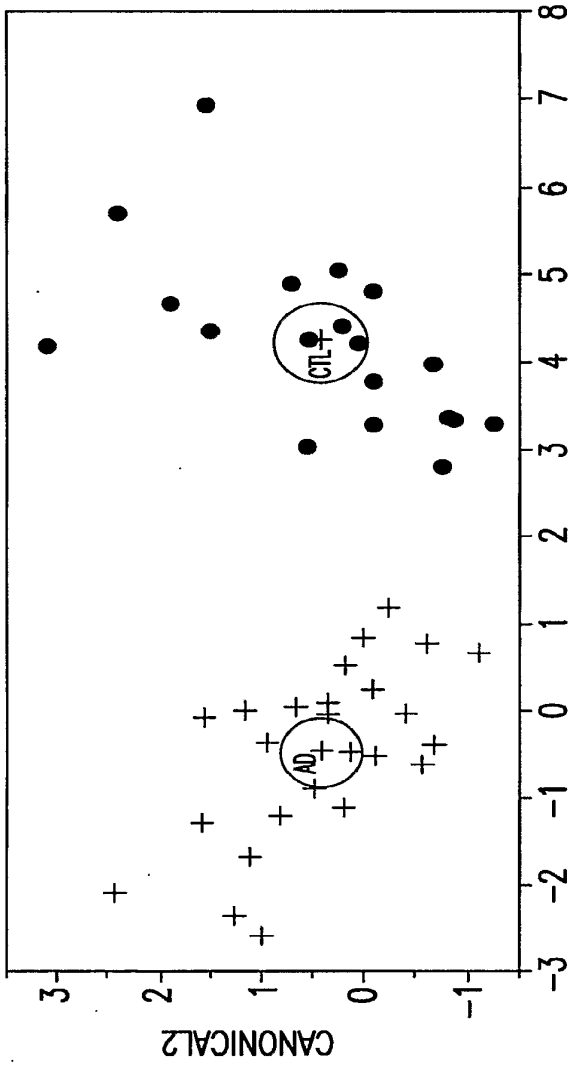



FIG.2

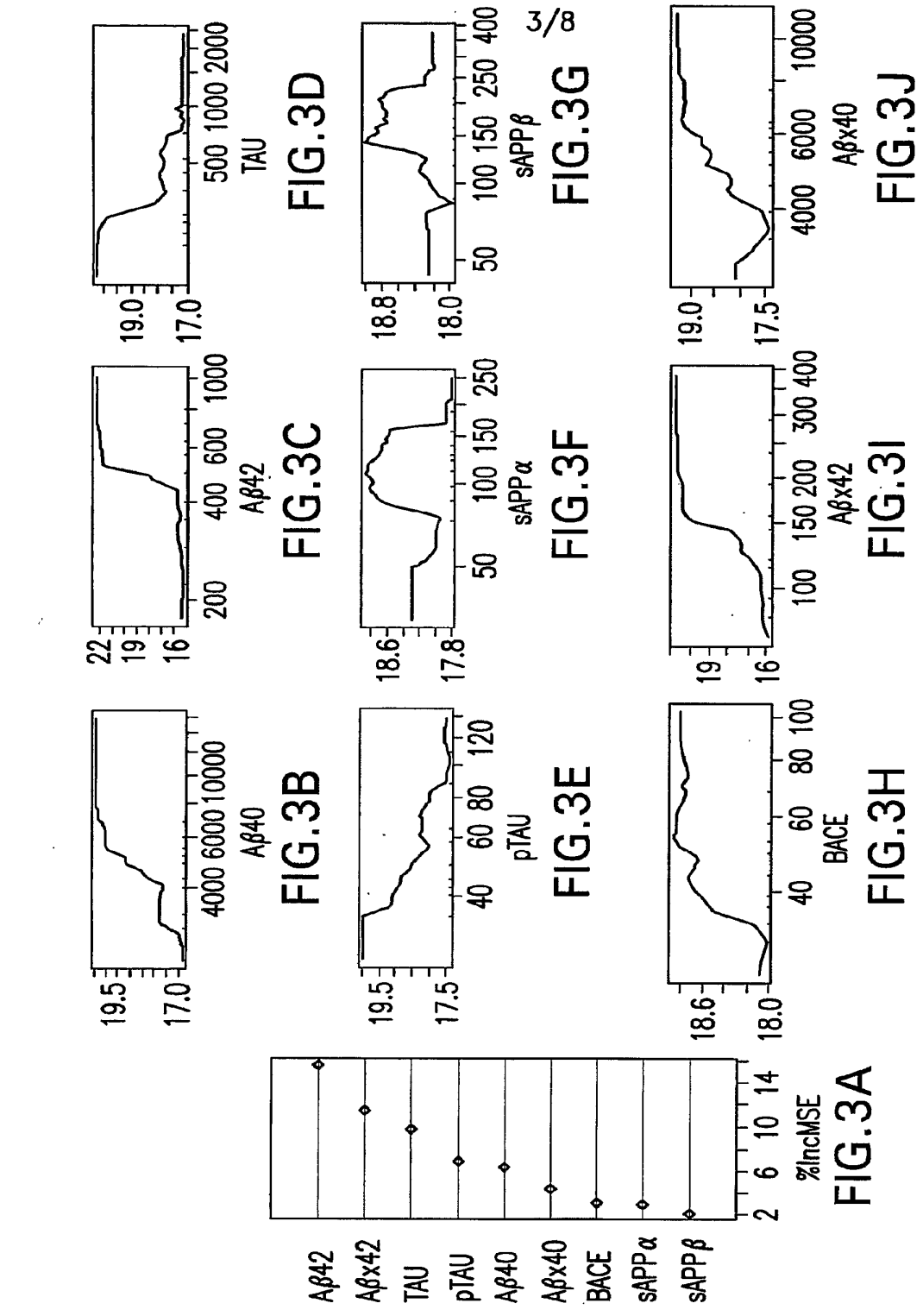



FIG.3A FIG.3B FIG.3C FIG.3D FIG.3E FIG.3F FIG.3G FIG.3H FIG.3I FIG.3J



Fujirebio Diagnostics, Inc. v. Quanterix Corp.
EX-1045
5905

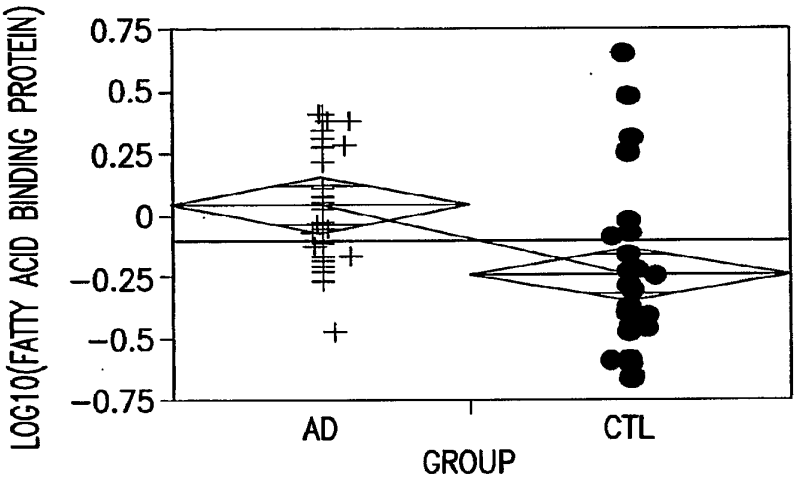



FIG.4A

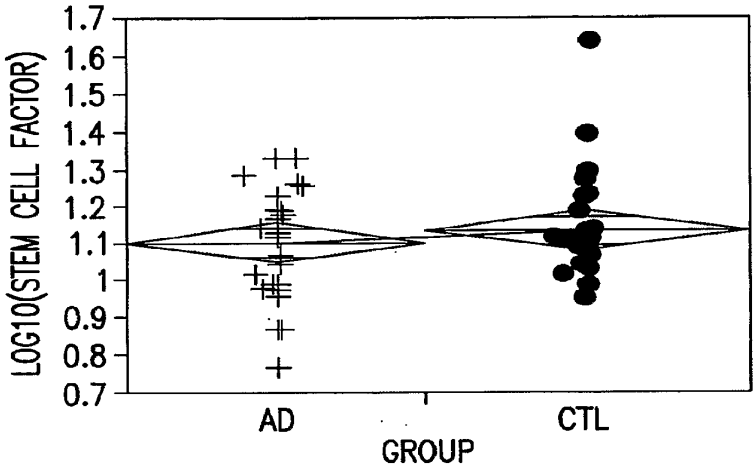



FIG.4B

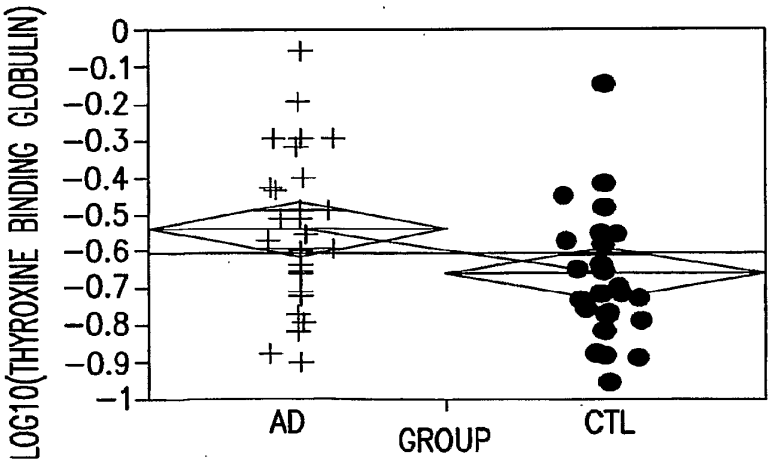



FIG.4C

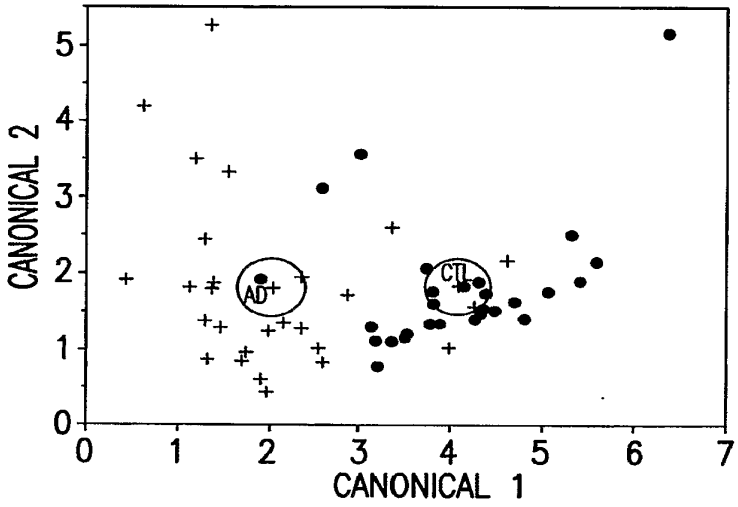

CANONICAL 2
CANONICAL 1
AD
CTL
0
1
2
3
4
5
6
7

FIG.5A

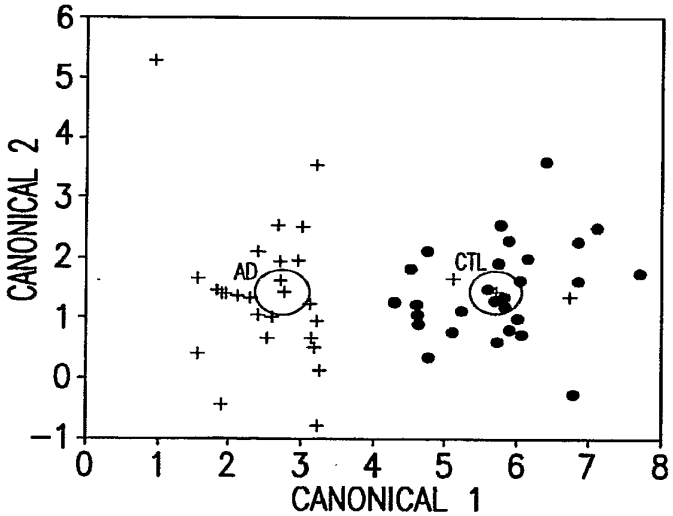

CANONICAL 2
CANONICAL 1
AD
CTL
−1
0
1
2
3
4
5
6
7
8

FIG.5B

| | RBM PANEL OF 90 MARKERS |
|---|---|
| 1 | ALPHA-1 ANTITRYPSIN |
| 2 | ADIPONECTIN |
| 3 | ALPHA-2 MACROGLOBULIN |
| 4 | ALPHA-FETOPROTEIN |
| 5 | APOLIPOPROTEIN A1 |
| 6 | APOLIPOPROTEIN CIII |
| 7 | APOLIPOPROTEIN H |
| 8 | BETA-2 MICROGLOBULIN |
| 9* | BRAIN-DERIVED NEUTROPHIC FACTOR |
| 10 | COMPLEMENT 3 |
| 11* | CANCER ANTIGEN 125 |
| 12* | CANCER ANTIGEN 19-9 |
| 13 | CALCITONIN |
| 14 | CD40 |
| 15 | CD40 LIGAND |
| 16* | CARCINOEMBRYONIC ANTIGEN |
| 17 | CREATINE KINASE-MB |
| 18 | C REACTIVE PROTEIN |
| 19* | EGF |
| 20* | ENA-78 |
| 21 | ENDOTHELIN-1 |
| 22 | EN-RAGE |
| 23 | EOTAXIN |
| 24* | ERYTHROPOIETIN |
| 25 | FATTY ACID BINDING PROTEIN |
| 26* | FACTOR VII |
| 27 | FERRITIN |
| 28* | FGF BASIC |
| 29 | FIBRINOGEN |
| 30* | G-CSF |
| 31* | GROWTH HORMONE |
| 32 | GM-CSF |
| 33* | GLUTATHIONE S-TRANSFERASE |
| 34 | HAPTOGLOBIN |
| 35 | ICAM-1 |
| 36 | IFN-GAMMA |
| 37 | IgA |
| 38 | IgE |
| 39* | IGF-1 |
| 40 | IgM |
| 41 | IL-10 |
| 42* | IL-12p40 |
| 43* | IL-12p70 |
| 44 | IL-13 |

FIG.6

| | |
|---|---|
| 45* | IL-15 |
| 46 | IL-16 |
| 47* | IL-18 |
| 48 | IL-1ALPHA |
| 49* | IL-1BETA |
| 50 | IL-1RA |
| 51* | IL-2 |
| 52* | IL-3 |
| 53* | IL-4 |
| 54 | IL-5 |
| 55 | IL-6 |
| 56 | IL-7 |
| 57 | IL-8 |
| 58* | INSULIN |
| 59 | LEPTIN |
| 60 | LIPOPROTEIN (a) |
| 61* | LYMPHOTACTIN |
| 62 | MCP-1 |
| 63* | MDC |
| 64 | MIP-1ALPHA |
| 65 | MIP-1BETA |
| 66 | MMP-2 |
| 67 | MMP-3 |
| 68* | MMP-9 |
| 69* | MYELOPEROXIDASE |
| 70 | MYOGLOBIN |
| 71 | PAI-1 |
| 72 | PROSTATIC ACID PHOSPHATASE |
| 73 | PAPP-A |
| 74 | PROSTATE SPECIFIC ANTIGEN, FREE |
| 75 | RANTES |
| 76 | SERUM AMYLOID P |
| 77 | STEM CELL FACTOR |
| 78 | SGOT |
| 79 | SHBG |
| 80 | THYROXINE BINDING GLOBULIN |
| 81 | TISSUE FACTOR |
| 82 | TIMP-1 |
| 83 | TNF RII |
| 84 | TNF-ALPHA |
| 85* | TNF-BETA |
| 86 | THROMBOPOIETIN |
| 87 | THYROID STIMULATING HORMONE |
| 88 | VCAM-1 |
| 89 | VEGF |
| 90 | VON WILLEBRAND FACTOR |

FIG.6-1

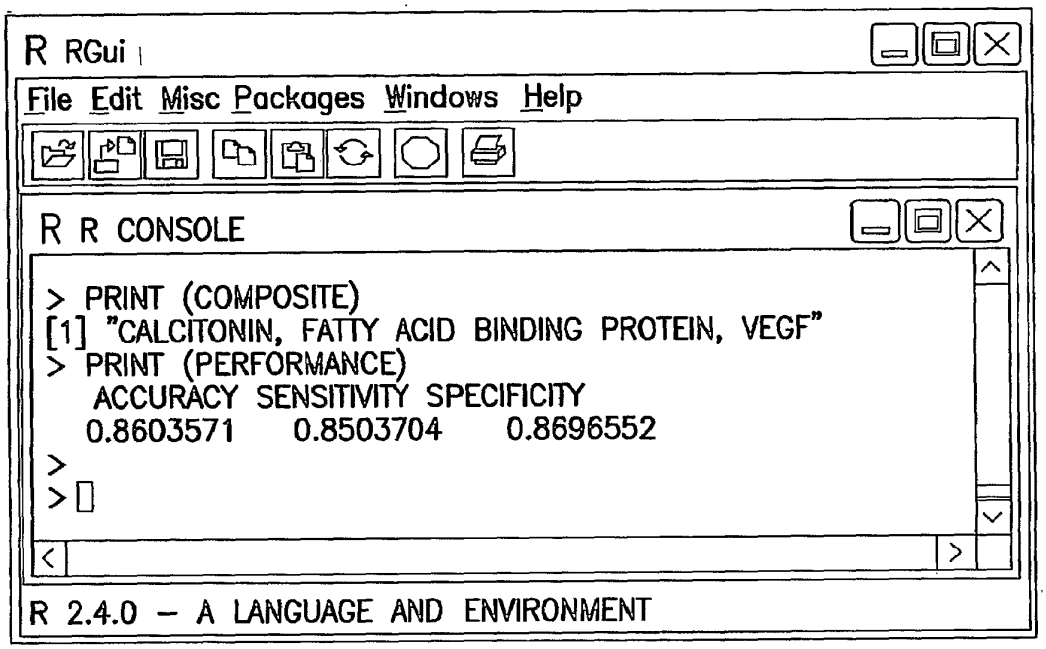

R RGui
File Edit Misc Packages Windows Help
R R CONSOLE
> PRINT (COMPOSITE)
[1] "CALCITONIN, FATTY ACID BINDING PROTEIN, VEGF"
> PRINT (PERFORMANCE)
ACCURACY SENSITIVITY SPECIFICITY
0.8603571 0.8503704 0.8696552
>
>
R 2.4.0 – A LANGUAGE AND ENVIRONMENT

FIG.7A

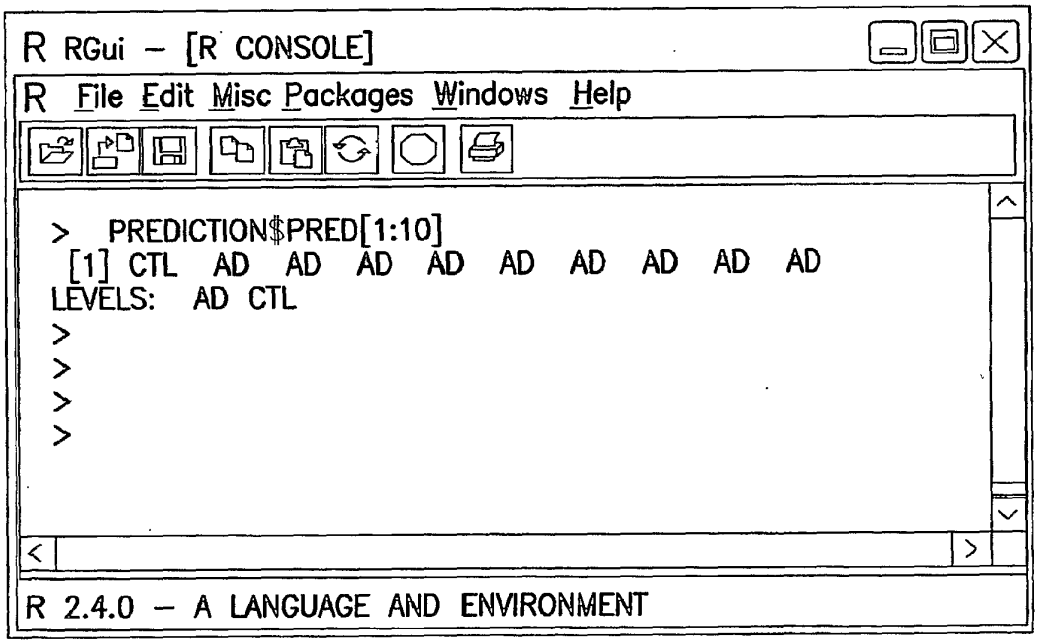

R RGui – [R CONSOLE]
R File Edit Misc Packages Windows Help
> PREDICTION$PRED[1:10]
[1] CTL AD AD AD AD AD AD AD AD AD
LEVELS: AD CTL
>
>
>
>
R 2.4.0 – A LANGUAGE AND ENVIRONMENT

FIG.7B

(12) INTERNATIONAL APPLICATION PUBLISHED UNDER THE PATENT COOPERATION TREATY (PCT)

(19) World Intellectual Property Organization
International Bureau

(43) International Publication Date
6 March 2008 (06.03.2008)

PCT

(10) International Publication Number
WO 2008/027017 A1

(51) International Patent Classification:
*A61K 38/02* (2006.01) *G01N 33/50* (2006.01)
*A61P 25/00* (2006.01)

(21) International Application Number:
PCT/SG2007/000283

(22) International Filing Date: 29 August 2007 (29.08.2007)

(25) Filing Language: English

(26) Publication Language: English

(30) Priority Data:
60/841,630 31 August 2006 (31.08.2006) US

(71) Applicant *(for all designated States except US)*: **SINGAPORE HEALTH SERVICES PTE LTD** [SG/SG]; 1, Third Hospital Avenue, #07-00 SNEC Building, Singapore 168821 (SG).

(72) Inventors; and
(75) Inventors/Applicants *(for US only)*: **XIAO, Zhi Cheng** [CA/SG]; c/o Singapore General Hospital, Department of Clinical Research, Outram Road, Singapore 169608 (SG). **MA, Quan-Hong** [CN/SG]; c/o Singapore General Hospital, Department of Clinical Research, Outram Road, Singapore 169608 (SG). **LI, Shao** [CN/SG]; c/o Singapore General Hospital, Department of Clinical Research, Outram Road, Singapore 169608 (SG). **DAWE, Gavin Stewart** [GB/SG]; c/o National University of Singapore, 21 Lower Kent Ridge Road, Singapore 119077 (SG).

(74) Agent: **MATTEUCCI, Gianfranco**; Lloyd Wise, Tanjong Pagar, P.O. Box 636, Singapore 910816 (SG).

(81) Designated States *(unless otherwise indicated, for every kind of national protection available)*: AE, AG, AL, AM, AT, AU, AZ, BA, BB, BG, BH, BR, BW, BY, BZ, CA, CH, CN, CO, CR, CU, CZ, DE, DK, DM, DO, DZ, EC, EE, EG, ES, FI, GB, GD, GE, GH, GM, GT, HN, HR, HU, ID, IL, IN, IS, JP, KE, KG, KM, KN, KP, KR, KZ, LA, LC, LK, LR, LS, LT, LU, LY, MA, MD, ME, MG, MK, MN, MW, MX, MY, MZ, NA, NG, NI, NO, NZ, OM, PG, PH, PL, PT, RO, RS, RU, SC, SD, SE, SG, SK, SL, SM, SV, SY, TJ, TM, TN, TR, TT, TZ, UA, UG, US, UZ, VC, VN, ZA, ZM, ZW.

(84) Designated States *(unless otherwise indicated, for every kind of regional protection available)*: ARIPO (BW, GH, GM, KE, LS, MW, MZ, NA, SD, SL, SZ, TZ, UG, ZM, ZW), Eurasian (AM, AZ, BY, KG, KZ, MD, RU, TJ, TM), European (AT, BE, BG, CH, CY, CZ, DE, DK, EE, ES, FI, FR, GB, GR, HU, IE, IS, IT, LT, LU, LV, MC, MT, NL, PL, PT, RO, SE, SI, SK, TR), OAPI (BF, BJ, CF, CG, CI, CM, GA, GN, GQ, GW, ML, MR, NE, SN, TD, TG).

**Declaration under Rule 4.17:**
— *of inventorship (Rule 4.17(iv))*

**Published:**
— *with international search report*
— *with sequence listing part of description published separately in electronic form and available upon request from the International Bureau*

WO 2008/027017 A1

(54) Title: MODULATION OF NEURAL ACTIVITY AND/OR CONDITION

(57) Abstract: There is provided methods to modulate biological or/and medical activities (functions), events and/or conditions. The biological or medical activities, events or conditions may include predisposition to, and onset and progression of neurological conditions, myelination and demyelination of neurons, and/or differentiation of neural stem cells. In particular, the present invention provides method(s) to modulate the expression and/or activity of amyloid precursor protein (APP) and/or its derivatives or fragments. The present invention also provides methods to modulate the expression and/or activity of molecules, such as sodium channels and/or TAG-1 , which interact with APP and its derivatives or fragments.

# Modulation of Neural Activity and/or Condition

## Field of the invention

The present invention generally relates to the field of medical and biological science. In particular, the present invention relates to methods to modulate neural conditions, activities and/or events.

## Background of the invention

Amyloid precursor protein (APP) is well known as a molecule that is involved in the pathogenesis of Alzheimer's disease (AD) and of other forms of dementia, such as Down's syndrome. The exact mechanisms by which APP contributes to the development of dementia are unknown but is it thought that cleavage of APP by secretases leading to formation of the smaller peptide, the beta amyloid (Aβ), is a crucial step.

Deposition of Aβ, has been suggested to be related to the pathology of AD and associated with other pathological markers of AD conditions such as cell death in the central nervous system (CNS), accumulation of amyloid plaques, and the appearance of neurofibrillary tangles. Reduction or prevention of Aβ deposition is widely believed to be desirable for slowing the progress of, or preventing the development of, AD. While reduction of Aβ deposition is thought to be desirable, there is no teaching or suggestion in the literature on how this may be achieved.

Previous research had suggested that release of Aβ may be activity dependent, but the reasons for this activity dependence were unknown. The release of component peptides of APP, including Aβ deposition, has also been thought to occur predominantly at synapses. However, although APP is enriched in axons and presynaptic terminals (Ferreira, 1993), its distribution and function along

myelinated neurons have yet to be elucidated. Further, although some of the potential interactions of APP had been explored, the interacting partners of APP were assumed to be synaptic proteins.

In AD patients, the entorhinal cortex, from where the perforant pathway originates, is one of the most severely affected areas, particularly at the earliest stages of the disease. Moreover, electrical activity within the pathway modulates interstitial fluid β-amyloid (Aβ) levels, which can be blocked by tetrodotoxin (TTX), a specific sodium channel blocker (Cirrito et al, 2005).

There is some evidence pointing to deficits in adult neurogenesis in AD and this has lead to considerable interest in the role of APP in regulating stem cell function. However, the mechanisms by which APP modulate stem cell functions such as proliferation and differentiation remain unknown. In particular, the interacting or binding partners of APP in the stem cell niche are unknown.

As such, any contribution to the understanding of the role of APP in the brain will be useful and will add to knowledge of neural functions and/or events, as well as to treatment of neurological conditions.

## Summary of the invention

The present invention addresses the problems above, and in particular, provides new methods to modulate at least one biological or medical condition, activity (function) and/or events.

Accordingly, the present invention provides a method of treating at least one medical condition in a subject, the method comprising modulating the expression and/or activity (function) of amyloid precursor protein (APP), APP derivative or APP fragment. In particular, the modulating may be by decreasing

the expression and/or activity (function) of amyloid precursor protein (APP), APP derivative or APP fragment.

The modulation of APP, its derivative or a fragment thereof may comprise modulating at least one molecule, protein, and/or peptide that interacts with amyloid precursor protein (APP), APP derivative or APP fragment. For example, the modulation may comprise modulating at least one cellular component that interacts with amyloid precursor protein (APP), APP derivative or APP fragment. The at least one cellular component may be selected from TAG-1, sodium channels, and sodium channel complex protein.

Accordingly, the modulation may comprise modulating at least one cellular component selected from Caspr2, NgR, TN-R, TN-C, MAG, Nogo-A, phosphacan, F3, OMgp, RPTPβ NG2 and Go protein(s).

According to a further aspect, the modulating according to the invention comprises administering at least one pharmaceutically and/or therapeutically effective amount of amyloid precursor protein (APP), APP derivative or APP fragment. Preferably, the APP derivative or APP fragment is Aβ, soluble APP (sAPP), APP-695, AICD or VTPEER peptide. The modulating may comprise administering a pharmaceutically and/or therapeutically effective amount of at least one drug, protein, peptide, antibody or molecule that interacts with amyloid precursor protein (APP), APP derivative or APP fragment, TAG-1, sodium channels, or sodium channel complex protein(s). The modulating may also comprise administering a pharmaceutically and/or therapeutically effective amount of at least one drug, protein, peptide, antibody or molecule that interacts with amyloid precursor protein (APP), APP derivative or APP fragment, TAG-1, sodium channels, TAG-1 complex protein(s), sodium channels complex protein(s), Caspr2, NgR, potassium channels, TN-R, TN-C, MAG, Nogo-A, phosphacan, F3, OMgp, RPTPβ and NG2. The modulating may also comprise administering a pharmaceutically and/or therapeutically effective amount of at

least one compound selected from the group consisting of TAG-1, anesthetic(s), toxin(s) and Go protein(s). In particular, the modulating may comprise administering a pharmaceutically and/or therapeutically effective amount of at least one drug or molecule selected from local anaesthetic(s), veratridine, batrachotoxin, scorpion toxins, sea anemone toxin, conus toxins, saxitoxin, tetrodotoxin, antiepileptic drug(s), antiarrhythmic drug(s), antibodies to sodium channel proteins, antibodies to Caspr, and peptide fragments of APP.

The modulation of amyloid precursor protein (APP), APP derivative or APP fragment may be to prevent and/or reduce beta amyloid (Aβ) deposition, improve and/or facilitate nervous tissue repair, improve and/or facilitate myelination, to modulate stem cell function(s) and/or to modulate sodium channel function(s). The at least one medical condition may be selected from the group consisting of Alzheimer's disease, multiple sclerosis, brain injury, spinal cord injury, axonal injury-related disorders, epilepsy, neurodegenerative disorders and demyelination disorders. The modulating may result in modulation of axonal conduction of action potential(s) for the treatment of pain and/or epilepsy. The modulating may result in the induction of analgesia and/or local anaesthesia.

The APP derivative may be soluble APP (sAPP) and the APP fragment may be beta amyloid (Aβ).

The present invention also provides a method of detecting and/or quantitating the presence of, predisposition to, and/or severity of, a neurological condition in a subject, the method comprising: (a) providing at least one sample from a subject; (b) determining the expression or activity of amyloid precursor protein (APP), APP derivative or APP fragment; (c) comparing the expression or activity of amyloid precursor protein (APP), APP derivative or APP fragment, with that of at least one control, a difference in expression and/or activity indicating the

presence of, or predisposition to, and/or severity of a neurological condition in the subject.

There is also provided a method of monitoring the efficacy of a treatment for a neurological condition in a subject, the method comprising: (a) providing at least two samples from a subject, each sample obtained at different time points; (b) determining the expression and/or activity (function) of amyloid precursor protein (APP), APP derivative or APP fragment; and (c) comparing the expression and/or activity (function) of amyloid precursor protein (APP), APP derivative or APP fragment, in the at least two samples.

There is also provided a method of prognosticating the outcome of a neurological condition in a subject, the method comprising: (a) providing at least one sample from a subject; (b) determining the expression and/or activity (function) of amyloid precursor protein (APP), APP derivative or APP fragment; (c) comparing the expression and/or activity (function) of amyloid precursor protein (APP), APP derivative or APP fragment, with that of at least one control, a difference in expression and/or activity (function) indicating the prognosis of a neurological condition in the subject.

There is also provided a a method of inducing analgesia and/or anesthesia in a subject, the method comprising modulating the expression and/or activity (function) of amyloid precursor protein (APP), APP derivative or APP fragment. The modulating may comprise decreasing the expression and/or activity (function) of amyloid precursor protein (APP), APP derivative or APP fragment.

The present invention also provides an in vitro or in vivo method of modulating proliferation, differentiation and/or function (activity) of at least one stem cell, the method comprising modulating the expression and/or activity (function) of amyloid precursor protein (APP), APP derivative or APP fragment, in the at least one stem cell. The present invention also provides a method of detecting and/or quantitating the presence of, predisposition to, and/or severity of, at least

one condition related to beta amyloid (Aβ) deposition and/or sodium channel dysfunction in a subject, the method comprising: (a) measuring the nerve and/or axon conduction velocity in the subject; (b) comparing the nerve and/or axon conduction velocity with that of at least one control, a difference in velocity indicating the presence of, or predisposition to, and/or severity of at least one condition related to Aβ deposition and/or sodium channel dysfunction in the subject. The method may be for detecting and/or quantitating the presence of, predisposition to, and/or severity of Alzheimer's disease (AD).

The present invention also provides an in vitro or in vivo method of modulating at least one activity (function) of amyloid precursor protein (APP), APP derivative or APP fragment, comprising administering at least one drug, protein, peptide, antibody or molecule that interacts with amyloid precursor protein (APP), APP derivative or APP fragment, TAG-1, sodium channels, or sodium channel complex protein(s). The modulating may comprise administering a pharmaceutically and/or therapeutically effective amount of at least one compound selected from the group consisting of TAG-1, anesthetic(s), toxin(s) and Go protein(s). The method may be for treating at least one condition selected from the group consisting of Alzheimer's disease, multiple sclerosis, brain injury, spinal cord injury, axonal injury-related disorders, epilepsy, neurodegenerative disorders and demyelination disorders.

The present invention also provides an in vitro or in vivo method of modulating sodium channel(s) activity(ies) (function/s) comprising administering at least one drug, protein, peptide, antibody or molecule that interacts with amyloid precursor protein (APP), APP derivative or APP fragment, TAG-1, sodium channel(s), or sodium channel complex protein(s). The method may be for modulating at lease one APP activity (function), and/or for the treatment of at least one neurological disorder. The method may be for the treatment of acute and/or chronic pain disorder(s), induction of analgesia, treatment of epilepsy

and/or convulsion(s), treatment of disorder(s) of the rhythm of the heart, and/or induction of anaesthesia and/or analgesia.

The present invention also provides at least one pharmaceutical composition for treating at least one APP and/or sodium channel related medical condition comprising at least one compound selected from the group consisting of: APP, APP derivative, APP fragment, antibody to APP, TAG-1, , a TAG-1 homologous protein or fragment thereof, antibody to TAG-1, sodium channel(s), at least one sodium channel complex protein, Caspr, Caspr derivative, Caspr fragment, anesthetic(s), toxin(s) and Go protein(s); and optionally at least one pharmaceutically acceptable diluent, carrier and/or excipient. The medical condition may be selected from the group consisting of Alzheimer's disease, multiple sclerosis, brain injury, spinal cord injury, axonal injury-related disorders, epilepsy, neurodegenerative disorders and demyelination disorders.

The present invention also provides use of at least one compound selected from the group consisting of: APP, APP derivative, APP fragment, antibody to APP, TAG-1, at least one TAG-1 complex protein, a TAG-1 homologous protein or fragment thereof, antibody to TAG-1, sodium channel(s), at least one sodium channel complex protein, Caspr, Caspr derivative, Caspr fragment, anesthetic(s), toxin(s) and Go protein(s), for the preparation of a medicament for the treatment of an APP and/or sodium channel related medical condition.

The present invention also provides a compound selected from the group consisting of: APP, APP derivative, APP fragment, antibody to APP, TAG-1, at least one TAG-1 complex protein, a TAG-1 homologous protein or fragment thereof, antibody to TAG-1, sodium channel(s), at least one sodium channel complex protein, Caspr, Caspr derivative, Caspr fragment, anesthetic(s), toxin(s) and Go protein(s) for the treatment of an APP and/or sodium channel related medical condition

The present invention also provides a kit comprising at least one compound selected from the group consisting of: APP, APP derivative, APP fragment, antibody to APP, TAG-1, at least one TAG-1 complex protein, a TAG-1 homologous protein or fragment thereof, antibody to TAG-1, sodium channel(s), at least one sodium channel complex protein, Caspr, Caspr derivative, Caspr fragment, anesthetic(s) and toxin(s), for the detection and/or diagnosis of at least one APP and/or sodium channel related medical condition and/or for the treatment of at least one APP and/or sodium channel related medical condition.

Preferably, the APP derivative or fragment is Aβ, soluble APP (sAPP), App-695, AICD or VTPEER peptide.

Brief description of the figures

Figure 1 shows that APP is expressed by axons during myelination. It also shows the interaction between APP and TAG-1, Caspr2, NgR, and K+ channels.

Figure 2 shows that APP is expressed at nodes of Ranvier. Interaction with Sodium channels places APP in the context of TN-R, TN-C, MAG, Nogo-A, phosphacan, F3, Omgp, RPTOß and NG2 complexes.

Figure 3 shows that TAG-1 is expressed in the stem cell niche and that APP interacts with TAG-1.

Figures 4-8 show that APP locates at NORs in the CNS.

Figure 4 shows that APP was detected at NORs in the spinal cord. a-k: Normal adult rat spinal cord were prepared for double IF, using polyclonal antibodies to APP (green; a-k) and monoclonal antibodies against Kv1.2 (Kch; red; a d, f, and g) or Tn-R (red; b, h j, and k) or Na+ channels (Nach; red; c), respectively. g and k: Orthogonal slices. Scale bars: 10 µm in a-c, f, g, j, and k.

Figures 5(a, b) show that APP evenly distributed along sciatic nerve. Normal adult rat sciatic nerves (SN) were prepared for double IF, using polyclonal antibodies to APP (Green) and monoclonal antibodies against NF200 (red; a) or Kv1.2 (red; b), respectively. Scale bars: 10 μm in a and b.

Figures 5(c, d, e) show disappearance of APP clustering in the spinal cord of APP knock-out mice. Adult spinal cord from APP knock-out mice (KO) was prepared for double IF, using polyclonal antibodies to APP (Green; a) or Caspr (Green; b and c) and monoclonal antibodies against Tn-R (red; a and b) and Nach (red; c), respectively. Scale bars: 10 μm in a, b.

Figure 6 shows the results of immunohistochemical studies of longitudinal sections of rat spinal cords at P6, P10, P15, and P21. Double labellings using antibodies against pan-Na+ channels (Nach, red; a) and K+ channel (Kch, red; b to d) showed that APP clustering commences at P10 and becomes prevalent by P15. Insert boxes show images with higher magnification from the respective lower magnification images.

Figure 7 shows quantification of double IFs of APP and K+ channels performed in spinal cords. Nodal APP labellings in relation to Kv1.2 in spinal cord were counted (n = 200) from at least three animals (e). The ratios were detected as 52.08 ± 7.29% at P10, 66.94 ± 0.9% at P15, 68.97 ± 2.3% at p21, and 90.16 ± 3.05% at 2 months. Scale bars: 10 μm in a-d.

Figure 8 shows quantification of double IF labelling of APP and K+ channels performed in spinal cords. Nodal APP labellings in relation to Kv1.2 in spinal cord were counted (n = 200) from at least three animals. The ratio was detected as 90.16 + 3.05%.

Figures 9-12 show myelination in APP knock-out and transgenic mice (Scale bars: 0.5 μm in Aa, Ab, Ca, and Cb; 5 μm in Ba, Bb. Error bars represent +SEM in Ac, Bc, and Cc. ** $p < 0.001$).

Figure 9 shows the results of EM studies in cross sections revealed the ultrastructure of myelin sheaths in spinal cords (SC) of wild-type littermates (WT; a) versus APP knock-out mice (KO; b) (all aged 3 months). The myelin thickness as indicated by g ratio (c) was significantly reduced in APP knock-out mice, in comparison with wild-type littermates.

Figure 10 shows the results of EM studies on the ultrastructure of myelin sheaths in sciatic nerve (SN). Cross sections revealed that wild-type littermates (WT; a) versus APP knock-out mice (KO; b) (all aged 3 months). The myelin thickness as indicated by g ratio (c) was significantly reduced in APP knock-out mice, in comparison with wild-type littermates.

Figure 11 shows the results of EM studies in cross sections revealed the ultrastructure of myelin sheaths in spinal cords (SC) of wild-type littermates (WT; a) versus APP transgenic mice (TG; b) (all aged 3 months). The myelin thickness as indicated by g ratio (c) was significantly increased in APP transgenic mice, in comparison with wild-type littermates.

Figure 12 shows the results of APP knock-out and overexpression showed the opposite effects on both axon (a) and fiber (b) diameters and the myelin thickness as indicated by g ratio (c), in mice after normalizing with wild-type littermates, respectively.

Figures 13-16 show that APP modulates the expression of Na+ channel Nav1.6 in *Xenopus* oocytes. Two-electrode voltage clamp recordings of Na+ currents in *Xenopus* oocytes expressing Nav1.6 in oocytes expressing: Figure 13, the α subunit alone and with APP; Figure 14, the α + β1 subunits without and with APP; Figure 15, the α + β2 subunits without and with APP; and Figure 16, α + β1 + β2 subunits without and with APP Traces (a) to (d).

Figure 13 illustrates the effects of APP on voltage-gated sodium channels.

**a.** Normalized current-voltage relationships of currents in oocytes expressing Nav1.6 α subunits alone (open squares) and together with APP (closed circles).

**b.** Activation of sodium currents in oocytes expressing Nav1.6 α subunits alone (open squares) and together with APP (closed circles). The activation curves were fitted by a Boltzmann equation, $G_{Na} / G_{Na,max}=1/[1+\exp(V_{1/2} - V_m)/k]$, where $V_{1/2}$ is the voltage of half-maximal $Na^+$ conductance and k is a slope factor.

**c.** Normalized inactivation of sodium currents in oocytes expressing Nav1.6 α subunit alone (open squares) and together with APP (closed circles). The inactivation data were fitted to a Boltzmann function, $I_{Na}/I_{Na,max}=1/[1+\exp((V_m-V_{1/2})/k)$, where $V_{1/2}$ is the voltage of half-maximal availability and k is a slope factor.

**d.** Recovery from inactivation was measured using a two-pulse protocol with a variable interval in oocytes expressing the Nav1.6 α subunit alone (open squares) and together with APP (closed circles). The data were fitted with a single rising exponential function.

**e.** Normalized current-voltage relationships of sodium currents in oocytes expressing Nav1.5 α subunit alone (open squares) and together with APP (closed circles).

**f.** Normalized current-voltage relationships of sodium currents in oocytes expressing Nav1.6 α subunit alone (open squares) and together with control injection of cRNA for the reverse APP sequence (closed circles).

Insert: Representative examples of sodium current responses elicited by depolarizing voltage steps.

For figures 14-16

a shows representative examples of Na+ current responses elicited by depolarizing voltage steps.

b shows normalized current-voltage relationships of Na+ currents in oocytes expressing Na+ channels alone (open circles) and together with APP (closed circles).

c shows activation of Na+ currents in oocytes expressing Na+ channels alone (open circles) and together with APP (closed circles). The activation curves were fitted by the Boltzmann equations GNa / GNa,max=1/[1+exp(V1/2 - Vm)/k] and INa/INa,max=1/[1+exp((Vm-V1/2)/k), respectively, where V1/2 is the voltage of half-maximal Na+ conductance and half-maximal availability, respectively, and k is a slope factor.

d shows normalized inactivation of Na+ currents in oocytes expressing Na+ channels alone (open circles) and together with APP (closed circles). The inactivation data were fitted to a Boltzmann function GNa / GNa,max=1/[1+exp(Vm – V1/2)/k] and INa/INa,max=1/[1+exp((Vm-V1/2)/k), as described above.

e shows recovery from inactivation measured using a two-pulse protocol with a variable interval in oocytes expression sodium channels alone (open circles and together with APP (solid circles).

Figures 17-18 show electrophysiological properties in APP-knock-out mice.

Figure 17 shows whole cell recordings of voltage-gated Na+ currents in acutely dissociated DRG neurons. a, Na+ current responses elicited by depolarizing voltage steps in a neuron from an APP knockout mouse (top). Normalized current-voltage curves of peak Na+ currents in wild-type mice (solid circles) and APP knockout mice (open circles). pF = picofarads. b, activation (circle symbols) and steady-state inactivation (triangle symbols) curves of Na+ currents in neurons from wild-type mice (dash line) and APP knockout mice (solid line). The activation and inactivation curves were fitted by the Boltzmann equations Gna / GNa,max = 1/[1+exp(V1/2 - Vm)/k] and

INa/INa,max=1/[1+exp((Vm-V1/2)/k), respectively, where V1/2 is the voltage of half-maximal Na+ conductance and half-maximal availability, respectively, and k is a slope factor. c; recovery from inactivation measured using a two-pulse protocol with a variable interval in neurons from wild-type mice (open circles) and APP knockout mice (solid circles). Data points indicate the amplitude of the second Na+ current response after normalization to the amplitude of the first response. Data in recordings from 9 neurons from four wild-type mice and 19 neurons from five APP knockout mice in b - c summarize recordings from 16 neurons from eight wild-type mice and 24 neurons from eight APP knockout mice. *, $p < 0.05$. **, $p < 0.01$.

Figure 18 shows the determination of conduction velocities of compound action potentials in APP-knock-out and wild-type mice. Representative CAPs from spinal cord recordings of APP knock-out (KO) and wild-type (WT) mice. Records were taken at 24°C, 32°C and 37°C for spinal cord (a). The conduction velocity measured in wild-type mouse spinal cord (a; n =8) was consistently higher than that seen in APP knock-out mice (a; n =12) at all temperatures measured. The conduction velocity measured in wild-type mouse sciatic nerves (b; n = 6) was slightly higher than that seen in APP knock-out mice (a; n =11) at all temperatures measured, but the difference was not significant. Significance values were calculated using the Student's t test and were as follows: 24°C, $p < 0.05$; 32°C, $p < 0.05$; and 37°C, $p < 0.005$. Error bars represent +SEM.

Figure 19A shows APP expression during development. Protein extracts of rat whole brains at various postnatal developmental stages (P0, P5, P7, P8, P10, P15, P21, P30 and adult) were subjected to Western blotting analyses using antibodies against APP and γ-tubulin (as loading control). Figure 19B shows that APP clustering was disrupted in the spinal cord of PLP transgenic mice (arrow). APP is still clustering at node of Ranvier in the unaffected myelinated fiber (arrowhead). Adult spinal cords from both mice were prepared for double

IF, using polyclonal antibodies to APP (green) and monoclonal antibodies against K+ channels (red) respectively. Scale bars: 10 μm.

Figures 20-22 show effects on axon and fiber diameters. (Note that increment of g ratio in KO mice is significant in almost all axons. ** $p < 0.001$; *$p < 0.05$. Error bars represent +SEM.)

Figure 20 shows that both axon (a) and fiber (b) diameters were significantly reduced in APP knock-out mice, in comparison with wild-type littermates. The distribution of the g ratio, representing the myelin thickness, in the spinal cord (c) was plotted against different axon diameters, comparing APP KO to WT mice.

Figure 21 shows the distribution of G ratio representing the myelin thickness of sciatic nerve was plotted against different axon diameters, comparing in APP KO and WT mice.

Figure 22 shows that both axon (a) and fiber (b) diameters were significantly increased in APP transgenic mice, in comparison with wild-type littermates.

Figure 23 shows effect of co-expression of APP on peak Na+ currents of oocytes expressing the Nav1.6 with a, α subunit; b, α + β1 subunit; c, α + β2 subunit; and d, α + β1 + β2 subunit; ** $p < 0.005$.

Figure 24 shows a western blot analyses of protein extracts from the brains of adult $APP^{+/+}$, $APP^{+/-}$, and $APP^{-/-}$ mice. Antibodies used were directed against Nav1.6 and γ-tubulin (as loading control).

Figure 25 shows a schematic representation of APP (Full-length APP695; SEQ ID NO: 2, cDNA; SEQ ID NO: 3, peptide), APP intracellular domain (AICD50; SEQ ID NO: 4, cDNA; SEQ ID NO: 7, peptide), APP C31 domain (C31; SEQ ID NO: 8, cDNA; SEQ ID NO: 10, peptide), APP Go protein binding domain (G0BD; SEQ ID NO: 11, cDNA; SEQ ID NO: 14, peptide), Fe65 binding domain

(Fe65BD; SEQ ID NO: 15, cDNA; SEQ ID NO: 18, peptide) and VTPEER peptides ($Val^{667}$-$Arg^{672}$; SEQ ID NO: 19, cDNA; SEQ ID NO: 22, peptide).

Figure 26 shows the effects of distinct APP intracellular domains and peptides on voltage-gated sodium channels.

Normalized current-voltage relationships of currents in oocytes expressing Nav1.6 α subunits alone (open squares) and together with APP intracellular domain (AICD50; **a**; closed circles), APP Go protein binding domain (G0BD; **b**; closed circles), Fe65 binding domain (Fe65BD; **c**; closed circles), APP C31 domain (C31; **d**; closed circles), and VTPEER peptide (VTPEER; **e**; closed circles). Normalized current-voltage relationships of currents in the cells expressing Nav1.6 α subunits before (**f**; open squares) and after (**f**; closed circles) VTPEER treatment. Insert: Representative examples of sodium current responses elicited by depolarizing voltage steps.

Figure 27 shows the effects of Go protein on the APP-induced sodium current expression.

**a.** Sodium channels and APP alone (open squares) and together with a G203T dominant negative mutant of the Go protein α subunit (GoDN; closed circles).

**b.** Sodium channels and AICD alone (open squares) and together with GoDN (closed circles).

**c.** Sodium channels and the Go protein-binding domain (GB) of APP alone (open squares) and together with GoDN (closed circles).

**d.** Sodium channels and the Fe65 binding domain (Fe65BD) of APP alone (open squares) and together with GoDN (closed circles).

**e.** Sodium channels and the C31 domain (C31) of APP alone (open squares) and together with GoDN (closed circles).

**f.** Sodium channels and the VTPEER peptide of APP alone (open squares) and together with GoDN (closed circles).

Figure 28 shows the effects of APP distinct domains and peptides on Nav1.6 electrophyshiological properties

Activation of sodium currents in oocytes expressing Nav1.6 α subunits alone (open squares) and together with AICD (**a**), Go binding domain (GB; **d**), C31 (**g**), and VTPEER peptides (**j**; closed circles), respectively. The activation curves were fitted by a Boltzmann equation, $G_{Na} / G_{Na,max}=1/[1+\exp(V_{1/2} - V_m)/k]$, where $V_{1/2}$ is the voltage of half-maximal $Na^+$ conductance and k is a slope factor.

Normalized inactivation of sodium currents in oocytes expressing Nav1.6 α subunit alone (open squares) and together with AICD (**b**), Go binding domain (GB; **e**), C31 (**h**), and VTPEER peptides (**k**; closed circles), respectively. The inactivation data were fitted to a Boltzmann function, $I_{Na}/I_{Na,max}=1/[1+\exp((V_m-V_{1/2})/k)$, where $V_{1/2}$ is the voltage of half-maximal availability and k is a slope factor.

Recovery from inactivation was measured using a two-pulse protocol with a variable interval in oocytes expressing the Nav1.6 α subunit alone (open squares) and together with AICD (**c**), Go binding domain (GB; **f**), C31 (**i**), and VTPEER peptides (**l**; closed circles), respectively. The data were fitted with a single rising exponential function.

Figure 29 shows the relationship between the amplitude of normalized sodium currents and the APP concentration.

Nav1.6 was co-expressed with full length APP in various molar ratios in oocytes. The graph shows the normalized mean peak sodium current amplitude ± SEM in oocytes injected with the indicated concentrations by molar ratio of Nav1.6 and APP cRNA. The effect of APP on the sodium current remained

constant over a wide range of APP concentrations suggesting that the effect on the sodium current does not depend upon a binding of the sodium channel with APP as a beta subunit or accessory protein. The data were obtained from between 18 and 42 oocytes from 4 frogs at each concentration.

Figure 30 illustrates that APP and TAG-1 are binding partners.

A. Cell adhesion assay. TAG-1 transfected CHO cells (**a**), but not F3 transfected CHO cells (**d**) and CHO cells (**e**), adhered to APP-Fc protein spots. Adhesion of TAG-1 transfected CHO cells to APP-Fc was blocked by antibodies against TAG-1 (**b**) and APP (**c**). APP transfected CHO cells (**f**, **g**, **h**, **j** and **l**), but not CHO cells (**i**, **k**, **m**, and **n**), adhered to spots coated with TAG-1-Fc protein (**f**), TAXIg-GST (**j**), and TAXFNII-GST (**l**), but not GST (**n**). Adhesion of APP transfected CHO cells to TAG-1-Fc was blocked by antibodies against TAG-1 (**g**) and APP (**h**). Bar in **n** is 20 μm (for **a-n).** ** $p<0.001$.

B. Quantification of TAG-1 transfected CHO cells adhering to APP-Fc substrate, APP transfected CHO cells adhering to TAG-1-Fc substrate, and the effects of blocking with antibodies against TAG-1 and APP . Error bars represent standard deviations.

Figure 31 shows that (**a**) APP and TAG-1 associate as a protein complex. Co-immunoprecipitation of APP with TAG-1. Mouse brain lysates were co-immunoprecipitated using anti-TAG-1 antibodies and non-immune IgG and probed with anti-APP antibody. Reciprocal assays used anti-APP antibody or APP-Fc to capture the protein complex and anti-TAG-1 antibodies to detect the binding partner. (**b**) GST Pulldown assay to analyze the interaction between TAX and APP. Mouse brain, APP/CHO, and CHO cell lysates were precipitated using TAXFNIII-GST, TAXIg-GST, and GST and probed with anti-APP antibody.

Figure 32 shows that AICD transcriptional activity in TAG-1- and TAX-transfected CHO cells and expression of APP and TAG-1 in the fetal neural stem cell niche. A. **(a)** CHO cells and L1 (CHOL1), TAX (CHOTAX) and TAG-1 (CHOTAG1) transfected CHO cells were transiently co-transfected in 24-well culture dishes with pG5E1B plasmid, APP-Gal4-responsive luciferase reporter gene, Fe65 plasmid, and luciferase internal control plasmid. Normalized luciferase activities in whole-cell lysates were determined in triplicate and expressed relative to activity in lysates prepared from CHO cells. **(b)** AICD transcriptional activity in TAG-1 transfected CHO cells was significantly reduced by a γ-secretase inhibitor (2 μM and 4 μM). ** $p<0.001$. Error bars represent standard deviations.

Figure 33 shows double immunostaining for nestin (red, **a, a', d,** and **d'; c, c', f, and f'** are the merged images) and APP (green, **b, b', c,** and **c'**) or TAG-1 (green, **e, e', f,** and **f'**) in the walls of the lateral ventricles in E14 mouse brain. Double immunostaining for APP (green, **h and h'; i and i'** are the merged images) and TAG-1 (red, **g, g', i,** and **i'**) in the walls of the lateral ventricles in E14 mouse brain. Bars in c, f, and i are 50μm (for a, b, d, e, g, and h); Bars in c', f', i' are 20 μm (for a', b', d', e', g', and h').

Figure 34 shows the expression of APP and TAG-1 in neural progenitor cells (NPCs). NPCs isolated from the lateral ventricles of E14 mouse brain were double-stained for APP (green; **a'** and red; **c' and e**) and/or TAG-1 (green; **b' and e'** and red; **d'**) and with neural precursor cell markers, nestin (red; **a** and **b**) or Sox2 (green; **c** and **d**). a" to e" are merged images. Mouse brain samples and the NPCs lysate were blotted with antibodies against TAG-1 and APP, respectively (**f**). Bars are 20 μm in a" (for a and a'); b" (for b and b'); c" (for c and c'); d" (for d and d'); and e" (for e and e').

Figure 35 shows the neurogenesis in APP and TAG-1 deficient mice.

A. NPCs were isolated from APP +/+ mice (APP WT) and APP -/- mice (APP KO). After 7-8 days in vitro culture differentiation, the cells were double-stained for TUJ1 (**a** and **b**) or MAP2 (d) and DAPI (**a** and **b**). The number of TUJ1 (**c**) and MAP2 (**d**) positive cells were counted and expressed as a percentage of the total number of DAPI positive cells. Bar in b is 100 µm (for a).

B. NPCs isolated from TAG-1 +/+ mice (TAG-1 WT) and TAG-1 -/- mice (TAG-1 KO) were double-stained for TUJ1 (**a** and **b**) or MAP2 (d) and DAPI (**a** and **b**). The number of TUJ1 (**c**) and MAP2 (**d**) positive cells were counted and expressed as a percentage of the total number of DAPI positive cells. Bar in b is 100 µm (for a).

** $p<0.001$. Error bars represent standard deviations.

Figure 36 shows TAG-1 triggered AICD transcriptional activity in NPCs, neurogenesis in TAG-1/APP double deficient mice and a putative model of the TAG-1/APP pathway.

A. NPCs isolated from APP$^{-/-}$/TAG-1$^{-/-}$ mice were transiently co-transfected with pG5E1B plasmid, a APP-Gal4-responsive luciferase reporter gene, Fe65 plasmid, and luciferase internal control plasmid (**a**). The transfected NPCs were cultured in 24-well culture dishes substrate-coated with laminin, F3-Fc, L1-Fc, and TAG1-Fc as indicated. Normalized luciferase activities in whole-cell lysates were determined in triplicate and expressed relative to the activity in lysates prepared from laminin treated cells. AICD transcriptional activity in APP$^{-/-}$/TAG-1$^{-/-}$ NPCs was significantly reduced by a γ-secretase inhibitor (2 µM and 4 µM, respectively; **b**). ** $p<0.001$. Error bars represent standard deviations.

**B.** NPCs isolated from APP$^{+/+}$/TAG-1$^{+/+}$ mice (WT) (**a**) and TAG-1$^{-/-}$/APP$^{-/-}$ mice (**b**) were double-stained for TUJ1 and DAPI. The percent of TUJ1/DAPI positive cells were counted (e). ** $p<0.001$. Error bars represent standard deviations. Bar in b is 100 µm (for a).

Figure 37 shows a putative model of the TAG-1/APP pathway. TAG-1 interacts with APP on the cell surface to activate the APP signaling pathway through γ-secretase-dependent cleavage. This is followed by the processing of APP and release of AICD into cytoplasm, where AICD may bind with Fe65 or other modifiers. The complex further translocates to the nucleus, where it interacts with other transcription-related proteins, such as Tip60, and thereby activates target genes. Thus, neurogenesis is negatively modulated by AICD transcriptional activity triggered by the TAG-1/APP interaction.

Detailed description of the invention

Bibliographic references mentioned in the present specification are for convenience listed in the form of a list of references and added at the end of the examples. The whole content of such bibliographic references is herein incorporated by reference.

Definitions

Medical or biological activity (function), event and/or condition – These are events, activities (functions) and/or conditions in humans and/or animals. Since such events, activities (functions) and/or conditions are homologous or equivalent in both humans and animals, and/or share many similar causations, processes or pathways, the present invention may be applicable to either humans or animals or to both. Accordingly, events, activities (functions) and/or conditions referred to in humans also refer to homologous or equivalent events, functions or conditions in animals.

Neural/neurological activity (function) – Neural activities (functions) are activities (functions) controlled by the nervous system. These include the functioning of the nervous system, sensing of changes in both the internal and external environments, the interpretation of those changes and the coordination of responses. Neural activities (functions) may comprise of one or more neural events. For the purpose of the present invention the terms "activity" or

"function" are assumed to have the same meaning and are used interchangeably. Further, any reference to the term in singular form, for example, "activity" or "function" also encompasses the plural term, that is, "activities" or "functions".

Neural event – events taking place in the nervous system such as myelination, differentiation, growth, changes and cell death and includes generation and propagation of action potentials. Neural events can either be normal or abnormal.

Neurological condition – the state of a part of, or the entire nervous system. It usually refers more to abnormal or disease conditions than normal conditions.

APP, APP derivative or APP fragment – For ease of description, in the present application, any reference to APP may also apply to any APP derivative as well as to any APP fragment which maintain the same, similar, equivalent or comparable biological activity (function) of APP.

APP expression and/or activity – APP expression related to the expression of the APP encoded by the APP gene. APP activity (also indicated as "function" as defined above) relates to the APP biological activity (function). In particular, to the neural/neurological activity (function), as defined above, of APP. For instance, to the APP capacity to interact with other cellular proteins and/or exogen drug(s) or compound(s) and to modulate their or its activity (function). For example, it relates to APP capacity to modulate the activity (function) of sodium channel(s) and TAG-1. As a further example, the APP activity (function) also encompasses the cleavage of APP and the formation of the beta amyloid (Aβ).

Modulating – varying or changing a state, level, system or event. For example, in certain aspects, modulation may be by increasing or decreasing the level or expression of a molecule in a system.

Expression – The conversion of a gene into a gene product which may be RNA or protein. Accordingly, the expression of a gene product may be controlled at two levels: at the transcription level or at the translation level, to obtain a change in the prevalence of the molecular product.

Cellular component – Any part of a cell including structural and non-structural components.

Protein - A polymer of amino acids linked via peptide bonds and which may be composed of one or more polypeptide chains. A protein may also have other non-amino acid components such as carbohydrates or lipids associated with it or may be post-translationally modified (e.g. by glycosylation or phosphorylation). A protein may be processed in or outside the cell (ie *in vivo* or *in vitro*) to obtain derivatives or cleaved to form one or more protein fragments. A protein may be purified from natural sources or artificially synthesized. A protein under the present invention includes proteins that are substantially identical to it. By "substantially identical", it is meant a protein exhibiting at least 50%, preferably 85%, more preferably 90%, and most preferably 95% sequence identity to the reference protein.

Homologous – For the purpose of the present invention, a molecule is said to be homologous to a reference molecule if that molecule is able to exert or elicit a similar response in a cell or biological system as that exerted or elicited by the reference molecule. For example, a synthetic molecule having an active site similar to that of a biologically-active reference molecule may be able to exert or elicit a similar response in a cell or biological system without the synthetic molecule having to possess a similar overall chemical structure as that of the reference molecule.

Interacts/interaction – Two biological molecules are said to interact with one another when either of them causes a change in the other molecule or to itself. The change may be a physical change or a change in biological properties.

Accordingly, the interaction may be direct wherein the two molecules come into direct physical contact or the interaction may be indirect when the interaction is via one or more intermediate molecules.

Sodium channel complex refers to a complex comprising molecules which interact with sodium channel. The molecules include but are not limited to Caspr2, NgR, potassium channels, Tn-R, Tn-C, MAG, Nogo-A, phosphacan, F3, OMgp, RPTPβ, NG2 and Go protein(s).

TAG-1 complex refers to a complex comprising molecules which interact with TAG-1. The molecules include but are not limited to APP, Caspr2, NgR, K+ channels, Tn-R, Tn-C, MAG, NogoA, phosphacan, F3, OMgp, RPTPβ, NG2 and Fe65.

Description

Myelinated axons in the central nervous system (CNS) are characterized by their segmental structures: the node of Ranvier (NOR), paranode, juxtaparanode, and internode. The present inventors have surprisingly found that, contrary to previously held beliefs, APP is localized and/or aggregated at the nodes of Ranvier (NORs) of axons in the central nervous system (CNS), but not the peripheral nervous system (PNS), and interacts with sodium channels and/or TAG-1. This localization and interaction with TAG-1 reveals novel activities (functions) for APP. In particular, it reveals novel activities (functions) for APP in myelination. The interaction with at least sodium channels and/or TAG-1 also provides novel target(s) for the modulation of APP function. It also provides novel targets for the modulation of Aβ deposition in Alzheimer's disease and other diseases associated to the modulation of APP, sodium channels or TAG-1. In particular, it provides novel target(s) for diseases related with Aβ deposition. Thus, according to the method of the present invention, the inventors provide method(s) to modulate biological and/or medical events, activities (functions) and/or conditions, such as neural activities (functions),

events and/or neurological conditions, by modulating the activity (function) and/or expression of APP, its derivative or a fragment thereof, or a molecule that interacts with APP, its derivative or a fragment thereof.

The inventors also found that TAG-1 is an interacting partner of APP in the stem cell niche and accordingly provides novel target(s) for modulation of stem cell activity (function). In addition to directly revealing sodium channel(s) and TAG-1 as target(s) for modulating APP activity (function) in axons and/or stem cells, association of APP with TAG-1 and sodium channel(s) reveals numerous other targets for modulation of APP by the known association of TAG-1 and sodium channels with protein complexes. These protein complexes involve numerous molecules including Caspr2, NgR, K+ channels, TN-R, TN-C, MAG, Nogo-A, phosphacan, F3, OMgp, RPTPβ and NG2. Additionally, the findings also suggest novel means of modulating sodium channel activity (function) and hence axonal conduction that may have application in treatment of pain, in local anaesthesia, or in the treatment of neurological disorders such as epilepsy.

In particular, the inventors have found that:

(a) APP is localized at the nodes of Ranvier in the myelinated axons of the central nervous system.

(b) APP interacts with sodium channels.

(c) APP interacts with TAG-1.

(d) TAG-1 is localized on stem cells and in the stem cell niche in the brain.

The finding revealed novel targets for modulation of APP and its functions in health and disease (e.g. to treat AD or to manipulate stem cells) and novel activities (functions) of APP in myelination (e.g. in the treatment of brain or

spinal injury and MS). The invention also provides novel target(s) for modulating sodium channel activity(ies) (function/s) (e.g. to achieve analgesia, local anaesthesia, or in the treatment of neurological disorders such as epilepsy).

As mentioned above, the release of component peptides of APP, including Aβ deposition, had been thought to occur at synapses. Although some of the potential interactions of APP had been explored, the interacting partners of APP were believed to be synaptic proteins. Therefore there was no knowledge that APP interacted with sodium channels and no knowledge of the intra- and intercellular protein-protein interactions of APP with TAG-1. In addition to forming Aβ after cleavage by secretases, APP can be cleaved by to release soluble APP (sAPP). The exact activities (functions) of sAPP were unknown but it has been suggested that sAPP may act as trophic factor. Together with evidence that there are deficits in adult neurogenesis in AD, this has lead to considerable interest in the role of APP in regulating stem cell function. However, the mechanisms by which APP modulate stem cell activities (functions) such as proliferation and differentiation was unknown. In particular, the interacting or binding partners of APP in the stem cell niche were unknown.

As shown in Figure 1, the present inventors have found that APP is expressed by axons during myelination and interactions with TAG-1 places APP in the TAG-1, Caspr2, NgR, K+ channel complex and reveals targets for modulation of myelination (e.g. in treatment of multiple sclerosis or spinal inury). Figure 2 shows that APP is expressed at nodes of Ranvier and interactions with sodium channels places APP in the context of TN-R, TN-C, MAG, Nogo-A, phosphacan, F3, OMgp, RPTPβ and NG2 complexes and reveals both novel targets for modulation of APP activity (function) including amyloid deposition (e.g. in treatment of Alzheimer's disease) and novel targets for sodium

channel modulation (e.g. in analgesia, local anaesthesia and treatment of epilepsy). Figure 3 shows that TAG-1 is expressed in the stem cell niche and that APP interacts with TAG-1 reveals novel targets for modulation of stem cell activity (function) (e.g. in cytotherapeutic brain repair).

Accordingly, the present inventors provide novel means to modulate at least (a) APP, its derivative or fragment thereof, (b) Myelination, (c) Sodium channel(s) and/or (d) stem cell(s).

In particular, the present invention provides the use of drugs, peptides or other molecules interacting with sodium channel(s) to modulate APP activity (function). The modulation of APP function may be used to prevent amyloid deposition (e.g. treatment of AD), to improve and/or facilitate nervous tissue repair (e.g. treatment of spinal injury), to improve and/or facilitate myelination (e.g. in the treatment of MS), or to modulate stem cell activity (function) (e.g. for brain repair). Examples of such drugs and molecules include but are not limited to local anaesthetics (e.g. lidocaine), veratridine, batrachotoxin, scorpion toxins, sea anaemone toxin, conus toxins, saxitoxin, tetrodotoxin, antiepileptic drugs (e.g. carbamazepine and phenytoin), antiarrhythmic drugs (e.g. quinidine), antibodies to sodium channel proteins, and peptide sequences derived from APP.

There is also provided the use of APP or peptides derived from the APP sequence to modulate sodium channel function. The modulation of sodium channel activity (function) may include modulation of APP expression and/or activity (function), treatment of acute or chronic pain disorders, induction of analgesia, treatment of epilepsy or convulsions, treatment of disorder of the rhythm of the heart, or induction of local anaesthesia.

There is also provided the use of drugs, peptides or other molecules interacting with TAG-1 to modulate APP function. The modulation of APP activity (function) may either be used to prevent amyloid deposition (e.g. treatment of AD), to improve and/or facilitate nervous tissue repair (e.g. treatment of spinal injury), to improve and/or facilitate myelination (e.g. in the treatment of MS), to modulate stem cell function (e.g. for brain repair), or to modulate sodium channel activity (function) (e.g. treatment of epilepsy or induction of local anaesthesia). Examples of such molecules include but are not limited to antibodies to TAG-1 and peptides derived from APP or Caspr.

There is also provided the use of TAG-1 or peptides which mimic part of the sequence of TAG-1 to modulate APP activity (function). The modulation of APP activity (function) may either be used to prevent amyloid deposition (e.g. treatment of AD), to facilitate nervous tissue repair (e.g. treatment of spinal injury), to improve and/or facilitate myelination (e.g. in the treatment of MS), to modulate stem cell function (e.g. for brain repair), or to modulate sodium channel activity (function) (e.g. treatment of epilepsy or induction of local anaesthesia). Examples of such molecules include but are not limited to full length TAG-1 and peptides comprising subset of the TAG-1 protein sequence.

There is also provided the use of drugs, peptides or other molecules interacting with TAG-1 or sodium channel peptide complex proteins to modulate APP function. The modulation of APP activity (function) may either be used to prevent amyloid deposition (e.g. treatment of AD), to improve and/or facilitate nervous tissue repair (e.g. treatment of spinal injury), to improve and/or facilitate myelination (e.g. in the treatment of MS), to modulate stem cell function (e.g. for brain repair), or to modulate sodium channel activity (function) (e.g. treatment of epilepsy and/or induction of local anaesthesia). TAG-1 or sodium channel peptide complex proteins include but are not limited to Caspr2, NgR, K+ channels, TN-R, TN-C, MAG, Nogo-A, phosphacan, F3, OMgp, RPTPβ and

NG2. Examples of drugs, peptides or other molecules include but are not limited to peptide fragments of or antibodies to Caspr, NgR, K+ channels, TN-R, TNB-C, MAG, Nogo, phosphacan, F3, OMgp, RPTPβ and NG2.

The present invention also provides a method of detecting and/or quantitating the presence of, predisposition to, and/or severity of, a neurological condition in a subject, the method comprising: (a) providing at least one sample from a subject; (b) determining the expression and/or activity of amyloid precursor protein, its derivative or a fragment thereof; (c) comparing the expression and/or activity of the amyloid precursor protein, its derivative or a fragment thereof, with that of at least one control, a difference in expression and/or activity indicating the presence of, or predisposition to, and/or severity of a neurological condition in the subject.

The present invention also provides a method of monitoring the efficacy of a treatment for a neurological condition in a subject, the method comprising: (a) providing at least two samples from a subject, each sample obtained at different time points; (b) determining the expression or activity of amyloid precursor protein, its derivative or a fragment thereof; and (c) comparing the expression and/or activity of the amyloid precursor protein, its derivative or a fragment thereof, in the at least two samples.

The present invention also provides a method of prognosticating the outcome of a neurological condition in a subject, the method comprising: (a) providing at least one sample from a subject; (b) determining the expression and/or activity of amyloid precursor protein, its derivative or a fragment thereof; (c) comparing the expression and/or activity of the amyloid precursor protein, its derivative or a fragment thereof, with that of at least one control, a difference in expression and/or activity indicating the prognosis of a neurological condition in the subject.

The present invention also provides a method of inducing analgesia and/or anesthesia in a subject, the method comprising modulating the expression and/or activity of amyloid precursor protein, its derivative or a fragment thereof.

The present invention also provides a method of modulating differentiation of at least one stem cell, the method comprising decreasing expression and/or activity of amyloid precursor protein, its derivative or a fragment thereof, in the at least one stem cell. The decreasing may comprise administering an effective amount of a compound selected from the group consisting of TAG-1, anesthetics, toxins and Go protein(s).

There is also provided the use of conduction velocity measures as a marker for APP-sodium channel interactions and hence as a biomarker for APP malfunction and propensity for Alzheimer's disease or other amyloid-related dementia. In particular, there is also provided a method of detecting and/or quantitating the presence of, predisposition to, and/or severity of, at least one condition related to beta amyloid (Aβ) deposition and/or sodium channel dysfunction in a subject, the method comprising: (a) measuring the nerve and/or axon conduction velocity in the subject; (b) comparing the nerve and/or axon conduction velocity with that of at least one control, a difference in velocity indicating the presence of, or predisposition to, and/or severity of at least one condition related to Aβ deposition and/or sodium channel dysfunction in the subject. The method may be for detecting and/or quantitating the presence of, predisposition to, and/or severity of Alzheimer's disease (AD).

The present invention also provides at least one pharmaceutical composition for treating at least one APP and/or sodium channel related medical condition comprising at least one compound selected from the group consisting of: APP, APP derivative, APP fragment, antibody to APP, TAG-1, a TAG-1 homologous protein or fragment thereof, antibody to TAG-1, sodium channel(s), at least one

sodium channel complex protein, Caspr, Caspr derivative, Caspr fragment, anesthetic(s) toxin(s) and Go protein(s); and optionally at least one pharmaceutically acceptable diluent, carrier and/or excipient. The medical condition may be selected from the group consisting of Alzheimer's disease, multiple sclerosis, brain injury, spinal cord injury, axonal injury-related disorders, epilepsy, neurodegenerative disorders and demyelination disorders.

The present invention also provides use of at least one compound selected from the group consisting of: APP, APP derivative, APP fragment, antibody to APP, TAG-1, at least one TAG-1 complex protein, a TAG-1 homologous protein or fragment thereof, antibody to TAG-1, sodium channel(s), at least one sodium channel complex protein, Caspr, Caspr derivative, Caspr fragment, anesthetic(s) toxin(s) and Go protein(s), for the preparation of a medicament (or pharmaceutical composition) for the treatment of an APP and/or sodium channel related medical condition.

The pharmaceutical composition may further comprise at least one pharmaceutically acceptable carrier, diluent, adjuvant, excipients, or a combination thereof. Examples of suitable excipients are water, saline, dextrose, glycerol, ethanol and the like as well as combinations thereof. Such a pharmaceutical composition may consist of the active ingredient alone, in a form suitable for administration to a subject, or alternatively the pharmaceutical composition may comprise the active ingredient and one or more pharmaceutically acceptable carrier, excipient and/or diluent. Excipients normally employed for such formulations, includes mannitol, lactose, starch, magnesium stearate, sodium saccharine, cellulose, magnesium carbonate, and the like. Further carrier, diluent, adjuvant, excipient or a combination thereof known in the art may also be used for the purpose of the present invention.

The pharmaceutical composition may be for local, subcutaneous, intravenal, parenteral and/or oral administration. The pharmaceutical composition may be administered through subcutaneous and/or intramuscular injection. For oral administration, the pharmaceutical composition may be formulated as solutions, suspensions, emulsions, tablets, pills, capsules, sustained release formulations, aerosols, powders, or granulates. The dosage required depends on the choice of the route of administration; the nature of the formulation; the nature of the subject's illness; the subject's size, weight, surface area, age, and sex; other drugs being administered; and the judgment of the attending physician. Wide variations in the needed dosage are to be expected in view of the variety of compounds available and the different efficiencies of various routes of administration.

The present invention also provides a kit comprising at least one compound selected from the group consisting of: APP, APP derivative, APP fragment, antibody to APP, TAG-1, at least one TAG-1 complex protein, a TAG-1 homologous protein or fragment thereof, antibody to TAG-1, sodium channel(s), at least one sodium channel complex protein, Caspr, Caspr derivative, Caspr fragment, anesthetic(s) toxin(s) and Go protein(s), for the detection and/or diagnosis of at least one APP and/or sodium channel related medical condition and/or for the detection and/or diagnosis of at least one APP and/or sodium channel related medical condition and/or or treating and/or preventing at least one APP and/or sodium channel related medical condition.

Having now generally described the invention, the same will be more readily understood through reference to the following examples which are provided by way of illustration, and are not intended to be limiting of the present invention.

EXAMPLES

Standard molecular biology techniques known in the art and not specifically described were generally followed as described in Sambrook and Russel, Molecular Cloning: A Laboratory Manual, Cold Springs Harbor Laboratory, New York (2001).

Materials and Methods for Examples 1-10.

Antibodies

Rabbit polyclonal antibodies against Caspr (Nie et al, 2003) and monoclonal antibodies against TN-R (596, 619) (Xiao et al, 1998) and APP (Selkoe et al, 1988) were described previously. The antibodies recognise specifically APP intracellular domain (Selkoe et al., 1988). Rabbit polyclonal anti-Nav1.6, Nav$\beta_2$, pan-Nav (Alomone laboratories, Israel), monoclonal antibodies against pan-$Na^+$ channel (K58/35; Sigma), potassium channels Kv1.2 (K14/16) (Upstate, USA), and γ-tubulin (GTU88; Sigma) were obtained from the respective commercial sources.

Mutant mice

The APP knock-out (Zheng et al, 1995), APP transgenic (Hsiao et al, 1995) and PLP transgenic (Inoue et al, 1996) mice have been previously described. APP knock-out mice exhibit decreased locomotor activity and forelimb grip strength (Zheng et al., 1995), consistent with myelinated axon-related abnormalities. APP transgenic mice over-express human APP driven by the prion promoter. APP protein expression in these transgenic mice depends upon copy number (Hsiao KK, et al., 1995). The PLP transgenic mouse (PLP tg; Inoue et al., 1996; Rasband et al., 2003) is an animal model of severe demyelination.

All experiments involving mice were approved by the Institutional Animal Care and Use Committee (IACUC) of Singapore General Hospital. The experiments

involving *Xenopus laevis* oocytes were approved by the IACUC of the National University of Singapore.

Immunofluorescence (IF) labelling

Animals were perfused transcardially with 0.1M Ringer's solution and 4% paraformaldehyde in 0.1M phosphate buffer, pH 7.4 (PB) sequentially. Spinal cords were removed immediately for different subsequent preparations. For cryosection, tissues were immersed, first in 15% sucrose and then in 30% sucrose in PB. Ten micrometer-thick sections were mounted onto gelatin or poly-l-lysine coated glass slides. After being air-dried, slides were kept at -20°C for later use.

For immunofluorescence staining, tissue slices were first immersed in absolute acetone at -20°C for 20 min. Slices were then thoroughly washed in 0.1M phosphate buffered saline (PBS, pH 7.6) containing 0.3% Triton X-100. After blocking with 10% normal goat serum (NGS) diluted in PB for 1 hr, tissue slices were incubated with primary antibodies at their optimum dilutions, either overnight or 2 hrs at room temperature (RT). Cy2- or Cy3-conjugated secondary antibodies (Amersham) corresponding to the primary antibodies were used for further incubation at RT for 1 hr. For double labelling, one more cycle of labelling was similarly conducted for second primary antibodies. All labeled slices were visualized and photographed under a Leica RXA2 upright fluorescence microscope or an LSM5 Carl Zeiss confocal microscopic system.

Western blot analysis

To prepare whole extracts, frozen tissues (spinal cords and brains) were homogenized in a lysis buffer (50 mM Tris-HCl pH 7.5, 5 mM EDTA, 1% Triton X-100, and protease inhibitors (Roche Diagnostics). After ultracentrifugation (150,000 g, 4°C, 45 min), the supernatants were collected and stored at -80°C for future use. Alternatively, membrane fractions were prepared as previously

described (Nie et al, 2003). Brain tissue or cells were homogenized in ice-cold homogenizing buffer (320 mM sucrose, 10 mM Tris-HCl pH 7.4, 1 mM $NaHCO_3$ pH 7.4, 1 mM $MgCl_2$) supplemented with 1% protease inhibitor cocktail (Amersham), and subsequently centrifuged at 5,000 g for 15 min. The supernatant was collected and spun at 60,000 g (Beckman ultracentrifuge) for 60 min at 4 °C. Pellets were then dissolved in a lysis buffer (10 mM Tris-HCl pH9, 150 mM NaCl, 0.5% Triton X-100, 1% sodium deoxycholate (DOC), 0.5% SDS, 2 mM EDTA, and 1% protease inhibitor cocktail. All samples were subjected to Bradford protein assay.

Equal amounts of protein were separated on acrylamide gels and transferred onto nitrocellulose membranes. Western blotting was performed under standard conditions, applying rabbit polyclonal antibodies against APP (1:1000) and mouse monoclonal antibodies against γ-tubulin (1:1000). The latter protein was used for loading normalization. Either anti-mouse, or anti-rabbit peroxidase-conjugated secondary antibodies were applied at 1:10,000 and blots were visualized with an ECL™ detection kit (Amersham).

Electromicroscopy

Animals were transcardially perfusion-fixed with 2% paraformaldehyde - 3% glutaraldehyde in 0.1 M cacodylate buffer (pH 7.4) for electron microscopy. Spinal cords and sciatic nerves were removed and post-fixed in the same fixative solution for 2 hrs. After being finely trimmed, the samples were immersion-washed overnight. Tissue blocks were further post-fixed in 1% osmium tetroxide ($OsO_4$) containing 1.5% potassium ferrocyanide for 2 hrs, and thereafter subjected to dehydration in ascending series of alcohol and acetone. After undergoing gradual infiltration with Araldite 502 (EMS), the blocks were embedded and polymerized overnight at 60°C. Ultrathin sections (~90 nm in thickness) were placed on 200-mesh copper grids and counterstained with uranyl acetate and lead citrate. All samples were examined and photographed

under a Jeol 1220 electron microscope. The *g* ratios were calculated from more than 50 myelinated axons per mouse (n = 3).

Plasmid construction and cRNA transcription

The vector pD4GL, a modified version of the pcDNA4A vector (Invitrogen) that contains the *Xenopus* β-globin untranslated regions, was used to boost expression in oocytes. Here, the *Xenopus* β-globin 5′ and 3′ untranslated regions were subcloned into the pcDNA4A vector. cDNAs encoding the rat β1 and β2 subunits (provided by Lori Isom, University of Michigan), the AICD domain (SEQ ID NO: 4 cDNA; SEQ ID NO: 7,peptide), C-terminal fragment C31 domain (SEQ ID NO: 8, cDNA; SEQ ID NO: 10, peptide), G protein Go binding domain (SEQ ID NO: 11; SEQ ID NO: 14, peptide), Fe65 binding domain (SEQ ID NO: 15, cDNA; SEQ ID NO: 18, peptide) and a short peptide motif Val667-Arg672 (SEQ ID NO: 19 cDNA;SEQ ID NO:22, peptide) were inserted between these two regions. To facilitate translational recognition by ribosomes, a Kozak sequence was added to around the start codon (GCCACCATGG) (SEQ ID NO:1) for oocyte expression. The pLCT1-Scn8a plasmid containing mouse Nav1.6 cDNA was provided by Dr. Alan L. Goldin (University of California, Irvine). The plasmid containing cDNA of Nav1.5 α subunit of sodium chanenels was provided by Dr. A. L. George (Vanderbilt University, Nashville). The plasmid encoding the human App695 cDNA was provided by Dr. Carsten Schmidt (University of Hamburg).

The AICD domain (forward primer: 5'-TTTGGTG AAGCTT GCCACCATG GTG ATG CTG AAG AAG AAA CAG TAC-3' (SEQ ID NO: 5); reverse primer: 5'-GGCG GCGGCCGC CTA GTT CTG CAT CTG CTC AAA GA-3' (SEQ ID NO: 6) G protein Go binding domain (forward primer: 5'-GCGC AAGCTT GCCACC ATG CATCATGGTGTGG TGGAGGTTG-3' (SEQ ID NO: 12); reverse primer: 5'- GGCG GCGGCCGC CTA CTT GGA CAG GTG GCG CTC CTC-3(SEQ ID

NO: 13), C-terminal C31 domain (forward primer: 5'-GCGC AAGCTT GCCACC ATG GCCGCTGTCACCCCAGAGGAG-3' (SEQ ID NO: 9); reverse primer: 5'GGCG GCGGCCGC CTA GTTCTGCATCTGCTCAAAGA-3'(SEQ ID NO: 6), Fe65 binding domain (forward primer: 5'-GCGC AAGCTT GCCACC ATG GTCACCCCAGAGGAGCGCCAC-3'(SEQ ID NO: 16); reverse primer: 5'-GGCG GCGGCCGC CTA CTTGTAGGTTGGATTTTCGT-3' (SEQ ID NO: 17), Val667-Arg672 motif (forward primer: 5'-AGCTT GCCACC ATG GTC ACC CCA GAG GAG CGC TAG GC-3'(SEQ ID NO: 19); reverse primer: 5'-GGCCGC CTA GCG CTC CTC TGG GGT GAC CAT GGTGGC A-3'(SEQ ID NO: 20) were obtained from the full length human APP-695(SEQ ID NO: 2).

Plasmids were purified using QIAGEN Plasmid Maxi Kit (QIAGEN). All these purified constructs were linearized, and cRNAs were synthesized in vitro using the mMESSAGE mMACHINETM T7 cRNA synthesis kit (Ambion). The concentration of cRNA was determined from OD (260 nm).

Expression and electrophysiological recording in oocytes

Stage V oocytes were surgically removed from mature female *Xenopus laevis* (Xenopus Express, France) anaesthetized with 1 g/L tricane methanesulphonate (Sigma, USA). Segments of ovarian lobe were removed by a small abdominal incision. The follicular layer was removed by digestion for 90 min with 2 mg/ml collagenase type V (Sigma, USA) in $Ca^{2+}$-free Barth's solution containing (mmol/L) NaCl 88, KCl 1, $NaHCO_3$ 2.4, $MgSO_4$ 0.82, Tris/HCl 5; pH 7.4 with NaOH; supplemented with 50 µg/ml gentamicin sulphonate). The oocytes were placed in 96-well plates and incubated at 19°C in Barth's solution overnight. On the following day oocytes were injected (Roboocyte, Multichannel Systems, Germany) with cRNAs. RNA was dissolved in 1 mM Tris-HCl, pH 7.5. The molar ratio of α to β subunits was 1:10, while that of the α subunit to APP was 1:1. The oocytes were then incubated at 19°C. Membrane currents were recorded from oocytes with the two-microelectrode voltage-clamp technique at

room temperature (19°C to 21°C) 2 to 3 days after injection of cRNA. Both injection and recording were performed using Roboocyte (Multi Channel Systems, Germany). Current injecting and potential measuring electrodes had resistances of 0.1 to 0.7MΩ when filled with 3 mol/L KCl. Data acquisition was performed with a GeneClamp 500B two-electrode voltage clamp amplifier connected to a Digidata 1322A interface and controlled with pClamp 9.2 software (all from Axon Instruments, Inc., Foster City, CA). Oocytes were perfused with ND96 solution containing (mmol/L) NaCl 96, KCl 2, $CaCl_2$ 1.8, $MgCl_2$ 1, and HEPES 5 (adjusted to pH 7.4 with NaOH). Oocytes were kept in current-clamp mode for at least 2 minutes before switching to voltage-clamp mode. All recordings were obtained after stable baseline and ionic current levels were achieved. Data was sampled at 50 kHz after filtering at 5 kHz with a 4-pole Bessel filter. The leakage current was digitally subtracted on-line using hyperpolarizing control pulses, applied before the test pulse, of one-fourth-test pulse amplitude (–P/4 procedure).

Oocytes were held at -100 mV and 45 ms steps to command potentials between -75 mV and 40 mV were made in 5 mV increments to assess the current-voltage (I-V) relationship. Activation was assessed by calculating conductance using the equation $G = I/(V-E_{Na})$ (where I is the peak current amplitude at command potential V and $E_{Na}$ is the equilibrium potential for $Na^+$ under our experimental conditions) and fitting the data to a Boltzmann distribution function: $G_{Na} / G_{Na,max}=1/[1+\exp(V_{1/2} - V_m)/k]$, where $G_{Na}$ is the voltage-dependent sodium conductance, $G_{Na,max}$ is the maximal sodium conductance, $V_{1/2}$ is the potential at which activation is half-maximal, $V_m$ is the membrane potential, and k is the slope. For statistical analysis, the peak current amplitude was recorded for each oocyte. Inactivation was assessed with a series of pre-pulses (-120 to 10mV) lasting 500 ms from the holding potential of -100mV, followed by a 25 ms depolarization to -10 mV. The normalized curves were fitted using a Boltzmann distribution equation ($G_{Na} / G_{Na,max}=1/[1+\exp(V_m$ -

$V_{1/2}$)/k]). Recovery from inactivation was assessed with two 50 ms pulses to -10 mV from the holding potential of -100 mV, with a variable recovery time period at -100 mV, in the range of 1 to 30 ms. Curves were fitted with a single rising exponential function.

All data are expressed as mean ± SEM. Student's *t* test was used to test for statistical significance of effects on peak current amplitude and $V_{1/2}$. Two-way ANOVA for effects of APP and recovery time was used to analyze the data on recovery from inactivation. A value of $p < 0.05$ was considered significant.

Electrophysiological recordings of dorsal root ganglion neurons

Acutely isolated dorsal root ganglion (DRG) neurons were prepared from the sensorimotor cortex of anesthetized and then decapitated adult $APP^{+/+}$ and $APP^{-/-}$ C57BL mice. The lumbar segments of vertebrate column were dissected. The DRGs, together with the nerve roots, were quickly removed and transferred immediately into Dulbecco's modified Eagle's Medium (DMEM, Gibco, Carlsbad, CA). After removal of attached nerves and surrounding connective tissues, the DRGs were minced with fine spring scissors and the ganglion fragments were placed in a flask containing 1.5 ml of DMEM in which trypsin (type III, 0.5 mg/ml, Sigma, St. Louis, MO), collagenase (type I, 1 mg/ml, Sigma) and DNase (type I, 0.1 mg/ml, Sigma) had been dissolved. After incubation at 35°C in a shaking water bath for 30 min, soybean trypsin inhibitor (type II-s, 1.25 mg/ml, Sigma) was then added to stop trypsin digestion. DRGs were carefully removed by Pasteur pipette and placed in bath solution containing (in mM): 140 NaCl, 3 KCl, 1 $MgCl_2$, 1 $CaCl_2$, 0.1 $CdCl_2$, and 20 HEPES, pH 7.3 adjusted to 320 mosmol/l with glucose. The DRGs were mechanically dispersed (5 strokes up and down) with a 1-ml pipette and plated onto a 35- mm culture dish and kept for at least 30 min before electrophysiological recordings. All recordings were made at room temperature (20-24°C) within 10 h after dissociation to keep the experiment as similar to *in vivo* as possible.

Current signals from acutely isolated DRG neurons, recorded in whole cell voltage clamp mode, were sampled at 20 kHz and filtered at 5 kHz using a MultiClamp 700A amplifier in conjunction with a Digidata 1322A interface and pClamp 8.1 software (all from Axon Instruments, Inc., Foster City, CA). Micropipettes were pulled from borosilicate glasses (Boralex) with a Flaming Brown micropipette puller (P2000, Sutter Instrument, Novato, CA) an electrode resistance ranging from 2 to 5 MΩ. The pipette solution contained (in mM) 140 CsF, 1 EGTA, 10 NaCl, and 10 HEPES, pH 7.3, and was adjusted to 310 mosmol/l with glucose. $CdCl_2$ in bath solution was used to block $Ca^{2+}$ currents. To eliminate the small residual sustained outward current that was seen at very depolarizing pulses, in some experiments we included 10 and 20 mM TEA in bath and pipette solutions, respectively, and CsF concentration was decreased to 120 mM in the pipette solution. The pipette potential was zeroed before seal formation, and the voltages were not corrected for liquid junction potential. Capacity transients were cancelled, and series resistance was compensated (75–80%) as necessary. The leakage current was digitally subtracted on-line using hyperpolarizing control pulses, applied before the test pulse, of one-fourth test pulse amplitude (P/4 procedure). Data are presented as means ± S.E and statistical analyses were performed using the Student's t test (significance at least $p < 0.05$).

Voltage protocols were as follows. Standard current–voltage (I–V) families were obtained using 50 msec pulses from a holding potential of -110 mV to a range of potentials (-60 to 50 mV) in 10-mV increments. The peak value at each potential was plotted to form I–V curves. Activation curves were fitted with the following Boltzmann distribution equation: $G_{Na} / G_{Na,max}=1/[1+\exp(V_{1/2} - V_m)/k]$, where $G_{Na}$ is the voltage-dependent sodium conductance, $G_{Na,max}$ is the maximal sodium conductance, $V_{1/2}$ is the potential at which activation is half-maximal, $V_m$ is the membrane potential, and k is the slope. Availability protocols consisted of a series of pre-pulses (-100 to 10mV) lasting 100 ms from the

holding potential of -70mV, followed by a 100 ms depolarization to -10 mV. The normalized curves were fitted using a Boltzmann distribution equation: $I_{Na}/I_{Na,max}=1/[1+\exp((V_m-V_{1/2})/k)]$, where $I_{Na,\ max}$ is the peak sodium current elicited after the most hyperpolarized prepulse, $V_m$ is the preconditioning pulse potential, $V_{1/2}$ is the half-maximal sodium current, and k is the slope factor. For recovery from inactivation experiments, two 40 ms stimuli were given to -10 mV from the holding potential of -110 mV, with a variable recovery time period at -110 mV, in the range of 1 to 400 ms. Curves were fitted with a double rising exponential function.

Conduction velocity recording

Electrophysiology for spinal cord

Conduction properties of myelinated axons were examined in acutely isolated spinal cords of C57BL/6 mice, using a double grease-gap technique (Coetzee et al, 1996). The spinal cord was placed in a Plexiglas chamber, with the central channel (15 mm wide) superfused by flowing, oxygenated Krebs' solution and the two ends isolated by grease gaps in chambers containing isotonic (120mM) potassium chloride solution. Silver/silver chloride electrodes were used to record the potential across one gap and to stimulate the spinal cord across the other. This provided a stable recording and stimulating arrangement with a fixed conduction distance of 15 mm for the spinal cord. The animals were anesthetized, and then decapitated and the spinal cord extracted by rapid laminectomy and washed in oxygenated Krebs' solution (NaCl 119mM, KCl 2.5mM, $NaH_2PO_4$ 1mM, $MgSO_4$ 1.3mM, $CaCl_2$ 2.5mM, D-glucose 11mM, $NaHCO_3$ 26.2mM, equilibrated with 95% $O_2$, 5%$CO_2$). The cord was incubated in Krebs' solution at room temperature for at least 1 hr, and then mounted in a recording chamber. The temperature of chamber was raised to 32°C and 37°C, and a series of recordings were made to stimulation that was adjusted to 10%

above the level that elicited a maximum response. The data were digitized at 20 kHz for subsequent analysis.

Electrophysiology for sciatic nerve

Sciatic nerves were dissected immediately after animals were killed and placed in oxygenated Krebs' solution. Nerves were then transferred to a recording chamber that was continuously perfused with oxygenated Krebs' solution. Stimulation was delivered onto one end of nerve by a concentric bipolar electrodes (Frederick Haer Co., Bowdoinham, ME, USA) and the other end of the nerve was drawn into a suction electrode for recording action potentials (Stys et al, 1991). Compound action potential of nerve recorded by suction electrode (Weber, 1999).

Electrophysiological recordings of Nav1.6 cell line

Whole-cell voltage-clamp recordings were performed in a human embryonic kidney 293-cell line stably expressing human Nav1.6 (Oliveira et al., 2004) using a Port-a-Patch NPC1 (Nanion Technologies GmbH, Munich, Germany) and Multiclamp700A amplifier (Axon Instruments (Molecular Devices), CA, USA). The external, internal and seal enhancer solutions were as supplied by Nanion. The VTPEER peptide was synthesised (Anaspec) and dissolved in internal solution. Capacity transients were cancelled, and series resistance was compensated by 85–90%. Leakage current was digitally subtracted on-line using a hyperpolarizing potential supplied after the test pulse (P/4 procedure). Currents were acquired at a sampling rate of 20 kHz via a Digidata 1322A series interface (Axon Instruments (Molecular Devices), CA, USA) controlled by pClamp 9.2 software (Axon Instruments (Molecular Devices), CA, USA) and filtered at 5 kHz. All experiments were performed at room temperature (21–24°C).

Voltage protocols were implemented at predetermined intervals after going whole cell. Briefly, standard current–voltage (I–V) families were obtained using 40ms pulses from a holding potential of -120mV, to a range of potentials (-65 to-60mV) every 5s. The peak value was plotted to form I–V curves. To plot I-V relationship, the currents at each potential were normalized to pre-treatment peak current. Activation curves were fitted with the following Boltzmann distribution equation: $G_{Na}=G_{Na,max}/(1/\exp(V_{1/2}-V_m)/k)$, where $G_{Na}$ is the voltage-dependent sodium conductance, $G_{Na}$, max is the maximal sodium conductance, $V_{1/2}$ is the potential at which activation is half-maximal, $V_m$ is the membrane potential, and k is the slope. Availability protocols consisted of a series of prepulses (-120 to +20mV) lasting 500ms, from the holding potential of -90mV, followed by a 40ms depolarization to -10mV, every 10s.The normalized curves were fitted using a Boltzmann distribution equation: $I_{Na/INa,max}=1/(1/\exp((V_m-V_{1/2})/k))$, where $I_{Na,\ max}$ is the peak sodium current elicited after the most hyperpolarized prepulse, $V_m$ is the preconditioning pulse potential, $V_{1/2}$ is the half-maximal sodium current, and k is the slope factor. For recovery from inactivation experiments, two 40 ms stimuli were given to -10 mV from the holding potential of -120 mV, with a variable recovery time period at -120 mV; in the range of 1 to 400 ms. Curves were fitted with a double rising exponential function.

Example 1 – Distribution of APP

Myelinated axons in the CNS are characterized by their segmental structures: the node of Ranvier (NOR), paranode, juxtaparanode, and internode. We used an antibody against the APP intracellular domain to (Selkoe et al, 1988) to investigate the distribution of APP along myelinated axons of both CNS and PNS. In longitudinal sections of the ventral part of adult rat spinal cord, APP immunoreactivity (green) was confined specifically to NORs along myelinated axons (Fig. 4). As evidenced by double immunofluorescence (IF) labelling, the

APP staining (green) was flanked by juxtaparanodal K+ channels Kv1.214 (Kch; red; Fig. 4a, d, e, f, and g) and co-localized with Tn-R6 (red; Fig. 4b, h, i, j, and k) and Na+ channels (Nach; red; Fig. 4c), two specific nodal molecules. Similar nodal localization of APP was also observed in optic nerve and other brain areas (not shown). The specific labelling of APP in NORs was undetectable after the antibody was pre-incubated with APP protein. The number of nodes labelling for APP was quantified relative to labelling with an antibody to the axonal marker, Kv1.2. The ratio of APP to Kv1.2, reflecting the portion of APP in all NORs, was above 95 % (Fig. 8), implying that APP is located at almost every NOR in the CNS. As the APP antibody applied for the IF staining recognizes the intracellular domain and the axon is exposed at the NORs in the CNS, these observations indicate that the clustered nodal APP is most likely mainly in axons. APP is also expressed in the PNS (Golde et al, 1990). However, in contrast to APP's nodal location in the CNS, APP immunoreactivity (green) was evenly distributed (Fig. 5) along adult rat sciatic nerve. This was shown by double IF labelling with NF200 (red; Fig. 5a), an axonal marker, or juxtaparanodal K+ channels Kv1.2 (red; Fig. 5b). Moreover, the nodal location of APP in the CNS was further investigated in longitudinal sections of the ventral part of spinal cords from APP knock-out mice16 by double IF labelling of Tn-R and APP or Caspr, a specific paranodal molecule, or Caspr and Nach (sodium channels). At NORs, APP clusters were absent in sections from APP knock-out mice (Fig. 5c). However, Tn-R, Nach, and Caspr clusters remained in the mutant mice (Fig. 5d and e). These experiments demonstrate that axonal APP is a novel component of NORs and its clustering occurs specifically in the CNS, but not in the PNS. Further, these observations demonsrate that nodal APP has no effects on the clustering of Tn-R, sodium channels and caspr in the nodal regions of the CNS.

Example 2 - distribution and expression profile of APP during development

Myelination is a dynamic process mediated by bidirectional axoglial interactions that are involved in the clustering of axonal molecules, such as Na+ channels, F3/contactin, and OMgp, at NORs (Salzer 2003; Ma et al., 2007). We investigated the distribution and expression profile of APP during development, especially in relation to the advance of myelination and nodal formation. As illustrated by Western blotting analysis (Fig. 19A), APP was expressed in brain as early as at birth (P0); however, it was greatly up-regulated between postnatal day 5 (P5) to day 21 (P21). The time course of APP appearance parallels the time frame for myelination (Huber et al, 2002), suggesting a role for APP in myelination. Moreover, IF studies were performed to correlate aggregation of APP with Na+ and K+ channel clustering during nodal maturation. At P6, when Na+ channels start clustering at NORs, APP was diffusely distributed along axons (Fig. 6a). APP was distributed along axons and appeared to start clustering in the NORs around P10 (Fig. 6b) and was prevalent at nodes after P15, when the nodal structure has been formed (Fig. 6c and d). These observations indicate that APP clustering lags behind the Na+ channel clustering in the CNS. The intensity of APP nodal clustering was quantified in relation to Kv1.2 during development. The ratio of APP to Kv1.2, reflecting the developmental progress of APP clustering in the population of axons, was 50% at P10, 60% at P15 and P21, and 90% at 2 months (Fig. 7), implying that APP clustering also occurs latter than the K+ channel clustering in the CNS.

Example 3 - nodal accumulation of APP relies on the integrity of distinct axonal domains

APP has long been utilized as a marker for axonal degeneration following neural injury (Kuhlmann et al, 2002). In the spinal cord of EAE mice, APP co-localizes extensively with Nav1.6 and to a lesser extent with Nav1.2 sodium

channels at sites of axonal injury. This is evidenced by diffuse distribution of both APP, Nav 1.6 and, to a lesser extent, Nav1.2 along demyelinated axons and an increase in the number of diffusely APP-positive axons (Craner et al, 2004). These observations suggest a spatial relationship between APP and these two nodal channels in this pathological condition. IF was performed using the spinal cord of 7-month-old PLP transgenic mice (PLP tg) (Rasband, 2003; Inoue et al.,1996), an animal model of severe demyelination. In PLP tg mice, double labelling of K+ channels (red) or the 200 kDa neurofilament (red), two axonal markers, with APP (green) revealed that APP clustering completely disappeared in demyelinated axons (Fig. 19B). Given that APP clustering along axons is severely disrupted in PLP tg mice as well as in the EAE model, these results support the notion that nodal accumulation of APP relies on the integrity of distinct axonal domains. Together, the above observations in both physiological and pathological animal models demonstrate that, similar to the clustering of Na+ channels and other axonal molecules at NORs, APP nodal aggregation along CNS myelinated axons requires axoglial interactions.

Example 4 – APP regulates axonal size and myelin thickness

APP knock-out mice exhibit decreased locomotor activity and forelimb grip strength (Zheng et al, 1995), consistent with myelinated axon-related abnormalities. Given the nodal location of APP and its expression pattern in the CNS during myelination, we analyzed the spinal cord from 3-month-old APP knock-out mice by electron microscopy (EM) to investigate that APP plays a role in the development of myelinated axons. No axonal swelling was found in mutant mice at this age (Fig. 9b). Both axon and fiber diameters were significantly reduced in the spinal cord of the knock-out mice versus wild-type mice (Fig. 20a and b; Fig. 9c). However, the g ratio (the numeric ratio between the diameter of the axon and the outer diameter of the myelinated fiber (Michailov, 2004) was significantly increased in the spinal cord of the knock-out

mice 0.829 ± 0.002) in comparison to wild-type mice (0.817 ± 0.002) (Fig. 9c; p < 0.001). To thoroughly characterize the role of APP in determining myelin thickness, we grouped the myelinated fibers by the axon diameter (<1.0 μm; 1.0~1.5 μm; 1.5~2.0 μm; 2.0~2.5 μm, 2.5~3.0 μm; 3.0~4.0 μm; and >4.0 μm). The g ratio showed that the hypomyelination in APP knockout mice was significant in all axons (Fig. 20c). These observations suggest that, as an axonal molecule, APP not only regulates axonal size, but also myelin thickness.

Moreover, the degree of peripheral myelination in the sciatic nerve from APP wild-type and knock-out mice was analysed by using EM. In wild-type mice, the average g ratio was 0.715 ± 0.002 whereas myelin in APP-/- mice was significantly thinner (p < 0.001) with a g ratio of 0.754 ± 0.038 (Fig. 10), indicating a thinner myelin sheath encapsulating the axons. The analysis of g ratios across all axon sizes was done. The reduction in the myelin sheaths occurred in nearly all axons, as illustrated by increased g ratios in axons of all sizes, but was more significant in small to medium sized axons (2.0 μm to 7.0 μm; p< 0.01; Fig. 21). Thus, APP plays a common role in promoting myelination in both CNS and PNS.

Example 5 – APP plays a role in myelination of axons

We analyzed spinal cords from 3-month-old transgenic mice that overexpress human APP. Driven by the prion promoter, APP protein expression in these transgenic mice was previously reported to depend upon copy number (Hsiao et al, 1995). No axonal swelling was found in these mutant mice at this age (Fig. 11b). Interestingly, both axon and fiber diameters were significantly increased (FIG. 22a and b), while the g ratio was significantly decreased in the transgenic mice (Fig. 11c) compared to wild-type mice. Although the APP knock-out and transgenic over expression mice have different strain backgrounds (C57BL/6 and FVB/N, respectively), the reversible changes in axon and fiber diameters

and myelin thickness between these two mutants have been confirmed after normalization with their respective wild-type littermates (Fig. 12a, b, and c). Together, these data demonstrate that APP plays a positive role in the development of myelinated axons.

Example 6 – APP interacts with sodium channels

Voltage-gated Na+ channels consist of a pore-forming α subunit and at least one β subunit that regulates channel behavior and surface expression (Catterall, 2000). Among the nine functionally expressed members of the α subunit family, Nav1.6 produces both transient and persistent currents (Rush et al, 2005) and localizes predominantly at adult NORs, but not in the internodal region of myelinated axons (Caldwell, 2000). Na+ channel β1 and β2 subunits also localize at NORs (Chen et al, 2004).

The inventors coexpressed Nav1.6 with full length APP in various molar ratios in *Xenopus laevis* oocytes to investigate whether APP could act as a β subunit of sodium channels. Notably, the increase in the sodium current in the presence of APP was not in a dose dependent manner, indicating that APP does not act as a β subunit of sodium channels (Fig. 28).

Sodium channesl $\beta_1$ and β2 were previously reported to localize at NORs (McEwen and Isom, 2004). To investigate these interactions of APP with Nav1.6 and the roles of β subunits in regulation of APP dependent sodium currents, the inventors co-expressed full length APP with the Nav1.6 α subunit alone or together with the β1 and β2 subunits either individually or in combination in *Xenopus laevis* oocytes. The inventors also co-expressed APP with Nav1.5 α subunit. Na+ currents were activated by stepped depolarisations. Greater currents were obtained in the presence of APP than in the absence of APP for all subunit combinations (Fig. 13a and b, 14a and b, 15a and b, and 16a and b). Greater currents were obtained for Nav1.6 in the presence of APP

(Fig. 13b), but not after control injection of cRNA for the reverse sequence (Fig. 13g) nor for Nav1.5 (Fig. 13f) Populations of oocytes were sampled from four frogs for each expression combination. To plot the current-voltage (I-V) relationship, the currents were normalised to the mean peak current in the absence of APP for each frog. The I-V curves confirmed that the currents were greater in the presence of APP than in the absence of APP (Fig. 13b, 14b, 15b, and 16b). For statistical analysis, the peak current in each oocyte was determined. APP increased the peak current 1.74 ± 0.11 fold on expression of the α subunit alone (FIG. 23a; $p < 0.001$), 2.38 ± 0.55 fold on expression of the α subunit and β1 subunit in combination (FIG. 23b; $p < 0.001$), 1.84 ± 0.21 fold on expression of the α subunit and β2 subunit in combination (FIG. 23c; $p < 0.001$), and 2.47 ± 0.22 fold on expression of the α subunit together with both β1 and β2 subunits (FIG. 23d; $p < 0.001$). The increase in the current in the presence of APP appeared to be greater when the β1 subunit was expressed as the sole β subunit (Fig. 14b, FIG. 23b) or in combination with the β2 subunit (Fig. 16b, FIG. 23d). Conductance was calculated from the I-V data and activation curves were fitted with a Boltzmann function to estimate V1/2, the potential at which activation is half-maximal (Fig. 13c, 14c, 15c, and 16c).

APP had no significant effect on activation when expressed together with the α subunit alone (Fig. 13c) or the α and β2 subunits (Fig. 15c), but shifted V1/2 to the left when the β1 subunit was expressed together with the α subunit (from –41.03 ± 2.3 in the absence of APP to –47.86 ± 1.60 in the presence of APP; $p < 0.005$; Fig. 14c) or together with the α and β2 subunits (from -42.80 ± 1.68 in the absence of APP to –51.67 ± 1.60 in the presence of APP; $p < 0.005$; Fig. 16c).

Inactivation protocols consisted of a series of pre-pulses followed by a short depolarisation. The normalized curves were fitted using a Boltzmann distribution equation. The presence of APP had no significant effect on the Na+ inactivation currents (Fig. 13d, 14d, 15d, and 16d). For recovery from inactivation

experiments, two pulses were applied with a variable recovery time (1 to 30 ms) at a holding potential of -100 mV. Curves were fitted with an exponential function. The presence of APP had no significant effect on the recovery from inactivation currents in the presence of the α subunit alone (Fig. 13e) or together with the β1 subunit (Fig. 14e). However, APP accelerated recovery in the presence of the β2 subunit when expressed as the sole beta subunit (ANOVA APP effect, $F_{1,1080} = 147.4$, $p < 0.001$; Fig. 15e) or together with the β1 (ANOVA APP effect, $F_{1,1200} = 115.1$, $p < 0.001$; Fig. 16e).

These data demonstrate that APP specifically increased Nav1.6 currents in *Xenopus* oocytes whether the channel was expressed with the α subunit alone or with the β1 or β2 subunits present. APP appeared to cause a greater increase in Na+ currents and produced a shift in the activation current towards more negative potentials only in the presence of the β1 subunit, whether as the only β subunit or in combination with the β2 subunit. APP accelerated recovery from inactivation only in the presence of the β2 subunit, whether as the only β subunit or in combination with the β1 subunit. Together these data suggest that APP interacts both with the α subunit alone and with the β subunits.

Example 7 – Whole cell recordings from DRG neurons

Next, we performed whole cell recordings from DRG neurons that were acutely isolated from APP knockout and wild type mice. After pharmacological suppression of voltage-dependent Ca2+ and K+ currents with Cd2+ and Cs+, respectively, fast Na+ currents were activated by stepped depolarizations (Fig. 4Aa top). To determine the I-V relationship of the Na+ current, the peak current amplitude at each voltage step was normalized to the neuron's capacitance and plotted as a function of the command potential (Fig. 17a bottom). As capacitance is related to cell size, correction for capacitance in this manner should reflect changes that are attributable to difference in cell size in the knockout mice .

Na+ current densities were significantly decreased in DRG neurons from APP knockout mice versus wild-type mice ($p < 0.05$). The activation curve of the Na+ conductance was constructed from the current-voltage relationship. There was no difference in the activation of Na+ currents in the wild type and APP-deficient mice ($p > 0.05$; Fig. 17b). Steady-state inactivation of Na+ currents was determined. Current amplitudes were expressed as a fraction of the maximal current amplitude and plotted as a function of the prepulse potential. Steady-state inactivation did significantly differ between the wild-type and APP-deficient mice (Fig. 17c). Recovery from inactivation was studied by gradually increasing the interval (1 to 400ms) between two depolarising test pulses.

The peak amplitude of the second Na+ current response divided by the response at the maximal interval was then plotted as a function of the interpulse interval. As shown in Fig. 17d, there was no significant difference in recovery from inactivation between the two groups. Thus, these observations indicate that APP positively modulates Na+ current density in mammalian cells. The β subunit-dependent effects of APP on activation and recovery from inactivation suggested by the experiments in *Xenopus* oocyte were not replicated in the mammalian cells. This may be explained by differences in Nav1.6 regulation in *Xenopus* oocytes and mammalian DRG or by the presence of additional native Na+ channel subtypes in the mammalian DRG. Nevertheless, the observations on Na+ current amplitude in *Xenopus* oocytes and mammalian DRG are consistent and indicate that APP positively modulates Na+ currents. The effect of APP on Na+ currents is unlikely to be due to changes in cell size as, in the DRG recordings, changes were still seen in current densities corrected for whole-cell capacitance. The effect of APP on Na+ currents reflects either increased expression of Na+ channels in the cell membrane or increased conductance of individual Na+ channels in the presence of APP.

Example 8 – APP modulates CNS action potentials

The congregation of specific ion channels and cell recognition molecules, such as Na+ channels and F3/contactin, at NORs, is critical for the rapid saltatory conduction of nerve impulses. To further explore the physiological role of clustered APP in the CNS, we recorded compound action potentials of APP knock-out versus wild-type mice. We used a double grease-gap chamber (fixed conduction distance (Coetzee et al, 1996) and suction electrode (Kazarinova-Noyes, et al., 2001) to measure CAPs from spinal cord and sciatic nerve, respectively. The time-to-peak for each trace was then measured and converted to a conduction velocity.

The average velocity in wild-type mice was faster than those from the mutant mice at all temperatures measured. At 24°C, the conduction velocity of control spinal cord was 12.83 ± 0.42 ms-1 (n = 8) and that of APP-deficient spinal cords was 11.34 ± 0.49 ms-1 (n = 11) ($p < 0.05$; Fig. 18a). At 37°C, the conduction velocities were 22.69 ± 0.10 ms-1 (n = 8) in wild-type mice and 18.53 ± 0.77 ms-1 (n = 11) in APP-deficient mice ($p < 0.005$, Fig. 18a). Moreover, we tested sciatic nerves from APP knock-out and wild-type mice as a control using suction electrodes to measure CAPs from sciatic nerves.

The conduction velocities at 24°C in nerves from the wild-type mouse averaged 22.23 ± 1.71 ms-1 (n = 6); in the APP-deficient mouse they averaged 20.24 ± 1.31 ms-1 (n = 11). At 37°C, the velocities were 33.05 ± 2.13 ms-1 (n = 6) in the wild-type mouse and 29.93 ± 1.48 ms-1 (n = 11) in the APP-deficient mouse. In these experiments the APP-deficient mouse consistently had a slight slower conduction velocity, but the difference was not significant (Fig. 18b). Given that APP clustering only occurs in the CNS, the significant change of nerve conduction in the mutant spinal cord, but not sciatic nerve, implies that the clustered APP is an important factor that plays a specific role in modulation of the CNS action potentials.

According to the present invention, by influencing the expression of APP, its fragments and derivatives, and that of molecules, cellular components, drugs and/or antibodies that interact with APP, its fragments and derivatives, many biological and medical events, functions and conditions, particularly neurological conditions, may be treated.

The expression of Nav1.6 sodium channel α subunit is abnormally downregulated in the CNS of APP null mice.

In the adult, Nav1.6 is the predominant_α subunit of sodium channels that locate at CNS NORs (Salzer, 2003). As the conduction velocities of compound action potentials is abberantly reduced in the *APP*$^{-/-}$ spinal cord, the present inventors ascertained as to whether there might be differences in the level of Nav1.6 expression between *APP*$^{-/-}$ mice and their wt littermates. Western blot results showed that the expression of Nav1.6 was abnormally decreased in the brain in *APP*$^{-/-}$ mice versus *APP*$^{+/+}$ and *APP*$^{+/-}$ littermates (Fig. 24). Together, the abnormal changes in locomotor activity, forelimb grip strength (Zheng et al., 1995), nerve conduction, and Nav1.6 expression in the *APP*$^{-/-}$ mice (Fig. 18 and Fig. 24) strongly imply that APP may act as a specific modulator of Nav1.6 at the CNS NORs.

Example 9 - VTPEER domain of APP increases sodium current expression in *Xenopus* oocytes expressing the Nav1.6 sodium channel α subunit.

The present inventors also determined which domain(s) in APP could involve in increment of sodium current expression in *Xenopus* oocytes expressing the Nav1.6 sodium channel a subunit. APP intracellular domain (AICD; X. Cao and Südhof (2001), Go protein-binding domain (GB; $H^{657}$-$K^{676}$ of APP-695; Nishimoto et al., 1993; Brouillet et al., 1999), Fe65 binding domain (Fe65BD; $V^{666}$-$Y^{686}$;Ermekova et al., 1997), and C31 domain (C31; $A^{664}$-$N^{695}$; Lu et al.,

2000; Figure 25) were constructed and coexpressed with the Nav1.6 a subunit in *Xenopus laevis* oocytes, respectively.

Interestingly, all the intracellular domains, including AICD, GB, Fe65BD, and C31, increased the peak sodium current (Fig. 26 a to d), but control injfection of cRNAs for their reverse sequences did not.

Given that VTPEER is a common overlapped peptide sequence in the AICD, GB, Fe65BD, and C31, the inventors further coexpressed this peptide with the Nav1.6 a subunit in *Xenopus laevis* oocytes. Notably, similar to full length APP and other intracellular domains, VTPEER increased the peak sodium current as well (Fig. 26e; Figure 25). All the intracellular domains had no significant effect on activation, inactivation or recovery from inactivation (Figure 28). To further confirm the role of the peptide in modulating sodium currents, the inventors chemically synthesised VTPEER peptide and measured its effects in a human embryonic kidney 293-cell line stably expressing human Nav1.6 (Oliveira et al., 2004). Consistently, the expression level of sodium current was also significantly increased in the Nav1.6-transfected 293-cells after treatment with the synthesised peptide in comparison with before peptide treatment (Fig. 26f). These data demonstrate that VTPEER peptide mediates the effects of APP on sodium currents.

Example 10 - Go protein is involved in the modulation of sodium currents by APP.

Various sodium channels are modulated by G proteins (Komwatana et al., 1996; Ma et al., 1997; Lu et al., 1999). The APP intracellular portion contains a Go protein-binding (GB) domain, $His^{657}$-$Lys^{676}$ of APP-695 (Nishimoto et al., 1993; Lang et al., 1995; Okamoto et al., 1995; Brouillet et al., 1999).

Further to their finding that APP GB domain increases the sodium current expression, the inventors postulated that Go protein might mediate the APP-dependent modulation of sodium currents. The inventors tested this by coexpressing the Nav1.6 α subunit and a G203T dominant-negative mutant of the human G-protein α oB subunit (GoDN) together with: (i) APP (Fig. 27a); (ii) AICD (Fig. 27b); (iii) GB (Fig. 27c), (iv) Fe65BD (Fig. 27d), (v) C31 (Fig. 27e), and (vi) VTPEER (Fig. 27f), respectively, in *Xenopus laevis* oocytes. Co-expression with GoDN reduced the sodium current in the presence of APP and all its intracellular domains as well as the VTPEER peptide (Fig.27). Control injection of GoDN and the Nav1.6 α subunit without APP did not change the sodium current. Accordingly, these data demonstrate that the effects of APP on sodium currents involve Go proteins.

**Discussion for Examples 1-10**

The present inventors have found that APP is clustered specifically at the NORs in the CNS, but not PNS. Consistently, conduction velocities are significantly impaired only in the CNS, but not PNS, in APP mutant mice. Moreover, APP positively modulates the function of sodium channels, increasing sodium currents through its intracellular VTPEER peptide via a Go protein-coupled pathway.

APP is a novel component at the CNS NORs.

During myelination, various axonal and glial molecules redistribute themselves to take up defined domains through dynamic axoglial interaction (Salzer 2003). Over the past decades, the molecular composition corresponding to the morphological domains of the myelinated axon has been extensively studied, with a major focus on the cell adhesion molecules. For instance, F3/contactin, a

member of the immunoglobulin superfamily, has been implicated in molecular communication in both nodal and paranodal sites of the CNS, via interacting with sodium channels and Caspr/paranodin, respectively. TAG-1/TAX, from the same L1 cell adhesion molecule subfamily as F3/contactin, has been suggested to be a constituent of juxtaparanodal formation (Traka et al., 2002 and Poliak et al., 2003). The sodium channel β subunits, which associate with α subunits of voltage-gated sodium channels at the NORs, have an extracellular immunoglobulin-like loop and act as cell adhesion molecules (McEwen and Isom, 2004). APP is expressed predominantly in axons and is upregulated on neural injury and has been utilized as a marker for axonal degeneration. The present work shows that APP is aggregated specifically at the NORs in the CNS, but not PNS. The clustering of APP occurs later than the clustering of sodium and potassium channels. This aggregation requires the integrity of distinct axonal domains as evidenced in both physiological and pathological conditions. Conversely, APP is not required for clustering of other nodal molecules such as tenascin-R, Caspr and sodium channels, as clustering of these molecules still occurs in APP null mice. APP clustering starts from P10 during myelination and disappears after demyelination in two animal models. Thus, nodal APP clustering in the CNS may be the most important factor related to the phenotype of reduced conduction velocities in the CNS, but not PNS, in APP mutant mice. However, the molecular mechanisms underlying the clustering of APP at CNS NORs remain to be explored.

Potential role of APP in modulating sodium channels

The structure of the NORs is formed by the halt of lateral expansions of two apposing oligodendrocytes in the CNS. The voltage-gated sodium channels are highly concentrated at this region with a density of 1,500 molecules/$\mu m^2$, but of less than 100 molecules/$\mu m^2$ in the non-nodal areas (Rosenbluth 1999). Since the myelin sheath insulates the wrapped portion of the axon, the action potential is conducted in a saltatory manner, thus significantly increasing the conduction

speed. Sodium channels are responsible for depolarizing and repolarizing events during transmission of the action potential along axons. The fine modulation of sodium channels at the NORs is essential for precise saltatory conduction along myelinated axons. At nodal regions, sodium currents are positively modulated by axonal molecules, such as F3/contactin, β subunits of sodium channels, and glia-derived molecules, such as tenascin-R and -C (Kazarinova-Noyes et al., (2001); Isom et al., (1995); Srinivasan et al., (1998); and Ma et al., (2007). APP does not act as a β subunit of sodium channels, as the increase in the sodium current in the presence of APP was not in a dose dependent manner (Figure 29). The increase in the sodium current did not require the β subunits of the sodium channel but was augmented by the β subunits. In the presence of the $\beta_1$ subunit, APP also induced a shift to the right in the activation of the channel while, in the presence of the $\beta_2$ subunit, APP accelerated current recovery from inactivation (Figures 14-16). Tenascin-R and its neuronal receptor, F3/contactin, which are extracellular molecules, interact with sodium channels at the NORs (Kazarinova-Noyes et al., 2001). As positive modulators of sodium channels, tenascin-R acts in a β subunit-dependent manner and F3/contactin increases membrane insertion of the α subunit. Similar to tenascin-R and F3/contactin, APP clusters at CNS NORs and increases Nav1.6 sodium currents in oocytes. The APP-induced increase in the sodium currents is mediated by its intracellular VTPEER peptide, a common domain shared by AICD, GB, Fe65BD, and C31. Consistent with the augmentation of sodium currents by APP, spinal conduction velocities are impaired in APP null mice.

The APP-induced increase in the sodium currents is also mediated by the $His^{657}$-$Lys^{676}$ Go protein binding domain in the AICD of APP-695 and appears to involve the heterotrimeric G protein Go. This G protein binding domain is known to selectively activate the heterotrimeric G protein Go with which it complexes (Nishimoto et al., 1993; Brouillet et al., 1999). Although APP modulation of

Nav1.6 via G protein has not previously been reported, our findings are consistent with G protein-mediated modulation of various other sodium channels (Komwatana et al., 1996; Ma et al., 1997; Lu et al., 1999).

The nodal Aß hypothesis.

Models of amyloid deposition in Alzheimer's disease have envisaged exclusively synaptic accumulation. Notably, specific APP clustering at the CNS NORs implicates a potential role for the NORs in the pathogenesis of AD. The exact mechanisms by which APP contributes to the development of dementia are unknown but it is thought that cleavage of APP by secretases leading to formation of a smaller peptide, ß amyloid (Aß), is a crucial step. Deposition of Aß, is considered to be a marker of the pathology of AD and is associated with other pathological markers of AD such as cell death in the CNS, accumulation of amyloid plaques, and the appearance of neurofibrillary tangles. APP is enriched in presynaptic terminals (Ferreira et al 1993). Although the release of component peptides of APP, including Aß deposition, has been thought to occur predominantly at synapses (Ferreira et al (1993), increasing evidence strongly suggests that an important component of AD is damage to myelin. ß1 and ß2 subunits of sodium channels, two nodal molecules, have been recently reported to be substrates of ß site amyloid precursor protein-cleaving enzyme (BACE1) and γ-secretase (Kim et al., 2005 and Wong et al., 2005). It has recently been reported that BACE1 controls myelination in the PNS (Willem et al. (2006). In AD patients, the entorhinal cortex, from where the perforant pathway originates, is one of the most severely affected areas, particularly at earlier stages of the disease. Moreover, electrical activity within the pathway modulates interstitial fluid Aß levels, which can be blocked by tetrodotoxin (TTX), a specific sodium channel blocker (Cirrito et al., 2005). NORs are the naked regions of the axolemma and intermittently distribute along myelinated axons, implying potential interactions between exposed axonal molecules and the extracellular partners. According to the observation that APP is specifically located at the CNS NORs, we propose a nodal Aß hypothesis for AD: that the NORs are important Aß releasing sites, which correlate with its deposition along the perforant pathway at the onset of AD.

Example 11

TAG-1 acts as a functional ligand for APP to trigger AICD transcriptional activation and negatively modulate neurogenesis

The present inventors have identified TAG-1 (contactin-2), a member of the F3/contactin family of glycolphosphatidylinositol-linked immunoglobulin superfamily adhesion molecules, as a functional ligand of APP. Cell adhesion assays and biochemical approaches established that TAG-1 and APP interact to trigger AICD's transcriptional activity in a γ-secretase-dependent manner. Further, both APP and TAG-1 were shown to co-localize in the neural stem cell niche of the fetal ventricular zone and in addition, neurogenesis is enhanced in neural precursor cells isolated from TAG-1-null, APP-null and TAG-1/APP double knock-out mice.

Cell adhesion assay

The following cell adhesion assays suggest a potential role between APP and TAG-1 in contrast to F3. When F3-transfected CHO (Fig. 30Ad and Fig. 30B) or control non-transfected CHO cells (Fig. 30Ae and Fig. 28B) were seeded onto APP-Fc (recombinant APP extracellular domain in fusion with the Fc part of the Fc part of immunoglobulin) spotted culture dishes, little adhesion was observed.

Interestingly, when TAG-1, or TAX (the human homolog of TAG-1), transfected CHO cells were seeded onto the culture dish dotted with APP-Fc, cells readily adhered to the APP protein spot (Fig. 30Aa and Fig. 30B), indicating that APP binds to TAG-1 or TAX. This adhesion could be blocked by pre-treating the cells with anti-TAG-1 antibody (Fig. 30Ab, Fig. 30B) or the culture dish with anti-APP antibody (22C11; Fig. 30Ac, Fig. 30B), indicating that the interaction of TAG-1 with APP contributes to the adhesion.

The reciprocal adhesion assays were performed by plating APP-transfected CHO cells onto culture dishes with TAG-1-Fc protein spots. Similar adhesion of the cells to the protein spot were observed (Fig. 30Af and Fig. 30B), and the adhesion was blocked by neutralization of coated TAG-1 protein spots (Fig. 30Ag and Fig. 30B) or cell membrane-bound APP (Fig. 30Ah and Fig. 30B) with their respective antibodies. Similarly, control non-transfected CHO cells did not adhere to the TAG-1 protein spot (Fig. 30Ai and Fig. 30B).

To identify the APP binding domains in TAX, GST fusion proteins of the 6 immunoglobulin Ig domains (TAXIg-GST) and 4 fibronectin type III (FNIII) repeats (TAXFNIII-GST) of TAX were used as coated protein substrates for APP-transfected CHO cells. The cells bound to spots of both proteins (Fig. 28Aj and i), indicating that APP has at least two binding sites located in the TAG-1 Ig domains and FNIII repeats. Consistently, control non-transfected CHO cells adhered to neither these two proteins (Fig. 30Ak and m) nor GST (Fig. 30An).

GST or Fc pull down assay

Immunoprecipitation and Fc or GST pull-down assays were performed in adult mouse brains to further confirm the interaction between TAG-1 and APP. The results showed that TAG-1 antibodies could precipitate APP from the mouse brain and vice versa (Fig. 31a). Consistent with the cell adhesion results, APP-Fc precipitated TAG-1 from the mouse brain (Fig. 31a) and both TAXIg-GST and TAXFNIII-GST precipitated APP from the mouse brain as well as APP transfected CHO cells (Fig. 31b). Together, these results demonstrate that APP and TAG-1 bind to each other.

TAG-1 and AICD's transcriptional activity

The activation of AICD release and transcriptional activity is thought to be triggered by external cues. However, ligands for the extracellular portion of APP

that affects its proteolytic processing and signalling cascade have not been functionally characterised.

The inventors studied the effect of TAG-1 on AICD's tracnsciptional activity. A previously reported luciferase reporter system where Gal4 is fused to the C-terminal of APP (Cao and Südhof 2001) was introduced into CHO and L1-, or TAG-1- or TAX-transfected CHO cells. A significant upregulation of the reporter activity was observed in both TAG-1- and TAX-transfected CHO cells, but not in the control CHO cells as well as L1-transfected CHO cells (Fig. 32a). Notably, a specific γ-secretase inhibitor reduced the TAG-1 triggered AICD transcriptional activity in a dose-dependent manner (Fig. 32b). That AICD luciferase activity is significantly increased by transfection with APP in both TAG and TAX transfected CHO cells suggest that the interaction between APP and TAG-1 is a critical step in triggering AICD activated transcription.

Co-localisation of APP and TAG-1

The expression of TAG-1 amd APP in E14 brain was studied by immunofluorescence (IF) labelling using antibodies against TAG-1 (a polyclonal anti-TAG-1) and APP (C7). In the E14 mouse brain, IF showed that APP (Fig. 33b, b', c and c') or TAG-1 (Fig. 33e, e', f and f') were co-localized with nestin (Fig. 33a and d), a neural progenitor marker, in the walls of the lateral ventricles (LV). Moreover, double IF showed that APP (Fig. 33h and h') and TAG-1 (**Fig.** 33g and g') were co-expressed (Fig. 33i and i') in the LV walls. These results demonstrate that both TAG-1 and APP are expressed by NPCs in the neural stem cell niche.

In addition, NPCs from E14 mouse telencephalic ventricular walls were isolated. These cells were double-stained for APP (Fig. 34a' and c') or TAG-1 (Fig. 34b' and d') and the neural progenitor markers nestin (Fig. 34a and b) or Sox2 (Fig.

34c and d). The results suggest that both APP and TAG-1 are expressed by the NPCs.

Further, the cells were double-stained for APP (Fig. 34e) and TAG-1 (Fig. 34e'), and the results indicate that APP and TAG-1 are co-localized in NPCs. Consistent with these observations, Western blot analysis showed that TAG-1 and APP bands were detected in total mouse brain and NPCs (Fig. 34f). Together, these results demonstrate that APP and TAG-1 are coexpressed in fetal NPCs.

TAG-1 /APP signaling pathway in modulation of neurogenesis.

NPCs were isolated from the E14 telencephalic ventricular walls of APP$^{-/-}$ (Fig. 35A) and TAG-1$^{-/-}$ (Fig. 35B) mice, respectively. After 7 to 8 days *in vitro* differentiation, cells were double-stained for TUJ1 (green; Fig. 35Aa and b; 35Ba and b) or MAP2, two markers for mature neurons (not shown), and DAPI (blue; Fig. 35Aa and b; Ca and b). Both TUJ1- and MAP2-positive cells are significantly increased in APP (about 40%; Fig. 35Bc and d) and TAG-1 (about 45%; Fig. 35Bc and d) deficient mice compared with wild-type littermates. These results demonstrate that the TAG-1/APP signaling pathway negatively modulates neurogenesis.

The inventors generated TAG-1-/-/APP-/- mice to confirm that TAG-1/APP signaling plays a negative role in modulating neurogenesis. Using the TAG-1-/-/APP-/- fetal NPCs, the inventors studied whether AICD transcriptional activity could be also modulated by the TAG-1/APP interaction. After transfection with the APP luciferase reporter system, TAG-1-/-/APP-/- NPCs were cultured as monolayers loaded onto culture dishes co-coated with TAG-1-Fc, F3-Fc, or L1-Fc and laminin. Interestingly, TAG-1-Fc, but not F3-Fc, L1-Fc, and laminin, strongly triggered AICD reporter activity (Fig. 36Aa). A specific γ-secretase

inhibitor blocked the induction of AICD transcriptional activity by TAG-1 in a dose-dependent manner (Fig. 36Ab), indicating that the γ-secretase is involved in the TAG-1 triggered RIP process in the TAG-1-/-/APP-/- fetal NPCs.

Similar to the observations in both TAG-1- and TAX-transfected CHO cells, these experiments further demonstrate that AICD transcriptional activity is also regulated by the interaction of TAG-1 and APP in NPCs. Notably, consistent with our observations in singly deficient mice, TUJ1- positive cells were significantly increased in TAG-1-/-/APP-/- (about 40 %; Fig. 34Bb and c) mice compared with wild-type littermates (Fig. 36Ba and c). Thus, given that neurogenesis is significantly promoted in NPC cultures isolated from TAG-1 and APP deficient mice as well as TAG-1/APP doubly deficient mice, the results strongly support the view that the TAG-1/APP signaling pathway negatively regulates neurogenesis during early CNS development.

The molecular structure and dimerization of APP suggest that APP is a cell surface receptor that can be activated by ligand binding (Kang et al 2004). In the present study, the inventors have shown that TAG-1, a member of F3/contactin family, is a functional ligand of APP. Similar to F3/contactin triggered NICD transcriptional activity, this binding promotes AICD transcriptional activity in a γ-secretase-dependent manner (Fig. 37). Moreover, the inventors have demonstrated that the TAG-1/APP signaling pathway is involved in negatively modulating neurogenesis (Fig. 37). These findings are important in the context of AD because abnormal processing of APP could also lead to aberrant AICD generation, which may be linked to abnormal gene expression.

## Experimental Procedures

### Antibodies

Antibodies used in this study were: rabbit TAG-123; mouse TAG-1 (4D7; Dr. A. Furley); goat TAG-1 (R&D system; Santa cruz); mouse APP (22C11; Chemicon); rabbit APP (C8; Dr. DJ Selkoe); rabbit APP C-terminal (751-770; C20), goat APP (Calbiochem); nestin, sox2, MAP2 (Chemicon); GFAP (Dako); ß tubulinIII (Tuj1; Sigma).

### Production of Fc and GST fusion proteins

Mouse APP 695 cDNA encoding for the neuronal isoform of APP (Dr S. Sisodia, University of Chicago, USA) was subcloned into the pblue Bac vector using the BamHI and SacI restriction sites. To generate the fusion protein containing the extracellular domain of APP with the Fc part of human immunoglobulin G at its COOH-terminal end (APP-Fc), primers for the SacI restriction site at the 5´end (CTGACGGAACCAAGACCACCG; SEQ ID NO: 23) and for the COOH terminal end of the APP extracellular domain (terminating at amino acid position 624; SWISS-Prot accession number P12023) at the 3´ end (GCTGAAGATGTGGGTTCGAACAAA; SEQ ID NO: 24) were used, introducing a new BclI restriction site at the 3´end. This vector was used to stably transfect CHO K1 cells according to published procedures (Chen et al 1999).

A soluble form of TAG-1-Fc recombinant protein was produced in 293T cells. The signal sequence of the GPI-anchor of mouse TAG-1 was substituted with human IgG-Fc followed by a termination codon. The recombinant cDNA was inserted at the Hind III-Not I sites of pDX, a modified pcDNA3 vector with an amplification-promoting sequence (APS) upstream of the CMV site (Hemann et al 1994). The vector was introduced into 293T cells.

Fc proteins were purified via the Fc-tag using Protein-A column chromatography as described (Chen et al 1999). The sequences of Ig and FNIII domains of TAG-1 were inserted into the pGEXKG vector to produce the GST-tagged fusion proteins. The recombinant vectors were introduced into the TOP10 strain of *E. coli*, which was subsequently induced by IPTG (Bio-Rad). The recombinant GST fusion proteins were purified by using GST beads (Sigma) as instructed by the manufacturer.

**Cell adhesion assays**

CHO cells were stably transfected with pcDNA 3.1(-) containing the human cDNA sequence of APP 695, the predominantly neuronal expressed isoform of APP. APP, F3, TAX, TAG-1 and mock transfected CHO cells were cultured in DMEM containing 10% fetal calf serum. 35mm tissue culture petri dishes (Becton Dickinson) were coated with methanol solubilized nitrocellulose and then with proteins (12μM) for 2 hours at 37°C in a humidified atmosphere. Subsequently, the dishes were washed and blocked overnight with 2% heat-inactivated fatty acid-free BSA (Sigma). After rinsing the dishes, cells (TAG-1-transfected CHO or APP-transfected CHO) were plated in 2 ml of DMEM (Gibco) containing 10% fetal calf serum at a density of 1.5 x 106cells/ml. At 0.5 hour (in the adhesion test), the cells were gently washed and fixed with 2.5% glutaraldehyde and stained with 0.5% toluidine blue (Sigma) in 2.5% sodium carbonate. Blockage of adhesion was carried out using polyclonal anti-TAG-1 (1:100) or anti-APP (1:100) antibodies for 0.5 h pre-incubation. Cells adhering to the various spots were photographed and counted. The results were analyzed by Newman-Keuls test with $p<0.05$ being considered significant.

**GST or Fc pull-down assays**

Freshly prepared cerebral hemispheres of adult rats were harvested and solubilized in 2% Triton X-100. The buffer homogenate was centrifuged at 13,000g for 1 hour at 4 °C and the supernatant was incubated for 45 min at room temperature with the glutathioneagarose or protein A-coupled agarose beads that had been incubated with TAG-1-Fc or APP-Fc. After washing the beads, proteins were eluted with SDS-PAGE sample buffer and immunoblotted with anti-APP or anti-TAG-1 antibodies, respectively.

**Co-immunoprecipitation and Western blot analysis**

Mice brains were lysed with RIPA buffer containing protease inhibitor cocktail (Roche). For immunoprecipatation, lysates were precleared with protein A-coupled agarose beads for 1 hrs and incubated with APP or TAG-1 antibodies together with protein A-coupled agarose for overnight at 4 °C. Samples were washed with washing buffer before the beads were re-suspend in SDS buffer and boiled for 3-5 mins. Samples were subjected to SDSPAGE.Western blot analysis was performed and developed with ECL reagents (Amersham).

**Luciferase assays**

The APP-Gal4 assay system has been previously described15. L1-, TAG-1-, TAXtransfected CHO cells as well as CHO cells were cotransfected with the following plasmids (i) pG5E1B-luc (Gal4 reporter plasmid, 0.1 µg DNA); (ii) pCMV-LacZ (ß-galactosidase control plasmid, 0.05 µg DNA); (iii) pMstAPP (Gal4) (0.1 µg DNA); (iv) pCMV5-Fe65 (Fe65) (0.1 µg DNA), in 24-well dishes using an Effectene Transfection kit (Qiagen). Additionally, cells cultured in 24-well dishes were used for AICD-Gal4 luciferase reporter assays. For the transactivation assay in NPCs, wells were coated with L1-Fc, TAG1-Fc, F3-Fc or laminin protein (8nM), respectively. Each well received 10 times the amount

of DNA as used for the CHO cells and the transfection was performed using a Nucleofector System (Amaxa). To examine the function of γ–secretase in this transactivation, two different concentrations (2 or 4μM) of a γ–secretase inhibitor (L-685, 458; Calbiochem) were applied to tansfected cells, while DMSO was used as a control. The ß-galactosidase expression plasmid pCMV/ß-Gal was included to monitor the transfection efficiency. Cells were lysed at 24 hours after transfection and assayed using the Steady-Glo Luciferase Assay Kit (Promega).

**APP- and TAG-1-deficient mice**

$APP^{-/-}$ mice 26 and TAG-$1^{-/-}$ mice27 have been described previously. APP/TAG-1 doubly deficient mice were generated by intercrossing APP homozygous and TAG-1 homozygous ($APP^{-/-}$ X TAG-$1^{-/-}$). Animals heterozygous for both loci were intercrossed to each other (TAG-$1^{+/-}$/APP+/- X TAG-$1^{+/-}$/$APP^{+/-}$) to generate APP and TAG-1 doubly deficient (TAG-1-/-/APP-/-) offspring.

**Culture of neural progenitor cells**

Telencephalic lateral ventricle walls isolated from E14 embryos were dissociated and neurosphere forming cells were cultured in DMEM/F12 (Gibco) containing N2 supplement, 20ng/ml bFGF and 20ng/ml EGF. For differentiation assay, second passage neurospheres were collected and dissociated into single cells. The cell suspension was seeded into 24-well dishes with 20,000 cells per well and was induced in DMEM/F12 culture medium containing N2 and 0.5% fetal calf serum for 7-8 days.

**Immunocytochemistry and quantitation**

Immunocytochemistry on cultured cells and immunostaining on tissue sections were performed as previously described25. For quantitation of immunofluorescence, images of fields of cultured cells were captured by digital photomicrograph under a 1.6x10X objective systematically from top-to-bottom and left-to-right across the entirety of each coverslip.

All labeled cells were then counted in each photomicrograph. The proportion of neurons was quantified as the numbers of Tuj1+ or MAP2+ cells divided by the total number of DAPI+ cells in the same fields. Each experiment was repeated on 3 to 7 mice.

The statistics were performed using one-way-ANOVA or Student's t test, as appropriate. In all the graphs, the error bars indicate standard error of the mean (SEM). *: $P<0.05$;**: $P<0.001$.

Although the present invention has been described in detail with reference to examples above, it is understood, that various modifications can be made without departing from the spirit of the invention. Accordingly, the invention is only limited by the following claims. All cited patents, patent applications and publications referred to in this application are herein incorporated by reference in their entirety.

## References

Brouillet E., Trembleau A., Galanaud D., Volovitch M. and Bouillot CThe amyloid precursor protein interacts with Go heterotrimeric protein within a cell compartment specialized in signal transduction. J Neurosci 19, 1717-1727 (1999)

Caldwell, J. H., Schaller, K.L., Lasher, R.S., Peles, E. and Levinson, S.R. Sodium channel Na(v)1.6 is localized at nodes of ranvier, dendrites, and synapses. *Proc. Natl. Acad. Sci. USA* 97, 5616-5620 (2000).

Cao, X. And Südhof, T. C. A transcriptional active complex of APP with Fe645 and histone acetyltransferase Tip60. Science 293, 115-120 (2001).

Catterall, W. A. From ionic currents to molecular mechanisms: the structure and function of voltage-gated sodium channels. Neuron 26, 13-25 (2000).

Chen, S., Mantei, N. Dong, L. and Schachner, M. Prevention of neural cell death by neural adhesion molecules L1 and CHL1. J. Neurobiol. 38, 428-439 (1999)

Chen, C, et al. Mice lacking sodium channel beta1 subunits display defects in neuronal excitability, sodium channel expression, and nodal architecture. J. Neurosci. 24, 4030-4042 (2004).

Cirrito, J. R, et al. Synaptic activity regulates interstitial fluid amyloid-beta levels in vivo. Neuron 48, 913-922 (2005).

Coetzee, T, et al. Myelination in the absence of galactocerebroside and sulfatide: normal structure with abnormal function and regional instability. Cell 86, 209-219 (1996).

Craner, M. J., Hains, B. C., Lo, A. C., Black, J. A., & Waxman, S. G. Co-localization of sodium channel Nav1.6 and the sodium-calcium exchanger at sites of axonal injury in the spinal cord in EAE. Brain 127, 294-303 (2004).

Ermekova K.S., Zambrano N., Linn H., Minopoli G., Gertler F., Russo T. and Sudol M. The WW domain of neural protein FE65 interacts with proline-rich motifs in Mena, the mammalian homolog of Drosophila enabled. J Biol. Chem. 72(52), 32869-77 (1997). Ferreira, A., Caceres, A., & Kosik, K. S. Intraneuronal compartments of the amyloid precursor protein. J. Neurosci. 13, 3112-3123 (1993).

Golde, T. E., Estus, S., Usiak, M., Younkin, L. H., & Younkin, S. G. Expression of beta amyloid protein precursor mRNAs: recognition of a novel alternatively spliced form and quantitation in Alzheimer's disease using PCR. Neuron 4, 253-267 (1990).

Hemann, C., Gartner, E., Weidle, U. H. and Grummt, F. High-copy expression vector based on amplification-promoting sequences. DNA Cell Biol. 13, 437-445 (1994).

Hsiao, K. K, et al. Age-related CNS disorder and early death in transgenic FVB/N mice overexpressing Alzheimer amyloid precursor proteins. Neuron 15, 1203-1218 (1995).

Huber, A. B., Weinmann, O., Brosamle, C., Oertle, T., & Schwab, M. E. Patterns of Nogo mRNA and protein expression in the developing and adult rat and after CNS lesions. J. Neurosci. 22, 3553-3567 (2002).

Inoue, Y., Kagawa, T., Matsumura, Y., Ikenaka, K., & Mikoshiba, K. Cell death of oligodendrocytes or demyelination induced by overexpression of proteolipid protein depending on expressed gene dosage. *Neurosci. Res.* 25, 161-172 (1996).

Isom L.L., Ragsdale, D. S., De Jongh, K. S., Westernbroek, R. E., and Reber, B. F. Structure and function of the beta 2 subunit of brain sodium channels, a transmembrane glycoprotein with a CAM motif. Cell 83, 433-442 (1995).

Kang, J. et al. The precursos of Alzheimer's disease amuloid A4 protein resembles a cell-surface receptor. Nature 325, 733-736 (1987).

Kazarinova-Noyes, K, et al. Contactin associates with Na+ channels and increases their functional expression. J. Neurosci. 21, 7517-7525 (2001).

Kim D. Y., Ingano L. A., Carey B. W., Pettingell W. H. and Kovacs D. M. Presinilin/gamma-secretase-mediated cleavage of the voltage-gated sodium channel b2-subunit regulates cell adhesion and migration. J. Biol. Chem., 280, 23251-23261 (2005).

Komwatana P., Dinudom A., Young J.A. and Cook D.I. Cytosolic Na+ controls and epithelial Na+ channel via the Go guanine nucleotide-binding regulatory protein. Proc Natl Acad Sci USA, 93, 8107-8111 (1996).

Kuhlmann, T., Lingfeld, G., Bitsch, A., Schuchardt, J., & Bruck, W. Acute axonal damage in multiple sclerosis is most extensive in early disease stages and decreases over time.Brain 125, 2202-2212 (2002).

Lang, J., Nishimoto, I., Okamoto, T., Regazzi, R., Kiraly, C., Weller, U. and Wollheim, C.B. Direct control of exocytosis by receptor-mediated activation of the heterotrimeric GTPases Gi and G(o) or by the expression of their active G alpha subunits. EMBO J 4(15): 3635-44 (1995).

Lu T., Lee H.C., Kabat J.A. and Shibata E.F. Modulation of rat cardiac sodium channel by the stimulatory G protein α subunit. J. Physiol. 518, 371-384 (1999).

Lu D.C., Rabizadeh S., Chandra S., Shayya R.F., Ellerby L.M., Ye X., Salvesen G.S., Koo E.H., Bredesen D.E. A second cytotoxic proteolytic peptide derived from amyloid beta-protein precursor. Nat. Med., 4, 397-404 (2000).

Ma J.Y., Catterall W.A. and Scheuer T. Persistent sodium currents through brain sodium channels induced by G-protein subunits. Neuron 19, 443-452 (1997).

Ma, Q.H., Yang, W. L., Nie, W. Y., Dawe, G. S. and Xiao, Z. C. Physiological roles of neurite outgrowth inhibitors at myelinated axons in the central nervous system-implications for the therapeutic neutralization of neurite outgrowth inhibitos. Curr. Pharm. Des. In press (2007).

McEwen, D.P. and Isom, L. L. Heterophilic interactions of sodium channel β1 subunits with axonal and glial cell adhesion molecules. J. Ciol. Chem. 279, 52744-52752 (2004).

Michailov, G. V, et al. Axonal neuregulin-1 regulates myelin sheath thickness. Science 304, 700-703 (2004).

Nie, D. Y, et al. Nogo-A at CNS paranodes is a ligand of Caspr: possible regulation of K (+) channel localization. EMBO J. 22, 5666-5678 (2003).

Nishimoto I. Okamoto T., Matsuura Y., Takahashi S. and Okamoto T. Alzheimer amyloid protein precursor complexes with brain GTP-binding protein G(o). Nature 362, 75-79 (1993). Oliveira J.S., Redaelli E., Zaharenko A.J., Cassulini R.R., Konno K., Pimenta D.C., Freitas J.C., Clare J.J. and Wanke, E. Binding specificity of sea anemone toxins to Nav 1.1-1.6 sodium channels: unexpected contributions from differences in the IV/S3-S4 outer loop. E.J Biol Chem 279(32): 33323-35 (2004).

Okamoto M., Ueda Y., Takahashi K., Nakazawa H. amd Doi, T. Direct enantiomeric separation of platelet-activating factor receptor antagonist SM-10661 by ligand-exchange high-performance liquid chromatography with a copper (II) N,S-dioctyl-D-penicillamine complex. Biosci, Biotechnol, Biochem., 59, 1740-1741 (1995)

Poliak, S., Saloman, D., Elhanany, H., Sabanay, H. and Kiernan, B. Juztaparanodal clustering of Shaker-like K+ channels in myelinated axons depends on Caspr2 and TAG-1. J. Cell. Biol. 162, 1149-1160 (2003).

Rasband, M. N., Kagawa, T., Park, E. W., Ikenaka, K., & Trimmer, J. S. Dysregulation of axonal sodium channel isoforms after adult-onset chronic demyelination. J. Neurosci. Res. 73, 465-470 (2003).

Rosenbluth J. A brief history of myelinated nerve fibers: one hundred and fifty years of controversy. J. Neurocytol. 28, 251-262 (1999).

Rush, A. M., Dib-Hajj, S. D., & Waxman, S. G. Electrophysiological properties of two axonal sodium channels, Nav1.2 and Nav1.6, expressed in mouse spinal sensory neurones. J. Physiol. 564, 803-815 (2005).

Salzer J. L Polarized domains of myelinated axons. Neuron. 40, 297-318 (2003).

Selkoe D. J, et al. Beta amyloid precursor protein of Alzheimer disease occurs as 110- to 135-kilodalton membrane-associated proteins in neural and nonneural tissues. Proc. Natl. Acad. Sci. USA 85, 7341-7345 (1988).

Srinivasan J., Schachner M. and Catterall, W. A. Interaction of voltage-gated sodium channels with the extracellular matrix molecules tenascin-C and tenascin-R. Proc Natl Acad Sci USA 95, 15753-15757 (1998)

Stys, P. K., Ransom, B. R., & Waxman, S. G. Compound action potential of nerve recorded by suction electrode: a theoretical and experimental analysis. Brain Res. 546, 18-32 (1991).

Traka, M., Dupree, J. L., Popko, B. and Karagogeos, D. The neuronal adhesion protein TAG-1 is expressed by Schwann cells and oligodendrocytes and is localized to the juxtaparanodal region of myelinated fibers. J. Neurosci., 22, 3016-3024 (2002)

Weber, P, *et al.* Mice deficient for tenascin-R display alterations of the extracellular matrix and decreased axonal conduction velocities in the CNS. *J. Neurosci.* 19, 4245-4262 (1999).

Willem M., Garrart A.N. Novak B., Citron M. And Kaufmann S. Control of peripheral nerve myelination by the β-secretase BACE1. Science, 314, 664-666 (2006).

Wong H. K., Sakurai, T., Oyama F., Kaneko J. And Wada K. β subuits of voltage-gated sodium channels are novel subsrates of β-site amyloid precursor protein-cleaving enyme (BACE1) and gamma-secretase. J. Biol. Chem., 280, 23009-23017 (2005)

Xiao, Z. C, et al. Defasciculation of neurites is mediated by tenascin-R and its neuronal receptor F3/11. J. Neurosci. Res. 52, 390-404 (1998).

Zheng, H, et al. beta-Amyloid precursor protein-deficient mice show reactive gliosis and decreased locomotor activity. Cell 81, 525-531 (1995).

Claims

1. A method of treating at least one medical condition in a subject, the method comprising modulating the expression and/or activity of amyloid precursor protein (APP), APP derivative or APP fragment.

2. The method according to claim 1, wherein the modulating is by decreasing the expression and/or activity of amyloid precursor protein (APP), APP derivative or APP fragment.

3. The method according to claim 1 or 2, wherein the modulation of APP, its derivative or a fragment thereof is by modulating at least one molecule, protein, and/or peptide that interacts with amyloid precursor protein (APP), APP derivative or APP fragment.

4. The method according to any one of the preceding claims, wherein the modulation of amyloid precursor protein (APP), APP derivative or APP fragment comprises modulating at least one cellular component that interacts with amyloid precursor protein (APP), APP derivative or APP fragment.

5. The method according to claim, wherein the at least one cellular component that interacts with amyloid precursor protein (APP), APP derivative or APP fragment is selected from TAG-1, sodium channels, and sodium channel complex protein.

6. The method according to any one of the preceding claims, wherein the modulation of amyloid precursor protein (APP), APP derivative or APP fragment comprises modulating at least one cellular component selected from the group consisting of TAG-1, Caspr2, NgR, TN-R, TN-C, MAG, Nogo-A, phosphacan, F3, OMgp, RPTPβ, NG2, sodium channel and Go protein(s).

7. The method according to any one of the preceding claims, wherein the modulating comprises administering a pharmaceutically and/or therapeutically effective amount of at least one drug, protein, peptide, antibody or molecule that interacts with amyloid precursor protein (APP), APP derivative or APP fragment, TAG-1, sodium channels, or sodium channel complex protein(s)

8. The method according to any one of the preceding claims, wherein the modulating comprises administering a pharmaceutically and/or therapeutically effective amount of at least one drug, protein, peptide, antibody or molecule that interacts with amyloid precursor protein (APP), APP derivative or APP fragment, TAG-1, sodium channels, TAG-1 complex protein(s), sodium channels complex protein(s), Caspr2, NgR, potassium channels, TN-R, TN-C, MAG, Nogo-A, phosphacan, F3, OMgp, RPTPβ and NG2.

9. The method according to any one of the preceding claims, wherein the modulating comprises administering at least one pharmaceutically and/or therapeutically effective amount of amyloid precursor protein (APP), APP derivative or APP fragment.

10. The method according to claim 9, wherein the APP derivative or APP fragment is Aβ, soluble APP (sAPP), APP-695, AICD or VTPEER peptide

11. The method according to any one of the preceding claims 1 to 8, wherein the modulating comprises administering a pharmaceutically and/or therapeutically effective amount of at least one compound selected from the group consisting of TAG-1, anesthetic(s), toxin(s) and Go protein(s).

12. The method according to any one of claims 1 to 8, wherein the modulating comprises administering a pharmaceutically and/or therapeutically effective amount of at least one drug or molecule selected from local anaesthetic(s), veratridine, batrachotoxin, scorpion toxins, sea anemone toxin, conus toxins, saxitoxin, tetrodotoxin, antiepileptic drug(s), antiarrhythmic drug(s), antibodies to sodium channel proteins, antibodies to Caspr, and peptide fragments of APP.

13. The method according to any one of the preceding claims, wherein the modulation of amyloid precursor protein (APP), APP derivative or APP fragment is to prevent and/or reduce beta amyloid (Aβ) deposition, improve and/or facilitate nervous tissue repair, improve and/or facilitate myelination, to modulate stem cell function(s) and/or to modulate sodium channels function(s).

14. The method according to any one of the preceding claims, wherein the at least one medical condition is selected from the group consisting of Alzheimer's disease, multiple sclerosis, brain injury, spinal cord injury, axonal injury-related disorders, epilepsy, neurodegenerative disorders and demyelination disorders.

15. The method according to any one of the preceding claims, wherein the modulating results in modulation of axonal conduction of action potential(s) for the treatment of pain and/or epilepsy.

16. The method according to any one of the preceding claims, wherein the modulating results in the induction of analgesia and/or local anaesthesia.

Fujirebio Diagnostics, Inc. v. Quanterix Corp.
EX-1045
5985

17. A method of detecting and/or quantitating the presence of, predisposition to, and/or severity of, a neurological condition in a subject, the method comprising:

(a) providing at least one sample from a subject;

(b) determining the expression and/or activity of amyloid precursor protein (APP), APP derivative or APP fragment;

(c) comparing the expression and/or activity of amyloid precursor protein (APP), APP derivative or APP fragment, with that of at least one control, a difference in expression and/or activity indicating the presence of, or predisposition to, and/or severity of a neurological condition in the subject.

18. A method of monitoring the efficacy of a treatment for a neurological condition in a subject, the method comprising:

(a) providing at least two samples from a subject, each sample obtained at different time points;

(b) determining the expression and/or activity of amyloid precursor protein (APP), APP derivative or APP fragment; and

(c) comparing the expression and/or activity of amyloid precursor protein (APP), APP derivative or APP fragment, in the at least two samples.

19. A method of prognosticating the outcome of a neurological condition in a subject, the method comprising:

(a) providing at least one sample from a subject;

(b) determining the expression and/or activity of amyloid precursor protein (APP), APP derivative or APP fragment;

(c) comparing the expression and/or activity of amyloid precursor protein (APP), APP derivative or APP fragment, with that of at least one control, a difference in expression and/or activity indicating the prognosis of a neurological condition in the subject.

20. A method of inducing analgesia and/or anesthesia in a subject, the method comprising modulating the expression and/or activity of amyloid precursor protein (APP), APP derivative or APP fragment.

21. The method according to claim 20, wherein the modulating comprises decreasing the expression and/or activity of amyloid precursor protein (APP), APP derivative or APP fragment.

22. An *in vitro* or *in vivo* method of modulating proliferation, differentiation and/or activity of at least one stem cell, the method comprising modulating the expression and/or activity of amyloid precursor protein (APP), APP derivative or APP fragment, in the at least one stem cell.

23. The method according to claim 22, wherein the modulating comprises decreasing the expression and/or activity of amyloid precursor protein (APP), APP derivative or APP fragment, in at least one stem cell.

24. The method according to claim 20 to 23, wherein the modulating comprises administering a pharmaceutically and/or therapeutically effective amount of at least one compound selected from the group consisting of TAG-1, anesthetics, toxins and Go protein(s).

25. The method according to any one of claims 20-24, wherein the modulating comprises administering a pharmaceutically and/or therapeutically effective amount of at least one drug or molecule selected from local anaesthetic(s), veratridine, batrachotoxin, scorpion toxins, sea anemone toxin, conus toxins, saxitoxin, tetrodotoxin, antiepileptic drug(s), antiarrhythmic drug(s), antibodies to sodium channel proteins, antibodies to Caspr, and peptide fragments of APP.

26. The method according to any one of claims 20 to 25, wherein the method is for neural system repair in a subject.

27. A method of detecting and/or quantitating the presence of, predisposition to, and/or severity of, at least one condition related to beta amyloid (Aβ) deposition and/or sodium channel dysfunction in a subject, the method comprising:
(a) measuring the nerve and/or axon conduction velocity in the subject;
(b) comparing the nerve and/or axon conduction velocity with that of at least one control, a difference in velocity indicating the presence of, or predisposition to, and/or severity of at least one condition related to Aβ deposition and/or sodium channel dysfunction in the subject.

28. The method according to claim 27, wherein the method is for detecting and/or quantitating the presence of, predisposition to, and/or severity of Alzheimer's disease (AD).

29 An *in vitro* or *in vivo* method of modulating the activity of amyloid precursor protein (APP), APP derivative or APP fragment, comprising administering at least one drug, protein, peptide, antibody or molecule that interacts with amyloid precursor protein (APP), APP derivative or APP fragment, TAG-1, sodium channels, sodium channel complex protein(s).

30. The method according to claim 29, wherein the modulating comprises administering a pharmaceutically and/or therapeutically effective amount of at least one compound selected from the group consisting of TAG-1, anesthetic(s), toxin(s) and Go protein(s).

31. The method according to claim 29 or 30, wherein the method is for treating at least one condition selected from the group consisting of Alzheimer's disease, multiple sclerosis, brain injury, spinal cord injury, axonal injury-related disorders, epilepsy, neurodegenerative disorders and demyelination disorders.

32. An *in vitro* or *in vivo* method of modulating sodium channel(s) function(s) comprising administering at least one drug, protein, peptide, antibody or molecule that interacts with amyloid precursor protein (APP), APP derivative or APP fragment, TAG-1, sodium channels, or sodium channel complex protein(s).

33. The method according to claim 32, wherein the method is for modulating APP expression and/or activity), and/or for the treatment of at least one neurological disorder.

34. The method according to claim 32 or 33, wherein the method is for the treatment of acute and/or chronic pain disorder(s), induction of analgesia, treatment of epilepsy and/or convulsion(s), treatment of disorder(s) of the rhythm of the heart, and/or induction of anaesthesia and/or analgesia.

35. A pharmaceutical composition for treating at least one APP and/or sodium channel related medical condition comprising at least one compound selected from the group consisting of: APP, APP derivative, APP fragment, antibody to APP, TAG-1, a TAG-1 homologous protein or fragment thereof, antibody to TAG-1, sodium channel(s), at least one sodium channel complex protein(s), Caspr, Caspr derivative, Caspr fragment, anesthetic(s), toxin(s) and Go protein(s); and optionally at least one pharmaceutically acceptable diluent, carrier and/or excipient.

36. A pharmaceutical composition according to claim 35 wherein the APP derivative or fragment is Aβ, soluble APP (sAPP), APP-695, AICD or VTPEER peptide.

37. The pharmaceutical composition according to claim 34 or 35, wherein the medical condition is at least one condition selected from the group consisting of Alzheimer's disease, multiple sclerosis, brain injury, spinal cord injury, axonal injury-related disorders, epilepsy, neurodegenerative disorders and demyelination disorders.

38. Use of at least one compound selected from the group consisting of: APP, APP derivative, APP fragment, antibody to APP, TAG-1, at least one TAG-1 complex protein, a TAG-1 homologous protein or fragment thereof, antibody to TAG-1, sodium channel(s), at least one sodium channel complex protein, Caspr, Caspr derivative, Caspr fragment, anesthetic(s), toxin(s) and Go protein(s), for the preparation of a medicament for the treatment of an APP and/or sodium channel related medical condition.

39. Use according to claim 38, wherein the APP derivative or APP fragment is Aβ, soluble APP (sAPP), APP-695, AICD or VTPEER peptide.

40. A compound selected from the group consisting of: APP, APP derivative, APP fragment, antibody to APP, TAG-1, at least one TAG-1 complex protein, a TAG-1 homologous protein or fragment thereof, antibody to TAG-1, sodium channel(s), at least one sodium channel complex protein, Caspr, Caspr derivative, Caspr fragment, anesthetic(s), toxin(s) and Go protein(s) for use in the treatment of an APP and/or sodium channel related medical condition.

Fujirebio Diagnostics, Inc. v. Quanterix Corp.
EX-1045
5990

41. A compound according to claim 40, wherein the APP fragment of derivative is Aβ, soluble APP (sAPP), APP-695, AICD or VTPEER peptide.

42. A compound, according to claim 40 or 41, for use in the treatment of Alzheimer's disease, multiple sclerosis, brain injury, spinal cord injury, axonal injury-related disorders, epilepsy, neurodegenerative disorders or demyelination disorders.

43. A kit comprising at least one compound selected from the group consisting of: APP, APP derivative, APP fragment, antibody to APP, TAG-1, at least one TAG-1 complex protein, a TAG-1 homologous protein or fragment thereof, antibody to TAG-1, sodium channel(s), at least one sodium channel complex protein, Caspr, Caspr derivative, Caspr fragment, anesthetic(s) toxin(s) and Go protein(s), for detecting and/or diagnosing at least one APP and/or sodium channel related medical condition or for the treatment of at least one APP and/or sodium channel related medical condition.

44. A kit according to claim 43, wherein the kit comprises Aβ, soluble APP (sAPP), APP-695, AICD or VTPEER peptide.

45. A kit according to claim 43 or 44, for the treatment of Alzheimer's disease, multiple sclerosis, brain injury, spinal cord injury, axonal injury-related disorders, epilepsy, neurodegenerative disorders or demyelination disorders.

# FIGURE 1

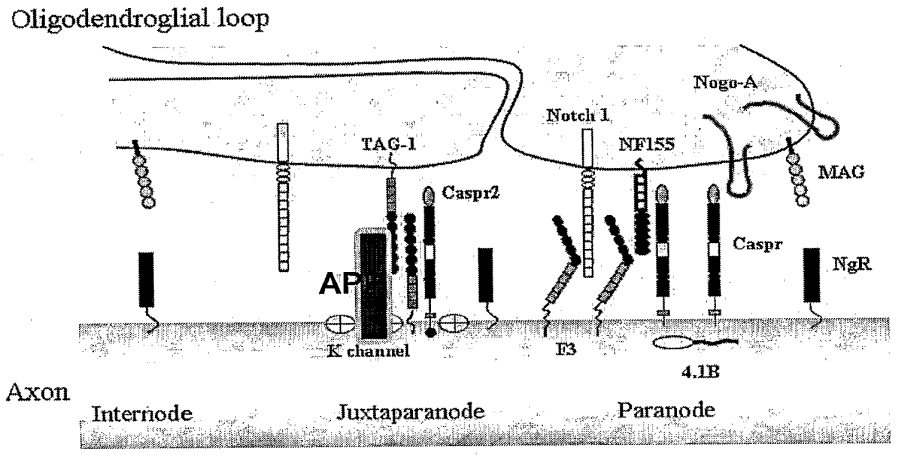
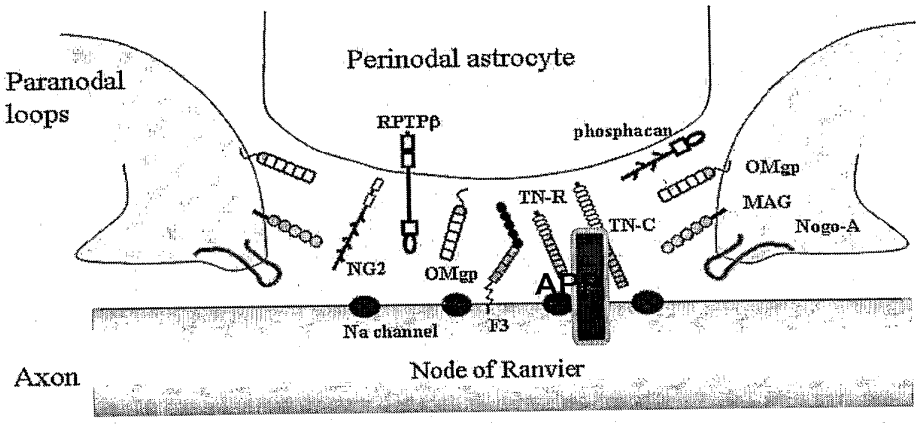

Oligodendroglial loop
Nogo-A
Notch 1
TAG-1
NF155
MAG
Caspr2
Caspr
NgR
AP
K channel
F3
4.1B
Axon
Internode
Juxtaparanode
Paranode

**FIGURE 2**




Fujirebio Diagnostics, Inc. v. Quanterix Corp.
EX-1045
5993

**FIGURE 3**

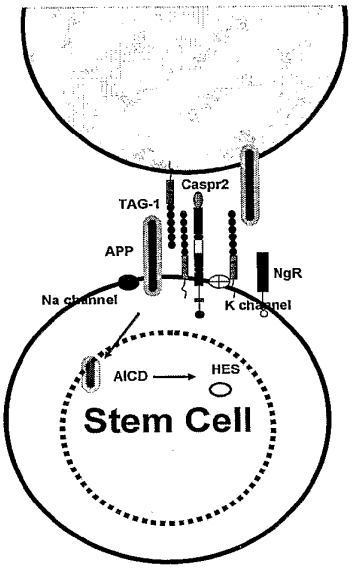


**FIGURE 4**

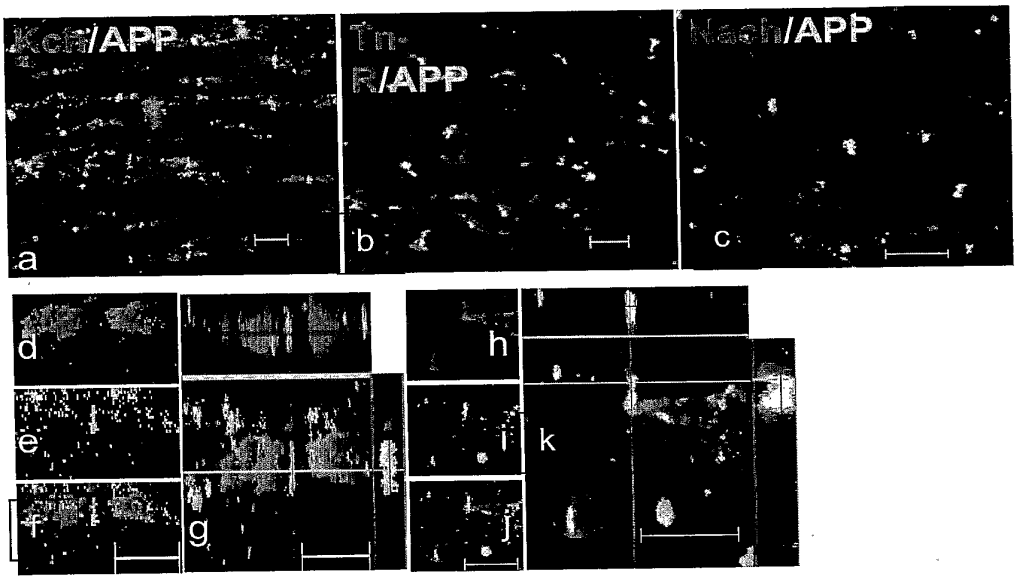


**FIGURE 5**

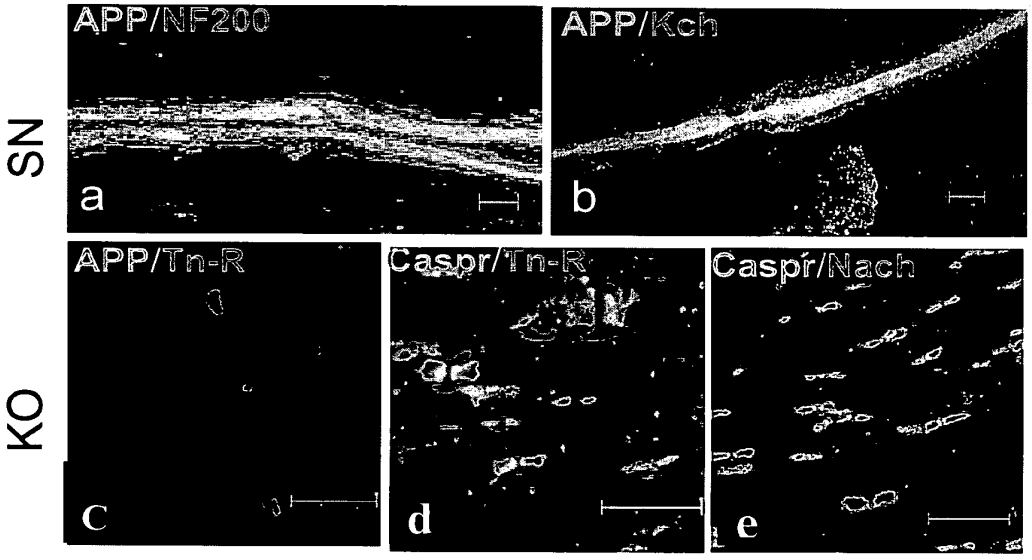


**FIGURE 6**

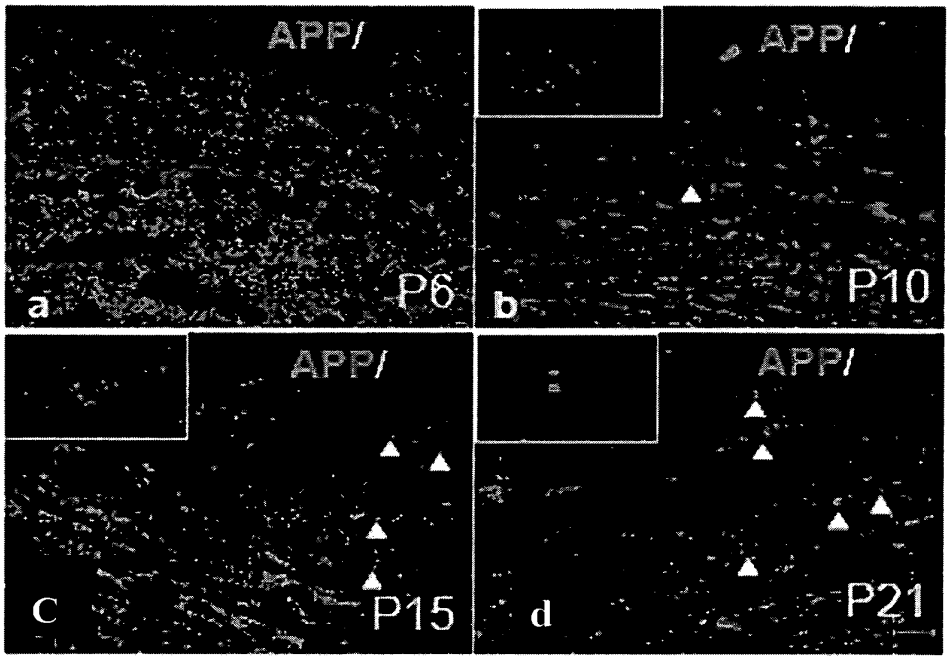


**FIGURE 7**

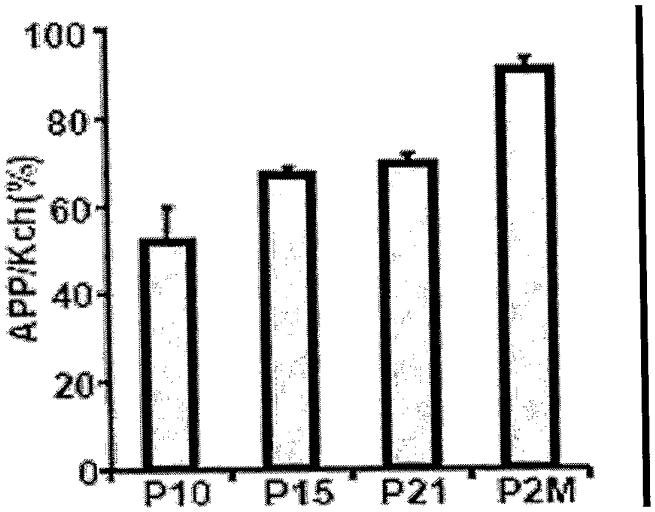



**FIGURE 8**

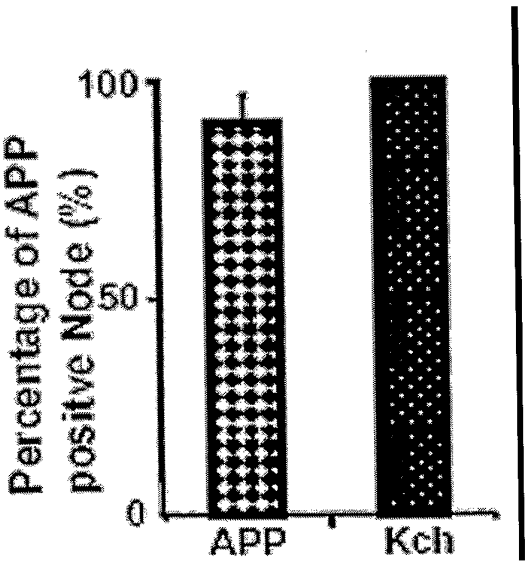
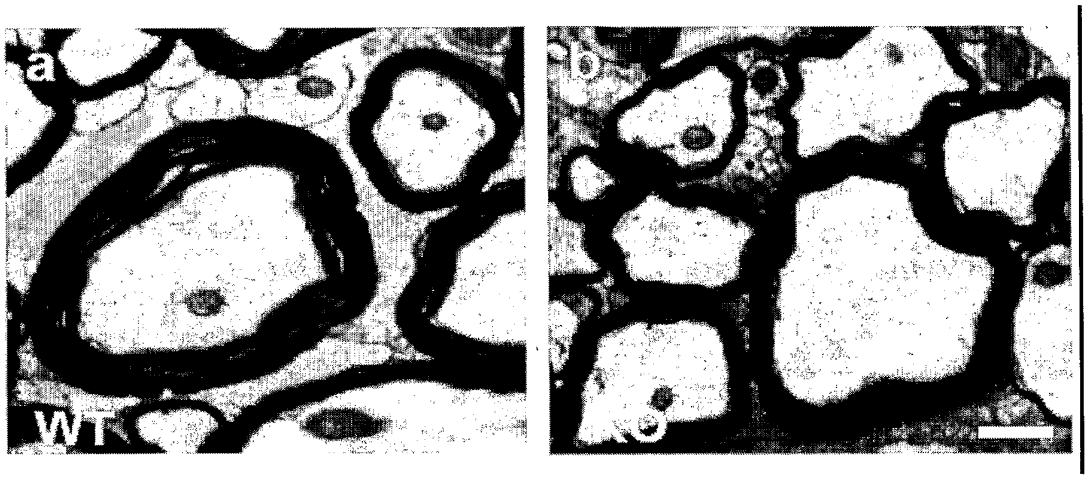


**FIGURE 9**



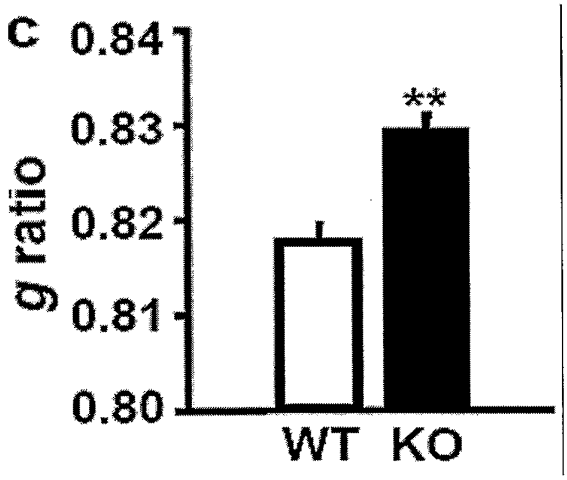
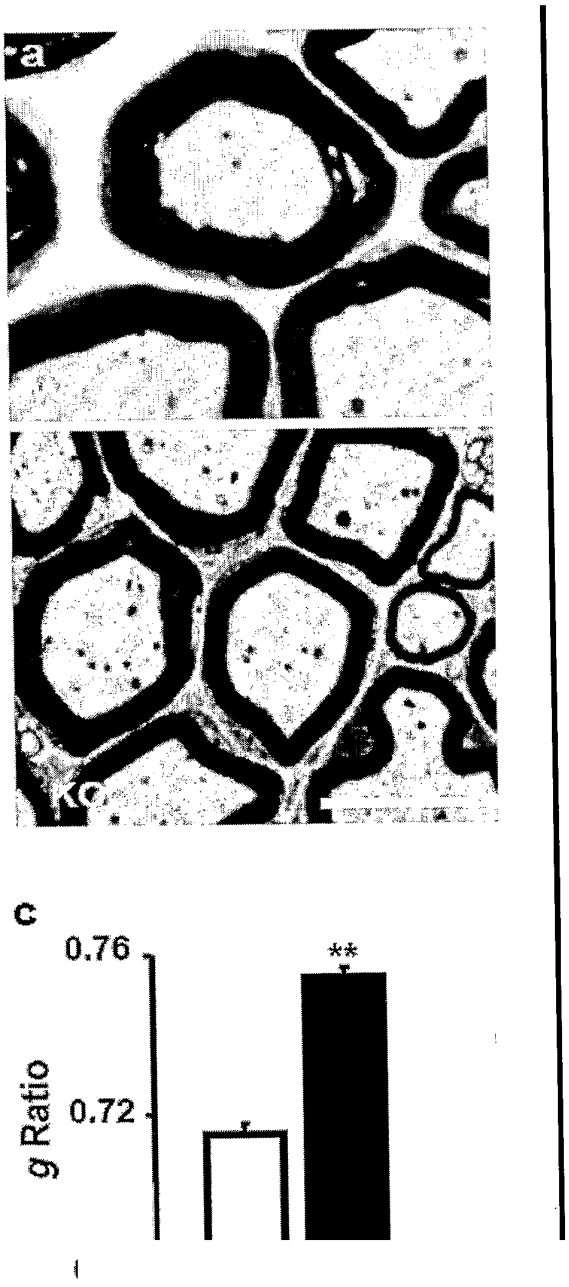



**FIGURE 10**




Fujirebio Diagnostics, Inc. v. Quanterix Corp.
EX-1045
6000